

SYNTHESIS OF INTERLOCKED MOLECULES BY OLEFIN METATHESIS

Thesis by

Paul Gregory Clark

In Partial Fulfillment of the Requirements

for the Degree of

Doctor of Philosophy

California Institute of Technology

Pasadena, California

2011

(Defended July 1, 2010)

© 2011

Paul Gregory Clark

All Rights Reserved

For My Family

## Acknowledgments

I have to begin by thanking Bob for these past five years. And I truly mean “thanking,” as my graduate school experience in your group has been beyond fantastic! Your encouragement and guidance these past five years have been an inspiration to me, and I feel truly blessed to have gotten the opportunity, the honor, to work in your group and become a member of the “Grubbs Research Family.” But I take away from Caltech so much more than a great education. I think it is rare (though not in your group) for a graduate student and advisor to form the kind of friendship I have with you. From river adventures where we have successfully harassed a very respectable number of fish (and even helped several gain a few extra inches of length!) to dinners of fresh trout enjoyed with you and Helen, it has been wonderful to get to enjoy so much time sharing my passion of fly fishing with you! You are well on your way to mastering the sport, and I look forward to taking you out to a “secret spot” whenever you get the chance to come back to Midland.

I would also like to thank my committee members, Prof. Peter Dervan, Prof. David Tirrell, and Prof. Jim Heath, for their advice about research projects and help with my job search this past fall. In addition, it was a pleasure to get to work with both Prof. Tirrell and Prof. Fraser Stoddart during the MURI collaboration. Prof. Wayne Steinmetz was a fantastic collaborator during the charm bracelet synthesis, and I was constantly amazed by his knowledge of NMR and the outdoors.

It is a sure thing that I would not be where I am without the constant support and love from my family. I think it goes without saying that these past five years have been as



challenging as they have been rewarding, and through it all, my family has been with me. Mom, you know I wouldn't be who I am without you! You have always been there to listen, wisely advise, and keep my feet on the path. No son has ever had a better mom, and no mother could have shown more love, patience, and self-sacrifice to her son than you have for me! Dad, you and I have so many wonderful memories of great times together, whether on the river, out back bar-b-queing dinner, or working in the garage on miscellaneous projects. You have helped shape me into the man I am today, and words can't express how much it means to me to be able to share this memory, too, with you. Mandi, you have been so much more than just my sister. You have been my friend, my coconut-bowling buddy, and my official source for all things "cool" ('cause I sure didn't have a clue!). I love you and thank you for always, always being there for me whenever I needed to talk, and for having an awesome apartment right near the beach! Last, but far from least, Gram and Papa...what can I say about you two that could ever do justice to the love you have for me and unceasing support and prayers you have given to me (and said *for* me) not just these past five years but for all my life? I cherish our nightly phone calls, and anxiously look forward to celebrating with you as soon as I am home again!

Several months ago, I received a much-anticipated invitation to a chili cook-off. The rest, they say, is "history", and my life has been so much brighter since that day. My Jo, you are my love, and I am so happy to have you with me to share in this celebration! You have brought balance and endless happiness to my life, and I can't imagine how I made it so long without you! You have supported me more than you know during all the

busy-ness these last several months, and you always have the ability to make me smile no matter how stressed I am. I love you more than I knew it was possible to love someone!

When I first arrived to California, I had the wonderfully good fortune to meet a group of great friends. Pam, Chris, and Zach, you have been my friends these past five years, and know, probably better than anyone, all of the ups and downs of the graduate school experience. We have been through it all together: classes, finals, candidacy, and so much more! I will miss you three very much, but I look forward to watching your successes and achievements (of which there will certainly be many!) in the future!

I simply cannot go any further without acknowledging my “California Family” and the support and love I have received from them. Zach, thank you for sharing your family with me! “Mom West”, I will always cherish all the hugs, morning coffee cake, and lazy days spent on the sundeck catching up on the latest happenings. You have welcomed me with open arms and made me feel like I was your own son! Thank you, too, for sharing Zach during the few times he has gotten back “across the pond”. Greg, dude, what can I say?! Thank you for opening your home, your beverage cupboard, and your hottub to this nerdy Caltech graduate student! I’ve never met someone so open and giving as you. You are, in fact, THE MAN!

At this point, I embark on an especially challenging section of the acknowledgments, and one I’m certain to cover in a very incomplete fashion. I have had the pleasure of working with some fantastic colleagues in a number of groups across the chemistry department. You all know who you are, and I hope that, over time, I’ve not forgotten to tell you how much your friendship has meant to me. With that said, please

do not be offended if I haven't included you in here! I think I must begin with my mentor in the group, Erin Guidry. I don't think I've ever met another person who was unfalteringly cheerful, sweet, and kind as Erin. She always greeted you with a smile, and after a visit with her, I found I couldn't help but smile too. On top of that, she was an incredibly talented chemist, and I feel fortunate to have had her as my lab mentor. And with Erin came Jean Li! I think Jean may be the last member in the group who has been here as long (or longer) than me. Jean, you have been a great sounding board for ideas, both chemistry and otherwise. You were a great softball manager, and have been an invaluable source for keeping me updated on all events Caltech, especially the social ongoings! My first baymate, Jason Jordan, had to put up with the brunt of my ignorance, and answered all my simple and stupid questions with infinite patience. Ron Walker, who was also a member of the Church 217 crew back before the remodel, was my lifting partner for quite some time. It was a pleasure to get "ripped and shredded" with you, Ron, and I'm lucky you were willing to put up with my crazy workouts! More recently, I've had the distinct pleasure of working with AJ on a few projects. But even before the start of ADMET polyrotaxanes, we were able to make frequent Subway/Rubios/"Beer Place" (aka, The Stuffed Sandwich) trips together. AJ, you are amazingly creative and smart, and these abilities are only surpassed, perhaps, by your ability to manage people. You will, without a doubt, be a rockstar in the chemistry world, and will, by your excellence, continue to elevate all those around you to the highest level.

I wouldn't dare to overlook those colleagues who have read so many pages of my writing these past couple of months. AJ, Jean, Renee, Rose, and Simon, thank you for reading my proposals and thesis and offering so many great suggestions!

There are a few "crews" here that I've been a part and that I must acknowledge. The Ath crew is probably first and foremost, as the Ath crew likes to drink! There have been far too many on this crew to name, and, though I'll forget some, I'll give it a try: Andy, Jacob, Erin, Tim, Ian, Pato, Daryl, Kevin, John, Matt, VWs, Keith, Renee, AJ, Rose, Vince, Jean, and all the others I'm blanking on! Relaxing on Friday afternoon (or the afternoon of any particularly-rough day!) with all of you was a great way to end the week! Another "crew" of which I was a member was the Stoltz lunch crew. Meeting at Ernie's, eating awesome food, and getting caught up on all the gossip was always a highlight of my day. There was also the "camping crew", which was composed of an elite group of us city slickers who would go up into mother nature and do our best not to get attacked by a bear. Going camping with all of you and with Bob have been some of my best memories, and will be a tradition I will greatly miss!

The Grubbs group has been fortunate to be blessed with athletic talent, and I've had the great joy (and sometimes pain!) of being a part of several sports teams. Beginning with my forays into softball, I've not only been a part of the "Imperial Palace" championship teams, but I've also been welcomed with open arms on the Stoltz group team, the "Stereoablators"! Playing with you all, win or lose, has been tons of fun, and a great way to take my mind off of chemistry for a few hours in the afternoon! Football has been a bit of a cruel mistress to me during my time here, but I love her just the same! All

I have to say is: “GO PLAYMAKERS!” While I didn’t play but a single game for the Grubbs group basketball team, I am proud to say that I was a part of the “Fuzzy Bunnies of Death.” I’m proud because the name is awesome, which more than makes up for the fact that the win/loss record is not.

One of the things I have most enjoyed about Caltech is the friendly interactions between all of the groups. I always enjoy getting to interact with all those in the Hsieh-Wilson group (that’s right, I’m especially thinking of you, Gloria, and you, Young In!), the Stoltz group (Mike, JT, Sandy, Kevin, Vlad, Dan, Chris, Pam, John, Narae, Amanda and Jon, Andy, Meyer and all the others), and the Reisman group. Friday IOS wouldn’t be the same without friends from all the other groups as well: Bercaw, Dougherty, Dervan, and Gray groups. And, as I said, there are so many other friends I’m sure I’m forgetting!

I would be remiss to end without acknowledging those who have impacted my success as a researcher, as well as my success at having a future career! Dave and Scott, your NMR expertise and constant patience have impacted my research more profoundly than I can describe. Thanks, Dave, for all the countless hours of sitting at FID, pouring over DOSY parameters or 2D analyses of my dimer! I am sure that my hood, not to mention all of our group electronics, would have fallen apart long ago if it weren’t for the unceasing efforts of the amazing Tom Dunn. Caltech will truly miss you when you enter your well-earned retirement. In equal fashion, my glassware would be especially sad if it weren’t for amazing skills of Rick in the glass shop. Mona and Naseem not only were fast and efficient at obtaining data for me, but patiently explained to me the intricacies of

mass spec and why my samples were so terrible! And speaking of terrible samples, my heart goes out to Larry and Mike, our beloved crystallographers. I'm pretty sure I owe each of them a bottle of something (aspirin or alcohol...the choice is theirs!) for the headache my dimer crystals caused them. I will say, to my credit, I heard the words "beautiful crystals" come out of Larry, but, to keep my ego in check, I also had Mike tell me: "You were going to have to shoot me in the head to get me to sign off on that crystal structure!" Last, but FAR from least, the office staff of the chemistry department and career center. Agnes and all the staff have been wonderful, helping with forms and all sorts of ridiculous requests and questions I come up with! I have to say a special thanks to two ladies in particular: Chris Smith and Kathy Miles. They both worked tirelessly on my behalf this past fall, giving advice and answering so many questions about the big, wide world of job hunting. I am sure my position at Dow is due in large part to all of the help I received from them!

Well, I think it's that time to wrap up this section. Before I call this section "finished", though, I want to explicitly state that reaching a goal of this magnitude is not accomplished by one person alone. There are always those working, too often behind the scenes, to support us as we go along our chosen path. I want to take this opportunity to say thank you to all those above, and to all I've not had the chance to mention. You all have my eternal love and gratitude, and, no matter whether we have the chance to cross paths again, I want you to know I always carry with me the example of kindness and friendship you have shown as I move forward in this journey of life!

**Abstract**

A large body of work in the Grubbs group has focused on the development of functional-group tolerant ruthenium alkylidene catalysts that perform a number of olefin metathesis reactions. These catalysts have seen application in a wide range of fields, including classic total synthesis as well as polymer and materials chemistry. One particular family of compounds, interlocked molecules, has benefitted greatly from these advances in catalyst stability and activity. This thesis describes several elusive and challenging interlocked architectures whose syntheses have been realized through the utilization of different types of ruthenium-catalyzed olefin metathesis reactions.

Ring-closing olefin metathesis has enabled the synthesis of a [c2]daisy-chain dimer with the ammonium binding site near the cap of the dimer. A deprotonated DCD possessing such a structural attribute will more forcefully seek to restore coordinating interactions upon reprotonation, enhancing its utility as a synthetic molecular actuator. Dimer functionalization facilitated incorporation into linear polymers, with a 48% size increase of an unbound, extended analogue of the polymer demonstrating slippage of the dimer units. Ongoing work is directed at further materials studies, in particular, exploring the synthesis of macroscopic networks containing the DCD units and analyzing the correlation between molecular-scale extension-contraction manipulations and resulting macro-scale changes.

A “clipping” approach to a polycatenated cyclic polymer, a structure that resembles a molecular “charm bracelet”, has been described. The use of ring-opening metathesis polymerization of a carbamate monomer in the presence of a chain transfer

agent allowed for the synthesis of a linear polymer that was subsequently functionalized and cyclized to the corresponding cyclic analogue. This cyclic polymer was characterized through a variety of techniques, and subjected to further functionalization reactions, affording a cyclic polyammonium scaffold. Diolefin polyether fragments were coordinated and “clipped” around the ammonium sites within the polymer backbone using ring-closing olefin metathesis, giving the molecular “charm bracelet”. Confirmation of the interlocked nature of the product was achieved via  $^1\text{H}$  NMR spectroscopy and two-dimensional diffusion ordered NMR spectroscopy.

A simple strategy for a one-pot, multi-component synthesis of polyrotaxanes using acyclic diene metathesis polymerization was developed. The polyrotaxanes were characterized by traditional  $^1\text{H}$  NMR spectroscopy as well as size exclusion chromatography, and the interlocked topology was confirmed using two-dimension diffusion-ordered NMR spectroscopy. The dynamic, self-correcting nature of the ADMET polymerization was also explored through the equilibration of a capped polyammonium polymer in the presence of dibenzo-24-crown-8 ether and olefin metathesis catalysts. The efficiency and ease with which these mechanically interlocked macromolecules can be assembled should facilitate rapid modulation to achieve versatile polyrotaxane architectures.

Flexible, switchable [c2]daisy-chain dimers (DCDs) were synthesized, where the macromer ammonium binding site was adjacent to the crown-type recognition structure and separated from the cap by an alkyl chain. A DCD of this topology is expected to have an extended structure in the bound conformation (when the ammonium was coordinated



to the crown). Several different macromer candidates were designed to allow access to DCDs with flexible alkyl chains between the ammonium binding site and the cap, and a number of synthetic routes were explored in an effort to access these challenging materials. While the first generation DCD structure proved to be unstable due to a labile ester linkage, work is continuing toward the development of several cap structures in an effort to replace the ester linkage with an ether linkage, which, in the second generation model systems, has proven much more stable to the acidic and basic conditions necessary to induce switching of the dimeric architecture.

One of the efforts in our lab is directed at the synthesis of  $^{18}\text{F}$ -labeled nanoparticles to be used as tumor imaging agents in positron emission tomography. We have been working to optimize fluorine incorporation while minimizing NP crosslinking. Because of evidence of NP side-reactions with the potassium carbonate base, we have begun to use potassium benzoate solid-state beads. To analyze the fluorinated NPs, various sorbents were explored. It was found that silica sorbents rapidly reacted and bound to the NPs, while the NPs remained unreactive and mobile on alumina. Further analysis of the NPs has been accomplished using 2D-DOSY NMR spectroscopy. Future work with the NPs will involve a systematic evaluation of the role of water on the extent of fluorination, as well as functionalization of the NPs with Cy5.5 dye for use in studies on eyes to be done in collaboration with researchers at the Mayo Clinic.

## Table of Contents

Acknowledgments.....	iv
Abstract.....	xi
Table of Contents.....	xiv
List of Figures.....	xvi
List of Schemes.....	xx
List of Abbreviations.....	xxiv

<b>Chapter 1: Introduction.....</b>	<b>1</b>
Introduction.....	2
Interlocked Molecules.....	2
Crown Ether/Ammonium Molecular Recognition.....	8
Dynamic Covalent Chemistry.....	11
Olefin Metathesis.....	13
References.....	22

<b>Chapter 2: [c2]Daisy-Chain Dimers, From Synthesis to Application in Materials.....</b>	<b>31</b>
Introduction.....	32
Dimer Synthesis and Analysis.....	35
Dimer Switching.....	40
Materials Synthesis.....	42
Conclusions.....	50
References.....	50
Experimental Information.....	55

<b>Chapter 3: Synthesis of a Molecular Charm Bracelet via Click Cyclization and Olefin Metathesis Clipping.....</b>	<b>164</b>
Introduction.....	165
Monomer Design and Synthesis.....	169
Polymer Synthesis and Characterization.....	170
Polymer Functionalization.....	176
Molecular “Charm Bracelet” Synthesis and Analysis.....	179
Conclusions.....	183
References.....	184
Experimental Information.....	192

<b>Chapter 4: Facile Synthesis of Polyrotaxanes via Acyclic</b>	
<b><i>Diene Metathesis Polymerization of Supramolecular Monomers</i>.....</b>	<b>265</b>
Introduction/Motivation.....	266
Results and Discussion.....	266
Continuing Work.....	271
Conclusions.....	273
References.....	273
 <b>Appendix 1: Flexible [c2]Daisy-Chain Dimers</b> .....	<b>275</b>
Introduction/Motivation.....	276
Synthesis of the First Generation Flexible [c2]Daisy-Chain Dimer.....	277
Macromer Modifications.....	284
Conclusions.....	289
References.....	290
Experimental Information.....	292
 <b>Appendix 2: Progress Toward <math>^{18}\text{F}</math> Labeled Nanoparticles</b>	
<b><i>as in vivo Imaging Agents</i>.....</b>	<b>309</b>
Recent Results and Discussion.....	310
Future Work.....	313

## List of Figures

### *Chapter 1: Introduction*

<b>Figure 1.1</b>	Graphical depiction of the simplest interlocked molecules, a [2]catenane, [2]rotaxane, and [2]pseudorotaxane.....	2
<b>Figure 1.2</b>	Supramolecular complex formation and important parameters that impact complexation.....	5
<b>Figure 1.3</b>	Graphical representation of exotic interlocked architectures that necessitate supramolecular templation.....	6
<b>Figure 1.4</b>	Graphical representation of [2]rotaxane and [2]catenane bistable molecular switches.....	6
<b>Figure 1.5</b>	Graphical representation of polyrotaxane and polycatenane interlocked architectures.....	7
<b>Figure 1.6</b>	Impact of crown ether structure on the association constants with ammonium ions <b>2</b> and <b>10</b> .....	10
<b>Figure 1.7</b>	Structures of some ruthenium-based olefin metathesis catalysts.....	14
<b>Figure 1.8</b>	Various olefin metathesis reactions and their products.....	16
<b>Figure 1.9</b>	Various ROMP monomers and their ring-strain energies.....	19

***Chapter 2: [c2]Daisy-Chain Dimers, From Synthesis to Application in Materials***

<b>Figure 2.1</b>	Graphical representation of switching of a bistable DCD and a terminal-ammonium DCD.....	32
<b>Figure 2.2</b>	Structure of macromer <b>1</b> -H·PF <sub>6</sub> .....	34
<b>Figure 2.3</b>	Solid-state structure of <b>20</b> -H <sub>2</sub> ·2PF <sub>6</sub> and analysis of $\pi$ - $\pi$ slipped-stacking interactions using the crystal structure and NMR spectra.....	39
<b>Figure 2.4</b>	Diastereomers formed during dimerization of <b>1</b> -H·PF <sub>6</sub> .....	39
<b>Figure 2.5</b>	NMR spectra of “switching” of dimer <b>18</b> -H <sub>2</sub> ·2PF <sub>6</sub> .....	41
<b>Figure 2.6</b>	Click gelation of <b>22</b> -H <sub>2</sub> ·2PF <sub>6</sub> to produce amorphous gels and gel cylinders.....	45
<b>Figure 2.7</b>	Relationship between copper catalyst loading and trialkyne/ <b>22</b> -H <sub>2</sub> ·2PF <sub>6</sub> gelation time.....	46
<b>Figure 2.8</b>	Small library of trialkynes used to tailor the stability and properties of the DCD click gels.....	46

***Chapter 3: Synthesis of a Molecular Charm Bracelet via Click Cyclization and Olefin Metathesis Clipping***

<b>Figure 3.1</b>	Graphical representation of the macrocyclization of an $\alpha,\omega$ -heterotelechelic polymer under high-dilution conditions.....	166
<b>Figure 3.2</b>	Ruthenium olefin metathesis catalysts <b>1</b> and <b>2</b> .....	166

<b>Figure 3.3</b>	Examples of a mechanically-interlocked [2]rotaxane and a [2]catenane synthesized using olefin metathesis.....	167
<b>Figure 3.4</b>	Graphical representations of various polycatenane structures, including main-chain, side-chain, and cyclic polycatenanes.....	168
<b>Figure 3.5</b>	GPC traces of linear bromide polymer <b>L-11</b> , linear azide polymer <b>L-12</b> , doubly-clicked linear polymer <b>L-15</b> , and cyclic polymer <b>C-13</b> .....	172
<b>Figure 3.6</b>	Proton NMR spectral analysis of polymer end-group resonances for <b>L-11</b> , <b>L-12</b> , and <b>C-13</b> .....	172
<b>Figure 3.7</b>	FT-IR spectrum for <b>L-11</b> , <b>L-12</b> , <b>L-15</b> , and <b>C-13</b> .....	173
<b>Figure 3.8</b>	Proton NMR spectral analysis of clicked polymer end-group resonances for <b>L-15</b> and <b>C-13</b> .....	175
<b>Figure 3.9</b>	Proton NMR spectral analysis of the threading interactions of 24-crown-8 ether with <b>C-13</b> and <b>L-15</b> .....	178
<b>Figure 3.10</b>	Two-dimensional DOSY $^1\text{H}$ NMR spectra of ring-closed crown <b>23</b> , cyclic polyammonium polymer <b>C-17-<math>n\text{H} \cdot n\text{PF}_6</math></b> , molecular charm bracelet <b>C-22-<math>n\text{H} \cdot n\text{PF}_6</math></b> , and a physical mixture of <b>C-22-<math>n\text{H} \cdot n\text{PF}_6</math></b> and <b>23</b> .....	182

## ***Chapter 4: Facile Synthesis of Polyrotaxanes via Acyclic Diene Metathesis***

### ***Polymerization of Supramolecular Monomers***

<b>Figure 4.1</b>	2D-DOSY NMR of polyrotaxane <b>6-mH</b> · <i>m</i> PF <sub>6</sub> .....	269
<b>Figure 4.2</b>	Data for ADMET polymerizations of various monomers to form polyrotaxane <b>6-mH</b> · <i>m</i> PF <sub>6</sub> .....	270

### ***Appendix 1: Flexible [c2]Daisy-Chain Dimers***

<b>Figure A1.1</b>	Graphical comparison of DCDs formed from a macromer with adjacent recognition moiety and binding site and the terminal-ammonium macromer from Chapter 2.....	276
<b>Figure A1.2</b>	First generation macromer <b>1-H</b> ·PF <sub>6</sub> .....	278
<b>Figure A1.3</b>	Second generation macromer <b>20-H</b> ·PF <sub>6</sub> .....	284
<b>Figure A1.4</b>	Cap structures <b>27</b> , <b>28</b> , and <b>29</b> that will be used to make DCDs presenting functional handles for incorporation in materials.....	286
<b>Figure A1.5</b>	Third generation macromer <b>30-H</b> ·PF <sub>6</sub> .....	287

### ***Appendix 2: Progress Toward <sup>18</sup>F Labeled Nanoparticles as in vivo Imaging Agents***

<b>Figure A2.1</b>	Two-dimensional DOSY <sup>1</sup> H NMR spectrum of fluorinated nanoparticles.....	313
<b>Figure A2.2</b>	General structure of Cy5.5 dye to be appended to NPs.....	314

## List of Schemes

### *Chapter 1: Introduction*

<b>Scheme 1.1</b>	Synthesis of the First [2]Catenane <b>1</b> .....	4
<b>Scheme 1.2</b>	“Perching” and “Nesting” Interactions Between Crown Ethers and Ammonium Ions.....	8
<b>Scheme 1.3</b>	Irreversible Kinetic and Reversible Dynamic Covalent Interlocking Reactions to Form a [2]Rotaxane.....	11
<b>Scheme 1.4</b>	Metal-Alkylidene Mediated Olefin Metathesis Mechanism...	13
<b>Scheme 1.5</b>	Synthesis of a Monodisperse Polymer and an End-Functionalized Telechelic Polymer via ROMP.....	20

### *Chapter 2: [c2]Daisy-Chain Dimers, From Synthesis to Application in Materials*

<b>Scheme 2.1</b>	Graphical Representation of DCD Synthesis via RCM or Capping.....	33
<b>Scheme 2.2</b>	Graphical DCD Synthesis and Possible Intramolecularly-Coupled Side-Products.....	34
<b>Scheme 2.3</b>	Synthesis of Crown-Biphenyl Fragment <b>3</b> .....	35
<b>Scheme 2.4</b>	Synthesis of Cap Fragment <b>12</b> .....	36
<b>Scheme 2.5</b>	Synthesis of DCD Macromer <b>1-H</b> ·PF <sub>6</sub> .....	37
<b>Scheme 2.6</b>	Synthesis of DCD <b>18-H</b> <sub>2</sub> ·2PF <sub>6</sub> and Ring-Closed Macromer <b>19-H</b> ·PF <sub>6</sub> .....	37
<b>Scheme 2.7</b>	Saturation of DCD <b>18-H</b> <sub>2</sub> ·2PF <sub>6</sub> .....	38



<b>Scheme 2.8</b>	Switching of DCD <b>18</b> -H <sub>2</sub> ·2PF <sub>6</sub> .....	40
<b>Scheme 2.9</b>	Synthesis of Azide Dimer <b>22</b> -H <sub>2</sub> ·2PF <sub>6</sub> .....	42
<b>Scheme 2.10</b>	Synthesis of Linear DCD Polymer <b>23</b> -H <sub>2n</sub> ·2nPF <sub>6</sub> , Neutral Polymer <b>24</b> , and Extended Acylated Analogue <b>25</b> .....	43
<b>Scheme 2.11</b>	Click Gelation of <b>22</b> -H <sub>2</sub> ·2PF <sub>6</sub> and Tripropargylamine.....	44
<b>Scheme 2.12</b>	Screened Conditions to Elongate DCD Gels.....	47
<b>Scheme 2.13</b>	Synthesis of Porous DCD Gel.....	49

### ***Chapter 3: Synthesis of a Molecular Charm Bracelet via Click Cyclization and Olefin***

#### ***Metathesis Clipping***

<b>Scheme 3.1</b>	Synthesis of 9-Membered Cyclic Carbamate Monomer <b>3</b> ....	169
<b>Scheme 3.2</b>	Synthesis of Linear Telechelic Dibromide Polymer <b>L-11</b> , Diazide Polymer <b>L-12</b> , and Cyclic Polymer <b>C-13</b> .....	171
<b>Scheme 3.3</b>	‘Click’ Removal of Linear Contaminants from Cyclic Polymer <b>C-13</b> Using Azide- and Alkyne-Functionalized Beads.....	174
<b>Scheme 3.4</b>	Synthesis of Doubly-Clicked Linear Polymer <b>L-15</b> .....	175
<b>Scheme 3.5</b>	Synthesis of Cyclic Polyammonium <b>C-17</b> -nH·nPF <sub>6</sub> and Linear Polyammonium <b>L-18</b> -nH·nPF <sub>6</sub> .....	177
<b>Scheme 3.6</b>	Screen Reaction to Determine Effect of Nitromethane Concentration on RCM Olefin Conversion.....	180

<b>Scheme 3.7</b>	Graphical Representation of the Synthesis of Molecular “Charm Bracelet” <b>C-22</b> · <i>n</i> H· <i>n</i> PF <sub>6</sub> .....	181
-------------------	---	-----

#### ***Chapter 4: Facile Synthesis of Polyrotaxanes via Acyclic Diene Metathesis***

##### ***Polymerization of Supramolecular Monomers***

<b>Scheme 4.1</b>	Synthesis of Dialkenyl Ammonium Salts <b>2a</b> and <b>2b</b> and Templation with DB24C8 to Provide Supramolecular Monomers <b>3a</b> and <b>3b</b> .....	267
<b>Scheme 4.2</b>	ADMET Polymerization of Supramolecular Monomers <b>3a</b> and <b>3b</b> to Form Polyrotaxane <b>6</b> · <i>m</i> H· <i>m</i> PF <sub>6</sub> .....	268
<b>Scheme 4.3</b>	One-Pot ADMET Polymerization to Form <b>6</b> · <i>m</i> H· <i>m</i> PF <sub>6</sub> .....	271
<b>Scheme 4.4</b>	Proposed Threading Equilibration Test of Capped Polyammonium Polymer <b>7</b> · <i>m</i> H· <i>m</i> PF <sub>6</sub> with Catalysts <b>4</b> and <b>8</b> .....	272

##### ***Appendix 1: Flexible [c2]Daisy-Chain Dimers***

<b>Scheme A1.1</b>	Synthesis of Crown Fragment <b>8</b> .....	278
<b>Scheme A1.2</b>	Synthesis of Flexible Cap Fragment <b>15</b> .....	280
<b>Scheme A1.3</b>	Synthesis of Macromer <b>1</b> ·H·PF <sub>6</sub> .....	281
<b>Scheme A1.4</b>	Dimerization of <b>1</b> ·H·PF <sub>6</sub> .....	282
<b>Scheme A1.5</b>	Synthesis of Macromer <b>20</b> ·H·PF <sub>6</sub> .....	285
<b>Scheme A1.6</b>	Dimerization of Macromer <b>20</b> ·H·PF <sub>6</sub> .....	286

<b>Scheme A1.7</b>	Synthesis of Third Generation Flexible Backbone-Cap <b>34</b> .....	288
--------------------	--	-----

***Appendix 2: Progress Toward  $^{18}\text{F}$  Labeled Nanoparticles as in vivo Imaging Agents***

<b>Scheme A2.1</b>	Fluorination of Mesylated Nanoparticles.....	310
<b>Scheme A2.2</b>	Synthesis of Resin-Bound Potassium Benzoate.....	312

**List of Abbreviations**

<b>24C8</b>	24-crown-8 ether
<b>Ac<sub>2</sub>O</b>	acetic anhydride
<b>ADMET</b>	acyclic diene metathesis
<b>Boc</b>	<i>tert</i> -butyl carbamate
<b>Boc<sub>2</sub>O</b>	di- <i>tert</i> -butyl dicarbamate
<b>CD<sub>3</sub>CN</b>	deuterated acetonitrile
<b>CDCl<sub>3</sub></b>	deuterated chloroform
<b>click</b>	Huisgen 1,3-dipolar cycloaddition
<b>CM</b>	cross metathesis
<b>COD</b>	cyclooctadiene
<b>COSY</b>	correlation spectroscopy
<b>CP</b>	cyclic polymer
<b>CsCO<sub>3</sub></b>	cesium carbonate
<b>CTA</b>	chain-transfer agent
<b>CuAAC</b>	copper-catalyzed alkyne-azide click
<b>CuBr</b>	copper(I) bromide
<b>DB24C8</b>	dibenzo-24-crown-8 ether
<b>DBU</b>	1,8-Diazabicyclo[5.4.0]undec-7-ene
<b>dc</b>	change in concentration
<b>DCC</b>	dynamic covalent chemistry
<b>DCD</b>	[c2]daisy-chain dimer

<b>DCM</b>	dichloromethane
<b>DMAP</b>	4-dimethylaminopyridine
<b>DMF</b>	N,N-dimethylformamide
<b>DMSO</b>	dimethylsulfoxide
<b>DMTS</b>	dimethylthexylsilyl
<b>dn</b>	change in refractive index
<b>D<sub>2</sub>O</b>	deuterium oxide
<b>DOSY (or 2D-DOSY)</b>	diffusion ordered nuclear magnetic resonance spectroscopy
<b>DP</b>	degree of polymerization
<b>DPTS</b>	N,N-dimethylaminopyridinium <i>p</i> -toluene-sulfonate
<b>D.-S.</b>	Dean-Stark
<b>EDC</b>	1-ethyl-3-(3-dimethylaminopropyl)-carbodiimide
<b>EI</b>	electrospray ionization
<b>Et<sub>3</sub>N</b>	triethylamine
<b>FAB</b>	fast atom bombardment
<b>FT-IR</b>	Fourier-transform infrared
<b>GPC</b>	gel permeation chromatography
<b><sup>1</sup>H</b>	proton
<b>HMBC</b>	heteronuclear multiple-bond correlation
<b>HPF<sub>6</sub></b>	hydrogen hexafluorophosphate
<b>HSQC</b>	heteronuclear spin quantum coherence

<b>K222</b>	kryptofix-222
<b><math>K_a</math></b>	association constant
<b><math>K_2CO_3</math></b>	potassium carbonate
<b>KOH</b>	potassium hydroxide
<b>kDa</b>	kilodaltons
<b>LAH</b>	lithium aluminum hydride
<b>M</b>	molarity
<b>MeNO<sub>2</sub></b>	nitromethane
<b>MALDI</b>	matrix-assisted laser-desorption/ionization
<b>MALLS</b>	multiangle laser light scattering
<b>MeOH</b>	methanol
<b>MgSO<sub>4</sub></b>	magnesium sulfate
<b><math>M_n</math></b>	number average molecular weight
<b><math>M_w</math></b>	weight average molecular weight
<b>MS</b>	mass spectrometry
<b>MsCl</b>	methanesulfonyl chloride
<b>MW</b>	molecular weight
<b>NaBH<sub>4</sub></b>	sodium borohydride
<b>NaOH</b>	sodium hydroxide
<b>NHC</b>	N-heterocyclic carbene
<b>NMR</b>	nuclear magnetic resonance
<b>NOESY</b>	nuclear Overhauser enhancement spectroscopy

<b>NP</b>	nanoparticle
<b>PCy<sub>3</sub></b>	tricyclohexylphosphine
<b>PDI</b>	polydispersity index
<b>PF<sub>6</sub></b>	hexafluorophosphate
<b>PMDETA</b>	<i>N,N,N',N'',N''</i> -pentamethyldiethylene-triamine
<b>PPh<sub>3</sub></b>	triphenylphosphine
<b><i>R<sub>g</sub></i></b>	radius of gyration
<b><i>R<sub>h</sub></i></b>	radius of hydration
<b>RCM</b>	ring-closing metathesis
<b>ROMP</b>	ring-opening metathesis polymerization
<b>r.t.</b>	room temperature
<b>TBDPS</b>	<i>tert</i> -butyldiphenylsilyl
<b>TBS</b>	<i>tert</i> -butyldimethylsilyl
<b>TBSCl</b>	<i>tert</i> -butyldimethylsilyl chloride
<b>TEA</b>	triethylamine
<b>TFA</b>	trifluoroacetic acid
<b>ThDMS</b>	thexyldimethylsilyl
<b>THF</b>	tetrahydrofuran
<b>THP</b>	tetrahydropyranyl
<b>TLC</b>	thin-layer chromatography
<b>TsCl</b>	<i>para</i> -toluenesulfonyl chloride

**TOF**

time-of-flight

**wt**

weight



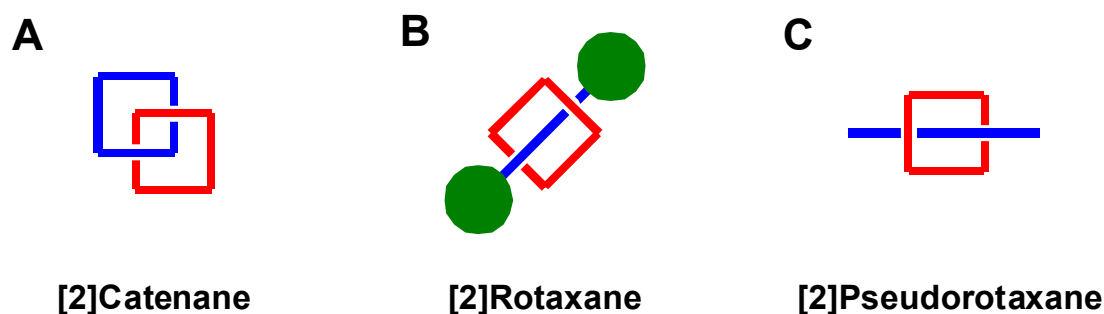
# **CHAPTER 1**

## **Introduction: Interlocked Molecules and Olefin Metathesis**

A large body of work in the Grubbs group has focused on the development of functional-group tolerant ruthenium alkylidene catalysts that perform a number of olefin metathesis reactions. These catalysts have seen application in a wide range of fields, including classic total synthesis as well as polymer and materials chemistry. One particular family of compounds, interlocked molecules, has benefitted greatly from these advances in catalyst stability and activity. This thesis describes several elusive and challenging interlocked architectures whose syntheses have been realized through the utilization of different types of ruthenium-catalyzed olefin metathesis reactions.

### ***Interlocked Molecules***

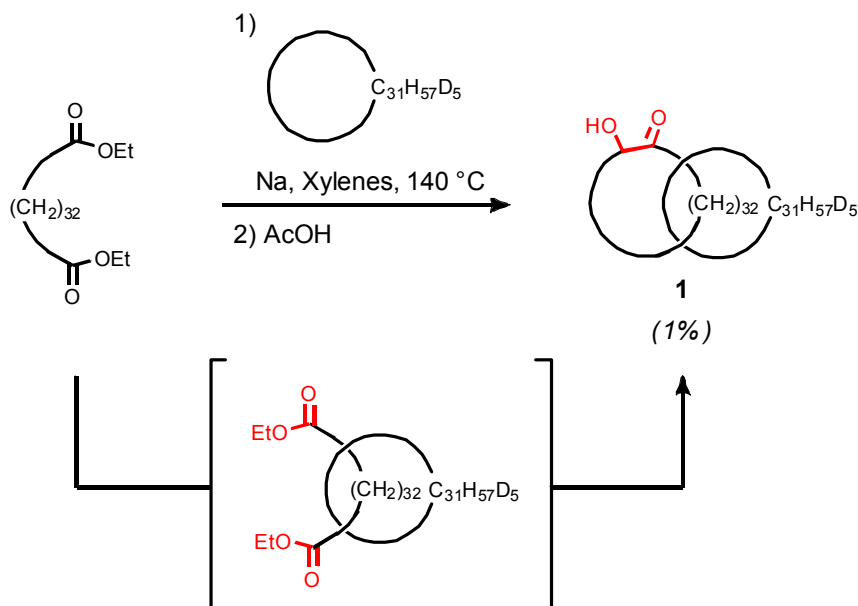
Interlocked molecules are defined as compounds composed of two or more discrete molecules that contain no covalent bonds between them, but that cannot be separated without cleavage of at least one covalent bond. The family of interlocked molecules<sup>1-5</sup> has two primary categories: catenanes and rotaxanes (Figure 1.1). Catenanes are structures composed of two or more rings threaded through one another,<sup>6-10</sup> and the simplest form is the [2]catenane (Figure 1.1A). In this nomenclature system, the number



**Figure 1.1:** Graphical depiction of the simplest interlocked molecules, the [2]catenane (A) and [2]rotaxane (B), and a non-interlocked precursor, the [2]pseudorotaxane (C).

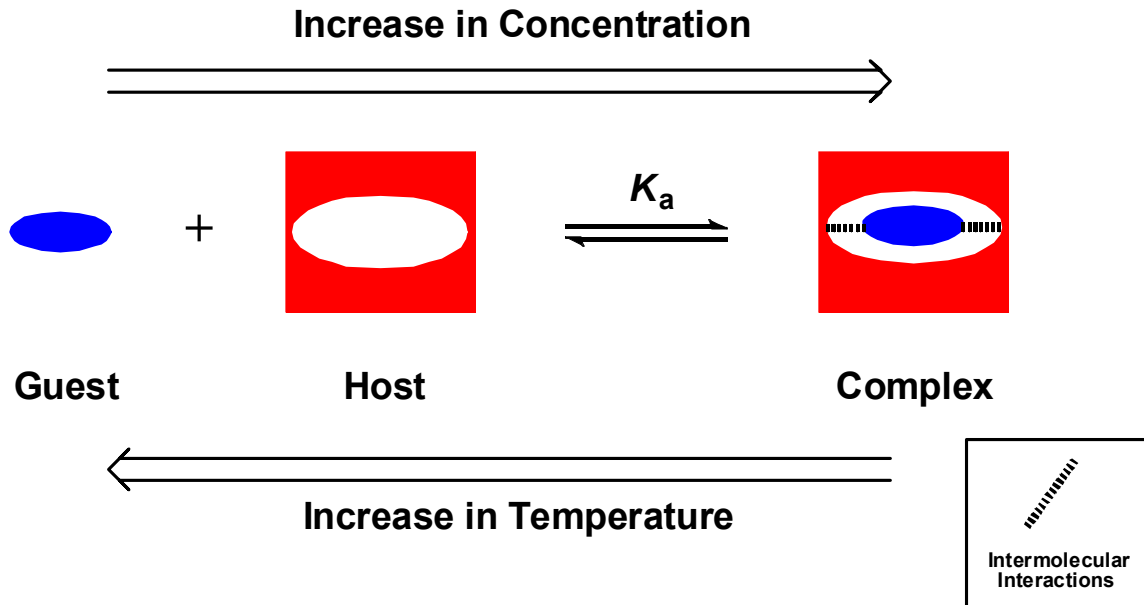
in brackets designates how many independent molecules are interlocked together. Rotaxanes are the second major class of interlocked molecules,<sup>11-17</sup> and are composed of a dumbbell-like rod encircled by one or more rings. Nomenclature of rotaxanes is the same as that for catenanes, with the lowest-complexity rotaxane, a [2]rotaxane (Figure 1.1B), having just a single ring encircling a rod-like structure. Often, the central rod has bulky groups on each end, as this prevents dethreading of the complex. A structure that lacks these “stoppers” is termed a pseudorotaxane (Figure 1.1B) due to the dynamic nature of the complex (the ring can slip off of the rod). Pseudorotaxanes are common precursors to both rotaxanes and catenanes. Though both rotaxanes and catenanes are interlocked molecules, catenanes are considered topological isomers since cleavage of a covalent bond is *required* to separate the rings, while rotaxanes are constitutional isomers, as it is theoretically possible to slip a ring over the blocking group and separate the molecules without covalent bond cleavage.

The first synthesis (Scheme 1.1) of an interlocked molecule, [2]catenane **1**, was reported by Wasserman and coworkers as Bell Laboratories in 1960,<sup>10</sup> and was the result of statistical threading of a linear chain through a macrocycle and the subsequent cyclization of that linear chain via an acyloin condensation. While the researchers were able to isolate interlocked product, they were only able to obtain a 1% yield of **1** due in part to the low-probability threading-cyclization process. Indeed, the syntheses of interlocked molecules have traditionally suffered from a low yield of desired product, and these low-yielding reactions created a two-fold problem: first, producing reasonable quantities of well-controlled interlocked structures was an intractable task, and, second,

**Scheme 1.1:** Synthesis of the First [2]Catenane **1**

the interlocked product had to be separated from the non-interlocked by-products. Many purification processes proved laborious and challenging, greatly increasing the time required to obtain bulk amounts of material and limiting the development of technologies employing mechanically interlocked structures as key building blocks.

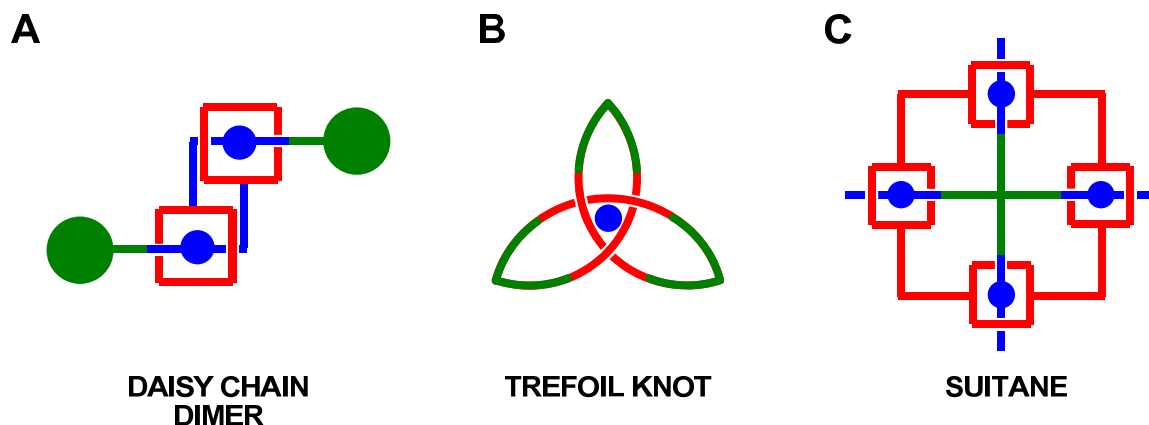
While interlocked molecules have always piqued the interest of researchers, these structures remained little more than intellectual curiosities for a long period of time. A major advance in the field occurred when supramolecular chemistry, also known as “host-guest” chemistry, was applied to the synthesis of interlocked structures.<sup>1-5,18,19</sup> Supramolecular chemistry enables assembly in solution of dynamic complexes composed of a number of different molecular constituents (Figure 1.2). These complexes are often held together by weak intra- or intermolecular interactions (such as hydrogen bonding<sup>20</sup> or  $\pi$ - $\pi$  stacking),<sup>21,22</sup> though strong metal coordination has also been exploited to produce supramolecular complexes with good success.<sup>23-25</sup> Regardless of the type of



**Figure 1.2:** Supramolecular complex formation and various parameters that impact the quantity of complex versus free guest and host.

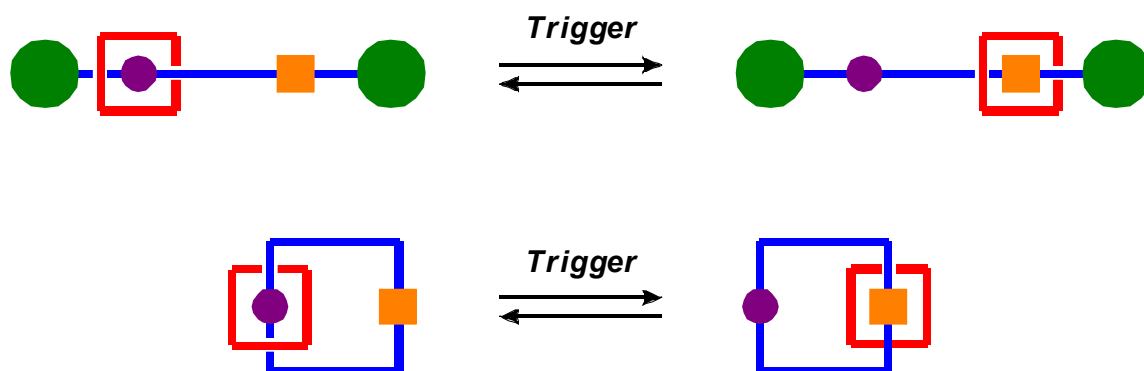
molecular recognition employed, the strength of the interaction between the pieces is denoted by the association constant,  $K_a$ , which has units of inverse concentration. The value of  $K_a$  determines whether, under specific conditions, a given system will favor the free constituents or the host-guest complex. Also, increasing the concentration of the host and guest structures favors complex formation, while increasing temperature decreases complexation.

Designing precursor molecules that contain precisely-located recognition moieties has enabled researchers to control the orientation of the pieces of a supramolecular architecture with respect to one another prior to the final covalent interlocking reaction. Such control has not only facilitated higher-yielding syntheses of simple interlocked

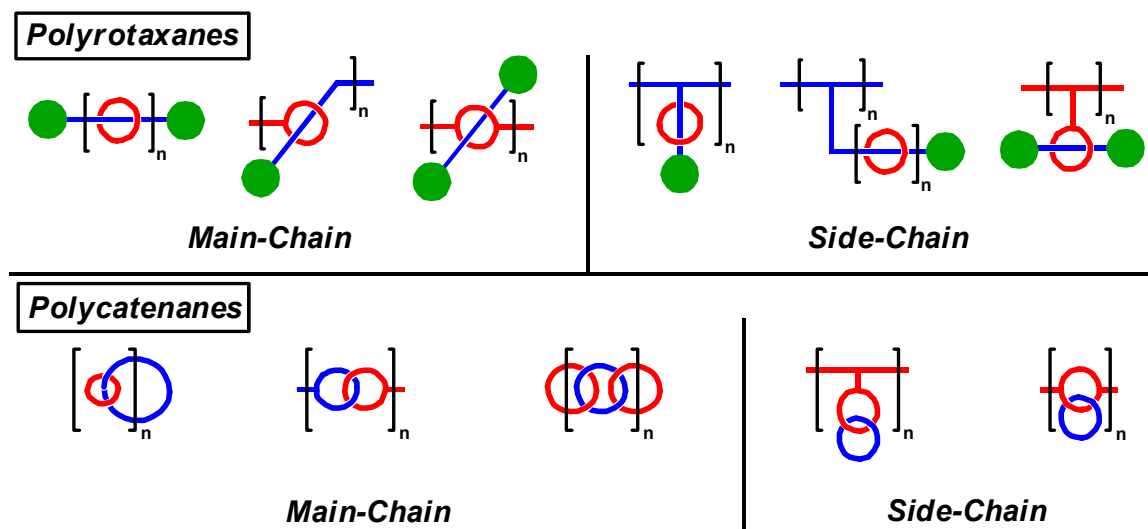


**Figure 1.3:** Graphical representation of various exotic interlocked structures whose syntheses necessitate the use of supramolecular host-guest templation

structures, but has also allowed the realization of beautiful and elegant structures (Figure 1.3) unattainable via statistical interlocking procedures.<sup>26-32</sup> While mechanically interlocked complexes are intellectually intriguing and pose significant synthetic challenge, recent advances in nanotechnology have indicated that structures are more than simple curiosities. Some design motifs enable coding of information using the topological orientation of the interlocked components, so-called molecular switches (Figure 1.4). In addition to molecular data storage, other types of interlocked structures



**Figure 1.4:** Graphical representation of bistable [2]rotaxanes and [2]catenanes that can be used as molecular switches.



**Figure 1.5:** Graphical representation of various polyrotaxane and polycatenane interlocked architectures.

such as daisy-chain dimers (Figure 1.3A)<sup>26-30</sup> can potentially behave as molecular machines, undergoing changes of dimension<sup>30</sup> and exerting forces on external surfaces. Regardless of the application, mechanically interlocked structures represent an intriguing subset of molecules that may allow control over device features on the nanoscale.<sup>33-45</sup> This type of “bottom-up” approach provides an attractive alternative to “top-down” fabrication techniques, such as microlithography.

When designing a synthetic route to a particular interlocked compound, whether a small molecule (Figure 1.1 and 1.3) or polymeric structure (Figure 1.5),<sup>46-51</sup> two parameters play the most significant role in the success (or failure) of the synthesis. The first involves the identity of the recognition motifs. Though utilizing a system with a high  $K_a$  is a worthy goal, further consideration of the type of molecular recognition is critical to not only the synthesis of the molecule but the subsequent “function” of the interlocked structure. Additionally, it is important to use a templation motif that is stable to the

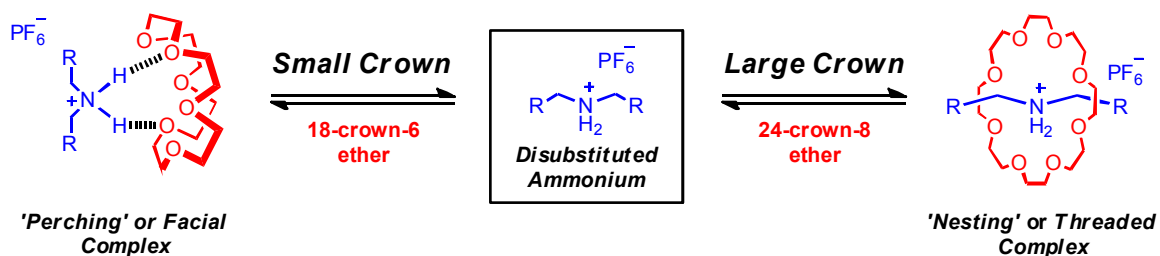
necessary interlocking reaction, which is the second critical component of the synthesis. Both of these topics warrant further elaboration, and will be discussed in more depth in this chapter as well as the individual chapters of this thesis.

### ***Crown Ether/Ammonium Molecular Recognition***

While many classes of intermolecular interactions have been employed in the supramolecular assembly and synthesis of interlocked compounds, hydrogen bonding has received particular attention. Nature has provided inspiration for a number of these motifs,<sup>52</sup> and some common biologically-based hydrogen bonding units exploited to template supramolecular complexes include base-pair hydrogen bonding<sup>53,54</sup> and amide hydrogen bonding.<sup>55-59</sup> In addition to these groups, hydrogen bonding between crown ethers and ammonium ions has a rich history in the interlocked molecules literature.<sup>1-5,20,60-62</sup> Throughout the subsequent chapters, the threaded interactions between crown ethers and disubstituted ammonium ions (Scheme 1.2) were harnessed to produce complex interlocked architectures.

Crown ethers are macrocyclic polyether structures containing a number of oxygen atoms within their skeleton. These structures were first discovered by Pederson<sup>63,64</sup> and,

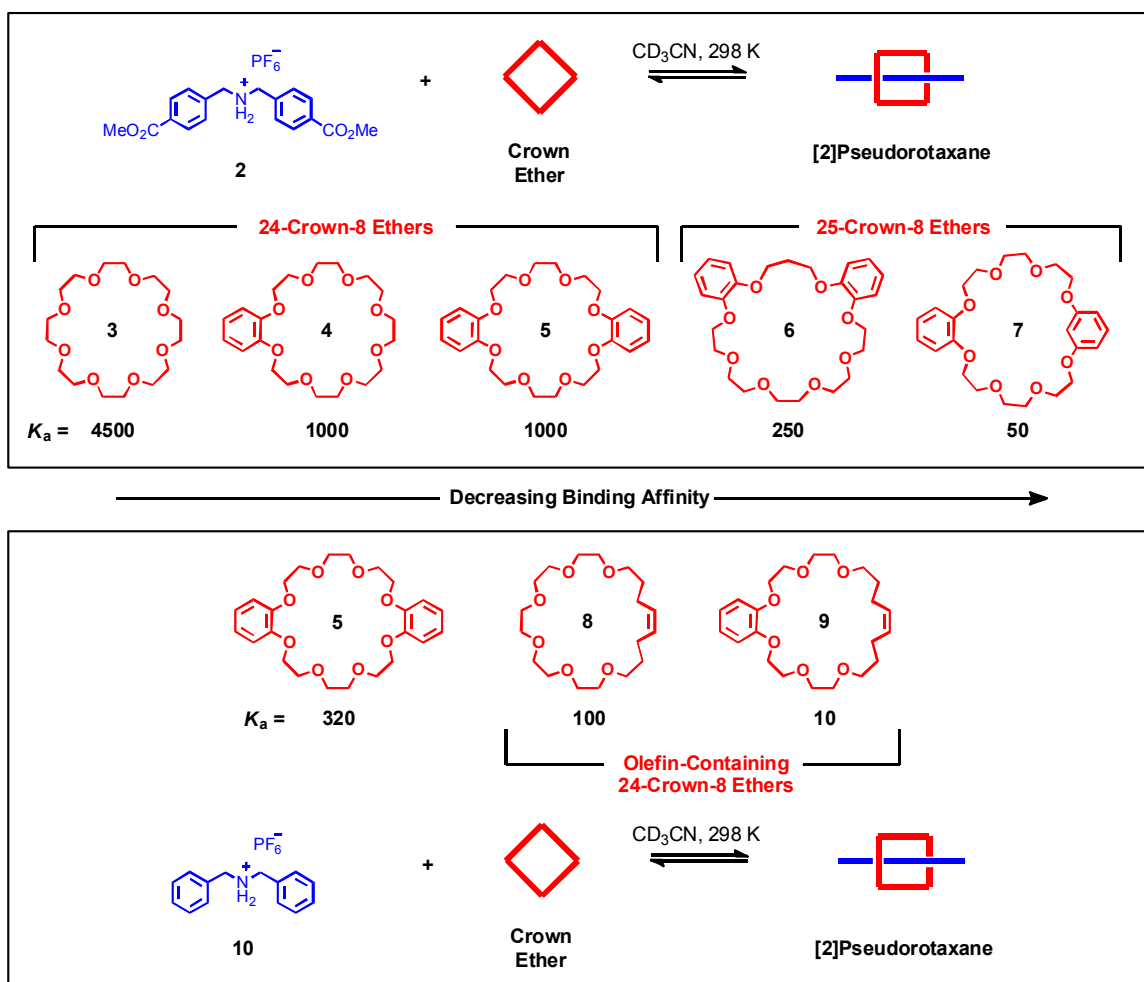
**Scheme 1.2:** “Perching” and “Nesting” Interactions Between Crown Ethers and Ammonium Ions





later, studied by Cram,<sup>65</sup> and their work with these structures earned them a Nobel Prize in 1987. It has been well-established that crown ethers bind metal cations (potassium, sodium, etc.), but these species can also form association complexes with mono- or dialkylated ammonium ions. Two conformations of such crown ether/ammonium complexes can be envisioned (Scheme 1.2): an external wrapping of the ammonium ion by the crown (a facial interaction) or a structure where the ammonium is encircled by the crown (a threading interaction). These complexation structures are called ‘perching’ and ‘nesting’, respectively, and the particular form adopted by the crown ether depends upon the size of the macrocycle. For instance, 18-crown-6 ether generally prefers to bind to ammonium ions in a perching fashion, while larger crown structures such as 24-crown-8 ether will usually form a nesting structure with the same cation.<sup>57</sup>

Not only does the size of the crown ether play a significant role in the type of complex formed, but the structure of the crown ether heavily influences the strength of the hydrogen bonding of the complex (the  $K_a$ ). This phenomenon has been extensively investigated (Figure 1.6), and it has been found that with dialkylammonium ion **2**, alkyl crown ethers (e.g., those crown ethers with dialkyl ether linkages) have the strongest bonding (ca.  $4500\text{ M}^{-1}$  for 24-crown-8 ether **3**). Introduction of phenolic oxygens (either one or two pairs of phenolic oxygens, crown ethers **4** and **5**, respectively) decreases the association constant of the crown ether (ca.  $1000\text{ M}^{-1}$  for dibenzo-24-crown-8 ether **5**). This decrease occurs because of two effects: first, phenolic oxygens are less basic and do not H-bond as strongly as alkyl ethers, and, second, it is likely that the structural rigidity introduced by aromatic linkages on one or both sides of the crown decreases the



**Figure 1.6:** Impact of crown ether structure on the association constants with ammonium ions **2** and **10**.

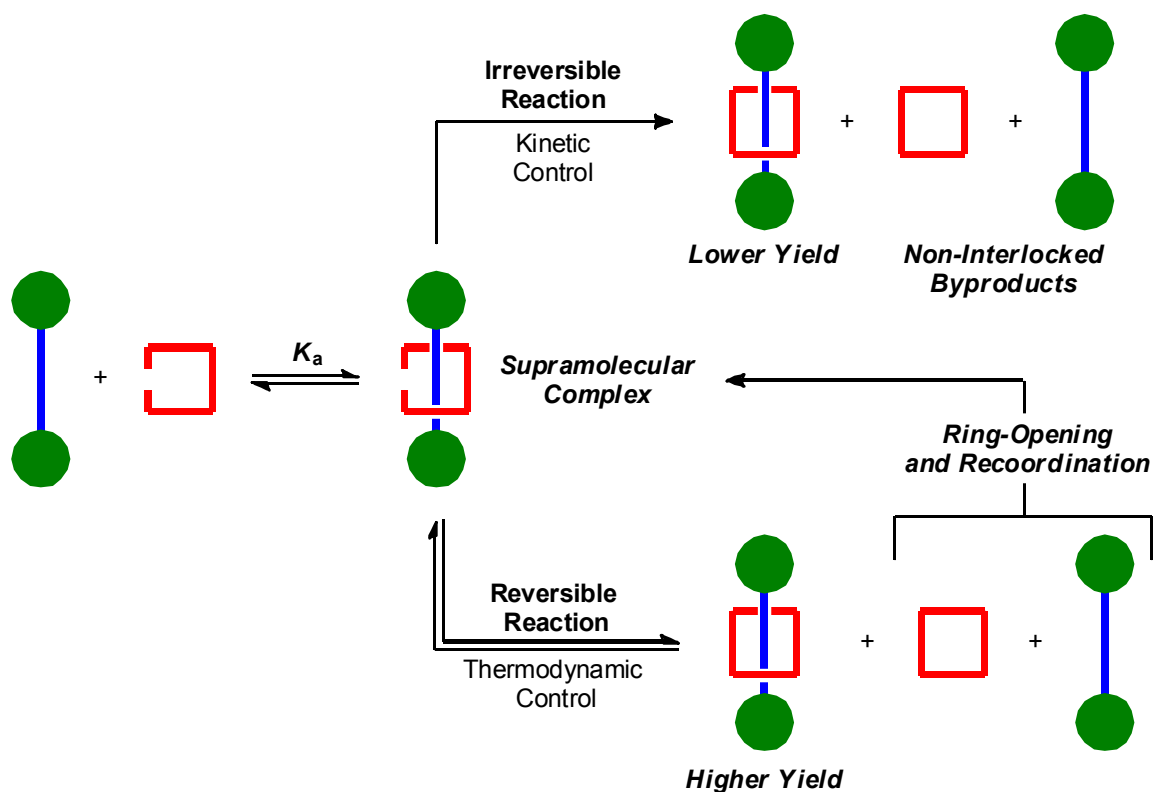
conformational flexibility of the crown ether and prevents maximized H-bonding with the complexed cation. Interestingly, while substitution of functionality around the crown affects the  $K_a$ , the crown ether association is impacted much more dramatically upon introduction of an additional methylene unit (crown ethers **6** and **7**) within the macrocycle. Such an effect is due to distortion of the array of oxygen atoms around the complexed ion and prevents the crown ether from adopting an optimized hydrogen-bonding geometry. The association of olefin-containing 24-crown-8 ether derivatives **8** and **9** has also been explored. Because of the absence of a pair of ethereal oxygens in the

ring, these structures form much weaker complexes with dibenzoammonium ion **10**. However, despite the lower association constant, the olefin functionality makes these crown-type structures highly versatile building blocks for interlocked compounds.

### *Dynamic Covalent Chemistry*

Generation of a supramolecular complex represents only the first step in the synthesis of an interlocked structure. Of equal importance to the success of the synthesis is the ability to perform the covalent interlocking of the supramolecular structure to afford the final mechanically interlocked compound. Traditionally, many of the final bond-forming events were irreversible reactions under kinetic control.<sup>66</sup> While these procedures do indeed afford some of the desired interlocked product (Scheme 1.3), the

**Scheme 1.3:** Irreversible Kinetic and Reversible Dynamic Covalent Interlocking Reactions to Form a [2]Rotaxane



reversible and incomplete formation of the supramolecular complex results in a number of non-interlocked by-products that, because of the irreversible nature of the reaction, must be removed from the desired interlocked structure. This results in challenging purification routes and decreased yield of product. Recently, the copper-catalyzed alkyne-azide “click” (CuAAC) reaction has emerged as promising interlocking procedure,<sup>67-71</sup> and, although kinetically controlled and irreversible, has afforded high yields of several interlocked architectures because of the exceptionally high fidelity of the alkyne-azide cycloaddition reaction.

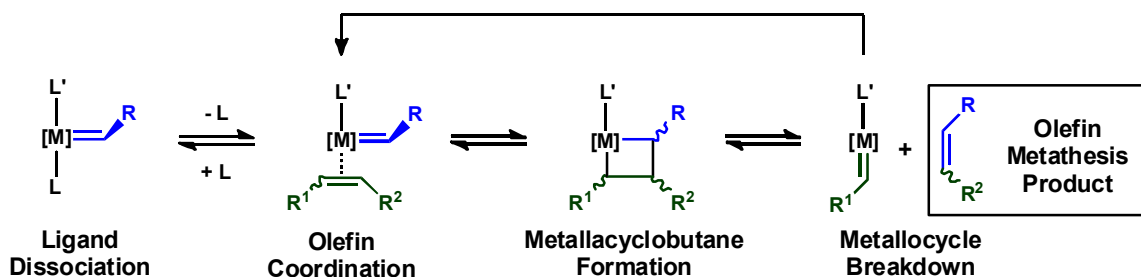
In contrast to irreversible reactions, much attention has been devoted to the development of a number of *reversible* covalent reactions, members of the dynamic covalent chemistry (DCC) family.<sup>60,72-78</sup> Employing a reversible reaction as the final bond-forming step in the synthesis of an interlocked compound enables error-checking to occur during the interlocking reaction, and allows the final yield of the interlocked product to reflect the thermodynamic stability of the interlocked material relative to non-interlocked components. Though non-interlocked impurities would initially form in the same quantities as in kinetic interlocking reactions (Scheme 1.3), the reversibility of dynamic covalent reactions enable these non-interlocked products to reverse to starting materials, coordinate to generate more supramolecular complex, and react again to interlock the additional supramolecular complex. In this way, the reversible reaction allows non-interlocked material to thermodynamically “funnel” to the interlocked product by allowing equilibrium to be reached, resulting in a higher yield of interlocked compound than would be obtained using an irreversible reaction under kinetic control.

Some common functional groups used in DCC reactions are disulfides,<sup>79-80</sup> imines,<sup>81-88</sup> and cyclic acetals.<sup>89</sup> The olefin metathesis reaction is another particularly powerful, reversible reaction under thermodynamic control, and is often performed by functional-group tolerant ruthenium catalysts, an important consideration given the high degree of functional complexity required for most molecular recognition motifs. Additionally, the olefin moiety is orthogonal to most functional groups used for templation, allowing the metathesis reaction to proceed without disrupting the supramolecular complex or interacting destructively with uncomplexed precursors. Lastly, one of the hallmarks of the olefin metathesis reaction is the number of substrate topologies that can be accommodated, making it an attractive choice to access a wide range of different interlocked architectures.

### *Olefin Metathesis*

One of the most widely-used and versatile carbon-carbon bond-forming reactions in current organic chemistry is the olefin metathesis reaction.<sup>90</sup> This process, mediated by a metal alkylidene complex, engages olefin-containing substrates and facilitates their conversion to new olefinic products via one of several possible reaction pathways. Chauvin first proposed the mechanism (Scheme 1.4)<sup>91</sup> of the olefin metathesis reaction in

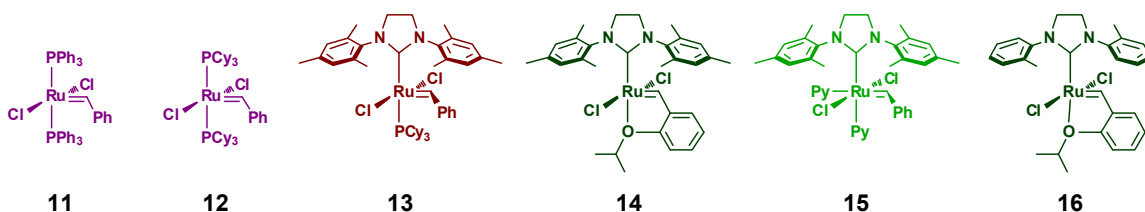
**Scheme 1.4:** Metal-Alkylidene Mediated Olefin Metathesis Mechanism



1970, a mechanism that has three steps. First, the olefin substrate coordinates to an open site on the metal center, and then, in the second step, undergoes a cyclization with the metal alkylidene to form a metallacyclobutane intermediate. At this point, metallacycle breakdown can regenerate the original starting materials (degenerate metathesis) or release a new olefin product (productive metathesis) and a new metal-alkylidene species capable of reentering the catalytic cycle. Typically, the reversible olefin metathesis reaction operates under thermodynamic control.<sup>91</sup>

The first metathesis catalysts were heterogeneous, ill-defined mixtures capable only of polymerizing highly strained cyclic olefin substrates.<sup>92</sup> More recent work has focused on the development of well-defined, highly active catalysts that are tolerant to a wide range of substrate structures and functionalities. A number of metals are capable of mediating the olefin metathesis reaction. Schrock and coworkers have expended considerable effort to develop molybdenum and tungsten olefin metathesis catalysts.<sup>93,94</sup> While these complexes are highly active for certain substrates, early transition metal complexes are extremely sensitive to both air and moisture impurities, and, because of the highly electrophilic nature of the metal, are, in general, intolerant of substrates containing polar functionality.

In contrast to these early transition metal catalysts, Grubbs and coworkers have developed a number of ruthenium olefin metathesis catalysts (Figure 1.7).<sup>95-97</sup> With

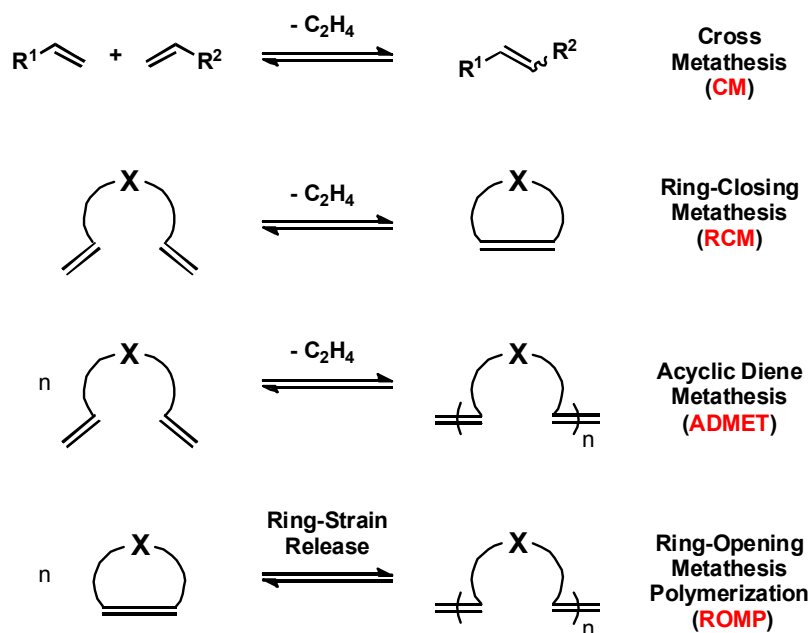


**Figure 1.7:** Structures of some ruthenium-based olefin metathesis catalysts.

certain ligand subsets, these ruthenium catalysts display not only high reactivity toward a wide range of olefin substrates, but are stable to both air and moisture impurities as well as many polar functional groups. Early ruthenium catalyst **11** did not have high activity, but could polymerize strained cyclic olefins.<sup>98</sup> Increasing the electron-donating ability of the ligand by substituting the triphenylphosphine (PPh<sub>3</sub>) ligands for tricyclohexylphosphine (PCy<sub>3</sub>) ligands<sup>99</sup> enhanced the activity of **12**. In addition to better activity, **12** also displayed greater functional group tolerance. Replacing one of the phosphine ligands with an N-heterocyclic carbene (NHC) ligand to produce **13** further enhanced the catalyst activity and expanded the substrate scope of the olefin metathesis reaction to include even electron-deficient olefins, such as acrylates.<sup>100</sup> The effect of the NHC ligand<sup>101,102</sup> and the origin of the increased activity and stability has been explored, and it was found that initiation of the complex (phosphine dissociation) is faster for **12**, but that **13** prefers to bind olefins ( $\pi$ -acidic substrates) in lieu of phosphine ligands ( $\sigma$ -donor species).<sup>97</sup> The stability of the catalyst complex improved upon introduction of a chelating isopropoxystyrene alkylidene (catalyst **14**) in place of the phosphine, albeit with a concomitant reduction in the rate of initiation of the complex.<sup>103,104</sup> By contrast, bipyridine catalyst **15** displays extremely fast initiation, and has proven particularly useful during the synthesis of well-defined polymeric materials.<sup>105</sup> This rapid initiation, however, comes with the cost of decreased catalyst lifetimes (with respect to similar NHC derivatives). Recently, *ortho*-methyl substituted NHC catalyst **15** has enabled olefin metathesis reactions of sterically hindered substrates to proceed to high conversion,<sup>106,107</sup> a challenge that, except for a few substrates,<sup>108</sup> had remained unsolved. A wide range of

additional catalyst structures has been explored in an effort to produce asymmetric olefin products,<sup>109</sup> afford high *cis:trans* product ratios, and effect water-based metathesis reactions.<sup>110-112</sup>

There are four primary categories of olefin metathesis reactions (Figure 1.8), and these classes of reactions are usually named by the type of structural transformation performed on the starting material in combination with the architecture of the generated product. Cross metathesis (CM) reactions produce coupled olefin material from two separate linear olefin precursors. By contrast, ring-closing metathesis (RCM) is the coupling of two olefin residues within the same molecule, often an  $\alpha,\omega$ -diene, to give a cyclic olefin product. Repeated couplings of  $\alpha,\omega$ -diene substrates in an iterative step-growth polymerization process produces linear polyalkenamers, a reaction termed acyclic diene metathesis (ADMET). Another metathesis polymerization technique, ring-opening



**Figure 1.8:** Various olefin metathesis reactions and their products.



metathesis polymerization (ROMP), involves the ring-opening of cyclic, olefin-containing monomers to yield a linear polymer. Because of the general reversibility of the olefin metathesis reaction, a driving force is required to favor product formation from starting material. Often, for CM, RCM, and ADMET reactions, this driving force is achieved via an irreversible expulsion of a small molecule olefin (such as ethylene) from the reaction mixture, a process that can be aided by application of high vacuum or an active purge of the reaction headspace. ROMP, by contrast, exploits the release of ring-strain energy of the cyclic monomers to favor the formation of linear polyalkenamers. Each of the classes of olefin metathesis reactions has unique advantages and disadvantages. Throughout this thesis, the application of an appropriate metathesis reaction will be used to generate a variety of interlocked molecular architectures. In the following sections, pertinent factors for several of the olefin metathesis reaction classes will be addressed.

### *Ring-Closing Metathesis*

Conversion of a linear diolefin to the closed cyclic olefin analogue necessitates several considerations. In general, RCM is limited to formation of sufficiently large rings that ring-strain energy of the product is negligible.<sup>113</sup> However, formation of smaller rings can be readily accomplished as well, especially if the linear structure has a high degree of chain substitution (which sterically forces the olefins in the same structure into close proximity with one another). Usually, RCM reactions are performed under high-dilution conditions (ca. 0.01 M solution of substrate) to favor intramolecular cyclization rather than intermolecular oligomerization of a number of substrate molecules. Also,

employing an  $\alpha,\omega$ -diene as the starting material can help drive the cyclization to higher conversion via release of a molecule of ethylene.

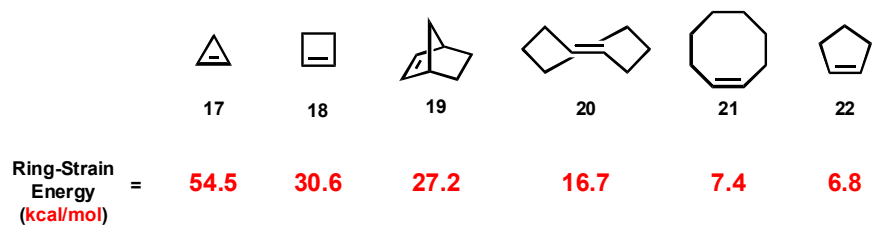
### *Acyclic Diene Metathesis*

In an antithetical approach to RCM reactions, which suppress intermolecular oligomerization of diene substrates via high-dilution conditions, ADMET reactions<sup>113</sup> are used to generate polymeric products via an iterative end-to-end oligomerization of monomer molecules (typically  $\alpha,\omega$ -dienes.) ADMET reactions are favored at high concentration of monomer (ideally performed in neat substrate), and often require vigorous efforts to remove ethylene in order to reach high conversion. Because of the step-growth nature of ADMET polymerization, high molecular weight (MW) polymeric material is only obtained at very high conversion,<sup>114</sup> and, in practice, reaching a polymer MW above ca. 20 kDa is exceptionally challenging. One significant barrier to the synthesis of high MW polymer via ADMET is the increase in viscosity of the reaction mixture as the MW increases, inhibiting ethylene removal and preventing quantitative conversion by dramatically slowing the diffusion of an ever-decreasing number of free chain ends. Because of the lack of control over the polymer initiation and propagation, the step-growth ADMET polymers tend to have poorly controlled molecular weight ranges and broad polydispersities, with a theoretical polydispersity index (PDI) of 2 at complete monomer conversion.

### Ring-Opening Metathesis Polymerization

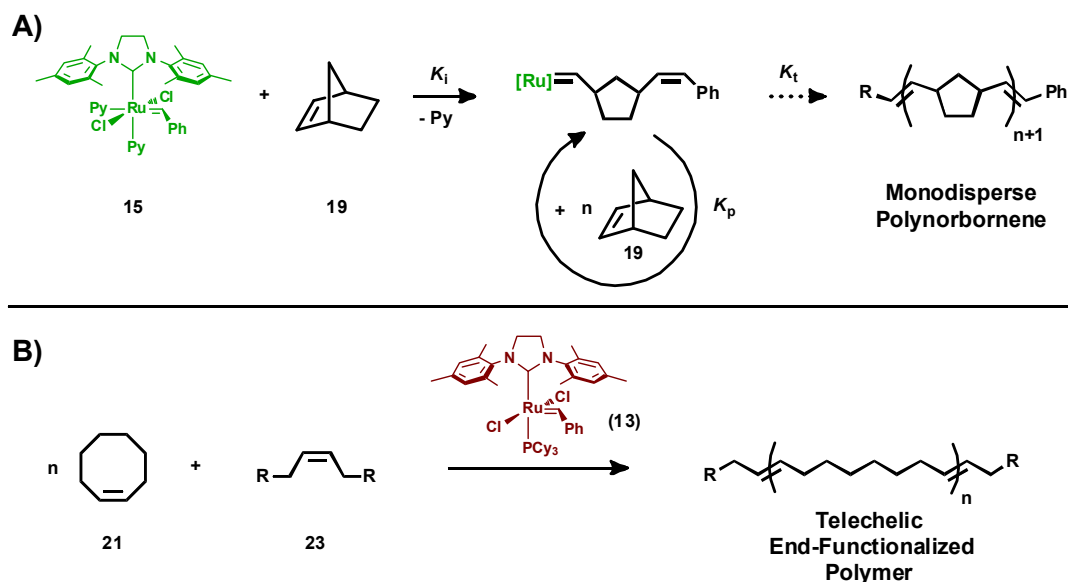
Unlike ADMET polymerizations, where removal of small molecule by-products (e.g., ethylene) provides the driving force for the formation of high MW material, ROMP relies on the release of ring-strain energy from the ring-opening of strained cyclic olefin monomers (Figure 1.9)<sup>115</sup> to favor formation of polymeric products. Another feature of ROMP that differs from ADMET is that ROMP is often performed in the presence of solvent. Though, in certain cases, ROMP can be performed in neat monomer, it is often advantageous to include some solvent, as this mitigates the impact of increasing solution viscosity on the kinetics of the polymerization.

Often, when polymerizing very highly strained monomers like norbornene **19**, fast initiating catalysts such as **15** (which have very labile pyridine ligands) are used to produce monodisperse polymer product (Scheme 1.5A).<sup>105</sup> Because the extreme ring-strain of monomer **19** results in a very rapid rate of propagation ( $K_p$ ), the rate of initiation ( $K_i$ ) should be, ideally, several orders of magnitude faster to maintain control over the polymer characteristics.<sup>114</sup> Thus, a rapidly initiating catalyst is essential to achieve a “living” (or “pseudo-living”) ROMP reaction, where polymer MW is determined by the catalyst to monomer ratio (assuming complete conversion) and the polymer product can



**Figure 1.9:** Various ROMP monomers and their ring-strain energies.

**Scheme 1.5:** Synthesis of a Monodisperse Polymer (A) and an End-Functionalized Telechelic Polymer (B) via ROMP



approach monodisperse (PDI approaching 1). However, controlling polymerization kinetics is not sufficient to fully control a polymerization. In addition, chain-breaking reactions must also be eliminated. Chain-breaking reactions involve “backbiting” of a reactive chain end with a functional group near the center of the same polymer chain or another polymer chain and disrupt the uniform growth of the chain, resulting in loss of control of the polymer MW and PDI. Because of the reversibility of metathesis reactions, the potential for backbiting reactions is significant and depends on the particular system (catalyst, monomer, temperature, concentration, etc.) being used.<sup>116-118</sup> As logic would indicate, the less hindered the olefin bonds within the polymer and the more active the catalyst used in the polymerization, the more prevalent backbiting reactions will be during the polymerization. To minimize these issues, ROMP reactions are typically stopped as soon as monomer conversion has reached completion. It is worth mentioning that polymers formed from some monomers, such as norbornene **19**, contain olefins that

are sufficiently sterically congested that backbiting is essentially negligible. Because of the absence of backbiting, production of block copolymers can be readily achieved via addition of a second monomer upon complete reaction of the first monomer.<sup>119</sup>

Though chain backbiting is often regarded as a detrimental side-reaction, these secondary polymer reactions (Scheme 1.5B) can be harnessed to afford functionalized polymers. By allowing a linear polymer to undergo numerous chain-breaking reactions in the presence of a chain-transfer agent (CTA, a structure such as **23**), the polymer structure equilibrates to the telechelic end-functionalized product.<sup>120-123</sup> In such a system, the ratio of CTA to monomer ratio dictates the MW of the polymer product, but the equilibration process means the PDI approaches the theoretical value of 2 (like a step-growth polymerization). Because the catalyst structure contained an initial alkylidene species that could also act as a chain end, in practice, it is important to not only carefully control the CTA-to-monomer ratio but also to keep the catalyst-to-CTA ratio low to minimize the number of non-CTA chain end-groups from catalyst alkylidene. Traditionally, only symmetric chain ends were able to be introduced. However, recent work has shown that introduction of different chain-transfer agents at strategic time points during the polymerization will produce a polymer containing two different end-groups.<sup>124</sup>

### References

- (1) Amabilino, D. B.; Stoddart, J. F. *Chem. Rev.* **1995**, *95*, 2725.
- (2) Raymo, F. M.; Stoddart, J. F. *Chem. Rev.* **1999**, *99*, 1643.
- (3) Stoddart, J. F. *Chem. Soc. Rev.* **2009**, *38*, 1802.
- (4) Schill, G. *Catenanes, Rotaxanes and Knots*; Academic Press: New York, 1971.
- (5) *Molecular Catenanes, Rotaxanes and Knots* Sauvage, J.-P.; Dietrich-Buchecker, C., Eds.; Wiley-VCH: Weinheim, 1999.
- (6) Wisner, J. A.; Beer, P. D.; Drew, M. G. B.; Sambrook, M. R. *J. Am. Chem. Soc.* **2002**, *124*, 12469.
- (7) Kilbinger, A. F. M.; Cantrill, S. J.; Waltman, A. W.; Day, M. W.; Grubbs, R. H. *Angew. Chem. Int. Ed.* **2003**, *42*, 3281.
- (8) Hannam, J. S.; Kidd, T. J.; Leigh, D. A.; Wilson, A. J. *Org. Lett.* **2003**, *5*, 1907.
- (9) Coumans, R. G. E.; Elemans, J. A. A. W.; Thordarson, P.; Nolte, R. J. M.; Rowan, A. E. *Angew. Chem., Int. Ed.* **2003**, *42*, 650.
- (10) Wasserman, E. *J. Am. Chem. Soc.* **1960**, *82*, 4433.
- (11) Kidd, T. J.; Leigh, D. A.; Wilson, A. J. *J. Am. Chem. Soc.* **1999**, *121*, 1599.
- (12) Weck, M.; Mohr, B.; Sauvage, J.-P.; Grubbs, R. H. *J. Org. Chem.* **1999**, *64*, 5463.
- (13) Mobian, P.; Kern, J.-M.; Sauvage, J.-P. *J. Am. Chem. Soc.* **2003**, *125*, 2016.
- (14) Iwamoto, H.; Itoh, K.; Nagamiya, H.; Fukazawa, Y. *Tetrahedron Lett.* **2003**, *44*, 5773.
- (15) Wang, L.; Vysotsky, M. O.; Bogdan, A.; Bolte, M.; Böhmer, V. *Science* **2004**, *304*, 1312.

- (16) Sambrook, M. R.; Beer, P. D.; Wisner, J. A.; Paul, R. L.; Cowley, A. R. *J. Am. Chem. Soc.* **2004**, *126*, 15364.
- (17) Guidry, E. N.; Cantrill, S. J.; Stoddart, J. F.; Grubbs, R. H. *Org. Lett.* **2005**, *7*, 2129.
- (18) Arico, F.; Badjić, J. D.; Cantrill, S. J.; Flood, A. H.; Leung, K. C.-F.; Liu, Y.; Stoddart, J. F. *Top. Curr. Chem.* **2005**, *249*, 203.
- (19) Fabio, A.; Chang, T.; Cantrill, S. J.; Khan, S. I.; Stoddart, J. F. *Chem. Eur. J.* **2005**, *11*, 4655.
- (20) Badjić, J. D.; Nelson, A.; Cantrill, S. J.; Turnbull, W. B.; Stoddart, J. F. *Acc. Chem. Res.* **2005**, *38*, 723.
- (21) Fyfe, M. C. T.; Stoddart, J. F. *Acc. Chem. Res.* **1997**, *30*, 393.
- (22) Ashton, P. R.; Baldoni, V.; Balzani, V.; Claessens, C. G.; Credi, A.; Hoffmann, H. D. A.; Raimo, F. M.; Stoddart, J. F.; Venturi, M.; White, A. J. P.; Williams, D. J. *Eur. J. Org. Chem.* **2000**, 1121.
- (23) Alexeev, Y. E.; Kharisou, B. I.; Garcia, T. C. H.; Garnovskii, A. D. *Coord. Chem. Rev.* **2010**, *254*, 794.
- (24) Dietrich-Buchecker, C. O.; Sauvage, J.-P. *Chem. Rev.* **1987**, *87*, 795.
- (25) Sauvage, J.-P. *Chem. Commun.* **2005**, 1507.
- (26) Jimenez, M. C.; Dietrich-Buchecker, C.; Sauvage, J.-P. *Angew. Chem.* **2000**, *39*, 3284.
- (27) Jimenez-Molero, M. C.; Dietrich-Buchecker, C.; Sauvage, J.-P. *Chem. Commun.* **2003**, 1613.

- (28) Wu, J.; Leung, K. C.-F.; Benitez, D.; Han, J.-Y.; Cantrill, S. J.; Fang, L.; Stoddart, J. F. *Angew. Chem. Int. Ed.* **2008**, *47*, 7470.
- (29) Guidry, E. N.; Li, J.; Stoddart, J. F.; Grubbs, R. H. *J. Am. Chem. Soc.* **2007**, *129*, 8944
- (30) Clark, P. G.; Day, M. W.; Grubbs, R. H. *J. Am. Chem. Soc.* **2009**, *131*, 13631.
- (31) Williams, A. R.; Northrop, B. H. ; Chang, T.; Stoddart, J. F.; White, A. J. P.; Williams, D. J. *Angew. Chem. Int. Ed.* **2006**, *45*, 6665.
- (32) Guo, J.; Mayers, P. C.; Breault, G. A.; Hunter, C. A. *Nat. Chem.* **2010**, *2*, 218.
- (33) Collier, C. P.; Mattersteig, G.; Wong, E. W.; Luo, Y.; Beverly, K.; Sampaio, J.; Raymo, F.; Stoddart, J. F.; Heath, J. R. *Science* **2000**, *289*, 1172.
- (34) Pease, A. R.; Jeppesen, J. O.; Stoddart, J. F.; Luo, Y.; Collier, C. P.; Heath, J. R. *Acc. Chem. Res.* **2001**, *34*, 433.
- (35) Luo, Y. Collier, C. P.; Jeppesen, J. O.; Nielsen, K. A.; Delonno, E.; Ho, G.; Perkins, J.; Tseng, H.-R.; Yamamoto, T.; Stoddart, J. F.; Heath, J. R. *ChemPhysChem* **2002**, *3*, 519.
- (36) Diehl, M. R.; Steuerman, D. W.; Tseng, H.-R.; Vignon, S. A.; Star, A.; Celestre, P. C.; Stoddart, J. F.; Heath, J. R. *ChemPhysChem* **2003**, *4*, 1335.
- (37) Tseng, H.-R.; Wu, D.; Fang, N. X.; Zhang, X.; Stoddart, J. F. *ChemPhysChem* **2004**, *5*, 111.
- (38) Steuerman, D. W.; Tseng, H.-R.; Peters, A. J.; Flood, A. H.; Jeppesen, J. O.; Nielsen, K. A.; Stoddart, J. F.; Heath, J. R. *Angew. Chem., Int. Ed.* **2004**, *43*, 6486.



- (39) Flood, A. H.; Ramirez, R. J. A.; Deng, W.-Q.; Muller, R. P.; Goddard III, W. A.; Stoddart, J. F. *Aust. J. Chem.* **2004**, *57*, 301.
- (40) Flood, A. H.; Peters, A. J.; Vignon, S. A.; Steuerman, D. W.; Tseng, H.-R.; Kang, S.; Heath, J. R.; Stoddart, J. F. *Chem. Eur. J.* **2004**, *10*, 6558.
- (41) Flood, A. H.; Stoddart, J. F.; Steuerman, D. W.; Heath, J. R. *Science* **2004**, *306*, 2055
- (42) Jang, S. S.; Jang, Y. H.; Kim, Y.-H.; Goddard III, W. A.; Flood, A. H.; Laursen, B. W.; Tseng, H.-R.; Stoddart, J. F.; Jeppesen, J. O.; Choi, J. W.; Steuerman, D. W.; Delonno, E.; Heath, J. R. *J. Am. Chem. Soc.* **2005**, *127*, 1563.
- (43) Balzani, V.; Credi, A.; Silvi, S.; Venturi, M. *Chem. Soc. Rev.* **2006**, *35*, 1135.
- (44) Credi, A. *J. Phys.: Condens. Matter* **2006**, *18*, S1779.
- (45) Rescifina, A.; Zagni, C.; Iannazzo, D.; Merino, P. *Curr. Org. Chem.* **2009**, *13*, 448.
- (46) Wenz, G.; Han, B. H.; Muller, A. *Chem. Rev.* **2006**, *106*, 782.
- (47) Niu, Z.; Gibson, H. W. *Chem. Rev.* **2009**, *109*, 6024.
- (48) Godt, A. *Eur. J. Org. Chem.* **2004**, 1634.
- (49) Harada, A.; Hashidzume, A.; Yamaguchi, H.; Takashima, Y. *Chem. Rev.* **2009**, *109*, 5974.
- (50) Fustin, C.-A.; Bailly, C.; Clarkson, G. J.; De Groote, P.; Galow, T. H.; Leigh, D. A.; Robertson, D.; Slawin, A. M. Z.; Wong, J. K. Y. *J. Am. Chem. Soc.* **2003**, *125*, 2200.

- (51) Clark, P. G.; Guidry, E. N.; Chan, W. Y.; Steinmetz, W. E.; Grubbs, R. H. *J. Am. Chem. Soc.* **2010**, *132*, 3405.
- (52) Rescifina, A.; Zagni, C.; Iannazzo, D.; Merino, P. *Curr. Org. Chem.* **2009**, *13*, 448.
- (53) Seeman, N. C. *DNA Cell Biol.* **1991**, *10*, 475.
- (54) Mueller, J. E.; Du, S. M.; Seeman, N. C. *J. Am. Chem. Soc.* **1991**, *113*, 6306.
- (55) Hunter, C. A. *J. Chem. Soc., Chem. Commun.* **1991**, 749.
- (56) Hunter, C. A. *J. Am. Chem. Soc.* **1992**, *114*, 5303.
- (57) Vogtle, F.; Meier, S.; Hoss, R. *Angew. Chem., Int. Ed. Engl.* **1992**, *31*, 1619.
- (58) Hunter, C. A.; Purvis, D. H. *Angew. Chem., Int. Ed. Engl.* **1992**, *31*, 792.
- (59) Carver, F. J.; Hunter, C. A.; Shannon, R. J. *J. Chem. Soc., Chem. Commun.* **1994**, 1277.
- (60) Ashton, P. R.; Bartsch, R. A.; Cantrill, S. J.; Hanes, Jr., R. E.; Hickingbottom, S. K.; Lowe, J. N.; Preece, J. A.; Stoddart, J. F.; Talanov, V. S.; Wang, Z.-H. *Tetrahedron Lett.* **1999**, *40*, 3661.
- (61) Cantrill, S. J.; Fulton, D. A.; Heiss, A. M.; Pease, A. R.; Stoddart, J. F.; White, A. J. P.; Williams, D. J. *Chem. Eur. J.* **2000**, *6*, 2274.
- (62) Schalley, C. A.; Weilandt, T.; Brüggemann, J.; Vögtle, F. *Topics Curr. Chemistry* **2004**, *248*, 141.
- (63) Pedersen, C. J. *J. Am. Chem. Soc.* **1967**, *89*, 2495.
- (64) Pedersen, C. J. *Science* **1988**, *241*, 536.
- (65) Cram, D. J.; Cram, J. M. *Acc. Chem. Res.* **1978**, *11*, 8.

- (66) Dichtel, W. R.; Miljanic, O. S.; Zhang, W.; Spruell, J. M.; Patel, K.; Aprahamian, I.; Heath, J. R.; Stoddart, J. F. *Acc. Chem. Res.* **2008**, *41*, 1750.
- (67) Megiatto, J. D.; Schuster, D. I. *J. Am. Chem. Soc.* **2008**, *130*, 12872.
- (68) Coutrot, F.; Romuald, C.; Busseron, E. *Org. Lett.* **2008**, *10*, 3741-3744.
- (69) Megiatto, J. D.; Schuster, D. I. *Chem. Eur. J.* **2009**, *15*, 5444.
- (70) Goldup, S. M.; Leigh, D. A.; Long, T.; McGonigal, P. R.; Symes, M. D.; Wu, J. *J. Am. Chem. Soc.* **2009**, *131*, 15924.
- (71) Hanni, K. D.; Leigh, D. A. *Chem. Soc. Rev.* **2010**, *39*, 1240.
- (72) Glink, P. T.; Oliva, A. I.; Stoddart, J. F.; White, A. J. P.; Williams, D. J. *Angew. Chem., Int. Ed.* **2001**, *40*, 1870.
- (73) Rowan, S. J.; Cantrill, S. J.; Cousins, G. R. L.; Sanders, J. K. M.; Stoddart, J. F. *Angew. Chem., Int. Ed.* **2002**, *41*, 898.
- (74) Aricó, F.; Chang, T.; Cantrill, S. J.; Khan, S. I.; Stoddart, J. F. *Chem. Eur. J.* **2005**, *11*, 4655.
- (75) Haussmann, P. C.; Khan, S. I.; Stoddart, J. F. *J. Org. Chem.* **2007**, *72*, 6708.
- (76) Meyer, C. D.; Joiner, C. S.; Stoddart, J. F. *Chem. Soc. Rev.* **2007**, *36*, 1705.
- (77) Wu, J.; Leung, K. C.-F.; Stoddart, J. F. *Proc. Natl. Acad. Sci. U.S.A.* **2007**, *104*, 17266.
- (78) Haussmann, P. C.; Stoddart, J. F. *Chem. Record* **2009**, *9*, 136.
- (79) Kolchinski, A. G.; Alcock, N. W.; Roesner, R. A.; Busch, D. H. *Chem. Commun.* **1998**, 1437.

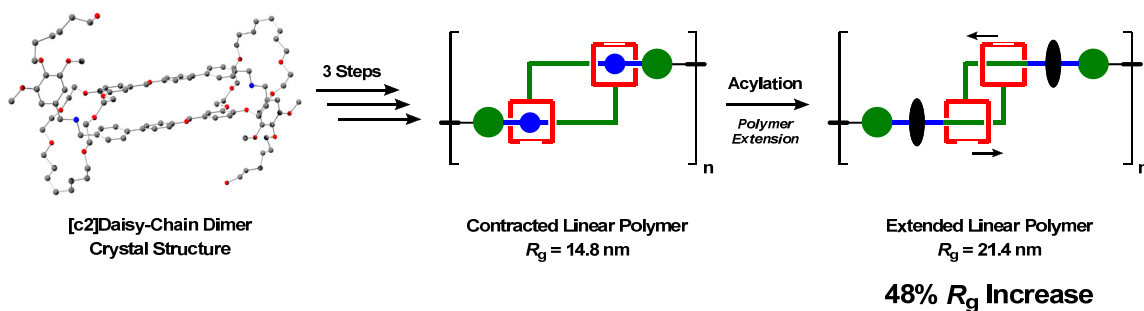
- (80) Furusho, Y.; Oku, T.; Hasegawa, T.; Tsuboi, A.; Kihara, N.; Takata, T. *Chem. Eur. J.* **2003**, *9*, 2895.
- (81) Cantrill, S. J.; Rowan, S. J.; Stoddart, J. F. *Org. Lett.* **1999**, *1*, 1363.
- (82) Rowan, S. J.; Stoddart, J. F. *Org. Lett.* **1999**, *1*, 1913.
- (83) Glink, P. T.; Oliva, A. I.; Stoddart, J. F.; White, A. J. P.; Williams, D. J. *Angew. Chem., Int. Ed.* **2001**, *40*, 1870.
- (84) Horn, M.; Ihringer, J.; Glink, P. T.; Stoddart, J. F. *Chem. Eur. J.* **2003**, *9*, 4046.
- (85) Chichak, K. S.; Cantrill, S. J.; Pease, A. R.; Chiu, S.-H.; Cave, G. W. V.; Atwood, J. L.; Stoddart, J. F. *Science* **2004**, *304*, 1308.
- (86) Hogg, L.; Leigh, D. A.; Lusby, P. J.; Morelli, A.; Parsons, S.; Wong, J. K. Y. *Angew. Chem., Int. Ed.* **2004**, *43*, 1218.
- (87) Schalley, C. A. *Angew. Chem., Int. Ed.* **2004**, *43*, 4399.
- (88) Cantrill, S. J.; Chichak, K. S.; Peters, A. J.; Stoddart, J. F. *Acc. Chem. Res.* **2005**, *38*, 1.
- (89) Fuchs, B.; Nelson, A.; Star, A.; Stoddart, J. F.; Vidal, S. B. *Angew. Chem., Int. Ed.* **2003**, *42*, 4220.
- (90) Grubbs, R. H. *Tetrahedron* **2004**, *60*, 7117.
- (91) Herisson, J.-L.; Chauvin, Y. *Makromol. Chem.* **1971**, *141*, 161.
- (92) Truett, W. L.; Johnson, D. R.; Robinson, I. M.; Montague, B. A. *J. Am. Chem. Soc.* **1960**, *82*, 2337.
- (93) Schrock, R. R.; Hoveyda, A. H. *Angew. Chem., Int. Ed.* **2003**, *42*, 4592.
- (94) Schrock, R. R. *J. Molec. Catal. A: Chem.* **2004**, *213*, 21.

- (95) Trnka, T. M.; Grubbs, R. H. *Acc. Chem. Res.* **2001**, *34*, 18.
- (96) Kuhn, K. M.; Bourg, J.-B.; Chung, C. K.; Virgil, S. C.; Grubbs, R. H. *J. Am. Chem. Soc.* **2009**, *131*, 5313.
- (97) Vougioukalakis, G. C.; Grubbs, R. H. *Chem. Rev.* **2010**, *110*, 1746.
- (98) Nguyen, S. T.; Johnson, L. K.; Grubbs, R. H.; Ziller, J. W. *J. Am. Chem. Soc.* **1992**, *114*, 3974.
- (99) Schwab, P.; France, M. B.; Ziller, J. W.; Grubbs, R. H. *Angew. Chem., Int. Ed.* **1995**, *34*, 2039.
- (100) Scholl, M.; Ding, S.; Lee, C. W.; Grubbs, R. H. *Org. Lett.* **1999**, *1*, 953.
- (101) Sanford, M. S.; Ulman, M.; Grubbs, R. H. *J. Am. Chem. Soc.* **2001**, *123*, 749.
- (102) Sanford, M. S.; Love, J. A.; Grubbs, R. H. *J. Am. Chem. Soc.* **2001**, *123*, 6543.
- (103) Garber, S. B.; Kingsbury, J. S.; Gray, B. L.; Hoveyda, A. H. *J. Am. Chem. Soc.* **2000**, *122*, 8168.
- (104) Gessler, S.; Randl, S. *Tetrahedron Lett.* **2000**, *41*, 9973.
- (105) Sanford, M. S.; Love, J. A.; Grubbs, R. H. *Organometallics* **2001**, *20*, 5314.
- (106) Stewart, I. C.; Ung, T.; Pletnev, A. A.; Berlin, J. M.; Grubbs, R. H.; Schrodi, Y. *Org. Lett.* **2007**, *9*, 1589.
- (107) Stewart, I. C.; Douglas, C. J.; Grubbs, R. H. *Org. Lett.* **2008**, *10*, 441.
- (108) Berlin, J. M.; Campbell, K.; Ritter, T.; Funk, T. W.; Chlenov, A.; Grubbs, R. H. *Org. Lett.* **2007**, *9*, 1339.
- (109) Funk, T. W.; Berlin, J. M.; Grubbs, R. H. *J. Am. Chem. Soc.* **2006**, *128*, 1840.
- (110) Hong, S. H.; Grubbs, R. H. *J. Am. Chem. Soc.* **2006**, *128*, 3508.

- (111) Jordan, J. P.; Grubbs, R. H. *Angew. Chem., Int. Ed.* **2007**, *46*, 5152.
- (112) Burtcher, D.; Grela, K. *Angew. Chem., Int. Ed.* **2009**, *48*, 442.
- (113) Grubbs, R. H., Ed. *Handbook of Metathesis*; Wiley-VCH: Weinheim, Germany, 2003; Vol. 1.
- (114) Odian, G. *Principles of Polymerization*; Wiley-Interscience: Hoboken, New Jersey, USA, 2004; 4<sup>th</sup> Ed.
- (115) Schleyer, P. V. R.; Williams Jr., J. E.; Blanchard, K. R. *J. Am. Chem. Soc.* **1970**, *92*, 2377.
- (116) Bielawski, C. W.; Grubbs, R. H. *Angew. Chem., Int. Ed.* **2000**, *39*, 2903.
- (117) Bielawski, C. W.; Benitez, D.; Grubbs, R. H. *Macromolecules* **2001**, *34*, 8610.
- (118) Scherman, O. A.; Kim, H. M.; Grubbs, R. H. *Macromolecules* **2002**, *35*, 5366.
- (119) Choi, T.-L.; Grubbs, R. H. *Angew. Chem., Int. Ed.* **2003**, *42*, 1743.
- (120) Hillmyer, M. A.; Grubbs, R. H. *Macromolecules* **1993**
- (121) Hillmyer, M. A.; Laredo, W. R.; Grubbs, R. H. *Macromolecules* **1995**, *28*, 6311.
- (122) Maughon, B. R.; Morita, T.; Bielawski, C. W.; Grubbs, R. H. *Macromolecules* **2000**, *33*, 1929.
- (123) Morita, T.; Maughon, B. R.; Bielawski, C. W.; Grubbs, R. H. *Macromolecules* **2000**, *33*, 6621.
- (124) Matson, J. B.; Virgil, S. C.; Grubbs, R. H. *J. Am. Chem. Soc.* **2009**, *131*, 3355.

## CHAPTER 2

### [c2]Daisy-Chain Dimers: From Synthesis to Applications in Materials

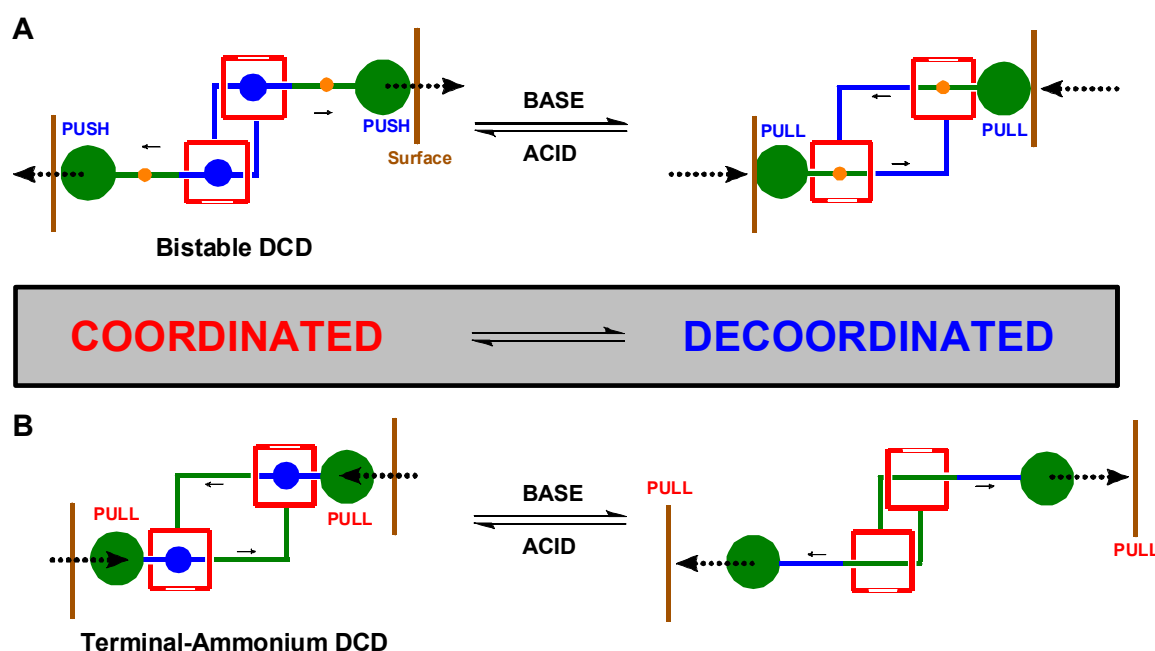


Portions of this chapter have previously appeared as: Clark, P. G.; Day, M. W.; Grubbs, R. H. *J. Am. Chem. Soc.* **2009**, *131*, 13631-13633.

## [c2]Daisy-Chain Dimers: From Synthesis to Applications in Materials

### *Introduction*

In an effort to miniaturize devices for a variety of applications, many researchers have begun to explore systems derived from examination of nature.<sup>1</sup> The elegance and complexity of biological systems provides a wealth of inspiration for synthetic chemists. A particularly intriguing challenge for materials scientists is mimicking the extension and contraction of natural fibers. One approach is to use switchable non-covalent interactions to guide the extending and contracting of macromolecules. Recently, the utilization of supramolecular chemistry to self-assemble complex molecular networks, coupled with dynamic covalent chemistry,<sup>2</sup> has facilitated the synthesis of a variety of interlocked molecules.<sup>3</sup> One class of these compounds, [c2]daisy-chain dimers<sup>4</sup> (DCDs, Figure 2.1), appeared to be a promising molecular actuator candidate due to the switchable



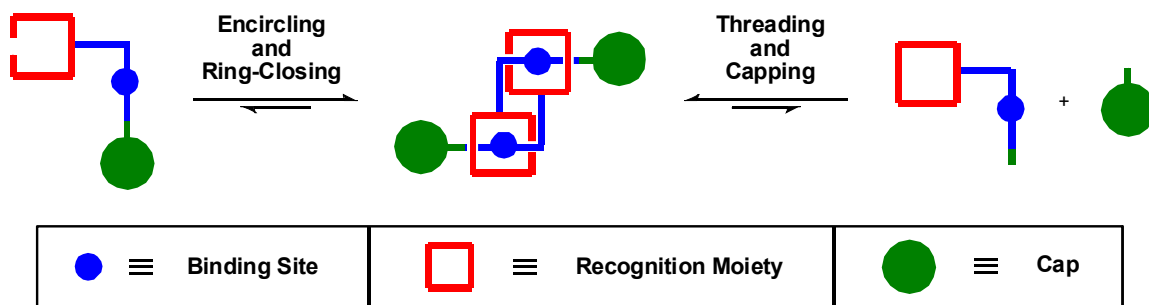
**Figure 2.1:** Graphical representation of binding and switching of a bistable DCD (**A**) and a DCD with ammonium binding sites near the caps, a “terminal ammonium” dimer (**B**).



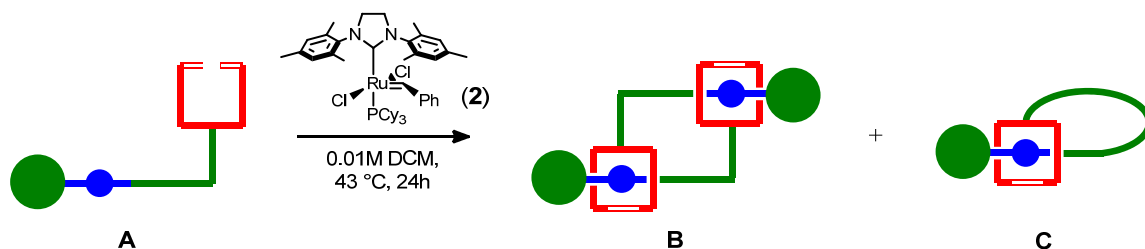
conformation<sup>5</sup> of the dimer upon removal of coordinating interactions. It has been proposed that incorporation of mechanically interlocked species into macromolecular materials will impart unique properties<sup>6</sup> to those materials not achievable via traditional covalent linkages. To this end, several reports of interlocked polymeric species have recently emerged.<sup>7,8</sup> Particularly, DCDs incorporated within polymers have shown facile switching behavior.<sup>8b</sup> Herein, we report the synthesis of a DCD whose structural topology enhances the stability of the contracted state, and the subsequent incorporation of this DCD into linear polymers that undergo a significant conformational change upon extension of the dimeric units.

Synthesis of a DCD (Scheme 2.1) involves the pairing and interlocking of two self-complementary macromers (molecules that contain both host and guest recognition moieties bound covalently within the same compound).<sup>4a,8</sup> One common process utilizes the threading of an ammonium-containing fragment through the dibenzo-24-crown-8 ether or other recognition moiety of a partner macromer followed by a “capping” reaction<sup>9</sup> to prevent dethreading of the complex. This technique gives DCDs in good yield, and allows introduction of a second, albeit significantly weaker, binding site near the cap of the dimer (Figure 2.1A).<sup>5a,d,8b</sup> The facile “switching” of such dimers from

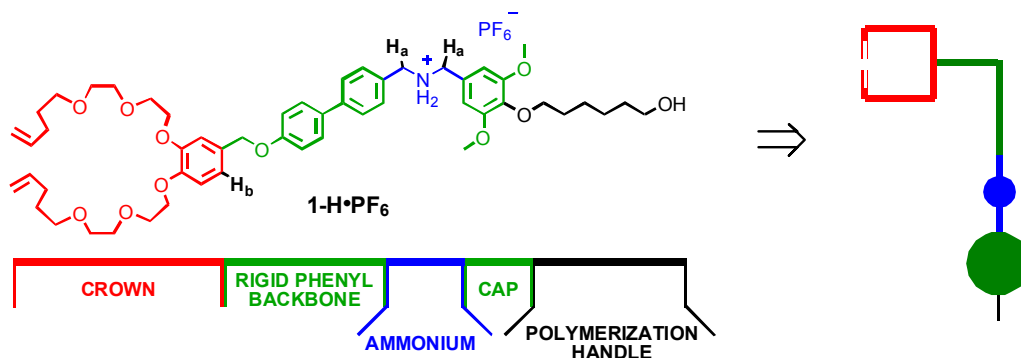
**Scheme 2.1:** Graphical Representation of DCD Synthesis via Ring-Closing or Capping



**Scheme 2.2:** Graphical DCD Synthesis and Possible Intramolecularly-Coupled Side-Products



extended to contracted conformations has been clearly demonstrated.<sup>5a-c,8b</sup> In contrast to reversible “capping” reactions, the dynamic ring-closing metathesis (RCM) reaction (Scheme 2.1), catalyzed by functional-group tolerant ruthenium alkylidene complexes,<sup>10</sup> has enabled the synthesis of [2]catenanes,<sup>11</sup> [2]rotaxanes,<sup>12</sup> and other interlocked species.<sup>13</sup> DCDs have also been synthesized by RCM, where the two diolefinic polyether fragments of each macromer encircle and close around an appropriately substituted dibenzylammonium ion of a partner macromer, thus interlocking the DCD.<sup>8a</sup> We believed that designing a DCD with a strongly coordinating binding site near the cap of the dimer would enhance the stability of the contracted state and produce a “stronger” molecular actuator (Figure 2.1B). With this criterion in mind, we envisaged macromer structure **1-H·PF<sub>6</sub>** (Figure 2.2) to be a promising target. A long, rigid biphenyl linker between the host and guest residues was incorporated to minimize the formation of self-



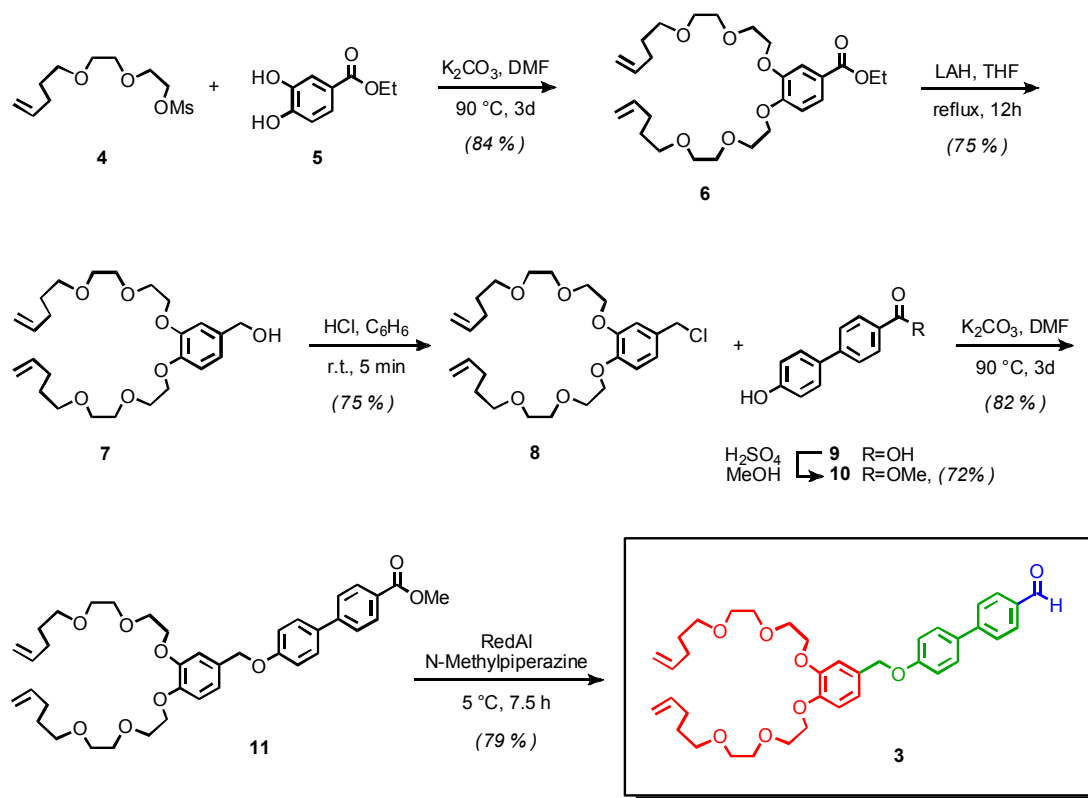
**Figure 2.2:** Structure of the targeted DCD macromer **1-HPF<sub>6</sub>**.

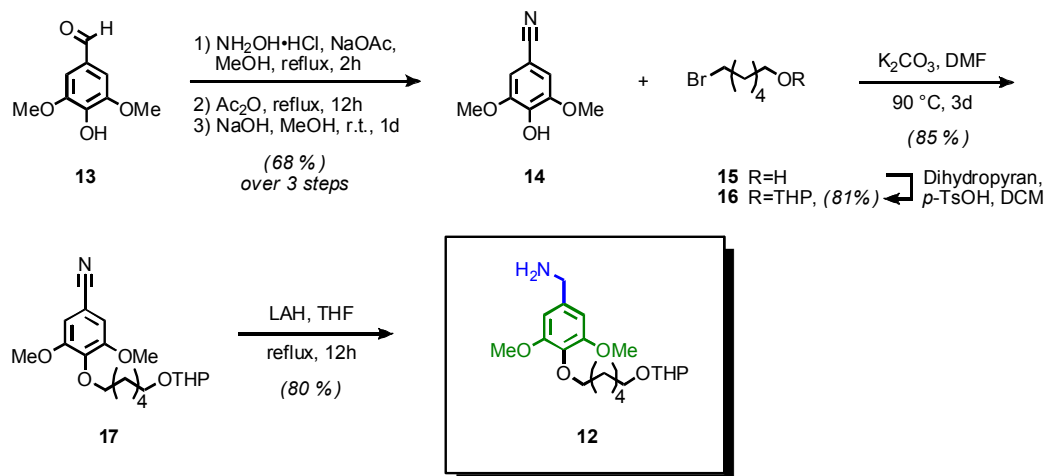
complexed monomer<sup>14</sup> (Scheme 2.2C), promote dimer preassembly via macromer-macromer  $\pi$ - $\pi$  slipped-stacking interactions, and enhance the linearity of the dimer, aiding elongation via slippage of the rod-like backbone through the closed crown ether-type rings.

### Dimer Synthesis and Analysis

Synthesis of **1**-H-PF<sub>6</sub> required 13 steps.<sup>15</sup> Retrosynthetically, it was most convenient to envision fragmentation of **1**-H-PF<sub>6</sub> at the ammonium, with a crown/backbone component and a cap component as individual targets. Crown-biphenyl fragment **3** (Scheme 2.3) was obtained in five steps. Alkylation of commercially available ethyl 3,4-dihydroxybenzoate (**5**) with mesylate **4** (synthesized via monoalkylation of

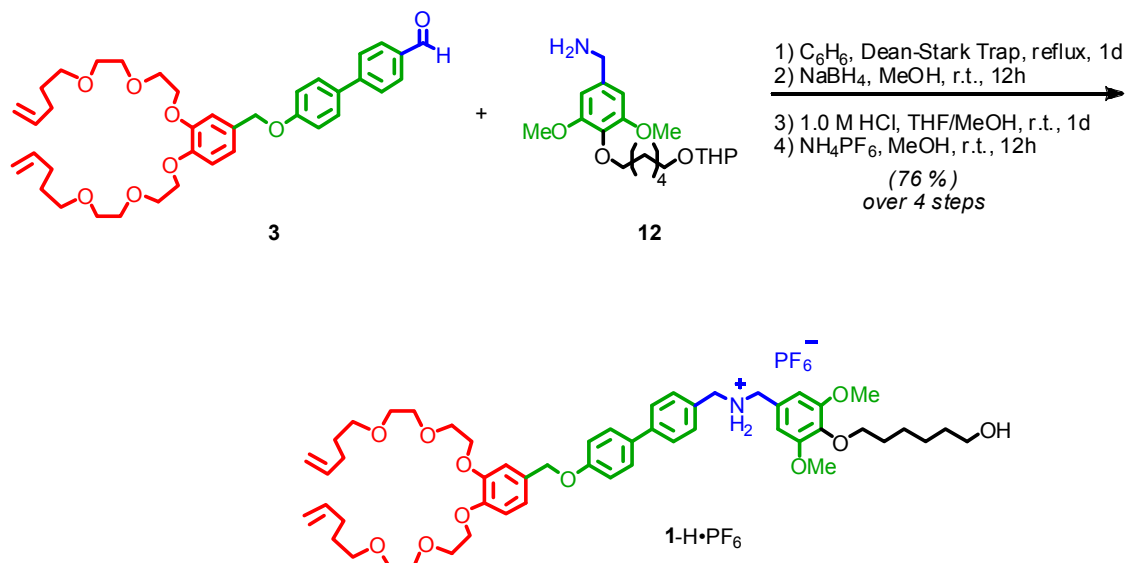
**Scheme 2.3:** Synthesis of Crown-Biphenyl Fragment **3**



**Scheme 2.4: Synthesis of Cap Fragment 12**


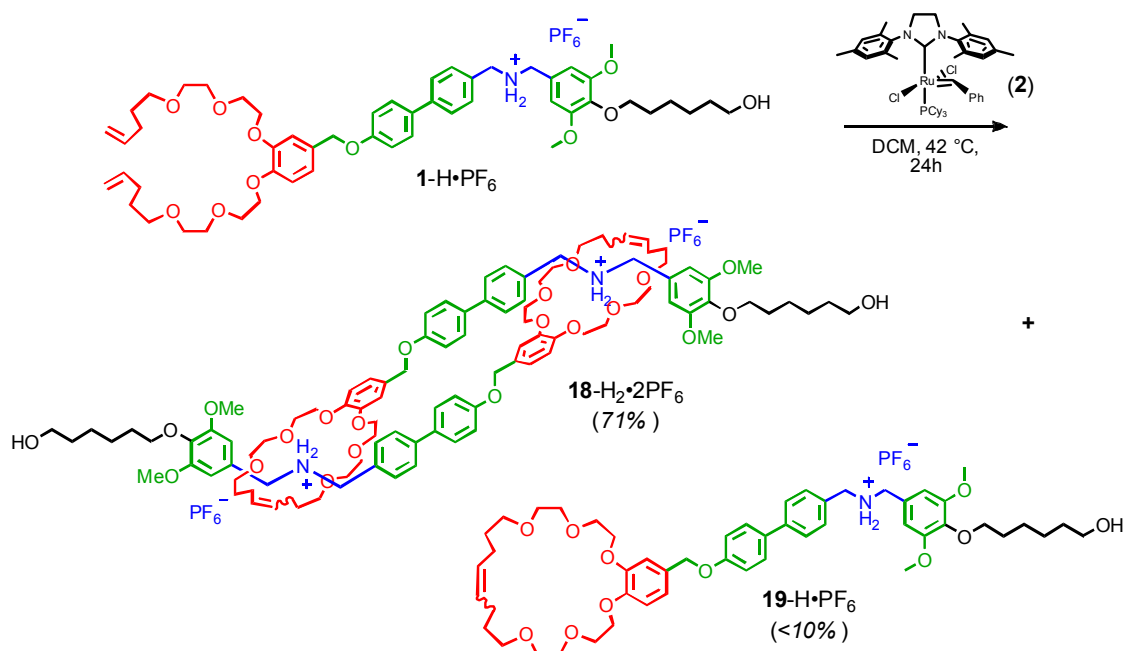
diethylene glycol with 5-bromo-1-pentene and subsequent mesylation of the resulting compound) produced ethyl ester **6**. Reduction of **6** using lithium aluminum hydride gave benzylic alcohol **7**, which could be readily converted to chloride analogue **8**. The commercially available 4'-hydroxy-4-biphenyl-carboxylic acid (**9**) was esterified to give **10**, followed by subsequent coupling with **8** to generate **11**. Reduction of methyl ester **11** produced the desired crown-biphenyl fragment **3**.

Cap synthesis (Scheme 2.4) began by transforming commercially available 3,5-dimethoxy-4-hydroxy-benzaldehyde (**13**) to nitrile **14**. Alkylation of **14** with **16** (obtained via THP-protection of commercially available 6-bromo-1-hexanol (**15**)) gave access to the cap precursor **17**. After reduction of nitrile **17** to amine **12**, subsequent coupling (Scheme 2.5) with **3** using standard Dean-Stark conditions produced the imine-linked product. The imine was reduced using sodium borohydride, followed by a tandem amine-protonation and THP-deprotection using hydrochloric acid. Counterion exchange with ammonium hexafluorophosphate completed the synthesis of **1-H·PF<sub>6</sub>**. Hexafluorophosphate counterions have been shown to increase the binding constant

**Scheme 2.5:** Synthesis of DCD Macromer **1-H·PF<sub>6</sub>**

between crown etherether–typetype species and ammonium ions, and also enhance the solubility of the charged complex in organic solvents.<sup>16</sup>

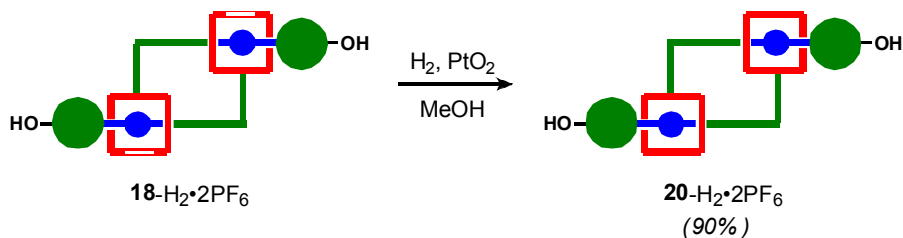
Treatment of self-complementary macromer **1-H·PF<sub>6</sub>** with olefin metathesis catalyst (H<sub>2</sub>IMes)(PCy<sub>3</sub>)(Cl)<sub>2</sub>Ru=CHPh (**2**) furnished the desired interlocked DCD **18-H<sub>2</sub>·2PF<sub>6</sub>** in 71 % isolated yield (Scheme 2.6). Additionally, some ring-closed macromer

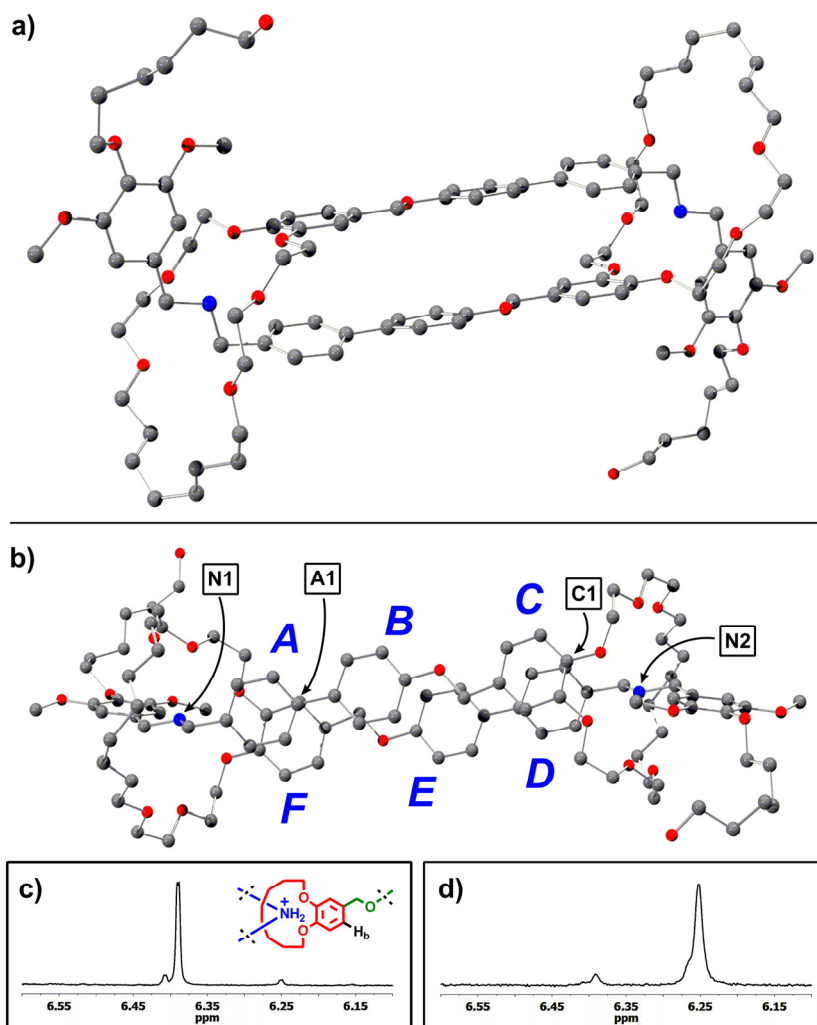
**Scheme 2.6:** Synthesis of DCD **18-H<sub>2</sub>·2PF<sub>6</sub>** and Ring-Closed Macromer **19-H·PF<sub>6</sub>**

**19-H**·PF<sub>6</sub> was also obtained (<10%).

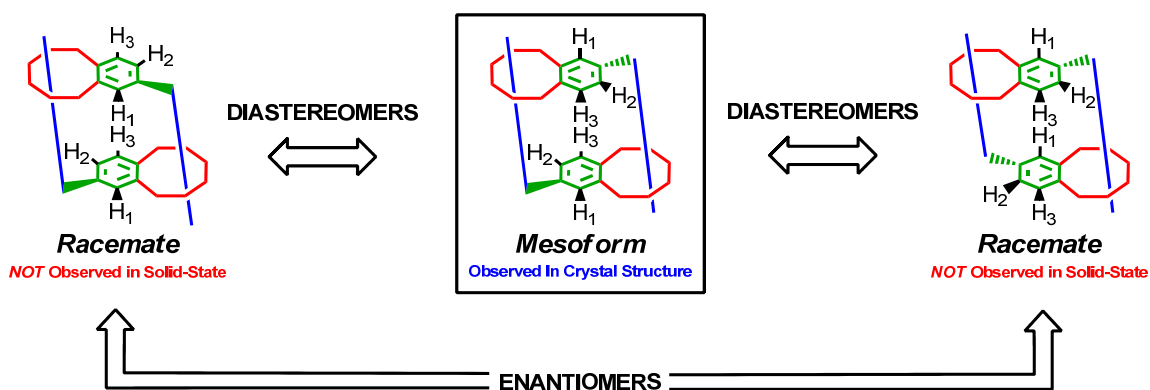
Confirmation of the interlocked nature of the product was achieved through a variety of characterization techniques. High-resolution mass spectrometry showed a dicationic species corresponding to the proposed DCD **18-H**<sub>2</sub>·2PF<sub>6</sub>. Further evidence for the interlocked nature of the product was observed in the increased complexity of the <sup>1</sup>H NMR spectrum, a result of the presence of both (*E*) and (*Z*) olefin isomers and a mixture of diastereomers.<sup>4a</sup> Full assignment of the <sup>1</sup>H NMR spectrum was accomplished using a complementary set of two-dimensional NMR techniques.<sup>15</sup> In addition to NMR spectroscopy and mass spectrometry characterization of **18-H**<sub>2</sub>·2PF<sub>6</sub>, we prepared the saturated analogue **20-H**<sub>2</sub>·2PF<sub>6</sub> (Scheme 2.7), which readily produced x-ray quality crystals (Figure 2.3a and 2.3b).<sup>17</sup> The solid-state structure unambiguously confirmed the interlocked nature of **20-H**<sub>2</sub>·2PF<sub>6</sub>, with the crown ether-type arms encircling the ammonium of a partner macromer. In contrast to other reports of such compounds,<sup>4a,8a</sup> we observed the mesoform of **20-H**<sub>2</sub>·2PF<sub>6</sub> in the solid-state structure (Figure 2.4). We attribute this phenomenon to the presence of strong  $\pi$ - $\pi$  slipped-stacking interactions<sup>18</sup> (average inter-“backbone” distance of 3.4 Å) between rings **A** and **F** as well as **C** and **D** (Figure 2.2b), imparting enhanced stability to the mesoform of the dimer. Due to inversion of one crown-aryl ring (either **A** or **D**) prior to interlocking, the racemic form of

**Scheme 2.7:** Saturation of DCD **18-H**<sub>2</sub>·2PF<sub>6</sub>





**Figure 2.3:** ORTEP representation of  $20\text{-H}_2\cdot 2\text{PF}_6$ : side-on view (a) and top-down view (b), showing  $\pi$ - $\pi$  slipped-stacking interactions between rings A and F as well as C and D (average interplanar distance: 3.4 Å). Hydrogen atoms, counterions, and solvent molecules have been omitted for clarity. Partial  $^1\text{H}$  NMR spectrum of  $20\text{-H}_2\cdot 2\text{PF}_6$  corresponding to the signal from  $\text{H}_b$  of the racemate (c) and mesoform (d).



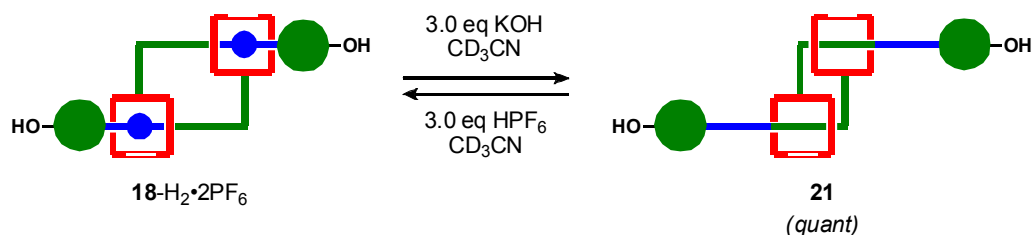
**Figure 2.4:** Different diastereomers formed during dimerization of  $1\text{-H}\cdot \text{PF}_6$ .

**20**-H<sub>2</sub>·2PF<sub>6</sub> is likely unable to simultaneously engage in extensive  $\pi$ - $\pi$  slipped-stacking interactions and strong crown ether-ammonium hydrogen bonding interactions, resulting in limited crystallinity. Evidence for the distinct environment of crown-aryl proton H<sub>b</sub> of each diastereomer is observed in the <sup>1</sup>H NMR spectrum (Figure 2c and 2d), confirming the altered alignment of the crown-aryl rings. Evidence from the crystal structure provided insight into the expected extension distance of the deprotonated forms of **18**-H<sub>2</sub>·2PF<sub>6</sub> and **20**-H<sub>2</sub>·2PF<sub>6</sub>. One scenario would involve sliding of the dimer backbone through the crown-type macrocycles until ring **A** aligned over ring **D** in a conformation similar to ring **C** in the bound state. In this case, the measured distance between A1 to C1 (a 10.7 Å extension distance) can be related to the binding-site-to-binding-site dimer length from N1 to N2 (18.3 Å), giving an extension of 58%. This value closely approximates the largest known extension percent of synthetic interlocked molecular actuators (66%).<sup>19</sup>

### *Dimer Switching*

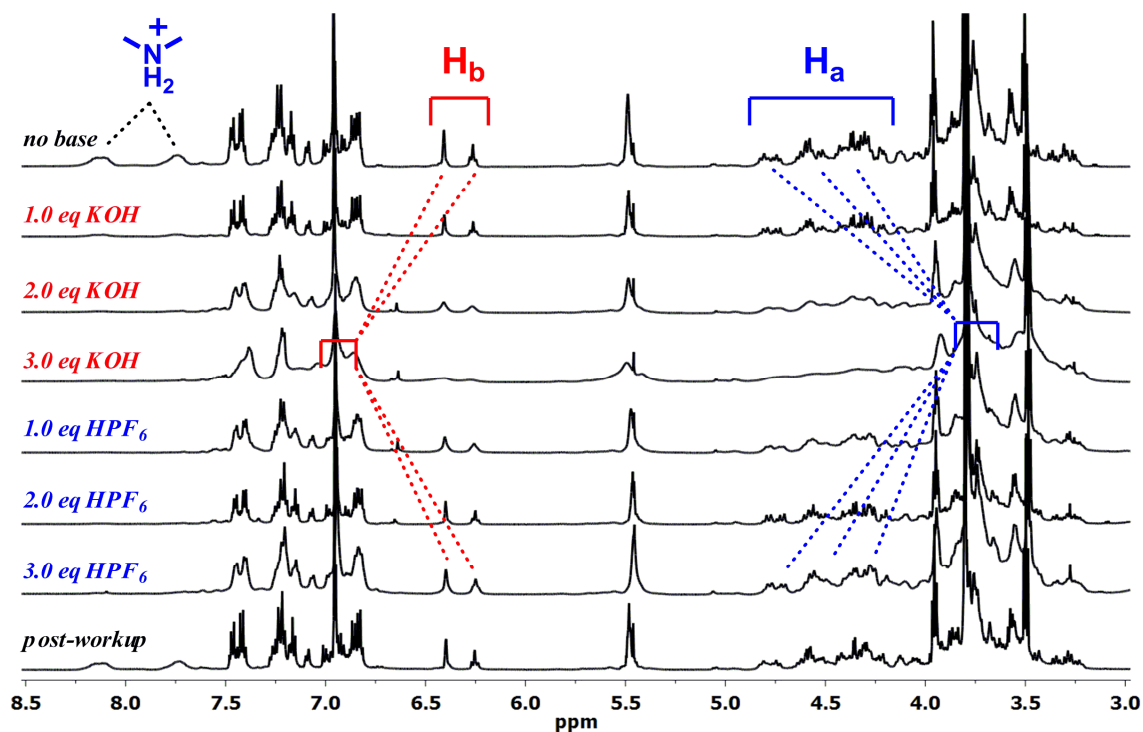
To demonstrate utility as a molecular actuator, switching between bound and unbound conformations of **18**-H<sub>2</sub>·2PF<sub>6</sub> must be facile and rapid. Addition of a solution of potassium hydroxide in D<sub>2</sub>O to **18**-H<sub>2</sub>·2PF<sub>6</sub> in CD<sub>3</sub>CN (Scheme 2.8) quickly affected ammonium deprotonation to give the unbound analogue **21**. Due to the absence of a secondary binding site, the <sup>1</sup>H NMR spectrum broadens significantly upon deprotonation

**Scheme 2.8:** Switching of Dimer **18**-H<sub>2</sub>·2PF<sub>6</sub>

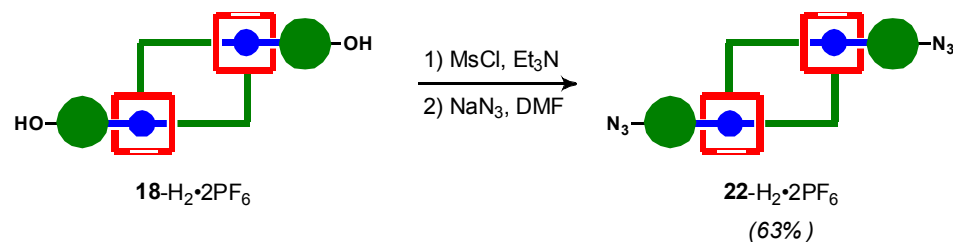




(Figure 2.5), indicating conformational heterogeneity possible only upon removal of crown-ammonium coordinating interactions. Heteronuclear single quantum coherence (HSQC) NMR analysis<sup>15</sup> of the deprotonated dimer confirmed an upfield shift (from 4.5 ppm to 3.7 ppm) of the resonance of the benzylic protons  $H_a$  adjacent to the ammonium, suggesting deprotonation. Furthermore, the resonance of proton  $H_b$  shifts downfield to 7.0 ppm and coalesces, indicating the presence of a variety of conformations distinct from the native forms of  $\mathbf{18-H_2 \cdot 2PF_6}$ . Upon addition of an equivalent amount of hexafluorophosphoric acid, the original  $^1\text{H}$  NMR spectrum of  $\mathbf{18-H_2 \cdot 2PF_6}$  was restored, completing the switching and showing facile return of the dimer to the contracted, bound conformation.



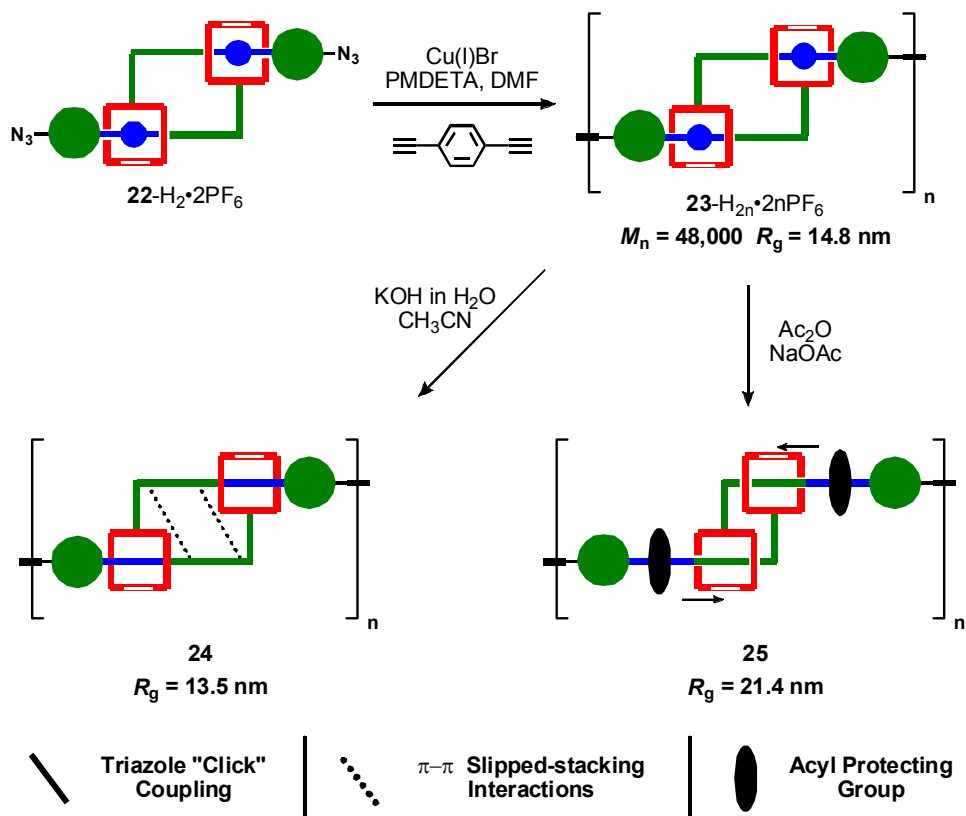
**Figure 2.5:** Partial 600 MHz  $^1\text{H}$  NMR spectrum of  $\mathbf{18-H_2 \cdot 2PF_6}$  depicting the switching from bound to unbound conformations upon addition of 3.0 eq KOH, and subsequent recoordination upon addition of 3.0 eq HPF<sub>6</sub>. An aqueous workup restores ammonium proton resonances.

**Scheme 2.9:** Synthesis of Azide Dimer **22**-H<sub>2</sub>·2PF<sub>6</sub>

### Materials Synthesis

In preparation for materials synthesis, the terminal alcohols of **18**-H<sub>2</sub>·PF<sub>6</sub>, were converted to mesylates and subsequently treated with sodium azide to give diazide **22**-H<sub>2</sub>·2PF<sub>6</sub> (Scheme 2.9). Use of a copper catalyst and N,N,N',N'',N''-pentamethyldiethylenetriamine ligand facilitated the Huisgen 1,3-dipolar cycloaddition “click” reaction<sup>20</sup> between **22**-H<sub>2</sub>·2PF<sub>6</sub> and 1,4-diethynylbenzene to give the step-growth linear polymer **23**-H<sub>2n</sub>·2nPF<sub>6</sub> (Scheme 2.10). Gel permeation chromatography (GPC)<sup>21</sup> coupled with multiangle laser light scattering (MALLS) detection analysis of **23**-H<sub>2n</sub>·2nPF<sub>6</sub> showed that the polymer had a molecular weight (MW) of 48,000 g mol<sup>-1</sup> and a radius of gyration (*R<sub>g</sub>*) of 14.8 nm. Since each DCD unit is about 2.5 nm and the degree of polymerization is approximately 22, we would expect the polymer to have an *R<sub>g</sub>* value of 27.5 nm if it were fully extended. The measured value (14.8 nm) indicates that the polymer, while not perfectly rod-shaped, appears to be mostly linear and is not excessively folded. Like the monomeric dimer, the polymer could be readily deprotonated to produce neutral analogue **24** (Scheme 2.10). Reprotonation of **24** to regenerate **23**-H<sub>2n</sub>·2nPF<sub>6</sub> was rapidly achieved upon treatment with HPF<sub>6</sub>, and five cycles of switching were performed with excellent polymer stability. By MALLS analysis, **24** had a *R<sub>g</sub>* of 13.5 nm, indicating the dimeric units within the deprotonated polymer

**Scheme 2.10:** Synthesis of Linear DCD Polymer **23**-H<sub>2n</sub>·2nPF<sub>6</sub>, Neutral Polymer **24**, and Extended Acylated Analogue **25**

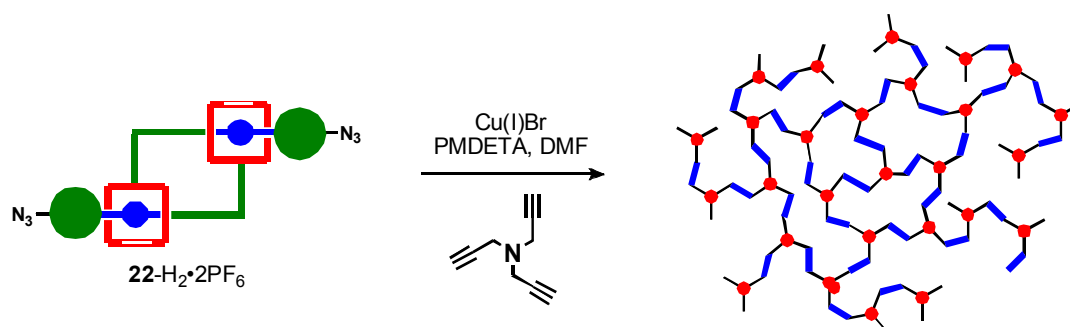


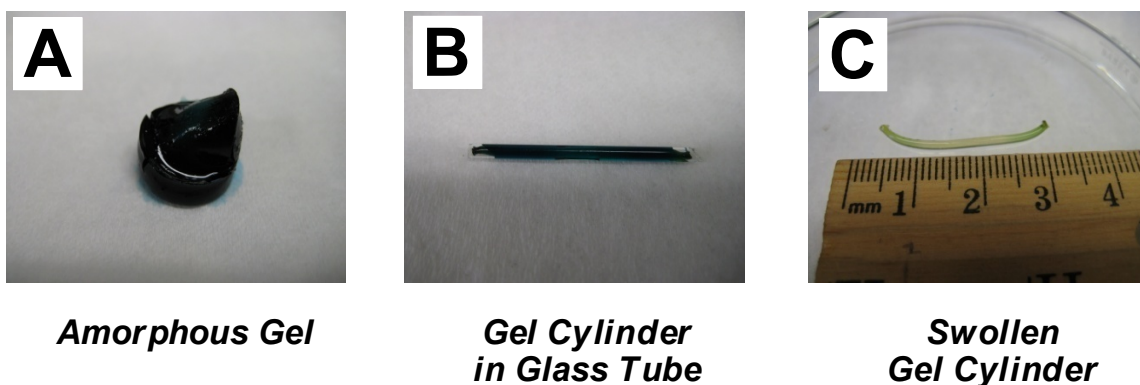
remained in the contracted conformation. This effect is likely due to a combination of  $\pi$ - $\pi$  slipped-stacking interactions of the dimer aryl rings and limited solubility in the GPC eluent<sup>21</sup>, favoring the collapsed, contracted conformation of the polymer and preventing systematic extension of the dimeric units. Additionally, the similar dimensions of bound polymer **23**-H<sub>2n</sub>·2nPF<sub>6</sub> and deprotonated polymer **24** implies that the solvent effect on both charged and neutral polymers is similar, and does not impact polymer shape in solution. However, <sup>1</sup>H NMR analysis of **24** in a good solvent (DCM)<sup>15</sup> revealed conformational heterogeneity similar to that observed in the monomeric dimer, confirming the ability of the dimer units in the polymer to slide upon deprotonation. In application, the DCD-containing materials will be placed under an external load, readily

inducing a lengthening of the dimeric units. To mimic the effect of such a force and demonstrate the extension ability of the DCD polymer, we employed acylation of **18**-H<sub>2n</sub>·2nPF<sub>6</sub> to increase the steric bulk of the amines and force slippage of the crown-type rings to give extended analogue **25** (Scheme 2.10). MALLS showed **25** had a *R<sub>g</sub>* of 21.4 nm, which indicated a size increase of 48% compared to the contracted analogue. This value closely matched the anticipated dimer extension percent, and showed that the polymer dimensions were dramatically impacted by the switchable DCD units.

Upon confirmation that the linear DCD polymer chains undergo physical change when the DCD units are extended, we began to explore the incorporation of diazide dimer **22**-H<sub>2</sub>·2PF<sub>6</sub> into larger, macroscopic materials. To achieve this goal, we substituted a trialkyne crosslinker for the linear 1,4-diethynylbenzene unit (Scheme 2.11). Commercially available tripropargylamine and **22**-H<sub>2</sub>·2PF<sub>6</sub> formed an amorphous, solid gel (Figure 2.6A) in the presence of copper catalyst. Based on isolated mass of the gel relative to the original components, we observed a quantitative incorporation of dimer and trialkyne. This click gel is composed of 96 wt% mechanically interlocked material, much higher than many other non-covalently linked gels.<sup>22</sup> Though amorphous gel

**Scheme 2.11:** Click Gelation of **22**-H<sub>2</sub>·2PF<sub>6</sub> and Tripropargylamine



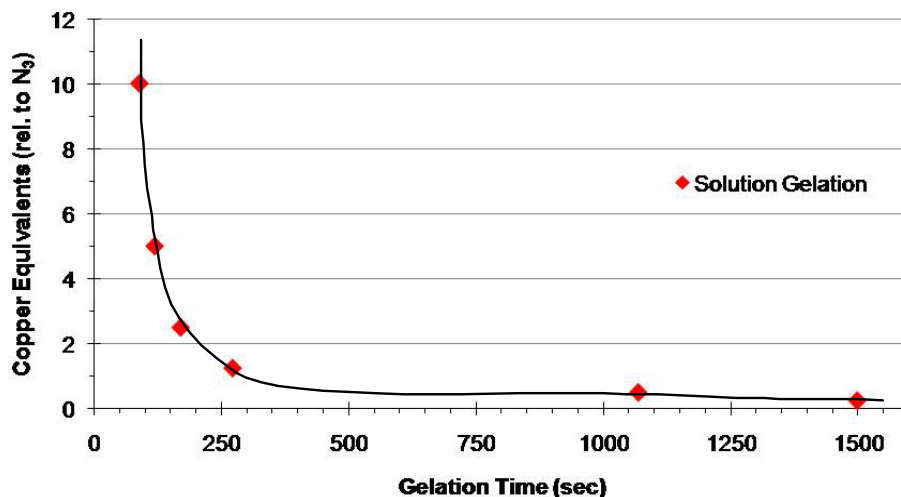


**Figure 2.6:** Click gelation of  $22\text{-H}_2\cdot 2\text{PF}_6$  and tripropargylamine produces amorphous gels (A), or, prior to gelation, the reaction solution can be flowed into glass tubes to produce uniform gel cylinders (B). These cylinders can be removed from the glass mold and swollen to several centimeters in length (C).

materials containing DCD interlocked units can be readily formed, a measure of control over the gel architecture requires sufficient time between catalyst addition and gel formation to manipulate the solution into a form or mold. Thus, a study of the relationship between catalyst loading and gel time was undertaken (Figure 2.7). By keeping the ratio of copper to azide equivalents near 2.5, the gelation time can be slowed to facilitate any necessary operations on the mixture.

While gel structure and crosslinking events are, generally, random processes control over at least the final architecture of the gel must be achieved if uniform materials are to be repeatedly synthesized. Having an understanding of the relationship between gelation time and catalyst loading allows the molding of the gel solution prior to solidification. Utilizing this knowledge, we have demonstrated that the reaction mixture can be flowed into a glass melting-point tube before the gelation event (Figure 2.6B). After allowing the reaction to proceed for several days at elevated temperature ( $50\text{ }^\circ\text{C}$ ), the crosslinked product can be removed from the capillary to yield a long, cylindrical gel

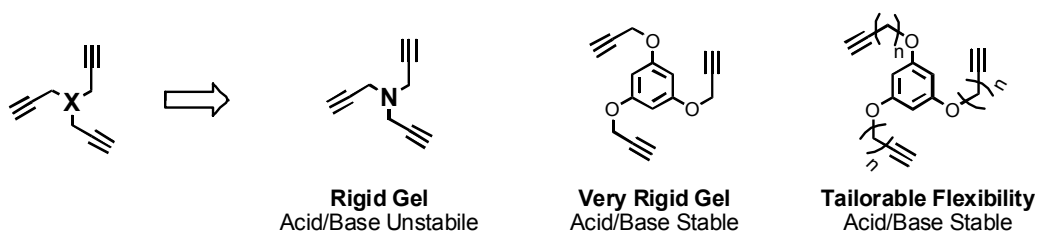
## Copper Equivalents vs. Gelation Time



**Figure 2.7:** Relationship between copper catalyst loading and trialkyne/**22**-H<sub>2</sub>·2PF<sub>6</sub> gelation time.

fragment. After swelling with solvent, the gel becomes nearly colorless due to leaching of copper and ligand out of the material (Figure 2.6C).

Though the glass capillary tubes enable control over the shape of the gel cylinders, we found that similar deprotonation/reprotonation conditions to those employed for switching of polymer **23**-H<sub>2n</sub>·2nPF<sub>6</sub> resulted in decomposition of the tripropargylamine crosslinking units and destruction of the gel. As a result of this instability, we explored alternate trialkyne structures (Figure 2.8). Gels formed with the short-chain alkyne units displayed good stability to acidic and basic conditions but were

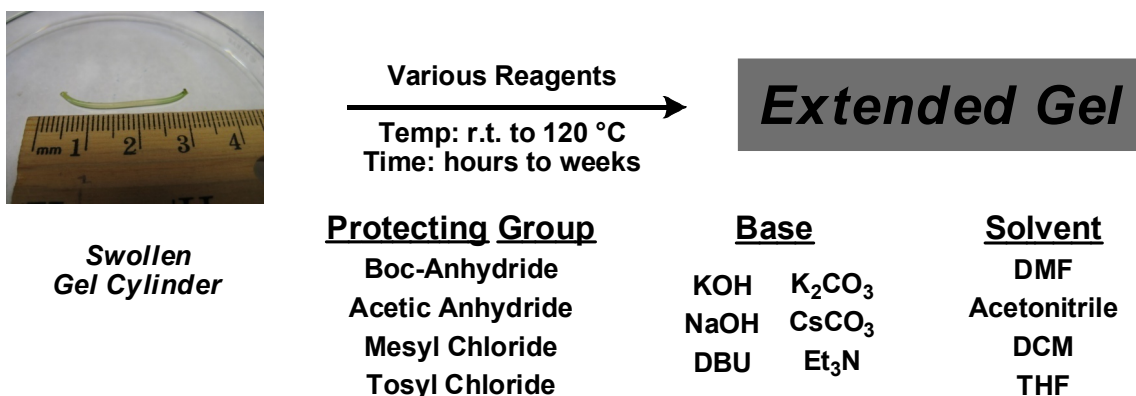


**Figure 2.8:** Small library of trialkyne structures to tailor the stability and properties of the DCD click gels.

brittle and not well suited for materials studies. However, when the longer-chain trialkyne crosslinker was employed, the resulting gels had similar stability as observed for the short-chain trialkyne but had increased flexibility and could be handled and manipulated without fracture.

Despite successfully obtaining DCD-rich gels that were stable to a range of switching conditions, we have been unable to induce dimensional elongation of the gels via deprotonation of the DCD units using a large number of reaction conditions (Scheme 2.12). This result is not entirely surprising given that the deprotonated DCD polymer **24** did not readily elongate. Consequently, we believed a more promising process would involve the forced elongation of the incorporated DCD units within the gel via a similar amine protection scheme as was employed with **25**. First, we subjected the gels to neat acetic anhydride at elevated temperature, but the gels contracted due to poor solubility. Addition of a 50:50 mix of DMF and acetic anhydride allowed the gels to remain swollen with solvent, but no significant dimensional changes were observed. At this point, we screened (Scheme 2.12) several common protecting groups (acetate and boc), and also

**Scheme 2.12:** Screened Conditions to Elongate DCD-Gels

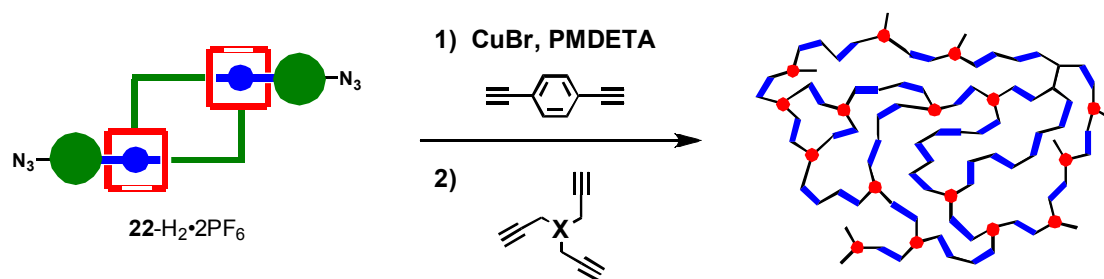


tried other suitable reagents, including tosyl chloride and mesyl chloride, which had been shown to react with ammoniums in  $\mathbf{18}\cdot\text{H}_2\cdot 2\text{PF}_6$ . We have tried a number of bases (Scheme 2.12), such as sodium and potassium hydroxide, potassium and cesium carbonate, sodium acetate, DBU, triethylamine, and sodium hydride, but none have met with success. To favor the swollen state of the gel and facilitate transfer of reagents to DCD units in the core of the gel cylinders, we explored a number of solvents and solvent systems (Scheme 2.12), and tried a range of temperatures (up to 120 °C). Unfortunately, none of these systems resulted in observable dimension changes of the gel.

The inability to *observe* lengthening of the DCD gels does not imply that these DCD gel tubes cannot extend. Instead, it is likely that the DCD gels simply do not facilitate diffusion of the protecting groups ( $\text{Ac}_2\text{O}$ ,  $\text{Boc}_2\text{O}$ , etc.) or the base to the DCD ammoniums located within the center of the gel. While the polymer DCD units are readily accessed by these small-molecule protecting agents, the gels often contract and shrink in the presence of such solvents/reagents as acetic anhydride. These gels have proven to be less of a chemical challenge and more of an engineering challenge.

To visualize gel elongation, it is likely that the DCDs will have to be aligned in a uniform direction within the gel. In this way, the gel would elongate *primarily* in a single direction, not in a three-dimensional fashion as would be anticipated with a randomly oriented DCD gel network. Successfully aligning the DCD units within the gel will require a secondary mechanical force applied to the solution during the gelation process. Such forces could be introduced via fiber “pulling,” where a DCD gel fiber is produced by withdrawing a portion of the solution at the moment of gelation. The motion of “pulling”



**Scheme 2.13:** Synthesis of Porous DCD Gel

the fiber from solution would be expected to align the DCD units parallel to the force of the fiber elongation. In a complementary fashion, injection of a gelling into a non-solvent reservoir may facilitate alignment of the DCD units. To produce a bulk quantity of DCD gel with aligned interlocked units, a solution of click-gel components could be subjected to flow in a uniform direction, possibly producing a gel sheet, tube, etc. containing highly-oriented DCD units.

In addition to aligning the DCD units, it might also be possible to enhance the permeability of the DCD gels by incorporating small linear sections of DCD chains (Scheme 2.13), which would separate the crosslinking units from one another and increase the pore size of the gel. This would enable faster and more facile diffusion of protecting or deprotonating reagents to the core of the gel. Tailoring the ratio of linear dialkyne to trialkyne crosslinker would enable control of the extent of gelation, and determining this ratio could prove critical to successfully obtaining a gel. Also, the duration of time between start of the linear oligomerization and the addition of the trialkyne will be important to prevent side-products from forming once the oligomerization has completed.

## Conclusions

In conclusion, utilization of olefin metathesis has enabled the synthesis of a [c2]daisy-chain dimer with the ammonium binding site near the cap of the dimer. A deprotonated DCD possessing such a structural attribute will more forcefully seek to restore coordinating interactions upon reprotonation, enhancing its utility as a synthetic molecular actuator. Dimer functionalization facilitated incorporation into linear polymers, with a 48% size increase of an unbound, extended analogue of the polymer demonstrating slippage of the dimer units. Ongoing work is directed at further materials studies. In particular, we are exploring the synthesis of macroscopic networks containing the DCD units and analyzing the correlation between molecular-scale extension-contraction manipulations and resulting macro-scale changes.

## References

- (1) Rescifina, A.; Zagni, C.; Iannazzo, D.; Merino, P. *Curr. Org. Chem.* **2009**, *13*, 448.
- (2) (a) Meyer, C. D.; Joiner, C. S.; Stoddart, J. F. *Chem. Soc. Rev.* **2007**, *36*, 1705.  
 (b) Haussmann, P. C.; Stoddart, J. F. *Chem. Record* **2009**, *9*, 136. (c) Rowan, S. J.; Cantrill, S. J.; Cousins, G. R. L.; Sanders, J. K. M.; Stoddart, J. F. *Angew. Chem. Int. Ed.* **2002**, *41*, 898.
- (3) (a) Bilig, T.; Oku, T.; Furusho, Y.; Koyama, Y.; Asai, S.; Takata, T. *Macromolecules* **2008**, *41*, 8496. (b) Bugler, J.; Sommerdijk, N. A. J. M.; Visser, A. J. W. G.; van Hoek, A.; Nolte, R. J. M.; Engbersen, J. F. J.; Reinhoudt, D. N.

- J. Am. Chem. Soc.* **1999**, *121*, 28. (c) Hirotsu, K.; Higuchi, T.; Fujita, K.; Ueda, T.; Shinoda, A.; Imoto, T.; Tabushi, I. *J. Org. Chem.* **1982**, *47*, 1143. (d) Liu, Y.; Li, L.; Fan, Z.; Zhang, H.-Y.; Wu, X.; Guan, X.-D.; Liu, S.-X. *Nano Lett.* **2002**, *2*, 257. (e) Liu, Y.; You, C.-C.; Zhang, M.; Weng, L.-H.; Wada, T.; Inoue, Y. *Org. Lett.* **2000**, *2*, 2761. (f) Wu, J.; Leung, K. C.-F.; Stoddart, J. F. *Proc. Natl. Acad. Sci. U.S.A.* **2007**, *104*, 17266.
- (4) (a) Cantrill, S. J.; Youn, G. J.; Stoddart, J. F.; Williams, D. J. *J. Org. Chem.* **2001**, *66*, 6857. (b) M. Consuelo Jiménez, M. C.; Dietrich-Buchecker, C.; Sauvage, J.-P.; De Cian, A. *Angew. Chem. Int. Ed.* **2000**, *39*, 1295. (c) Yamaguchi, N.; Devdatt, S.; Nagvekar, D. S.; Gibson, H. W. *Angew. Chem. Int. Ed.* **1998**, *37*, 2361. (d) Peter R. Ashton, P. R.; Baxter, I.; Cantrill, S. J.; Fyfe, M. C. T.; Glink, P. T.; Stoddart, J. F.; White, A. J. P.; Williams, D. J. *Angew. Chem. Int. Ed.* **1998**, *37*, 1294.
- (5) (a) Coutrot, F.; Romuald, C.; Busseron, E. *Org. Lett.* **2008**, *10*, 3741. (b) Wu, J.; Leung, K. C.-F.; Benitez, D.; Han, J.-Y.; Cantrill, S. J.; Fang, L.; Stoddart, J. F. *Angew. Chem. Int. Ed.* **2008**, *47*, 7470-7474. (c) Jiménez, M. C.; Dietrich-Buchecker, C.; Sauvage, J.-P. *Angew. Chem.* **2000**, *39*, 3284. (d) Elizarov, A. M.; Chiu, S.-H.; Stoddart, J. F. *J. Org. Chem.* **2002**, *67*, 9175. (e) Pease, A. R.; Jeppesen, J. O.; Stoddart, J. F.; Luo, Y.; Collier, C. P.; Heath, J. R. *Acc. Chem. Res.* **2001**, *34*, 433.

- (6) (a) Fustin, C. A.; Clarkson, G. J.; Leigh, D. A.; Van Hoof, F.; Jonas, A. M.; Bailly, C. *Macromolecules* **2004**, *37*, 7884. (b) Fustin, C.-A.; Bailly, C.; Clarkson, G. J.; Galow, T. H.; Leigh, D. A. *Macromolecules* **2004**, *37*, 66.
- (7) (a) Fustin, C.-A.; Bailly, C.; Clarkson, G. J.; De Groote, P.; Galow, T. H.; Leigh, D. A.; Robertson, D.; Slawin, A. M. Z.; Wong, J. K. Y. *J. Am. Chem. Soc.* **2003**, *125*, 2200. (b) Watanabe, N.; Ikari, Y.; Kihara, N.; Takata, T. *Macromolecules* **2004**, *37*, 6663. (c) Werts, M. P. L.; van den Boogaard, M.; Tsivgoulis, G. M.; Hadziioannou, G. *Macromolecules* **2003**, *36*, 7004.
- (8) (a) Guidry, E. N.; Li, J.; Stoddart, J. F.; Grubbs, R. H. *J. Am. Chem. Soc.* **2007**, *129*, 8944. (b) Fang, L.; Hmadeh, M.; Wu, J.; Olson, M. A.; Spruell, J. M.; Trabolsi, A.; Yang, Y.-W.; Elhabiri, M.; Albrecht-Gary, A.-M.; Stoddart, J. F. *J. Am. Chem. Soc.* **2009**, *131*, 7126.
- (9) (a) Chiu, S.-H.; Rowan, S. J.; Cantrill, S. J.; Stoddart, J. F.; White, A. J. P.; Williams, D. J. *Chem. Commun.* **2002**, 2948. (b) Rowan, S. J.; Cantrill, S. J.; Stoddart, J. F.; White, A. J. P.; Williams, D. J. *Org. Lett.* **2000**, *2*, 759. (c) Ueng, S.-H.; Hsueh, S.-Y.; Lai, C.-C.; Liu, Y.-H.; Peng, S.-M.; Chiu, S.-H. *Chem. Commun.* **2008**, 817. (d) Hoshino, T.; Miyauchi, M.; Kawaguchi, Y.; Yamaguchi, H.; Harada, A. *J. Am. Chem. Soc.* **2000**, *122*, 9876.
- (10) (a) Trnka, T. M.; Grubbs, R. H. *Acc. Chem. Res.* **2001**, *34*, 18. (b) Scholl, M.; Ding, S.; Lee, C. W.; Grubbs, R. H. *Org. Lett.* **1999**, *1*, 953.
- (11) (a) Kidd, T. J.; Leigh, D. A.; Wilson, A. J. *J. Am. Chem. Soc.* **1999**, *121*, 1599. (b) Weck, M.; Mohr, B.; Sauvage, J.-P.; Grubbs, R. H. *J. Org. Chem.* **1999**, *64*,

5463. (c) Mobian, P.; Kern, J.-M.; Sauvage, J.-P. *J. Am. Chem. Soc.* **2003**, *125*, 2016. (d) Sambrook, M. R.; Beer, P. D.; Wisner, J. A.; Paul, R. L.; Cowley, A. R. *J. Am. Chem. Soc.* **2004**, *126*, 15364. (e) Guidry, E. N.; Cantrill, S. J.; Stoddart, J. F.; Grubbs, R. H. *Org. Lett.* **2005**, *7*, 2129.
- (12) (a) Wisner, J. A.; Beer, P. D.; Drew, M. G. B.; Sambrook, M. R. *J. Am. Chem. Soc.* **2002**, *124*, 12469. (b) Kilbinger, A. F. M.; Cantrill, S. J.; Waltman, A. W.; Day, M. W.; Grubbs, R. H. *Angew. Chem. Int. Ed.* **2003**, *42*, 3281. (c) Hannam, J. S.; Kidd, T. J.; Leigh, D. A.; Wilson, A. J. *Org. Lett.* **2003**, *5*, 1907.
- (13) (a) Coumans, R. G. E.; Elemans, J. A. A. W.; Thordarson, P.; Nolte, R. J. M.; Rowan, A. E. *Angew. Chem. Int. Ed.* **2003**, *42*, 650. (b) Badjić, J. D.; Cantrill, S. J.; Grubbs, R. H.; Guidry, E. N.; Orenes, R.; Stoddart, J. F. *Angew. Chem. Int. Ed.* **2004**, *43*, 3273. (c) Wang, L.; Vysotsky, M. O.; Bogdan, A.; Bolte, M.; Böhmer, V. *Science* **2004**, *304*, 1312. (d) Zhu, X.-Z.; Chen, C.-F. *J. Am. Chem. Soc.* **2005**, *127*, 13158.
- (14) Nielsen, M. B.; Hansen, J. G.; Becher, J. *Eur. J. Org. Chem.* **1999**, 2807.
- (15) See the supporting information for complete details.
- (16) (a) Ashton, P. R.; Cantrill, S. J.; Preece, J. A.; Stoddart, J. F.; Wang, Z.-H.; White, A. J. P.; Williams, D. J. *Org. Lett.* **1999**, *1*, 1917. (b) Montalti, M. *Chem. Commun.* **1998**, 1461. (c) Doxsee, K. M. *J. Org. Chem.* **1989**, *54*, 4712. (d) Jones, J. W.; Gibson, H. W. *J. Am. Chem. Soc.* **2003**, *125*, 7001.
- (17) Crystallographic data have been deposited at the CCDC: deposition number 734570. See supporting information for complete details.

- (18) Coates, G. W.; Dunn, A. R.; Henling, L. M.; Dougherty, D. A.; Grubbs, R. H. *Angew. Chem. Int. Ed.* **1997**, *36*, 248.
- (19) Liu, Y.; Flood, A. H.; Bonvallet, P. A.; Vignon, S. A.; Northrop, B. H.; Tseng, H.-R.; Jeppesen, J. O.; Huang, T. J.; Brough, B.; Baller, M.; Magonov, S.; Solares, S. D.; Goddard, W. A.; Ho, C.-M.; Stoddart, J. F. *J. Am. Chem. Soc.* **2005**, *127*, 9745.
- (20) (a) Kolb, H. C.; Finn, M. G.; Sharpless, K. B. *Angew. Chem. Int. Ed.* **2001**, *40*, 2004. (b) Lutz, J.-F. *Angew. Chem. Int. Ed.* **2008**, *47*, 2182.
- (21) All GPC/MALLS measurements were performed using 0.2 M LiBr in DMF in an effort to minimize the effects of charge on the polymers in solution and prevent aggregation of charged species on the columns.
- (22) Ito, K. *Polym. J.* **2007**, *39*, 489.

## *Experimental Information*

### **Supporting Information**

Experimental procedures and characterization data ( $^1\text{H}$  and  $^{13}\text{C}$  and 2D NMR, IR, HRMS, GPC) for all compounds and their precursors.

**General Information.** NMR spectra were obtained on either a Mercury 300 MHz spectrometer, an INOVA 500 MHz spectrometer equipped with an AutoX broadband probe with z-gradients, or an INOVA 600 MHz spectrometer equipped with an inverse HCN triple resonance probe with x-, y-, and z-gradients. All spectrometers were running Varian VNMRJ software. Chemical shifts for both  $^1\text{H}$  and  $^{13}\text{C}$  spectra are reported in per million (ppm) relative to  $\text{Si}(\text{CH}_3)_4$  ( $\delta=0$ ) and referenced internally to the proteo solvent resonance. Multiplicities are abbreviated as follows: singlet (s), doublet (d), triplet (t), quartet (q), quintet (qt), septuplet (sp), multiplet (m), and broad (br). MestReNova NMR 5.3.2 software was used to analyze all NMR spectra. Molecular mass calculations were performed with ChemBioDraw Ultra 11.0.1 (Cambridge Scientific). Mass spectrometry measurements (FAB, EI, and MALDI) were performed by the California Institute of Technology Mass Spectrometry Facility. Analytical thin-layer chromatography (TLC) was performed using silica gel 60 F254 precoated plates (0.25 mm thickness) with a fluorescent indicator. Visualization was performed using UV and iodine stain. Flash column chromatography was performed using silica gel 60 (230–400 mesh) from EM Science. Gel permeation chromatography (GPC) was carried out in 0.2 M LiBr in DMF on two I-series Mixed Bed Low MW ViscoGel columns (Viscotek) connected in series

with a DAWN EOS multiangle laser light scattering (MALLS) detector and an Optilab DSP differential refractometer (both from Wyatt Technology). No calibration standards were used, and  $dn/dc$  values were obtained for each injection assuming 100% mass elution from the columns. IR was obtained on a Perkin-Elmer BX-II FTIR spectrometer using thin-film techniques on NaCl plates.

**Materials and Methods.** Anhydrous N,N-dimethylformamide (DMF) was obtained from Acros (99.8% pure, Acrosealed). Dry tetrahydrofuran (THF), toluene, and dichloromethane (DCM) were purified by passage through solvent purification columns.<sup>1</sup> All water was deionized. 6-Bromo-1-hexanol (**10**, 97%), syringaldehyde (**12**, 98%), 5-bromo-1-pentene (**17**, 95%), protocatechuic acid ethyl ester (**20**, 97%), 4'-Hydroxy-4-biphenylcarboxylic acid (**24**, 99%), and 1,4-diethynylbenzene (96%) were purchased from Aldrich and used as received. Anhydrous potassium carbonate (J. T. Baker, 99.6%) was used as received. Grubbs second-generation catalyst ( $H_2IMes)(PCy_3)(Cl)_2Ru=CHPh$  (**2**) was obtained as a generous gift from Materia, Inc. All other compounds were purchased from Acros or Aldrich and used as received.

**General Freeze-Pump-Thaw Procedure.** A flask charged with reagents and solvent was frozen with liquid nitrogen. After the solution had frozen, the headspace of the flask was evacuated under vacuum. The flask was sealed and allowed to thaw to room temperature. The headspace of the flask was then backfilled with argon. The flask was sealed and the reaction mixture frozen again with liquid nitrogen. This process was repeated twice. On the third cycle, the solution was frozen and the headspace evacuated



and backfilled with argon. Catalyst was quickly added to the top of the frozen solution, the headspace was again evacuated, and the solution allowed to warm to room temperature. The solution was backfilled with argon, refrozen, and subjected to another cycle for a total of four freeze-pump-thaw cycles.

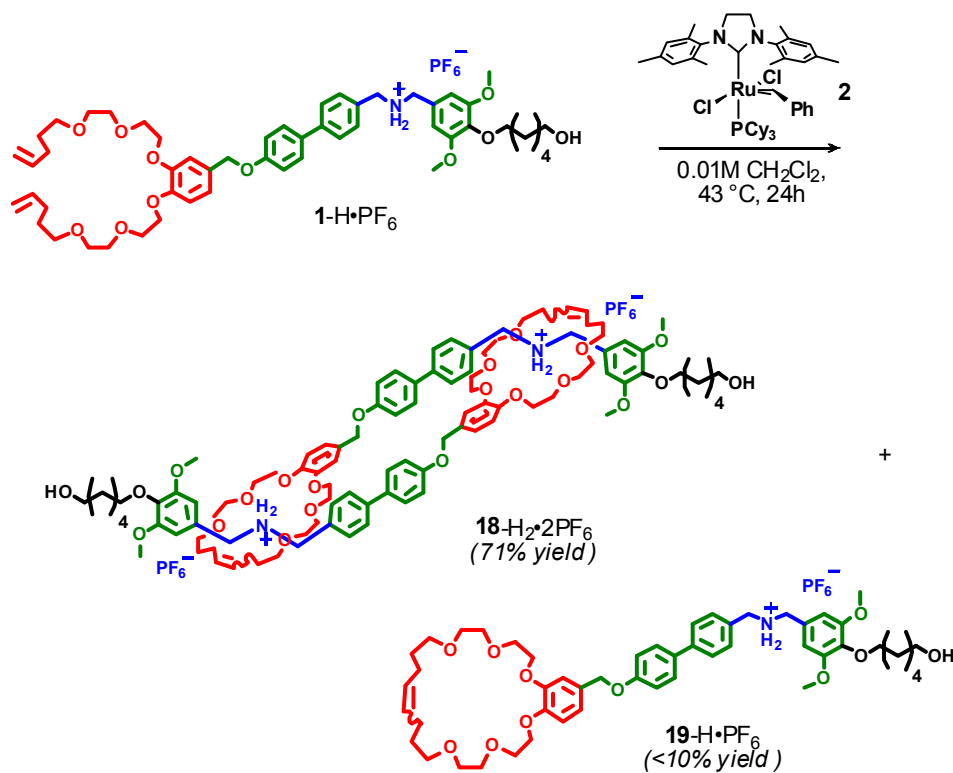
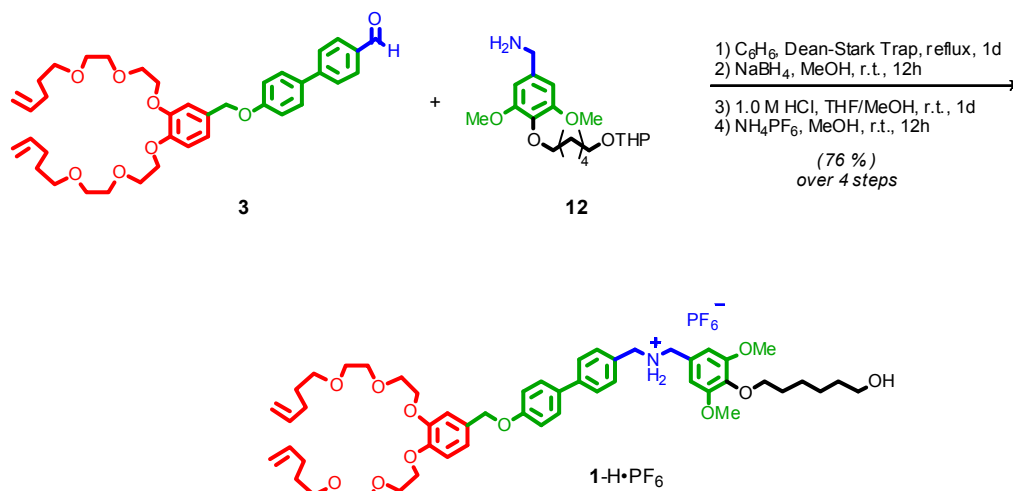
**General Phenol Alkylation Procedure.** To a cooled, flame-dried, two-neck round bottom flask, equipped with a stir bar and fitted with a septum, water-jacketed reflux condenser, and vacuum adapter was added, under argon, 3 equivalents (relative to each mole of phenol) of anhydrous potassium carbonate, anhydrous DMF (to make an ~0.1 M solution), and phenol at room temperature. To this stirring mixture was added the alkylating agent dissolved in a minimal amount of DMF. The reaction was heated to 90 °C in an oil bath for 2 to 3 days, and, upon completion, was stopped by cooling to room temperature. The reaction mixture was poured into a separatory funnel, and partitioned between water (5x original volume of DMF) and ethyl acetate (1x original volume of DMF). The aqueous layer was extracted three times with fresh portions of ethyl acetate (1x original volume of DMF), and the combined organic layers were washed three times with fresh portions of water and brine (1x original volume of DMF). The washed organic layer was dried over anhydrous magnesium sulfate ( $\text{MgSO}_4$ ), filtered through filter paper, and evaporated to dryness under reduced pressure to give the alkylation product. Purification was achieved by silica gel flash chromatography using various eluents.

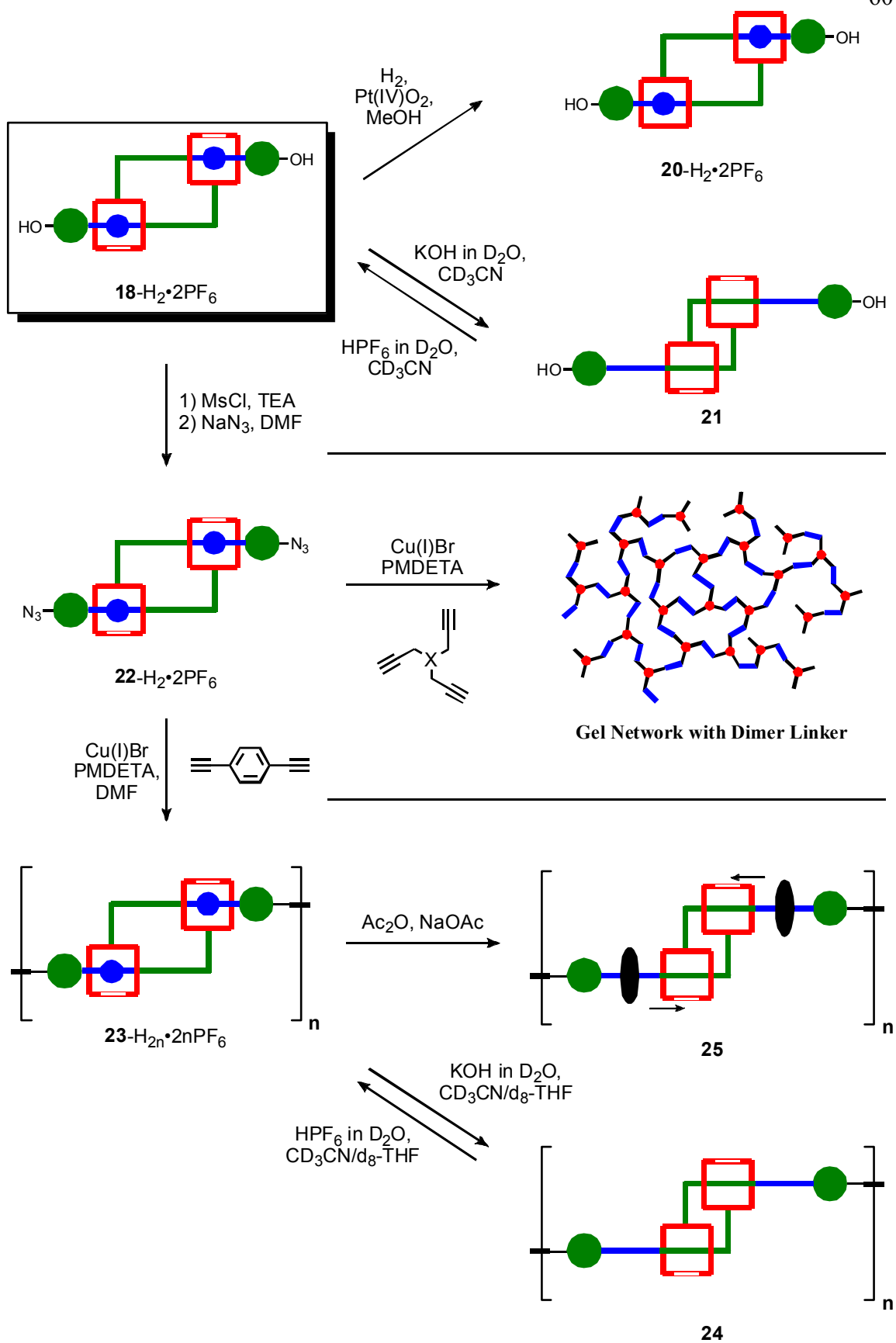
**General Lithium Aluminum Hydride Reduction Procedure.** To a cooled, flame-dried 2-neck flask, equipped with a stir bar and fitted with a septum, water-jacketed reflux

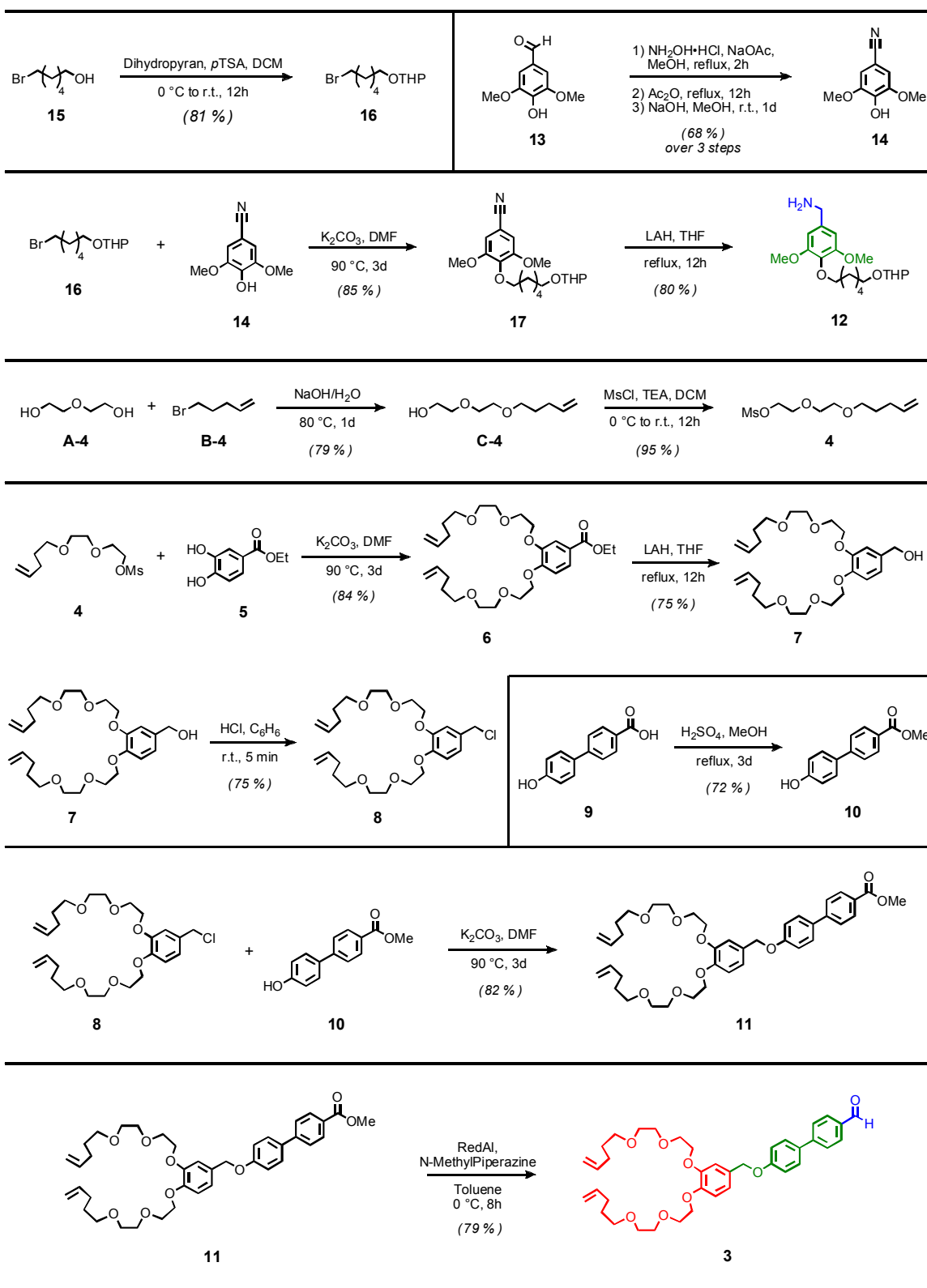
condenser, and vacuum adapter was added, under argon and at 0 °C, 3 equivalents of lithium aluminum hydride (LAH) powder (95+%), dry THF, and, slowly, 1 equivalent of ester, acid, aldehyde, or nitrile dissolved in a minimal amount of dry THF. The reaction was heated to 87 °C overnight in an oil bath. To quench the reaction mixture, the oil bath was removed and the reaction cooled to 0 °C. Water (1 ml per gram of LAH) was added very slowly to the stirring mixture, followed by very slow addition of a 15% sodium hydroxide solution (1 ml per gram of LAH). Water (3 ml per gram of LAH) was added very rapidly, and the resulting slurry was allowed to stir for 4 hours at room temperature. After this time, a large excess of celite and anhydrous  $\text{MgSO}_4$  was added, and the mixture allowed to stir for an additional hour. The reaction was filtered, and the solvent removed by rotary evaporation. The product was redissolved in organic solvent (0.5x original volume of THF), and partitioned with water (1x original volume of THF) in a separatory funnel. The water layer was extracted three times with fresh solvent (0.25x original volume of THF), and the combined organic layer was washed with two fresh portions of water (0.5x original volume of THF), dried over anhydrous  $\text{MgSO}_4$ , filtered, and evaporated to dryness under reduced pressure to give the reduced product. The products were used with no further purification, or purified via specified protocols.

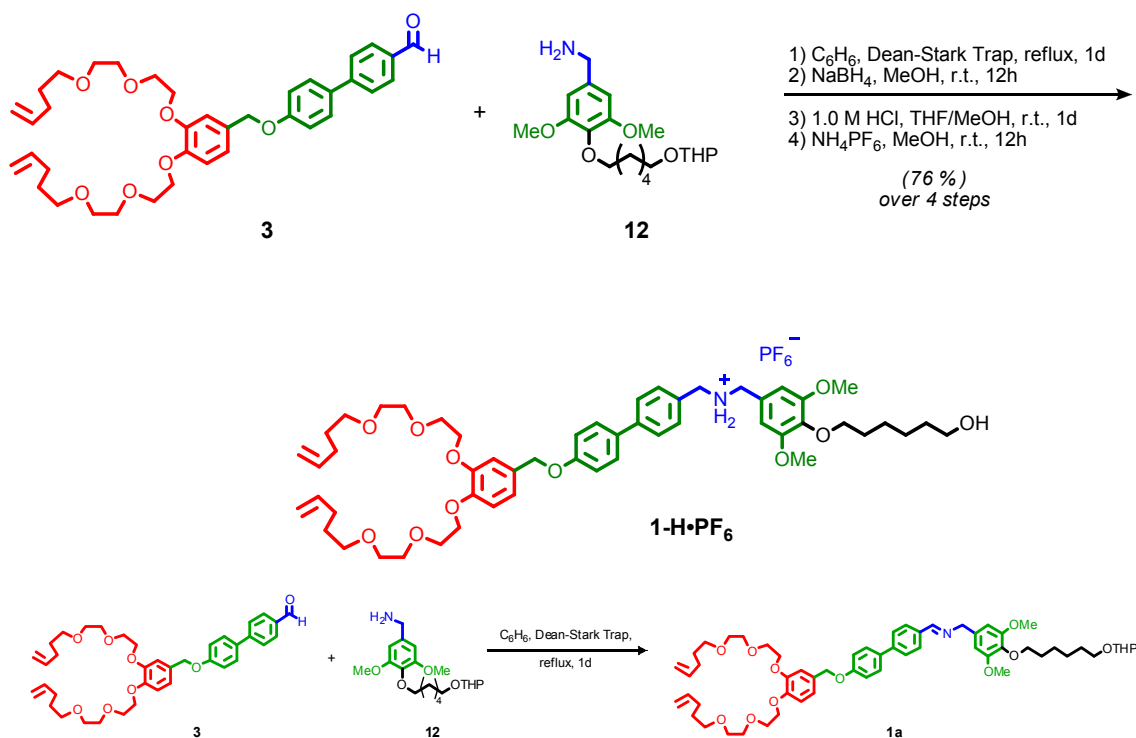
### ***References***

- (1) Pangborn, A. B.; Giardello, M. A.; Grubbs, R. H.; Rosen, R. K.; Timmers, F. J. *Organometallics* **1996**, *15*, 1518-1520.

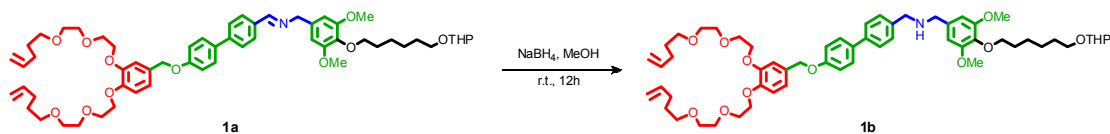
**EXPERIMENTAL SECTION**



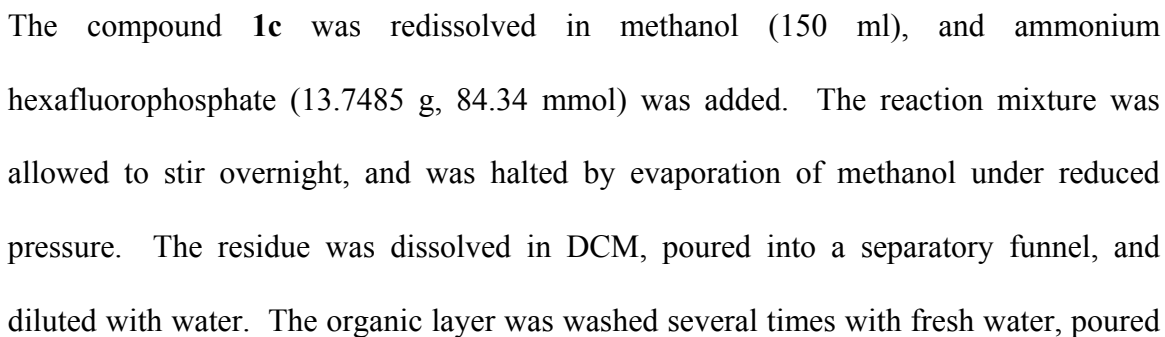
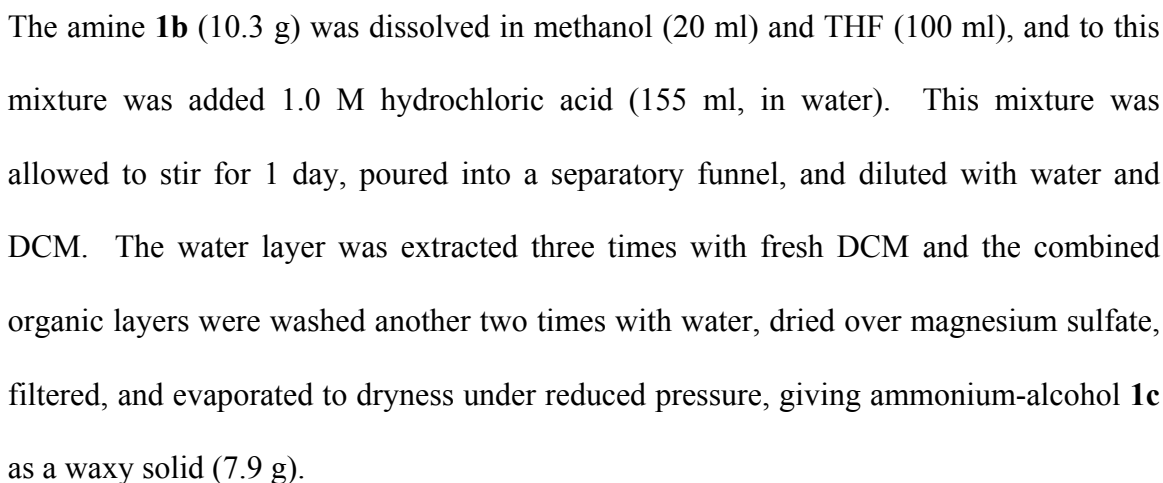




**Self-Complementary Macromer (1-H·PF<sub>6</sub>).** A flask equipped with a stir bar was charged with **3** (6.8249 g, 10.79 mmol, 1 eq), **12** (3.9635 g, 10.79 mmol, 1 eq), and benzene (250 ml). The flask was fitted with a Dean-Stark trap and reflux condenser, and heated to 100 °C. The trap was flushed several times over the course of the reaction. After 1 day, the reaction was cooled to room temperature and the benzene removed under reduced pressure to give imine **1a** as a viscous oil (10.59 g).

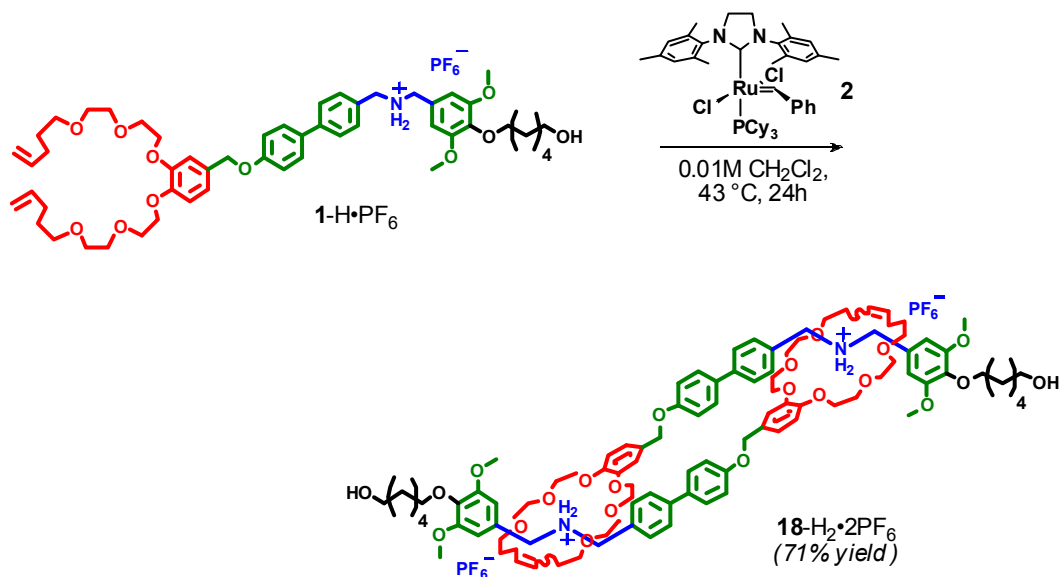


Imine **1a** (10.59 g) was dissolved in methanol (108 ml), and sodium borohydride (1.2241 g, 32.37 mmol) was added to the reaction. Stirring was continued at room temperature for 12 hours. The methanol was removed under reduced pressure, and the residue



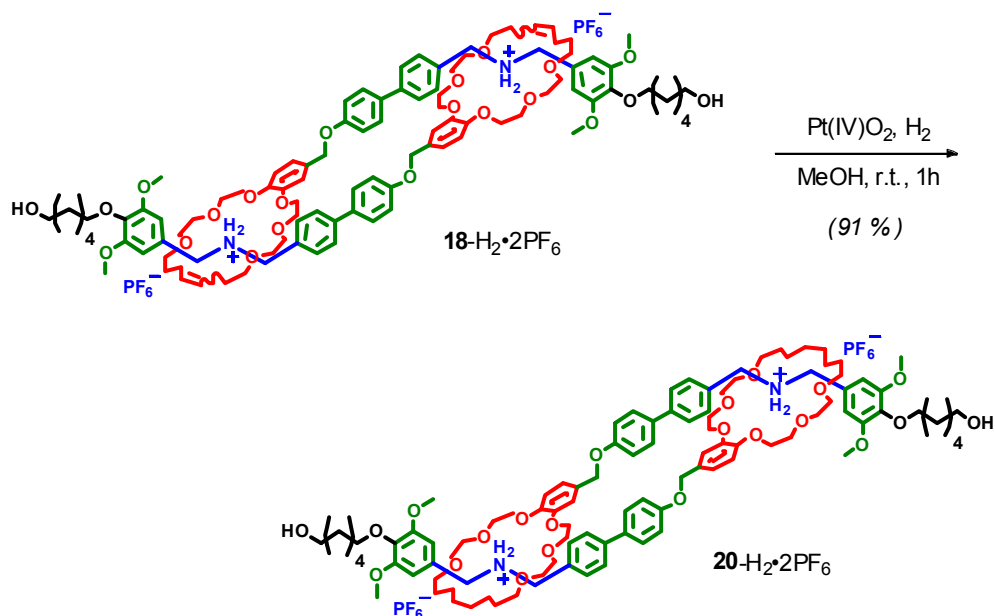
through filter paper, and evaporated to dryness under reduced pressure. Flash chromatography (SiO<sub>2</sub>: gradient from 2%, then 2.5%, then 10% DCM to methanol eluent) gave **1**-H·PF<sub>6</sub> (8.6 g, 76% yield over 4 steps) as a pale-yellow waxy solid. <sup>1</sup>H NMR (500 MHz, CDCl<sub>3</sub>): δ 7.37 (m, 6H), 6.91 (m, 4H), 6.78 (s, 1H), 6.70 (s, 2H), 5.76 (m, 2H), 5.05-4.86 (m, 4H), 4.74 (s, 2H), 4.48-3.98 (m, 4H), 3.91 (t, J = 6.50 Hz, 2H), 3.88-3.66 (m, 16H), 3.66-3.42 (m, 12H), 2.08 (m, 4H), 1.67 (sp, J = 1.67 Hz, 4H), 1.58-1.27 (m, 8H). <sup>13</sup>C NMR (126 MHz, CDCl<sub>3</sub>): δ 158.42, 153.70, 146.50, 145.99, 141.44, 137.88, 137.72, 137.44, 131.86, 130.52, 130.03, 128.23, 127.82, 126.48, 126.35, 119.65, 115.14, 114.92, 112.30, 110.80, 105.89, 73.28, 71.18, 71.02, 70.94, 70.72, 69.85, 69.76, 69.53, 69.34, 68.53, 67.66, 62.64, 56.14, 52.41, 32.47, 30.08, 30.01, 29.86, 28.58, 28.46, 25.49, 25.38. HRMS-FAB (m/z): [M – PF<sub>6</sub>] calcd for C<sub>53</sub>H<sub>74</sub>NO<sub>11</sub>, 900.5262; found, 900.5245.





**[c2]Daisy-Chain Dimer (**18-H<sub>2</sub>·2PF<sub>6</sub>**).** A cooled, flame-dried flask equipped with a stir bar, gas port, and septum was charged, under argon, with **1-H·PF<sub>6</sub>** (10.00 g, 9.56 mmol, 1 eq) and dry DCM (960 ml, 0.01 M). This mixture was sparged with argon for 30 minutes, and catalyst (H<sub>2</sub>IMes)(PCy<sub>3</sub>)(Cl)<sub>2</sub>Ru=CHPh **2** (406 mg, 0.478 mmol, 5 mol %) was added. The reaction was heated to 43 °C for 24 hours and was then quenched by addition of 5 ml of ethyl vinyl ether, which was allowed to stir for 30 minutes at elevated temperature. The solvent was removed under reduced pressure to give crude **18-H<sub>2</sub>·2PF<sub>6</sub>** as a brown foam (9.2650 g, 91.4% recovered). A 100.0 mg portion of the foam was purified by flash chromatography (SiO<sub>2</sub>: gradient from pure DCM to 0.5% methanol in DCM to 1.0% methanol in DCM to 2% methanol in DCM to 5% methanol in DCM) to afford pure **18-H<sub>2</sub>·2PF<sub>6</sub>** as a white foam (77.6 mg, 71% overall isolated yield). Note: see <sup>1</sup>H spectra for full assignment. <sup>1</sup>H NMR (600 MHz, CD<sub>3</sub>CN): δ 8.10 (br s, 2H), 7.75 (br s, 2H), 7.48-7.35 (m, 4H), 7.30-7.12 (m, 8H), 7.09 (d, J = 7.6 Hz, 1H), 7.02-6.75 (m,

11H), 6.38 (m, 1H), 6.25 (m, 1H), 5.75-5.39 (m, 4H), 4.88-3.12 (br m, 72H), 2.44 (t, J = 5.3 Hz, 2H), 2.41-1.99 (br m, 8H), 1.91-1.55 (m, 8H), 1.67 (qt, J = 7.0 Hz, 4H), 1.54-1.43 (m, 8H), 1.41-1.32 (m, 4H).  $^{13}\text{C}$  NMR (126 MHz,  $\text{CD}_3\text{CN}$ ):  $\delta$  159.96, 159.87, 155.30, 147.41, 147.26, 146.89, 146.81, 142.47, 139.18, 133.46, 133.36, 132.78, 132.69, 132.06, 132.01, 131.93, 131.59, 131.48, 131.33, 131.27, 130.90, 130.85, 130.25, 129.30, 129.27, 128.46, 127.43, 127.29, 120.35, 119.82, 116.20, 116.16, 113.52, 113.24, 111.42, 111.02, 107.71, 107.27, 74.31, 73.45, 73.25, 73.07, 72.85, 72.80, 72.51, 72.41, 72.11, 72.05, 71.41, 71.23, 71.15, 71.00, 70.96, 70.77, 70.56, 70.48, 69.72, 69.46, 69.11, 68.90, 62.97, 57.30, 57.27, 53.66, 53.43, 33.98, 31.79, 31.75, 31.25, 30.44, 30.35, 29.71, 29.67, 29.58, 29.19, 29.09, 29.07, 26.93, 26.80, 26.66, 25.95. FTIR (NaCl,  $\text{cm}^{-1}$ ): 3594.29, 3445.56, 3143.46, 3008.55, 2936.49, 2870.07, 2625.68, 2249.01, 1949.63, 1721.96, 1607.67, 1594.00, 1514.17, 1502.65, 1463.46, 1433.21, 1391.50, 1372.07, 1354.31, 1334.36, 1291.77, 1249.20, 1195.92, 1181.75, 1162.97, 1128.93, 1100.34, 1050.97, 993.38, 973.95, 948.94, 913.43, 842.34, 780.57, 763.77, 730.64, 697.31, 673.00, 647.63, 619.96. ESI-TOF MS (m/z):  $[\text{M} + 2\text{H} - 2\text{PF}_6]^{+2}$  calcd for  $\text{C}_{51}\text{H}_{70}\text{NO}_{11}$ , 872.9966; found 872.9941.

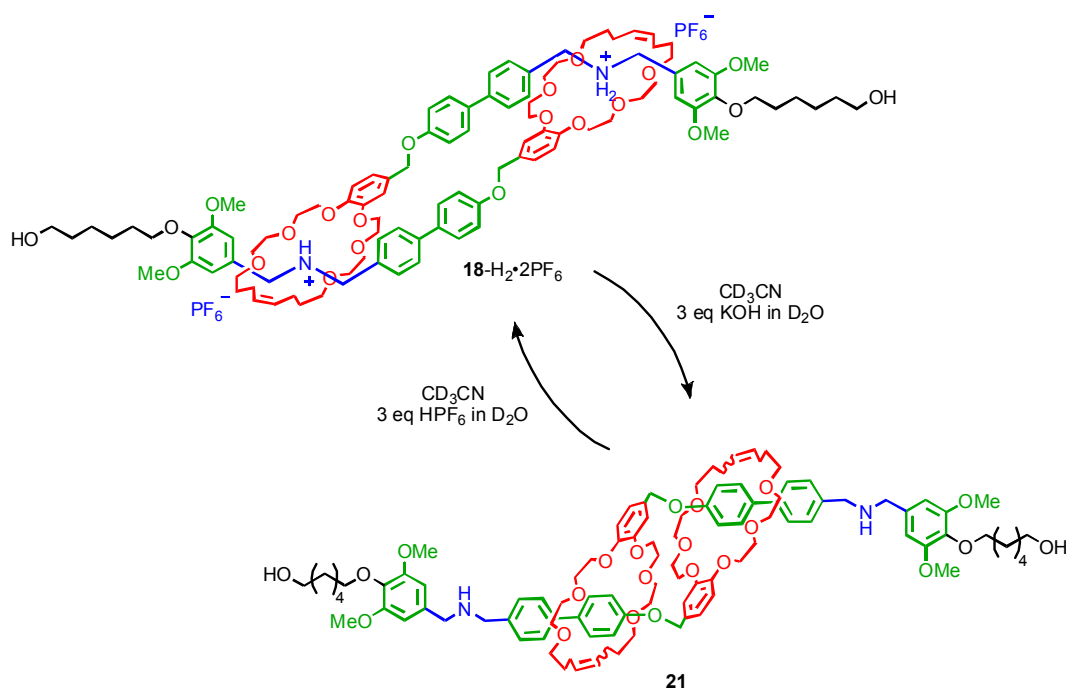


**Saturated [c2]Daisy-Chain Dimer (20-H<sub>2</sub>·2PF<sub>6</sub>).** To a round bottom flask equipped with a stir bar was added **18-H<sub>2</sub>·2PF<sub>6</sub>** (40.0 mg, 19.6 μmol, 1 eq) and methanol (25 ml). The dimer was dissolved in the methanol via heating, then allowed to cool to room temperature. To the solution, “Adam’s Catalyst” platinum(IV) oxide (89 mg, 0.393 mmol, 20 eq) was added in one portion. The flask was sealed with a septum, and, with stirring, was vigorously sparged with hydrogen gas for 15 minutes. The catalyst changed color from brown to black-gray. After the sparging was complete, a balloon of hydrogen was placed into the septum, and a positive pressure of hydrogen was maintained throughout the course of the reaction. The reaction was stirred very vigorously for one hour then filtered through a pad of celite to give the saturated dimer **20-H<sub>2</sub>·2PF<sub>6</sub>** as a white solid (36.4 mg, 91% yield). (see <sup>1</sup>H of **3-H<sub>2</sub>·2PF<sub>6</sub>** for proton letter assignments) <sup>1</sup>H NMR (600 MHz, CD<sub>3</sub>CN): δ 8.10 (br s, 2H), 7.75 (br s, 2H), 7.45 (d, J = 8.7 Hz, 1.6H,

$H_{n\ m}$ ), 7.41 (d,  $J = 8.7$  Hz, 2.4H,  $H_{n\ r}$ ), 7.30-7.24 (m, 4H,  $H_p$ ), 7.21 (d,  $J = 8.2$  Hz, 1.6H,  $H_{q\ m}$ ), 7.17 (d,  $J = 8.2$  Hz, 2.4H,  $H_{q\ r}$ ), 7.8 (d,  $J = 6.7$  Hz, 0.9H,  $H_{l\ m}$ ), 6.98 (d,  $J = 8.5$  Hz, 0.9H,  $H_{k\ m}$ ), 6.96-6.93 (s + d, 5.2H,  $H_r + H_{l\ r}$ ), 6.89 (d,  $J = 8.5$  Hz, 1.3H,  $H_{k\ r}$ ), 6.86 (d,  $J = 8.7$  Hz, 1.6H,  $H_{o\ m}$ ), 6.82 (d,  $J = 8.7$  Hz, 2.4H,  $H_{o\ r}$ ), 6.40 (m, 1.2 H,  $H_{b\ r}$ ), 6.26 (m, 0.8H,  $H_{b\ r}$ ), 4.85-4.25 (m, 12H,  $H_a + H_j$ ), 4.15-3.40 (m +  $t_{3.95} + s_{3.79} + t_{3.47}$ , 60H, [ $m = H_f - H_j$ ] + [ $t_{3.95} = H_t$ ] + [ $s_{3.79} = H_s$ ] + [ $t_{3.47} = H_y$ ]), 2.44 (t,  $J = 5.3$  Hz, 2H,  $H_z$ ), 1.73-1.33 (br m, 40 H,  $H_u - H_x + H_c - H_e$ ).  $^{13}\text{C}$  NMR (126 MHz,  $\text{CD}_3\text{CN}$ ):  $\delta$  159.96, 159.87, 155.29, 147.34, 147.24, 146.71, 146.66, 142.41, 142.28, 139.05, 133.34, 133.28, 131.98, 131.82, 131.60, 131.47, 130.23, 129.26, 128.49, 128.47, 127.44, 127.31, 120.24, 119.83, 118.69, 116.13, 113.35, 113.07, 111.31, 111.02, 107.32, 74.28, 73.44, 73.19, 73.15, 72.88, 72.83, 71.76, 71.36, 71.11, 70.12, 69.93, 69.68, 69.40, 68.95, 68.78, 62.95, 57.29, 53.80, 53.73, 33.97, 31.24, 30.88, 30.83, 30.53, 30.49, 29.10, 29.08, 28.96, 26.92, 26.79, 26.74, 26.73, 26.57, 26.55. FTIR (NaCl,  $\text{cm}^{-1}$ ): 3593.99, 3433.21, 3137.28, 2933.11, 2860.90, 1952.15, 1593.24, 1514.07, 1501.41, 1463.66, 1435.55, 1393.10, 1372.52, 1353.85, 1334.80, 1293.11, 1248.93, 1196.12, 1181.25, 1162.76, 1128.62, 1099.00, 1048.90, 1001.31, 974.66, 906.59, 842.20, 780.29, 763.75, 735.51, 701.04, 672.30, 619.80, 588.82, 557.65, 528.46. ESI-TOF MS ( $m/z$ ):  $[\text{M} - \text{PF}_6]^{1+}$  calcd for  $\text{C}_{102}\text{H}_{144}\text{N}_2\text{O}_{22}\text{F}_6\text{P}$ , 1893.9853; found, 1893.9867.

Crystals suitable for x-ray diffraction were obtained for the mesoform via slow evaporation of a solution of **20**- $\text{H}_2 \cdot 2\text{PF}_6$  (10.7 mg) in 3:3:1 hexanes:ethyl acetate:acetonitrile (0.5 ml, 0.5 ml, 0.17 ml, respectively). The racemic mixture

remained soluble and did not crystallize (see  $^1\text{H}$  NMR of each diastereomer in spectra section). The solid-state structure was deposited in the CCDC: 734570. See the CIF file for complete details.



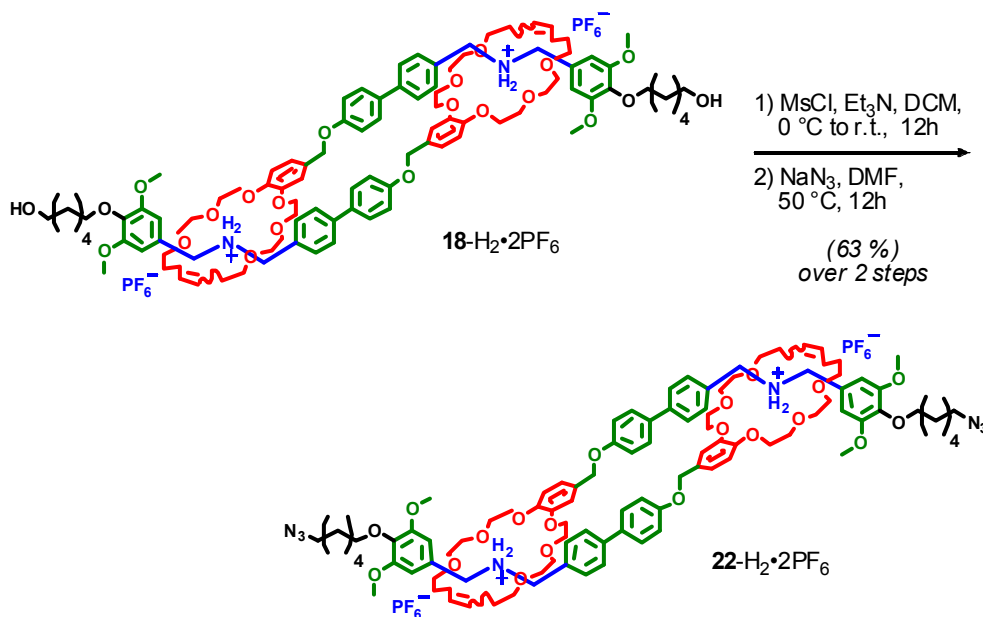
**Deprotonated [c2]Daisy-Chain Dimer (21).** To a vial was added **18**- $\text{H}_2\cdot 2\text{PF}_6$  (44.3 mg, 21.8  $\mu\text{mol}$ , 1 eq) and deuterated acetonitrile (0.5 ml), and this solution was transferred via pipet to a 5 mm NMR tube. To a separate vial was added potassium hydroxide (122 mg, 2.18 mmol, 100 eq) and deuterium oxide (0.50 ml). Using a 25  $\mu\text{l}$  syringe (Hamilton 1700 Series Gastight Syringe), 5  $\mu\text{l}$  injections (total of 3 injections) of the  $\text{KOH}/\text{D}_2\text{O}$  solution was added to the NMR tube. After each injection, the tube was vigorously shaken for 10–15 seconds, and then reinserted into the spectrometer. Deprotonation was complete after addition of 3 equivalents of potassium hydroxide, giving **21**. The sample

remained stable for 36 h, with an unchanged  $^1\text{H}$  NMR spectrum, and was subjected to reprotonation with no purification.  $^1\text{H}$  NMR (600 MHz,  $\text{CD}_3\text{CN}$ ):  $\delta$  7.75-7.30 (br m, 5H), 7.30-7.15 (m, 4H), 7.15-6.19 (br m, 17H), 5.85-5.15 (br m, 4H), 4.87-3.15 (br m, 74H), 2.45-2.00 (br m, 8H), 1.83-1.53 (br m, 12H), 1.53-1.42 (m, 8H), 1.34 (qt, 4H).  $^{13}\text{C}$  NMR (126 MHz,  $\text{CD}_3\text{CN}$ ):  $\delta$  159.48, 154.59, 148.98, 148.78, 147.07, 141.84, 140.98, 140.10, 139.12, 136.49, 134.58, 131.68, 131.10, 130.54, 130.02, 128.94, 126.69, 120.72, 116.51, 116.18, 112.85, 107.55, 107.29, 74.05, 72.76, 71.85, 71.49, 71.04, 70.77, 70.60, 70.42, 70.01, 69.70, 69.03, 68.47, 62.72, 56.99, 56.89, 54.86, 53.48, 33.74, 31.73, 31.10, 30.40, 29.71, 27.68, 26.81, 26.66.

A third vial was charged with deuterium oxide (0.5 ml) and hexafluorophosphoric acid (296  $\mu\text{l}$ , 2.18 mmol, 100 eq, 60 wt% in  $\text{H}_2\text{O}$ ). Using the same 25  $\mu\text{l}$  syringe, 5  $\mu\text{l}$  injections (total of 3 injections) of this solution were added to the NMR tube containing **21**, restoring the  $^1\text{H}$  NMR spectrum corresponding to **18**- $\text{H}_2\cdot 2\text{PF}_6$  and completing the “switching” of the dimer. (see  $^1\text{H}$  NMR spectral information for **18**- $\text{H}_2\cdot 2\text{PF}_6$ ) Note: Spectra were taken immediately after appropriate locking and shimming protocols with no extra time allowed for additional reaction. All deprotonation and reprotonation reactions were complete by the time the necessary NMR protocols were complete (<3 min).

After the switching was complete, the NMR sample was transferred to a vial and the solvent was removed under reduced pressure. The residue was dissolved in DCM (10

ml), and water was added (20 ml). The aqueous layer was extracted with fresh DCM (2 x 5 ml), and the combined organic layer further washed with fresh water (2 x 5 ml). The organic layer was poured through filter paper, and the solvent removed via rotary evaporation to return **18**-H<sub>2</sub>·2PF<sub>6</sub> (37.5 mg, 85% recovery). See <sup>1</sup>H NMR spectral characterization information for **18**-H<sub>2</sub>·2PF<sub>6</sub>.

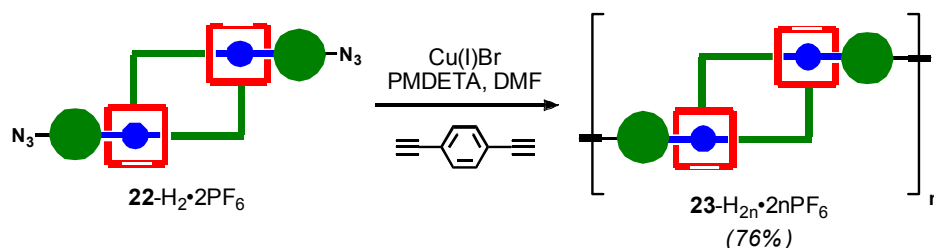


**Diazide [c2]Daisy-Chain Dimer (6-H<sub>2</sub>·2PF<sub>6</sub>).** Crude **3**-H<sub>2</sub>·PF<sub>6</sub> was mixed with ethyl acetate (5 ml) and vigorously sonicated for 15 minutes giving a tan oil. The ethyl acetate was decanted, and a fresh portion of ethyl acetate (5 ml) was added. The suspension was again sonicated vigorously for 15 minutes, and the ethyl acetate was decanted to give a pale tan powder. This terminal diol [c2]daisy-chain dimer **18**-H<sub>2</sub>·PF<sub>6</sub> powder (2.58 g, 1.27 mmol, 1 eq) was dissolved in DCM (12.7 ml, 0.1 M) and triethylamine (1.1 ml, 7.62 mmol, 6 eq), and cooled to 0 °C. To this stirring solution, mesyl chloride (0.60 ml, 7.62

mmol, 6 eq) was added dropwise. The reaction was warmed to room temperature for 12 h, then poured into a separatory funnel and diluted with water (100 ml) and DCM (25 ml). The aqueous layer was extracted with fresh DCM (2 x 25 ml), and the combined organic layer was washed with fresh water (50 ml). The organic layer was poured through filter paper, and evaporated to dryness. The resulting foam was mixed with ethyl acetate (5 ml) and subjected to sonication for 15 minutes. The ethyl acetate was decanted, and another 5 ml of fresh ethyl acetate was added. The suspension was sonicated for an additional 15 minutes, the ethyl acetate decanted, and the tan powder (2.24 g) was used without further purification.  $^1\text{H}$  NMR (500 MHz,  $\text{CDCl}_3$ ):  $\delta$  8.08 (br m, 2H), 7.68 (br m, 2H), 7.43-7.27 (m, 4H), 7.22-7.02 (m, 8 H), 7.02-6.60 (m, 12 H), 6.32-6.10 (m, 2H), 5.68-5.21 (br m, 4 H), 5.05-4.01 (br m, 19 H), 3.96 (t,  $J = 6.4$  Hz, 4H), 3.93-3.10 (br m, 48 H), 2.97 (s, 4H), 2.42-1.93 (br m, 8 H), 1.90-1.31 (br m, 24 H). The dimesylated dimer (2.24 g, 1.02 mmol, 1 eq) was added to a flame-dried flask equipped with a stir bar and under a positive argon atmosphere, and dry DMF (50 ml, 0.02 M) was added. Sodium azide (0.80 g, 12.24 mmol, 12 eq) was added in one portion, and the reaction mixture was heated to 50 °C for 12 h. The solution was poured into a separatory funnel and diluted with ethyl acetate (100 ml) and water (50 ml). The aqueous layer was extracted with fresh ethyl acetate (4 x 25 ml), and the combined organic layer was washed with fresh water (50 ml). The organic layer was poured through filter paper and evaporated to dryness. The resulting foam was sonicated with ethyl acetate (2 x 5 ml) to give **22**- $\text{H}_2\cdot 2\text{PF}_6$  (1.67 g, 63%) as a pale-tan foam that was used without further purification.  $^1\text{H}$  NMR (500 MHz,  $\text{CDCl}_3$ ):  $\delta$  8.10 (br s, 2H), 7.65 (br s, 2H), 7.42-7.30

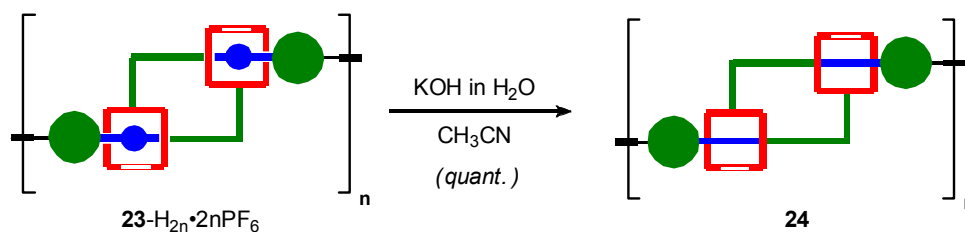


(m, 4H), 7.20-7.05 (m, 8H), 7.04 (d,  $J = 7.8$  Hz, 1H), 6.95-6.70 (m, 11H), 6.28 (m, 1H), 6.15 (m, 1H), 5.61-5.29 (m, 4H), 4.82-3.18 (br m, 72H), 2.41-1.90 (br m, 8H), 1.90-1.35 (m, 24H).  $^{13}\text{C}$  NMR (126 MHz,  $\text{CDCl}_3$ )  $\delta$  158.54, 158.48, 154.06, 154.01, 145.86, 145.70, 145.31, 145.18, 141.53, 137.94, 131.62, 131.13, 130.61, 129.98, 128.24, 127.86, 127.13, 126.23, 119.28, 118.75, 114.97, 111.89, 111.75, 109.89, 109.57, 105.94, 105.30, 77.48, 77.23, 76.98, 73.57, 73.47, 71.83, 71.36, 71.22, 71.16, 71.04, 70.36, 70.04, 69.88, 69.80, 69.40, 69.30, 68.67, 68.25, 67.93, 67.90, 67.57, 67.47, 62.89, 56.44, 56.40, 52.31, 52.27, 51.51, 32.79, 30.62, 30.54, 30.11, 30.05, 29.18, 29.14, 28.90, 28.39, 28.34, 28.15, 28.01, 26.59, 25.71, 25.62, 25.52, 24.96, 24.91. FTIR ( $\text{NaCl}$ ,  $\text{cm}^{-1}$ ): 3956.56, 3659.54, 3592.45, 3141.56, 3008.82, 2936.76, 2623.29, 2530.03, 2360.09, 2343.93, 2096.21, 1952.38, 1593.87, 1505.34, 1455.83, 1393.37, 1372.65, 1353.86, 1335.16, 1249.54, 1195.47, 1181.54, 1162.53, 1125.38, 1048.91, 973.99, 898.13, 838.37, 779.95, 763.92, 734.50, 701.42, 672.28, 644.56, 632.82, 619.78, 588.90, 557.67, 528.21. ESI-TOF MS ( $m/z$ ):  $[\text{M} + 2\text{H} - 2\text{PF}_6]^{+2}$  calcd for  $\text{C}_{51}\text{H}_{69}\text{N}_4\text{O}_{10}$ , 897.5013; found 897.5054. GPC (DMF with 0.2 M LiBr):  $M_n = 3123$  g/mol;  $M_w = 3868$  g/mol; PDI = 1.24;  $dn/dc = 0.121$  ;  $R_{gz} = n/a$ .



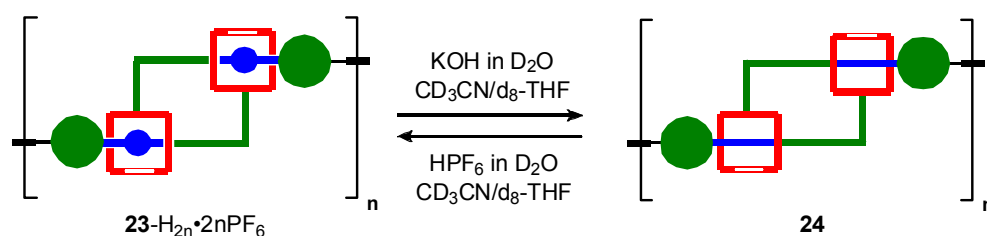
**[c2]Daisy-Chain Dimer Polymer ( $23\text{-H}_{2n}\cdot 2n\text{PF}_6$ ).** To a flame-dried vial equipped with a stir bar and septum cap was added  $22\text{-H}_2\cdot 2\text{PF}_6$  (75.0 mg, 35.9  $\mu\text{mol}$ , 1 eq), 1,4-diethynylbenzene (4.5 mg, 35.9  $\mu\text{mol}$ , 1 eq), *N,N,N',N'',N''*-pentamethyldiethylenetriamine (37.5  $\mu\text{l}$ , 179.8  $\mu\text{mol}$ , 5 eq), and dry DMF (360  $\mu\text{l}$ , 0.1M). This mixture was subjected to standard freeze-pump-thaw protocol, with addition of copper(I) bromide (26.4 mg, 179.8  $\mu\text{mol}$ , 5 eq) after the third freeze. After the fourth freeze-pump-thaw cycle was completed, the vial was placed in a 50  $^\circ\text{C}$  oil bath for 24 h. The viscous reaction mixture was cooled to room temperature, and added dropwise to a stirring solution of methanol (40 ml). The precipitate was collected, dried, redissolved in dichloromethane (0.5 ml), and subjected to a second precipitation in fresh methanol (40 ml). The solid was collected and dried under reduced pressure to afford  $23\text{-H}_{2n}\cdot 2n\text{PF}_6$  (60.4 mg, 76% yield) as an off-white powder. The product was used with no further purification.  $^1\text{H}$  NMR (500 MHz,  $\text{CDCl}_3$ ):  $\delta$  8.10 (br m, 4H), 7.91 (s, 4H), 7.82 (d,  $J$  = 7.7 Hz, 0.6 H), 7.70 (br s, 2H), 7.55 (d,  $J$  = 8.1 Hz, 0.6 H), 7.48-7.35 (m, 5H), 7.28-7.02 (m, 11H), 7.01-6.75 (m, 13H), 6.45-6.15 (m, 2H), 5.71-5.35 (m, 4H), 4.85-3.08 (br m, 88H), 2.50-1.80 (br m, 10H), 1.80-1.35 (m, 28H + HDO).  $^1\text{H}$  NMR (500 MHz,  $\text{CD}_2\text{Cl}_2$ ):  $\delta$  8.12 (br m, 2H), 7.89 (s, 3H), 7.80 (d,  $J$  = 8.1 Hz, 0.5 H), 7.68 (br s, 2H), 7.53 (d,  $J$  = 7.3 Hz, 0.6 H), 7.48-7.30 (m, 4H), 7.28-7.08 (m, 9H), 7.05-6.60 (m, 11H), 6.40-6.10 (m,

2H), 5.71-5.35 (m, 4H), 4.90-3.08 (br m, 72H), 2.50-1.80 (br m, 12H), 1.80-1.35 (m, 22H + HDO). FTIR (NaCl,  $\text{cm}^{-1}$ ): 3645.89, 3436.49, 3275.37, 3140.73, 3047.82, 3007.96, 2935.65, 2867.49, 2626.16, 2362.05, 2103.24, 1949.57, 1593.01, 1513.78, 1501.17, 1463.53, 1432.12, 1389.82, 1371.32, 1353.86, 1333.98, 1291.59, 1248.54, 1195.05, 1181.27, 1163.07, 1128.14, 1100.30, 1048.58, 973.32, 899.38, 842.74, 780.23, 763.80, 734.32, 700.48, 672.09, 644.03, 632.82, 619.48, 588.59, 557.58, 528.37. GPC (0.2 M LiBr in DMF):  $M_n = 47,940$  g/mol;  $M_w = 141,100$  g/mol; PDI = 2.94;  $dn/dc = 0.116$ ;  $R_{gz} = 14.8$  nm.



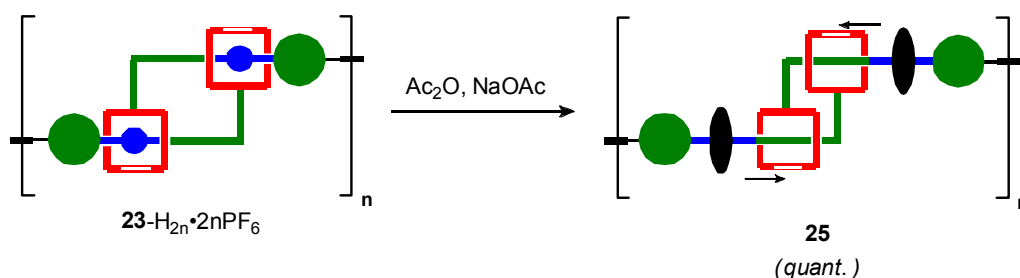
**Deprotonation of [c2]Daisy-Chain Dimer Polymer  $\mathbf{23-H_{2n} \cdot 2nPF_6}$  (**24**).** A vial was charged with  $\mathbf{23-H_{2n} \cdot 2nPF_6}$  (10 mg, 9  $\mu\text{mol}$ , 1 eq) and acetonitrile (2 ml). To this mixture was added a 1.0 M solution of aqueous potassium hydroxide (1.8 ml), resulting in immediate precipitation of an off-white solid. The solution was decanted, and the solid was washed with fresh acetonitrile (2 x 2 ml). The deprotonated polymer **24** (9 mg, quant. yield) was analyzed with no further purification. The  $\text{CD}_2\text{Cl}_2$  used in the NMR study was passed through a plug of basic alumina prior to addition to the deprotonated polymer sample.  $^1\text{H}$  NMR (500 MHz,  $\text{CD}_2\text{Cl}_2$ ):  $\delta$  7.92-7.82 (m, 3.8H), 7.80 (d,  $J = 7.7$

Hz, 0.4H), 7.53 (d,  $J = 7.9$  Hz, 0.4H), 7.48-6.20 (m, 26H), 5.65-5.35 (m, 4H), 4.86-3.05 (br m, 72H), 2.55-1.55 (br m, 32H + H<sub>2</sub>O signal). GPC (0.2 M LiBr in DMF):  $M_n = 41,680$  g/mol;  $M_w = 125,800$  g/mol; PDI = 3.02;  $dn/dc = 0.148$ ;  $R_{gz} = 13.5$  nm.



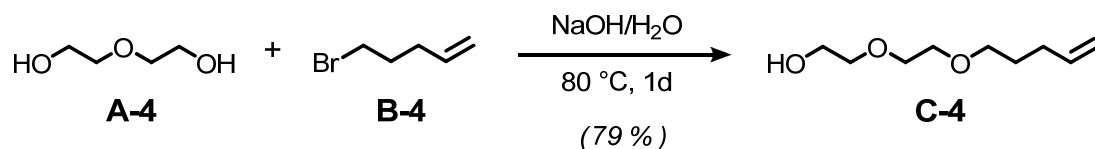
**5x Switching of Polymer 23-H<sub>2n</sub>·2nPF<sub>6</sub>.** A vial was charged with **23-H<sub>2n</sub>·2nPF<sub>6</sub>** (11.6 mg, 5.3  $\mu$ mol, 1 eq), and the polymer was dissolved in CD<sub>3</sub>CN (0.4 ml) and loaded in an NMR tube. To the tube was added d<sub>8</sub>-THF (0.4 ml), and the mixture was shaken vigorously for several seconds. The switching was performed via addition of a stock solution of KOH in D<sub>2</sub>O (Stock Solution: 180 mg KOH in 0.5 ml D<sub>2</sub>O; 5  $\mu$ l injection volume, 6 eq) followed by vigorous shaking for 15 seconds to give **24**, and, after analysis, subsequent reprotonation via addition of a stock solution of HPF<sub>6</sub> in D<sub>2</sub>O (450  $\mu$ l 65% HPF<sub>6</sub> in 0.5 ml D<sub>2</sub>O; 5  $\mu$ l injection volume, 6 eq) to regenerate **23-H<sub>2n</sub>·2nPF<sub>6</sub>**. See **21** for syringe specifications. After five cycles of deprotonation and reprotonation were completed, the polymer solution was transferred to a vial and the solvent was removed under reduced pressure. The residue was washed with water (2 x 2 ml) and dried under high vacuum, returning **23-H<sub>2n</sub>·2nPF<sub>6</sub>** as a white solid (11.6 mg, quant. yield). Protonated Polymer: <sup>1</sup>H NMR (500 MHz, 1:1 CD<sub>3</sub>CN/d<sub>8</sub>-THF):  $\delta$  8.25-8.02 (m, 2.8 H),

7.92 (m, 2.6H), 7.85 (d,  $J = 8.0$  Hz, 0.4H), 7.75 (br s, 2H), 7.53 (d,  $J = 8.1$  Hz, 0.4H), 7.48-7.35 (m, 4H), 7.32-7.13 (m, 8H), 7.12-6.75 (12H), 6.47-6.18 (m, 2H), 5.75-5.35 (m, 4H), 4.86-3.15 (br m, 72H +  $d_8$ -THF), 2.55-1.70 (m, 18H +  $CD_3CN$  +  $d_8$ -THF signal), 1.70-1.32 (m, 14H).



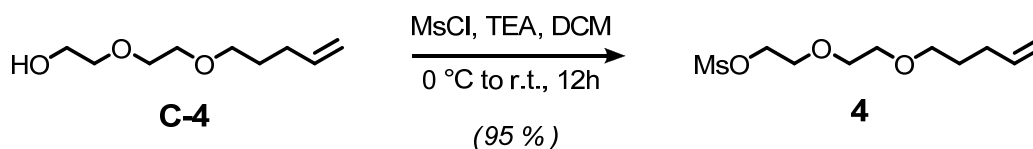
**Acylated [c2]Daisy-Chain Dimer Polymer (25).** To a vial equipped with a stir bar was added **23**-H<sub>2n</sub>·2nPF<sub>6</sub> (10.0 mg, 208 nmol, 1 eq), sodium acetate (18.5 mg, 225 μmol, 25 eq per ammonium), and acetic anhydride (500 μl). This solution was placed under a positive pressure of argon and heated to 90 °C for 2 hours. The acetic anhydride was removed under reduced pressure, and the resulting residue washed with water (3 x 2 ml) to give the acylated derivative **25** (9.1 mg, quant. yield) as an off-white powder. The product was used with no further purification. <sup>1</sup>H NMR (500 MHz, CD<sub>2</sub>Cl<sub>2</sub>):  $\delta$  7.82-7.68 (m, 5H), 7.67-7.48 (m, 8H), 7.48-6.67 (br m, 15H), 6.45-6.15 (m, 6H), 5.50-4.98 (m, 4H), 4.60-4.15 (m, 16H), 4.09-3.05 (br m, 62H), 2.50-1.55 (br m, 30H), 1.50-1.28 (m, 10H). GPC (0.2 M LiBr in DMF):  $M_n = 26,870$  g/mol;  $M_w = 117,200$  g/mol; PDI = 4.36; dn/dc = 0.133;  $R_{gz} = 21.8$  nm.

Note on GPC Analysis: All polymer GPC LS analyses were fitted using the Zimm Model. Though all polymers displayed limited solubility in the 0.2 M LiBr DMF eluent, efforts to use an alternate eluent without salt (DMF or THF) generated chromatographs unsuitable for analysis due to severe polymer aggregation on the SEC columns.



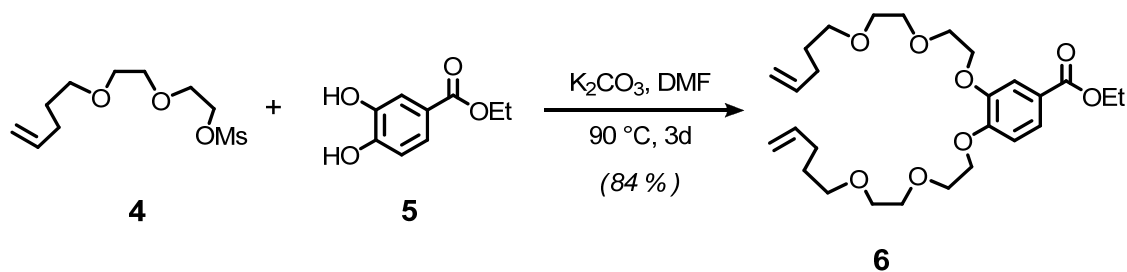
**2-(2-(Pent-4-enyloxy)ethoxy)ethanol (C-4).** A flask equipped with a stir bar was charged with diethylene glycol (**A-4**) (637 ml, 6.71 moles, 20 eq) and 5-bromo-1-pentene (**B-4**) (50 g, 0.37 moles, 1 eq). A solution of sodium hydroxide and water (67.1 g NaOH, 1.68 moles, 5eq; 67 ml of H<sub>2</sub>O) was added slowly over a period of one hour via an addition funnel, resulting in turbidity of the reaction mixture. The reaction was heated to 80 °C for one day, and after cooling to room temperature, the mixture was poured into a separatory funnel, diluted with methylene chloride (500 ml), water (500 ml), and brine (500 ml). The aqueous layer was extracted four times with fresh methylene chloride (4 x 250 ml), and the combined organic layers were washed two times with fresh water and brine (2 x 500 ml), dried over magnesium sulfate, filtered, and evaporated to dryness under reduced pressure. The resulting residue was purified by flash chromatography, (SiO<sub>2</sub>: gradient from 3:1 hexanes to ethyl acetate to 1:1 hexanes to ethyl acetate) to afford

pure **C-4** (46.8 g, 80% yield) as a clear oil.  $^1\text{H}$  NMR (600 MHz,  $\text{CDCl}_3$ ):  $\delta$  = 5.81 (m, center, 1 H), 5.05-4.94 (m, 2 H), 3.75-3.72 (m, 2 H), 3.69-3.66 (m, 2 H), 3.64-3.61 (m, 2 H), 3.61-3.58 (m, 2 H), 3.48 (t,  $J$  = 6.7, 2 H), 2.42 (t,  $J$  = 6.1 Hz, 1H), 2.14-2.09 (m, 2 H), 1.70 (qt,  $J$  = 7.1, 2 H);  $^{13}\text{C}$  NMR (125 MHz,  $\text{CDCl}_3$ ):  $\delta$  = 138.37, 115.02, 72.70, 70.99, 70.73, 70.43, 62.10, 30.41, 28.95. HRMS-EI ( $m/z$ ):  $[\text{M} + \text{H}]$  calcd for  $\text{C}_9\text{H}_{18}\text{O}_3$ , 174.1256; found 174.1262.



**2-(2-(Pent-4-enyloxy)ethoxy)ethyl methanesulfonate (4).** A cooled, flame-dried flask equipped with a stir bar and septum was charged with **C-4** (46.3 g, 0.266 moles, 1 eq) and dry DCM (300 ml, 0.9 M), then cooled to 0 °C. To the cooled reaction mixture was slowly added methanesulfonyl chloride (31 ml, 0.399 moles, 1.5 eq) and triethylamine (55.5 ml, 0.399 moles, 1.5 eq) alternately in several batches. The reaction was allowed to warm to room temperature and stirred overnight. Stirring was stopped and the reaction mixture poured into a separatory funnel and partitioned with water and brine (1 L). The aqueous layer was extracted three times with fresh DCM (3 x 300 ml), and the combined organic layers were washed three times with fresh water and brine (3 x 300 ml), dried over magnesium sulfate, filtered, and evaporated to dryness under reduced pressure. The resulting crude oil was purified by flash chromatography (plug of  $\text{SiO}_2$ : 3:2 hexanes to

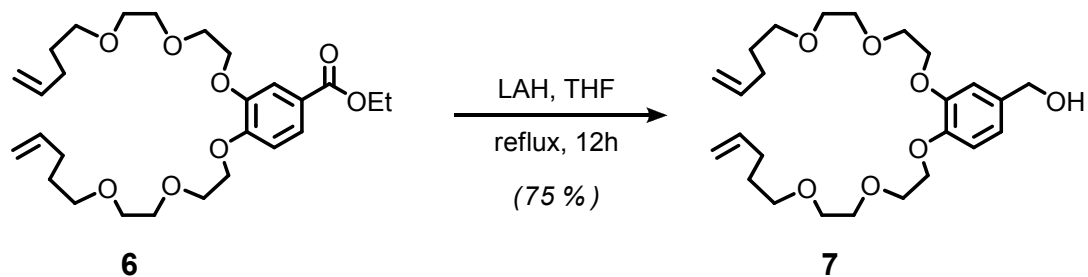
ethyl acetate) to give **4** (64.2 g, 96% yield) as a clear oil.  $^1\text{H}$  NMR (500 MHz,  $\text{CDCl}_3$ ):  $\delta$  = 5.80 ppm (m, 1 H), 5.04-4.94 (br m, 2 H), 4.39-4.37 (m, 2 H), 3.78-3.75 (m, 2 H), 3.67-3.64 (m, 2 H), 3.59-3.56 (m, 2 H), 3.45 (t,  $J$  = 6.6 Hz, 2 H), 3.06 (s, 1 H), 2.17-2.07 (m, 2 H), 1.67, (qt,  $J$  = 7.1 Hz, 2 H);  $^{13}\text{C}$  NMR (126 MHz,  $\text{CDCl}_3$ ):  $\delta$  = 138.34, 115.01, 70.93, 70.92, 70.25, 69.48, 69.25, 37.92, 30.40, 28.97. HRMS-EI ( $m/z$ ):  $[\text{M} + \text{H}]$  calcd for  $\text{C}_{10}\text{H}_{21}\text{O}_5\text{S}$ , 253.1110; found 253.1119.



**Ethyl Ester Crown-Type Recognition Fragment (6).** Standard alkylation conditions were used with protocatechuic acid ethyl ester **5** (12.6345 g, 69.35 mmol, 1 eq), **4** (35.0000 g, 0.139 moles, 2 eq),  $\text{K}_2\text{CO}_3$  (57.5217 g, 0.416 moles, 6 eq), and dry DMF (1 L, 0.07 M). After 3 days, the reaction was extracted and purified via flash chromatography ( $\text{SiO}_2$ : 4:1 hexanes to acetone), giving **6** (28.8 g, 84% yield) as a clear oil.  $^1\text{H}$  NMR (300 MHz,  $\text{CDCl}_3$ ):  $\delta$  7.60 (m, 1H), 7.53 (m, 1H), 6.86 (m, 1H), 5.75 (m, 2H), 5.05-4.84 (m, 4H), 4.28 (m, 2H), 4.16 (m, 4H), 3.84 (m, 4H), 3.68 (m, 4H), 3.54 (m, 4H), 3.41 (m, 4H), 2.13-1.98 (m, 4H), 1.62 (m, 4H), 1.31 (m, 3H).  $^{13}\text{C}$  NMR (75 MHz,  $\text{CDCl}_3$ ):  $\delta$  166.36, 152.90, 148.28, 138.32, 138.30, 123.98, 123.39, 115.00, 114.81, 114.79, 112.69, 71.04, 70.97, 70.82, 70.28, 70.27, 69.71, 69.61, 68.91, 68.68, 60.84,

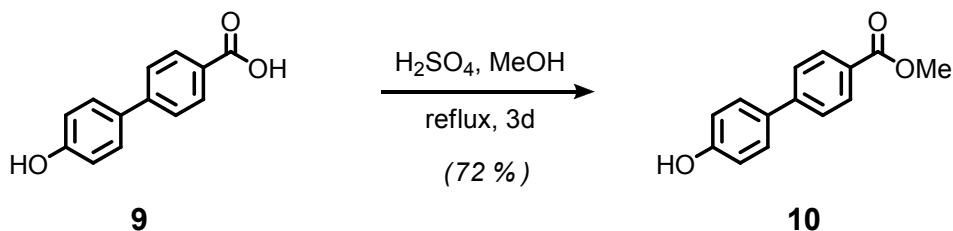


30.31, 28.85, 14.49. HRMS-TOF MS ( $m/z$ ):  $[M + Na]$  calcd for  $C_{27}H_{42}O_8Na$ , 517.2777; found 517.2796.



**Benzyl Alcohol Crown-Type Recognition Fragment (7).** Standard LAH reduction conditions were used with **6** (28.6 g, 63.24 mmol, 1 eq), LAH (7.1998 g, 0.190 moles, 3 eq), and dry THF (~630 ml, 0.1 M). The reaction was refluxed overnight, quenched, filtered, and extracted to give **7** (21.9 g, 75% yield) as a clear oil. The product was used with no further purification.  $^1H$  NMR (300 MHz,  $CDCl_3$ ):  $\delta$  6.94 (s, 1H), 6.87-6.79 (m, 2H), 5.79 (m, 2H), 5.04-4.85 (m 4H), 4.55 (s, 2H), 4.14 (m, 4H), 3.83 (t,  $J = 5.09$  Hz, 4H), 3.60 (m, 4H), 3.57 (m, 4H), 3.45 (t,  $J = 6.60$  Hz, 4H), 2.14 (s, 1H), 2.08 (q,  $J = 6.60$  Hz, 4H), 1.66 (qt,  $J = 6.60$  Hz, 4H).  $^{13}C$  NMR (75 MHz,  $CDCl_3$ ):  $\delta$  149.02, 148.33, 138.33, 134.74, 120.12, 114.83, 114.73, 113.75, 70.91, 70.85, 70.83, 70.25, 69.86, 69.83, 69.06, 68.84, 64.96, 30.31, 28.83. HRMS-TOF MS ( $m/z$ ):  $[M + Na]$  calcd for  $C_{25}H_{40}O_7Na$ , 475.2672; found 475.2649.



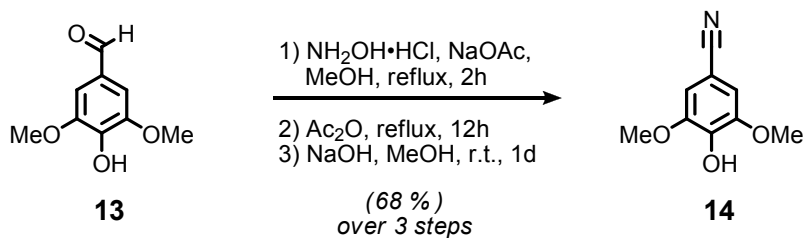


**Methyl Ester Backbone Fragment (10).** A flask equipped with a stir bar was charged with 4'-hydroxy-4-biphenylcarboxylic acid (**9**) (9.1003 g, 42.48 mmol, 1 eq) and methanol (40 ml, 1 M). The solution was cooled to 0 °C, and concentrated sulfuric acid (6 ml, 33.2 mmol, 0.8 eq) was added dropwise. The flask was fitted with a reflux condenser, and the reaction heated to reflux for 5 hours. After cooling to 0 °C in an ice bath, a 10% sodium hydroxide solution (150 ml) was added slowly to the reaction. The reaction mixture was poured into a separatory funnel, and diluted with ethyl acetate (250 ml) and water and brine (500 ml). The aqueous layer was extracted four times with ethyl acetate (4 x 100 ml), and the organic layers were combined, dried over magnesium sulfate, filtered, and evaporated to dryness under reduced pressure. Recrystallization from a minimum of hot ethyl acetate afforded **10** (7.0104 g, 72%) as a white crystalline solid. <sup>1</sup>H NMR (300 MHz, Acetone-d<sub>6</sub>): δ 8.64 (s, 1H), 8.04 (d, J = 8.53 Hz, 2H), 7.73 (d, J = 8.80 Hz, 2H), 7.61 (d, J = 8.80 Hz, 2H), 6.97 (d, J = 8.80 Hz, 2H), 3.89 (s, 3H). <sup>13</sup>C NMR (126 MHz, Acetone-d<sub>6</sub>): δ 167.22, 158.93, 146.31, 131.81, 130.83, 129.28, 129.08, 127.10, 116.84, 52.32. HRMS-FAB (m/z): [M + H] calcd for C<sub>14</sub>H<sub>12</sub>O<sub>3</sub>, 228.0786; found 228.0796.

**Methyl Ester Recognition-Backbone Fragment (11).** Standard alkylation conditions were used with **8** (14.4292 g, 31.91 mmol, 1.05 eq), **10** (6.7775 g, 29.69 mmol, 1 eq), K<sub>2</sub>CO<sub>3</sub> (12.3121 g, 89.07 mmol), and dry DMF (500 ml). The reaction was heated for 3 days, then extracted with ethyl acetate. The residue was purified via flash chromatography (SiO<sub>2</sub>: gradient from 12:1 to 8:1 to 6:1 to 4:1 to 2:1 hexane to acetone) as eluent to give **11** (16.1 g, 82% yield) as a white crystalline solid. <sup>1</sup>H NMR (300 MHz, CDCl<sub>3</sub>): δ 8.05 (d, J = 8.25 Hz, 2H), 7.60 (d, J = 8.25 Hz, 2H), 7.55 (d, J = 8.81 Hz, 2H), 7.03 (d, J = 8.80 Hz, 2H), 7.01-6.85 (m, 3H), 5.78 (m, 2H), 5.05-4.88 (m, 6H), 4.16 (m, 4H), 3.91 (s, 3H), 3.85 (t, J = 5.09 Hz, 4H), 3.70 (m, 4H), 3.58 (m, 4H), 3.45 (m, 4H), 2.08 (m, 4H), 1.66 (m, 4H). <sup>13</sup>C NMR (75 MHz, CDCl<sub>3</sub>): δ 167.22, 159.16, 149.24, 149.00, 145.32, 138.43, 132.73, 130.26, 130.11, 128.52, 128.38, 126.63, 121.09, 115.46, 114.89, 114.77, 114.42, 71.04, 70.93, 70.36, 70.17, 69.90, 69.11, 69.07, 52.26, 30.41, 28.94. HRMS-TOF MS (m/z): [M + Na] calcd for C<sub>39</sub>H<sub>50</sub>O<sub>9</sub>Na, 685.3353; found 685.3358.

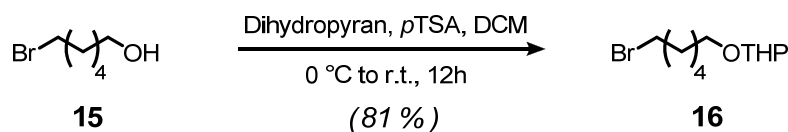
**Aldehyde Recognition-Backbone Fragment (3).** A cooled, flame-dried two-neck flask equipped with a stir bar, water condenser, gas port, and septum was charged, under argon at 0 °C, with RedAl (9.84 ml, 32.79 mmol, 1 eq) and dry toluene (16.4 ml). To this stirring mixture was added, slowly, N-methylpiperazine (4.01 ml, 36.07 mmol, 1.2), and the reaction allowed to stir for 30 minutes at 0 °C. A separate cooled, flame-dried two-neck flask equipped with a stir bar, water condenser, gas port, and septum was charged, under argon at 0 °C, with **11** (16.1 g, 24.29 mmol) and dry toluene (25 ml). After the 30 minute incubation time, the RedAl solution was added dropwise to the stirring solution of **11** in toluene. The reaction was allowed to stir for 8 hours at 0 °C, then quenched by addition of water (20 ml). The reaction was poured into a separatory funnel, and partitioned between ethyl acetate (100 ml) and water (200 ml) and brine (200 ml). The aqueous layer was extracted two times with DCM (2 x 100 ml), and the ethyl acetate and DCM layers were combined and washed with fresh water and brine (2 x 200 ml), dried with magnesium sulfate, filtered, and the solvent removed under reduced pressure. Flash chromatography (SiO<sub>2</sub>: 4:1 hexane to acetone) gave **3** (12.1 g, 79% yield) as a white crystalline solid. <sup>1</sup>H NMR (300 MHz, CDCl<sub>3</sub>): δ 9.93 (s, 1H), 7.82 (d, J = 8.25 Hz, 2H), 7.61 (d, J = 8.26 Hz, 2H), 7.49 (d, J = 8.80 Hz, 2H), 6.98 (d, J = 8.57 Hz, 2H), 6.95-6.79 (m, 3H), 5.73 (m, 2H), 5.05-4.88 (m, 6H), 4.12 (q, J = 5.04 Hz, 4H), 3.81 (t, J = 4.95 Hz,

4H), 3.67 (t,  $J = 4.68$ , 4H), 3.53 (t,  $J = 4.68$  Hz, 4H), 3.40 (m, 4H), 2.12-1.98 (m, 4H), 1.62 (m, 4H).  $^{13}\text{C}$  NMR (75 MHz,  $\text{CDCl}_3$ ):  $\delta$  192.04, 159.42, 149.27, 149.05, 146.87, 138.41, 134.81, 132.37, 130.46, 130.01, 128.64, 127.20, 121.09, 115.55, 114.88, 114.81, 114.47, 71.03, 70.91, 70.35, 70.17, 69.89, 69.13, 69.10, 30.39, 28.93. HRMS-FAB ( $m/z$ ):  $[\text{M} + \text{H} - \text{H}_2]$  calcd for  $\text{C}_{38}\text{H}_{47}\text{O}_8$ , 631.3271; found 631.325



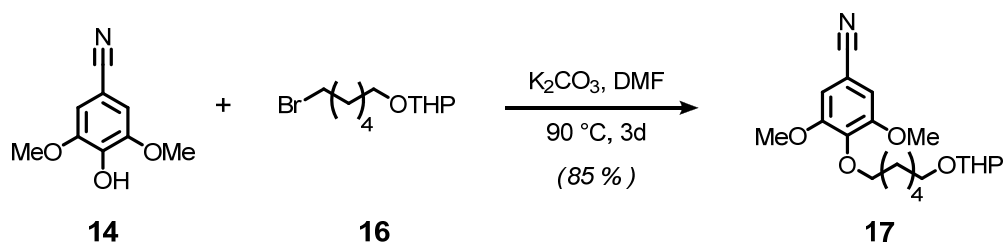
**Nitrile Cap Fragment (14).** To a flask fitted with a reflux condenser was added syringaldehyde (**13**) (5.0000 g, 27.44 mmol, 1 eq) and methanol. Sodium acetate (3.3999 g, 42.43 mmol, 1.51 eq) was added to the stirring solution, followed by hydroxylamine hydrochloride (2.8610 g, 41.16 mmol, 1.5 eq). The solution was heated to reflux for 2 h, then cooled to room temperature. The methanol was removed under reduced pressure, and the residue redissolved in ethyl acetate (100 ml) and added to a separatory funnel. Brine (50 ml) and an aqueous solution of citric acid (23.1 g, 109.8 mmol, 4 eq in 220 ml water, 0.5 M) were added, and the aqueous layer was extracted twice more with fresh ethyl acetate (2 x 50 ml). The combined organic layer was washed with brine (2 x 50 ml), dried over magnesium sulfate, filtered, and evaporated to dryness under reduced pressure to give a yellow solid (5.1273 g, 95%). The oxime was dissolved in acetic

anhydride (25 ml, 250 mmol, 10 eq) and heated to reflux for 1d. The acetic anhydride was removed under high vacuum, and the resulting black residue dissolved in ethyl acetate and mixed in a separatory funnel with saturated sodium bicarbonate and water. The aqueous layer was extracted with fresh ethyl acetate (2 x 100 ml), and the combined organic layers were dried over magnesium sulfate, filtered, and evaporated to dryness, giving a brown oil. Methanol (80 ml, 0.4 M) was added to the oil, followed by a 50 weight percent solution of sodium hydroxide (10.33 g, 250 mmol). After stirring overnight, the methanol was removed by rotary evaporation and the aqueous layer acidified with 2 M hydrochloric acid. Ethyl acetate was mixed with the aqueous layer, and the solution extracted with fresh ethyl acetate (3 x 50 ml). The combined organic layers were washed with water (2 x 100 ml), dried over magnesium sulfate, and evaporated under reduced pressure to give a thick oil that solidified upon standing. Purification was achieved by flash chromatography (SiO<sub>2</sub>: gradient from 6:1 to 4:1 to 2:1 hexanes to acetone) to give **14** as an off-white crystalline solid (3.1574 g, 68%). <sup>1</sup>H NMR (600 MHz, Acetone-d<sub>6</sub>):  $\delta$  8.20 (br s, 1H), 6.97 (s, 2H), 3.85 (s, 6H). <sup>13</sup>C NMR (75 MHz, Acetone-d<sub>6</sub>):  $\delta$  148.95, 141.51, 120.15, 110.41, 102.06, 56.91. HRMS-EI (m/z): [M + H] calcd for C<sub>9</sub>H<sub>10</sub>NO<sub>3</sub>, 180.0661; found 180.0643.

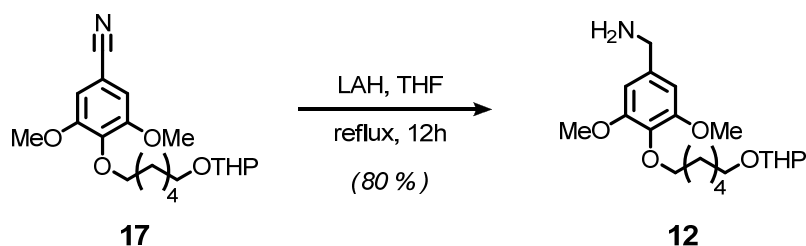


**2-(6-Bromohexyloxy)tetrahydro-2H-pyran (16).** A cooled, flame-dried round bottom flask equipped with a stir bar and septum was charged, under argon and at 0 °C, with 6-bromo-1-hexanol (**15**) (7.6551 g, 42.28 mmol, 1 eq), dry DCM (10 ml), dihydropyran (4.25ml, 46.51 mmol, 1.1 eq), and *p*-toluenesulfonic acid (0.4030 g, 2.12 mmol, 5 mol %). The reaction was allowed to stir at room temperature overnight, and was quenched by diluting with water (50 ml) and DCM (50 ml) in a separatory funnel. The organic layer was washed three times with brine (3 x 50 ml), dried (MgSO<sub>4</sub>), filtered, and evaporated to dryness under reduced pressure. Flash chromatography (SiO<sub>2</sub>: 15:1 hexanes to ethyl acetate) gave **16** (9.0902 g, 81% yield) as a clear oil. <sup>1</sup>H NMR (500 MHz, CDCl<sub>3</sub>): δ 4.56 (t, J = 2.75 Hz, 1H), 3.85 (m, 1H), 3.72 (m, 1H), 3.51 (m, 1H), 3.40 (m, 3H), 1.95-1.36 (br m, 14H). <sup>13</sup>C NMR (126 MHz, CDCl<sub>3</sub>): δ 99.05, 67.56, 62.54, 34.02, 32.92, 30.94, 29.73, 28.18, 25.67, 25.65, 19.87. HRMS-FAB (m/z): [M + H] calcd for C<sub>11</sub>H<sub>22</sub>O<sub>2</sub>Br, 265.0803; found 265.0804.



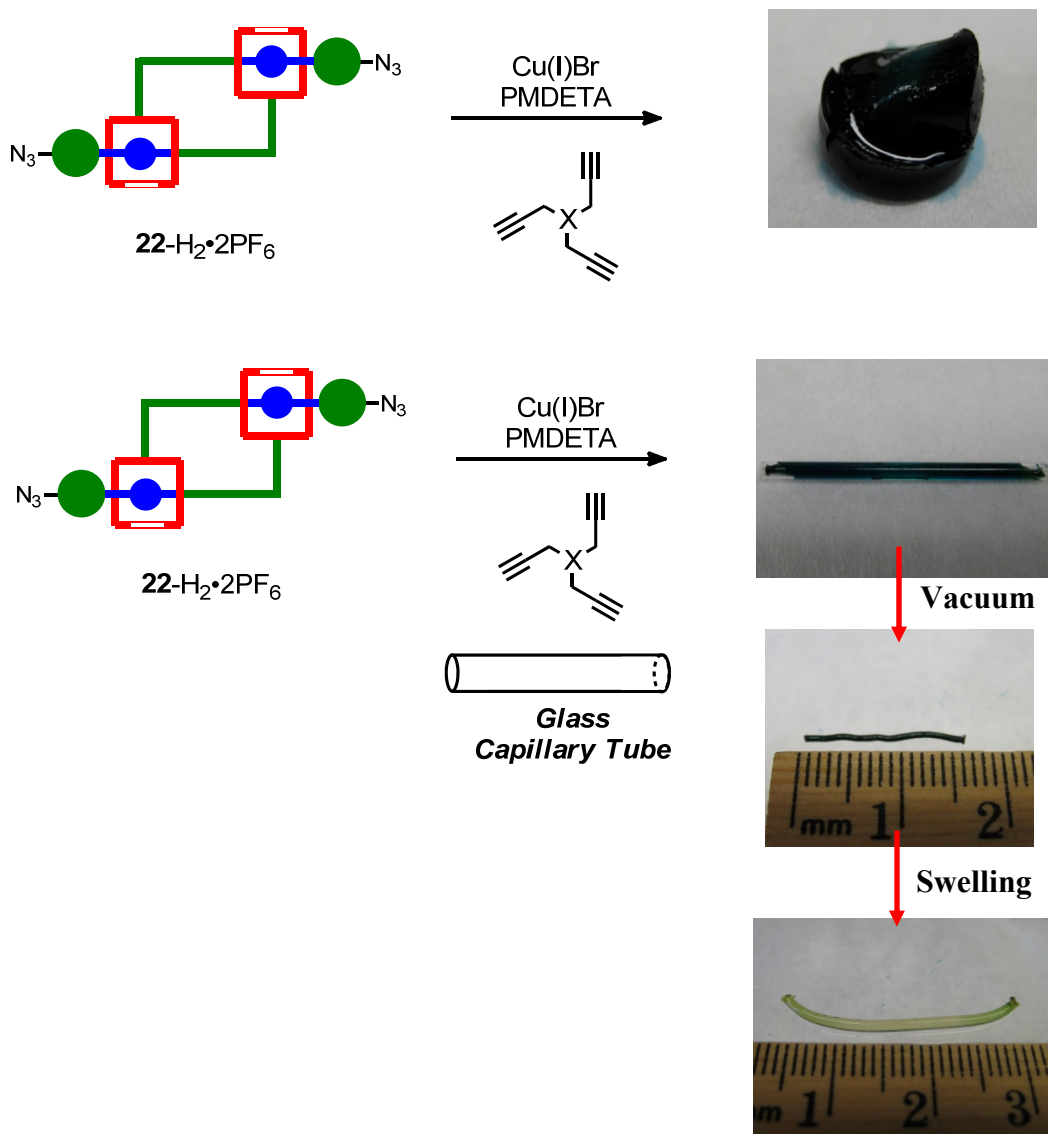


**Alkylated Nitrile Cap Fragment (17).** Standard alkylation conditions were used with **14** (2.8437 g, 15.87 mmol, 1eq), **16** (4.2089 g, 15.87 mmol, 1eq),  $K_2CO_3$  (6.5802 g, 47.61 mmol, 3eq), and dry DMF (150 ml, 0.1M). The reaction was heated for 3 days, followed by extraction with ethyl acetate. Flash chromatography ( $SiO_2$ : 4:1 hexanes to acetone) gave **17** (4.9 g, 85% yield) as a clear oil.  $^1H$  NMR (500 MHz,  $CDCl_3$ ):  $\delta$  6.78 (s, 2H), 4.49 (t,  $J = 2.75$  Hz, 1H), 4.95 (t,  $J = 6.74$  Hz, 2H), 3.80 (m, 1H), 3.78 (s, 6H), 3.65 (m, 1H), 3.41 (m, 1H), 3.31 (m, 1H), 1.91-1.32 (m, 14H).  $^{13}C$  NMR (126 MHz,  $CDCl_3$ ):  $\delta$  153.83, 141.77, 119.06, 109.50, 106.45, 98.90, 73.65, 67.55, 62.39, 56.39, 30.82, 30.03, 29.75, 26.02, 25.64, 25.53, 19.76. HRMS-EI ( $m/z$ ):  $[M + H]^+$  calcd for  $C_{20}H_{29}NO_5$ , 363.2046; found 363.2031.



**Alkylated Amine Cap Fragment (15).** Standard LAH reduction conditions were used with **17** (4.9 g, 13.48 mmol, 1 eq), LAH (1.5349 g, 40.44 mmol, 3 eq), and dry THF (200 ml, 0.07 M). After heating overnight, the reaction was quenched, filtered, and the solvent

removed under reduced pressure to give **12** (3.9635 g, 80% yield) as a clear oil.  $^1\text{H}$  NMR (500 MHz,  $\text{CDCl}_3$ ):  $\delta$  6.52 (s, 2H), 4.55 (t,  $J = 2.75$  Hz, 1H), 3.92 (m, 2H), 3.84 (m, 1H), 3.82 (s, 6H), 3.80 (s, 2H), 3.72 (m, 1H), 3.47 (m, 1H), 3.37 (m, 1H), 1.86-1.26 (m, 14H).  $^{13}\text{C}$  NMR (126 MHz,  $\text{CDCl}_3$ ):  $\delta$  153.58, 138.75, 136.09, 104.11, 98.89, 73.39, 67.66, 62.39, 56.15, 46.79, 30.84, 30.22, 30.08, 29.81, 26.13, 25.80, 25.56, 19.76. HRMS-FAB ( $m/z$ ):  $[\text{M} + \text{H}]$  calcd for  $\text{C}_{20}\text{H}_{34}\text{O}_5\text{N}$ , 368.2437; found 368.2450.



### Macroscopic Gel Synthesis.

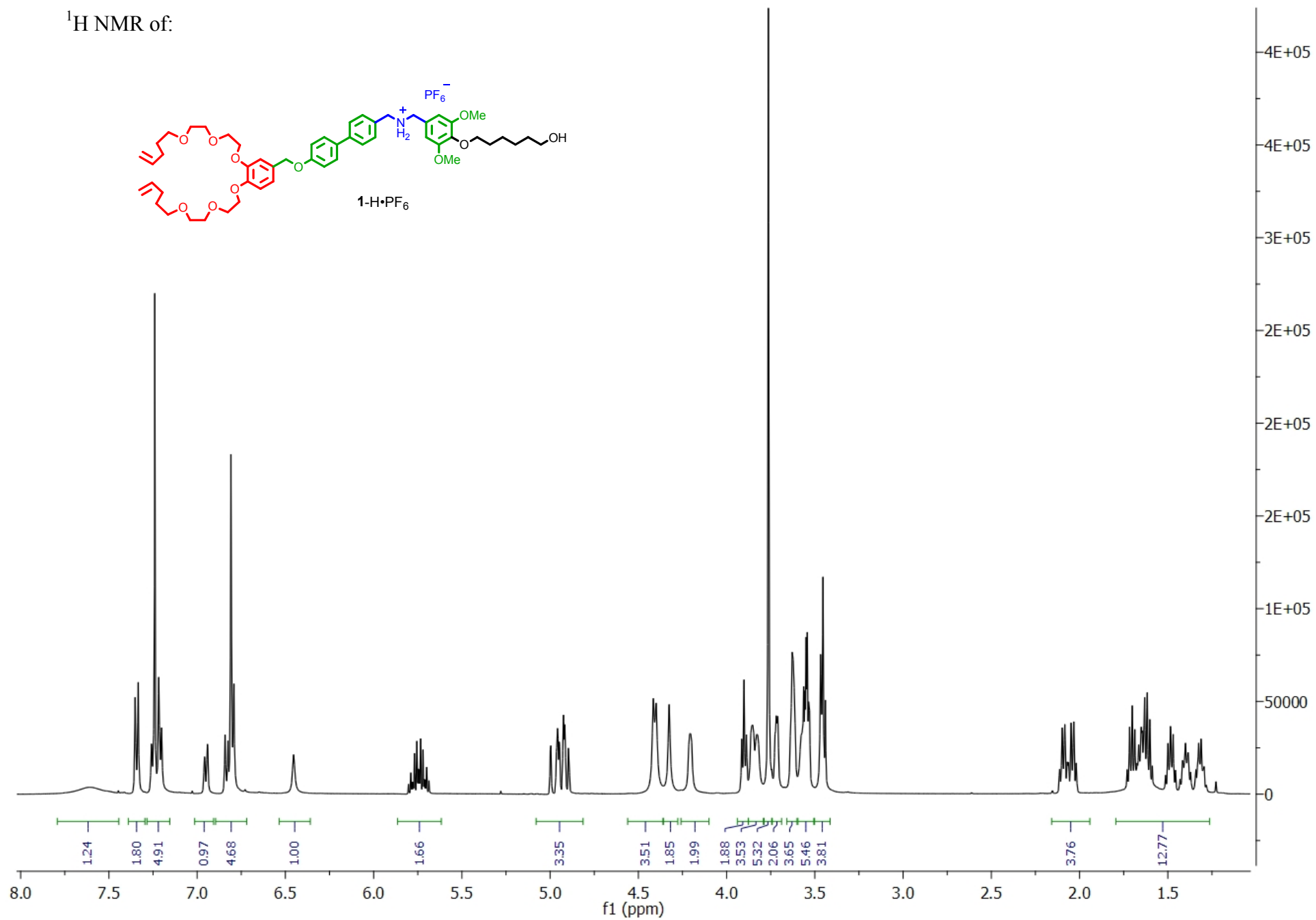
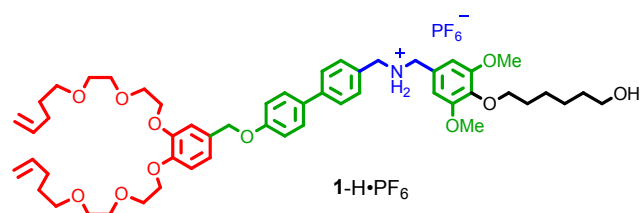
**(A) Amorphous Gel:** To an oven-dried vial equipped with a stir bar was added  $22\text{-H}_2\cdot 2\text{PF}_6$  (70.0 mg, 33.6  $\mu\text{mol}$ , 1 eq), tripropargylamine (3.0  $\mu\text{l}$ , 22.4  $\mu\text{mol}$ , 0.67 eq),  $N,N,N',N'',N'''$ -pentamethyldiethylenetriamine (35.1  $\mu\text{l}$ , 167.9  $\mu\text{mol}$ , 5 eq) and dry DMF (340  $\mu\text{l}$ , 0.1 M). This mixture was subjected to standard freeze-pump-thaw protocol, with addition of copper(I) bromide (48.2 mg, 33.6  $\mu\text{mol}$ , 1 eq) after the third freeze. After the

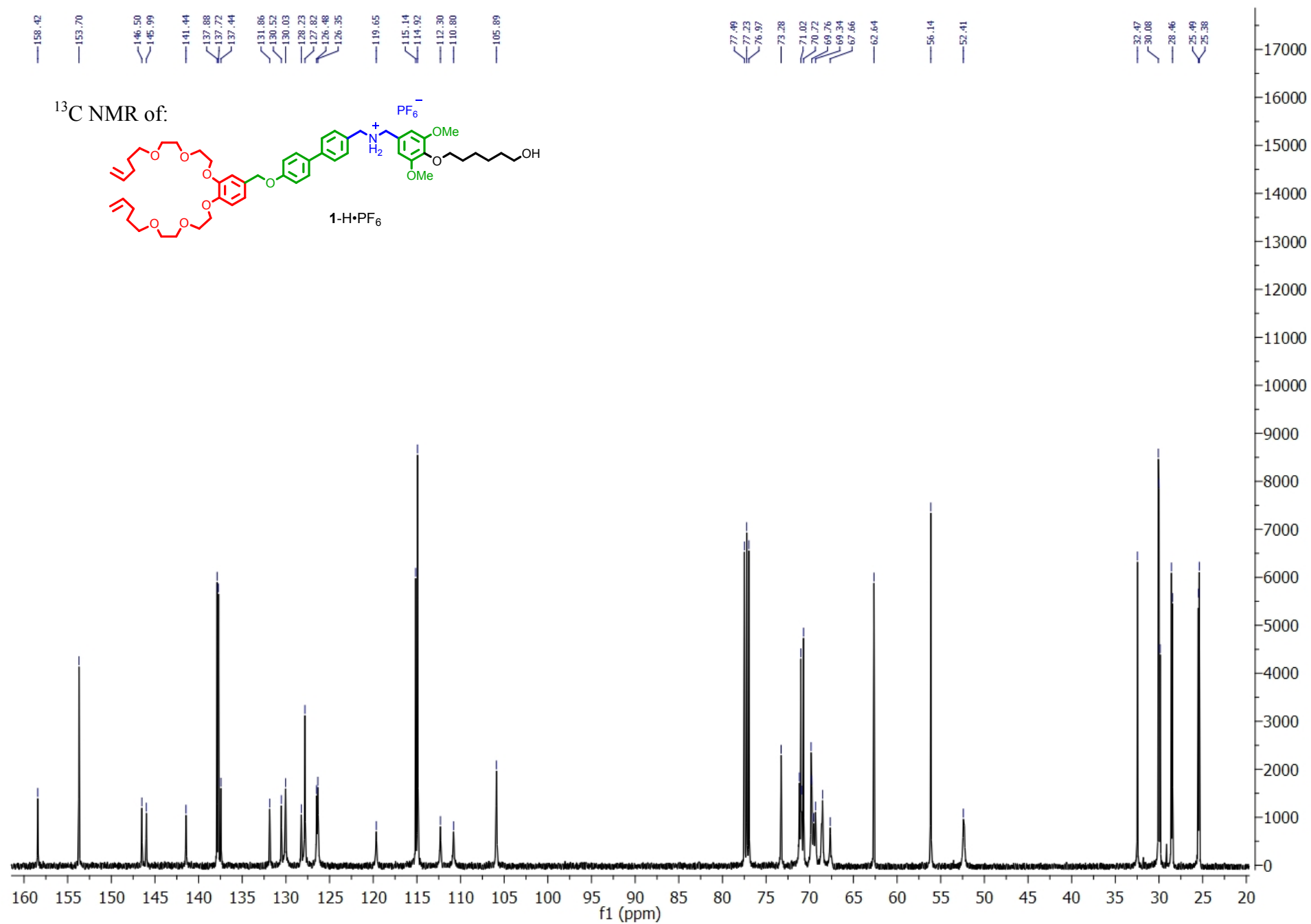
fourth freeze-pump-thaw cycle was completed, the solution was allowed to warm to room temperature. The solution became deep green and, after 30 seconds to 1 minute, became a solid gel (see video). The vial was placed in a 50 °C oil bath for 2 days to complete reaction, then cooled to room temperature. The DMF and other volatiles were removed under reduced pressure, and the resulting amorphous gel was placed in a vial containing fresh DMF (10 ml). The DMF was removed and fresh DMF was added (3 x 10 ml) to afford a pale-green gel. The volatiles were again removed to generate a hardened gel (73 mg, quant. yield).

**(B) Gel Cylinders:** To an oven-dried vial equipped with a stir bar was added **22**-H<sub>2</sub>·2PF<sub>6</sub> (100 mg, 47.9 μmol, 1 eq), tripropargylamine (4.5 μl, 32.0 μmol, 0.67 eq), *N,N,N',N'',N'''*-pentamethyldiethylenetriamine (50.1 μl, 239.7 μmol, 5 eq), and dry DMF (0.48 ml, 0.1 M). This mixture was subjected to standard freeze-pump-thaw protocol, with addition of copper(I) bromide (34.4 mg, 239.8 μmol, 5 eq) after the third freeze. After the fourth freeze-pump-thaw cycle was completed, the solution was allowed to warm to room temperature and was stirred for 30 seconds. The vial was rapidly opened and a glass capillary tube was added (cut to 20 mm long, 1.5–1.8 mm diameter, Kimax-51 Glass Capillary Tubes, Fischer Scientific Product Number #34505). The vial was turned horizontal and the solution was allowed to fill the capillary tube and solidify. After gelation, the vial was placed in a 50 °C oil bath for 2 days to complete reaction, then cooled to room temperature. The glass capillary tube with intercalated gel was removed from the surrounding amorphous gel, and placed in a vial under high vacuum.

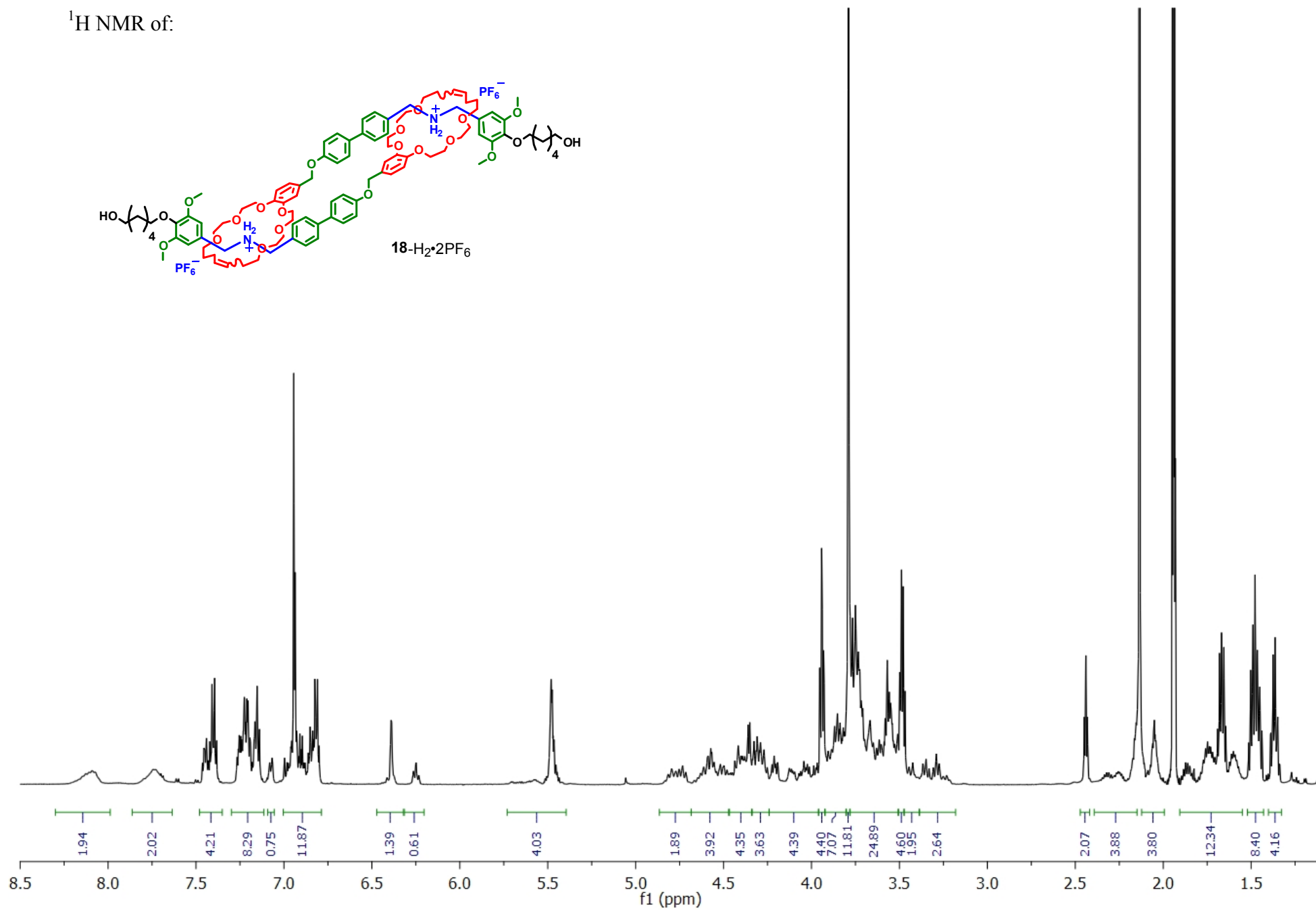
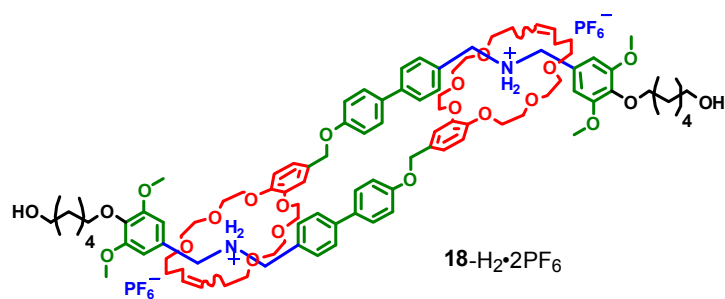
A blunt needle was used to carefully push the shrunken gel from the glass tube. After removal from the tube, the gel was subjected to repeated swellings with 1:1 DCM/Acteone (3 x 10 ml) to afford nearly-transparent gel cylinders.

$^1\text{H}$  NMR of:





$^1\text{H}$  NMR of:





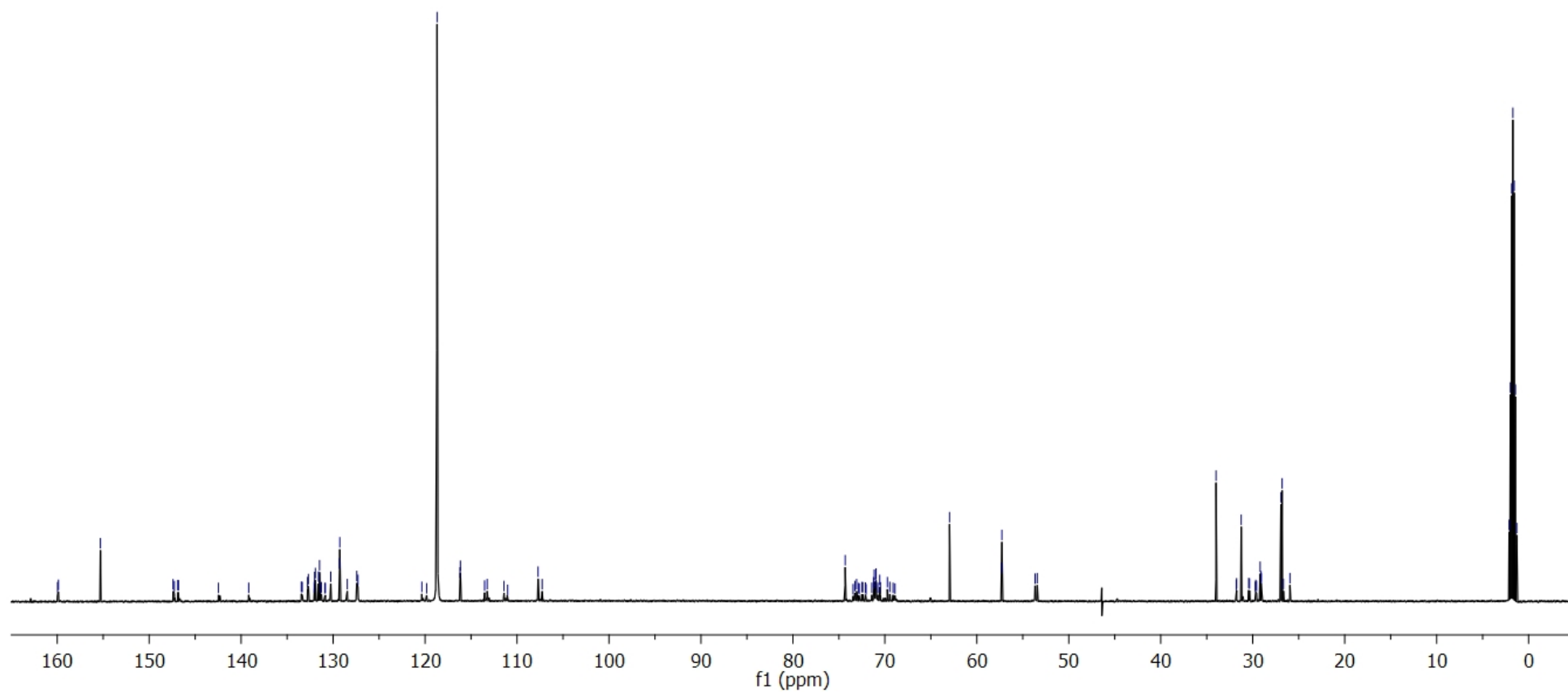
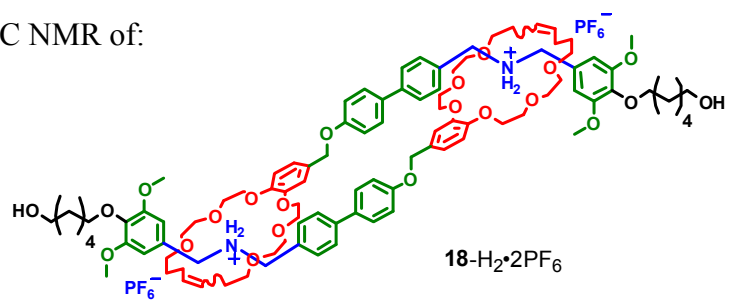
159.96  
159.87  
155.30  
147.41  
147.26  
146.89  
146.81  
142.47  
139.18  
132.78  
131.93  
131.48  
131.27  
130.85  
129.30  
128.46  
127.29  
120.35  
119.82  
118.69  
116.16  
113.24  
111.02  
107.71  
107.27

74.31  
72.41  
72.11  
72.05  
71.41  
71.23  
71.15  
71.00  
70.96  
70.77  
70.56  
70.48  
70.42  
69.72  
69.46  
69.11  
68.90  
62.97  
57.30  
57.27  
53.66  
53.43

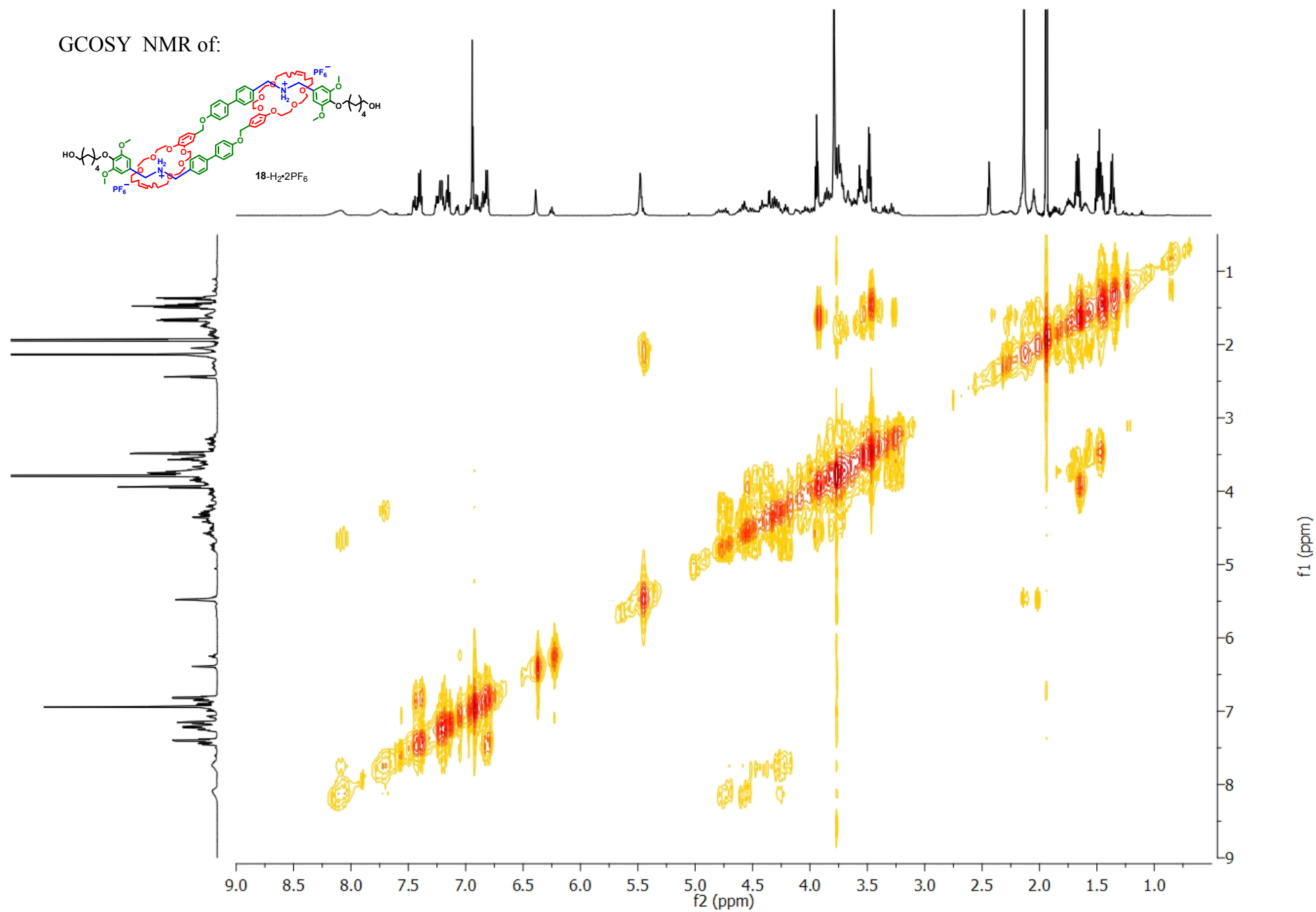
33.98  
31.79  
29.07  
26.93  
26.80  
26.66  
25.95

2.12  
1.98  
1.84  
1.70  
1.57  
1.43  
1.29

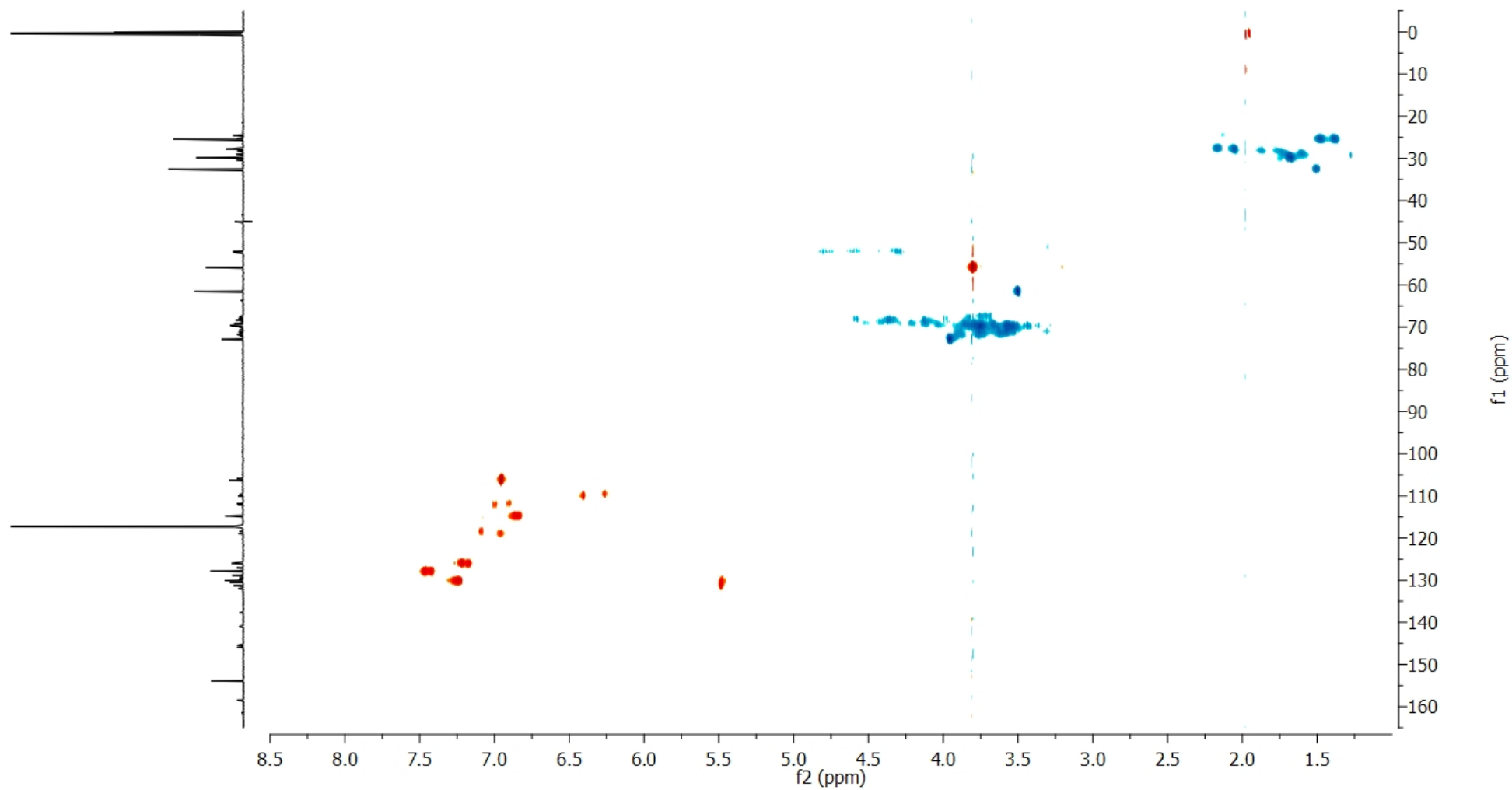
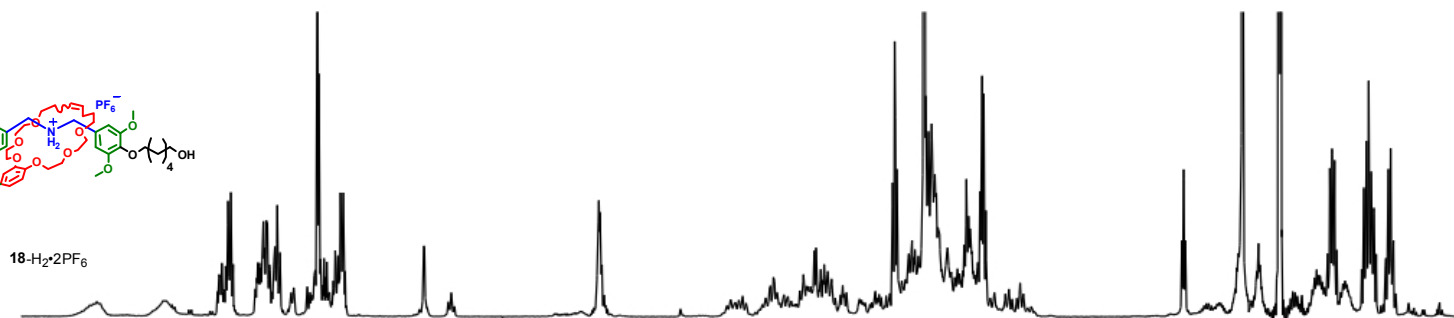
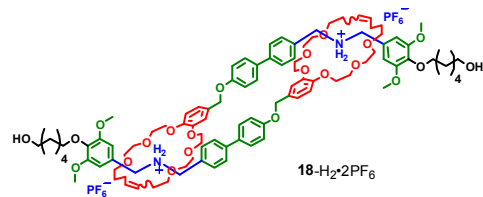
$^{13}\text{C}$  NMR of:



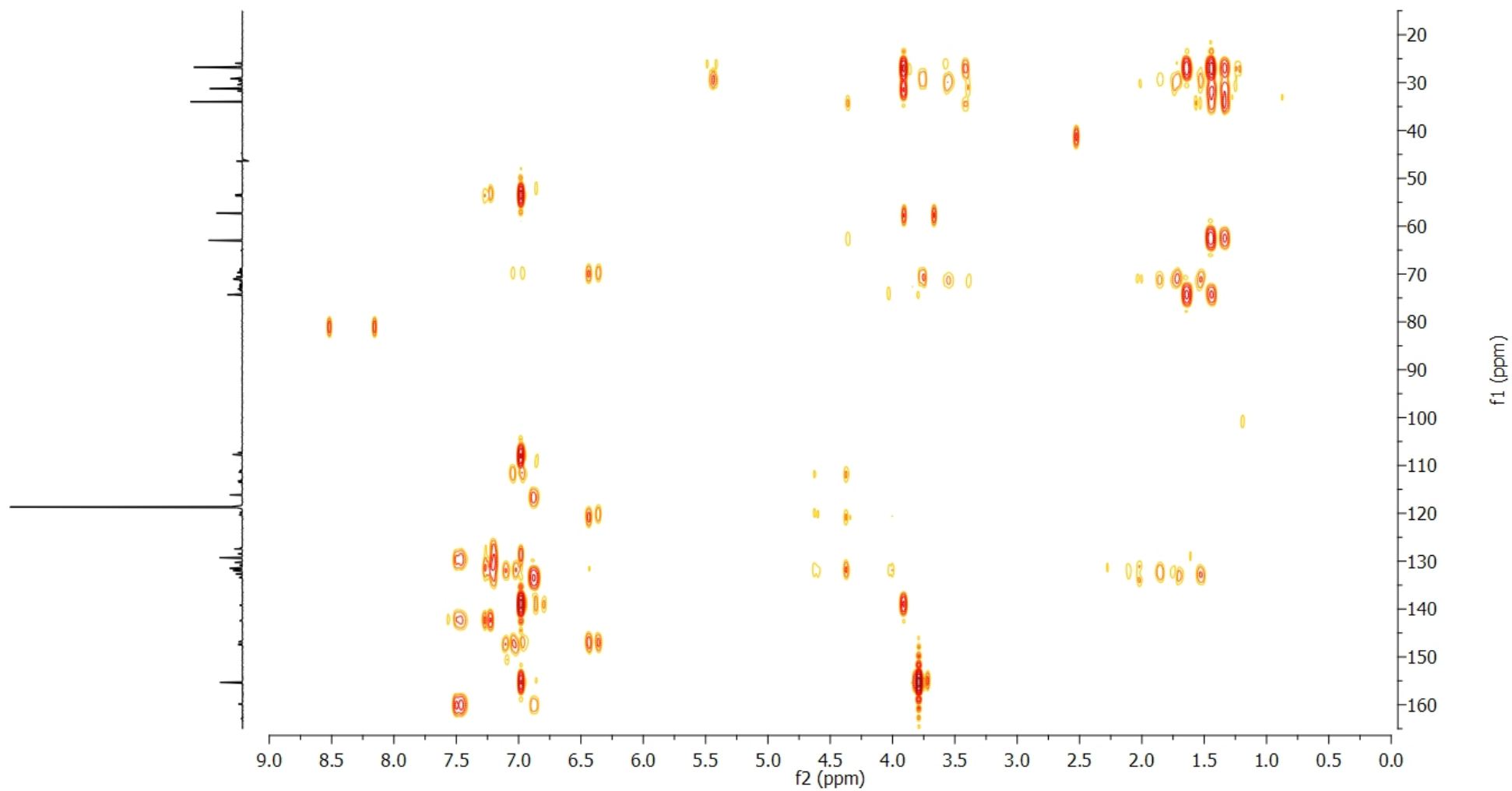
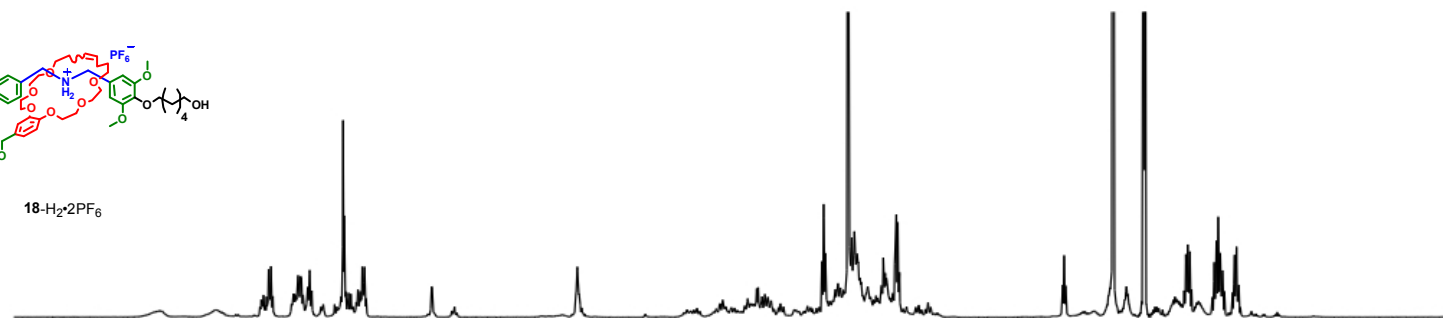
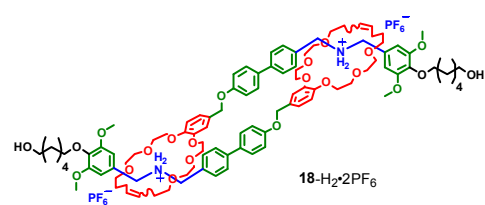
GCOSY NMR of:



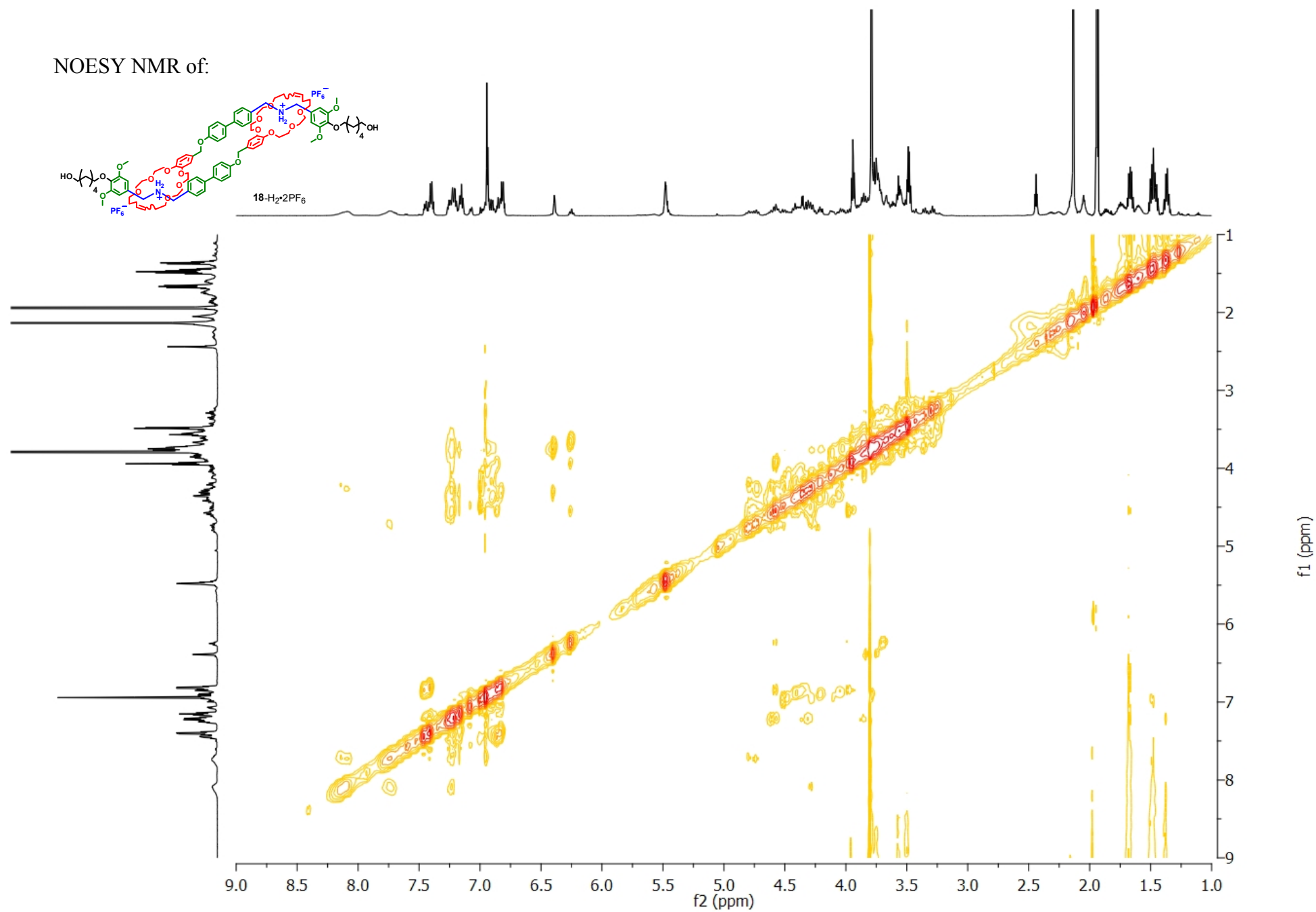
GHSQC NMR of:

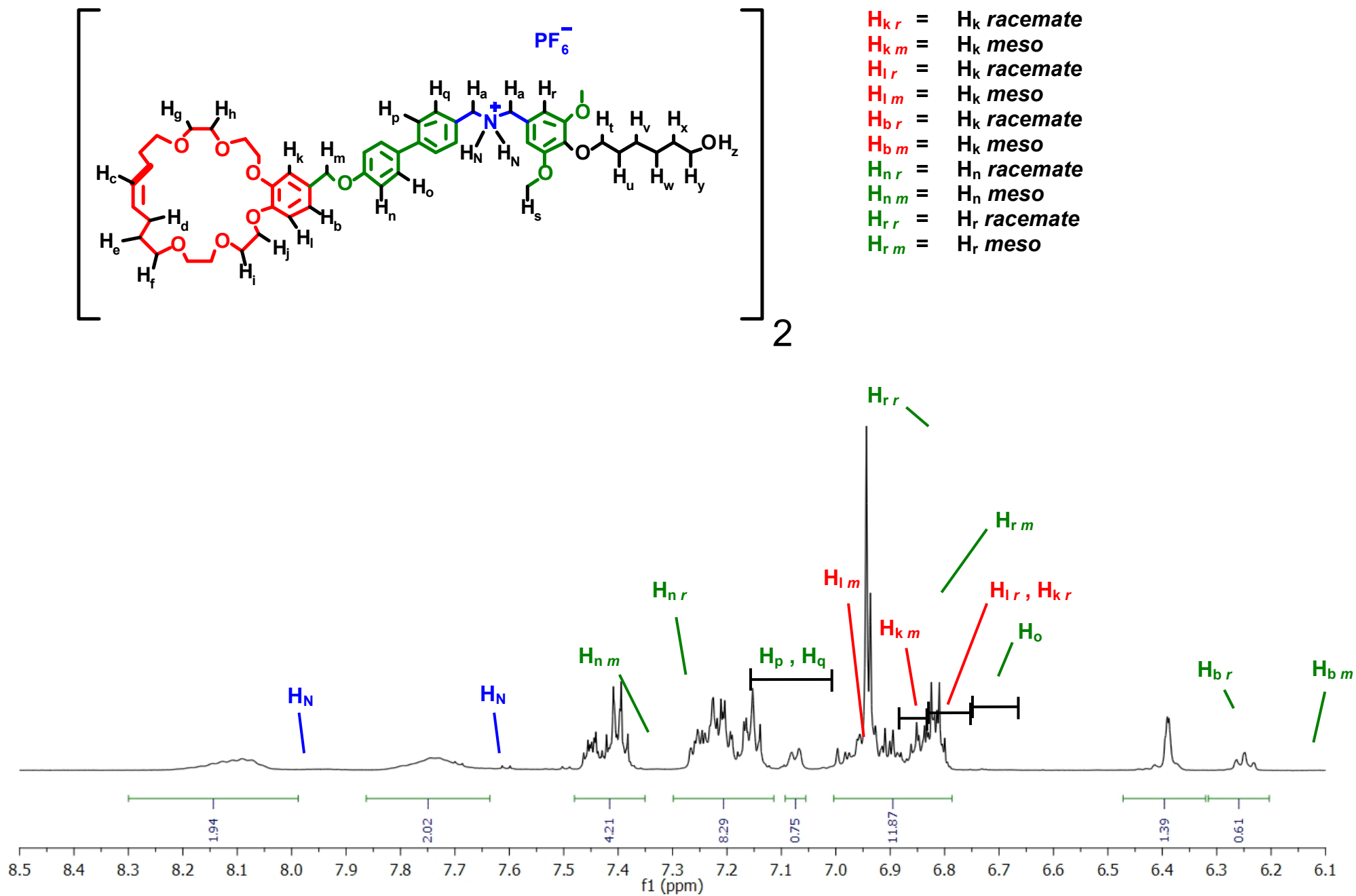


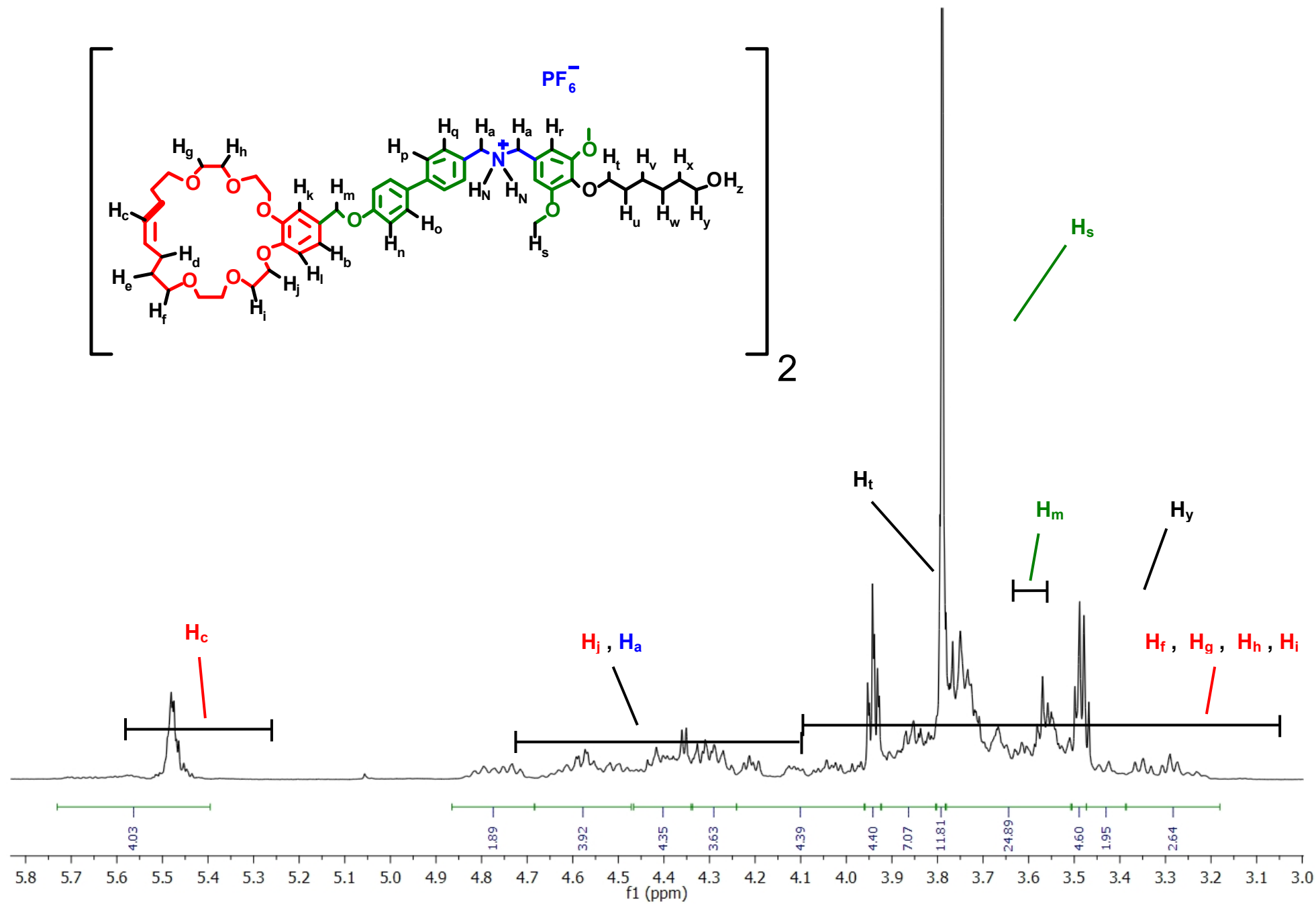
GHMBC NMR of:

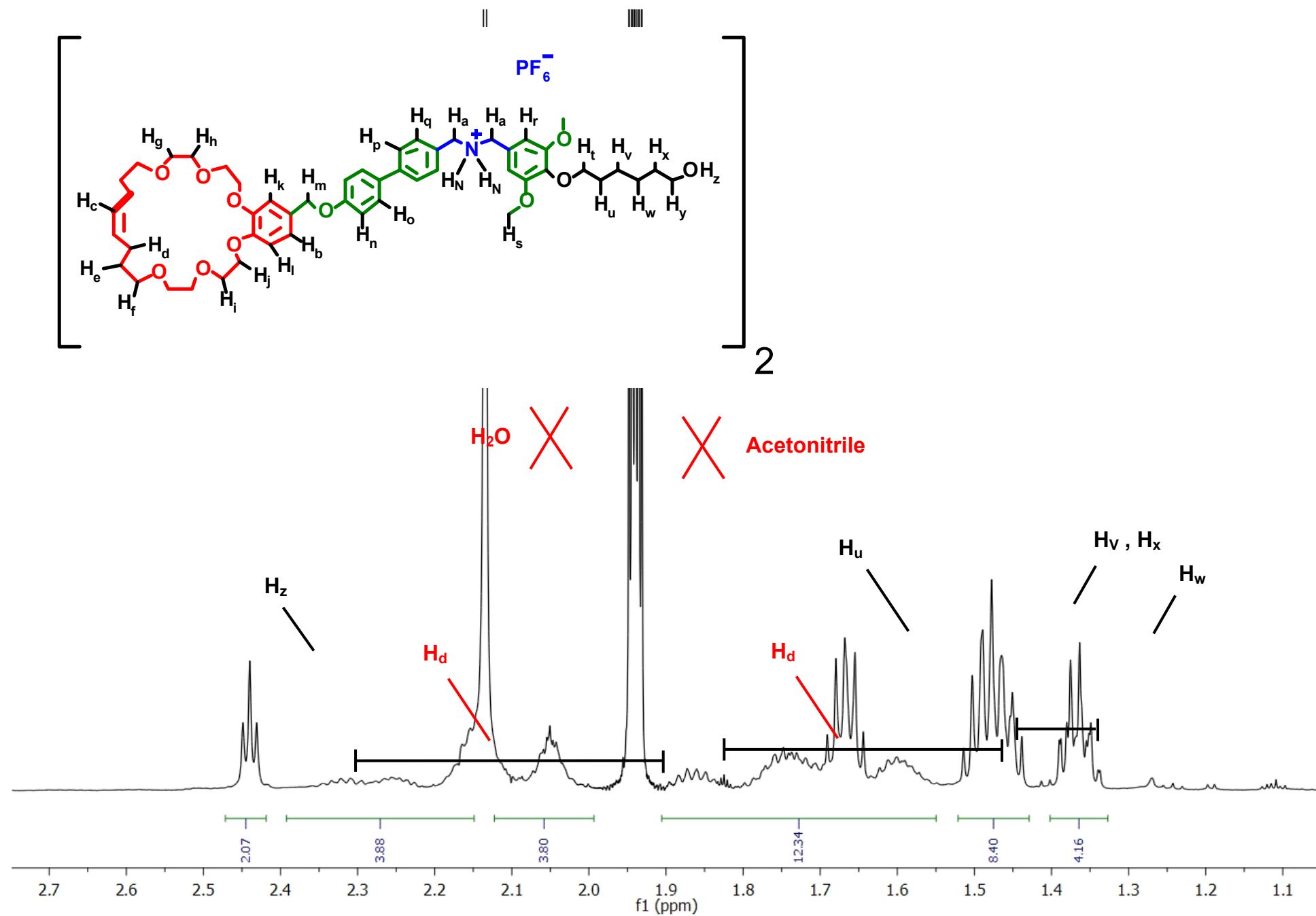


NOESY NMR of:

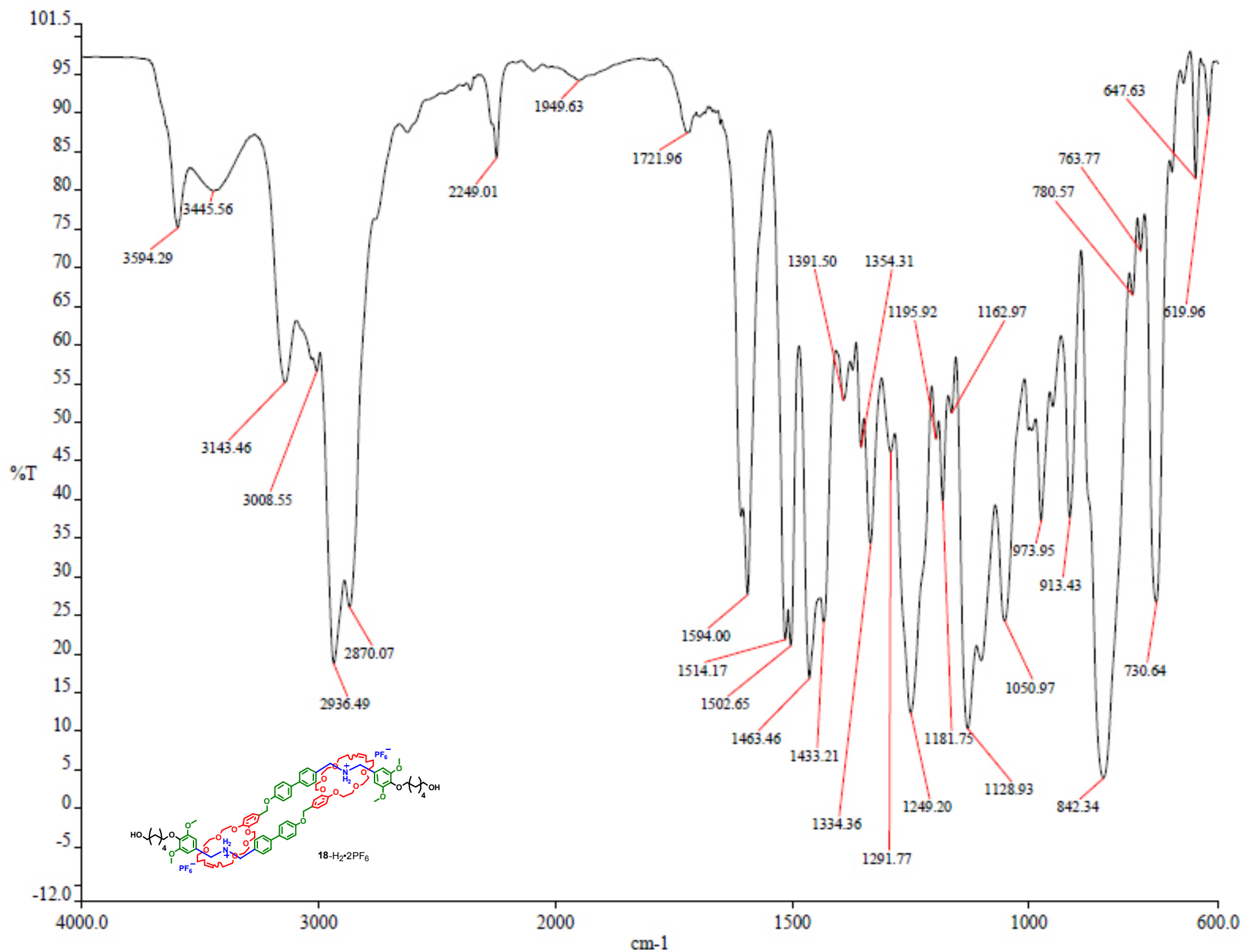




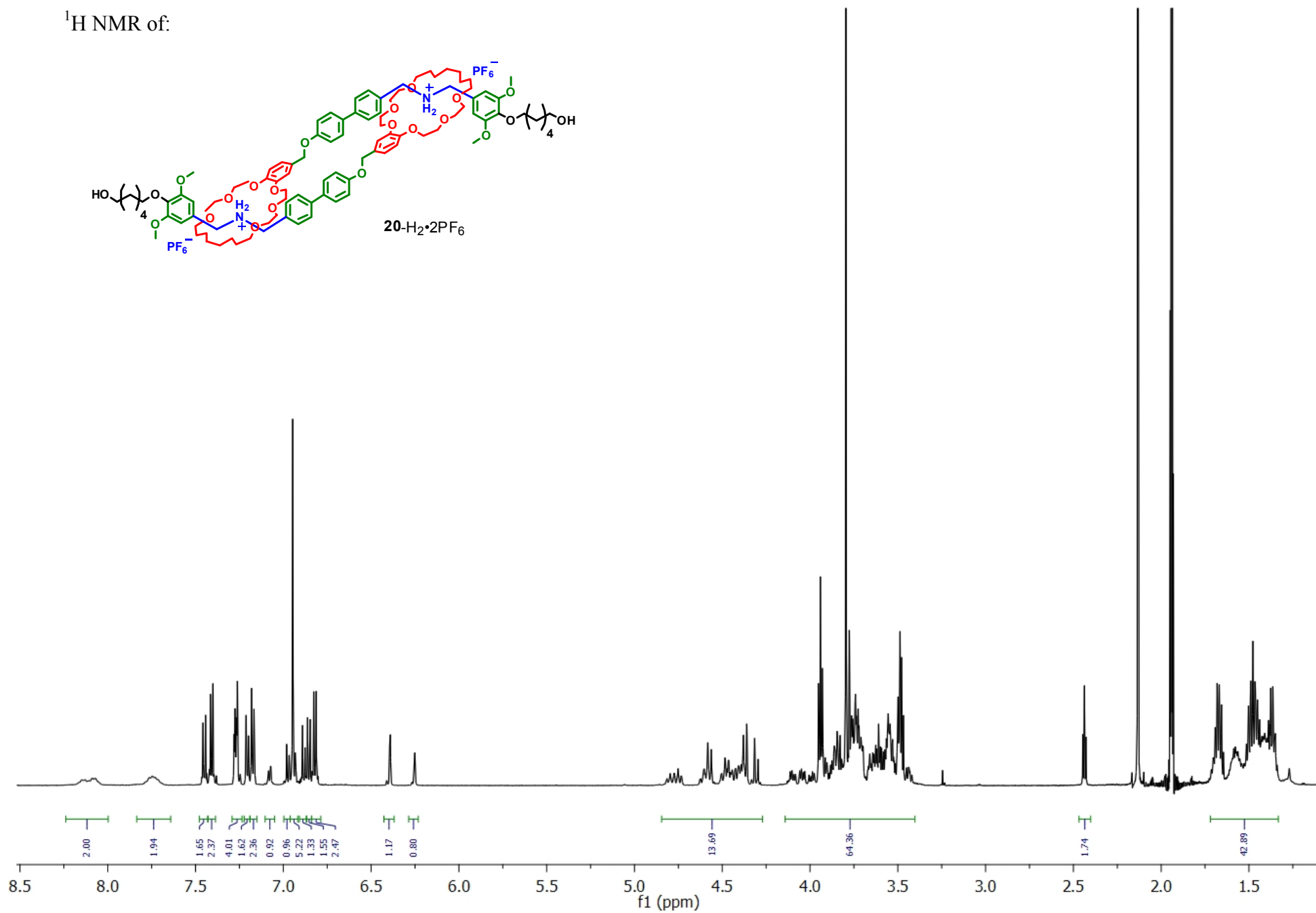
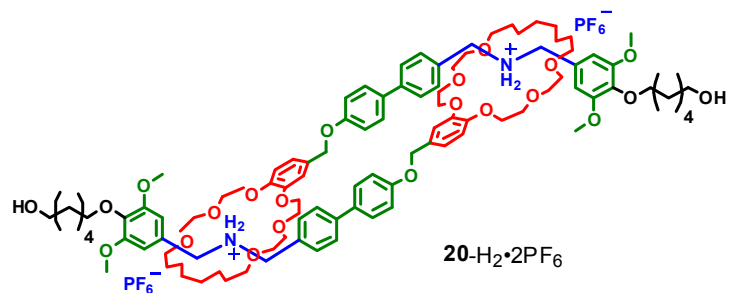




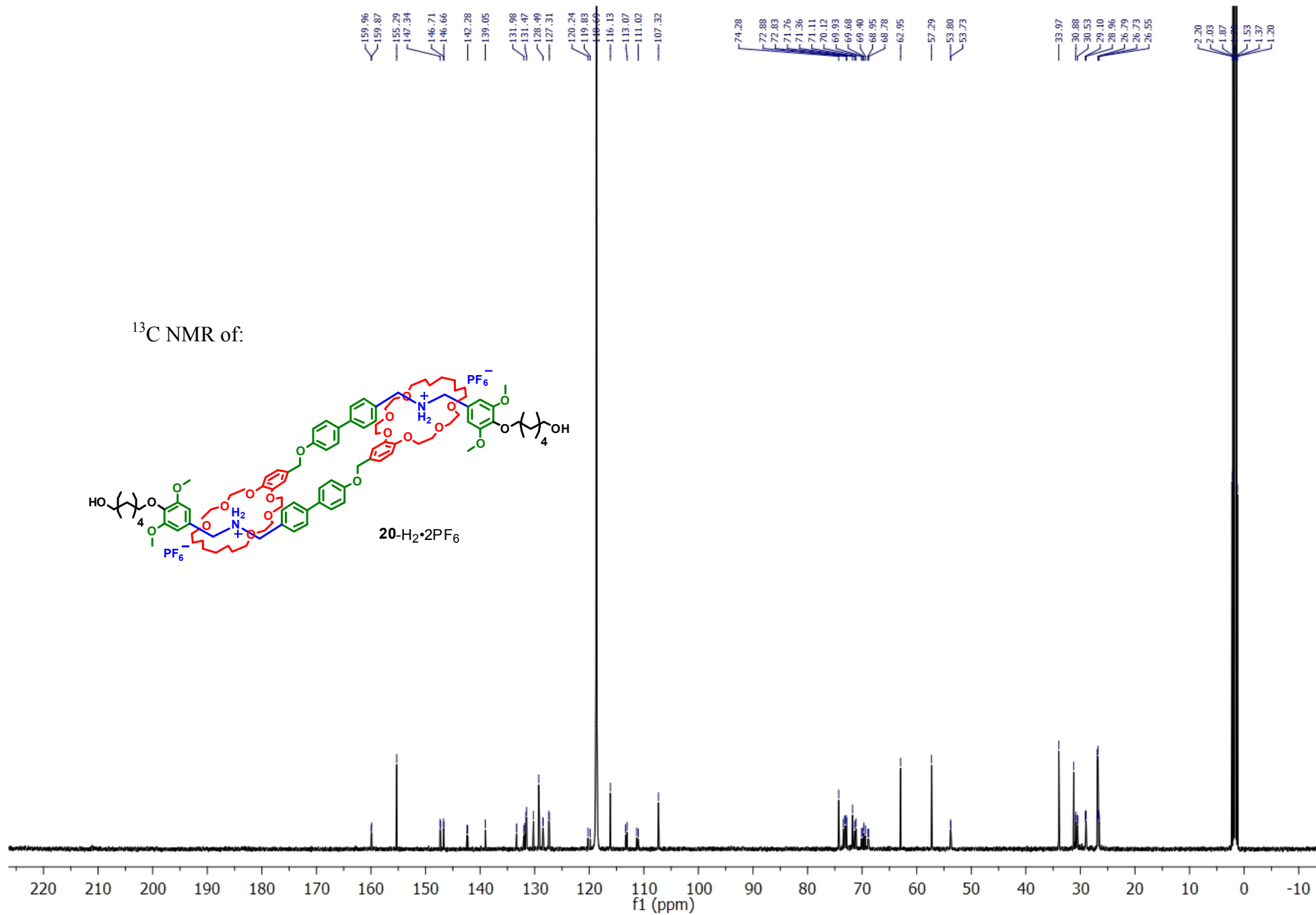
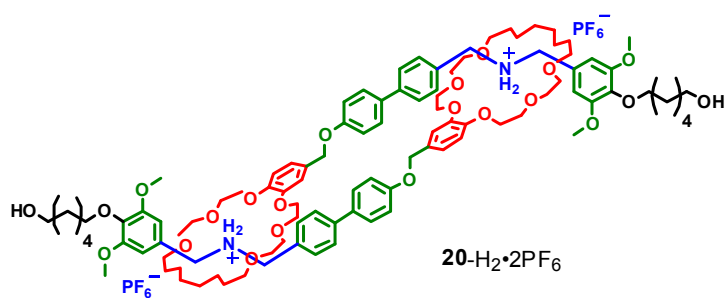


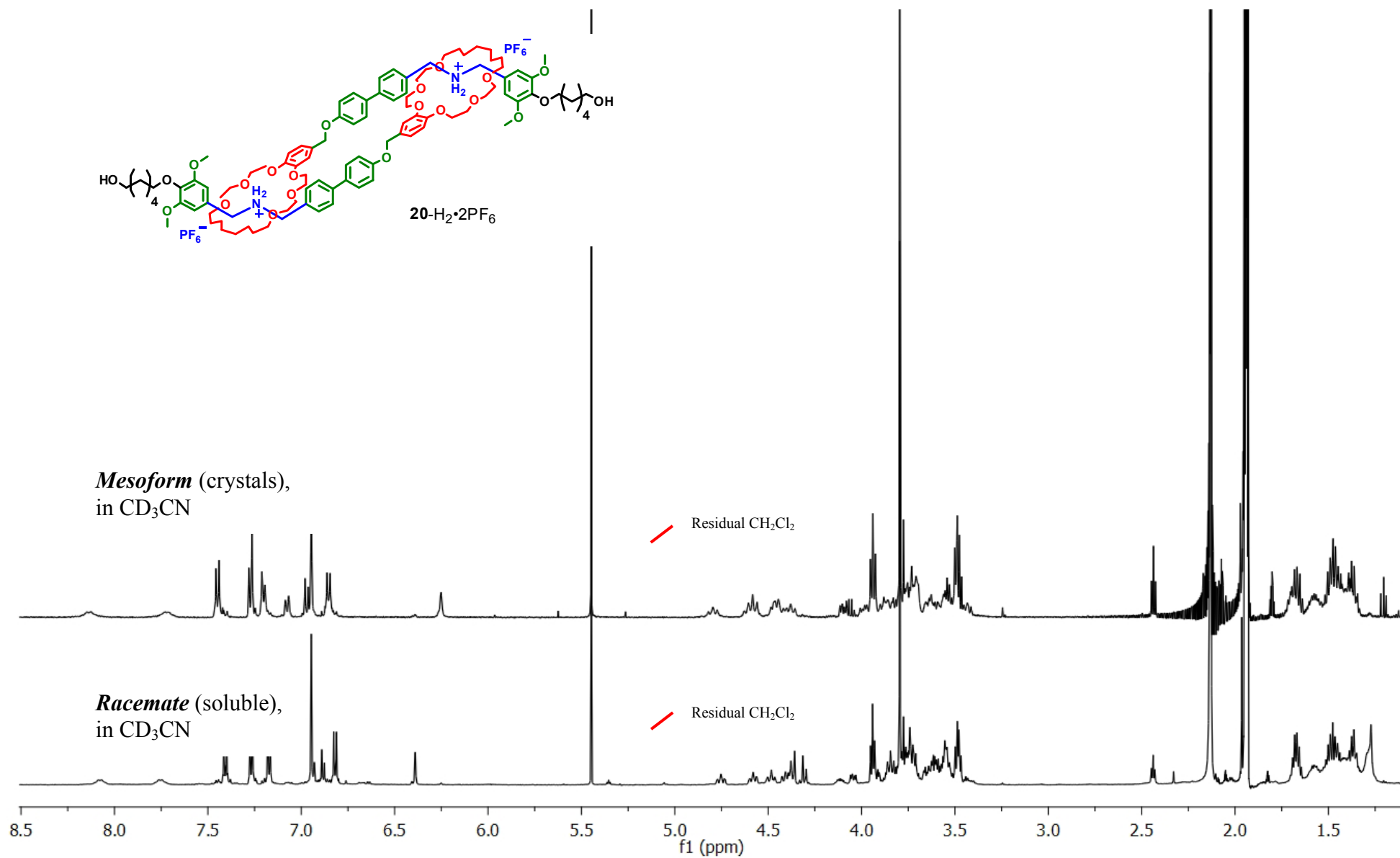


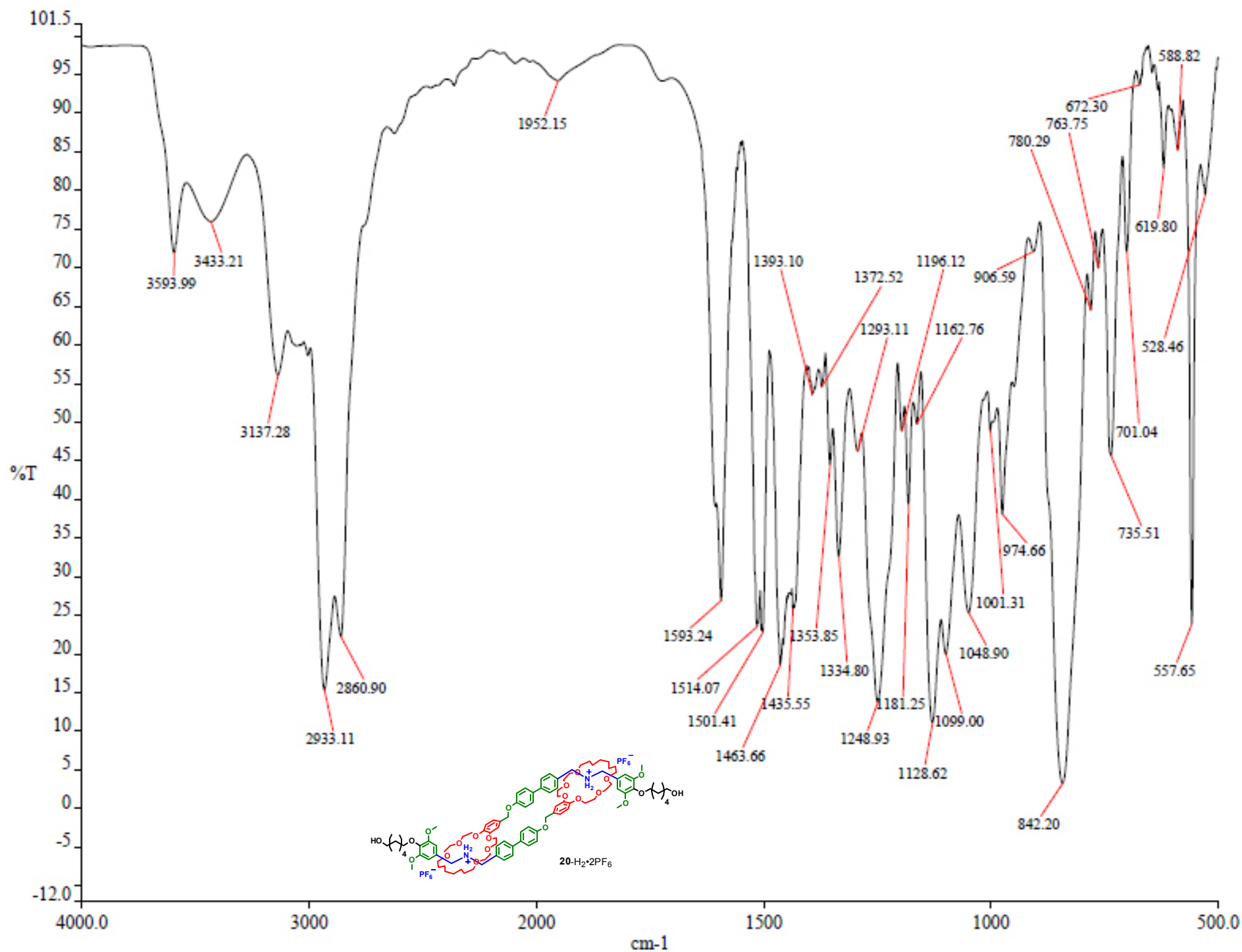
$^1\text{H}$  NMR of:



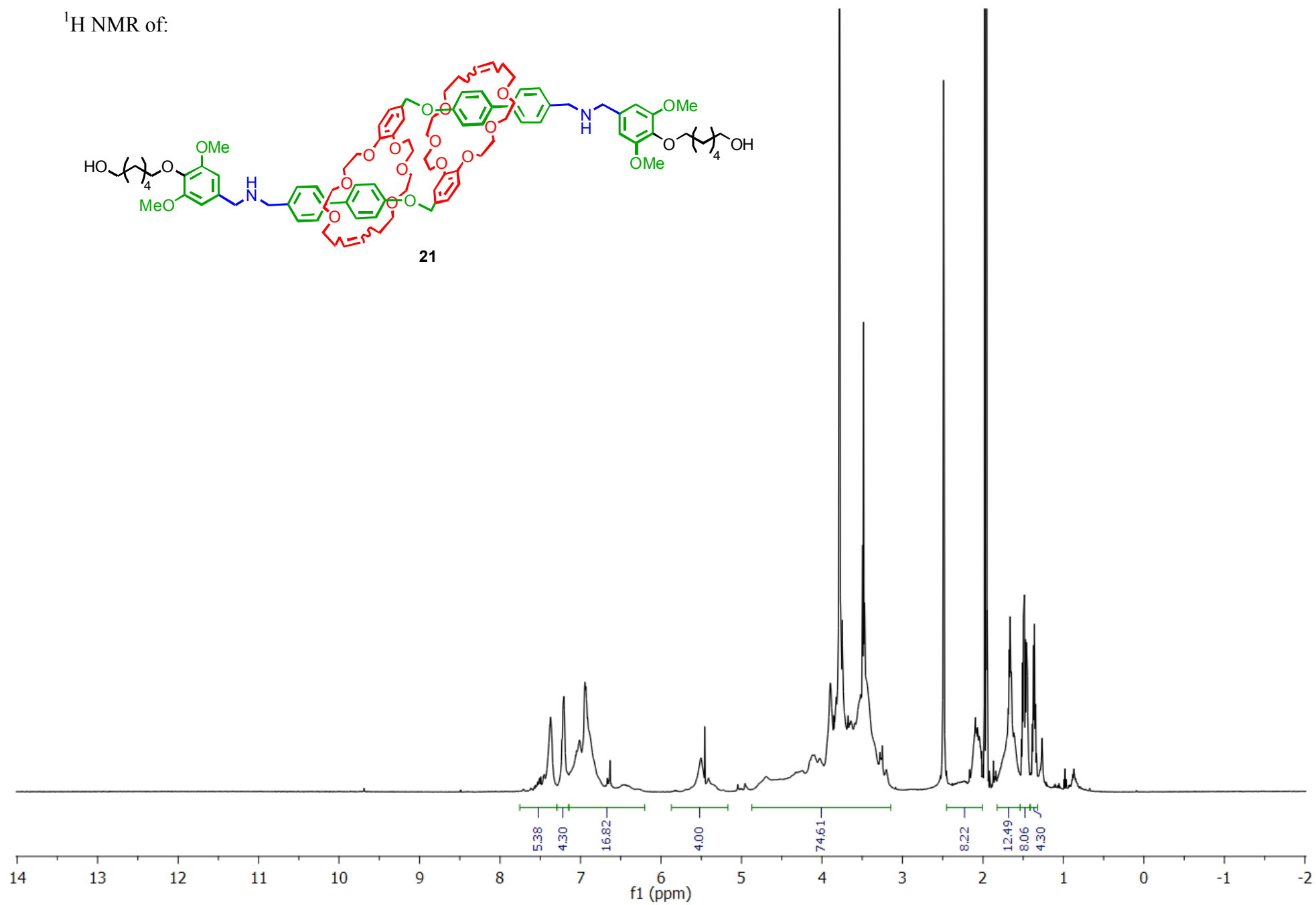
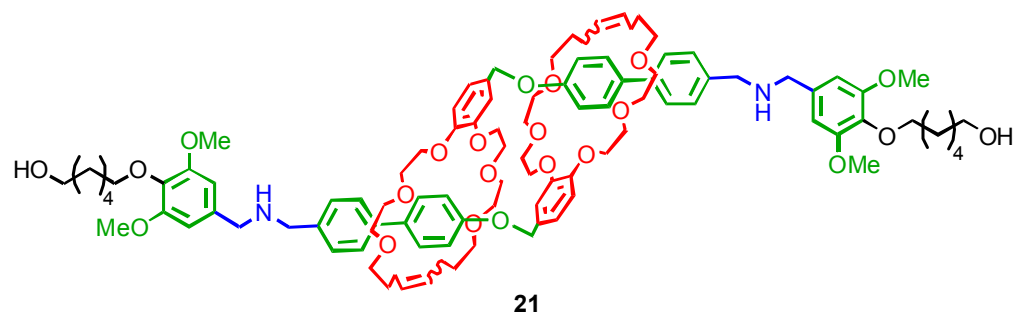
$^{13}\text{C}$  NMR of:







$^1\text{H}$  NMR of:

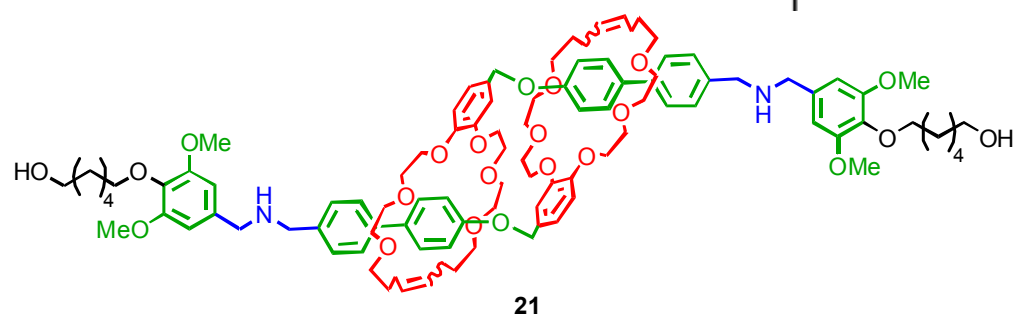


111

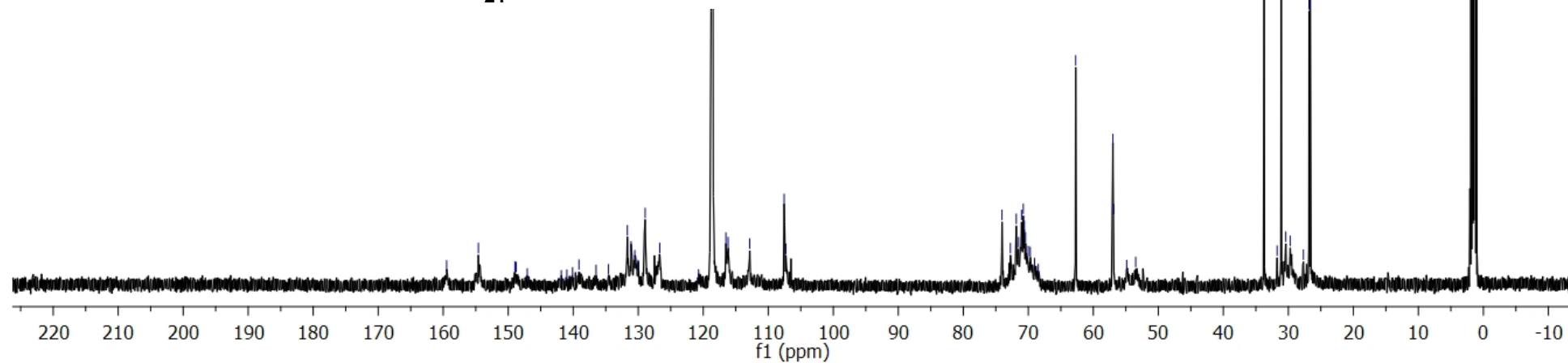


$^{13}\text{C}$  NMR (126 MHz,  $\text{cd}_3\text{cn}$ )  $\delta$  159.48, 154.59, 148.98, 148.78, 147.07, 141.84, 140.98, 140.10, 139.12, 136.49, 134.58, 131.68, 131.10, 130.54, 130.02, 128.94, 126.69, 120.72, 118.69, 116.51, 116.18, 112.85, 107.55, 107.29, 74.05, 72.76, 71.85, 71.49, 71.04, 70.77, 70.60, 70.42, 70.01, 69.70, 69.03, 68.47, 62.72, 56.99, 56.89, 54.86, 53.48, 33.74, 31.73, 31.10, 30.40, 29.71, 27.68, 26.81, 26.66, 2.05, 1.88, 1.72, 1.55, 1.39, 1.22, 1.06.

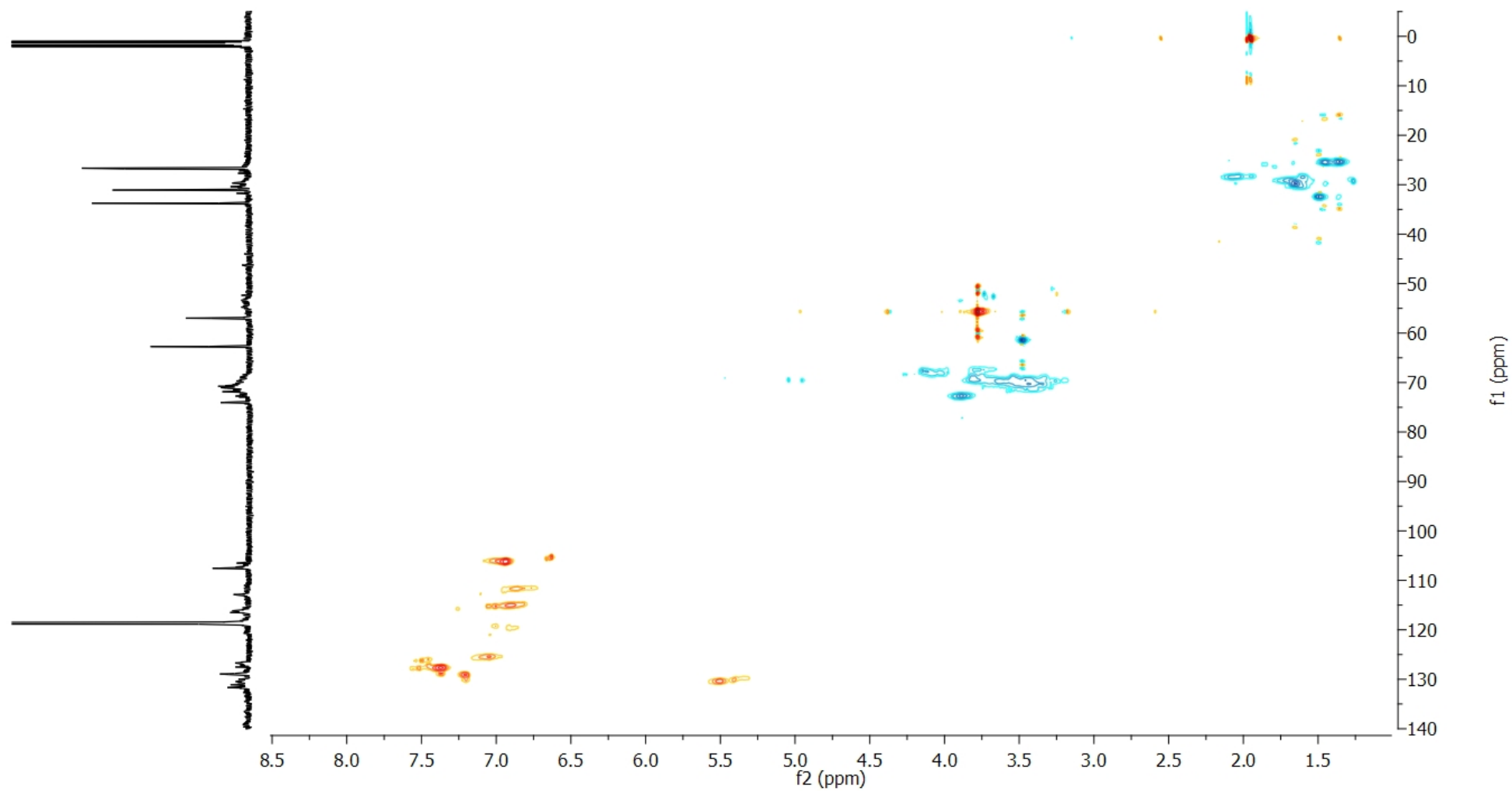
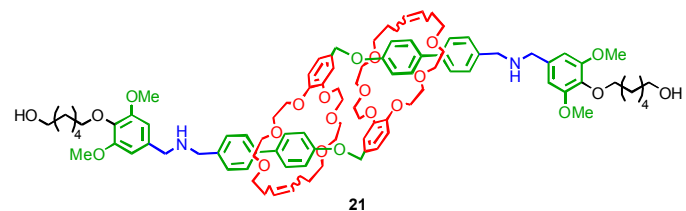
$^{13}\text{C}$  NMR of:



**21**

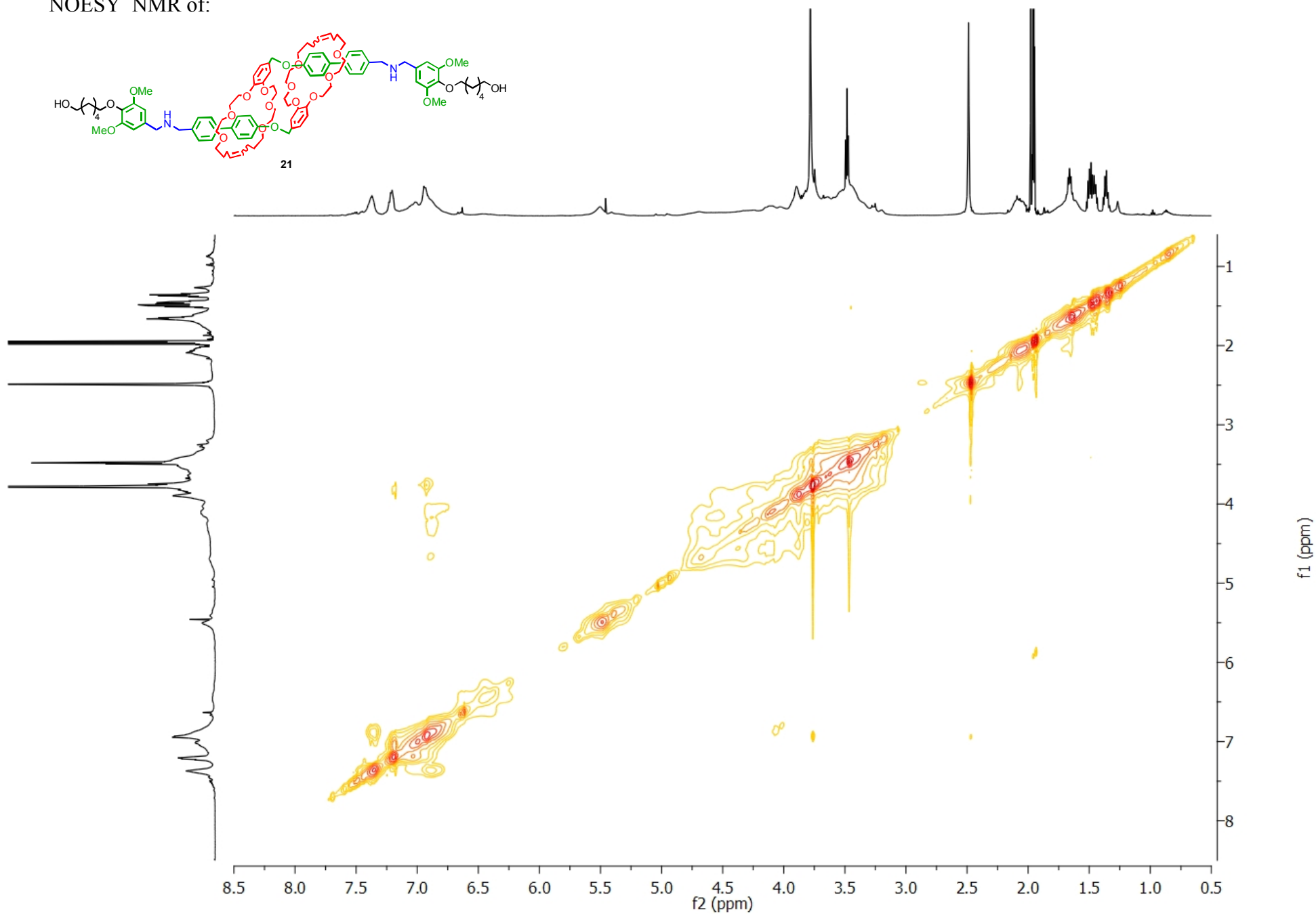


GHSQC NMR of:

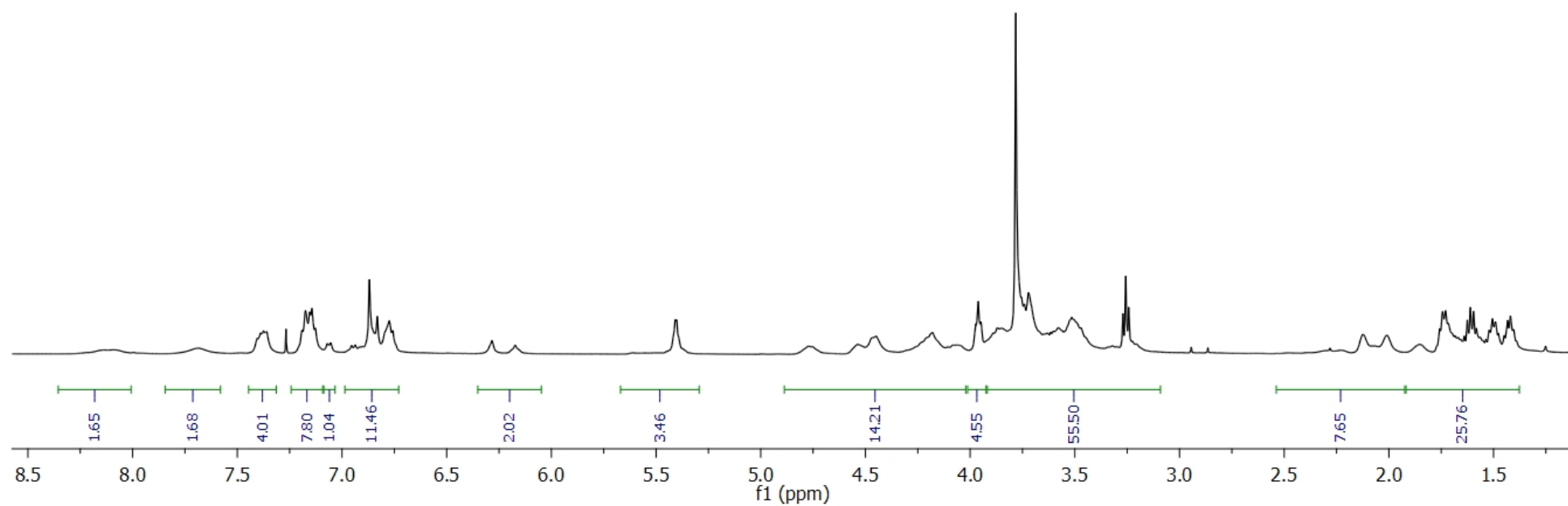
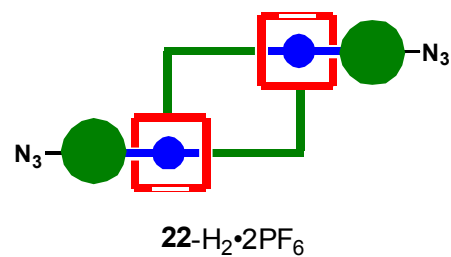


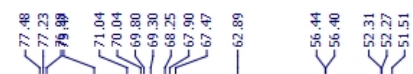
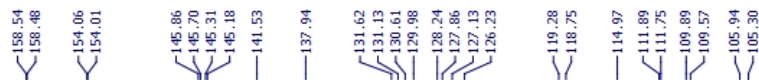


NOESY NMR of:

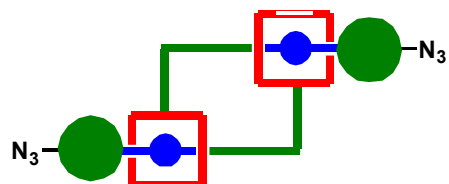


$^1\text{H}$  NMR of:



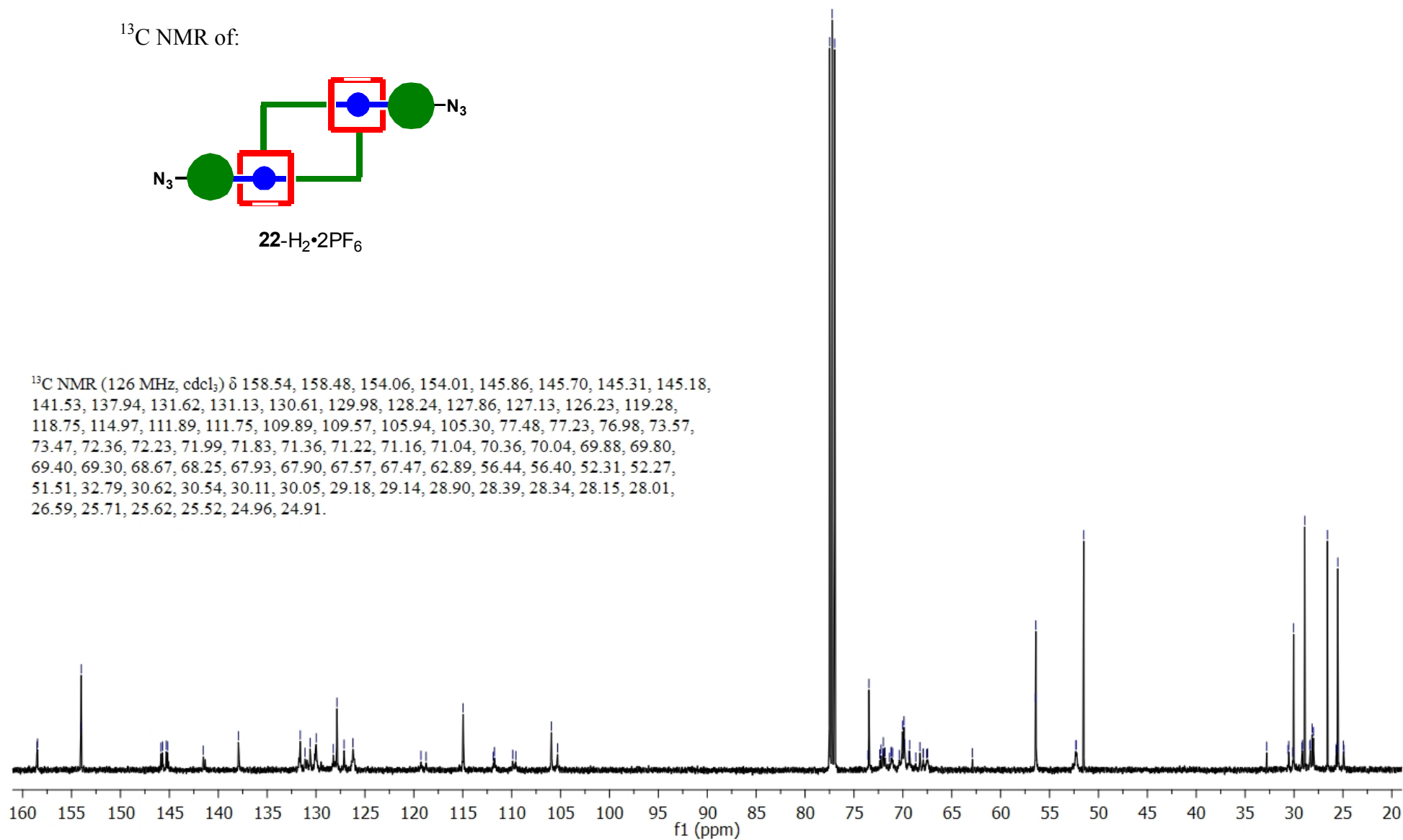


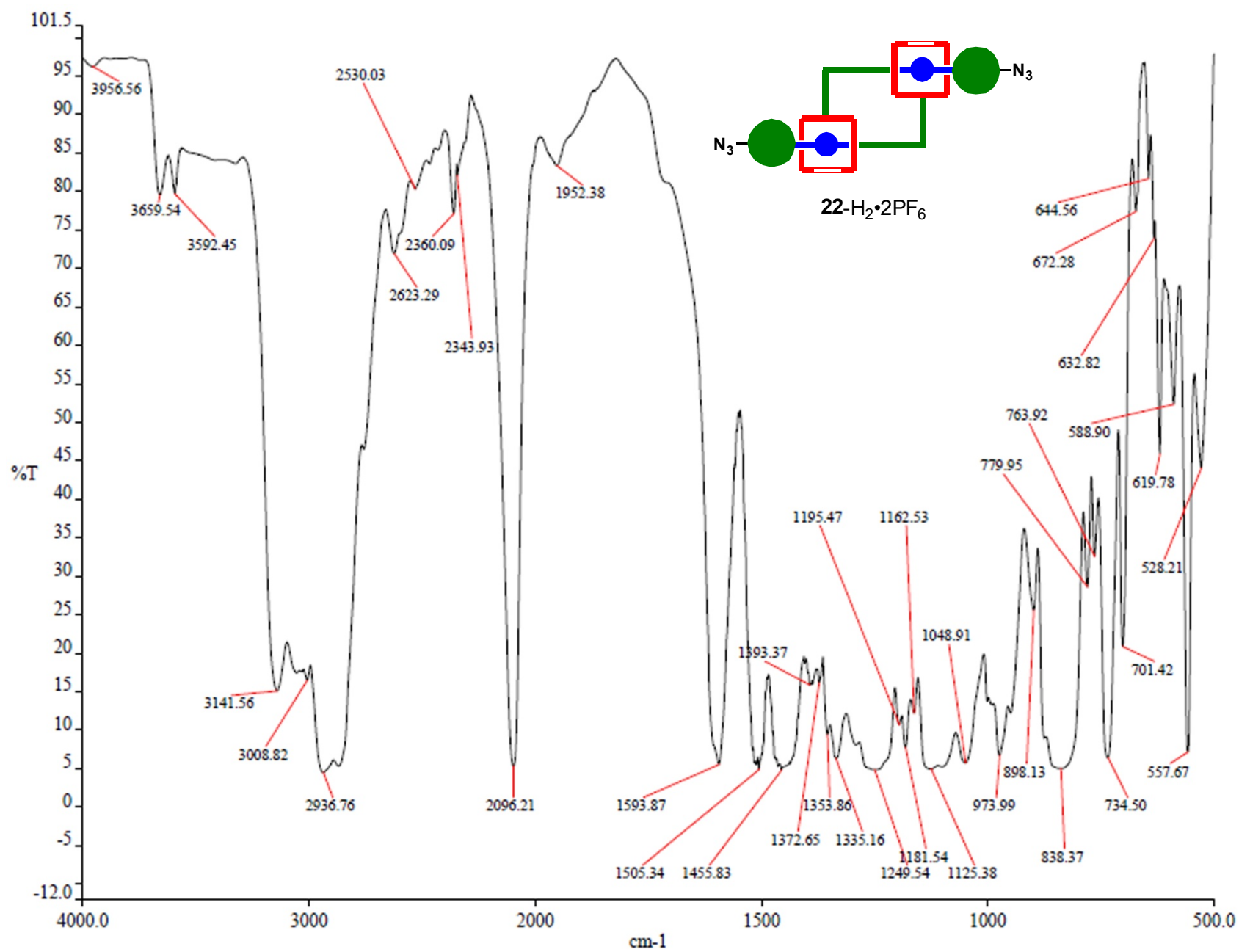
$^{13}\text{C}$  NMR of:



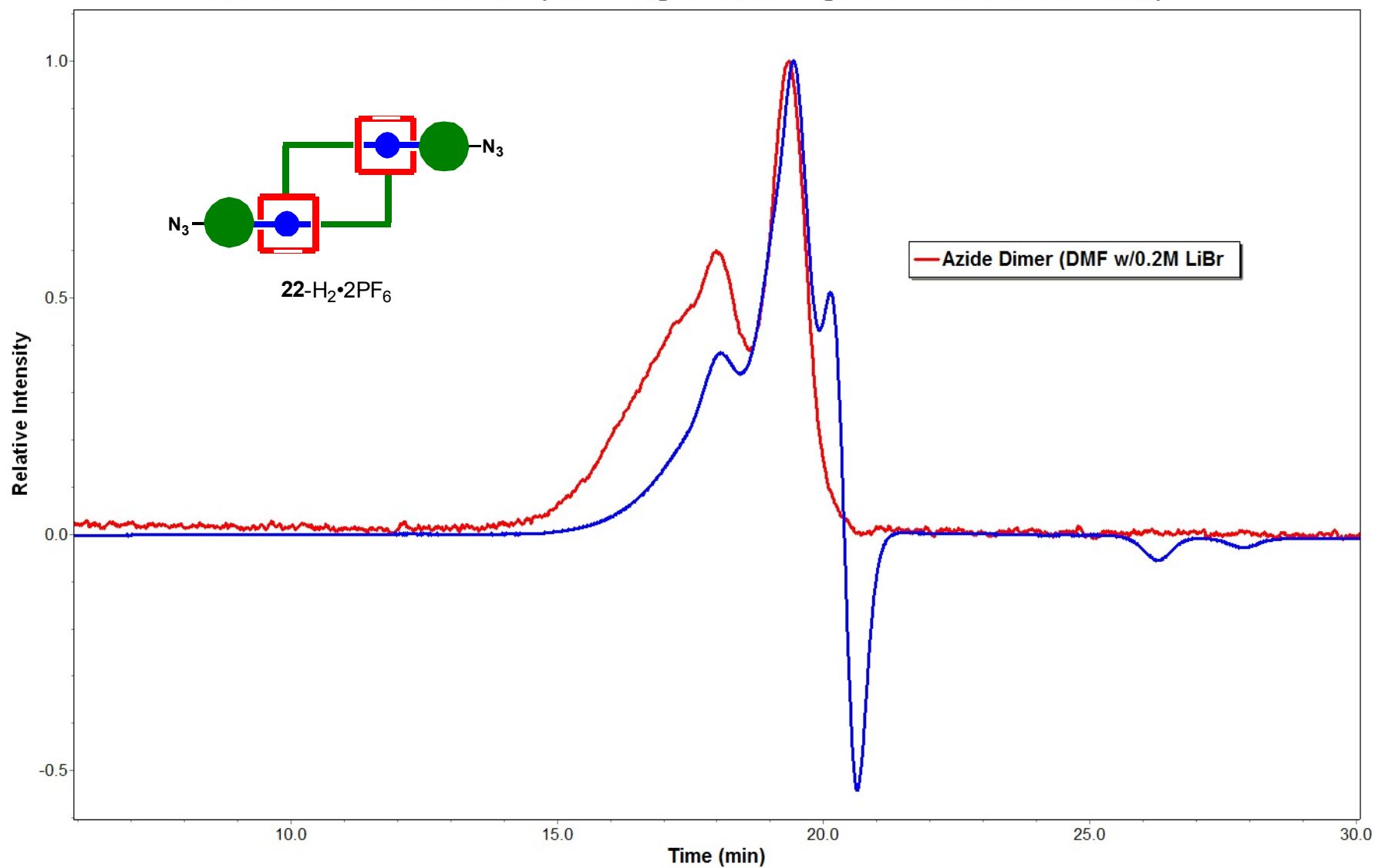
**22-H<sub>2</sub>·2PF<sub>6</sub>**

$^{13}\text{C}$  NMR (126 MHz,  $\text{cdCl}_3$ )  $\delta$  158.54, 158.48, 154.06, 154.01, 145.86, 145.70, 145.31, 145.18, 141.53, 137.94, 131.62, 131.13, 130.61, 129.98, 128.24, 127.86, 127.13, 126.23, 119.28, 118.75, 114.97, 111.89, 111.75, 109.89, 109.57, 105.94, 105.30, 77.48, 77.23, 76.98, 73.57, 73.47, 72.36, 72.23, 71.99, 71.83, 71.36, 71.22, 71.16, 71.04, 70.36, 70.04, 69.88, 69.80, 69.40, 69.30, 68.67, 68.25, 67.93, 67.90, 67.57, 67.47, 62.89, 56.44, 56.40, 52.31, 52.27, 51.51, 32.79, 30.62, 30.54, 30.11, 30.05, 29.18, 29.14, 28.90, 28.39, 28.34, 28.15, 28.01, 26.59, 25.71, 25.62, 25.52, 24.96, 24.91.

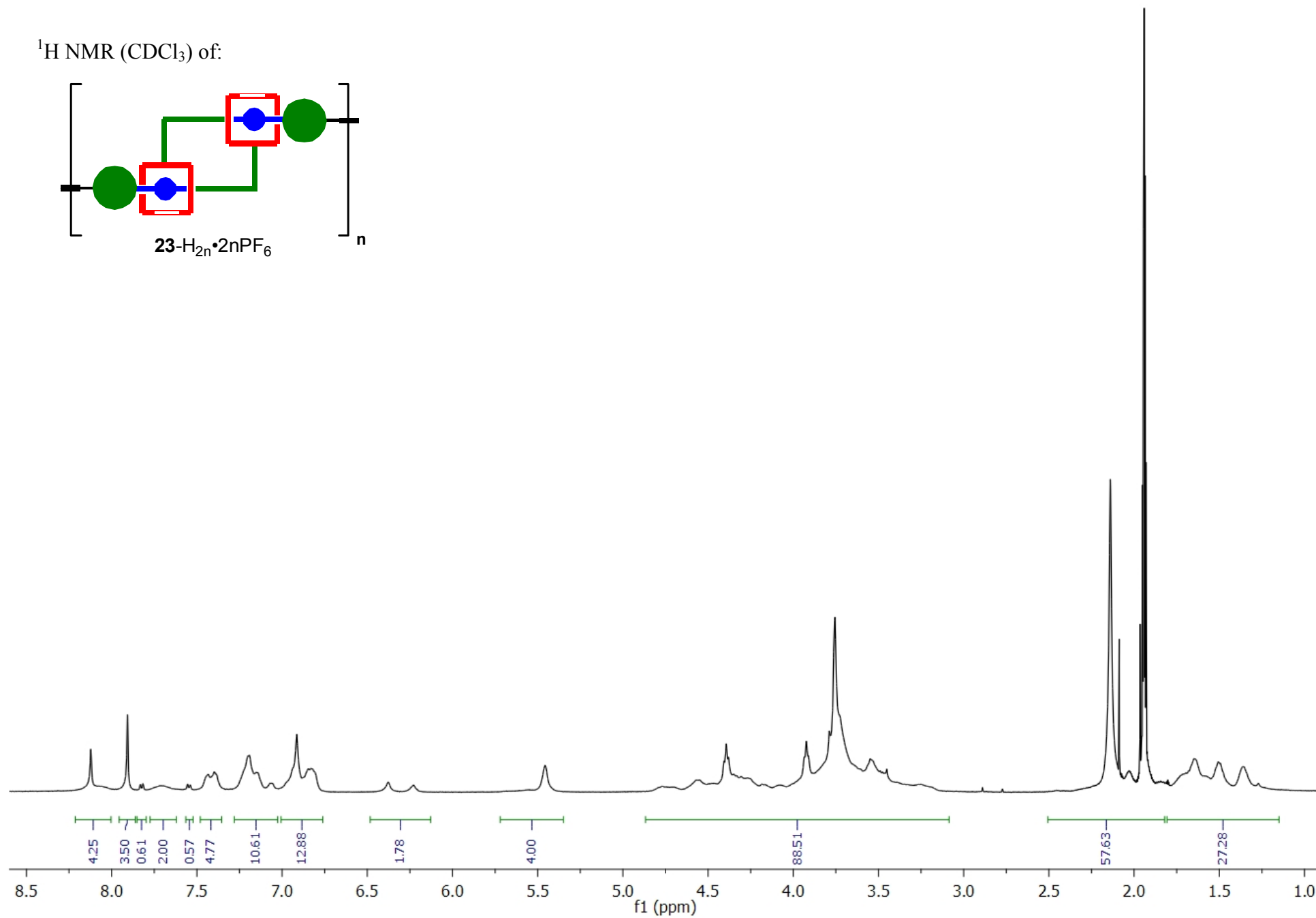
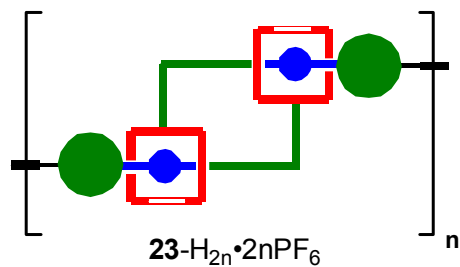




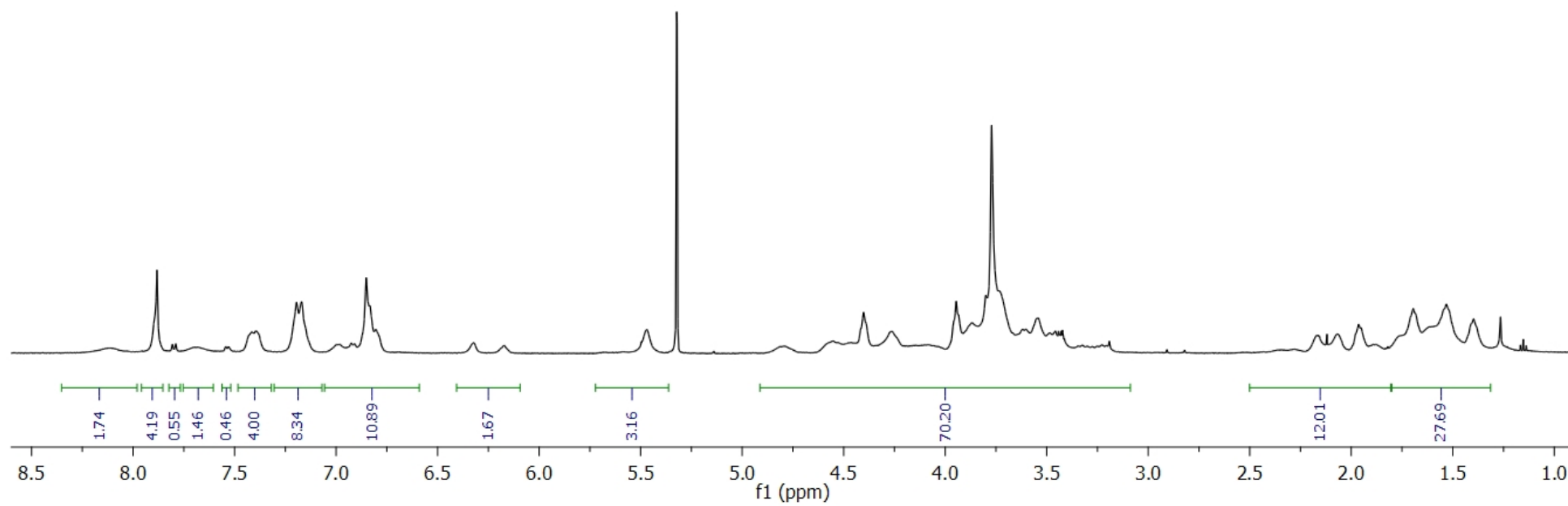
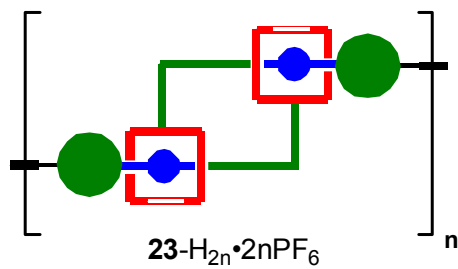
GPC of Pure Azide Dimer (Red = Light Scattering; Blue = Refractive Index)

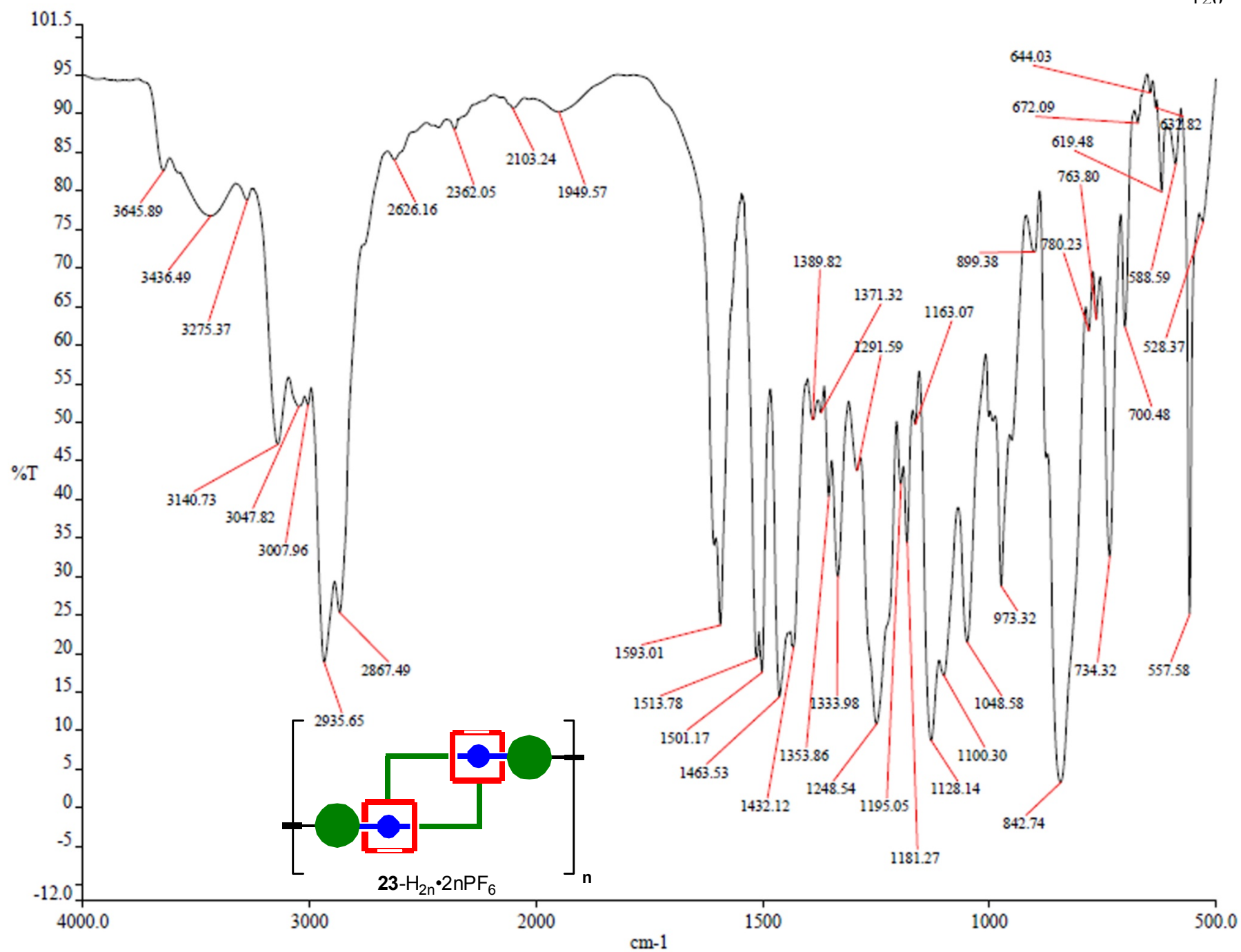


$^1\text{H}$  NMR ( $\text{CDCl}_3$ ) of:

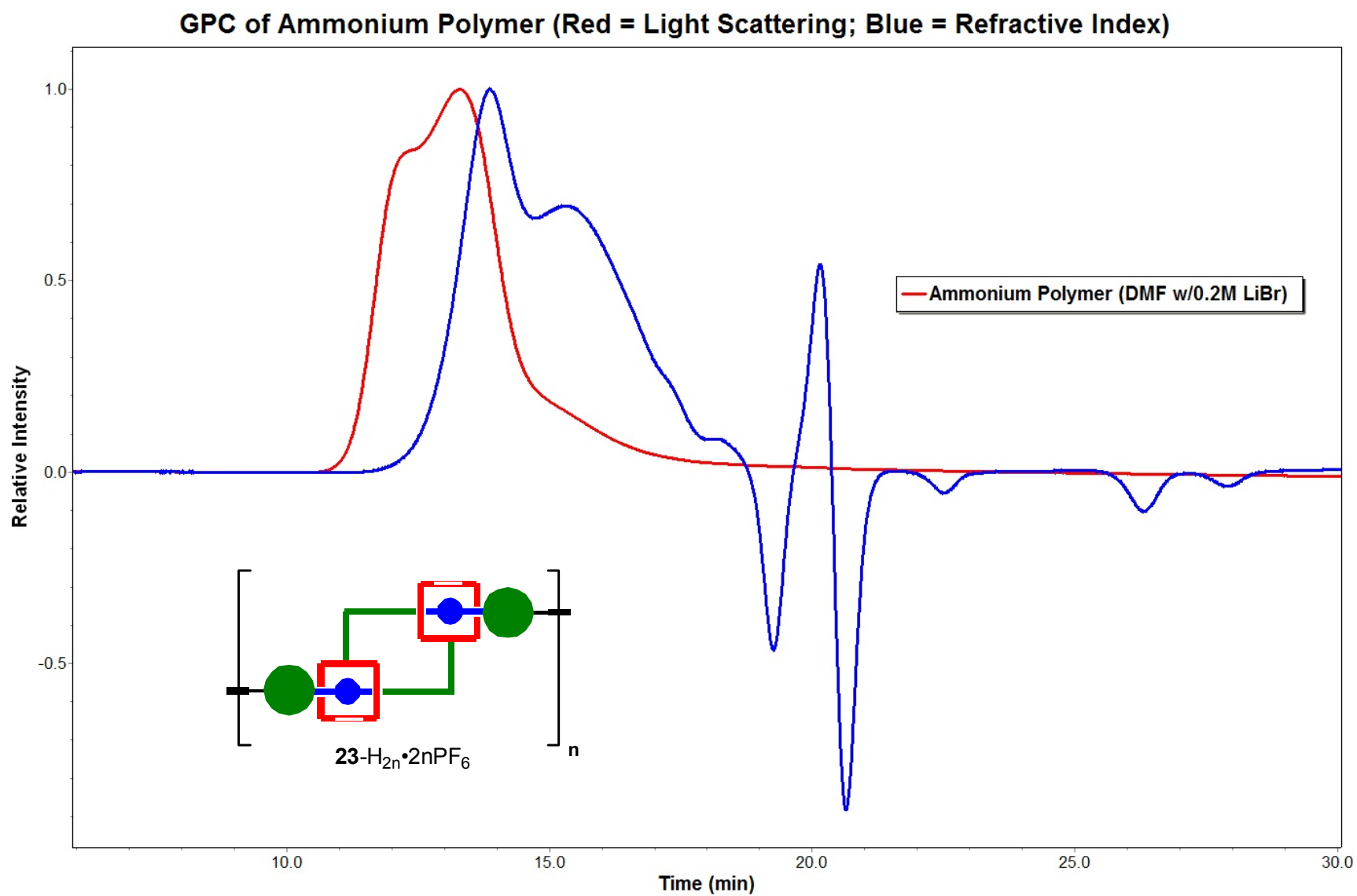


$^1\text{H}$  NMR ( $\text{CD}_2\text{Cl}_2$ ) of:

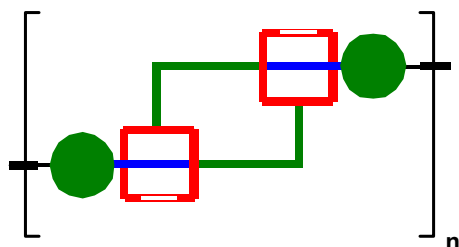




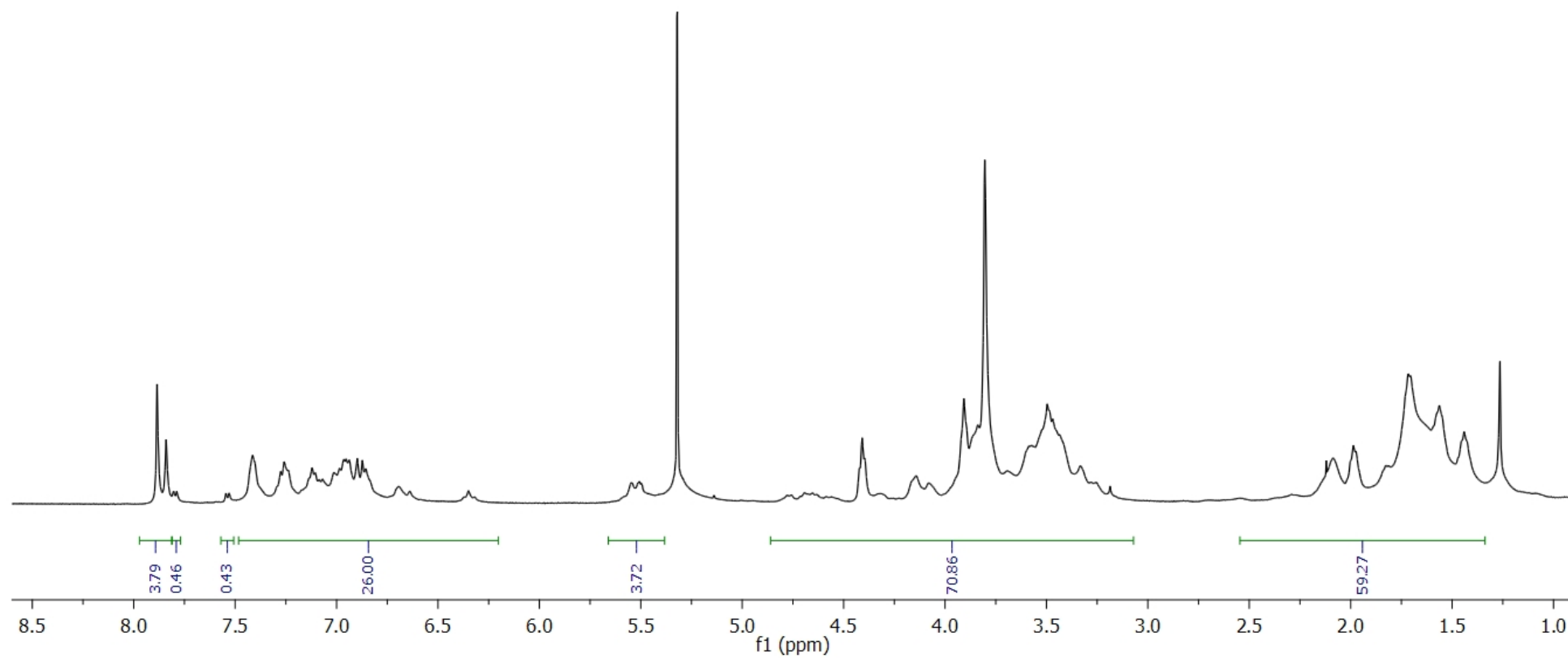




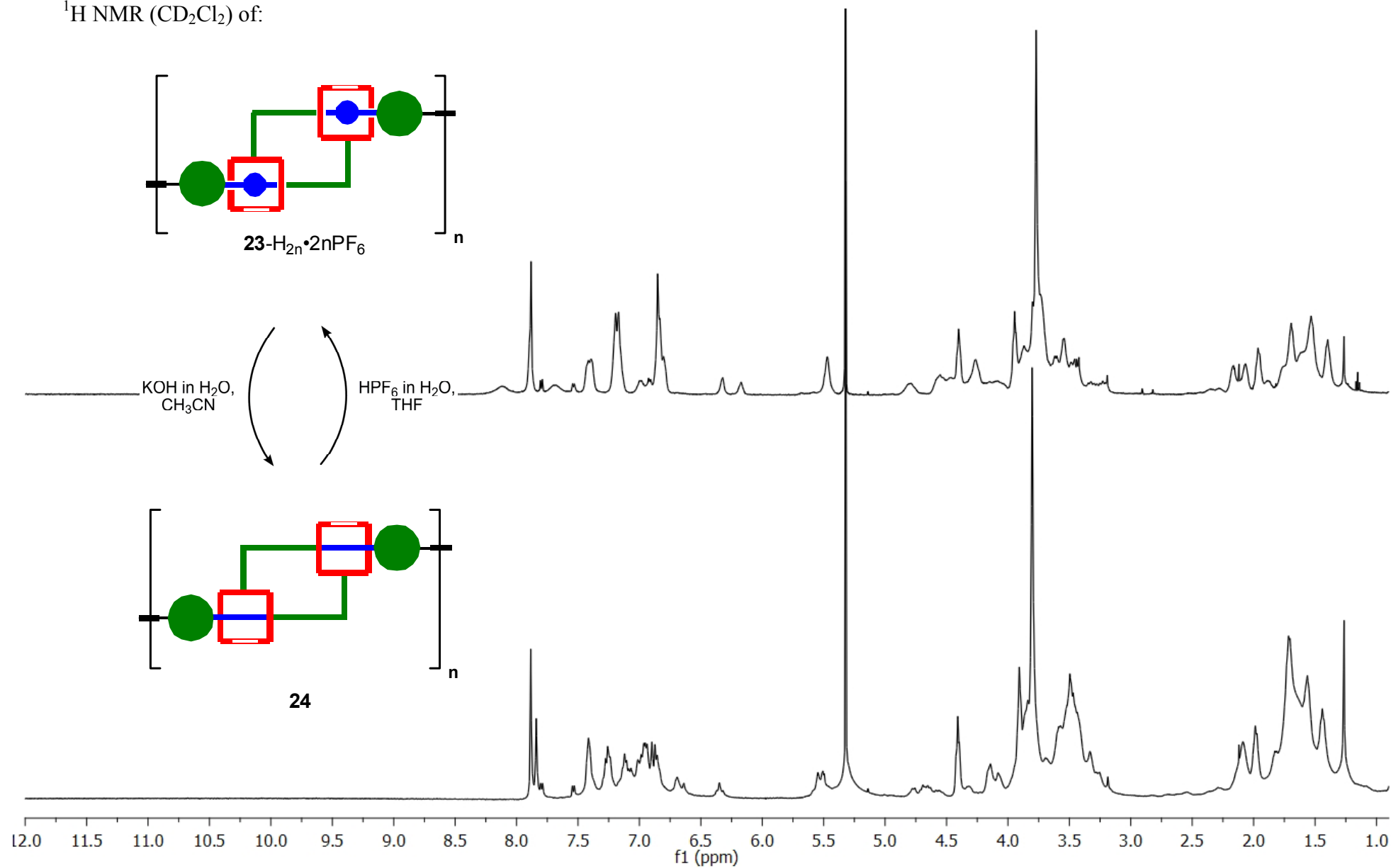
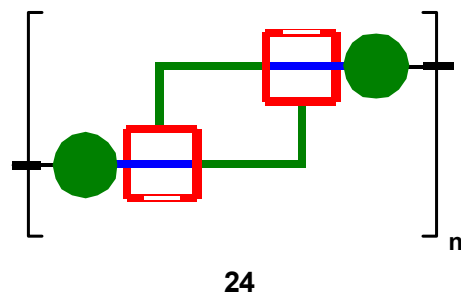
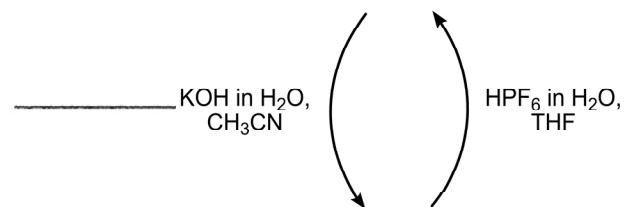
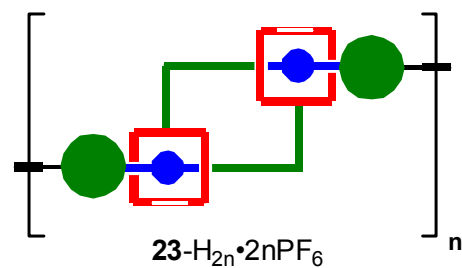
$^1\text{H}$  NMR of:



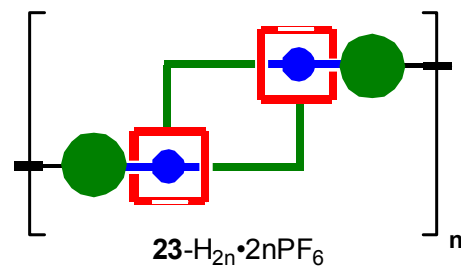
24



$^1\text{H}$  NMR ( $\text{CD}_2\text{Cl}_2$ ) of:

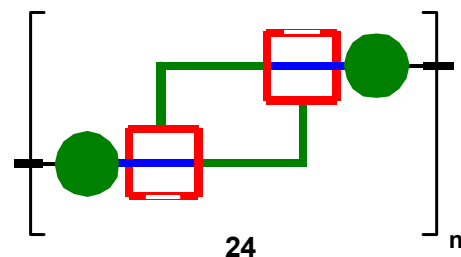


$^1\text{H}$  NMR (1:1  $\text{CD}_3\text{CN}/\text{d}_8\text{-THF}$ ) of:



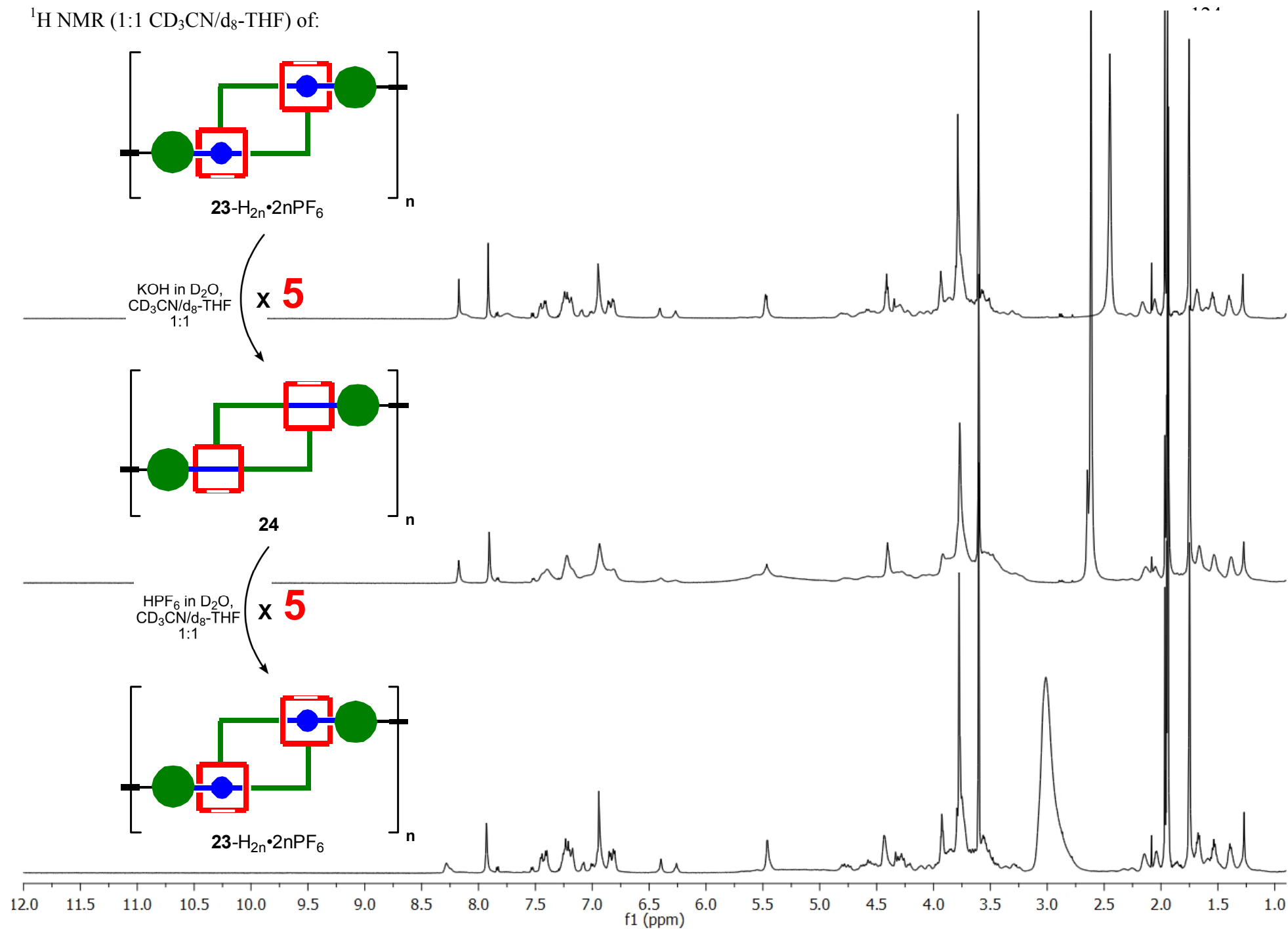
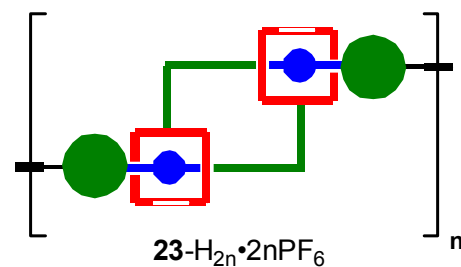
$\text{KOH in D}_2\text{O},$   
 $\text{CD}_3\text{CN}/\text{d}_8\text{-THF}$   
1:1

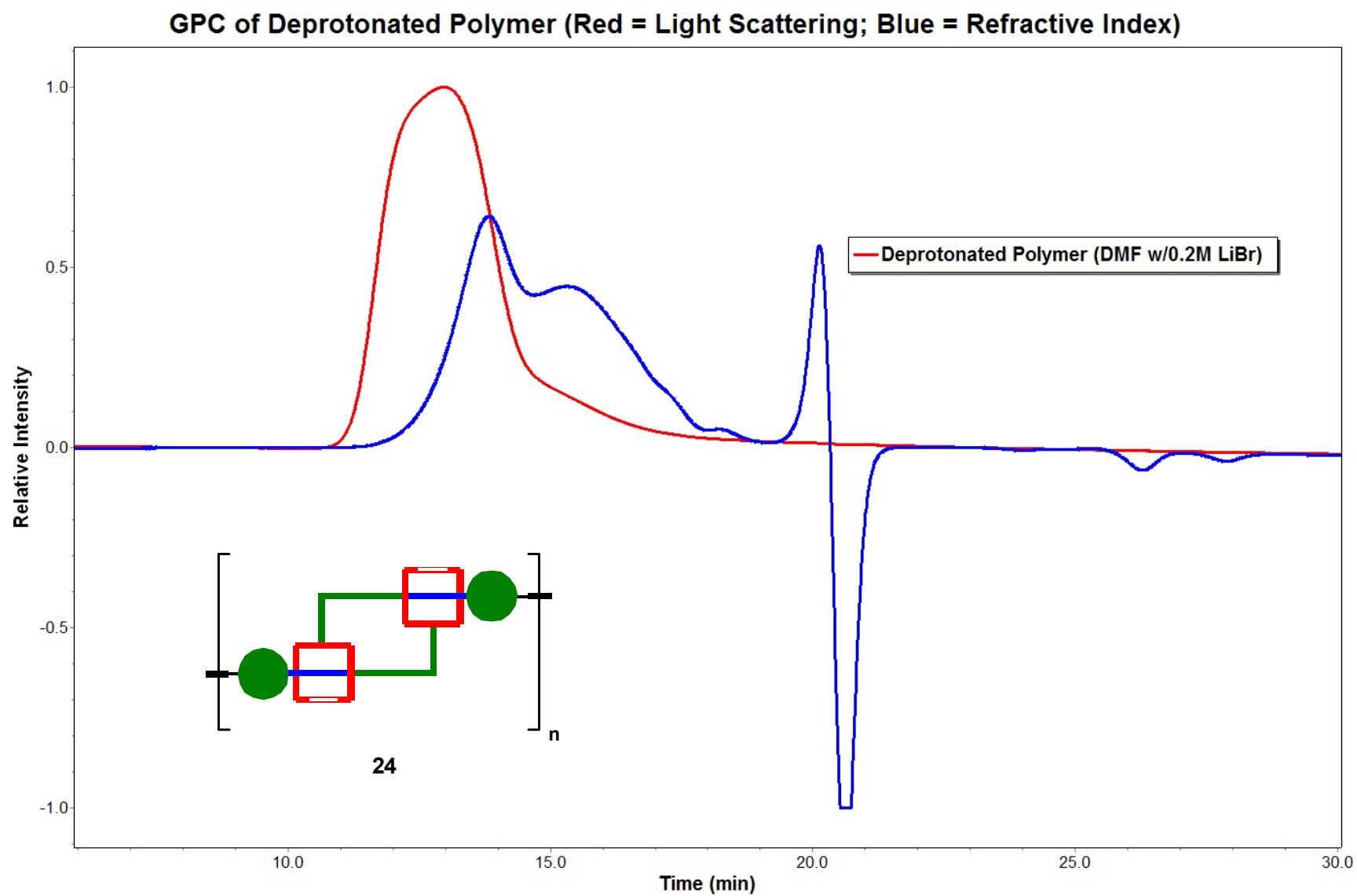
$\times 5$



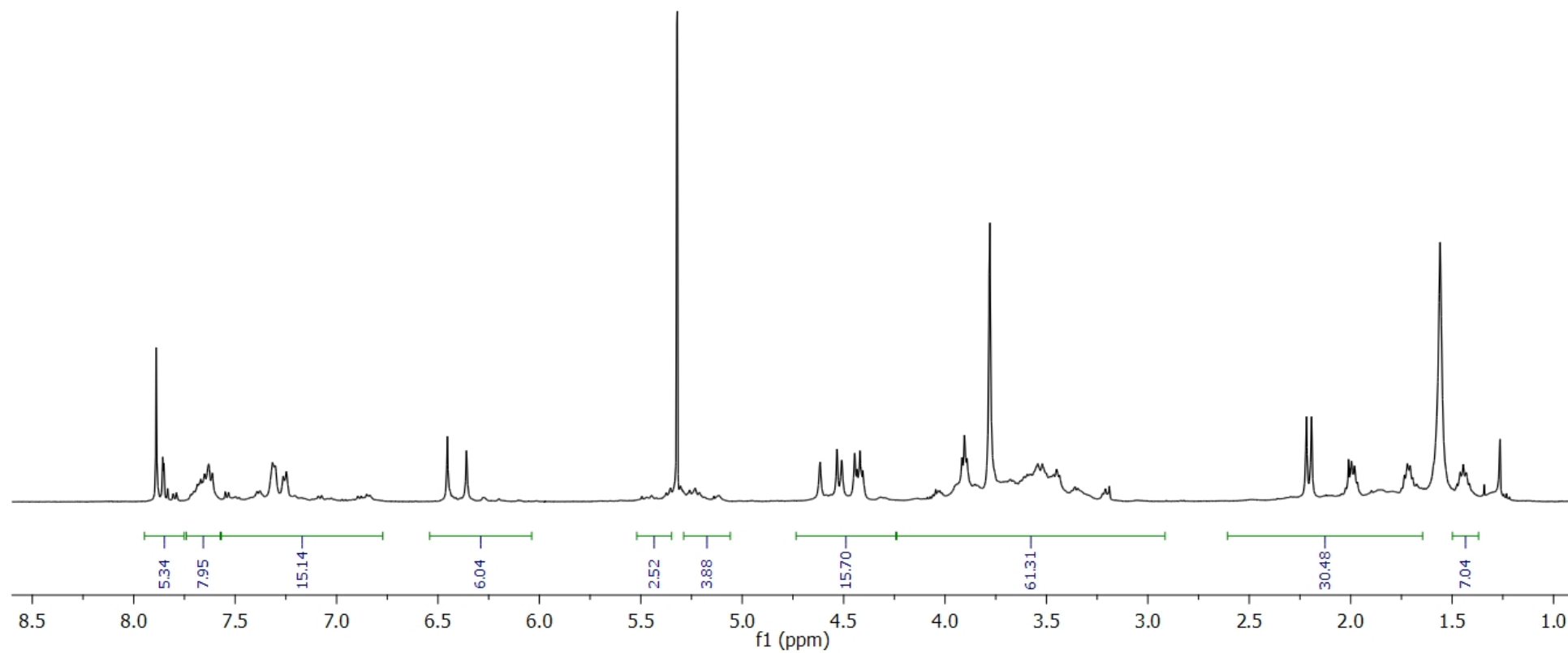
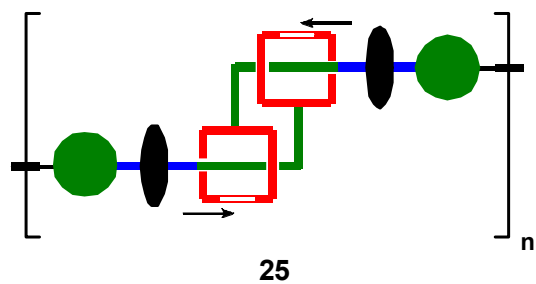
$\text{HPF}_6 \text{ in D}_2\text{O},$   
 $\text{CD}_3\text{CN}/\text{d}_8\text{-THF}$   
1:1

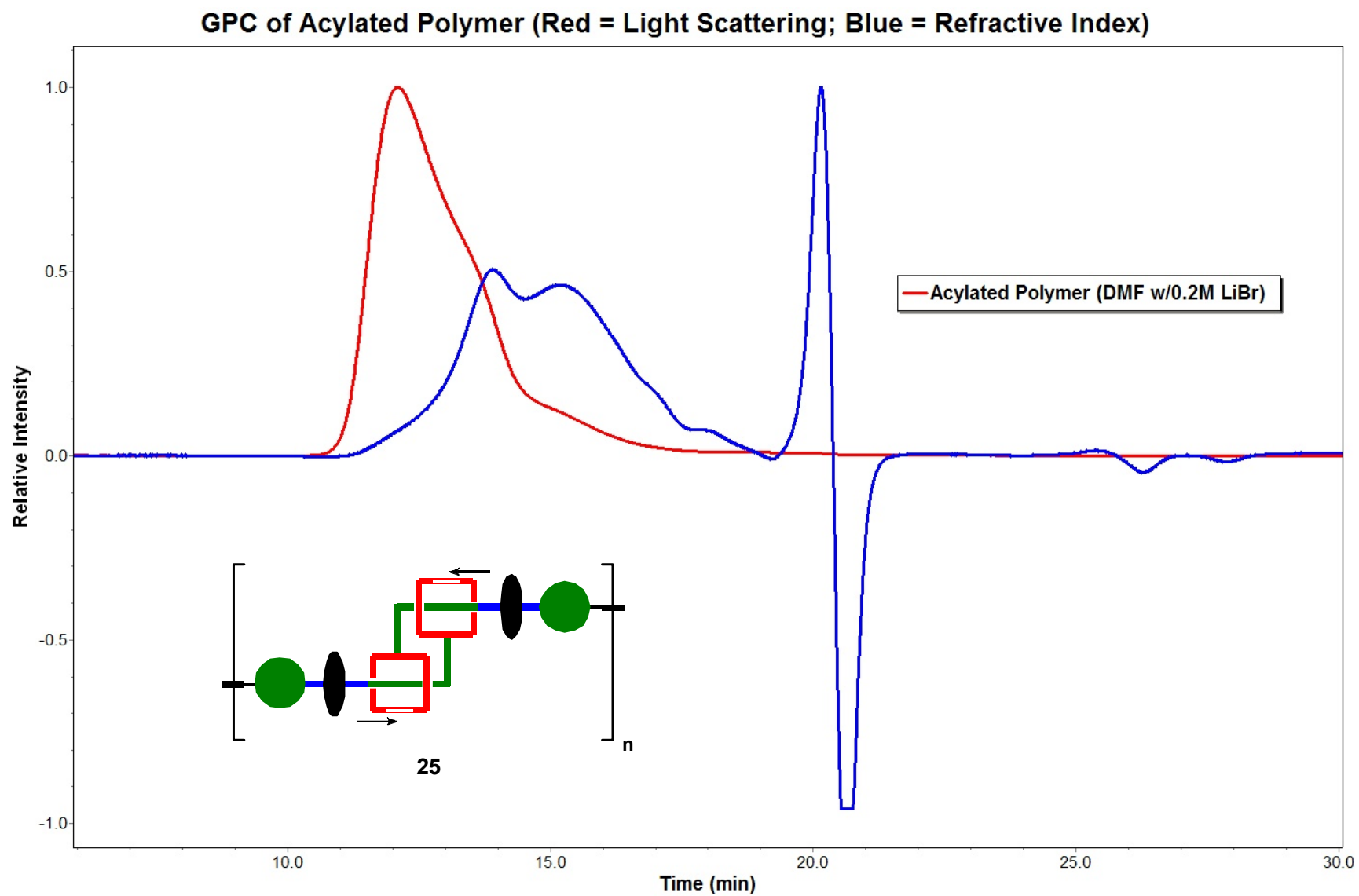
$\times 5$



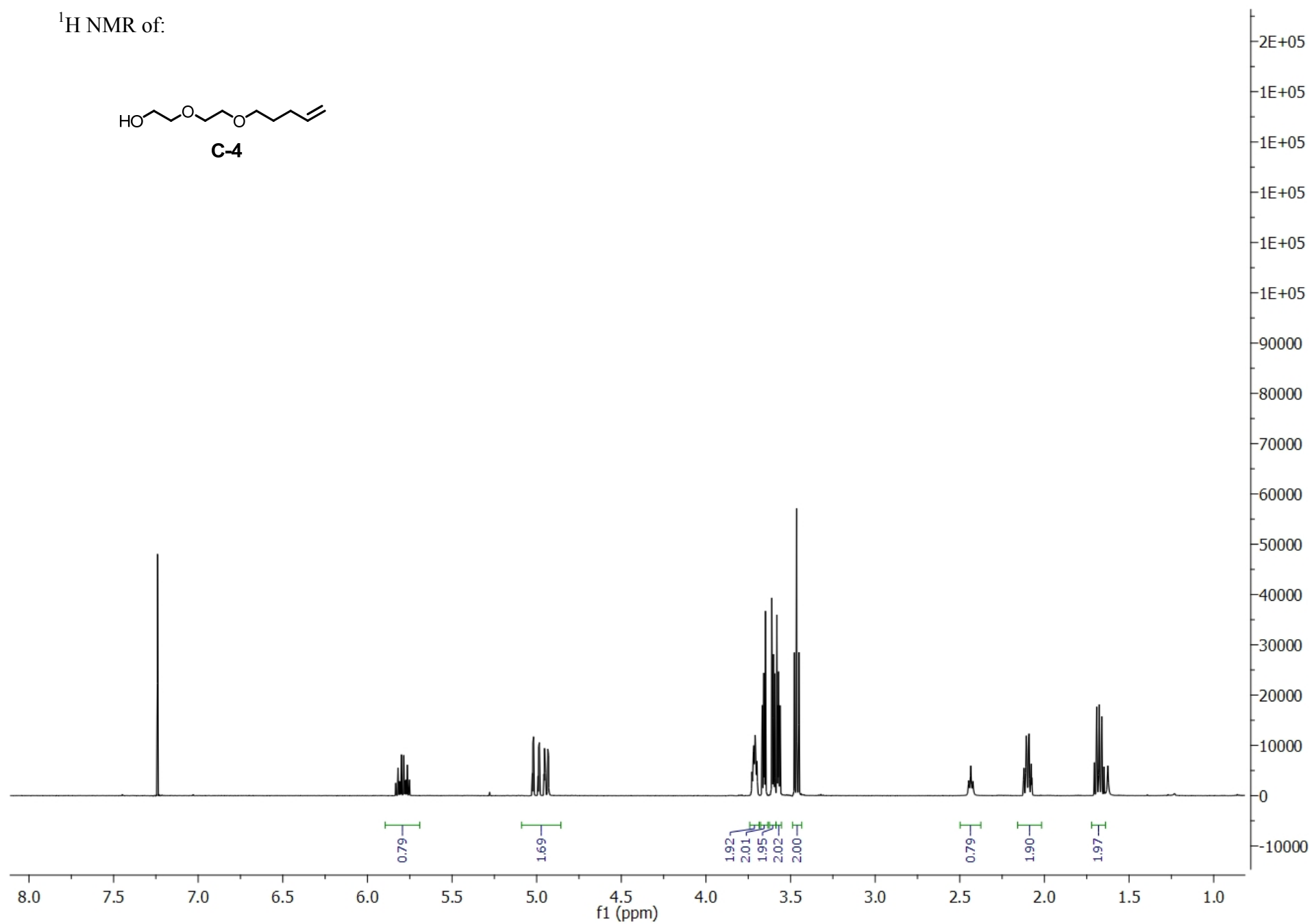
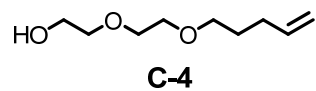


$^1\text{H}$  NMR of:



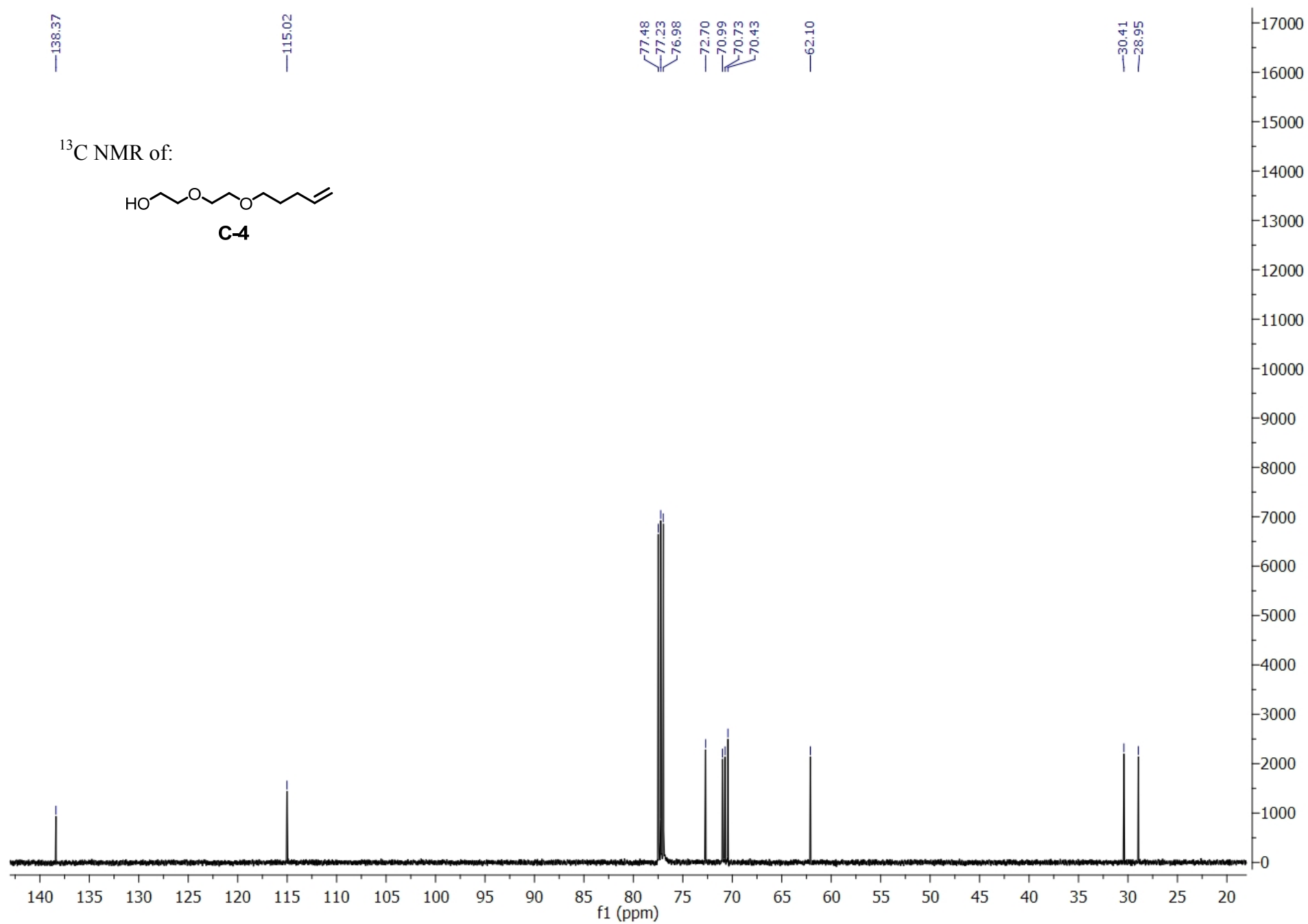
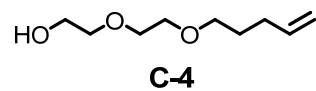


$^1\text{H}$  NMR of:

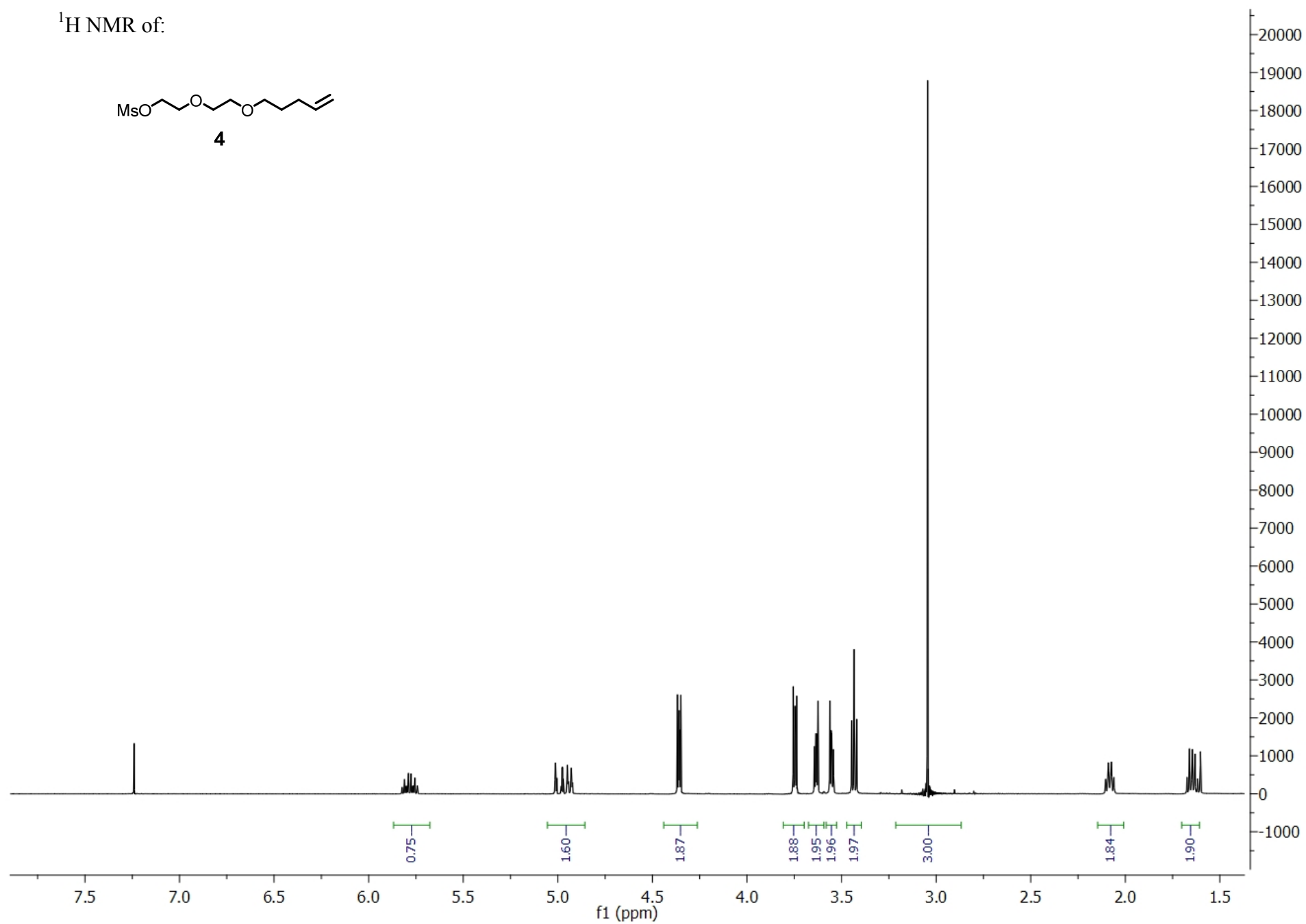
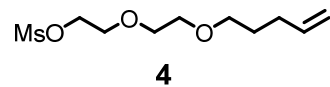




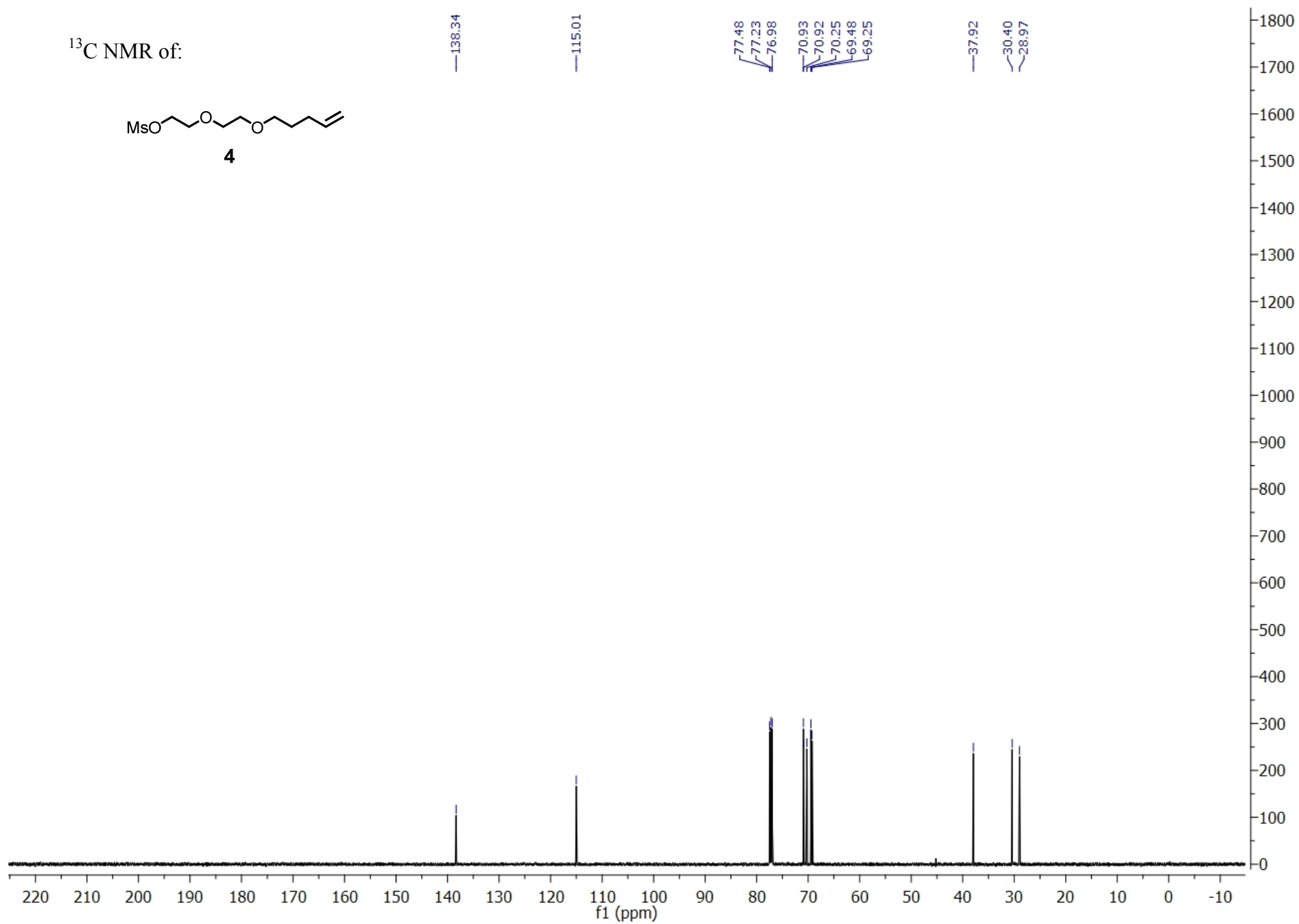
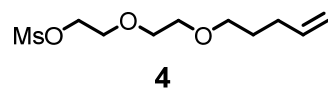
$^{13}\text{C}$  NMR of:



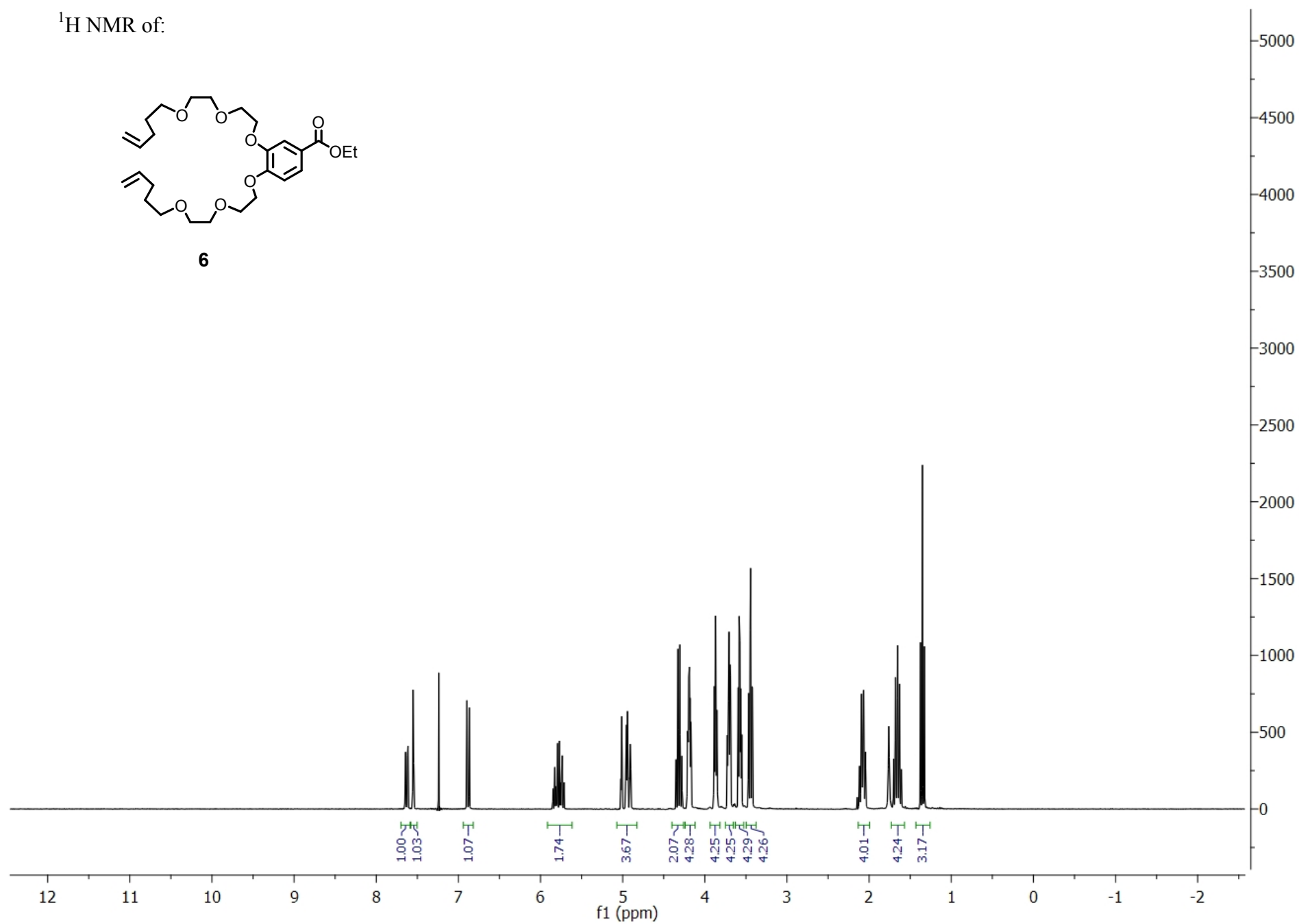
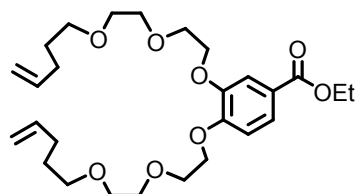
<sup>1</sup>H NMR of:



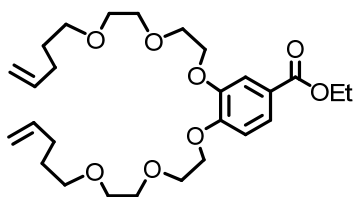
$^{13}\text{C}$  NMR of:



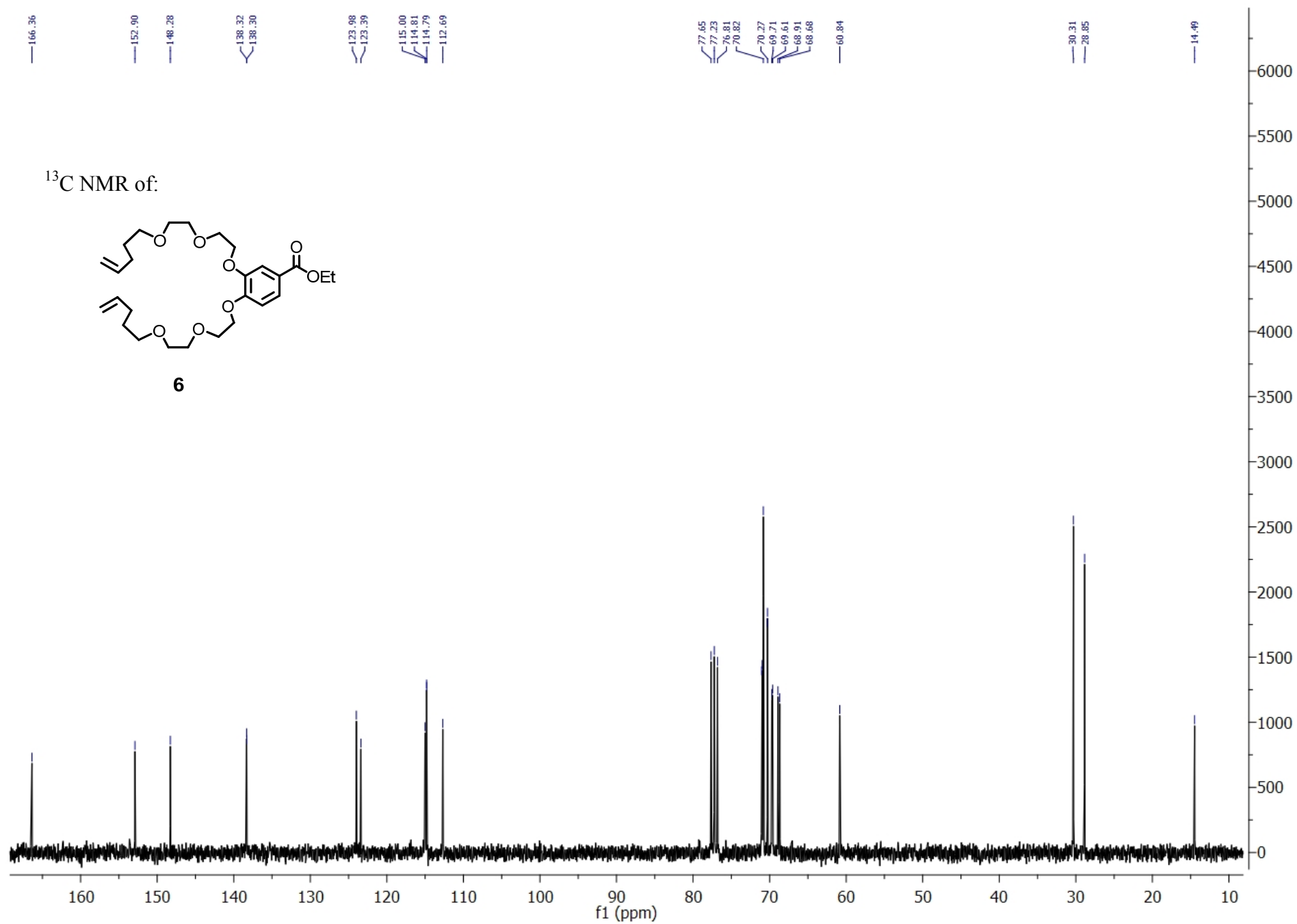
$^1\text{H}$  NMR of:



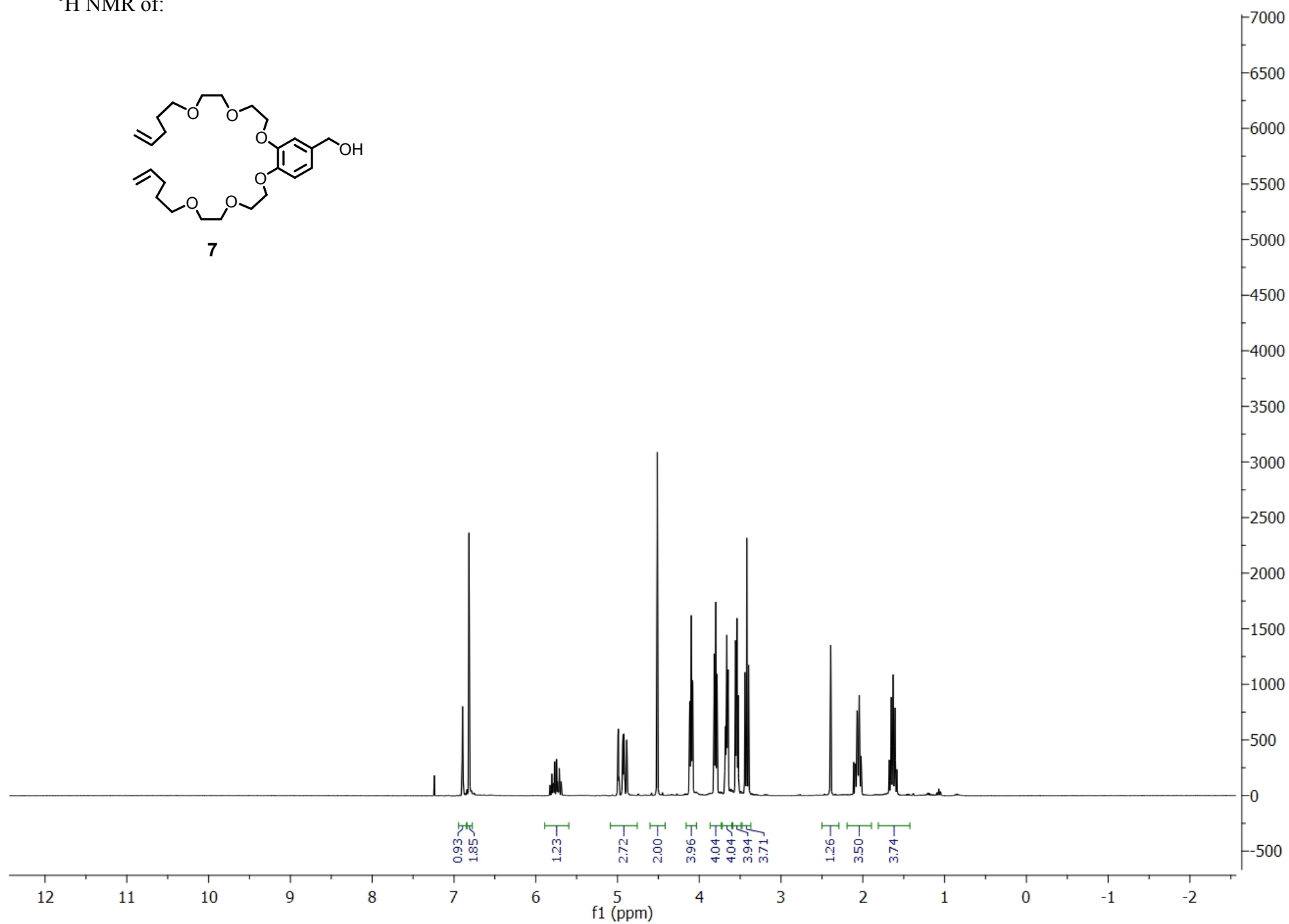
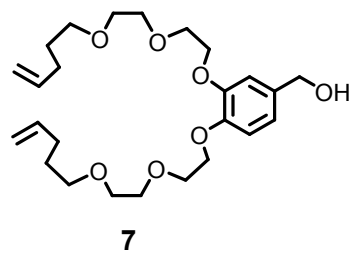
$^{13}\text{C}$  NMR of:

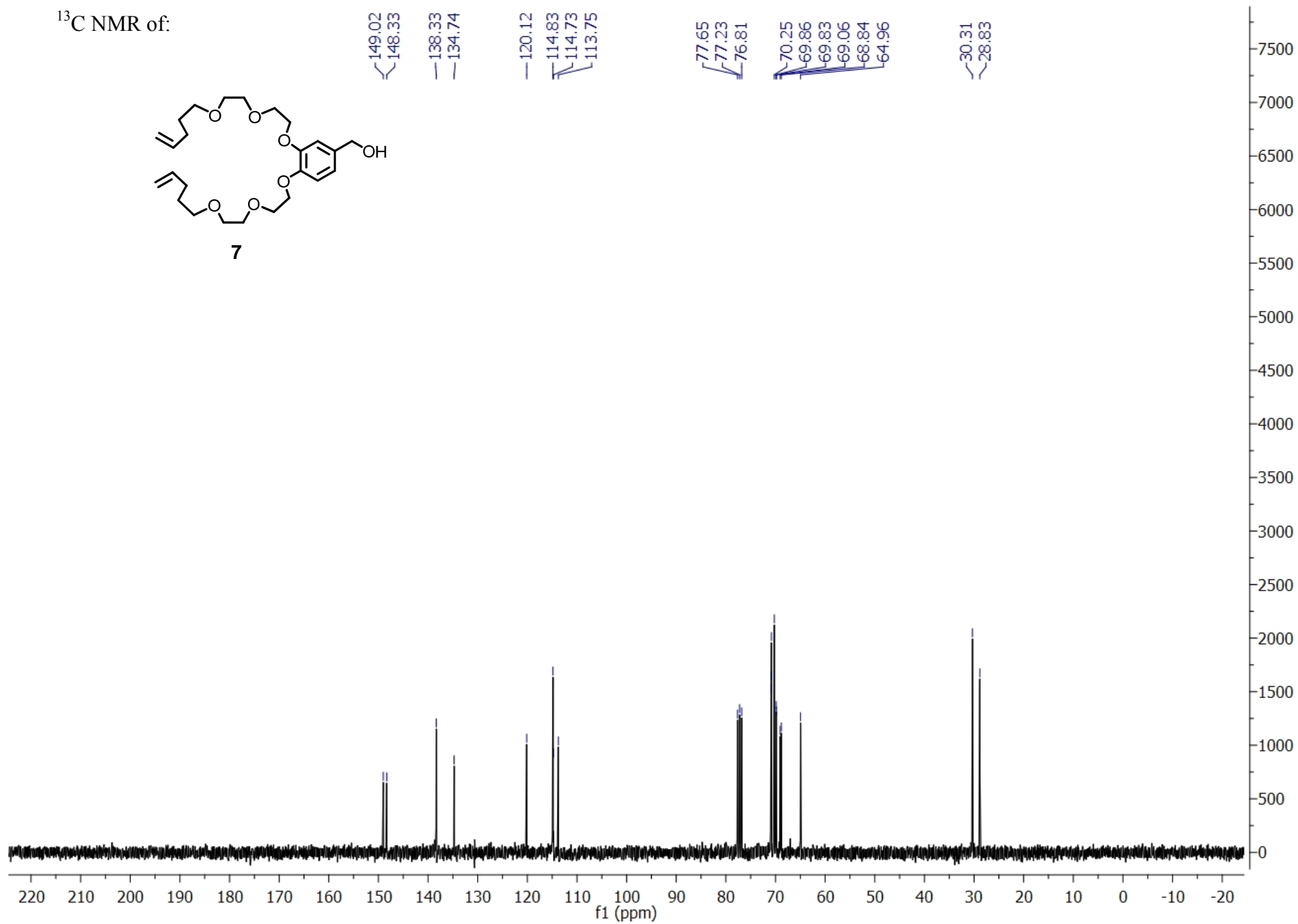
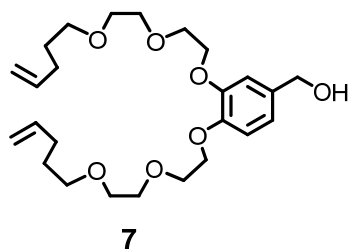


**6**

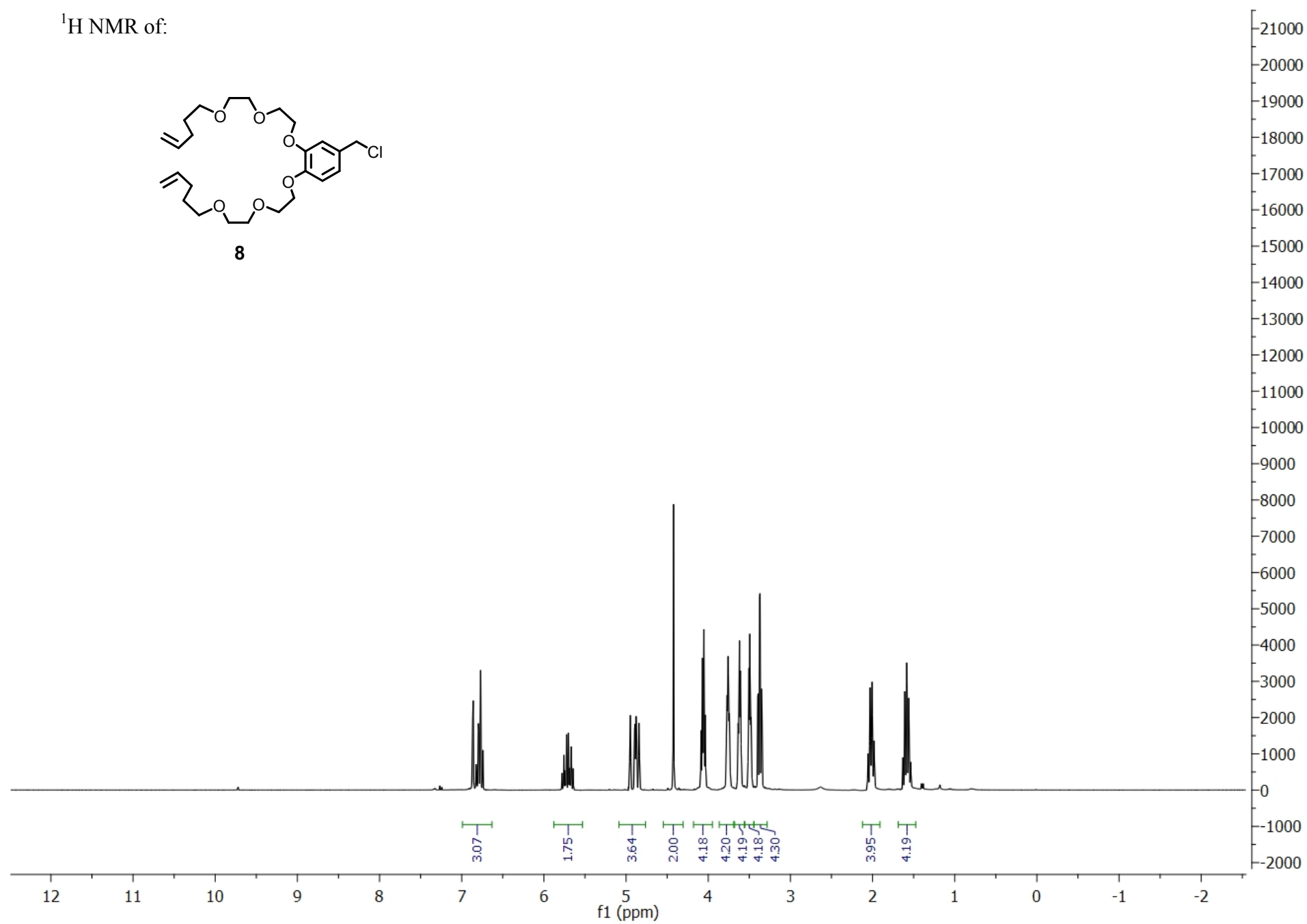
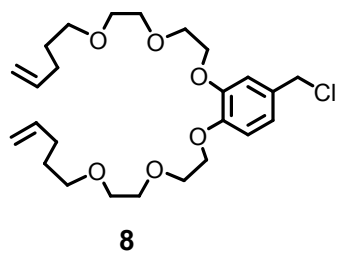


$^1\text{H}$  NMR of:



<sup>13</sup>C NMR of:

$^1\text{H}$  NMR of:





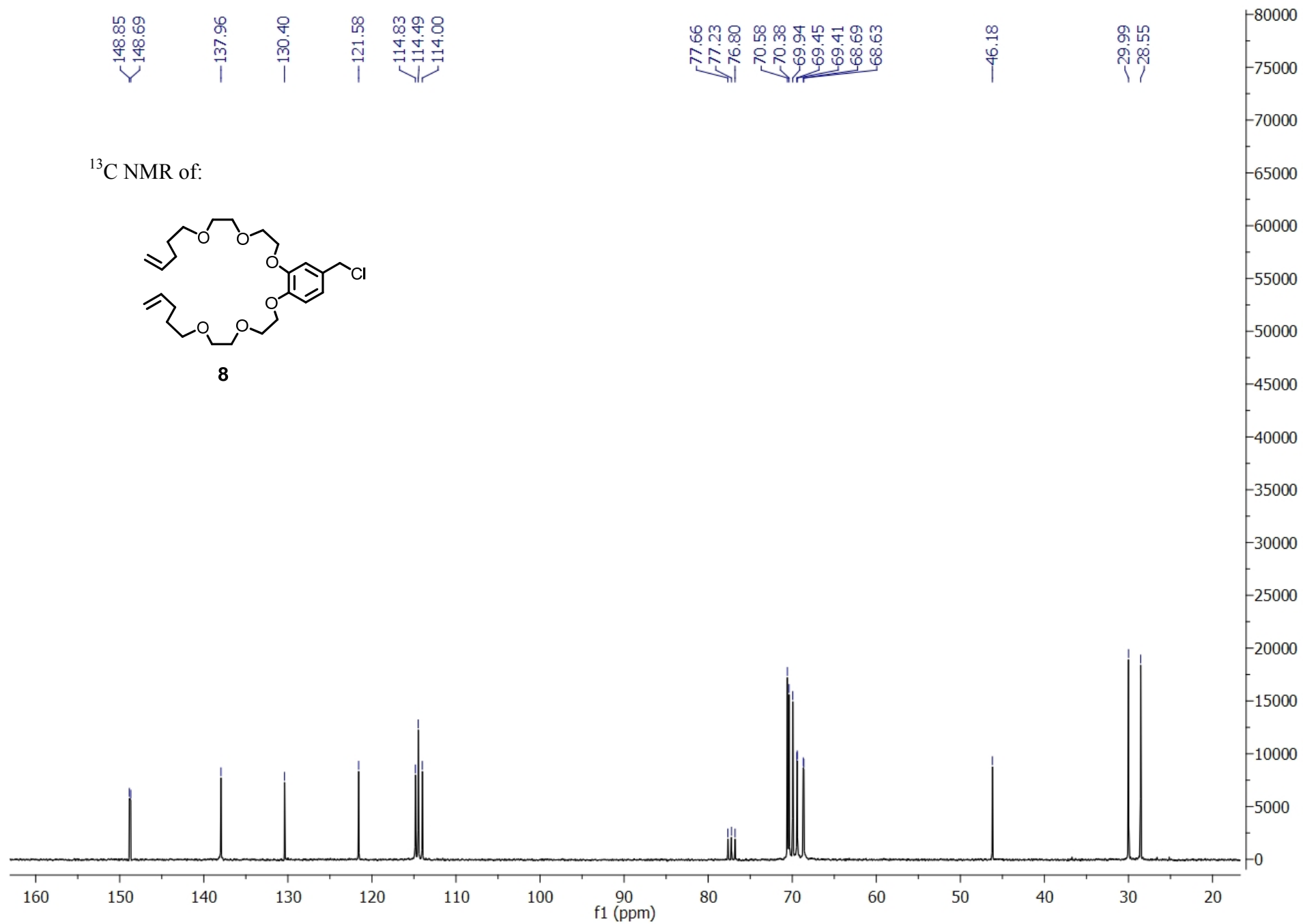
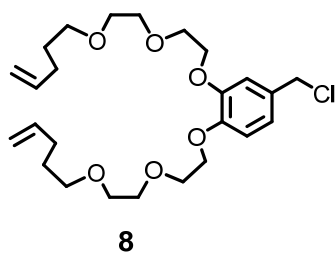
$\sim 148.85$   
 $\sim 148.69$   
 $\sim 137.96$   
 $\sim 130.40$   
 $\sim 121.58$   
 $\sim 114.83$   
 $\sim 114.49$   
 $\sim 114.00$

$\sim 77.66$   
 $\sim 77.23$   
 $\sim 76.80$   
 $\sim 70.58$   
 $\sim 70.38$   
 $\sim 69.94$   
 $\sim 69.45$   
 $\sim 69.41$   
 $\sim 68.69$   
 $\sim 68.63$

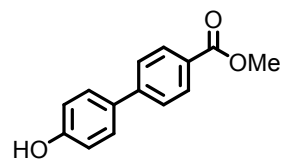
$\sim 46.18$

$\sim 29.99$   
 $\sim 28.55$

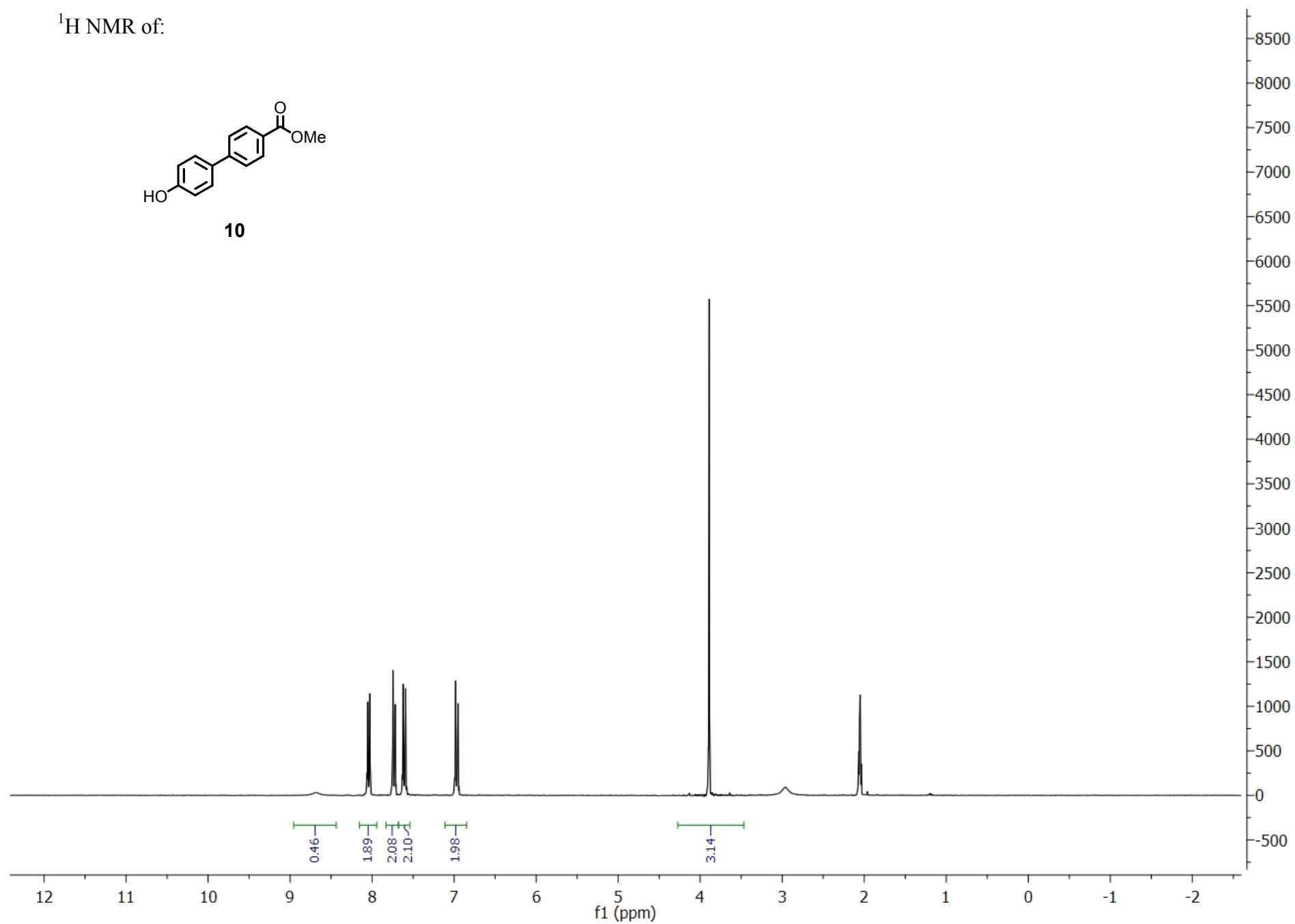
$^{13}\text{C}$  NMR of:

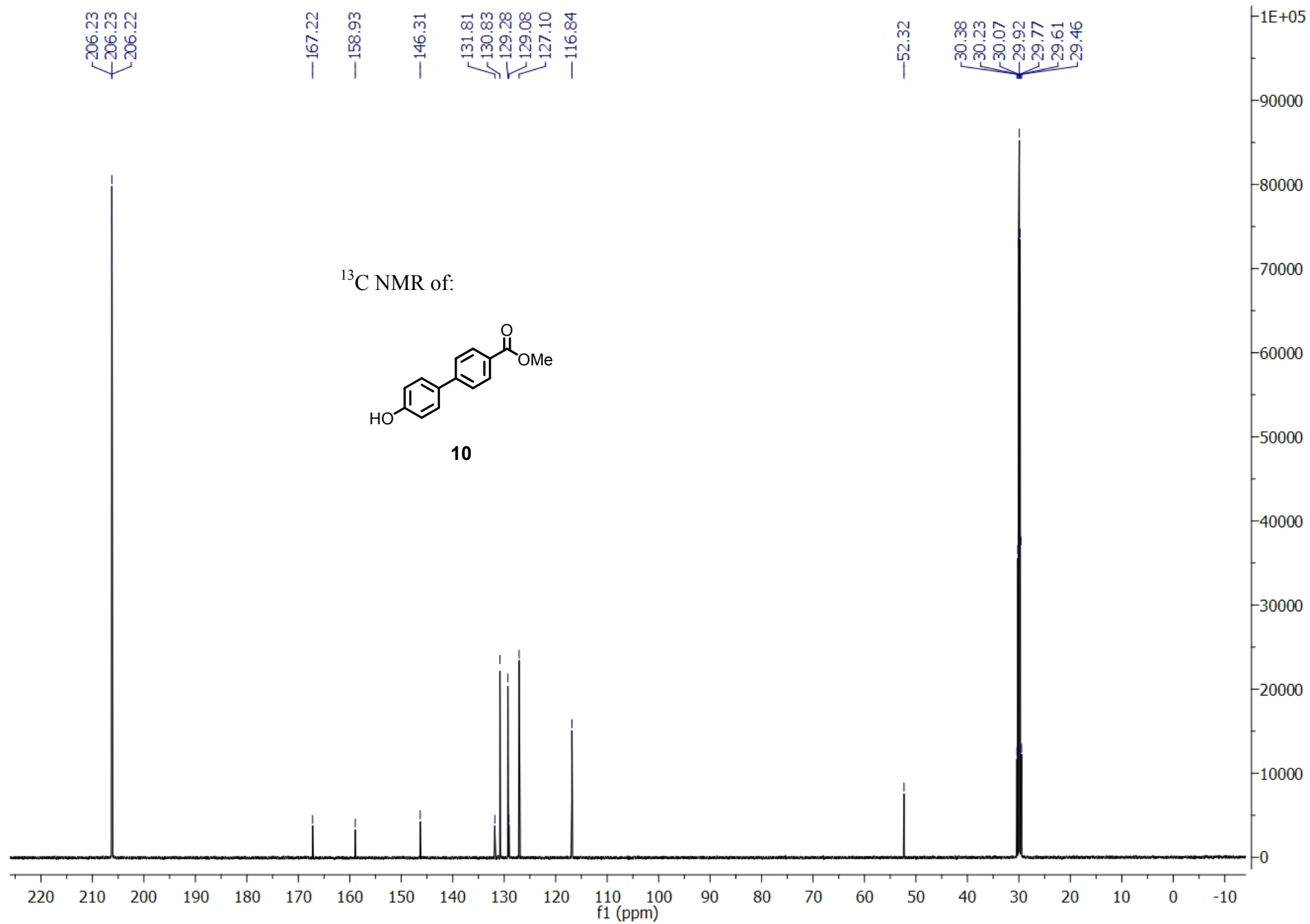


$^1\text{H}$  NMR of:

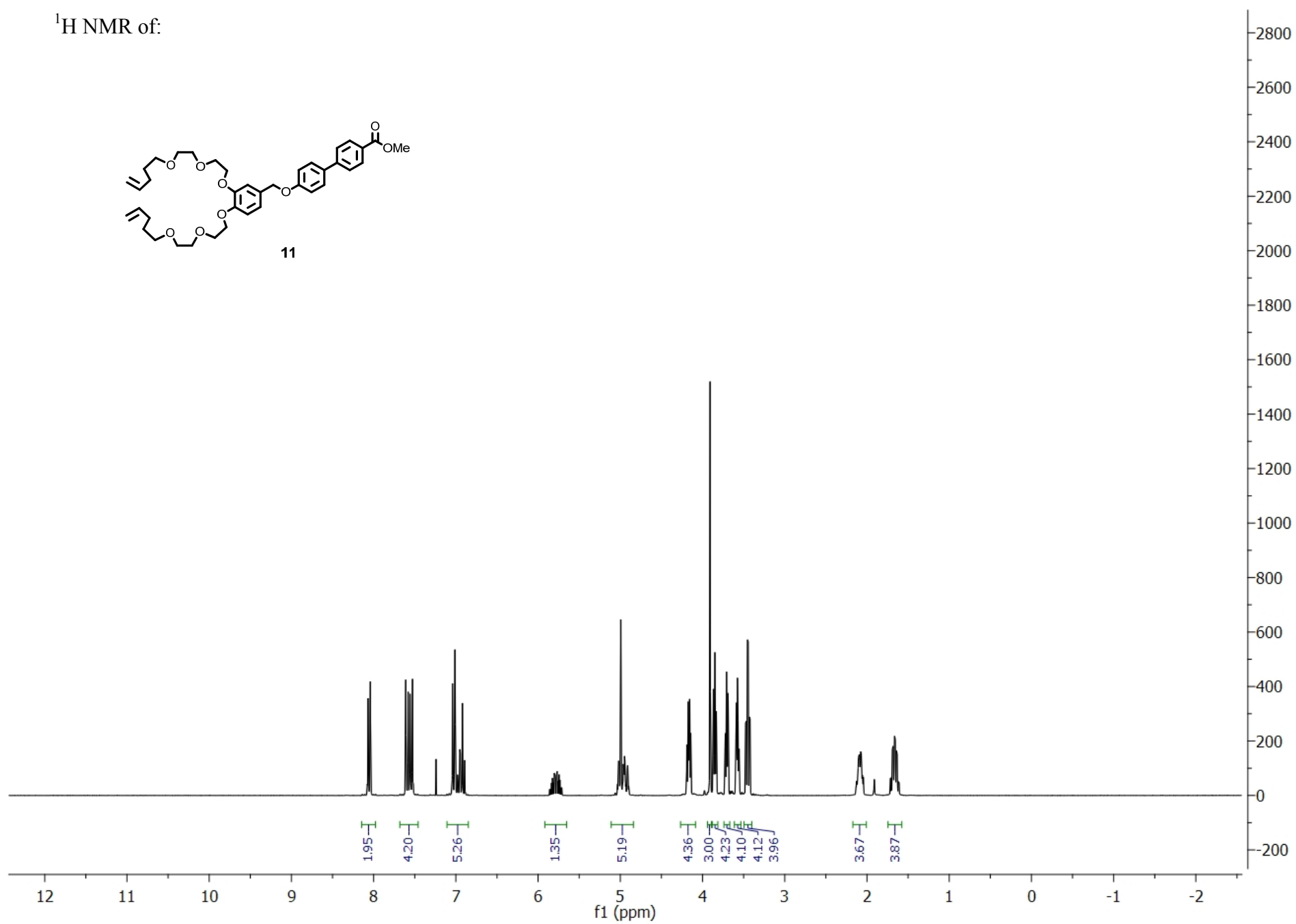
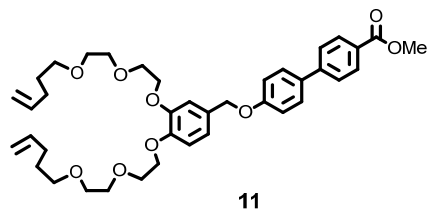


**10**

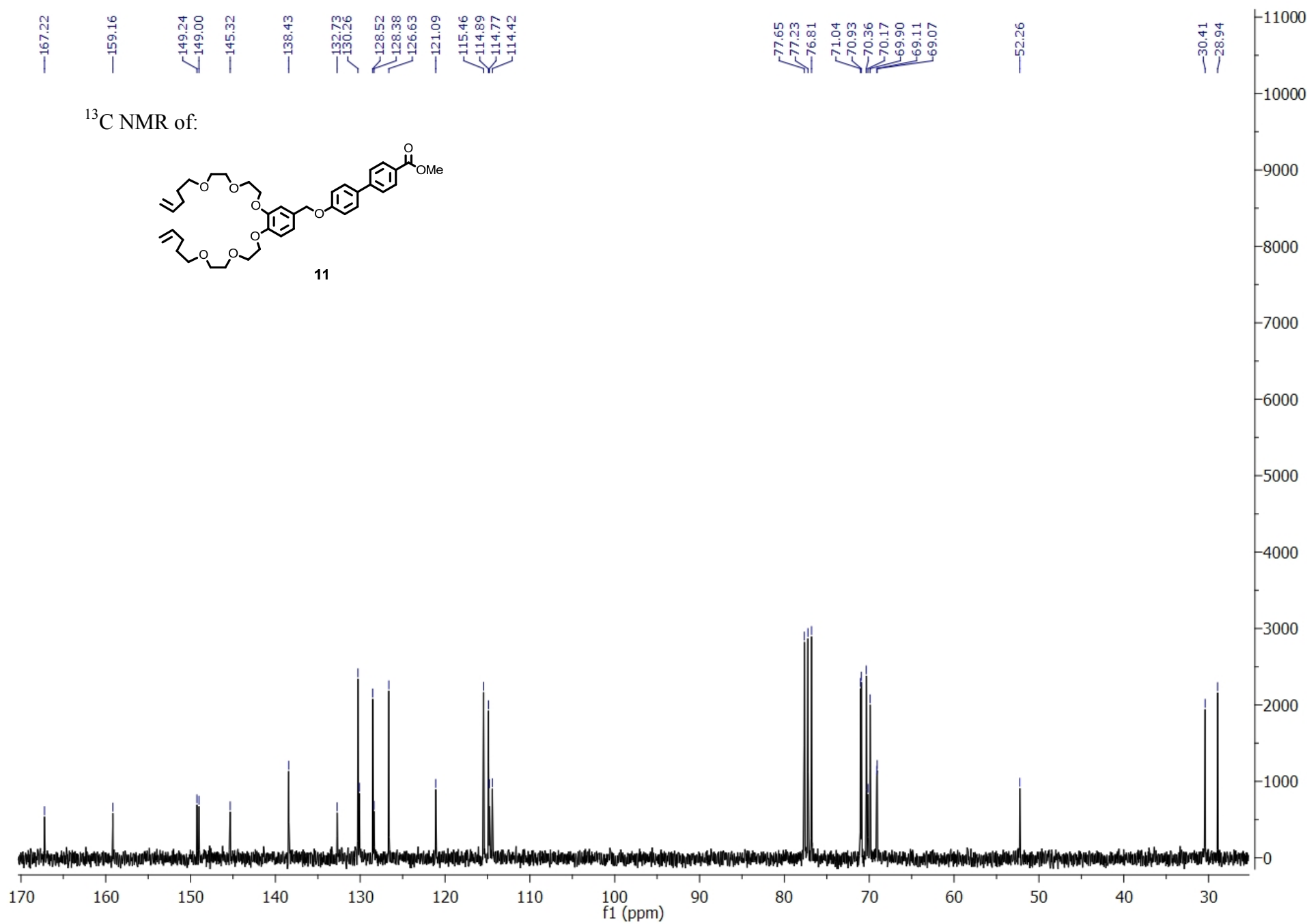
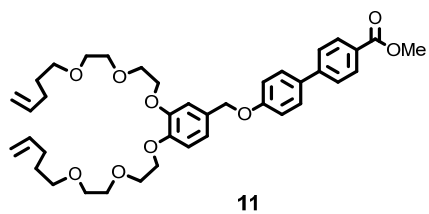


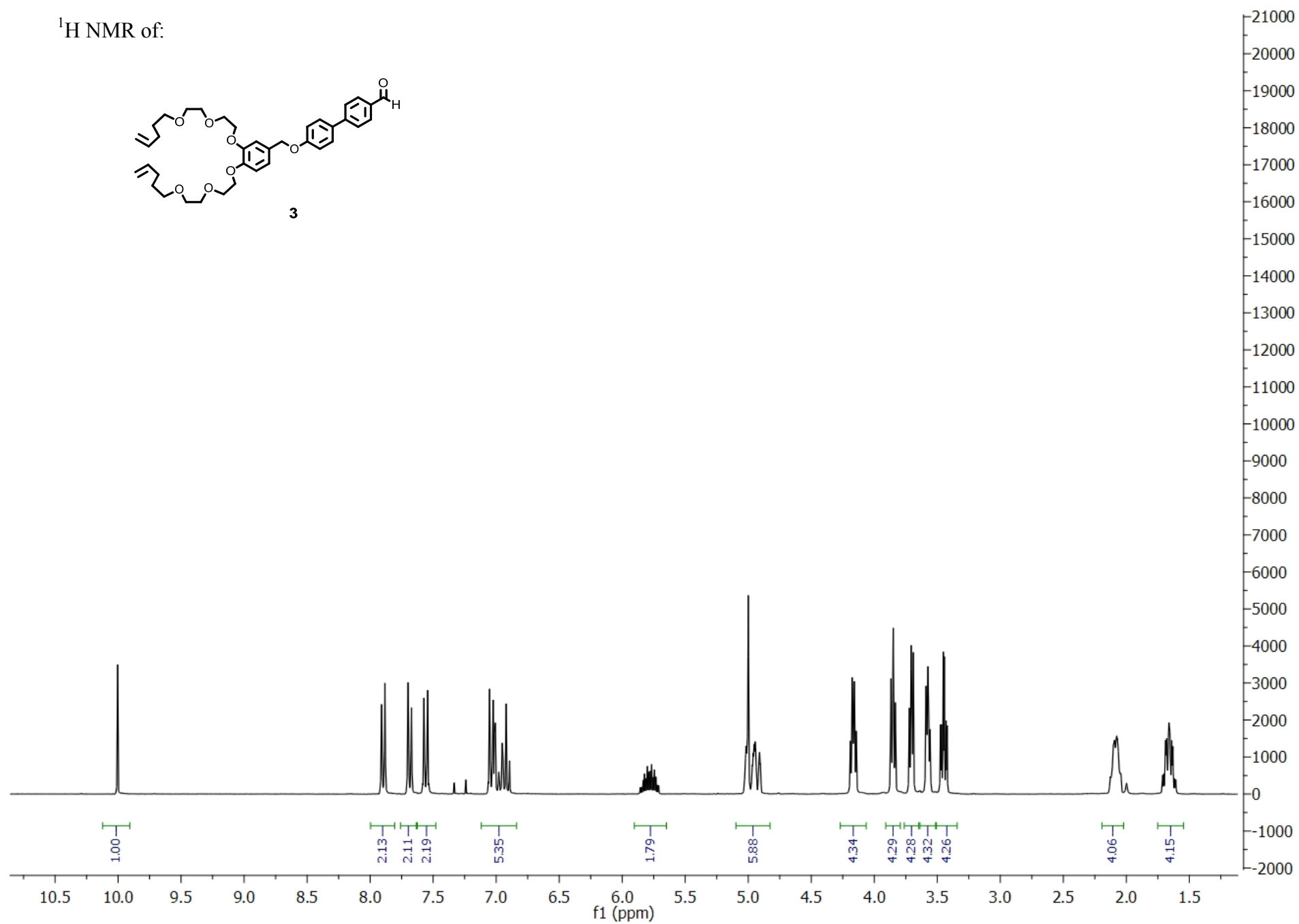
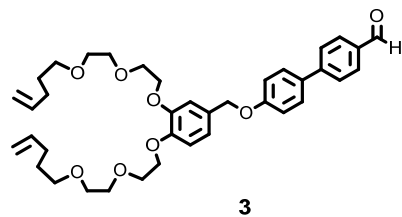


$^1\text{H}$  NMR of:

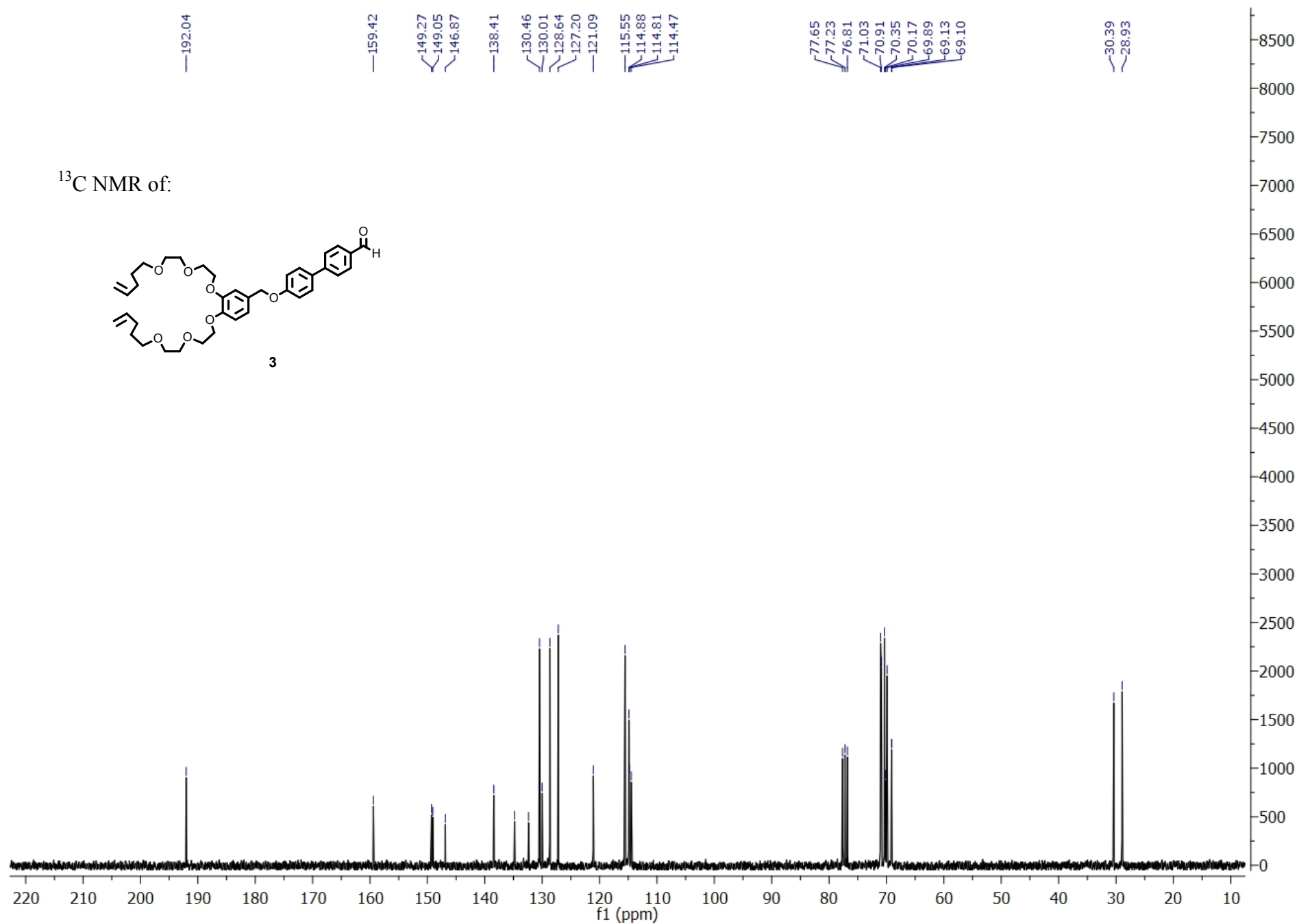
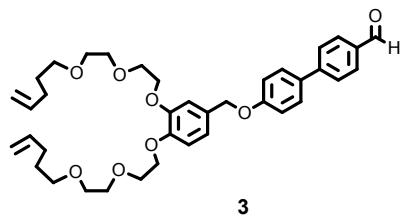


141

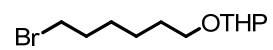
 $^{13}\text{C}$  NMR of:

<sup>1</sup>H NMR of:

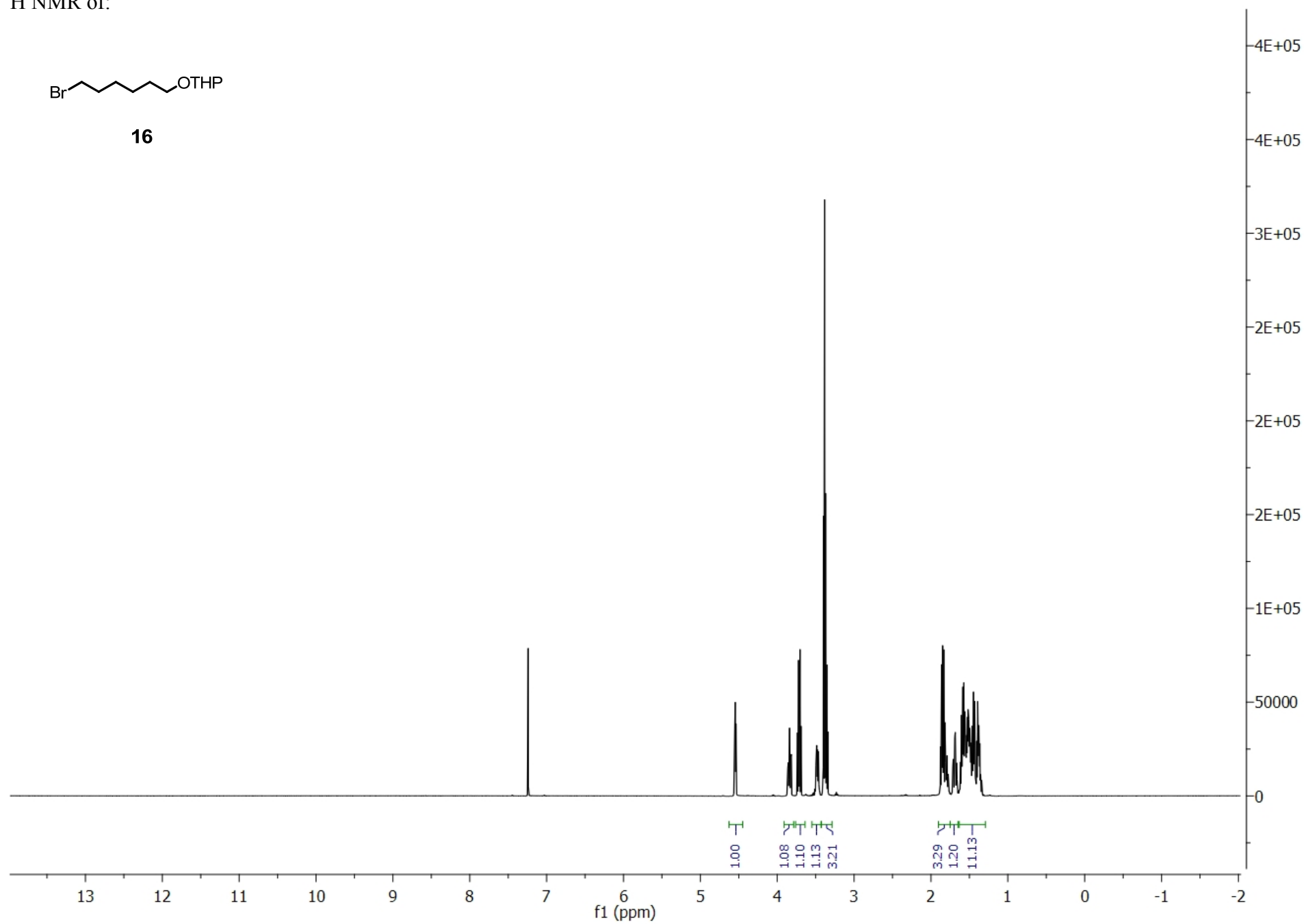
$^{13}\text{C}$  NMR of:



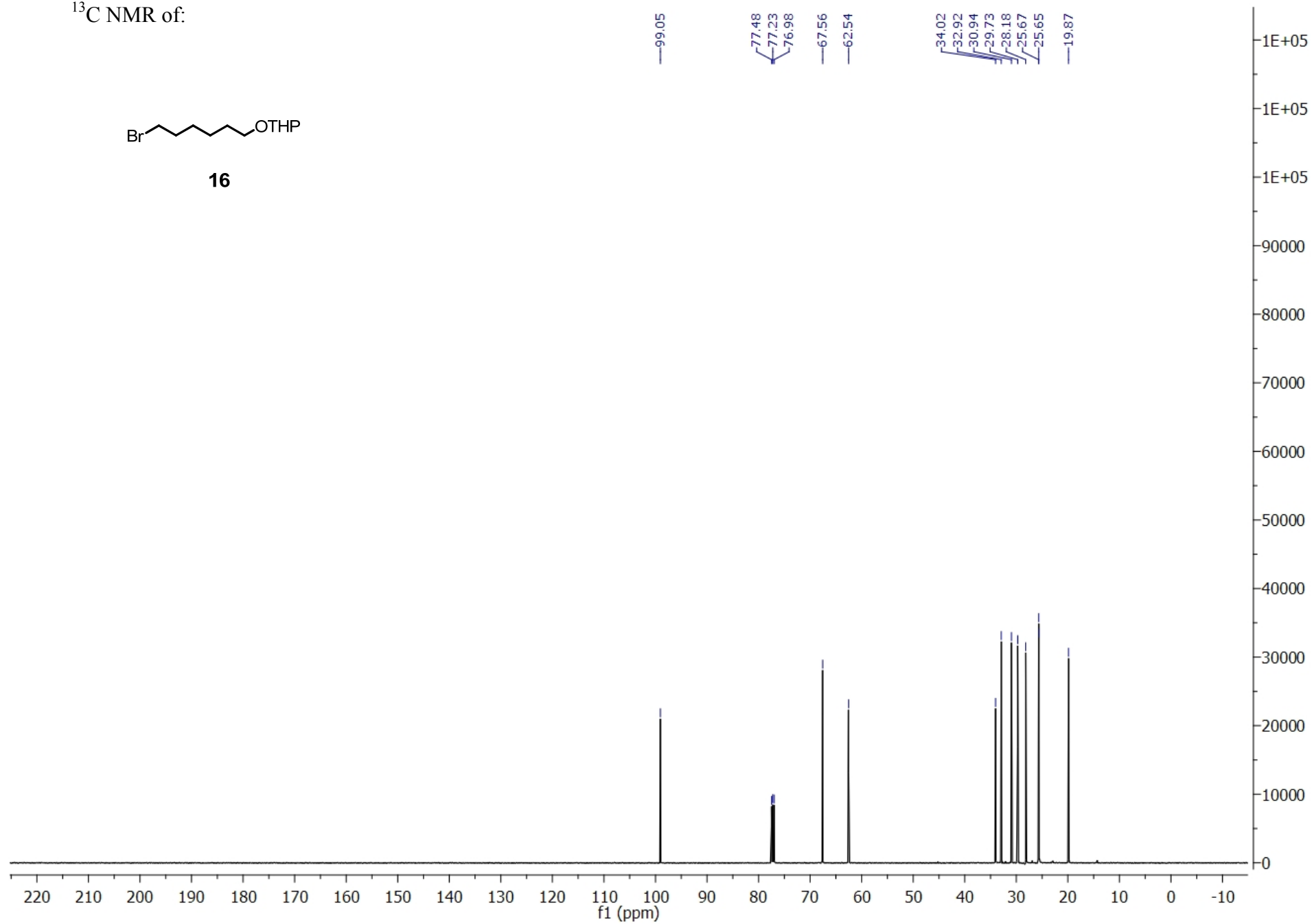
$^1\text{H}$  NMR of:



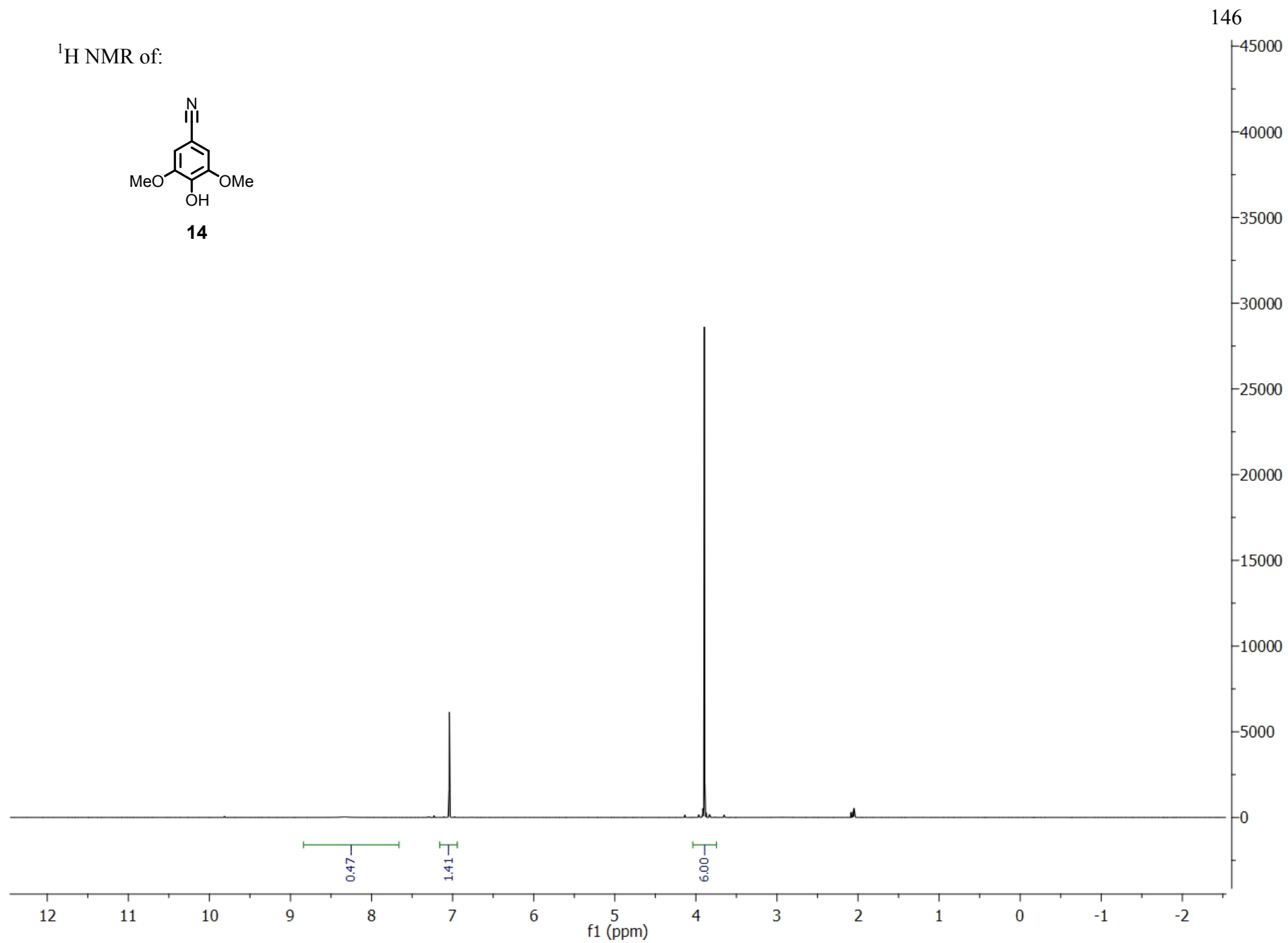
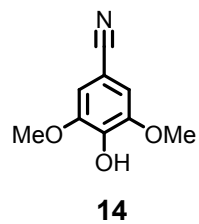
**16**



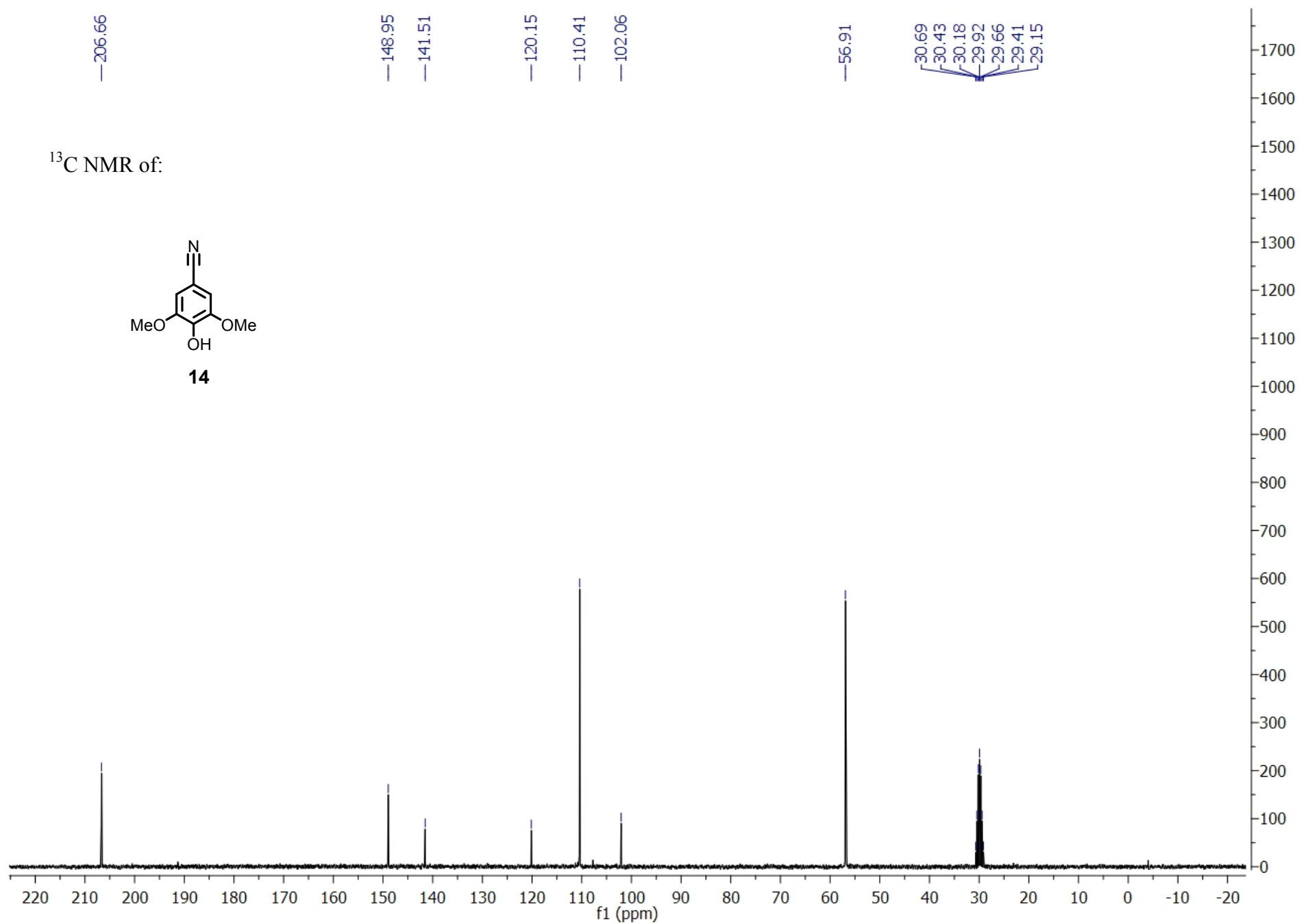
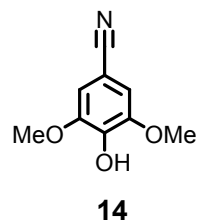


$^{13}\text{C}$  NMR of:**16**

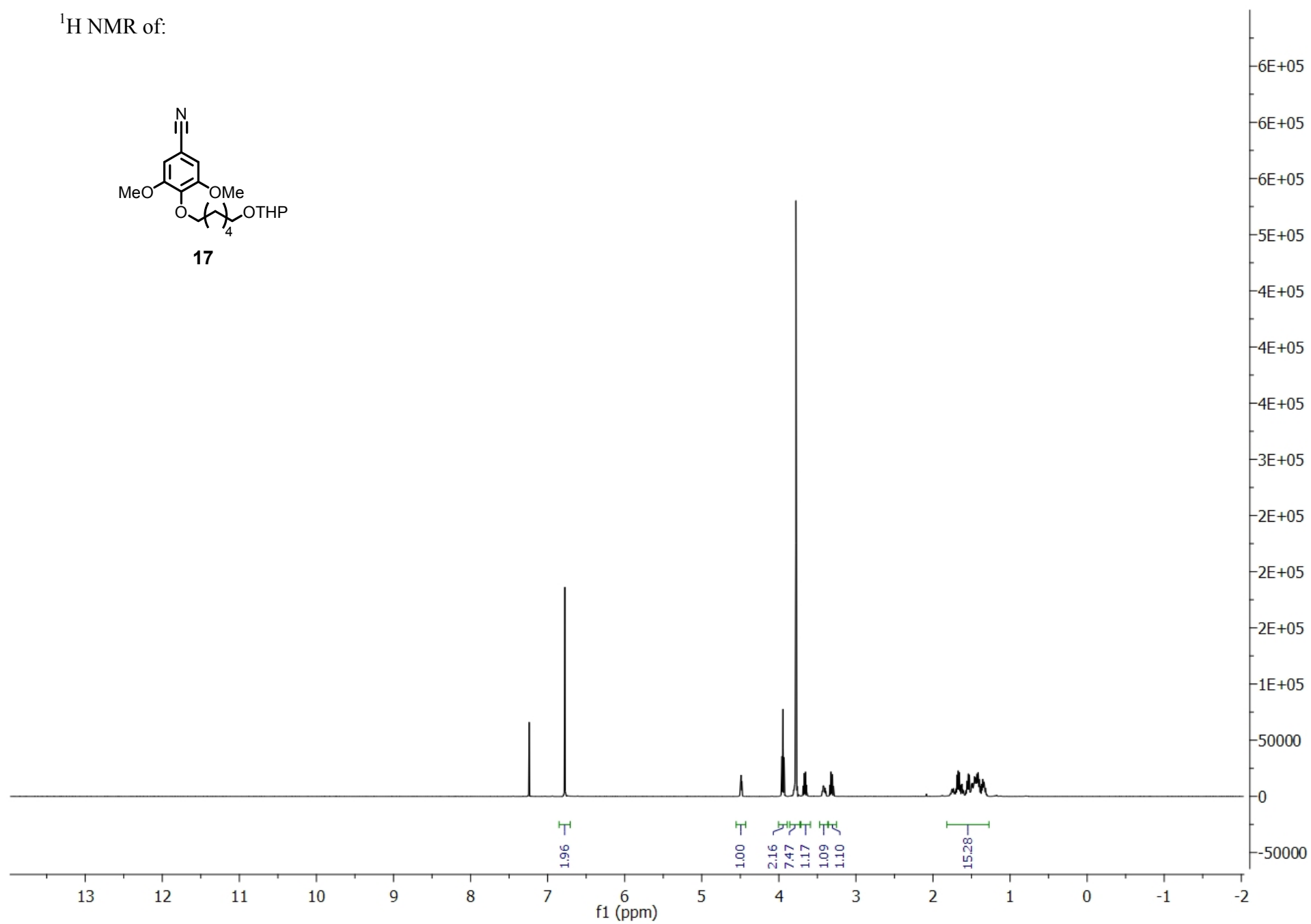
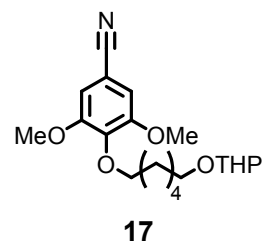
$^1\text{H}$  NMR of:



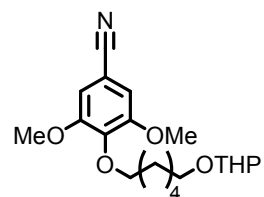
$^{13}\text{C}$  NMR of:



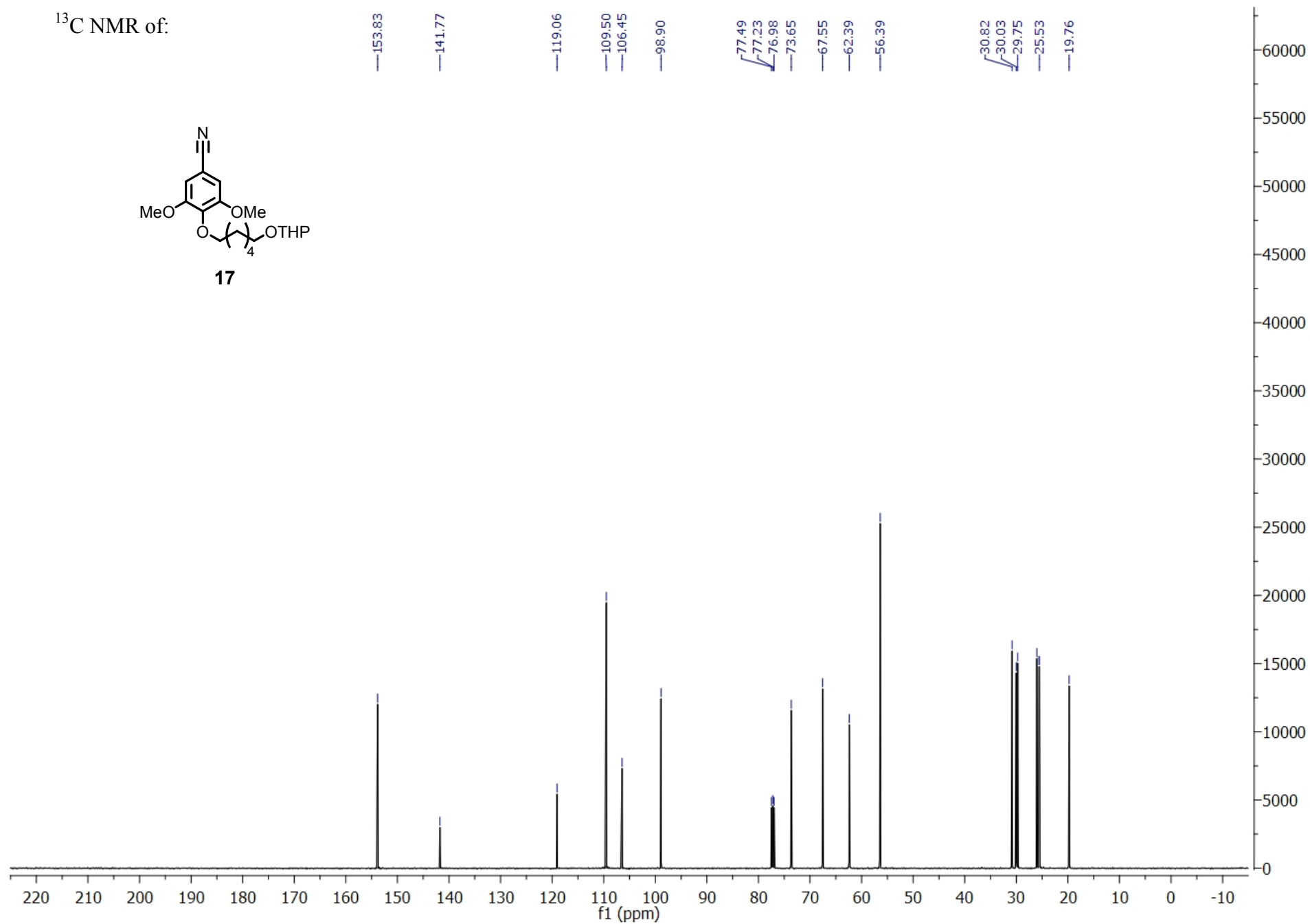
$^1\text{H}$  NMR of:



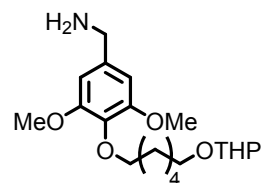
$^{13}\text{C}$  NMR of:



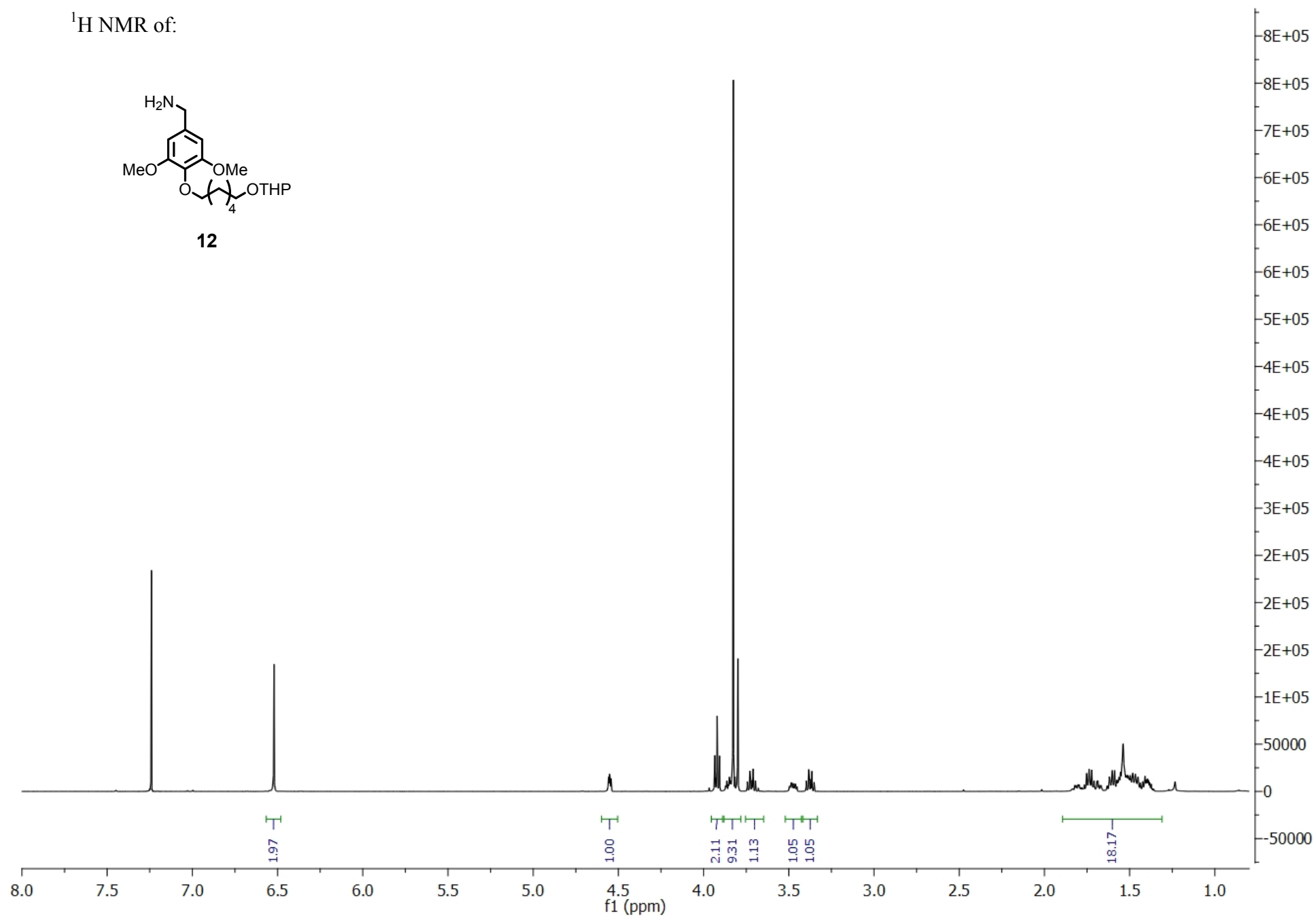
**17**



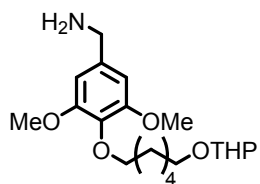
$^1\text{H}$  NMR of:



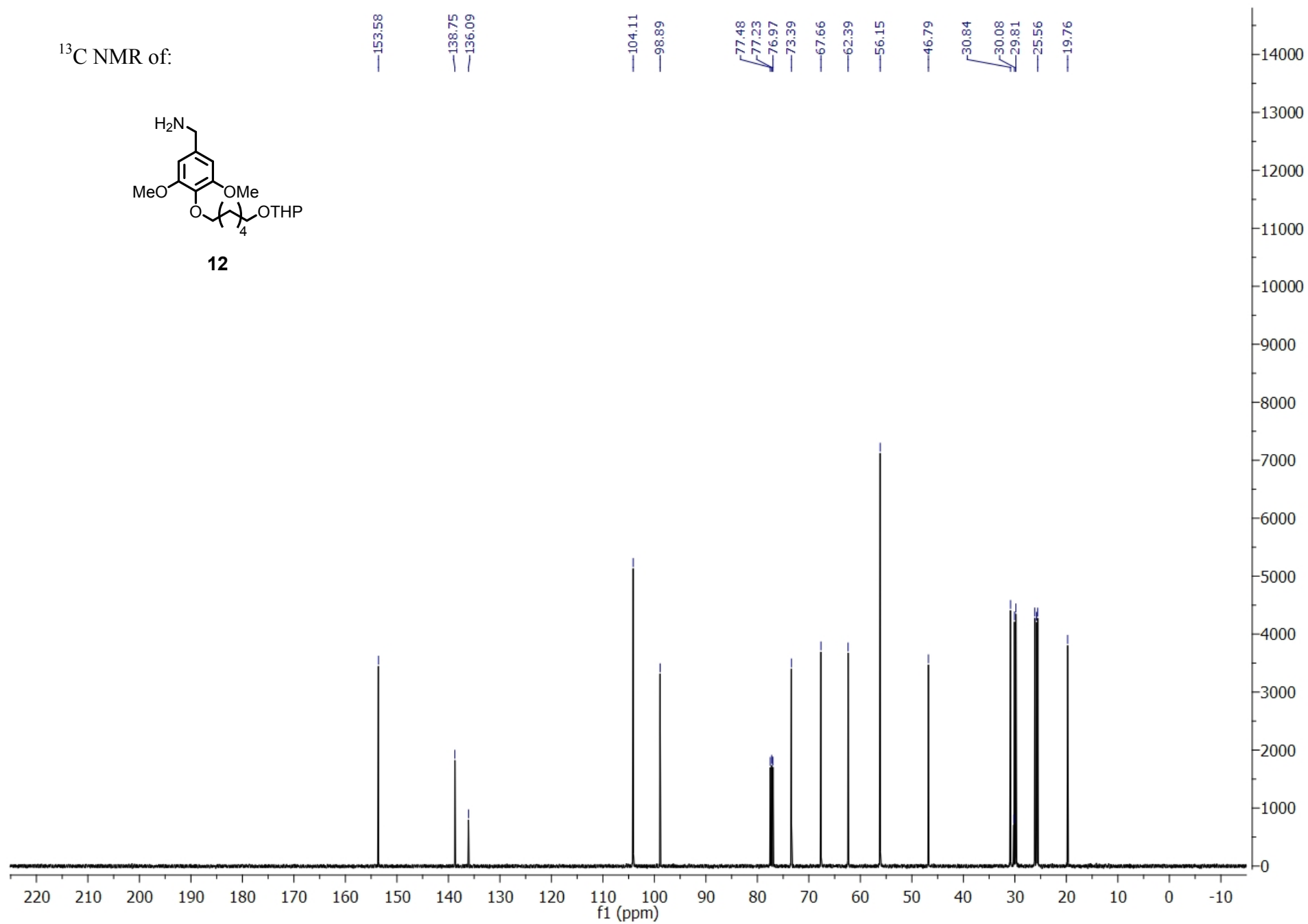
**12**



$^{13}\text{C}$  NMR of:



**12**



CALIFORNIA INSTITUTE OF TECHNOLOGY  
BECKMAN INSTITUTE  
X-RAY CRYSTALLOGRAPHY LABORATORY



Date 2 June 2009

**Crystal Structure Analysis of:**

**PGC05**

(shown below)

<b>For</b>	Investigator: Paul Clark	ext. 6019
	Advisor: R. H. Grubbs	ext. 6003
	Account Number:	RHG.MTMCH3-1-NSF.MTMCH3
<b>By</b>	Michael W. Day	116 Beckman ext. 2734 e-mail: mikeday@caltech.edu

Contents

Table 1. Crystal data

Figures Minimum overlap, dimmer (no hydrogen) and stereo view

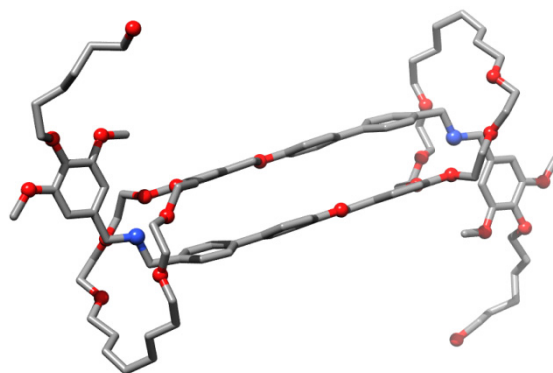
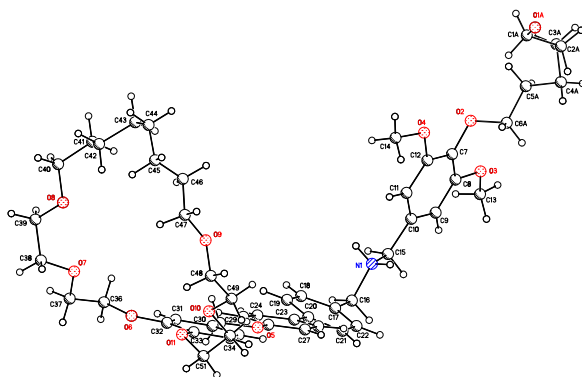
Table 2. Atomic Coordinates

Table 3. Full bond distances and angles

Table 4. Anisotropic displacement parameters

Table 5. Hydrogen bond distances and angles

Table 6. Observed and calculated structure factors (available upon request)



PGC05

**Note:** The crystallographic data have been deposited in the Cambridge Database (CCDC) and has been placed on hold pending further instructions from me. The deposition number is 734570. Ideally the CCDC would like the publication to contain a footnote of the type: "Crystallographic data have been deposited at the CCDC, 12 Union Road, Cambridge CB2 1EZ, UK and copies can be obtained on request, free of charge, by quoting the publication citation and the deposition number 734570."



**Table 1. Crystal data and structure refinement for PGC05 (CCDC 734570).**

Empirical formula	[C <sub>51</sub> H <sub>71</sub> NO <sub>11</sub> ] <sup>+</sup> (Hexafluorophosphate omitted)
Formula weight	874.09 (Hexafluorophosphate omitted)
Crystallization Solvent	Methanol/pentane
Crystal Habit	Plate
Crystal size	0.33 x 0.27 x 0.09 mm <sup>3</sup>
Crystal color	Colorless

**Data Collection**

Type of diffractometer	Bruker SMART 1000
Wavelength	1.54178 Å CuKα
Data Collection Temperature	325(2) K
θ range for 5815 reflections used in lattice determination	3.30 to 60.52°
Unit cell dimensions	a = 32.5892(12) Å b = 15.3988(6) Å c = 28.4571(10) Å
	β = 124.734(3)°
Volume	11736.0(8) Å <sup>3</sup>
Z	8
Crystal system	Monoclinic
Space group	C2/c
Density (calculated)	0.989 Mg/m <sup>3</sup> (Hexafluorophosphate omitted)
F(000)	3776 (1233 electrons recovered with SQUEEZE)
θ range for data collection	3.31 to 68.64°
Completeness to θ = 68.64°	87.2 %
Index ranges	-37 ≤ h ≤ 36, -17 ≤ k ≤ 17, -32 ≤ l ≤ 32
Data collection scan type	ω scans at 17 settings
Reflections collected	81248
Independent reflections	9453 [R <sub>int</sub> = 0.1374]
Absorption coefficient	0.555 mm <sup>-1</sup>
Absorption correction	None
Max. and min. transmission	0.9517 and 0.8379

**Table 1 (cont.)****Structure solution and Refinement**

Structure solution program	SHELXS-97 (Sheldrick, 2008)
Primary solution method	Direct methods
Secondary solution method	Difference Fourier map
Hydrogen placement	Geometric positions
Structure refinement program	SHELXL-97 (Sheldrick, 2008)
Refinement method	Full matrix least-squares on $F^2$
Data / restraints / parameters	9453 / 50 / 563
Treatment of hydrogen atoms	Riding
Goodness-of-fit on $F^2$	2.758
Final R indices [ $I > 2\sigma(I)$ , 5289 reflections]	$R1 = 0.1087$ , $wR2 = 0.1987$
R indices (all data)	$R1 = 0.1521$ , $wR2 = 0.2031$
Type of weighting scheme used	Sigma
Weighting scheme used	$w = 1/\sigma^2(F_o^2)$
Max shift/error	0.001
Average shift/error	0.000
Largest diff. peak and hole	0.531 and -0.448 e.Å <sup>-3</sup>

**Special Refinement Details**

Crystals were mounted on a glass fiber using Paratone oil then placed on the diffractometer under a nitrogen stream at 100K.

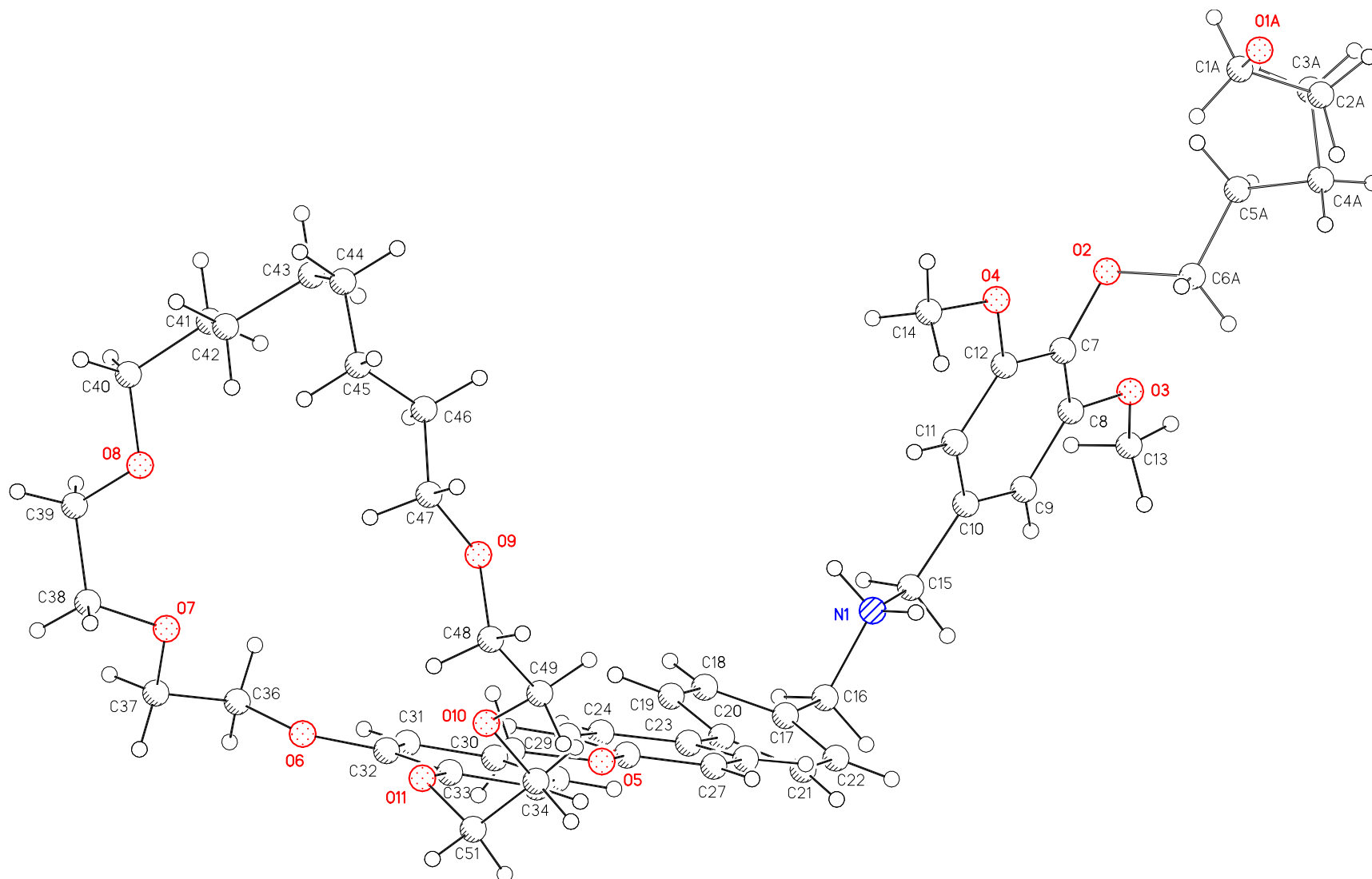
The hydroxy tail (O1-C6) is disordered and was modeled isotropically with geometry restraints.

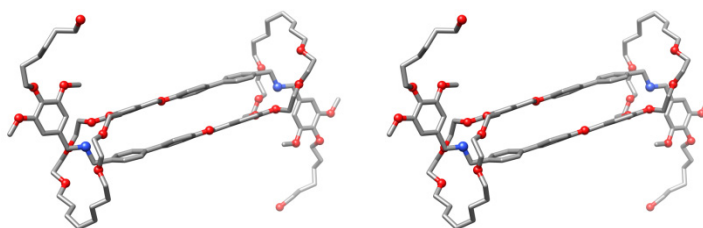
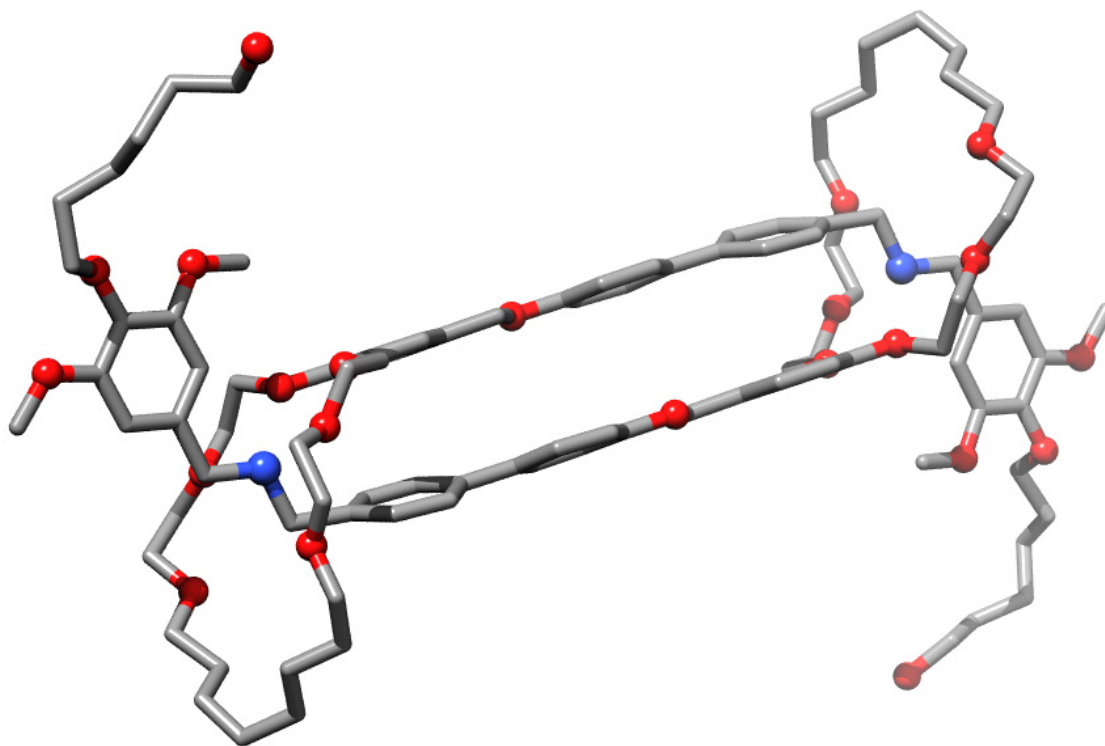
All anions and possible solvent molecules were removed from the coordinates and the program SQUEEZE<sup>1</sup> was used to adjust intensities so as to account for electrons in the solvent region without including them explicitly as discrete atoms. Approximately 1152 electrons (eight hexafluorophosphates) were excluded in this way and 1233 were recovered by the program. These were NOT included in the molecular weight, calculated density or  $F(000)$ .

Refinement of  $F^2$  against ALL reflections. The weighted R-factor ( $wR$ ) and goodness of fit ( $S$ ) are based on  $F^2$ , conventional R-factors ( $R$ ) are based on  $F$ , with  $F$  set to zero for negative  $F^2$ . The threshold expression of  $F^2 > 2\sigma(F^2)$  is used only for calculating R-factors(gt) etc. and is not relevant to the choice of reflections for refinement. R-factors based on  $F^2$  are statistically about twice as large as those based on  $F$ , and R-factors based on ALL data will be even larger.

All esds (except the esd in the dihedral angle between two l.s. planes) are estimated using the full covariance matrix. The cell esds are taken into account individually in the estimation of esds in distances, angles and torsion angles; correlations between esds in cell parameters are only used when they are defined by crystal symmetry. An approximate (isotropic) treatment of cell esds is used for estimating esds involving l.s. planes.

<sup>1</sup> SQUEEZE - Sluis, P. v.d.; Spek, A. L. Acta Crystallogr., Sect A 1990, 46, 194-201.





**Table 2. Atomic coordinates ( $\times 10^4$ ) and equivalent isotropic displacement parameters ( $\text{\AA}^2 \times 10^3$ ) for PGC05 (CCDC 734570) (CCDC 734570).  $U(\text{eq})$  is defined as the trace of the orthogonalized  $U^{\text{ij}}$  tensor.**

	x	y	z	$U_{\text{eq}}$	Occ
O(2)	12490(1)	6303(2)	13885(1)	63(1)	1
O(3)	13286(2)	5579(2)	14833(2)	71(1)	1
O(4)	11907(1)	5388(2)	12930(1)	58(1)	1
O(5)	9658(1)	-1359(2)	10049(1)	60(1)	1
O(6)	8504(1)	-2676(2)	7600(1)	46(1)	1
O(7)	8217(1)	-2302(2)	6500(1)	59(1)	1
O(8)	7573(2)	-1117(3)	5575(2)	88(1)	1
O(9)	6075(2)	-1331(4)	6301(2)	99(2)	1
O(10)	6741(1)	-2620(3)	7159(2)	78(1)	1
O(11)	7806(1)	-2940(2)	7751(1)	51(1)	1
N(1)	12578(1)	2266(2)	13385(2)	43(1)	1
O(1A)	10079(11)	7968(19)	12404(15)	460(20)	0.50
C(1A)	10639(11)	7950(50)	12769(14)	650(30)	0.50
C(2A)	10852(7)	8090(30)	13389(12)	470(20)	0.50
C(3A)	11396(8)	8322(13)	13744(10)	299(15)	0.50
C(4A)	11688(6)	7628(12)	14185(8)	186(8)	0.50
C(5A)	12073(6)	7388(7)	14076(8)	115(6)	0.50
C(6A)	12133(4)	6426(7)	14051(6)	76(4)	0.50
O(1B)	10001(9)	7438(19)	13120(13)	387(14)	0.50
C(1B)	10388(10)	7180(40)	13020(20)	690(40)	0.50
C(2B)	10822(9)	7790(30)	13280(20)	570(20)	0.50
C(3B)	11308(8)	7480(30)	13795(13)	439(18)	0.50
C(4B)	11697(8)	7315(18)	13679(9)	286(13)	0.50
C(5B)	12213(8)	7466(12)	14205(12)	309(15)	0.50
C(6B)	12498(8)	6626(14)	14388(5)	213(10)	0.50
C(7)	12600(2)	5436(3)	13890(2)	47(1)	1
C(8)	13008(2)	5063(3)	14354(2)	47(1)	1
C(9)	13128(2)	4196(3)	14350(2)	44(1)	1
C(10)	12826(2)	3719(3)	13853(2)	41(1)	1
C(11)	12422(2)	4094(3)	13374(2)	45(1)	1
C(12)	12306(2)	4960(3)	13395(2)	47(1)	1
C(13)	13751(2)	5255(4)	15282(2)	85(2)	1
C(14)	11633(2)	4911(3)	12399(2)	70(2)	1
C(15)	12978(2)	2788(3)	13842(2)	47(1)	1
C(16)	12718(2)	1324(3)	13411(2)	45(1)	1
C(17)	12288(2)	832(3)	12913(2)	39(1)	1
C(18)	12229(2)	777(3)	12406(2)	41(1)	1
C(19)	11810(2)	398(3)	11932(2)	41(1)	1
C(20)	11436(2)	44(3)	11974(2)	36(1)	1
C(21)	11508(2)	68(3)	12502(2)	43(1)	1
C(22)	11930(2)	470(3)	12972(2)	45(1)	1
C(23)	10978(2)	-323(3)	11467(2)	35(1)	1
C(24)	10952(2)	-559(3)	10986(2)	45(1)	1
C(25)	10520(2)	-892(3)	10492(2)	49(1)	1
C(26)	10106(2)	-1021(3)	10508(2)	44(1)	1
C(27)	10111(2)	-804(4)	10973(2)	57(2)	1
C(28)	10537(2)	-441(4)	11447(2)	56(2)	1

C(29)	9641(2)	-1595(3)	9563(2)	51(1)	1
C(30)	9141(2)	-1933(3)	9104(2)	39(1)	1
C(31)	9080(2)	-2141(3)	8587(2)	47(1)	1
C(32)	8610(2)	-2481(3)	8137(2)	41(1)	1
C(33)	8238(2)	-2607(3)	8210(2)	47(1)	1
C(34)	8305(2)	-2395(3)	8730(2)	56(2)	1
C(35)	8767(2)	-2059(3)	9170(2)	56(2)	1
C(36)	8859(2)	-2467(3)	7483(2)	55(1)	1
C(37)	8676(2)	-2761(4)	6915(2)	61(2)	1
C(38)	8031(2)	-2422(4)	5911(2)	76(2)	1
C(39)	7951(2)	-1586(4)	5606(2)	78(2)	1
C(40)	7506(4)	-330(7)	5298(4)	148(4)	1
C(41)	7226(5)	358(7)	5396(4)	157(4)	1
C(42)	6704(4)	153(7)	5088(4)	149(4)	1
C(43)	6435(5)	847(8)	5221(5)	196(5)	1
C(44)	5887(5)	677(9)	4973(5)	218(7)	1
C(45)	5753(5)	-111(10)	5099(7)	253(8)	1
C(46)	5961(5)	-202(9)	5673(4)	181(6)	1
C(47)	5787(4)	-1062(9)	5720(4)	174(5)	1
C(48)	5928(2)	-2145(6)	6403(4)	117(3)	1
C(49)	6261(2)	-2338(4)	7006(4)	107(3)	1
C(50)	7053(2)	-2856(4)	7755(3)	77(2)	1
C(51)	7460(2)	-3376(4)	7836(2)	61(2)	1

---

**Table 3. Bond lengths [Å] and angles [°] for PGC05 (CCDC 734570) (CCDC 734570).**

O(2)-C(7)	1.380(5)	C(23)-C(24)	1.372(6)
O(2)-C(6A)	1.498(2)	C(23)-C(28)	1.417(6)
O(2)-C(6B)	1.501(2)	C(24)-C(25)	1.402(6)
O(3)-C(8)	1.378(5)	C(25)-C(26)	1.389(6)
O(3)-C(13)	1.404(6)	C(26)-C(27)	1.354(6)
O(4)-C(12)	1.384(5)	C(27)-C(28)	1.387(6)
O(4)-C(14)	1.443(5)	C(29)-C(30)	1.484(6)
O(5)-C(26)	1.392(5)	C(30)-C(35)	1.348(6)
O(5)-C(29)	1.401(5)	C(30)-C(31)	1.404(6)
O(6)-C(32)	1.393(5)	C(31)-C(32)	1.424(6)
O(6)-C(36)	1.412(5)	C(32)-C(33)	1.356(6)
O(7)-C(38)	1.433(6)	C(33)-C(34)	1.403(6)
O(7)-C(37)	1.455(5)	C(34)-C(35)	1.399(7)
O(8)-C(39)	1.385(7)	C(36)-C(37)	1.440(6)
O(8)-C(40)	1.393(8)	C(38)-C(39)	1.490(7)
O(9)-C(47)	1.420(10)	C(40)-C(41)	1.524(11)
O(9)-C(48)	1.432(8)	C(41)-C(42)	1.436(11)
O(10)-C(49)	1.433(6)	C(42)-C(43)	1.559(12)
O(10)-C(50)	1.442(6)	C(43)-C(44)	1.523(13)
O(11)-C(33)	1.361(5)	C(44)-C(45)	1.404(14)
O(11)-C(51)	1.446(5)	C(45)-C(46)	1.372(16)
N(1)-C(15)	1.451(5)	C(46)-C(47)	1.475(14)
N(1)-C(16)	1.510(5)	C(48)-C(49)	1.445(10)
O(1A)-C(1A)	1.501(2)	C(50)-C(51)	1.450(7)
C(1A)-C(2A)	1.500(2)		
C(2A)-C(3A)	1.500(2)	C(7)-O(2)-C(6A)	111.2(5)
C(3A)-C(4A)	1.503(2)	C(7)-O(2)-C(6B)	116.6(9)
C(4A)-C(5A)	1.501(2)	C(6A)-O(2)-C(6B)	41.5(9)
C(5A)-C(6A)	1.501(2)	C(8)-O(3)-C(13)	117.1(4)
O(1B)-C(1B)	1.500(2)	C(12)-O(4)-C(14)	116.3(4)
C(1B)-C(2B)	1.500(2)	C(26)-O(5)-C(29)	117.0(4)
C(2B)-C(3B)	1.500(2)	C(32)-O(6)-C(36)	118.9(4)
C(3B)-C(4B)	1.500(2)	C(38)-O(7)-C(37)	116.3(4)
C(4B)-C(5B)	1.501(2)	C(39)-O(8)-C(40)	109.8(6)
C(5B)-C(6B)	1.502(2)	C(47)-O(9)-C(48)	114.6(8)
C(7)-C(8)	1.358(7)	C(49)-O(10)-C(50)	110.5(5)
C(7)-C(12)	1.378(6)	C(33)-O(11)-C(51)	119.5(4)
C(8)-C(9)	1.393(6)	C(15)-N(1)-C(16)	113.4(3)
C(9)-C(10)	1.387(6)	C(2A)-C(1A)-O(1A)	112.1(14)
C(10)-C(11)	1.371(6)	C(1A)-C(2A)-C(3A)	113.9(14)
C(10)-C(15)	1.521(6)	C(2A)-C(3A)-C(4A)	109.6(13)
C(11)-C(12)	1.397(6)	C(5A)-C(4A)-C(3A)	102.0(10)
C(16)-C(17)	1.512(6)	C(4A)-C(5A)-C(6A)	113.5(10)
C(17)-C(18)	1.344(6)	O(2)-C(6A)-C(5A)	106.5(7)
C(17)-C(22)	1.385(6)	C(2B)-C(1B)-O(1B)	113.6(13)
C(18)-C(19)	1.387(6)	C(3B)-C(2B)-C(1B)	116.9(15)
C(19)-C(20)	1.403(6)	C(2B)-C(3B)-C(4B)	112.9(13)
C(20)-C(21)	1.382(6)	C(3B)-C(4B)-C(5B)	111.2(12)
C(20)-C(23)	1.473(6)	C(4B)-C(5B)-C(6B)	109.4(11)
C(21)-C(22)	1.403(6)	O(2)-C(6B)-C(5B)	106.5(10)

C(8)-C(7)-C(12)	119.6(5)	C(42)-C(41)-C(40)	111.1(10)
C(8)-C(7)-O(2)	121.5(5)	C(41)-C(42)-C(43)	109.6(10)
C(12)-C(7)-O(2)	118.7(5)	C(44)-C(43)-C(42)	116.3(11)
C(7)-C(8)-O(3)	116.5(5)	C(45)-C(44)-C(43)	118.9(13)
C(7)-C(8)-C(9)	121.4(5)	C(46)-C(45)-C(44)	112.2(17)
O(3)-C(8)-C(9)	122.0(5)	C(45)-C(46)-C(47)	104.1(13)
C(10)-C(9)-C(8)	118.5(5)	O(9)-C(47)-C(46)	109.5(9)
C(11)-C(10)-C(9)	120.8(5)	O(9)-C(48)-C(49)	108.0(6)
C(11)-C(10)-C(15)	121.1(4)	O(10)-C(49)-C(48)	112.0(7)
C(9)-C(10)-C(15)	118.0(4)	O(10)-C(50)-C(51)	107.2(5)
C(10)-C(11)-C(12)	119.3(5)	C(50)-C(51)-O(11)	116.5(5)
C(7)-C(12)-O(4)	116.8(5)		
C(7)-C(12)-C(11)	120.3(5)		
O(4)-C(12)-C(11)	122.9(5)		
N(1)-C(15)-C(10)	113.8(4)		
C(17)-C(16)-N(1)	110.1(4)		
C(18)-C(17)-C(22)	119.2(4)		
C(18)-C(17)-C(16)	121.8(5)		
C(22)-C(17)-C(16)	118.9(4)		
C(17)-C(18)-C(19)	122.0(5)		
C(18)-C(19)-C(20)	120.2(4)		
C(21)-C(20)-C(19)	117.6(4)		
C(21)-C(20)-C(23)	121.7(4)		
C(19)-C(20)-C(23)	120.7(4)		
C(20)-C(21)-C(22)	121.0(5)		
C(17)-C(22)-C(21)	119.9(4)		
C(24)-C(23)-C(28)	116.1(4)		
C(24)-C(23)-C(20)	122.1(4)		
C(28)-C(23)-C(20)	121.7(4)		
C(23)-C(24)-C(25)	123.5(5)		
C(26)-C(25)-C(24)	117.3(4)		
C(27)-C(26)-C(25)	121.7(4)		
C(27)-C(26)-O(5)	115.5(4)		
C(25)-C(26)-O(5)	122.8(4)		
C(26)-C(27)-C(28)	119.8(5)		
C(27)-C(28)-C(23)	121.4(5)		
O(5)-C(29)-C(30)	111.5(4)		
C(35)-C(30)-C(31)	120.8(5)		
C(35)-C(30)-C(29)	123.7(4)		
C(31)-C(30)-C(29)	115.5(4)		
C(30)-C(31)-C(32)	117.7(5)		
C(33)-C(32)-O(6)	116.9(4)		
C(33)-C(32)-C(31)	120.8(4)		
O(6)-C(32)-C(31)	122.3(5)		
C(32)-C(33)-O(11)	115.6(4)		
C(32)-C(33)-C(34)	120.8(5)		
O(11)-C(33)-C(34)	123.6(5)		
C(35)-C(34)-C(33)	118.1(5)		
C(30)-C(35)-C(34)	121.8(5)		
O(6)-C(36)-C(37)	108.7(4)		
C(36)-C(37)-O(7)	109.7(4)		
O(7)-C(38)-C(39)	112.7(5)		
O(8)-C(39)-C(38)	110.0(5)		
O(8)-C(40)-C(41)	114.9(8)		



**Table 4. Anisotropic displacement parameters ( $\text{\AA}^2 \times 10^4$ ) for PGC05 (CCDC 734570) (CCDC 734570). The anisotropic displacement factor exponent takes the form:  $-2\pi^2 [h^2 a^{*2} U^{11} + \dots + 2 h k a^* b^* U^{12}]$**

	$U^{11}$	$U^{22}$	$U^{33}$	$U^{23}$	$U^{13}$	$U^{12}$
O(2)	990(30)	410(20)	560(20)	-129(18)	490(20)	-70(20)
O(3)	860(30)	600(30)	640(30)	-270(20)	420(20)	-170(20)
O(4)	690(30)	440(20)	540(20)	63(19)	310(20)	90(20)
O(5)	430(20)	940(30)	360(20)	-123(19)	175(17)	-130(20)
O(6)	399(19)	480(20)	440(20)	-64(16)	196(17)	-97(17)
O(7)	580(20)	740(30)	420(20)	-68(19)	274(19)	-30(20)
O(8)	730(30)	1290(40)	620(30)	210(30)	370(20)	100(30)
O(9)	630(30)	1200(40)	760(30)	-200(30)	180(30)	50(30)
O(10)	570(30)	750(30)	930(30)	-260(20)	380(20)	-180(20)
O(11)	440(20)	540(20)	420(20)	-71(17)	171(18)	-116(18)
N(1)	400(20)	370(20)	400(20)	-95(19)	160(20)	-50(20)
C(7)	680(40)	330(30)	460(30)	-70(30)	350(30)	-40(30)
C(8)	570(30)	470(30)	450(30)	-240(30)	340(30)	-250(30)
C(9)	360(30)	530(30)	440(30)	-80(30)	240(20)	-90(30)
C(10)	400(30)	420(30)	420(30)	-90(20)	240(30)	-80(30)
C(11)	440(30)	380(30)	380(30)	-110(20)	140(20)	-80(30)
C(12)	550(30)	420(30)	530(30)	0(30)	360(30)	-20(30)
C(13)	660(40)	1000(50)	630(40)	-430(40)	210(40)	-160(40)
C(14)	720(40)	570(40)	530(40)	80(30)	180(30)	10(30)
C(15)	320(30)	470(30)	430(30)	-140(20)	100(20)	-50(30)
C(16)	340(30)	350(30)	490(30)	-10(20)	130(20)	40(20)
C(17)	340(30)	320(30)	400(30)	-30(20)	150(20)	-10(20)
C(18)	350(30)	380(30)	430(30)	-30(20)	180(20)	-50(20)
C(19)	440(30)	370(30)	420(30)	10(20)	240(20)	60(30)
C(20)	430(30)	250(30)	350(30)	-50(20)	190(20)	10(20)
C(21)	460(30)	460(30)	410(30)	-20(20)	260(30)	-100(30)
C(22)	520(30)	370(30)	300(30)	-30(20)	150(20)	-50(30)
C(23)	300(30)	340(30)	400(30)	30(20)	190(20)	0(20)
C(24)	410(30)	540(30)	440(30)	-90(30)	270(30)	-120(30)
C(25)	440(30)	660(40)	330(30)	-100(30)	200(30)	-60(30)
C(26)	350(30)	540(30)	240(30)	-70(20)	50(20)	-70(30)
C(27)	300(30)	970(50)	370(30)	-40(30)	160(20)	-90(30)
C(28)	470(30)	850(40)	340(30)	-120(30)	210(30)	-60(30)
C(29)	490(30)	590(40)	400(30)	-80(30)	210(30)	-10(30)
C(30)	390(30)	400(30)	300(30)	-70(20)	150(20)	-100(20)
C(31)	400(30)	490(30)	400(30)	-20(20)	160(20)	40(30)
C(32)	430(30)	330(30)	340(30)	-60(20)	140(20)	-10(20)
C(33)	520(30)	420(30)	400(30)	-40(20)	230(30)	-90(30)
C(34)	680(40)	550(40)	500(30)	-50(30)	370(30)	-60(30)
C(35)	640(40)	540(40)	400(30)	-80(30)	230(30)	-20(30)
C(36)	520(30)	640(40)	450(30)	-30(30)	250(30)	40(30)
C(37)	530(30)	750(40)	610(40)	10(30)	370(30)	80(30)
C(38)	710(40)	990(50)	640(40)	-270(40)	420(40)	-290(40)
C(39)	720(40)	1010(60)	570(40)	10(40)	350(40)	-160(40)
C(40)	1880(100)	1380(90)	1260(80)	610(70)	940(80)	350(80)

C(41)	1890(120)	1330(90)	1070(80)	210(70)	590(80)	10(90)
C(42)	1300(90)	1490(100)	1110(80)	-330(70)	340(70)	-140(80)
C(43)	1470(110)	2110(140)	2020(120)	-670(110)	820(100)	-180(100)
C(44)	1800(140)	1690(130)	1790(120)	310(100)	270(100)	-50(120)
C(45)	2060(160)	2100(170)	2800(200)	720(170)	1030(160)	570(140)
C(46)	1510(100)	2360(150)	750(70)	660(90)	170(70)	390(100)
C(47)	1270(90)	2680(160)	770(70)	-360(90)	290(70)	590(100)
C(48)	470(40)	870(60)	1520(80)	-490(60)	190(50)	-100(40)
C(49)	650(50)	700(50)	1990(90)	-360(60)	840(60)	-150(40)
C(50)	680(40)	830(50)	730(40)	-230(40)	360(40)	-250(40)
C(51)	670(40)	630(40)	650(40)	10(30)	450(30)	-100(30)

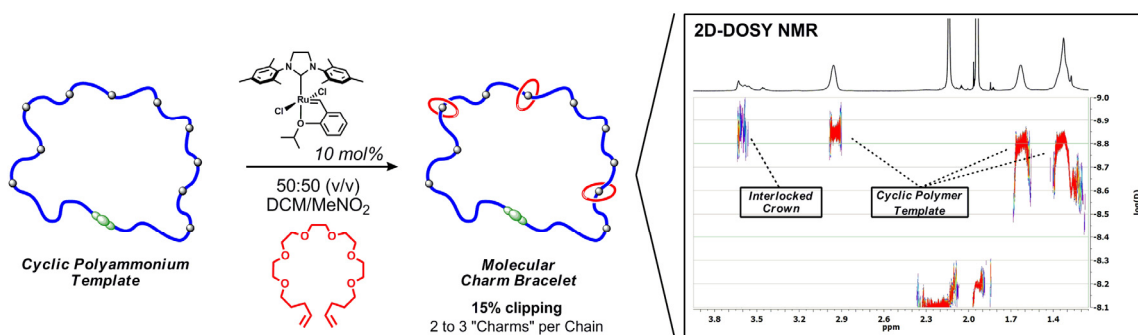
---

**Table 5. Hydrogen bonds for PGC05 (CCDC 734570) (CCDC 734570) [ $\text{\AA}$  and  $^\circ$ ].**

D-H...A	d(D-H)	d(H...A)	d(D...A)	<(DHA)
N(1)-H(1AA)...O(11)#1	0.90	2.02	2.914(5)	172.2
N(1)-H(1AB)...O(7)#1	0.90	1.90	2.793(5)	174.8

## CHAPTER 3

### Synthesis of a Molecular Charm Bracelet via Click Cyclization and Olefin Metathesis Clipping



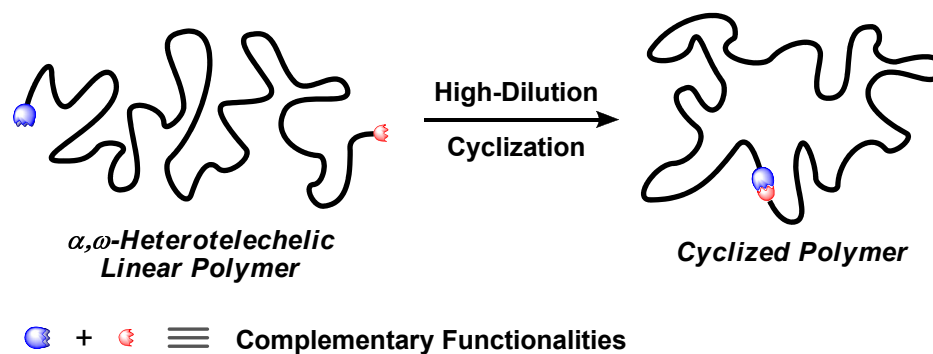
Portions of this chapter have previously appeared as: Clark, P. G.; Guidry, E. N.; Chan, W. Y.; Steinmetz, W. E.; Grubbs, R. H. *J. Am. Chem. Soc.* **2010**, *132*, 3405-3412.

## Synthesis of a Molecular Charm Bracelet via Click Cyclization and Olefin Metathesis Clipping

### *Introduction*

Novel polymer architectures have attracted significant interest from scientists in an unceasing quest to tailor the structural attributes of a material for specific applications. Cyclic polymers (CPs) have garnered particular attention due to a number of attractive traits, including desirable physical properties, increased functional-group density, and smaller hydrodynamic radii relative to linear polymer analogues.<sup>1-7</sup> Recent work by Fréchet, Szoka, and coworkers<sup>8</sup> has also indicated that CPs have potential biological applications, displaying better circulation half-lives than their linear counterparts and thus making them attractive candidates as possible drug carriers.

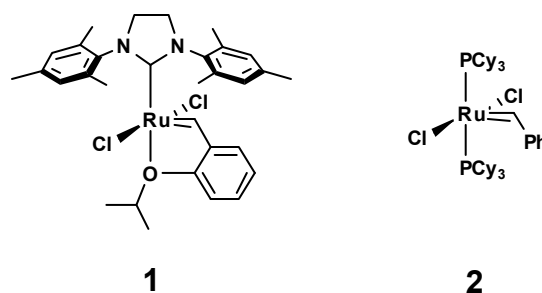
In addition to their intriguing properties, CPs also present a unique challenge to synthetic chemists, as there are few procedures that favor the formation of these “endless” polymers in high purity.<sup>9-12</sup> Traditionally, CPs have been synthesized via high-dilution cyclization of dianionic linear polymers and a two-site coupling agent. However, due to issues associated with polymer purity using this technique, modern efforts have focused on the development of a number of new routes to cyclic architectures, including macrocyclization of  $\alpha,\omega$ -heterotelechelic linear polymers (Figure 3.1)<sup>13-15</sup> or olefin-terminated polymers,<sup>16,17</sup> cyclization of electrostatically-templated telechelic polymers,<sup>18-25</sup> and ring-expansion reactions of cyclic species, including lactides<sup>26</sup> and olefin monomers.<sup>27-30</sup> Macrocyclization reactions of  $\alpha,\omega$ -heterotelechelic polymers often employ high-fidelity, high-conversion “click” reactions<sup>31-36</sup> such the Huisgen 1,3-dipolar cycloaddition between an alkyne and an azide, but necessitate high-dilution or pseudo-



**Figure 3.1:** Graphical representation of the macrocyclization of an  $\alpha,\omega$ -heterotelechelic polymer under high-dilution conditions.

high-dilution conditions to favor cycles rather than oligomers. By contrast, reactions such as ring-expansion metathesis polymerization<sup>27-30</sup> (REMP), catalyzed by cyclic ruthenium alkylidene species, overcome this limitation, and enable rapid synthesis of multigram quantities of pure cyclic polymer. In addition to the cyclic ruthenium catalysts used in REMP, a number of other functional-group tolerant ruthenium alkylidene catalysts, for example, catalysts **1** and **2** (Figure 3.2), have seen broad application in polymer synthesis.<sup>37-40</sup>

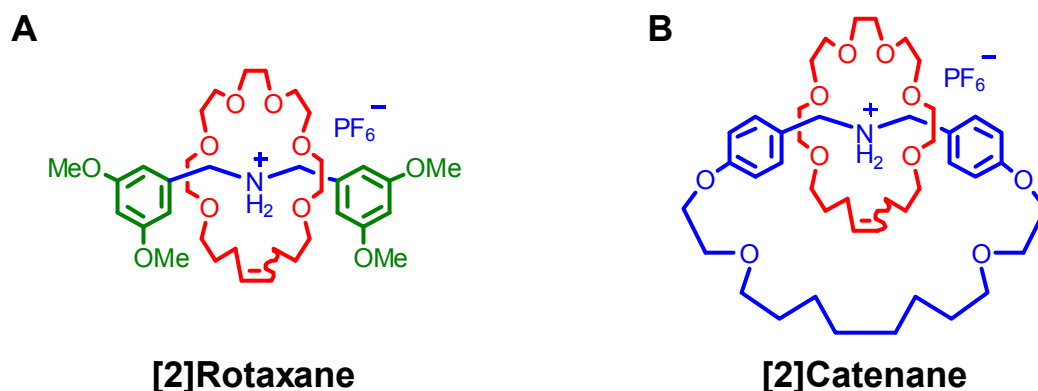
Another intriguing and challenging area of research is the synthesis of mechanically interlocked molecules.<sup>41-44</sup> Such structures contain two or more molecules that cannot be separated without covalent bond cleavage, but that do not contain any



**Figure 3.2:** Ruthenium olefin metathesis catalysts **1** and **2**.

covalent bonds between them. Utilizing a combination of supramolecular chemistry<sup>45-47</sup> (often involving hydrogen bonding interactions between crown ether-type species and secondary ammonium ions) to template the formation of preorganized structures and dynamic covalent chemistry<sup>48-54</sup> to induce interlocking of the resulting complex, high-yielding syntheses of rotaxanes<sup>55-58</sup> and catenanes<sup>59-65</sup> (Figure 3.3), as well as a variety of other, more complex architectures,<sup>66-72</sup> have been realized. One particularly effective strategy to synthesize mechanically interlocked molecules employs the dynamic, ruthenium-catalyzed ring-closing metathesis (RCM) reaction, whereby a diolefin polyether fragment is subjected to RCM conditions and “clipped” around a disubstituted ammonium ion (Figure 3.3).<sup>56,63,69</sup>

Due to the complexity of mechanically-linked structures, confirmation of the interlocked nature of the products can often prove difficult via standard characterization techniques. However, the use of two-dimensional diffusion ordered NMR spectroscopy<sup>73-79</sup> (2D-DOSY) facilitates the analysis of distinct complexes in solution

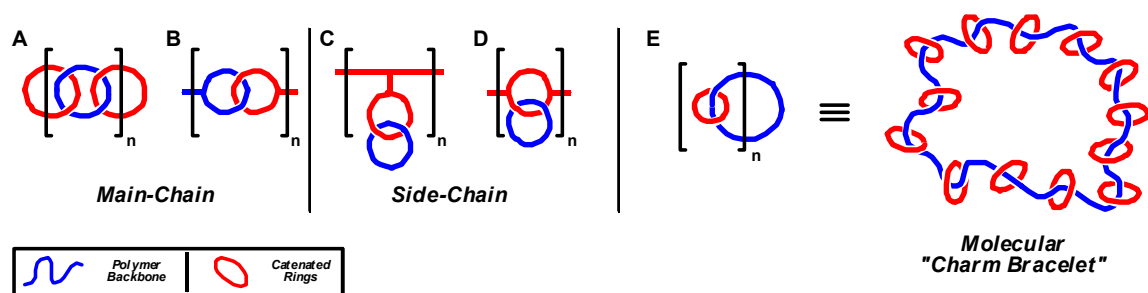


**Figure 3.3:** Examples of a mechanically interlocked [2]rotaxane (A) and a [2]catenane (B) that were synthesized using olefin metathesis.

based on their unique diffusion rate. Using this technique, small molecules with fast diffusion rates that are intimately associated (either covalently or mechanically) with a slowly diffusing macromolecule will diffuse at the speed of the larger structure to which they are appended. The application of this protocol to linear polymers with threaded rings has been demonstrated previously.<sup>80</sup>

The inclusion of interlocked moieties as a part of a larger macromolecular structure<sup>43,81</sup> has been shown to have an impact on both the solution state and bulk properties<sup>82-85</sup> of the resulting material, and, to this end, researchers have synthesized a number of polyrotaxanes,<sup>82,83</sup> as well as polycatenane species (Figure 3.4A-D).<sup>72,84,85</sup> The polycatenane “charm bracelet” structure (Figure 3.4E), however, has been particularly elusive.<sup>9-11,45,70</sup> Recently, a few reports have emerged describing smaller cyclic complexes containing threaded moieties,<sup>86-91</sup> and Harada has reported the cyclization of a threaded, capped polyrotaxane.<sup>92</sup>

In complement to these reports, we wanted to explore a “clipping” approach to such a polycatenated molecular “charm bracelet.” We synthesized a CP architecture via a



**Figure 3.4:** Graphic representation of various polycatenane structures, including main-chain polycatenanes (A and B), side-chain polycatenanes (C and D), and the targeted cyclic interlocked “charm bracelet” polycatenane (E).

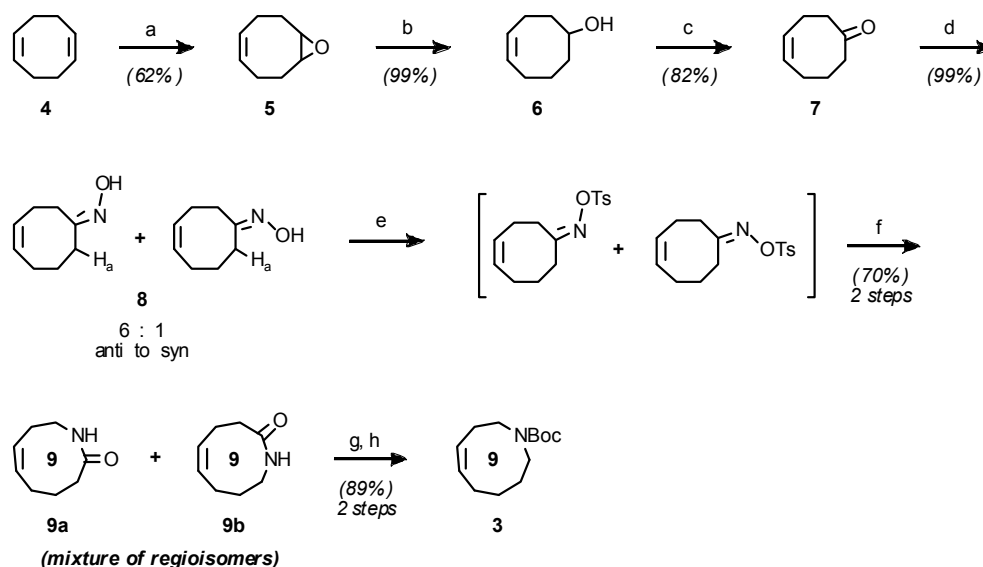


pseudo-high-dilution, two-component “click” macrocyclization, and subsequently converted this species to the polyammonium analogue. We were then able to “clip” diolefin crown ether–type rings around the ammonium sites of the polymer scaffold using RCM. Confirmation of the interlocked nature of the “charm bracelet” product was achieved via 2D-DOSY NMR.

### Results and Discussion

**Monomer Design and Synthesis.** We believed the nine-membered cyclic carbamate **3** (Scheme 3.1)<sup>93</sup> possessed sufficient ring strain to be a suitable metathesis polymerization monomer and would afford the desired polyammonium polymer upon removal of the boc-protecting group.

**Scheme 3.1:** Synthesis of Nine-Membered Cyclic Carbamate Monomer **3**<sup>a</sup>

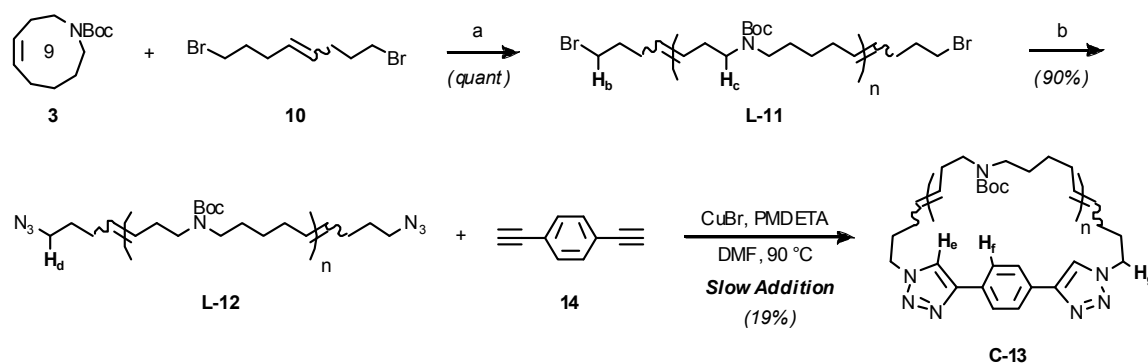


<sup>a</sup> Reagents and Conditions: (a) *m*-CPBA,  $\text{CHCl}_3$ , 0 °C to r.t., 12 h. (b) LAH, THF, 0 °C to reflux, 4 h. (c) Oxalyl chloride, DMSO, TEA, -78 °C to r.t., 4 h. (d)  $\text{NH}_2\text{OH}\cdot\text{HCl}$ ,  $\text{NaHCO}_3$ , MeOH, reflux, 4 h.; (e) TsCl, Pyr, DCM, 0 °C to r.t., 12 h. (f)  $\text{K}_2\text{CO}_3$ ,  $\text{H}_2\text{O}$ , THF, r.t., 12 h. (g) LAH, THF, reflux, 4 h.; (h)  $\text{Boc}_2\text{O}$ , TEA, DMAP, DCM, r.t. 24 h.

Synthesis of **3** was readily achieved in eight steps and 31% overall yield. *cis*-1,5-Cyclooctadiene (**4**) was treated with *meta*-3-chloroperoxybenzoic acid to afford monoepoxidized cyclooctene species **5**. Reduction of **5** with lithium aluminum hydride opened the epoxide to the corresponding alcohol **6**, which was subjected to Swern oxidation conditions, giving ketone **7**. Refluxing **7** in the presence of hydroxylamine hydrochloride generated oxime **8**, which was transiently converted to the tosyl oxime intermediate prior to undergoing a base-promoted Beckmann rearrangement that produced a regioisomeric mixture of lactams **9a** and **9b**. By <sup>1</sup>H NMR spectroscopic analysis, isomer **9b** appeared to dominate the product mixture, not entirely surprising given that, in **8**, the ratio of oxime *anti* to H<sub>a</sub> versus *syn* to H<sub>a</sub> was approximately 6 to 1, respectively. The mixture of lactams was reduced to the cyclic amine by lithium aluminum hydride, and subsequently boc-protected to yield the desired nine-membered unsaturated cyclic carbamate monomer **3**. Interestingly, despite the mixture of starting materials, only the non-symmetric regioisomer of **3** was isolated.

**Polymer Synthesis and Characterization.** Unfortunately, initial efforts to utilize REMP as the polymerization method proved challenging with monomer **3**. Thus, we turned our attention to ring-opening metathesis polymerization (ROMP) in the presence of a chain-transfer agent (CTA),<sup>94-98</sup> as a suitably-functionalized telechelic polymer would be structurally analogous to early dianionic polymers used in the synthesis of CPs.<sup>9,99</sup>

**Scheme 3.2:** Synthesis of Linear Telechelic Dibromide Polymer **L-11**, Diazide Polymer **L-12**, and Cyclic Polymer **C-13**<sup>a</sup>

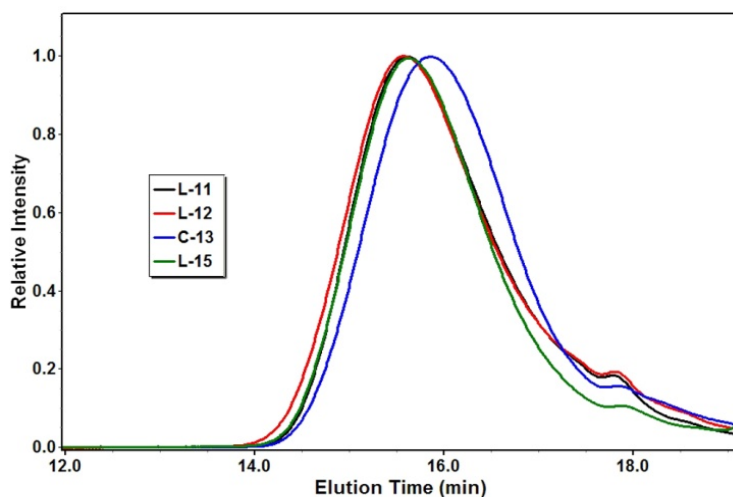


<sup>a</sup> Reagents and Conditions: (a) catalyst **1**, 1.0 M DCM, 43 °C, 1 d. (b) NaN<sub>3</sub>, DMF, 50 °C, 12 h.

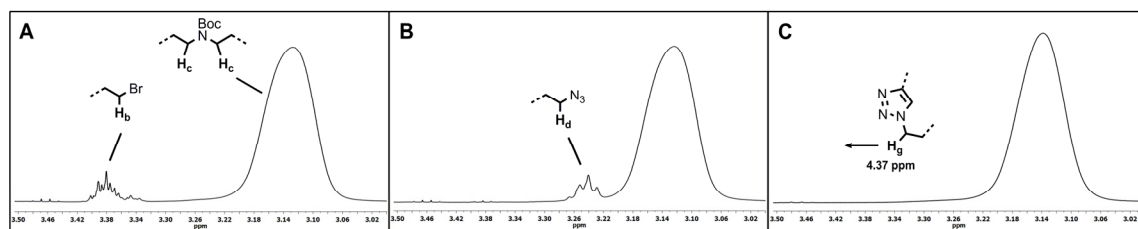
Given the successful application of the alkyne-azide “click” reaction to the synthesis of CPs,<sup>13-15</sup> we employed this protocol to cyclize our linear polymer. Our efforts to ROMP monomer **3** in the presence of a diazide CTA were unsuccessful. However, we readily accessed dibromo telechelic polymer **L-11** upon treatment of a solution of **3** and dibromo CTA **10** with catalyst **1** (Scheme 3.2).<sup>100</sup> Gel permeation chromatography (GPC, Figure 3.5) analysis of **L-11** revealed that the polymer had an  $M_n$  of 4.1 kDa, correlating to a degree of polymerization (DP) of 17, and a polydispersity index (PDI) of 1.49. By <sup>1</sup>H NMR end-group analysis (Figure 3.6A), the DP of **L-11** was found to be 19, in close agreement with the GPC results. Synthesis of the desired diazide telechelic polymer **L-12** was accomplished by treating dibromotelechelic polymer **L-11** with sodium azide (Scheme 3.2). The GPC traces for **L-11** and **L-12** overlapped closely (Figure 3.5), and polymer end-group conversion from bromide to azide was monitored by <sup>1</sup>H NMR spectroscopy (Figure 3.6B), which showed an upfield shift of the bromomethylene protons (from 3.37 to 3.23 ppm) after substitution with sodium azide. To verify that **L-12** contained azide functionalities, we studied polymers **L-11** and **L-12**

by FT-IR (Figure 3.7). As expected, the spectrum of **L-12** contained a strong band at  $2096\text{ cm}^{-1}$ , while no azide peak was observed in the spectrum of **L-11**.

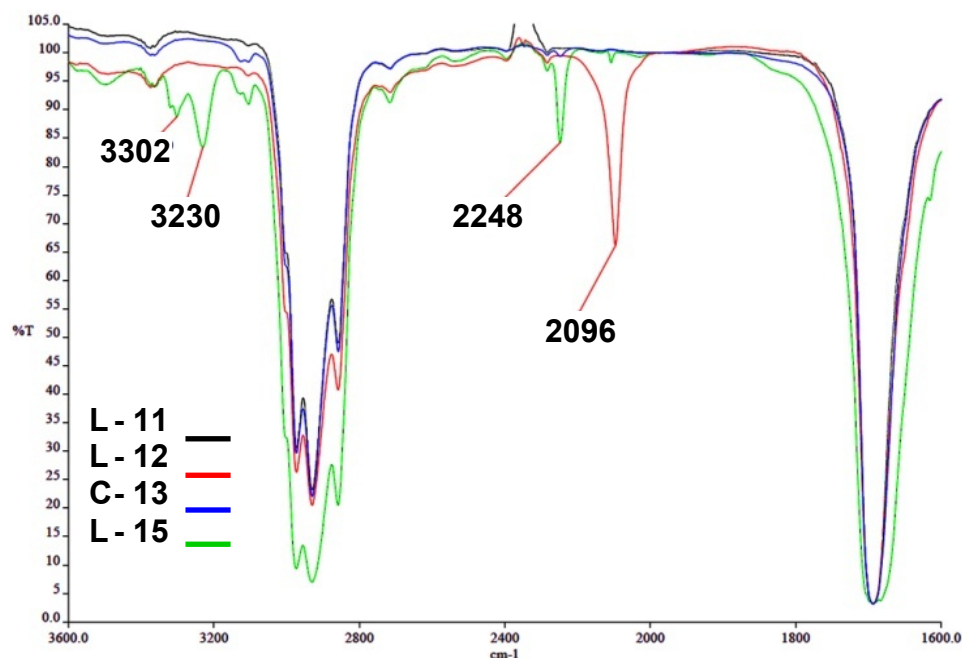
We effected the cyclization of the linear diazide polymer **L-12** to the targeted CP **C-13** via a slow-addition, pseudo-high-dilution process<sup>13-15</sup> (Scheme 3.2), whereby a solution of diazide linear polymer **L-12** and 1,4-diethynylbenzene (**14**) was added by syringe pump over several days to a well-stirred DMF reservoir containing Cu-catalyst and *N,N,N',N'',N''*-pentamethyl-diethylenetriamine (PMDETA) ligand. Rather than



**Figure 3.5:** GPC traces of linear bromide polymer **L-11** (black), linear azide polymer **L-12** (red), doubly-clicked linear polymer **L-15** (green), and cyclic polymer **C-13** (blue).



**Figure 3.6:** Partial 600 MHz  $^1\text{H}$  NMR spectrum at  $25\text{ }^\circ\text{C}$  in  $\text{CDCl}_3$  of polymer endgroup resonances showing conversion of the telechelic bromide **L-11** (A) to the diazide **L-12** (B) to the post-click cyclic species **C-13** (C). After cyclization, the endgroup signal shifts downfield to 4.37 ppm. Full spectra can be seen in the SI.

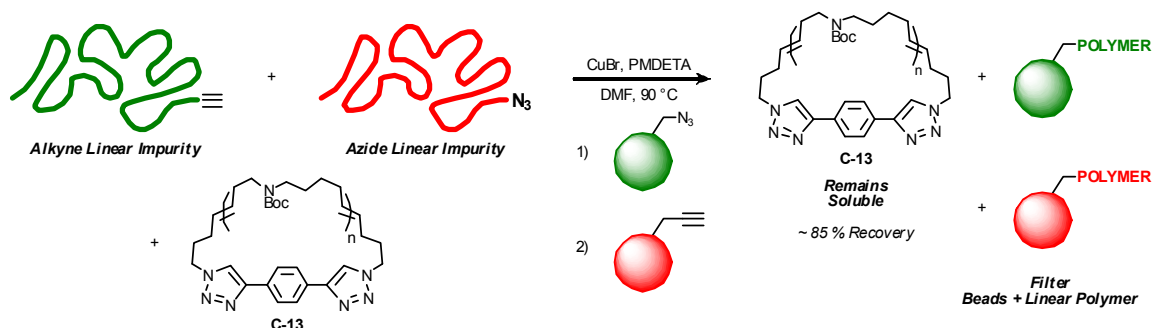


**Figure 3.7:** FT-IR spectrum for linear bromide polymer **L-11** (black), linear azide polymer **L-12** (red), cyclic polymer **C-13** (blue), and doubly-clicked linear polymer **L-15** (green).

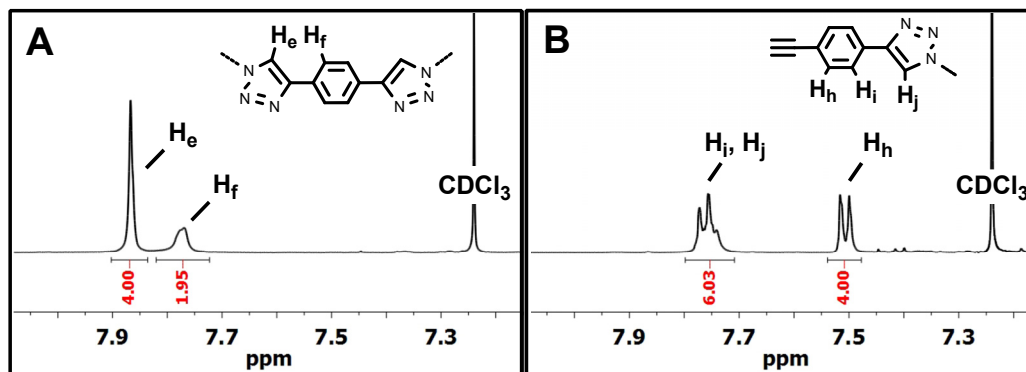
attempt to fractionally precipitate linear polymer impurities<sup>99</sup> from **C-13**, we instead utilized the high fidelity of the “click” reaction. Since any linear polymer contaminants would likely contain either an azide or an alkyne chain-end functionality, we subjected the crude cyclization products to a more concentrated “click” reaction in the presence of alkyne-functionalized polymer beads and azide-functionalized Merrifield resin (Scheme 3.3).<sup>100</sup> Filtration of the solid beads resulted in the concomitant removal of all linear contaminants from solution and afforded a solution of pure cyclic polymer **C-13**.

The cyclic topology of **C-13** was confirmed by <sup>1</sup>H NMR end-group analysis and shifting of GPC peak elution volume. Evidence for the success of the click reaction could be readily observed in the dramatic downfield shift of the azidomethylene proton (H<sub>d</sub>) signal from 3.23 to 4.37 ppm (Figure 3.6C), indicating conversion of the azide to a

**Scheme 3.3:** “Click” Removal of Linear Contaminants from Cyclic Polymer **C-13** Using Azide- and Alkyne-Functionalized Beads.



triazole functionality. IR spectroscopy of **C-13** (Figure 3.7) also showed that the strong azide band in the spectrum of **L-12** was no longer present. Inclusion of the 1,4-diethynylbenzene unit within the backbone of **C-13** was readily apparent in the  $^1\text{H}$  NMR spectrum (Figure 3.8A), with the phenyl protons of the linker ( $\text{H}_f$ ) generating a sharp singlet at 7.88 ppm that integrated to four protons upon assigning the end-group signal from the  $\alpha$ -triazole methylene proton  $\text{H}_g$  an integration value of four (Scheme 3.2). Absence of splitting of the aromatic signal indicated the symmetric nature of the “clicked” unit and implied click coupling at both ends of the 1,4-diethynylbenzene. The triazole moiety also produced a broad singlet at 7.78 ppm (Figure 3.8) that integrated to two protons. GPC analysis of **C-13** (Figure 3.5) showed the expected increase in peak retention time characteristic of cyclic polymers,<sup>9</sup> with no appreciable change in molecular weight (MW) except for the addition of the diethynylbenzene unit ( $M_n = 4.4$  kDa).<sup>101</sup> Additionally, end-group integration by  $^1\text{H}$  NMR remained identical to the linear species **L-11** and **L-12**. Though we attempted to confirm the MW of the polymers through matrix-assisted laser desorption ionization time-of-flight mass spectrometry (MALDI-TOF MS), the lability of the boc-groups, as well as the lability of the bromide and azide

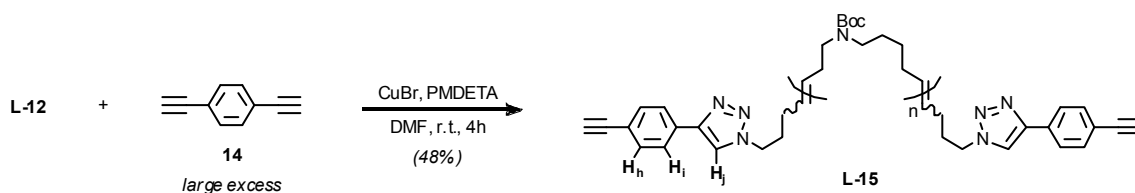


**Figure 3.8.** Partial 600 MHz  $^1\text{H}$  NMR spectra at 25  $^\circ\text{C}$  in  $\text{CDCl}_3$  of the clicked endgroups of the symmetric cyclic polymer **C-13** (A) and the nonsymmetric doubly-clicked linear polymer analogue **L-15** (B). Integration values in red were obtained by assigning the endgroup signal from  $\text{H}_g$  an integration value of four.

end-groups of the linear precursors, prevented accurate mass analysis due to complex and intractable fragmentation patterns.

To confirm that the observed increase in retention time upon cyclization was not an artifact of the click reaction, we synthesized a control polymer using the original diazide polymer **L-12**. We again subjected **L-12** to “click” conditions, but in the presence of a significant excess of dialkyne **14** to give linear, doubly-clicked analogue **L-15** (Scheme 3.4). The GPC trace for **L-15** (Figure 3.5) overlapped identically with both **L-11** and **L-12**, again with only a slight MW increase ( $M_n = 4.4$  kDa) due to the addition of the clicked units. In contrast to the symmetric singlet of the phenyl clicked endgroup of **C-13**, the signal from  $\text{H}_h$  and  $\text{H}_i$  of the phenyl group of the clicked units of **L-15**

**Scheme 3.4: Synthesis of Doubly-Clicked Linear Polymer L-15**



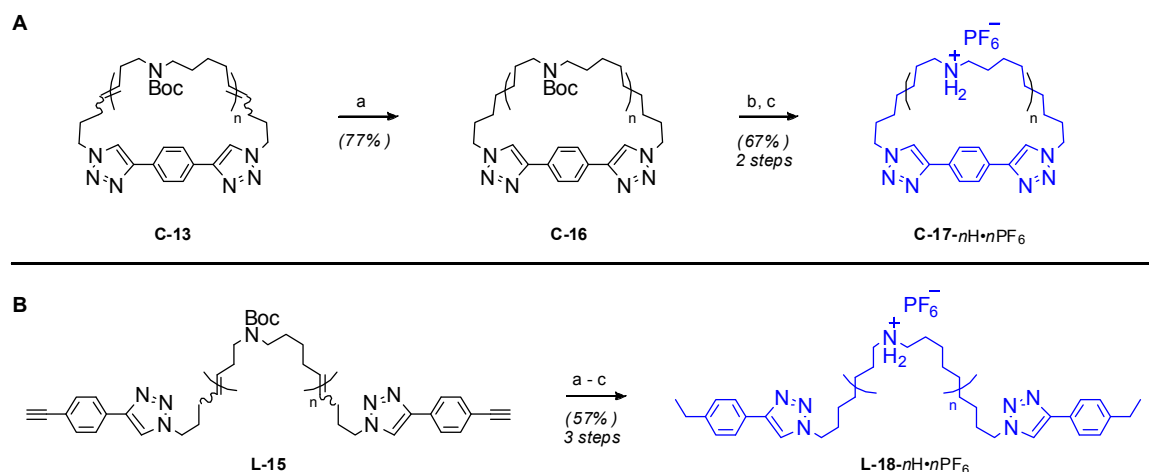
produced two doublets (Figure 3.8) with coincidental overlap of the triazole signal from  $H_j$  with the downfield doublet. Upon assigning the signal from  $H_g$  a value of four protons, each of the doublets from  $H_h$  and  $H_i$  integrated to four protons with an additional two protons from the triazole, confirming the clicking of two 1,4-diethynylbenzene units per polymer chain. IR spectroscopy (Figure 3.7) also showed no azide resonance after the “click” reaction, though peaks at 3300 and 2200  $\text{cm}^{-1}$  indicated the presence of remaining alkyne functionality. The alkyne protons, too, could be observed in the  $^1\text{H}$  NMR spectrum (3.10 ppm) as a sharp singlet extending above the broad signal from  $H_c$ .<sup>100</sup>

**Polymer Functionalization.** Once we had confirmed the cyclic structure of **C-13**, we began the process of functionalizing the polymer in preparation for the desired interlocking reaction. The use of the ruthenium olefin metathesis catalyst **1** to affect the final “clipping” RCM reaction necessitated hydrogenation of all olefin residues within the cyclic polymer backbone, and this was achieved by treating **C-13** with Wilkinson’s catalyst under high-pressure hydrogenation conditions (Scheme 3.5A) to give **C-16**. No remaining olefin residues at 5.40 ppm were observed by  $^1\text{H}$  NMR spectroscopy, indicating saturation of **C-13**.

To reveal the coordinating ammonium sites within the backbone of the polymer, we treated **C-16** with trifluoroacetic acid (TFA), removing the boc-protecting group. The ammonium-TFA adduct was then subjected to counterion exchange with ammonium hexafluorophosphate to produce **C-17- $n\text{H} \cdot n\text{PF}_6$** . Hexafluorophosphate counterions have been shown to increase the binding constant between crown ether–type species and



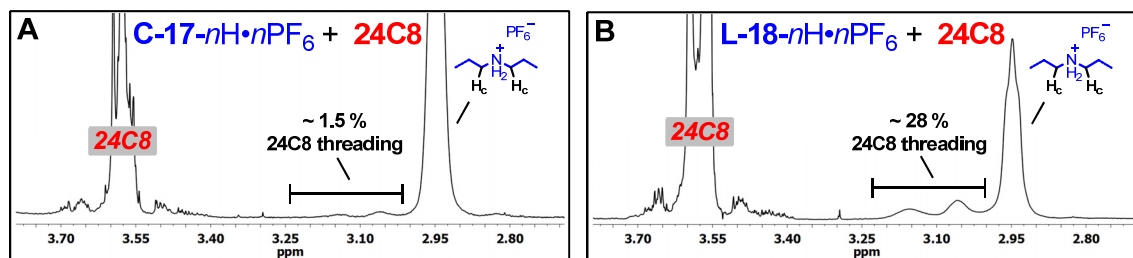
**Scheme 3.5:** Synthesis of (A) Cyclic Polyammonium **C-17-*n*H·*n*PF<sub>6</sub>** and (B) Linear Polyammonium **L-18-*n*H·*n*PF<sub>6</sub>**<sup>a</sup>



<sup>a</sup> Reagents and Conditions: (a) Wilkinson's catalyst ( $\text{Rh}(\text{PPh}_3)_3\text{Cl}$ ), 800 psi  $\text{H}_2$ , THF, 50 °C, 24 h. (b) TFA, DCM, r.t., 4 h. (c)  $\text{NH}_4\text{PF}_6$ , MeOH, r.t., 12 h.

ammonium ions, and also enhance the solubility of the charged complex in organic solvents.<sup>102-105</sup> Analysis of **C-17-*n*H·*n*PF<sub>6</sub>** by <sup>1</sup>H NMR spectroscopy showed a broad singlet (6.45 ppm) corresponding to the ammonium residues, and the sharp signal at 1.4 ppm corresponding to protons on the boc-group was no longer present. Additionally the  $\alpha$ -ammonium methylene proton signal from H<sub>c</sub> (Scheme 3.2) shifted upfield to 2.96 ppm (originally 3.13 ppm), an effect of the conversion of the boc-amine to an ammonium salt. Broadening and shifting of the triazole resonance (from 7.80 ppm to 8.14 ppm) suggested that the acidic conditions of the deprotection may have resulted in protonation of the triazole.

The linear doubly-clicked analogue **L-15** was subjected to the same hydrogenation conditions (Scheme 3.5B) as **C-13** to give the saturated product. Deprotection and anion exchange were also performed, generating linear polyammonium adduct **L-18-*n*H·*n*PF<sub>6</sub>**. Unfortunately none of the charged polymers were amenable to



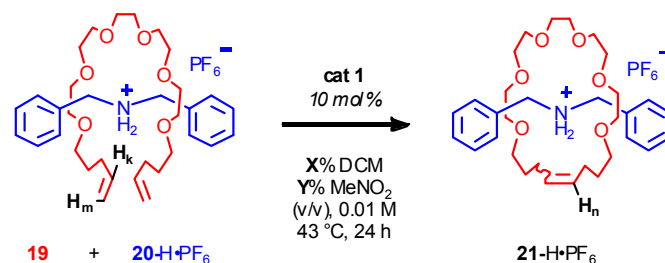
**Figure 3.9:** Partial 600 MHz  $^1\text{H}$  NMR spectrum at 25  $^\circ\text{C}$  in  $\text{CD}_3\text{CN}$  of (A) cyclic polyammonium **C-17- $n\text{H}_2 \cdot n\text{PF}_6$**  with 24-crown-8 ether (24C8) showing less than 1.5% threading, and (B) linear doubly-clicked polyammonium **L-18- $n\text{H}_2 \cdot n\text{PF}_6$**  with 24C8 showing more than 28% threading. (Note: approximately 0.5 equiv of 24C8 per ammonium, see Supporting Information for complete details.)

GPC analysis due to challenges associated with solubility. As an alternate protocol for cyclic/linear topology confirmation, we exploited the well-known hydrogen-bonding association between 24-crown-8 ether (24C8) and dialkylammonium ions. Upon encircling a dialkylammonium ion, the strongly-coordinating 24C8 causes a downfield shift of the signal from the protons on the carbons adjacent to that ammonium site. Correlating the integration values of the original signal with the shifted signals enables quantitation of the threading of the polymeric chains by 24C8. When a solution of the “endless” **C-17- $n\text{H}_2 \cdot n\text{PF}_6$**  was mixed with 24C8 (0.5 equivalents per ammonium site), barely-detectable threading ( $< 2\%$ ) was observed  $^1\text{H}$  NMR spectroscopy (Figure 3.9A, see Supporting Information for full details). However, linear analogue **L-19- $n\text{H}_2 \cdot n\text{PF}_6$**  engaged in significant threading interactions upon addition of the same amount of 24C8 (nearly 30% threading, Figure 3.9B). As expected, introduction of additional 24C8 (total of 2.0 equivalents per ammonium site) resulted in increased threading for both polymers, with coordination remaining low for **C-17- $n\text{H}_2 \cdot n\text{PF}_6$**  ( $\sim 10\%$ ) while **L-19- $n\text{H}_2 \cdot n\text{PF}_6$**  threaded to  $\sim 45\%$ . It is worth noting that, due to the dominance of cyclic architectures in

the sample of **C-17-*n*H·*n*PF<sub>6</sub>**, the effective concentration of available 24C8 would be much higher per ammonium site for any linear, threadable polymers, and could explain the proportionally greater increase in threading upon introduction of additional crown. This topologically-based threading protocol was particularly valuable, as it enabled quantitative determination that the presence of linear contaminants **C-17-*n*H·*n*PF<sub>6</sub>** was very low and unambiguously showed that the sample contained near or above 90% cyclic polymer.

**Molecular “Charm Bracelet” Synthesis and Analysis.** To enable “clipping” of CP **C-17-*n*H·*n*PF<sub>6</sub>**, we had to develop a suitable solvent system that would both solubilize the highly-charged polymer and facilitate the olefin metathesis reaction. Because the polymer displayed good solubility in nitromethane, we explored the possibility of using this as our RCM solvent. To test the efficacy of this system, we monitored the effect of nitromethane concentration on the conversion of protons H<sub>k</sub> and H<sub>m</sub> to H<sub>n</sub> upon “clipping” of diolefin crown ether–type fragment **19** around template **20-H·PF<sub>6</sub>** to form pseudorotaxane **21-H·PF<sub>6</sub>** (Scheme 3.6).<sup>100</sup> We observed that increased nitromethane volume fraction (relative to DCM) led to decreased olefin conversion. Consequently, we concluded that a 1:1 mixture (v/v) of dichloromethane to nitromethane would maximize the solubility of the polymer while still enabling reasonable olefin conversion.

**Scheme 3.6.** Screen Reaction to Determine Effect of Nitromethane Concentration on RCM Olefin Conversion

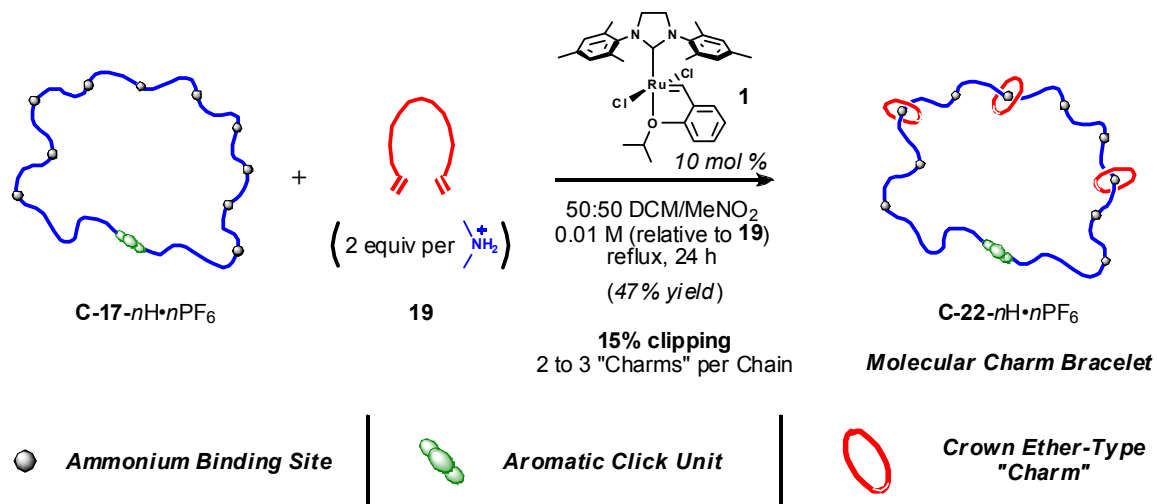


Entry	X % DCM	Y % MeNO <sub>2</sub>	Conversion [%] <sup>a</sup>
1	100	0	quant
2	95	5	90
3	90	10	90
4	80	20	85
5	50	50	62
6	25	75	54
7	0	100	30

<sup>a</sup> Conversion measured by <sup>1</sup>H NMR integration of H<sub>m</sub> relative to H<sub>n</sub> after 24 h.

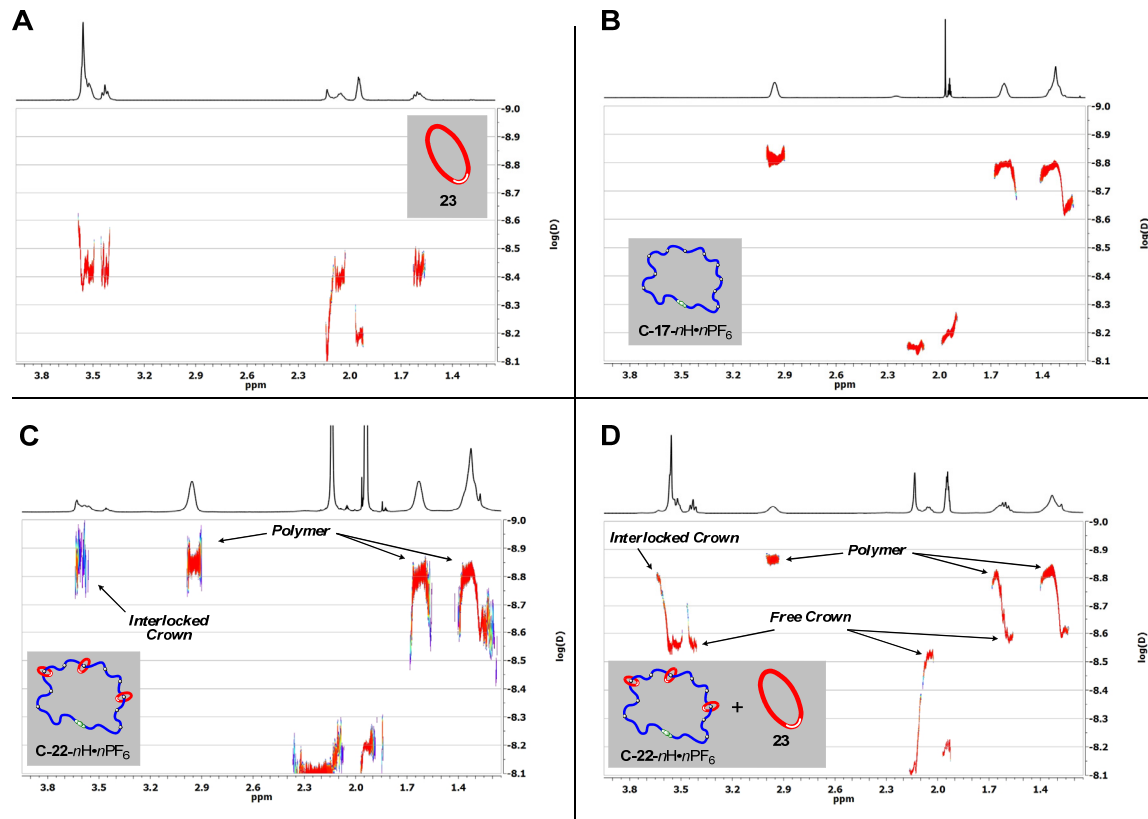
Synthesis of the molecular “charm bracelet” polymer (Scheme 3.7) was achieved via addition of catalyst **1** to a solution of **C-17-nH<sub>2</sub>·nPF<sub>6</sub>** and **19** in the 1:1 dichloromethane to nitromethane (v/v) solvent mixture. Simple precipitation of the polymer into pure dichloromethane and isolation of the insoluble material afforded the desired interlocked “charm bracelet” **C-22-nH·nPF<sub>6</sub>**. By <sup>1</sup>H NMR spectroscopic analysis, ~15% of the ammonium sites were clipped, indicating each polymer chain contained approximately two to three interlocked “charms.” We believe there are several factors that resulted in this low clipping percent. Because of the limited solubility of the polymer, the charged ammonium residues were likely concentrated in a dense core surrounded by the more-soluble alkyl components, severely limiting access of **19** and catalyst to the polymer binding sites and preventing extensive clipping. Also, the large amount of nitromethane solvent required to dissolve **C-17-nH<sub>2</sub>·nPF<sub>6</sub>** would significantly

**Scheme 3.7:** Graphical Representation of the Synthesis of Molecular “Charm Bracelet”  
**C-22-*n*H·*n*PF<sub>6</sub>**



decrease the association constant governing coordination of **19** to the ammonium sites, a phenomenon further compounded by the inherently lower binding constant of dialkylammonium species relative to their dibenzyl counterparts.<sup>45</sup>

Though efforts to neutralize **C-22-*n*H·*n*PF<sub>6</sub>** were unsuccessful, conclusive evidence for the interlocked nature of the molecular “charm bracelet” was obtained using <sup>1</sup>H and 2D-DOSY NMR spectroscopy. Analysis of the proton signals of the interlocked crown showed significant line broadening<sup>100</sup> relative to the free, non-interlocked ring-closed analogue, a phenomenon that is commonly observed for interlocked complexes<sup>56,63,69</sup> and arises from an increase in the rotational correlation time of the interlocked crown as a result of increased MW and volume (due to interlocking of the small ring with the large polymer). Additionally, a downfield shift in the –CH<sub>2</sub>– crown proton signals from 3.57 ppm to 3.64 ppm was observed, a phenomenon attributed to subtle electron-withdrawing effects from hydrogen bonding interactions occurring



**Figure 3.10:** 2D-DOSY  $^1\text{H}$  NMR spectra at 400 MHz and 25  $^\circ\text{C}$  in  $\text{CD}_3\text{CN}$  of free ring-closed crown **23** (A), cyclic polyammonium template **C-17-nH-nPF<sub>6</sub>** (B), purified molecular “charm bracelet” **C-22-nH-nPF<sub>6</sub>** (C), and a physical mixture of **C-22-nH-nPF<sub>6</sub>** and **23** (D). The units of the diffusion constant  $D$  are  $\text{m}^2 \text{s}^{-1}$ .

between the ammonium protons and crown oxygens. Though one-dimensional  $^1\text{H}$  NMR analysis suggested the interlocked nature of **C-22-nH-nPF<sub>6</sub>**, 2D-DOSY NMR provided convincing evidence. This technique enabled the direct detection of the diffusion rates of ring-closed product **23** after ring-closing in the absence and presence of polymer (Figure 3.10A and 3.10C, respectively). Typically, the diffusion values obtained from 2D-DOSY NMR are reported as  $\log(D)$ , where the diffusion constant,  $D$ , has units of  $\text{m}^2 \text{s}^{-1}$ . Thus, a smaller (more negative) diffusion value implies a slower diffusion rate. For example, the large macromolecular template **C-17-nH-nPF<sub>6</sub>** (Figure 3.10B) had a diffusion value of

$\log(D) = -8.83$  (slow), while free crown **23** (Figure 3.10A) had a faster diffusion value of  $\log(D) = -8.45$ , expected behavior for a small molecule. However, when the crown signals from **C-22-*n*H·*n*PF<sub>6</sub>**, were analyzed by 2D-DOSY NMR, a significant reduction in crown diffusion speed ( $\log(D) = -8.85$ ) was observed (Figure 3.10B). The alignment of crown and polymer signals at the same diffusion rate indicated an intimate association between the two species, only possible if **23** was interlocked around the cyclic polymer framework. To rule out the possibility of coincidental overlap between crown and polymer diffusion values observed in Figure 3.10B, a sample of **C-22-*n*H·*n*PF<sub>6</sub>** was spiked with non-interlocked **23**. If the slow diffusion rate of crown signals in the 2D-DOSY NMR of **C-22-*n*H·*n*PF<sub>6</sub>** (Figure 3.10C) originated from hydrogen bonding interactions between the crown and polymer and not from interlocking of the crown around the polymer backbone, we would expect to see the introduced, non-interlocked crown diffuse at a similarly slow rate as the interlocked crown in **C-22-*n*H·*n*PF<sub>6</sub>**. However, upon 2D-DOSY NMR analysis of a physical mixture of **C-22-*n*H·*n*PF<sub>6</sub>** and **23**, a distinct difference between diffusion rates of the two types of crown ( $\log(D) = -8.80$  and  $-8.52$ , bound and free, respectively) was observed (Figure 3.10D), confirming the interlocked nature of the crown in molecular “charm bracelet” **C-22-*n*H·*n*PF<sub>6</sub>**.

### Conclusions

We have described a “clipping” approach to a polycatenated cyclic polymer, a structure that resembles a molecular “charm bracelet.” We have shown that the use of ring-opening metathesis polymerization of a carbamate monomer in the presence of a chain transfer agent allows for the synthesis of a linear polymer that could be

subsequently functionalized and cyclized to the corresponding cyclic analogue. This cyclic polymer was characterized through a variety of techniques, and subjected to further functionalization reactions, affording a cyclic polyammonium scaffold. Diolefin polyether fragments were coordinated and “clipped” around the ammonium sites within the polymer backbone using ring-closing olefin metathesis, giving the molecular “charm bracelet.” Confirmation of the interlocked nature of the product was achieved via  $^1\text{H}$  NMR spectroscopy and two-dimensional diffusion-ordered NMR spectroscopy.

### **References**

- (1) McKenna, G. B.; Hadziioannou, G.; Lutz, P.; Hild, G.; Strazielle, C.; Straupe, C.; Rempp, P.; Kovacs, A. J. *Macromolecules* **1987**, *20*, 498.
- (2) Roovers, J.; Toporowski, P. M. *Macromolecules* **1983**, *16*, 843.
- (3) Semlyen, J. A. *Large Ring Molecules Chichester*; Wiley: New York, 1996.
- (4) Semlyen, J. A. *Cyclic Polymers*, 2nd Ed.; Kluwer Academic Publishers: Boston, 2000.
- (5) Zimm, B. H.; Stockmayer, W. H. *J. Chem. Phys.* **1949**, *17*, 1301.
- (6) Bensafi, A.; Maschke, U.; Benmouna, M. *Polym. Int.* **2000**, *49*, 175.
- (7) Subramanian, G.; Shanbhag, S. *Macromolecules* **2008**, *41*, 7239.
- (8) Nasongkla, N.; Chen, B.; Macaraeg, N.; Fox, M. E.; Fréchet, J. M. J.; Szoka, F. C. *J. Am. Chem. Soc.* **2009**, *131*, 3842.
- (9) Laurent, B. A.; Grayson, S. M. *Chem. Soc. Rev.* **2009**, *38*, 2202.
- (10) Kricheldorf, H. R. *Macromol. Rapid Commun.* **2009**, *30*, 1371.
- (11) Kricheldorf, H. R.; Schwarz, G. *Macromol. Rapid Commun.* **2003**, *24* 359.



- (12) Hadjichristidis, N.; Pitsikalis, M.; Pispas, S.; Iatrou, H. *Chem. Rev.* **2001**, *101*, 3747.
- (13) Laurent, B. A.; Grayson, S. M. *J. Am. Chem. Soc.* **2006**, *128*, 4238.
- (14) Eugene, D. M.; Grayson, S. M. *Macromolecules* **2008**, *41*, 5082.
- (15) Goldmann, A. S.; Quémener, D.; Millard, P.-E.; Davis, T. P.; Stenzel, M. H.; Barner-Kowollik, C.; Müller, A. H. E. *Polymer* **2008**, *49*, 2274.
- (16) Adachi, K.; Honda, S.; Hayashi, S.; Tezuka, Y. *Macromolecules* **2008**, *41*, 7898.
- (17) Tezuka, Y.; Ohtsuka, T.; Adachi, K.; Komiya, R.; Ohno, N.; Okui, N. *Macromol. Rapid Commun.* **2008**, *29*, 1237.
- (18) Oike, H.; Imaizumi, H.; Mouri, T.; Yoshioka, Y.; Uchibori, A.; Tezuka, Y. *J. Am. Chem. Soc.* **2000**, *122*, 9592.
- (19) Tezuka, Y.; Fujiyama, K. *J. Am. Chem. Soc.* **2005**, *127*, 6266.
- (20) Oike, H.; Kobayashi, S.; Mouri, T.; Tezuka, Y. *Macromolecules* **2001**, *34*, 2742.
- (21) Oike, H.; Mouri, T.; Tezuka, Y. *Macromolecules* **2001**, *34*, 6592.
- (22) Adachi, K.; Takasugi, H.; Tezuka, Y. *Macromolecules* **2006**, *39*, 5585.
- (23) Tezuka, Y. *J. Polym. Sci., Part A: Polym. Chem.* **2003**, *5*, 17.
- (24) Tezuka, Y.; Oike, H. *Macromol. Rapid Commun.* **2001**, *22*, 1017.
- (25) Tezuka, Y. *Chem. Rec.* **2005**, *5*, 17.
- (26) Culkin, D. A.; Jeong, W.; Csihony, S.; Gomez, E. D.; Balsara, N. P.; Hedrick, J. L.; Waymouth, R. M. *Angew. Chem., Int. Ed.* **2007**, *46*, 2627.
- (27) Boydston, A. J.; Xia, Y.; Kornfield, J. A.; Gorodetskaya, I. A.; Grubbs, R. H. *J. Am. Chem. Soc.* **2008**, *130*, 12775.

- (28) Xia, Y.; Boydston, A. J.; Yao, Y.; Kornfield, J. A.; Gorodetskaya, I. A.; Spiess, H. W.; Grubbs, R. H. *J. Am. Chem. Soc.* **2009**, *131*, 2670.
- (29) Bielawski, C. W.; Benitez, D.; Grubbs, R. H. *J. Am. Chem. Soc.* **2003**, *125*, 8424.
- (30) Bielawski, C. W.; Benitez, D.; Grubbs, R. H. *Science* **2002**, *297*, 2041.
- (31) Kolb, H. C.; Finn, M. G.; Sharpless, K. B. *Angew. Chem. Int. Ed.* **2001**, *40*, 2004.
- (32) Golas, P. L.; Tsarevsky, N. V.; Sumerlin, B. S.; Matyjaszewski, K. *Macromolecules* **2006**, *39*, 6451.
- (33) Lutz, J.-F. *Angew. Chem. Int. Ed.* **2008**, *47*, 2182.
- (34) Tsarevsky, N. V.; Sumerlin, B. S.; Matyjaszewski, K. *Macromolecules* **2005**, *38*, 3558.
- (35) Fournier, D.; Hoogenboom, R.; Schubert, U. S. *Chem. Soc. Rev.* **2007**, *36*, 1369.
- (36) Lutz, J.-F. *Angew. Chem., Int. Ed.* **2007**, *46*, 1018.
- (37) Trnka, T. M.; Grubbs, R. H. *Acc. Chem. Res.* **2001**, *34*, 18.
- (38) Love, J. A.; Sanford, M. S.; Day, M. W.; Grubbs, R. H. *J. Am. Chem. Soc.* **2003**, *125*, 10103.
- (39) Frenzel, U.; Nuyken, O. *J. Polym. Sci., Part A: Polym. Sci.* **2002**, *40*, 2895.
- (40) Bielawski, C. W.; Grubbs, R. H. *Prog. Polym. Sci.* **2007**, *32*, 1.
- (41) Huang, F.; Gibson, H. W. *Prog. Polym. Sci.* **2005**, *30*, 982.
- (42) Wenz, G.; Han, B.-H.; Müller, A. *Chem. Rev.* **2006**, *106*, 782.
- (43) Harada, A.; Hashidzume, A.; Yamaguchi, H.; Takashima, Y. *Chem. Rev.* **2009**, *109*, 5974.
- (44) Stoddart, J. F. *Chem. Soc. Rev.* **2009**, *38*, 1802.

- (45) Schalley, C. A.; Weilandt, T.; Brüggemann, J.; Vögtle, F. *Topics Curr. Chemistry* **2004**, 248, 141.
- (46) Cantrill, S. J.; Fulton, D. A.; Heiss, A. M.; Pease, A. R.; Stoddart, J. F.; White, A. J. P.; Williams, D. J. *Chem. Eur. J.* **2000**, 6, 2274.
- (47) Ashton, P. R.; Bartsch, R. A.; Cantrill, S. J.; Hanes Jr., R. E.; Hickingbottom, S. K.; Lowe, J. N.; Preece, J. A.; Stoddart, J. F.; Talanov, V. S.; Wang, Z.-H. *Tetrahedron Lett.* **1999**, 40, 3661.
- (48) Meyer, C. D.; Joiner, C. S.; Stoddart, J. F. *Chem. Soc. Rev.* **2007**, 36, 1705.
- (49) Haussmann, P. C.; Stoddart, J. F. *Chem. Record* **2009**, 9, 136.
- (50) Rowan, S. J.; Cantrill, S. J.; Cousins, G. R. L.; Sanders, J. K. M.; Stoddart, J. F. *Angew. Chem., Int. Ed.* **2002**, 41, 898.
- (51) Wu, J.; Leung, K. C.-F.; Stoddart, J. F. *Proc. Natl. Acad. Sci. U.S.A.* **2007**, 104, 17266.
- (52) Haussmann, P. C.; Khan, S. I.; Stoddart, J. F. *J. Org. Chem.* **2007**, 72, 6708.
- (53) Aricó, F.; Chang, T.; Cantrill, S. J.; Khan, S. I.; Stoddart, J. F. *Chem. Eur. J.* **2005**, 11, 4655.
- (54) Glink, P. T.; Oliva, A. I.; Stoddart, J. F.; White, A. J. P.; Williams, D. J. *Angew. Chem., Int. Ed.* **2001**, 40, 1870.
- (55) Wisner, J. A.; Beer, P. D.; Drew, M. G. B.; Sambrook, M. R. *J. Am. Chem. Soc.* **2002**, 124, 12469.
- (56) Kilbinger, A. F. M.; Cantrill, S. J.; Waltman, A. W.; Day, M. W.; Grubbs, R. H. *Angew. Chem. Int. Ed.* **2003**, 42, 3281.

- (57) Hannam, J. S.; Kidd, T. J.; Leigh, D. A.; Wilson, A. J. *Org. Lett.* **2003**, *5*, 1907.
- (58) Coumans, R. G. E.; Elemans, J. A. A. W.; Thordarson, P.; Nolte, R. J. M.; Rowan, A. E. *Angew. Chem., Int. Ed.* **2003**, *42*, 650.
- (59) Kidd, T. J.; Leigh, D. A.; Wilson, A. J. *J. Am. Chem. Soc.* **1999**, *121*, 1599.
- (60) Weck, M.; Mohr, B.; Sauvage, J.-P.; Grubbs, R. H. *J. Org. Chem.* **1999**, *64*, 5463.
- (61) Mobian, P.; Kern, J.-M.; Sauvage, J.-P. *J. Am. Chem. Soc.* **2003**, *125*, 2016.
- (62) Sambrook, M. R.; Beer, P. D.; Wisner, J. A.; Paul, R. L.; Cowley, A. R. *J. Am. Chem. Soc.* **2004**, *126*, 15364.
- (63) Guidry, E. N.; Cantrill, S. J.; Stoddart, J. F.; Grubbs, R. H. *Org. Lett.* **2005**, *7*, 2129.
- (64) Iwamoto, H.; Itoh, K.; Nagamiya, H.; Fukazawa, Y. *Tetrahedron Lett.* **2003**, *44*, 5773.
- (65) Wang, L.; Vysotsky, M. O.; Bogdan, A.; Bolte, M.; Böhmer, V. *Science* **2004**, *304*, 1312.
- (66) Badjić, J. D.; Cantrill, S. J.; Grubbs, R. H.; Guidry, E. N.; Orenes, R.; Stoddart, J. F. *Angew. Chem., Int. Ed.* **2004**, *43*, 3273.
- (67) Wang, L.; Vysotsky, M. O.; Bogdan, A.; Bolte, M.; Böhmer, V. *Science* **2004**, *304*, 1312-1314.
- (68) Zhu, X.-Z.; Chen, C.-F. *J. Am. Chem. Soc.* **2005**, *127*, 13158.
- (69) Guidry, E. N.; Li, J.; Stoddart, J. F.; Grubbs, R. H. *J. Am. Chem. Soc.* **2007**, *129*, 8944-8945.
- (70) Takata, T.; Kihara, N.; Furusho, Y. *Adv. Polym. Sci.* **2004**, *171*, 1.

- (71) Gibson, H. W.; Ge, Z.; Huang, F.; Jones, J. W.; Lefebvre, H.; Vergne, M. J.; Hercules, D. M. *Macromolecules* **2005**, *38*, 2626.
- (72) Endo, K.; Yamanaka, T. *Macromolecules* **2006**, *39*, 4038.
- (73) Gozowsky, E. K.; Gorenstein, D. G. *J. Mag. Reson. B* **1996**, *111*, 94.
- (74) Dötsch, V.; Wider, G. *J. Am. Chem. Soc.* **1995**, *117*, 6064.
- (75) Johnson, C. S. *Prog. NMR* **1999**, *34*, 203.
- (76) Sørland, G. H.; Aksnes, D. *Magn. Reson. Chem.* **2002**, *40*, 146.
- (77) Zhang, S. *J. Am. Chem. Soc.* **2006**, *128*, 4974.
- (78) Antalek, B. *Conc. Magn. Res.* **2002**, *14*, 225.
- (79) Wu, J.; Fang, F.; Lu, W.-Y.; Hou, J.-L.; Li, C.; Wu, Z.-Q.; Jiang, X.-K.; Li, Z.-T.; Yu, Y.-H. *J. Org. Chem.* **2007**, *72*, 2897.
- (80) Zhao, T.; Beckham, H. W.; Gibson, H. W. *Macromolecules* **2003**, *36*, 4833.
- (81) Niu, Z.; Gibson, H. W. *Chem. Rev.* **2009**, *109*, 6024.
- (82) Gibson, H. W.; Liu, S.; Lecavalier, P.; Wu, C.; Shen, Y. X. *J. Am. Chem. Soc.* **1995**, *117*, 852.
- (83) Gibson, H. W.; Liu, S.; Gong, C.; Ji, Q.; Joseph, E. *Macromolecules* **1997**, *30*, 3711.
- (84) Fustin, C. A.; Clarkson, G. J.; Leigh, D. A.; Van Hoof, F.; Jonas, A. M.; Bailly, C. *Macromolecules* **2004**, *37*, 7884.
- (85) Fustin, C.-A.; Bailly, C.; Clarkson, G. J.; Galow, T. H.; Leigh, D. A. *Macromolecules* **2004**, *37*, 66.

- (86) Ni, X.-L.; Lin, J.-X.; Zheng, Y.-Y.; Wu, W.-S.; Zhang, Y.-Q.; Xue, S.-F.; Tao, Z.; Day, A. I. *Cryst. Growth Des.* **2008**, *8*, 3446.
- (87) Chiu, S.-H.; Rowan, S. J.; Cantrill, S. J.; Ridvan, L.; Ashton, P. R.; Garrell, R. L.; Stoddart, J. F. *Tetrahedron* **2002**, *58*, 807.
- (88) Roh, S.-G.; Park, K.-M.; Park, G.-J.; Sakamoto, S.; Yamaguchi, K.; Kim, K. *Angew. Chem., Int. Ed.* **1999**, *38*, 637.
- (89) Heo, J.; Kim, S.-Y.; Whang, D.; Kim, K. *Angew. Chem., Int. Ed.* **1999**, *38*, 641.
- (90) Park, K.-M.; Whang, D.; Lee, E.; Heo, J.; Kim, K. *Chem. Eur. J.* **2002**, *8*, 498.
- (91) Ko, Y. H.; Kim, K.; Kang, J.-K.; Chun, H.; Lee, J. W.; Sakamoto, S.; Yamaguchi, K.; Fettinger, J. C.; Kim, K. *J. Am. Chem. Soc.* **2004**, *126*, 1932.
- (92) Okada, M.; Harada, A. *Macromolecules* **2003**, *36*, 9701.
- (93) Wilson, S. R.; Sawicki, R. A. *J. Org. Chem.* **1979**, *44*, 330.
- (94) Hillmyer, M. A.; Grubbs, R. H. *Macromolecules* **1993**, *26*, 872.
- (95) Hillmyer, M. A.; Laredo, W. R.; Grubbs, R. H. *Macromolecules* **1995**, *28*, 6311.
- (96) Maughon, B. R.; Morita, T.; Bielawski, C. W.; Grubbs, R. H. *Macromolecules* **2000**, *33*, 1929.
- (97) Morita, T.; Maughon, B. R.; Bielawski, C. W.; Grubbs, R. H. *Macromolecules* **2000**, *33*, 6621.
- (98) Matson, J. B.; Virgil, S. C.; Grubbs, R. H. *J. Am. Chem. Soc.* **2009**, *131*, 3355.
- (99) Gan, Y.; Dong, D.; Hogen-Esch, T. E. *Macromolecules* **2002**, *35*, 6799.
- (100) See Supporting Information for full details.

- (101) All GPC MW measurements were obtained through multiangle laser light scattering detection, giving the absolute MW of the polymer.
- (102) Ashton, P. R.; Cantrill, S. J.; Preece, J. A.; Stoddart, J. F.; Wang, Z.-H.; White, A. J. P.; Williams, D. J. *Org. Lett.* **1999**, *1*, 1917.
- (103) Montalti, M. *Chem. Commun.* **1998**, 1461.
- (104) Doxsee, K. M. *J. Org. Chem.* **1989**, *54*, 4712.
- (105) Jones, J. W.; Gibson, H. W. *J. Am. Chem. Soc.* **2003**, *125*, 7001.

### ***Experimental Section***

Experimental procedures and characterization data ( $^1\text{H}$  and  $^{13}\text{C}$  and 2D NMR, IR, HRMS, GPC) for all compounds and their precursors.

**General Information.** NMR spectra were obtained on either a Mercury 300 MHz spectrometer, an INOVA 500 MHz spectrometer equipped with an AutoX broadband probe with z-gradients, or an INOVA 600 MHz spectrometer equipped with an inverse HCN triple resonance probe with x-, y-, and z-gradients. All spectrometers were running Varian VNMRJ software. Chemical shifts for both  $^1\text{H}$  and  $^{13}\text{C}$  spectra are reported in per million (ppm) relative to  $\text{Si}(\text{CH}_3)_4$  ( $\delta=0$ ) and referenced internally to the proteo solvent resonance. Multiplicities are abbreviated as follows: singlet (s), doublet (d), triplet (t), quartet (q), quintet (qt), septuplet (sp), multiplet (m), and broad (br). MestReNova NMR 5.3.2 software was used to analyze all NMR spectra. Molecular mass calculations were performed with ChemBioDraw Ultra 11.0.1 (Cambridge Scientific). Mass spectrometry measurements (FAB, EI, and MALDI) were performed by the California Institute of Technology Mass Spectrometry Facility. Analytical thin-layer chromatography (TLC) was performed using silica gel 60 F254 precoated plates (0.25 mm thickness) with a fluorescent indicator. Visualization was performed using UV and iodine stain. Flash column chromatography was performed using silica gel 60 (230-400 mesh) from EM Science. Gel permeation chromatography (GPC) was carried in THF out on two PLgel 10  $\mu\text{m}$  mixed-B LS columns (Polymer Labs) connected in series with a DAWN EOS multiangle laser light scattering (MALLS) detector and an Optilab DSP differential refractometer (both from Wyatt Technology). No calibration standards were



used, and  $dn/dc$  values were obtained for each injection assuming 100% mass elution from the columns. IR was obtained on a Perkin-Elmer BX-II FTIR spectrometer using thin-film techniques on NaCl plates.

**DOSY Information.** The 2D-DOSY measurements were made at 400 MHz on a Bruker DPX spectrometer with a variable-temperature dual  $^1\text{H}/^{13}\text{C}$  dual probe and a DPX Avance console. Accessories relevant to the experiment included a GCU gradient shaping card, a GREAT gradient amplifier with a maximum gradient current of 10 A, and a single-axis gradient coil on the probe. Bruker XWINNMR was used to control the spectrometer and process the data. The execution of the experiment, which employs an automation program in addition to the `ledbpgp2s` pulse sequence, is described in a special Bruker document.<sup>1</sup> The coil constant for the probe was determined by applying the BP-LDE pulse sequence, which was developed for measuring the translational diffusion constant  $D_T$ , on a sample with a known  $D_T$ . Longworth accurately measured  $D_T$  of HDO in  $\text{D}_2\text{O}$ .<sup>2</sup> Accordingly, the HDO signal in 99.96 atom-%  $\text{D}_2\text{O}$  was observed with the BP-LDE method of Stejskal and Tanner modified by Wu et al., which employs bipolar gradient pulses and the LED pulse sequence.<sup>3</sup> The DOSY measurements were based on the 2D version of the BP-LDE method. The acquisition parameters were SW, 10.00 ppm; TD, 16k; NS, 512; AQ, 2.0447731 s;  $\Delta$  (the diffusion time), 500 ms;  $\tau$  (the gradient recovery), 0.2 ms;  $T_e$  (the eddy current delay), 5 ms;  $\delta/2$  (the gradient pulse), 0.5 ms. Sinusoidal gradient pulses and a quadratic ramp in gradient current were employed.

A quadratic ramp of 16 gradient currents ranging from 0.354% to 21.235% was employed.

**Materials and Methods.** Anhydrous N,N-dimethylformamide (DMF) was obtained from Acros (99.8% pure, Acroseal). Dry tetrahydrofuran (THF) and dichloromethane (DCM) were purified by passage through solvent purification columns.<sup>4</sup> All water was deionized. *cis*-1,5-Cyclooctadiene (**4**, 99%), 5-bromo-1-pentene (95%), and 1,4-diethynylbenzene (**14**, 96%), and nitromethane (95+%, ACS reagent) were purchased from Aldrich and used as received. Anhydrous potassium carbonate (J. T. Baker, 99.6%) was used as received. Grubbs second-generation catalyst (H<sub>2</sub>IMes)(PCy<sub>3</sub>)(Cl)<sub>2</sub>Ru=CHPh and Grubbs-Hoveyda second-generation isopropoxybenzylidene catalyst (H<sub>2</sub>IMes)(Cl)<sub>2</sub>RuCH(o-OiPrC<sub>6</sub>H<sub>4</sub>) (**1**) were obtained as a generous gift from Materia, Inc. All other compounds were purchased from Acros or Aldrich and used as received.

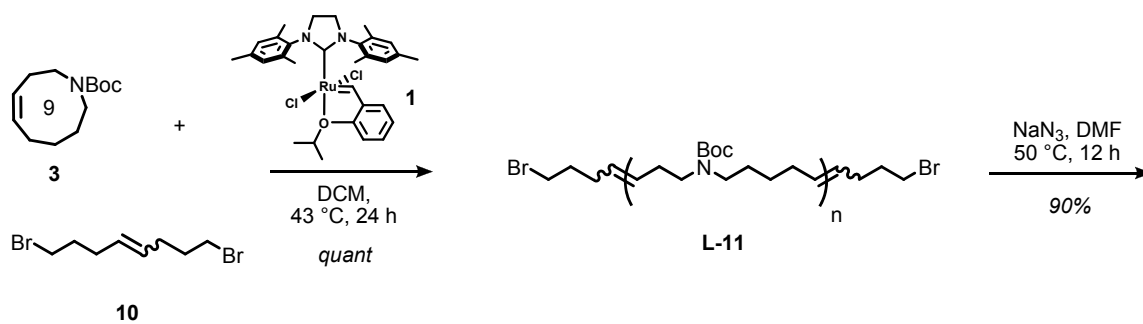
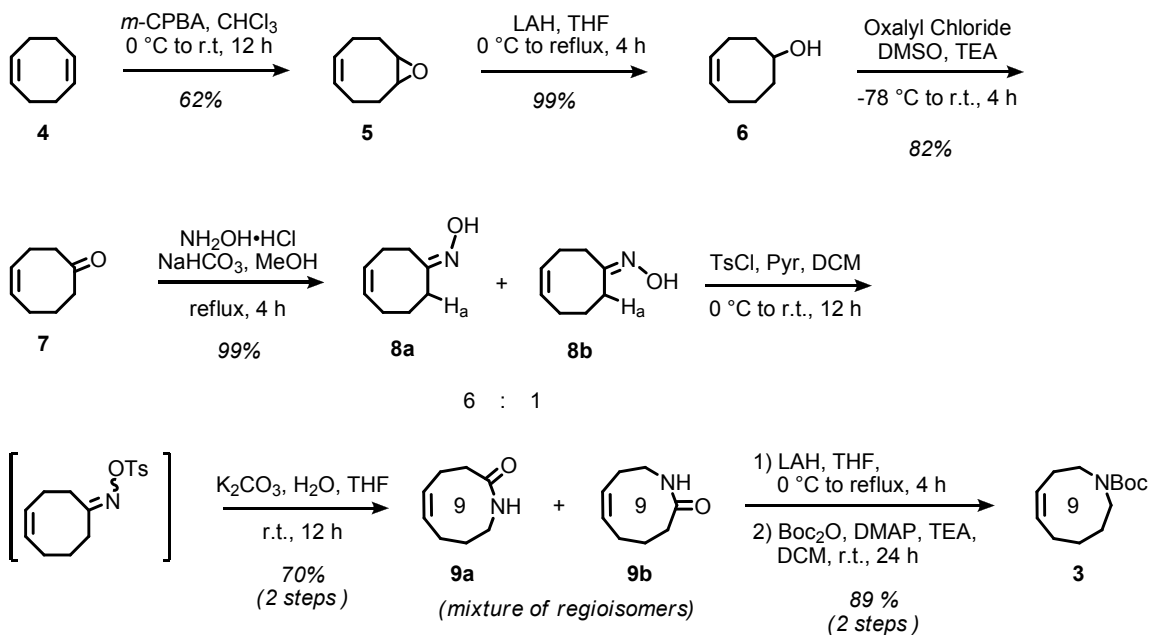
**General Freeze-Pump-Thaw Procedure.** A flask charged with reagents and solvent was frozen with liquid nitrogen. After the solution had frozen, the headspace of the flask was evacuated under vacuum. The flask was sealed and allowed to thaw to room temperature. The headspace of the flask was then backfilled with argon. The flask was sealed and the reaction mixture frozen again with liquid nitrogen. This process was repeated twice. On the third cycle, the solution was frozen and the headspace evacuated and backfilled with argon. Catalyst was quickly added to the top of the frozen solution,

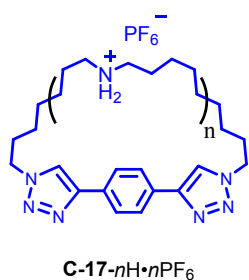
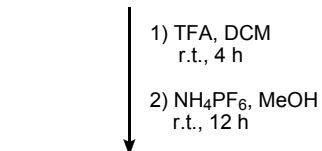
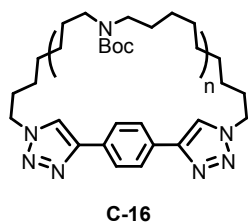
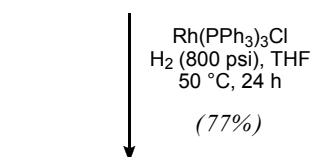
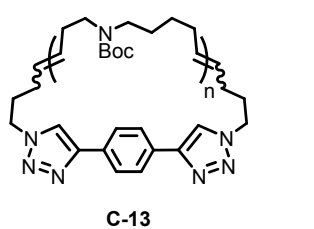
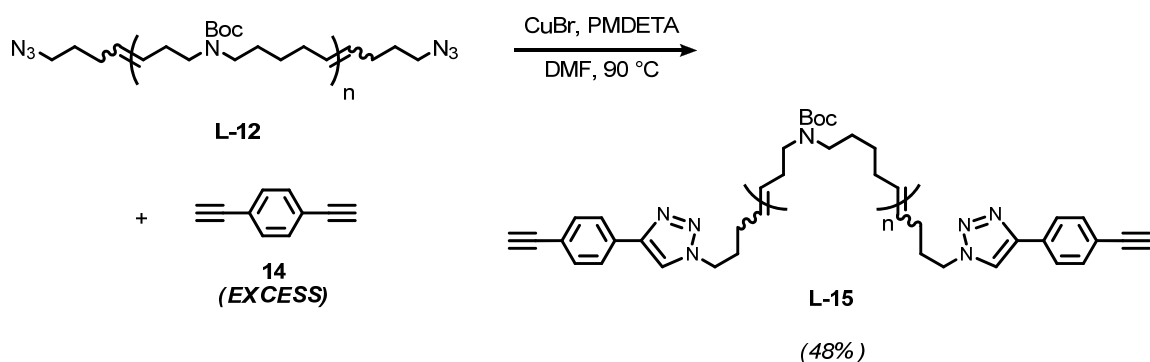
the headspace was again evacuated, and the solution allowed to warm to room temperature. The solution was backfilled with argon, refrozen, and subjected to another cycle for a total of four freeze-pump-thaw cycles.

---

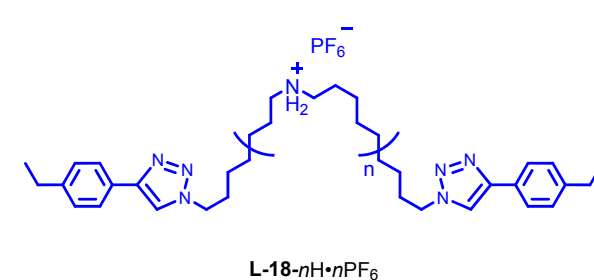
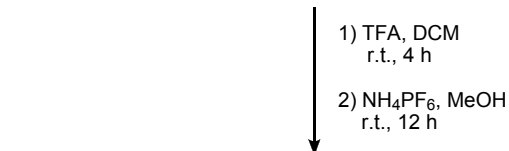
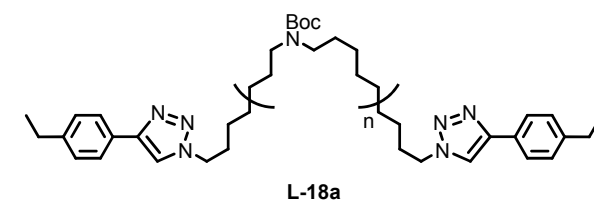
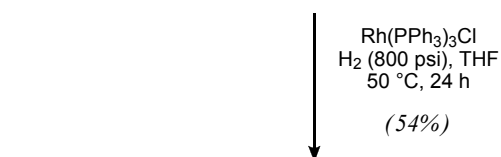
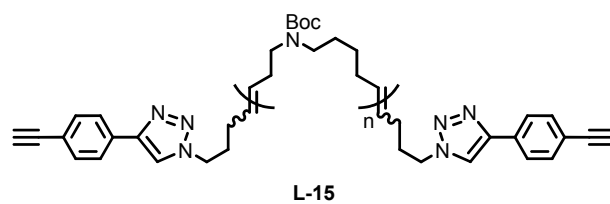
### ***References***

- 1) Kerssebaum, R. DOSY and Diffusion by NMR, Bruker Biospin, Rheinstetten, 2002.
- 2) Longworth, L. G. The Mutual Diffusion of Light and Heavy Water. *J. Phys. Chem.* **1960**, *64*, 1914.
- 3) Wu, D.; Chen, A.; Johnson, C. S. An Improved Diffusion-ordered Spectroscopy Experiment Incorporating Bipolar-Gradient Pulses. *J. Magn. Reson. A.* **1995**, *115*, 260.
- 4) Pangborn, A. B.; Giardello, M. A.; Grubbs, R. H.; Rosen, R. K.; Timmers, F. J. *Organometallics* **1996**, *15*, 1518-1520.

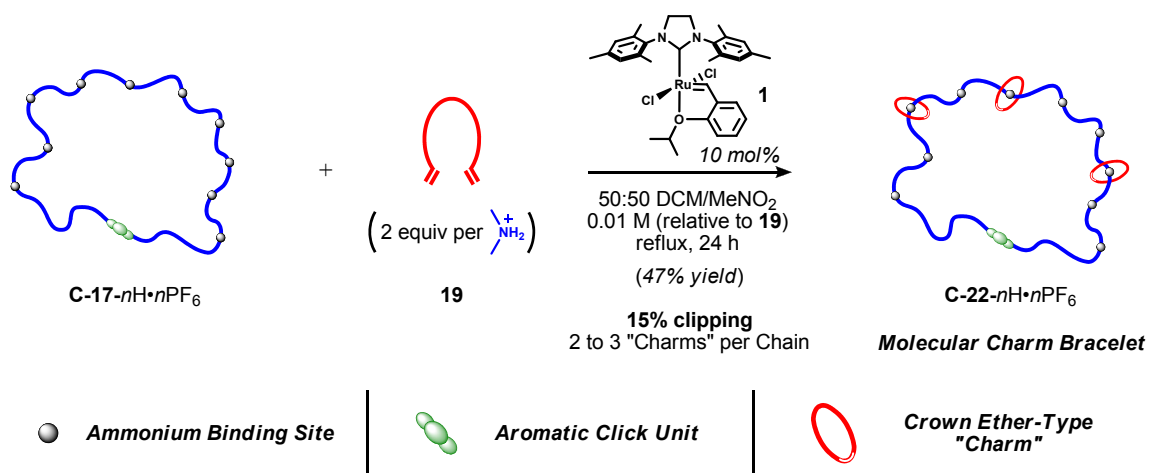


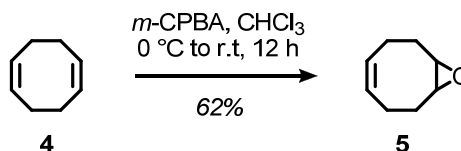


(67%)  
2 steps

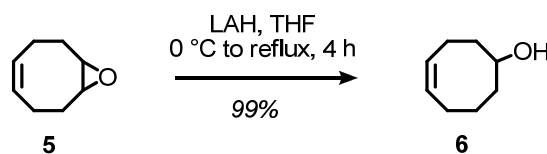


(91%)  
2 steps



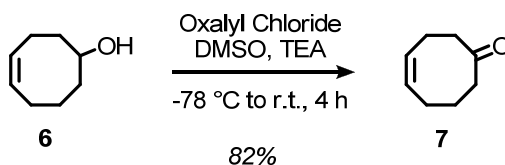


**Cyclooctene monoepoxide (5).** To a two-liter round bottom flask equipped with a stir bar was added *cis*-1,5- cyclooctadiene (50.0g, 0.41 mol, 1 eq). The flask was fitted with an addition funnel, and the round bottom flask was cooled in an ice bath. A solution of 3-chloroperoxybenzoic acid (124.5 g, 0.556 mol, 1.36 eq) in chloroform (1 L) was added slowly over 2 hours. The reaction was allowed to stir at room temperature overnight, then filtered. The solution was washed in a separatory funnel with saturated aqueous sodium bisulfate, then saturated aqueous sodium bicarbonate, then saturated sodium chloride. The organic layer was dried (MgSO<sub>4</sub>), filtered, and evaporated under reduced pressure. The crude oil was subjected to purification via flash chromatography (SiO<sub>2</sub>: eluting in 10:1 hexanes to ethyl acetate) to afford monoepoxide **5** as a clear, colorless oil (31.985 g, 62% yield). <sup>1</sup>H NMR (300 MHz, CDCl<sub>3</sub>):  $\delta$  5.55 (m, 2H), 3.02 (m, 2H), 2.42 (m, 2H), 2.20-1.90 (m, 6H). <sup>13</sup>C NMR (76 MHz, CDCl<sub>3</sub>):  $\delta$  129.06, 56.95, 28.31, 23.89. HRMS-EI (m/z): [M + H] calcd for C<sub>8</sub>H<sub>12</sub>O, 124.0888; found 124.0891.



**Cyclooct-4-enol (6).** To an oven-dried two-neck two-liter flask equipped with a stir bar, septum, and reflux condenser under argon was added lithium aluminum hydride powder (28.3 g, 0.747 mol, 3 eq). The flask was cooled in an ice bath, and dry THF (1 L) was added via cannulation. To this slurry, and at 0 °C, was slowly added cyclooctene

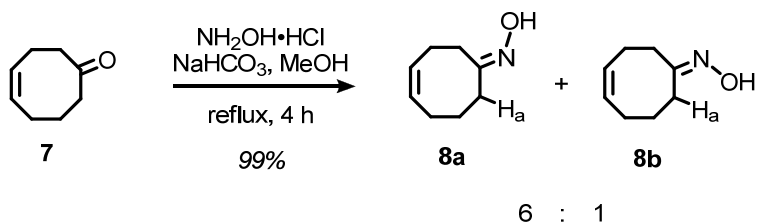
monoepoxide **5** (30.90 g, 0.249 mol, 1 eq) dissolved in dry THF (100 ml). The reaction was heated to reflux for 4 hours, then cooled to 0 °C. Water (28.3 ml) was added dropwise to the slurry, then a solution of 15 % aqueous sodium hydroxide (28.3 ml), and, finally, additional water (84.9 ml). This solution was allowed to stir at room temperature for 4 hours, and the gray salts slowly became white. An excess of celite and MgSO<sub>4</sub> were added and allowed to stir for 30 minutes. The salts were filtered, and the solution was concentrated by rotary evaporation to afford the desired alcohol **6** as a clear oil (31.29 g, 99% yield). The product was used with no further purification. <sup>1</sup>H NMR (500 MHz, CDCl<sub>3</sub>): δ 5.75-5.50 (m, 2H), 3.80 (m, 1H), 2.30 (m, 1H), 2.14 (m, 3 H), 1.97-1.80 (m, 2H), 1.77-1.58 (m, 2H), 1.52 (m, 2H). <sup>13</sup>C NMR (126 MHz, CDCl<sub>3</sub>): δ 130.34, 129.73, 72.93, 37.91, 36.47, 25.85, 25.07, 22.98. HRMS-EI (m/z): [M + H] calcd for C<sub>8</sub>H<sub>14</sub>, 126.1045; found 126.1043.



**Cyclooct-4-enone (7).** To an oven-dried two-neck two-liter flask equipped with a stir bar and fitted with an oven-dried addition funnel was added, under argon, dry dichloromethane (DCM, 850 ml) and dimethylsulfoxide (71.0 g, 0.909 mol, 4 eq), and the solution was cooled to -78 °C. Oxalyl chloride (57.7 g, 0.454 mol, 2 eq) was slowly added to the reaction, and the solution was allowed to stir for 30 minutes. Alcohol **6** (28.66 g, 0.227 mol, 1 eq) was added to the reaction as a solution in dry DCM (150 ml)

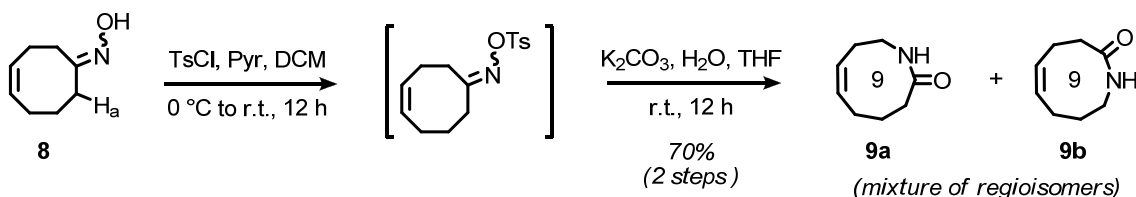


over 30 minutes. After stirring for another 30 minutes, anhydrous triethylamine (230 g, 2.27 mol, 10 eq) was added. The reaction was stirred for 10 minutes at -78 °C, then warmed to room temperature and stirred for 30 minutes. The salts were filtered, and the solvent removed by rotary evaporation. The crude oil was purified first by flash chromatography (SiO<sub>2</sub>: eluting in a gradient of 20:1 hexanes to acetone, then 10:1, then 4:1, then 1:2), and then via reduced pressure fractional distillation through a Vigreux column (10.0 torr, bp = 75-85 °C) to afford ketone **7** as a clear oil (23.134 g, 82%). <sup>1</sup>H NMR (500 MHz, CDCl<sub>3</sub>): δ 5.66 (m, 2H), 2.43 (m, 6H), 2.13 (m, 2H), 1.56 (m, 2H). <sup>13</sup>C NMR (126 MHz, CDCl<sub>3</sub>): δ 214.91, 130.95, 130.41, 47.43, 40.54, 26.50, 24.11, 22.02. HRMS-EI (m/z): [M + H] calcd for C<sub>8</sub>H<sub>12</sub>O, 124.0888; found 124.0847.



**Cyclooct-4-enone oxime (8).** To a one-liter round bottom flask equipped with a stir bar and reflux condenser was added ketone **7** (22.12 g, 0.178 mol, 1 eq), hydroxylamine hydrochloride (18.56 g, 0.267 mol, 1.5 eq), sodium bicarbonate (22.6 g, 0.269 mol, 1.51 eq), and methanol (600 ml). The solution was heated to reflux for 4 hours, then cooled to room temperature. The methanol was removed by rotary evaporation, and the residue redissolved in ethyl ether (300 ml) and partitioned with water (500 ml). The aqueous

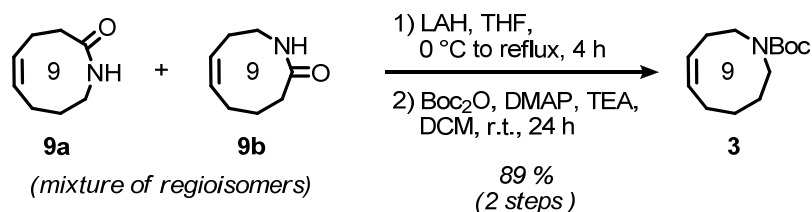
layer was extracted with fresh ether (300 ml x 1, 100 ml x 2), and the combined organic layers washed with fresh water (500 ml), dried ( $\text{MgSO}_4$ ), and filtered. The solvent was removed to give oxime **8** as a white crystalline solid (24.56 g, 99%). The product was used with no further purification.  $^1\text{H}$  NMR (600 MHz,  $\text{CDCl}_3$ ):  $\delta$  8.30 (br s, 1H), 5.66 (m, 2H), 2.57 (m, 0.3H, **8b**), 2.42 (m, 1.7H, **8a**), 2.28 (m, 4H), 2.11 (m, 2H), 1.71 (m, 1.7H, **8a**), 1.61 (m, 0.3H, **8b**).  $^{13}\text{C}$  NMR (76 MHz,  $\text{CDCl}_3$ ):  $\delta$  162.65, 131.28, 129.84, 36.25, 28.25, 26.43, 23.93, 22.76. HRMS-EI ( $m/z$ ):  $[\text{M} + \text{H}]$  calcd for  $\text{C}_8\text{H}_{13}\text{NO}$ , 139.0997; found, 139.0999.



**Lactam (9a and 9b).** Synthesis of the tosyl oxime intermediate was performed batchwise. Oxime **8** (12.00 g, 86.2 mmol, 1 eq) was added to a two-liter round bottom flask equipped with a stir bar and addition funnel, then dissolved in DCM (900 ml). Pyridine (17.05 g, 215.5 mmol, 2.5 eq) and dimethylaminopyridine (a few crystals) were added. Tosyl chloride (24.65 g, 129.3 mmol, 1.5 eq) was dissolved in DCM (500 ml) and added to the addition funnel. The reaction mixture was cooled to 0  $^\circ\text{C}$ , and the tosyl chloride solution was slowly added to reaction over 2 hours. After addition was complete, the reaction was warmed to room temperature and allowed to stir for 1 day. The reaction was poured into a separatory funnel and partitioned with water (500 ml). The aqueous

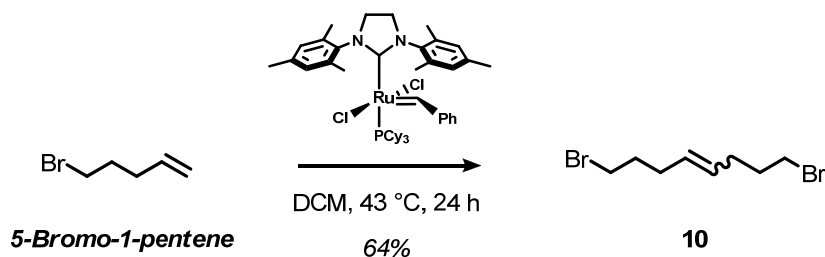
layer was extracted with fresh chloroform (4 x 100 ml), and the combined organic layers were dried (MgSO<sub>4</sub>), filtered, and evaporated to dryness under reduced pressure. The tosyl oxime product was used in the next reaction with no further purification.

Tosyl oxime (25.29 g, 86.21 mmol, 1 eq) was added to a flask, and a solution of aqueous potassium carbonate (11.32 g, 81.90 mmol, 0.95 eq in 688 ml H<sub>2</sub>O) was added. This was allowed to stir for 30 seconds, at which point tetrahydrofuran (360 ml) was added. The solution became bright yellow over several hours. The reaction was allowed to stir at room temperature for 1 day, then poured into a separatory funnel and partitioned between water and chloroform (250 ml). The aqueous layer was extracted with fresh chloroform (4 x 100 ml), and the combined organic layers were dried (MgSO<sub>4</sub>), filtered, and evaporated to dryness under reduced pressure. The product was purified by flash chromatography (SiO<sub>2</sub>: eluting in 2:1 hexanes to acetone) to give the lactams **9a** and **9b** as a white, fluffy powder (8.488 g, 70 % overall yield from oxime **8**). <sup>1</sup>H NMR (300 MHz, CDCl<sub>3</sub>):  $\delta$  7.33 (br s, 0.7 H), 6.15 (br s, 0.3 H) 5.70-5.20 (m, 2H), 3.50 (m, 0.3H), 3.10 (m, 1.4H), 2.60 (m, 0.3H), 2.30-1.80 (br m, 6H), 1.80-1.60 (br m, 2H). <sup>13</sup>C NMR (76 MHz, CDCl<sub>3</sub>):  $\delta$  178.07, 176.88, 134.12, 131.45, 128.82, 124.97, 42.17, 38.89, 36.39, 29.41, 28.86, 27.67, 26.72, 25.55, 25.41. HRMS-EI (m/z): [M + H] calcd for C<sub>8</sub>H<sub>13</sub>NO, 139.0997; found 139.0991.



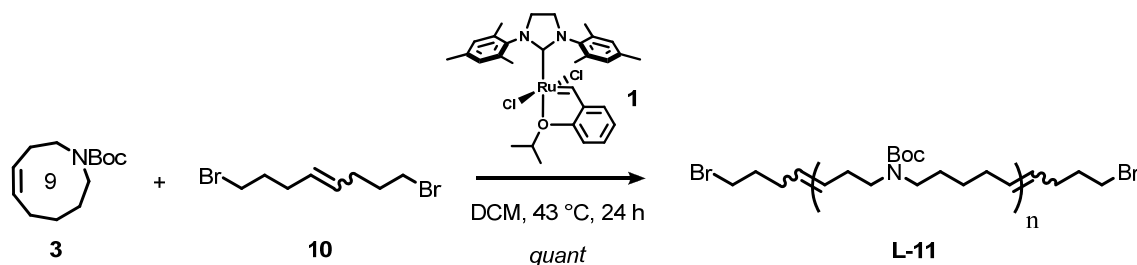
Carbamate (3). To an oven-dried flask equipped with a stir bar, septum, and reflux condenser under argon was added lithium aluminum hydride powder (3.27 g, 37.95 mmol, 3 eq). The flask was cooled in an ice bath, and dry THF (287 ml) was added via cannulation. To this slurry, and at 0 °C, was slowly added lactams 9a and 9b (3.50 g, 28.7 mmol, 1 eq) dissolved in dry THF (25 ml). The reaction was heated to reflux for 4 hours, then cooled to 0 °C. To quench the reaction, water (3.27 ml), 15 % NaOH/H<sub>2</sub>O (3.27 ml), and water (9.81 ml) were added sequentially, and the solution allowed to stir for 1 hour. An excess of celite and MgSO<sub>4</sub> were added, and the slurry was allowed to stir for 15 min. The salts were filtered, and the solvent removed by rotary evaporation to yield a clear oil. The crude amine was redissolved in DCM (287 ml), and dimethylaminopyridine (a few crystals), triethylamine (8.71 g, 86.1 mmol, 3 eq), and di-*tert*-butyl dicarbonate (6.89 g, 31.6 mmol, 1.1 eq) were added. The solution was stirred at room temperature for 12 hours, then poured into a separatory funnel and diluted with water (250 ml). The aqueous layer was extracted with fresh DCM (2 x 50 ml), and the combined organic layers were dried (MgSO<sub>4</sub>), filtered, and evaporated to dryness. The crude oil was purified by flash chromatography (SiO<sub>2</sub>: eluting in a gradient from 16:1 hexanes to acetone, then 8:1) to afford the carbamate monomer 3 as a clear oil (5.10 g, 89% overall yield from lactams 9a and 9b). Though <sup>1</sup>H NMR analysis of the crude reaction mixture showed the presence of both regioisomers, only regioisomer 3 was

isolated after column chromatography. The reported NMR and MS data are for this pure regioisomeric form.  $^1\text{H}$  NMR (500 MHz,  $\text{CDCl}_3$ ):  $\delta$  5.76 (tt,  $J = 8.0$  Hz, 1H), 5.43 (m, 1H), 3.36 (t,  $J = 5.7$  Hz, 1H), 3.27 (t,  $J = 5.7$  Hz, 1H), 3.15-3.05 (m, 2H), 2.33-2.22 (m, 2H), 2.12 (q,  $J = 7.1$  Hz, 2H), 1.60-1.48 (br m, 6H), 1.46 (s, 9H).  $^{13}\text{C}$  NMR (151 MHz,  $\text{CDCl}_3$ ):  $\delta$  156.09, 155.51, 131.99, 131.37, 129.16, 128.58, 79.23, 79.12, 48.42, 48.26, 47.89, 47.82, 28.63, 28.58, 26.91, 26.77, 26.68, 25.63, 25.54, 25.38, 24.29, 23.58. HRMS-EI ( $m/z$ ):  $[\text{M} + \text{H}]$  calcd for  $\text{C}_{13}\text{H}_{23}\text{NO}_2$ , 225.1729; found 225.1729.

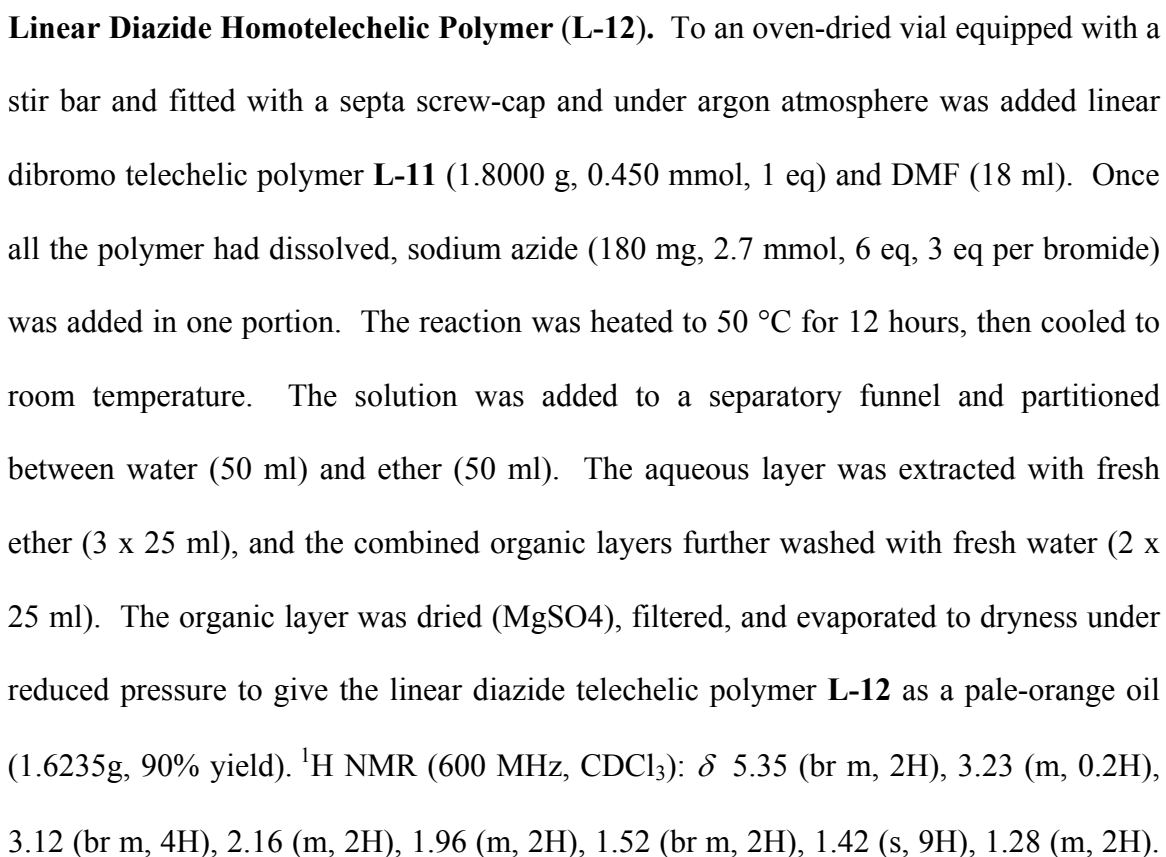


**Dibromo Chain-Transfer Agent (10).** To an oven-dried vial equipped with a stir bar and fitted with a septa screw-cap and under argon atmosphere was added 5-bromo-1-pentene (0.5 g, 3.36 mmol, 2 eq) and dry DCM (16.9 ml). This solution was sparged with argon with stirring for 15 minutes, and Grubbs second-generation ruthenium olefin metathesis catalyst ( $\text{H}_2\text{IMes}$ )( $\text{PCy}_3$ )( $\text{Cl}$ ) $_2$  $\text{Ru}=\text{CHPh}$  (0.1424 g, 0.168 mmol, 5 mol%) was quickly added. Sparging was continued for an additional 5 minutes, and the reaction heated to 41  $^\circ\text{C}$  for 24 h. The reaction was cooled to room temperature, and excess ethyl vinyl ether was added. Stirring was continued for 30 minutes, and the solution evaporated to dryness. The crude oil was purified by flash chromatography ( $\text{SiO}_2$ : eluting in hexanes) to afford the dibromo chain-transfer agent **10** as a clear oil (0.291 g,

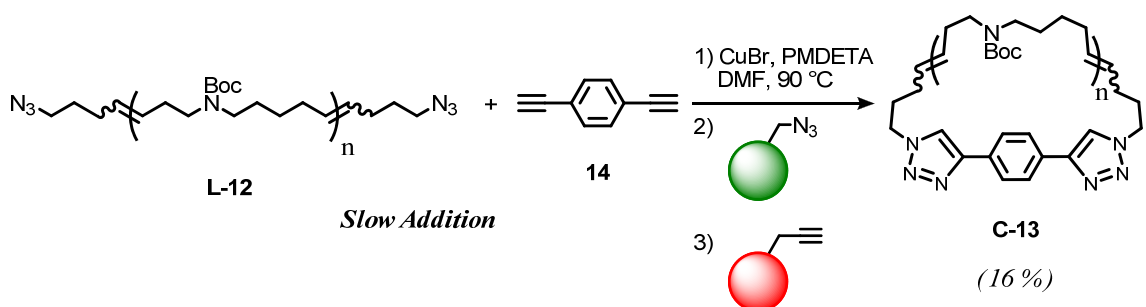
64% yield).  $^1\text{H}$  NMR (300 MHz,  $\text{CDCl}_3$ ):  $\delta$  5.42 (m, 2H), 3.38 (m, 4H), 2.52-2.05 (m, 4H), 2.05-1.75 (m, 4H).  $^{13}\text{C}$  NMR (76 MHz,  $\text{CDCl}_3$ ):  $\delta$  129.97, 129.49, 33.46, 32.46, 32.26, 31.03, 25.93. HRMS-EI ( $m/z$ ):  $[\text{M} + \text{H}]$  calcd for  $\text{C}_8\text{H}_{14}\text{Br}_2$ , 269.9442; found 269.9432.



**Linear Dibromo Homotelechelic Polymer (L-11).** To an oven-dried vial equipped with a stir bar and fitted with a septa screw-cap and under argon atmosphere was added monomer **3** (2.0000 g, 8.875 mmol, 180 eq), dibromo CTA **10** (0.1331 g, 0.4931 mmol, 10 eq), and dry DCM (8.9 ml, 1.0 M with respect to monomer). This solution was sparged with argon for 15 minutes, and Grubbs-Hoveyda second-generation isopropoxybenzylidene catalyst  $(\text{H}_2\text{IMes})(\text{Cl})_2\text{RuCH}(\text{o-OiPrC}_6\text{H}_4)$  **1** (30.9 mg, 49.3  $\mu\text{mol}$ , 1 eq) was quickly added. Sparging was continued for 10 minutes, and the reaction was then heated to 43  $^\circ\text{C}$  for 24 h. The reaction was cooled to room temperature, and excess ethyl vinyl ether was added. After stirring for 10 minutes, the solvent was removed under reduced pressure. The resulting viscous oil was added slowly to a vigorously stirring reservoir of hexanes (50 ml). The dark-colored precipitate was filtered off, and the solution was evaporated to dryness to afford linear dibromo telechelic polymer **L-11** as a pale-brown viscous oil (2.01 g, quant. yield).  $^1\text{H}$  NMR (600 MHz,



$^{13}\text{C}$  NMR (126 MHz,  $\text{CDCl}_3$ ):  $\delta$  155.72, 132.34, 130.42, 129.19, 127.28, 79.17, 77.48, 77.23, 76.98, 50.98, 47.25, 32.61, 31.75, 30.24, 29.74, 28.71, 28.42, 28.10, 27.16, 27.08, 26.92. FTIR (NaCl,  $\text{cm}^{-1}$ ): 3373.98, 2973.07, 2929.83, 2858.42, 2095.99, 1693.88, 1468.40, 1415.38, 1390.47, 1365.19, 1250.54, 1166.69, 968.23, 884.04, 771.85, 672.26. GPC (THF):  $M_n$  = 4.4 kDa;  $M_w$  = 7.1 kDa; PDI = 1.54.

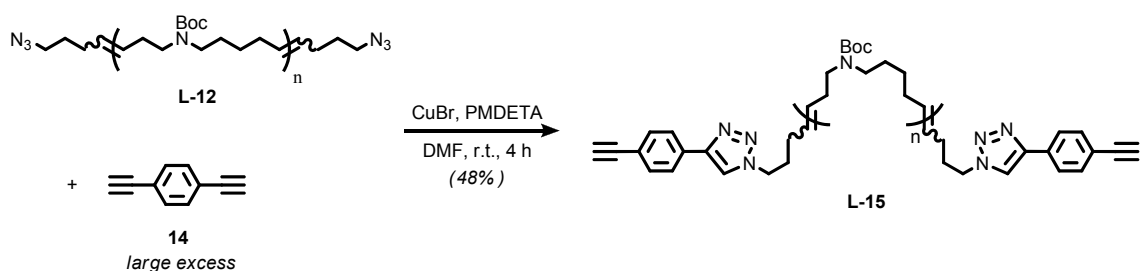


**Clicked Cyclic Polymer (C-13).** An oven-dried two-liter two-neck round bottom flask equipped with a stir bar and reflux condenser was charged, under argon, with dry DMF (1.12 L) and *N,N,N',N'',N'''*-pentamethyldiethylenetriamine (PMDETA, 0.4527 g, 2.61 mmol, 20 eq). This solution was sparged vigorously with argon for 30 minutes, and copper(I) bromide (0.3747 g, 2.61 mmol, 20 eq) was added. Sparging was continued for 10 minutes, and then the reservoir was heated to 90 °C. To a separate flame-dried flask was added linear diazide homotelechelic polymer **L-12** (0.5000 g, 0.1306 mmol, 1 eq) and 1,4-diethynylbenzene **14** (17.3 mg, 0.1375 mmol, 1.04 eq), and these compounds were dissolved in dry DMF (23.8 ml). This solution was sparged with argon for 20 minutes, then transferred to a 25 ml syringe. The polymer/dialkyne mixture was added via syringe pump to the reservoir of copper/PMDETA/DMF at a rate of 0.3 ml per hour.



Once the addition was complete, the reaction was allowed to stir for an additional 2 hours at elevated temperature. The DMF was removed via reduced pressure distillation, and the resulting residue was dissolved in ether (20 ml) and partitioned with water (100 ml). The aqueous layer was further extracted with fresh ether (3 x 20 ml), and the combined organic layers were washed with fresh water (2 x 25 ml). The organic layer was dried ( $\text{MgSO}_4$ ), filtered, and evaporated to dryness. The resulting residue was purified by flash chromatography ( $\text{SiO}_2$ : eluting in a gradient from hexanes, to 25% ether in hexanes, to 50% ether in hexanes, to pure ether) to afford a mixture of linear and cyclic polymer (94.1 mg). This crude polymer residue was redissolved in dry DMF (5.0 ml), and PMDETA (20.4 mg, 0.1176 mmol, 5 eq) and azide-functionalized beads (104 mg, 0.235 mmol azide, 10 eq) were added. The solution was sparged for 15 minutes, and copper(I) bromide (16.9 mg, 0.1176 mmol, 5 eq) was added. The mixture was heated to 90 °C for 6 h with very gentle stirring, and, after this time, alkyne-functionalized beads (235 mg, 0.235 mmol alkyne, 10 eq) were added. Heating and gentle stirring were continued for another 6 h, and the reaction was cooled and filtered. The solution was evaporated to dryness under reduced pressure, and the resulting residue was purified by flash chromatography ( $\text{SiO}_2$ : eluting in a gradient of 1:1 hexanes to ether, to pure ether) afford pure cyclic polymer **C-13** (80.0 mg, 16% yield) as a colorless oil.  $^1\text{H}$  NMR (600 MHz,  $\text{CDCl}_3$ ):  $\delta$  7.88 (s, 0.2H), 7.78 (s, 0.1H), 5.36 (br m, 2H), 4.37 (br s, 0.2H), 3.12 (br m, 4H), 2.17 (m, 2H), 1.96 (m, 2H), 1.42 (br m, 2H), 1.41 (s, 9H), 1.29 (m, 2H).  $^{13}\text{C}$  NMR (126 MHz,  $\text{CDCl}_3$ ):  $\delta$  155.68, 155.66, 147.49, 132.30, 131.72, 130.40, 129.87, 129.15, 128.26, 127.24, 126.56, 126.23, 119.80, 79.17, 79.13, 50.49, 49.87, 47.21, 46.95, 32.55,

31.73, 30.49, 30.18, 29.85, 29.48, 28.81, 28.66, 28.50, 28.38, 28.03, 27.17, 27.11, 27.00, 26.87. FTIR (NaCl,  $\text{cm}^{-1}$ ): 2973.04, 2929.76, 2858.00, 1693.68, 1468.24, 1415.67, 1390.40, 1365.27, 1301.11, 1250.58, 1167.26, 968.89, 883.92, 772.01, 733.43. GPC (THF):  $M_n = 4.4$  kDa; 6.3 Da; PDI = 1.45.

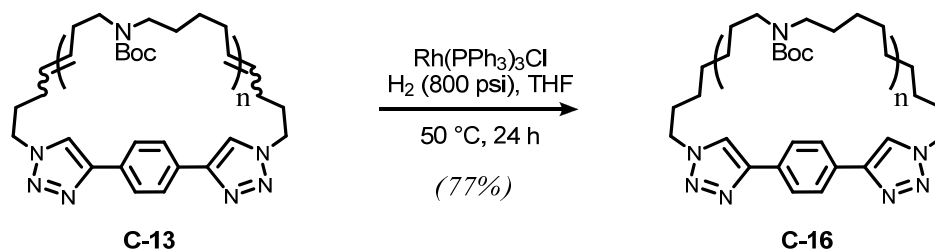


**Doubly-Clicked Linear Polymer (L-15).** To a flame-dried flask equipped with a stir bar and under argon atmosphere was added linear diazide homotelechelic polymer **L-12** (0.100 g, 26.12  $\mu\text{mol}$ , 1 eq), 1,4-diethynylbenzene **14** (0.330 g, 2.6 mmol, 100 eq), PMDETA (23 mg, 0.1306 mmol, 5 eq), and dry DMF (26 ml). This solution was sparged for 15 minutes, and copper(I) bromide (19 mg, 0.1306 mmol, 5 eq) was added. The solution was heated to 50  $^{\circ}\text{C}$  for 4h, then cooled to room temperature. The product was mixed with ether (50 ml) and partitioned with water (100 ml). The aqueous layer was extracted with fresh ether (2 x 50 ml), and the combined organic layer was washed with fresh water (2 x 25 ml). The organic layer was dried ( $\text{MgSO}_4$ ), filtered, and evaporated under reduced pressure. This crude mixture was purified by flash chromatography ( $\text{SiO}_2$ : eluting in a gradient from 1:1 hexanes to ether, to pure ether) to afford the doubly-clicked

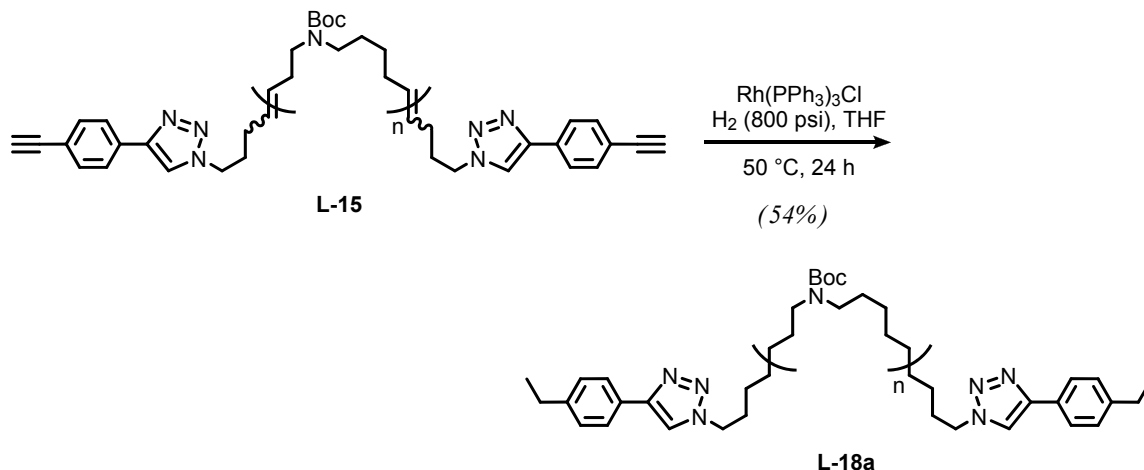
linear polymer **L-15** as a pale-yellow oil (50.9 mg, 48% yield).  $^1\text{H}$  NMR (500 MHz,  $\text{CDCl}_3$ ):  $\delta$  7.76 (d + s,  $J = 8.4$  Hz, 0.22H), 7.51 (d,  $J = 8.2$  Hz, 0.15 H), 5.34 (m, 2H), 4.36 (br s, 0.15H), 3.10 (br m + s, 4H), 2.15 (br m, 2H), 1.95 (br m, 2H), 1.45 (m, 2H), 1.41 (s, 9H), 1.27 (m, 2H).  $^{13}\text{C}$  NMR (126 MHz,  $\text{CDCl}_3$ ):  $\delta$  155.69, 155.67, 132.79, 132.32, 131.74, 131.28, 130.41, 129.90, 129.16, 128.20, 127.24, 125.64, 121.81, 120.07, 83.66, 79.18, 79.14, 78.07, 50.54, 49.92, 47.20, 46.95, 32.59, 31.71, 30.15, 29.88, 29.48, 28.68, 28.40, 28.05, 27.19, 27.13, 27.02, 26.89. FTIR ( $\text{NaCl}$ ,  $\text{cm}^{-1}$ ): 3301.80, 3230.47, 2973.68, 2930.41, 2858.54, 2247.99, 1693.99, 1469.67, 1416.84, 1390.93, 1365.54, 1250.77, 1166.70, 969.14, 923.02, 884.01, 772.35, 733.16, 672.20, 646.20. GPC (THF):  $M_n = 4.4$  kDa;  $M_w = 7.1$  kDa; PDI = 1.63.

**General Hydrogenation Protocol.** Polymer was added to a vial and dissolved in tetrahydrofuran (THF, 10 ml). To this mixture was added Wilkinson's catalyst ( $\text{Rh}(\text{PPh}_3)_3\text{Cl}$ ) (1 mol %), and the vial was sealed inside a stainless-steel high-pressure hydrogenation bomb. The bomb was subjected to three pressurization/release cycles (up to 400 psi  $\text{H}_2$  per cycle), then pressurized to 800 psi  $\text{H}_2$ . The bomb was placed in an oil bath set to 50 °C for 24 h. After the reaction time, the oil bath was removed, and the pressure released. The solvent was removed under reduced pressure, and the resulting residue slowly dripped into a reservoir of hexanes (50 ml). Once the solution had settled, the solids were removed via filtration, and the solvent again evaporated. The residue was purified by flash chromatography ( $\text{SiO}_2$ : eluting a gradient from pure

hexanes, to 25% ether in hexanes, to 50% ether in hexanes, to 75% ether in hexanes, to pure ether) to give the hydrogenated polymer as a clear oil.



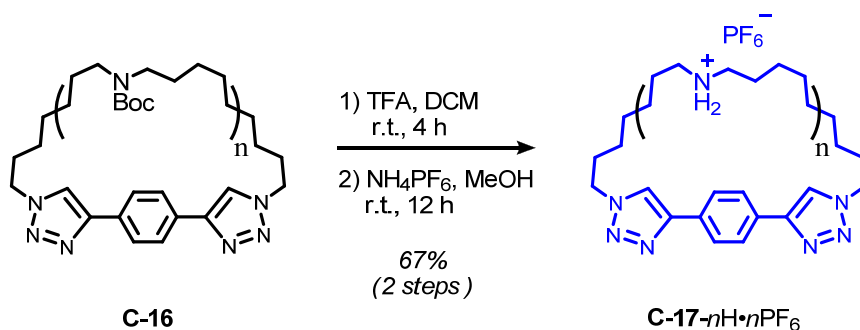
**Saturated Cyclic Product (C-16).** A portion of the cyclic polymer **C-13** (48.2 mg, 12.1  $\mu\text{mol}$ , 1 eq) and Wilkinson's catalyst (2.0 mg, 2.07  $\mu\text{mol}$ , 1 mol % relative to double bonds) were subjected to standard hydrogenation conditions and purification protocols to produce the saturated derivative **C-16** as a clear oil (37.6 mg, 77% yield).  $^1\text{H}$  NMR (600 MHz,  $\text{CDCl}_3$ ):  $\delta$  7.88 (s, 0.2H), 7.78 (s, 0.1H), 4.39 (br s, 0.2H), 3.11 (br s, 4H), 1.94 (m, 0.2H), 1.46 (br s, 4H), 1.42 (s, 9H), 1.35 (br s, 0.8H), 1.25 (m, 8H).  $^{13}\text{C}$  NMR (126 MHz,  $\text{CDCl}_3$ ):  $\delta$  155.81, 147.56, 130.60, 126.26, 119.66, 79.08, 79.05, 50.65, 47.20, 30.52, 29.90, 29.80, 29.65, 29.47, 28.86, 28.71, 28.54, 27.13, 27.08, 26.95, 26.69.



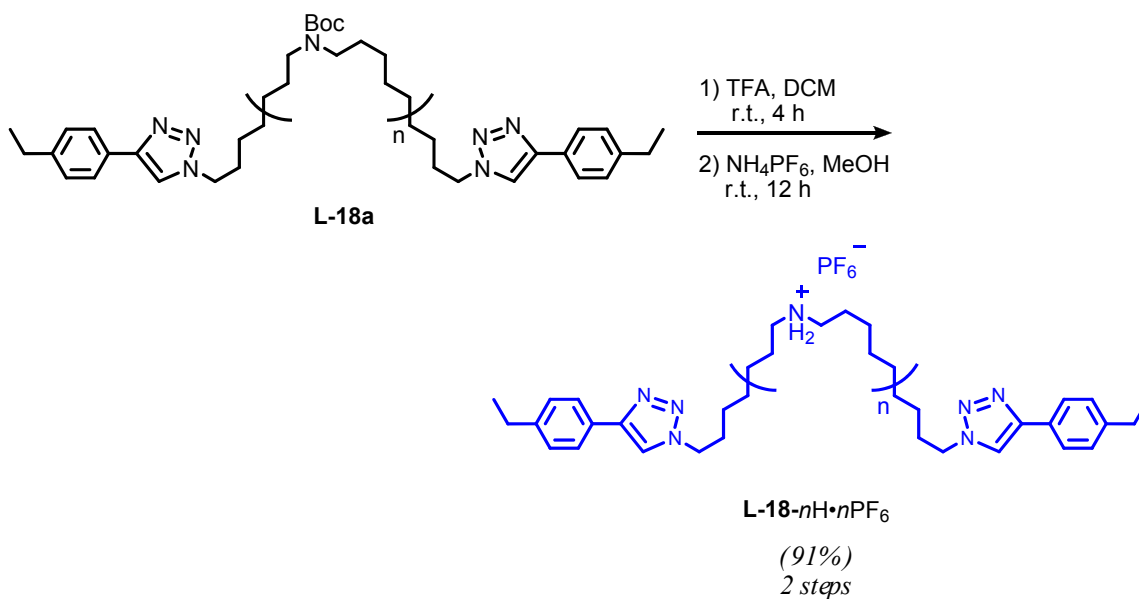
**Saturated Doubly-Clicked Linear Polymer (L-18a)** A portion of the linear doubly-clicked polymer **L-15** (49.9 mg, 12.5  $\mu\text{mol}$ , 1 eq) and Wilkinson's catalyst (2.4 mg, 2.57  $\mu\text{mol}$ , 1 mol % relative to double bonds) were subjected to standard hydrogenation conditions and purification protocols to produce the saturated derivative **L-18a** as a clear oil (29.2 mg, 58% yield).  $^1\text{H}$  NMR (600 MHz,  $\text{CDCl}_3$ ):  $\delta$  7.72 (d,  $J$  = 8.1 Hz, 0.15H), 7.68 (s, 0.08H), 7.23 (d,  $J$  = 8.2 Hz, 0.15H), 4.36 (t,  $J$  = 7.2 Hz, 0.15H), 3.10 (br m, 4H), 2.65 (q,  $J$  = 7.62 Hz, 0.15H), 1.92 (m, 0.15H), 1.46 (m, 4H), 1.42 (s, 9H), 1.23 (br m, 8H).

**General Deprotection and Anion Metathesis Protocol.** A vial was charged with a stir bar, saturated polymer, and DCM (10 ml). Trifluoroacetic acid (15 eq) was added, and the solution allowed to stir for 4 h. The solvent and TFA were removed *in vacuo*, and the deprotected TFA-ammonium polymer adduct dissolved in methanol (10 ml). Ammonium hexafluorophosphate (10 eq) was added, and the solution allowed to stir for 12 h. The solvent was removed under reduced pressure, and the solid residue was mixed

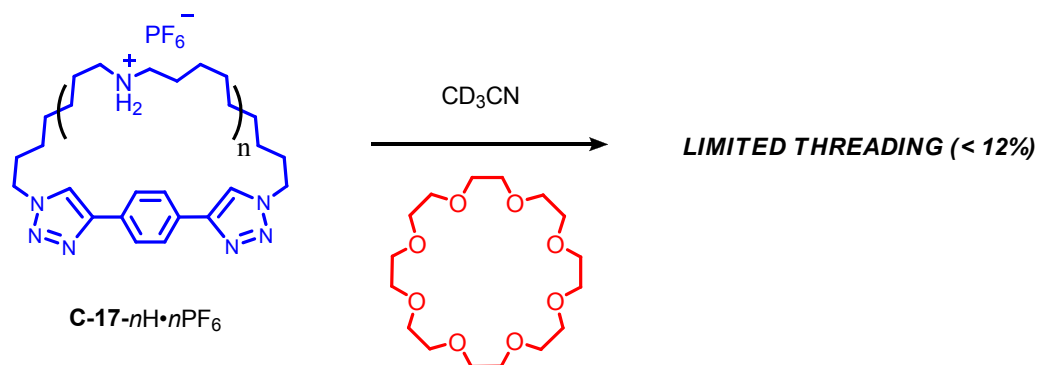
with water (10 ml). The water was decanted, and the remaining solid washed with fresh water (2 x 10 ml) to afford the desired polyammonium hexafluorophosphate polymer as a white solid.



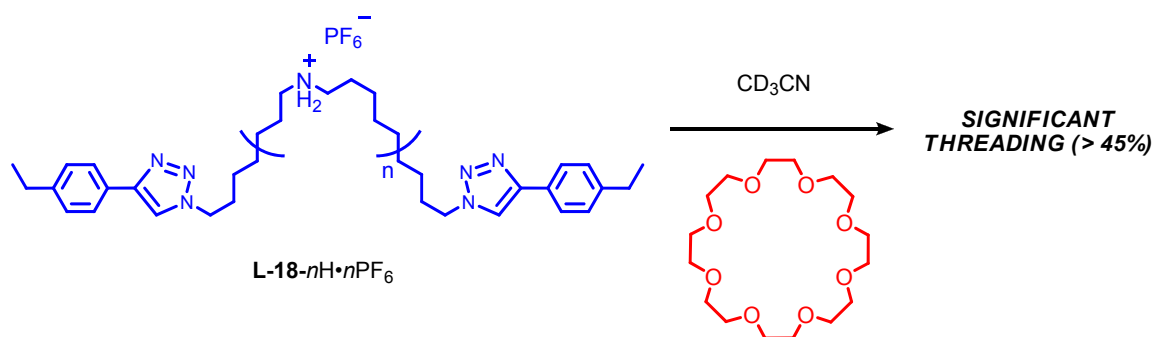
**Polyammonium Hexafluorophosphate Cyclic Polymer (C-17- $n\text{H} \cdot n\text{PF}_6$ ).** Standard deprotection and anion metathesis conditions were used. Hydrogenated cyclic polymer **C-16** (11.8 mg, 8.04  $\mu\text{mol}$ , 1 eq) was dissolved in DCM, and TFA was added (150  $\mu\text{l}$ , 15 eq per boc). The reaction was allowed to stir for 4 h, then pumped to dryness. Methanol and ammonium hexafluorophosphate (210 mg, 1.29 mmol, 10 eq per N) were added. The solution was stirred for 12 h, the methanol was removed, and the standard extraction protocol was performed to afford the cyclic polyammonium hexafluorophosphate polymer **C-17- $n\text{H} \cdot n\text{PF}_6$**  as a white solid (25.3 mg, 67% over two steps).  $^1\text{H}$  NMR (600 MHz,  $\text{CD}_3\text{CN}$ ):  $\delta$  8.13 (s, 0.1H), 7.91 (s, 0.2H), 6.47 (br s, 2H), 4.41 (s, 0.2H), 2.95 (s, 4H), 1.62 (s, 4H), 1.32 (br s, 8H).  $^{13}\text{C}$  NMR (126 MHz,  $\text{CD}_3\text{CN}$ ):  $\delta$  126.95, 121.91, 49.24, 49.03, 30.05, 29.74, 29.46, 27.04, 26.90, 26.66, 26.39, 26.34. 2D-DOSY NMR  $\log_{10}(\text{diffusion}) = -8.83$ .



**Polyammonium Hexafluorophosphate Doubly-Clicked Linear Polymer (L-18-*n*H·*n*PF<sub>6</sub>).** Standard deprotection and anion metathesis conditions were used. Hydrogenated linear doubly-clicked polymer **L-18a** (32.1 mg, 2.86 μmol, 1 eq) was dissolved in DCM, and TFA was added (150 μl). The reaction was allowed to stir for 4 h, then pumped to dryness. Methanol and ammonium hexafluorophosphate (75 mg, 450 μmol, 10 eq per N) were added. The solution was stirred for 12 h, the methanol was removed, and the standard extraction protocol was performed to afford the linear doubly-clicked polyammonium hexafluorophosphate polymer **L-18-*n*H·*n*PF<sub>6</sub>** as a white solid (13.6 mg, 98% over two steps). <sup>1</sup>H NMR (600 MHz, CD<sub>3</sub>CN): δ 8.04 (s, 0.1H), 7.74 (d, J = 8.2 Hz, 0.2H), 7.30 (d, J = 8.2 Hz, 0.2H), 6.37 (br s, 2H), 4.39 (m, 0.2H), 2.95 (br m, 4H), 2.67 (q, J = 7.6 Hz, 0.2H), 1.62 (br m, 4H), 1.32 (br m, 8H), 1.24 (t, J = 7.61 Hz, 0.35H).



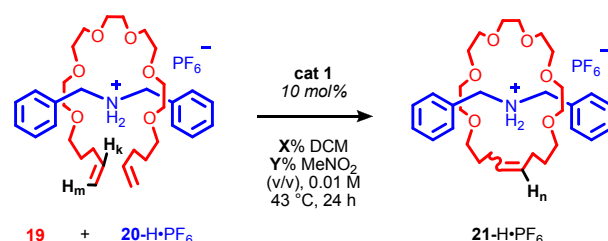
**24-Crown-8 Ether Threading of Cyclic Polymer C-17- $n\text{H}\cdot n\text{PF}_6$ .** A sample of C-17- $n\text{H}\cdot n\text{PF}_6$  (1.0 mg) was dissolved in acetonitrile (0.75 ml, 5 mM ammonium concentration) and mixed with 24-crown-8 ether (24C8, 0.5 eq per ammonium). After analysis, additional 24C8 (total of 2 eq per ammonium) was introduced, and the solution analyzed again. Threaded Peaks (0.5 eq 24C8):  $^1\text{H}$  NMR (600 MHz,  $\text{CD}_3\text{CN}$ , 25 °C):  $\delta$  3.25-3.00 (br m, 0.02H), 2.96 (br m, 1H); Threaded percent =  $(0.02 / 1) \times 100 = 2\%$ . Threaded Peaks (2.0 eq 24C8):  $^1\text{H}$  NMR (600 MHz,  $\text{CD}_3\text{CN}$ , 25 °C):  $\delta$  3.25-3.00 (br m, 0.12H), 2.96 (br m, 1H).



**24-Crown-8 Ether Threading of Hexafluorophosphate Doubly-Clicked Linear Polymer L-18- $n\text{H}\cdot n\text{PF}_6$ .** A sample of L-18- $n\text{H}\cdot n\text{PF}_6$  (1.0 mg) was dissolved in



deuterated acetonitrile (0.75 ml, 5 mM ammonium concentration) and mixed with 24-crown-8 ether (24C8, 0.5 eq per ammonium). After analysis, additional 24C8 (total of 2 eq per ammonium) was added, and the solution analyzed again. Threaded Peaks (0.5 eq 24C8):  $^1\text{H}$  NMR (600 MHz,  $\text{CD}_3\text{CN}$ , 25 °C):  $\delta$  3.25-3.00 (br m, 0.28H), 2.96 (br m, 1H); Threading Percent =  $(0.28 / 1) \times 100 = 28\%$  Threaded Peaks (2.0 eq 24C8):  $^1\text{H}$  NMR (600 MHz,  $\text{CD}_3\text{CN}$ , 25 °C):  $\delta$  3.25-3.00 (br m, 0.86H), 2.96 (br m, 1H).



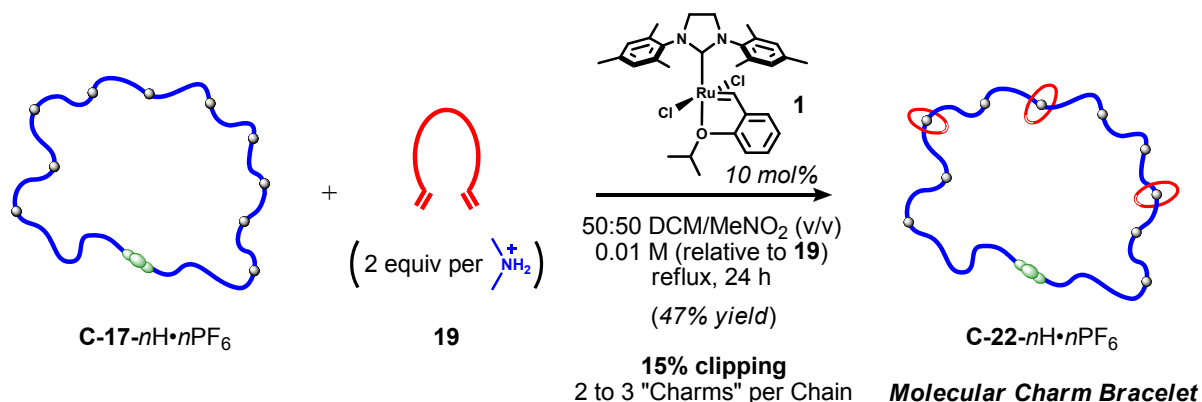
Entry	X % DCM	Y % MeNO <sub>2</sub>	Conversion [%] <sup>a</sup>
1	100	0	quant
2	95	5	90
3	90	10	90
4	80	20	85
5	50	50	62
6	25	75	54
7	0	100	30

<sup>a</sup> Conversion measured by  $^1\text{H}$  NMR integration of  $\text{H}_m$  relative to  $\text{H}_n$  after 24h.

#### Procedure for “Clipped” Pseudorotaxane (**21-H**·PF<sub>6</sub>). **ENTRY 5:**

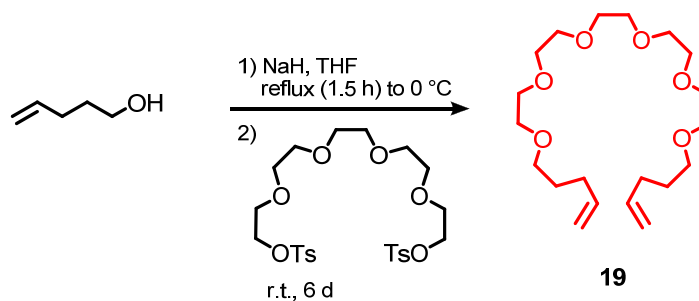
Dibenzylammonium hexafluorophosphate template **20-H**·PF<sub>6</sub> (10 mg, 29.15  $\mu\text{mol}$ , 1 eq) and diolefin crown ether–type species **19** (10.9 mg, 29.15  $\mu\text{mol}$ , 1 eq) were added to a flame dried vial equipped with a stir bar and under an argon atmosphere, then dissolved in solvent (50% DCM, 50% Nitromethane, 2.9 ml total volume, 0.01 M relative to **19**). The mixture was degassed via the standard freeze-pump-thaw protocol, backfilling with

argon. On the third freeze, ruthenium metathesis catalyst  $(\text{H}_2\text{IMes})(\text{Cl})_2\text{RuCH}(\text{o-OiPrC}_6\text{H}_4)$  **1** (1.9 mg, 2.9  $\mu\text{mol}$ , 10 mol %) was added. The headspace was evacuated, and the reaction subjected to one final freeze-pump-thaw cycle. The solution was heated to 43 °C for 24 h. The reaction was cooled to r.t., and ethyl vinyl ether (0.2 ml) was injected and allowed to stir for 30 minutes. The solvents were removed under reduced pressure, and the conversion of the crude product was analyzed with no further purification. Example  $^1\text{H}$  integration for determination of conversion percent (Entry 5):  $^1\text{H}$  (500 MHz,  $\text{CDCl}_3$ ):  $\delta$  5.85-5.72 (m, 1.74 H,  $\text{H}_\text{k}$ ), 5.40-5.25 (m, 3.21 H,  $\text{H}_\text{n}$ ), 5.03-4.88 (m, 4.00 H,  $\text{H}_\text{m}$ ). *Conversion %* =  $3.21 / (3.21 + (4.00 / 2)) = \sim 62\%$



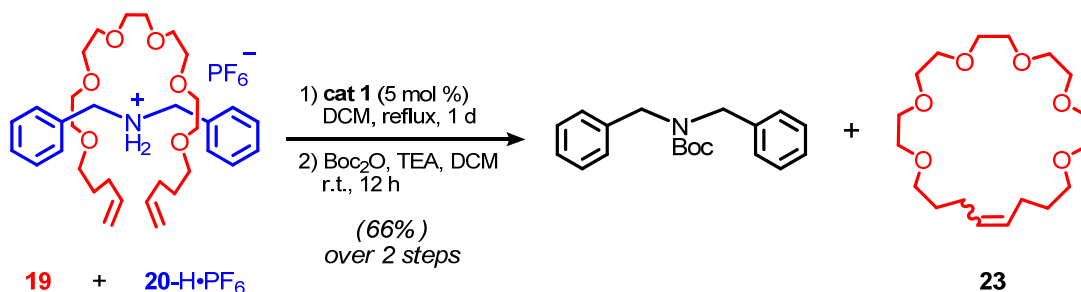
**Molecular “Charm Bracelet” ( $\text{C-22-}n\text{H}\cdot n\text{PF}_6$ ).** To a flame-dried vial equipped with a stir bar and under argon was added a portion of  $\text{C-17-}n\text{H}\cdot n\text{PF}_6$  (5.0 mg, 1.1  $\mu\text{mol}$ , 1 eq) and diolefin crown ether–type species **19** (12.7 mg, 33.9  $\mu\text{mol}$ , 32 eq, 2 eq per ammonium). To this mixture was added nitromethane (1.7 ml), followed by DCM (1.7 ml, total solvent concentration 0.01 M relative to **19**). The solution was degassed via sparging with argon for 15 minutes. Catalyst  $(\text{H}_2\text{IMes})(\text{Cl})_2\text{RuCH}(\text{o-OiPrC}_6\text{H}_4)$  **1** (2.2

mg, 3.39  $\mu\text{mol}$ , 10 mol% relative to **19**) was added, and the headspace quickly evacuated. Another freeze-pump-thaw cycle was completed, after which the reaction was heated to 43 °C for 24 h. The solution was cooled to r.t., and quenched via addition of excess ethyl vinyl ether (0.5 ml). The solvent was removed under reduced pressure, and the resulting solid was dissolved in a minimum of acetonitrile and added to a stirring reservoir of DCM (30 ml). The solvent was decanted to afford the molecular “charm bracelet” interlocked complex **C-22**· $n\text{H}$ · $n\text{PF}_6$  as a white solid (2.7 mg, 47% yield, 15% clipping, 2 to 3 charms per polymer).  $^1\text{H}$  NMR (600 MHz,  $\text{CD}_3\text{CN}$ ):  $\delta$  8.13 (br s, 0.6H), 7.92 (s, 0.12H), 6.72 (br s, 1H), 5.90 (br s), 5.58-5.20 (br m, 0.2H), 4.41 (m, 0.14H), 3.68-3.30 (m, 3.6H), 2.96 (m, 4H), 2.30 (m, 0.47 H), 1.63 (m, 4.8H), 1.33 (m, 12H). 2D-DOSY NMR for crown and polymer  $^1\text{H}$  signals:  $\log_{10}(\text{diffusion}) = -8.85$



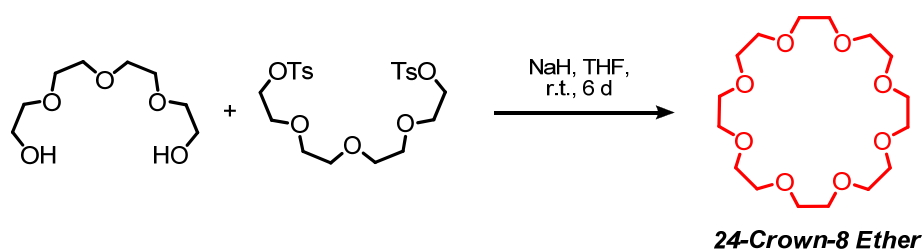
**Synthesis of Clipping Crown (19).** To a flame-dried flask equipped with a reflux condenser and stir bar and under an argon atmosphere was added sodium hydride (40 g, 1.0 moles, 5 eq, 60% dispersion in mineral oil) and dry THF (1 L), followed by 4-penten-1-ol (19.03 g, 221 mmol, 2.2 eq) dissolved in dry THF (110 ml). The solution was heated to reflux for 1.5 h, then cooled to 0 °C. The reflux condenser was replaced by an addition funnel charged with pentaethylene glycol ditosylate (54.9 g, 100.4 mmol, 1 eq) dissolved

in dry THF (110 ml), and this solution was slowly added over 1 h. The solution was allowed to stir at r.t. under an Ar atmosphere for 6 d, then quenched by slow addition of methanol. The volatiles were removed by rotary evaporation, and the oil dissolved in DCM (500 ml) and partitioned with water (500 ml) in a separatory funnel. The aqueous layer was further washed with ether (2 x 200 ml), and the combined organic layers were dried ( $\text{MgSO}_4$ ), filtered, and evaporated to dryness to give an orange oil. The crude product was purified by flash chromatography ( $\text{SiO}_2$ : eluting in 2:1 hexanes to ethyl acetate) to afford **19** a clear, colorless oil (18.41 g, 49% yield)  $^1\text{H}$  NMR (500 MHz,  $\text{CDCl}_3$ ):  $\delta$  5.78 (m, 2H), 4.97 (m, 4H), 3.65-3.50 (m, 20H), 3.44 (t,  $J = 6.7$  Hz, 4H), 2.08 (q,  $J = 7.2$  Hz, 4H), 1.65 (qt,  $J = 7.1$  Hz, 4H).  $^{13}\text{C}$  NMR (126 MHz,  $\text{CDCl}_3$ ):  $\delta$  138.49, 114.88, 70.91, 70.82, 70.80, 70.80, 70.31, 30.44, 28.98. HRMS-FAB ( $m/z$ ):  $[\text{M} + \text{H}]$  calcd for  $\text{C}_{20}\text{H}_{39}\text{O}_6$ , 375.2747; found 375.2733.



**Pure Ring-Closed Clipping Crown (23).** A flame-dried vial was charged with dibenzylammonium hexafluorophosphate template **20-H $\cdot$ PF<sub>6</sub>** (202 mg, 587  $\mu\text{mol}$ , 1.1 eq), diolefin polyether fragment **19** (200 mg, 534  $\mu\text{mol}$ , 1 eq), and dry DCM (53.4 ml, 0.01 M). The solution was sparged with argon for 20 min, and catalyst **1** (16.8 mg, 26.7

$\mu\text{mol}$ , 5 mol%) was introduced in one portion. Sparging was continued for 5 min, and the reaction heated to 43 °C for 24h. The solution was cooled to r.t., and quenched with ethyl vinyl ether. Volatiles were removed under reduced pressure, and the resulting residue was mixed with DCM (30 ml), triethylamine (328  $\mu\text{l}$ , 2.35 mmol, 4 eq), and boc-anhydride (270  $\mu\text{l}$ , 1.18 mmol, 2 eq). Reaction was allowed to continue for 12 h at r.t., and the solvent removed via rotary evaporation. The crude orange oil was subjected to flash chromatography (SiO<sub>2</sub>: eluting in a gradient of 20:1 hexanes to acetone, to 16:1, to 10:1 to 5:1), giving ring-closed product **23** as a clear, pale-yellow oil (0.1227 g, 66% yield over 2 steps). <sup>1</sup>H NMR (500 MHz, CDCl<sub>3</sub>):  $\delta$  5.45-5.35 (m, 2H), 3.75-3.55 (m, 20H), 3.48 (m, 4H), 2.15-2.05 (m, 4H), 1.65 (m, 4H). <sup>13</sup>C NMR (126 MHz, CD<sub>3</sub>CN):  $\delta$  130.49, 129.99, 71.03, 70.99, 70.95, 70.88, 70.67, 70.59, 70.41, 29.78, 29.40, 29.02, 23.93. 2D-DOSY NMR log<sub>10</sub>(D) = -8.45. HRMS-FAB (m/z): [M + H] calcd for C<sub>18</sub>H<sub>35</sub>O<sub>6</sub>, 347.2434; found 347.2422.

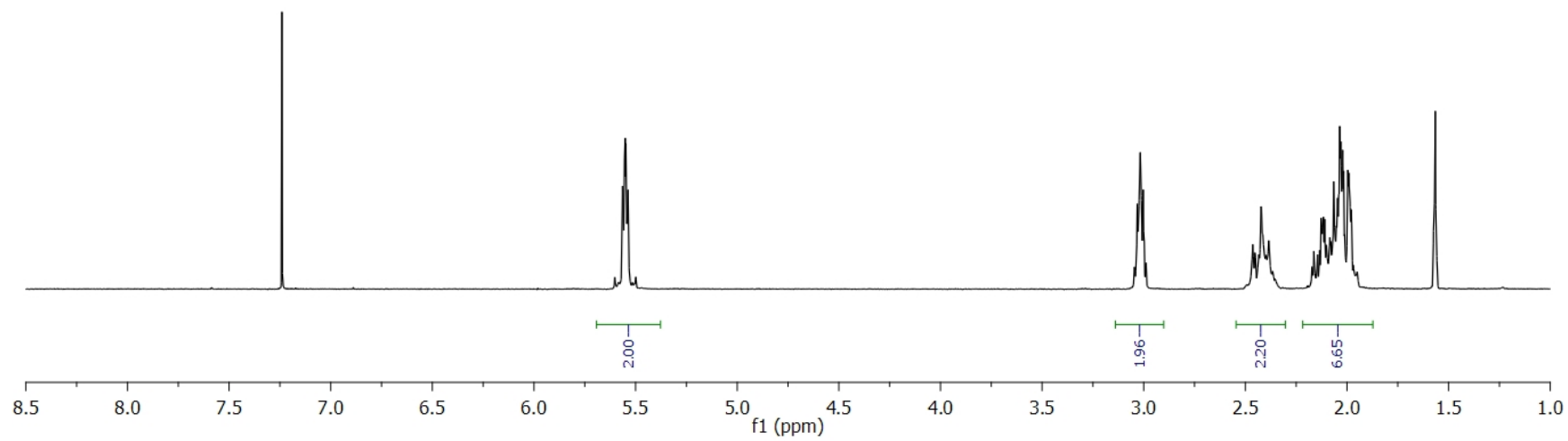
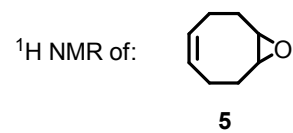


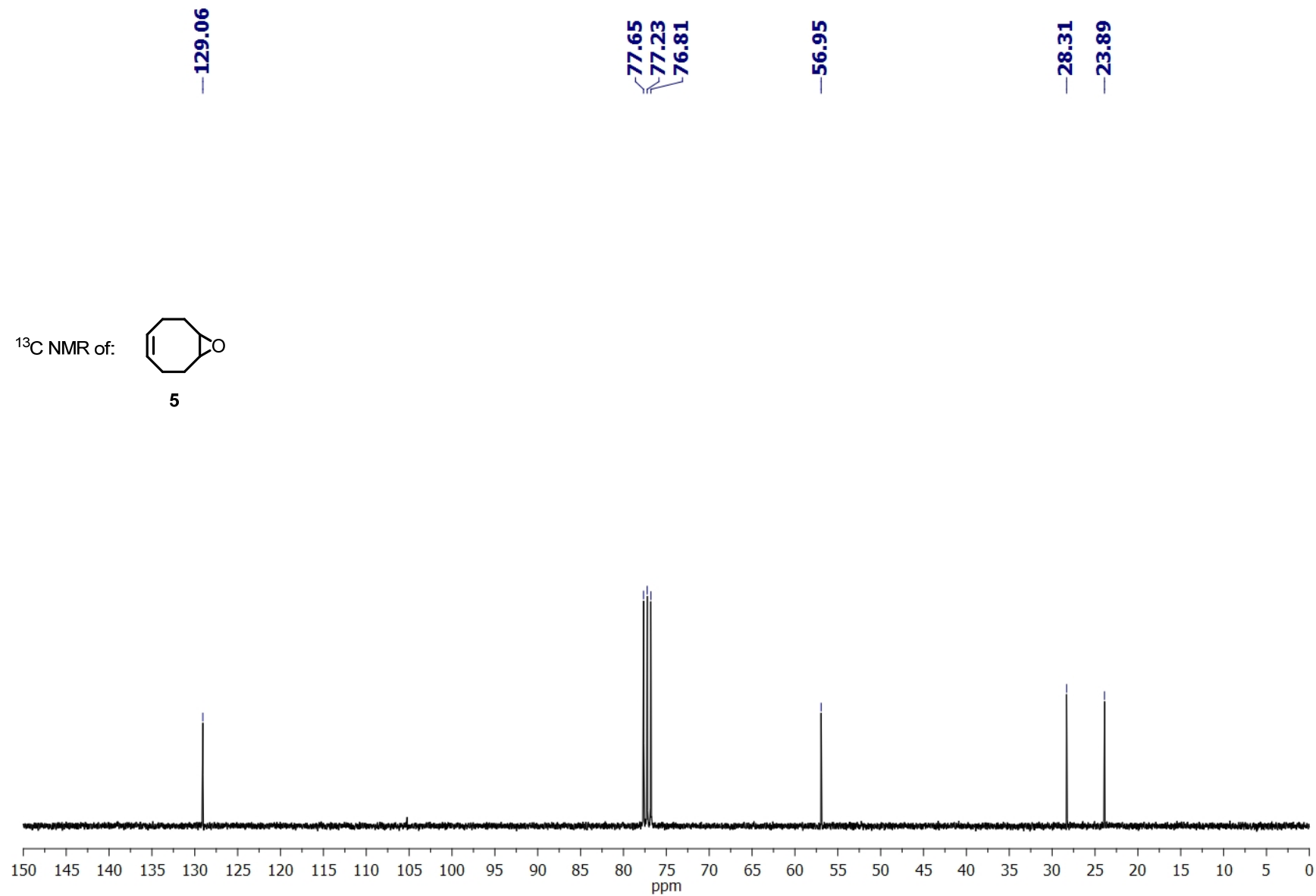
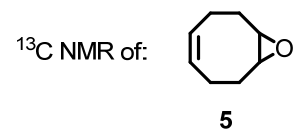
**Synthesis of 24-Crown-8 Ether (24C8).** 24C8 was prepared according to a literature procedure.<sup>5</sup> A flame-dried flask equipped with an addition funnel and stir bar, and under an argon atmosphere, was charged with sodium hydride (24 g, 600 mmol, 24 eq, 60% dispersion in mineral oil) and dry THF (100 ml). To the addition funnel was added a

solution of tetraethylene glycol ditosylate (12.94 g, 25.7 mmol, 1 eq) and tetraethylene glycol (5 g, 25.7 mmol, 1 eq) dissolved in dry THF (300 ml), and this was slowly introduced to the reservoir of THF/NaH at r.t. over 2 d. After addition was complete, the solution was allowed to stir for 1 week at r.t. under an argon atmosphere. The brown solution was quenched with water (12 ml), filtered (fritted glass) to remove salts, and evaporated to dryness under reduced pressure. The brown oil was dissolved in refluxing hexanes (1000 ml total, added in 4 portions of 500 ml, 300 ml, 100 ml, and 100ml) and poured through filter paper. The hexanes were removed via rotary evaporation, and the oil dissolved in acetonitrile (500 ml). After concentration to 100 ml of solution volume, the mixture was placed in the freezer overnight, resulting in precipitation of clear, colorless crystals. The crystals were quickly collected by decanting the supernatant, followed by several washings with fresh, cold acetonitrile. The crystals were placed under high vacuum to afford 24-crown-8 ether as a clear, colorless oil (1.8069 g, 20% yield).  $^1\text{H}$  NMR (500 MHz,  $\text{CDCl}_3$ ):  $\delta$  3.65 (s, 32H).  $^{13}\text{C}$  NMR (126 MHz,  $\text{CD}_3\text{CN}$ ):  $\delta$  71.05. HRMS-FAB ( $m/z$ ):  $[\text{M} + \text{H}]$  calcd for  $\text{C}_{16}\text{H}_{33}\text{O}_8$ , 353.2175; found 353.2192.

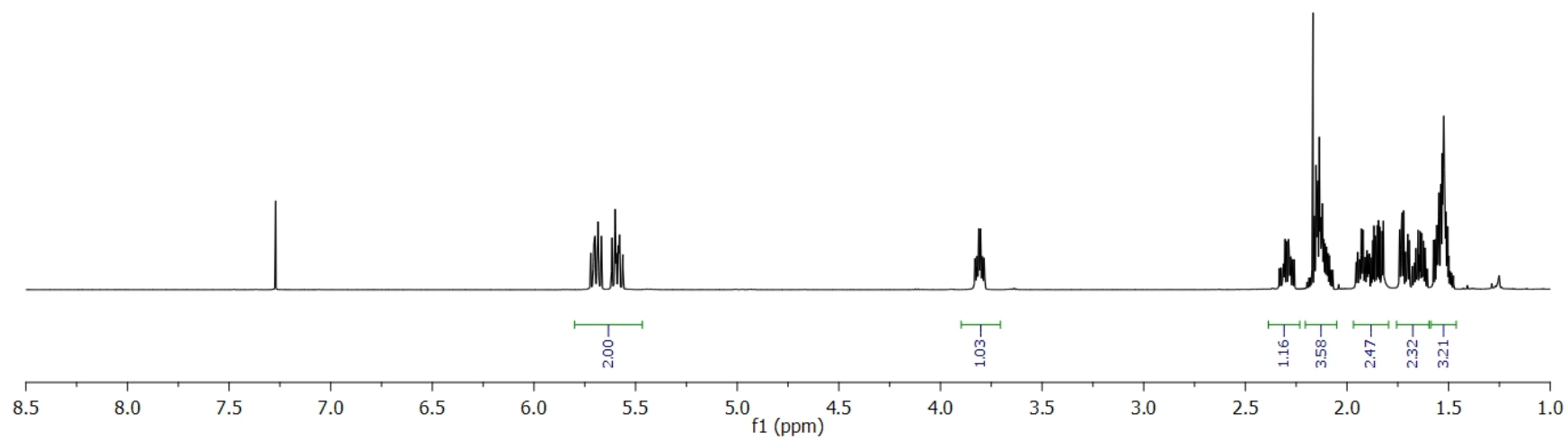
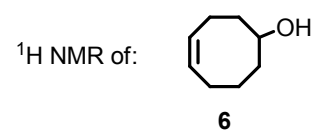
**Reference:**

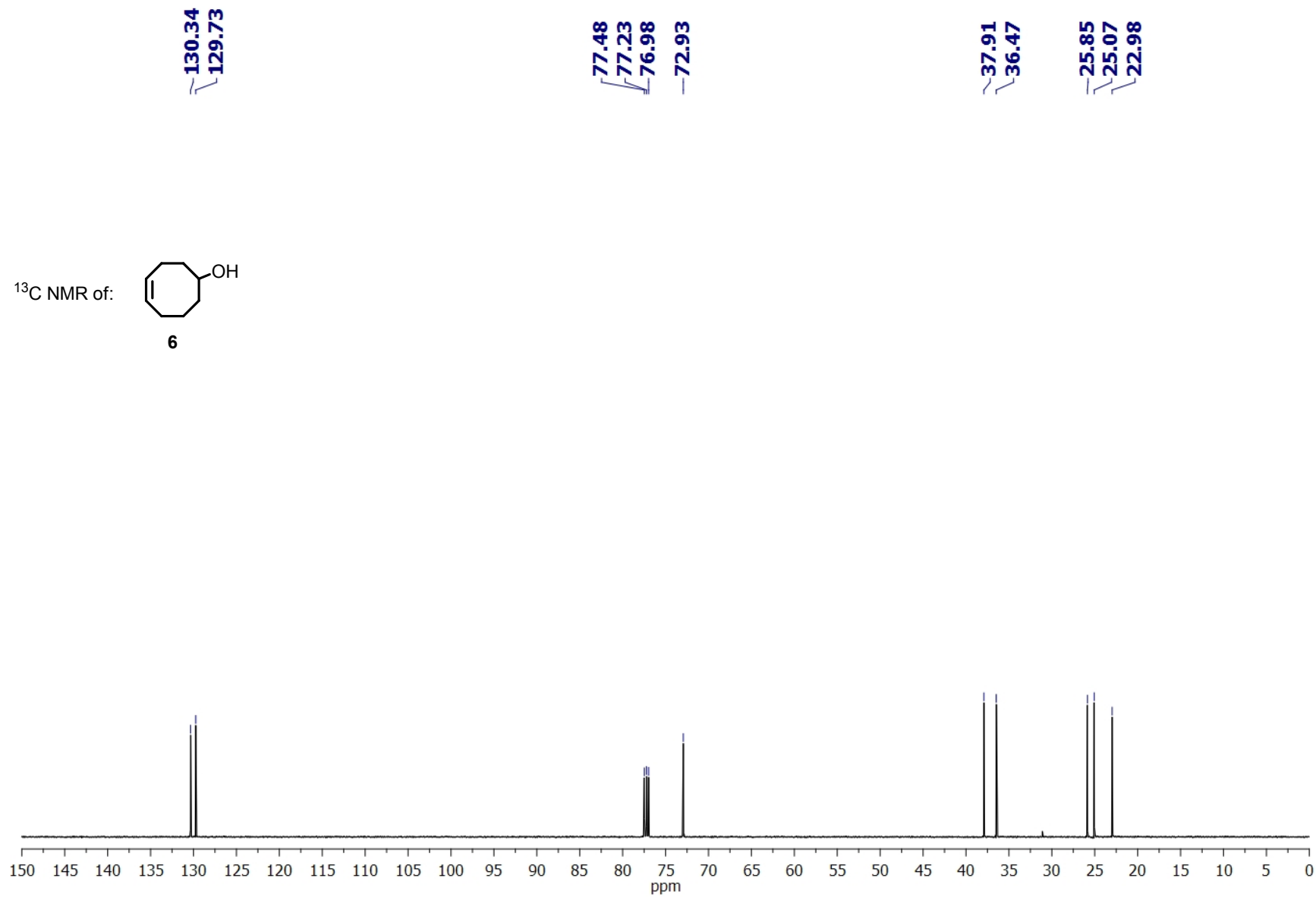
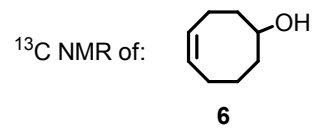
(5) Talanov, V. S.; Bartsch, R. A. *Synth. Commun.* **1999**, 29, 3555

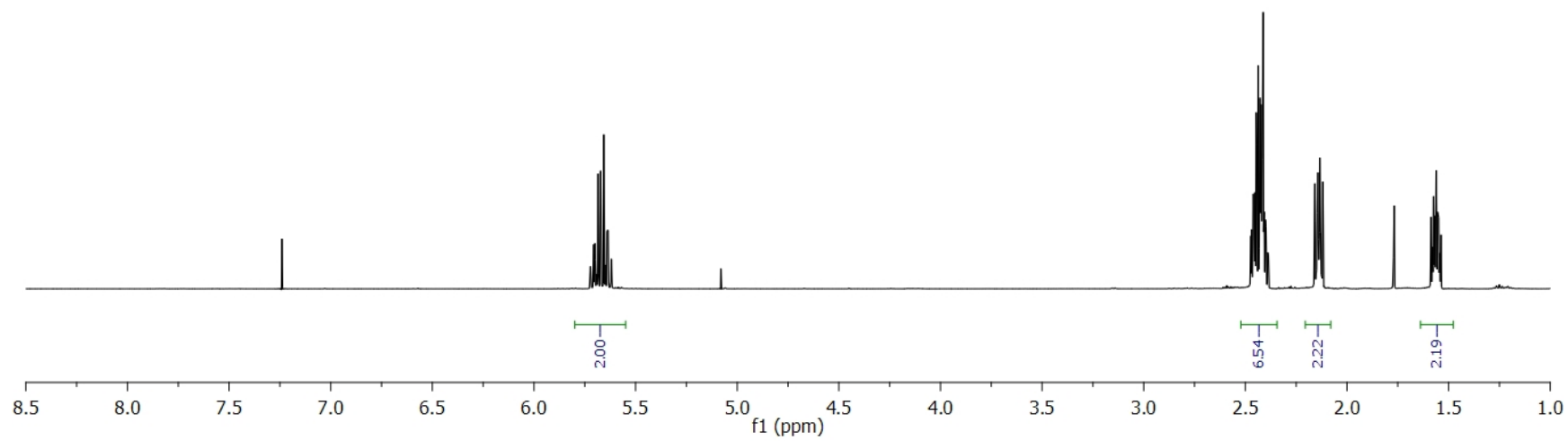
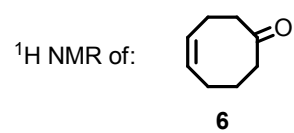


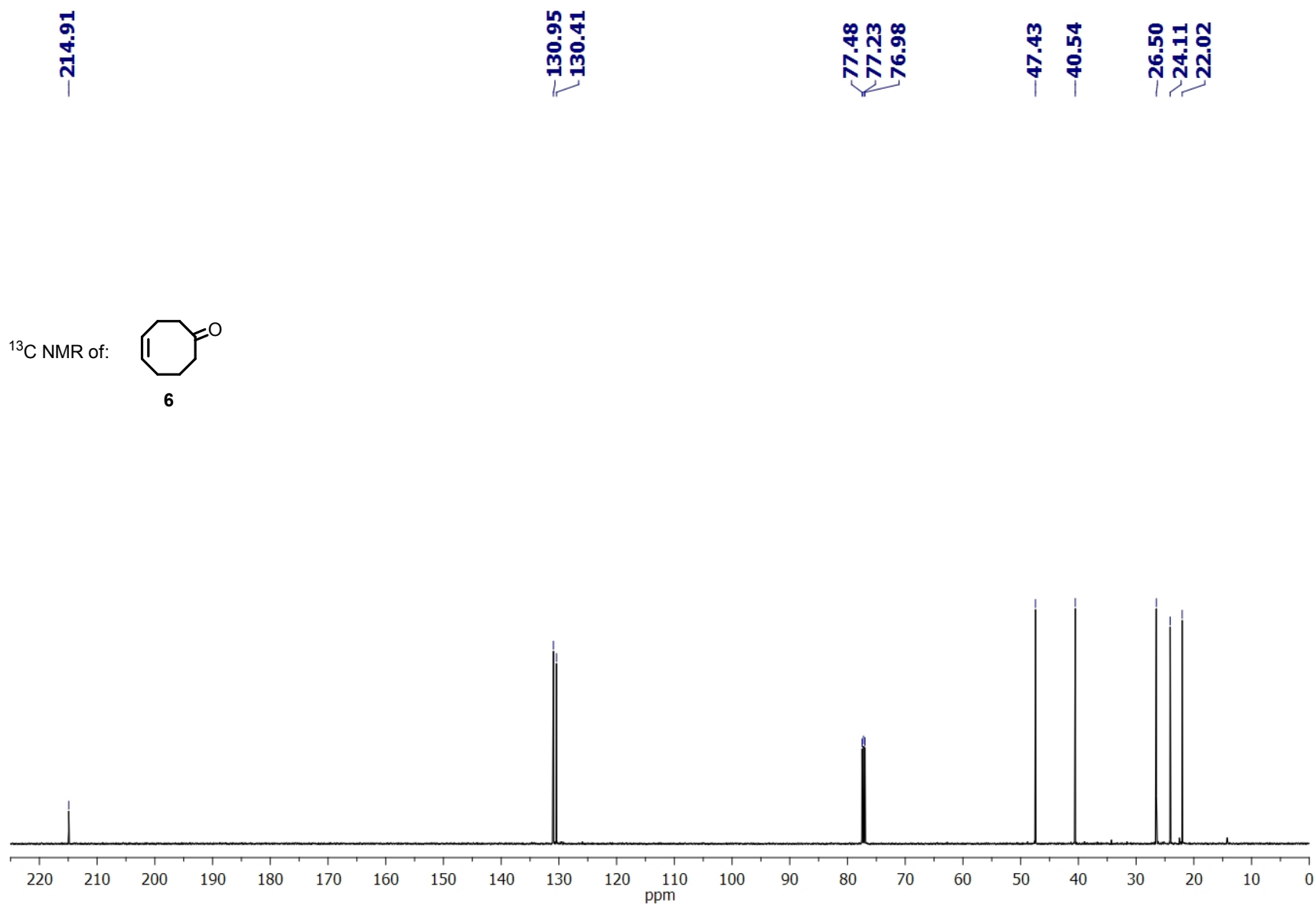


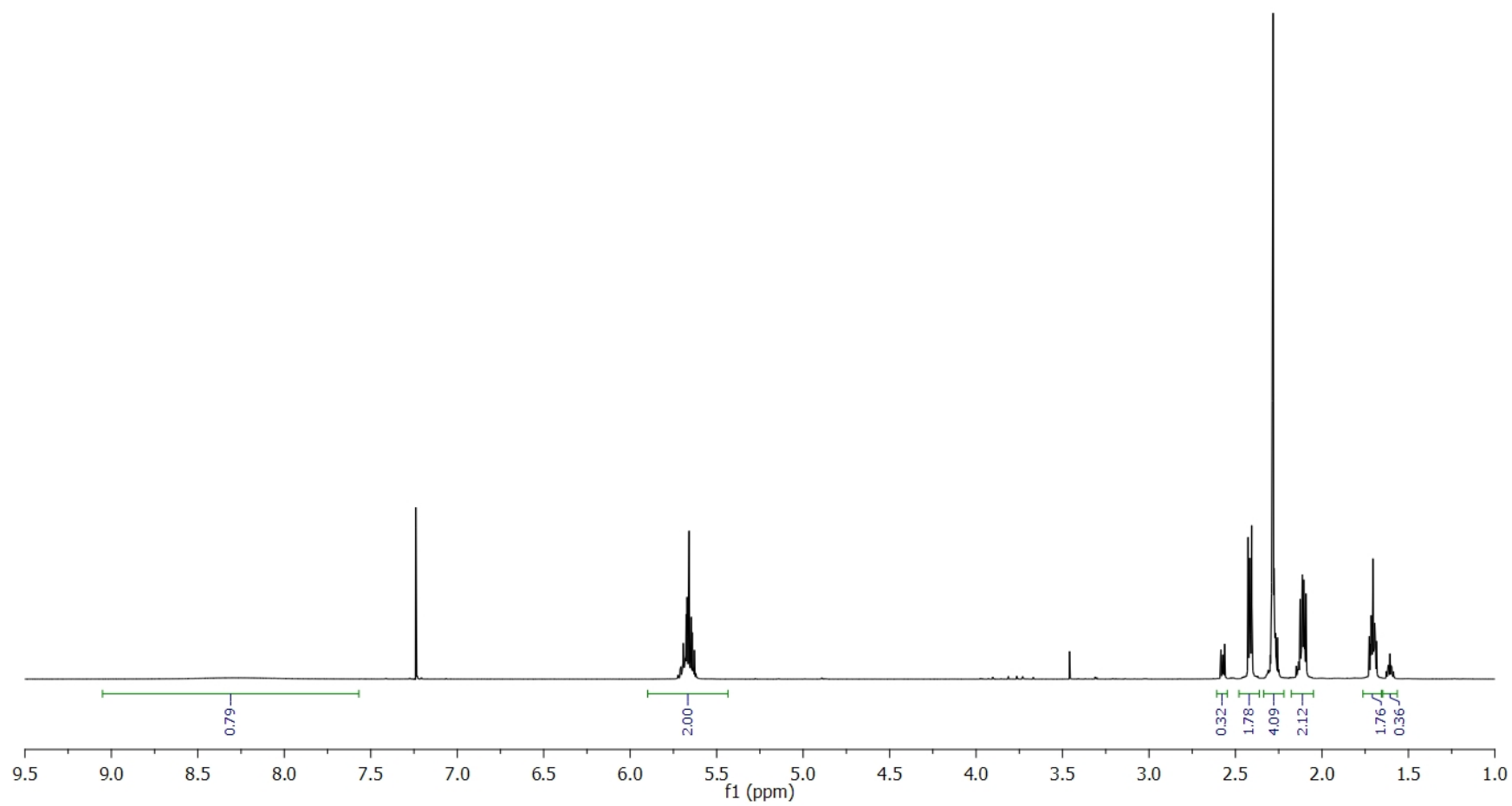
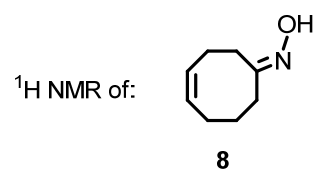


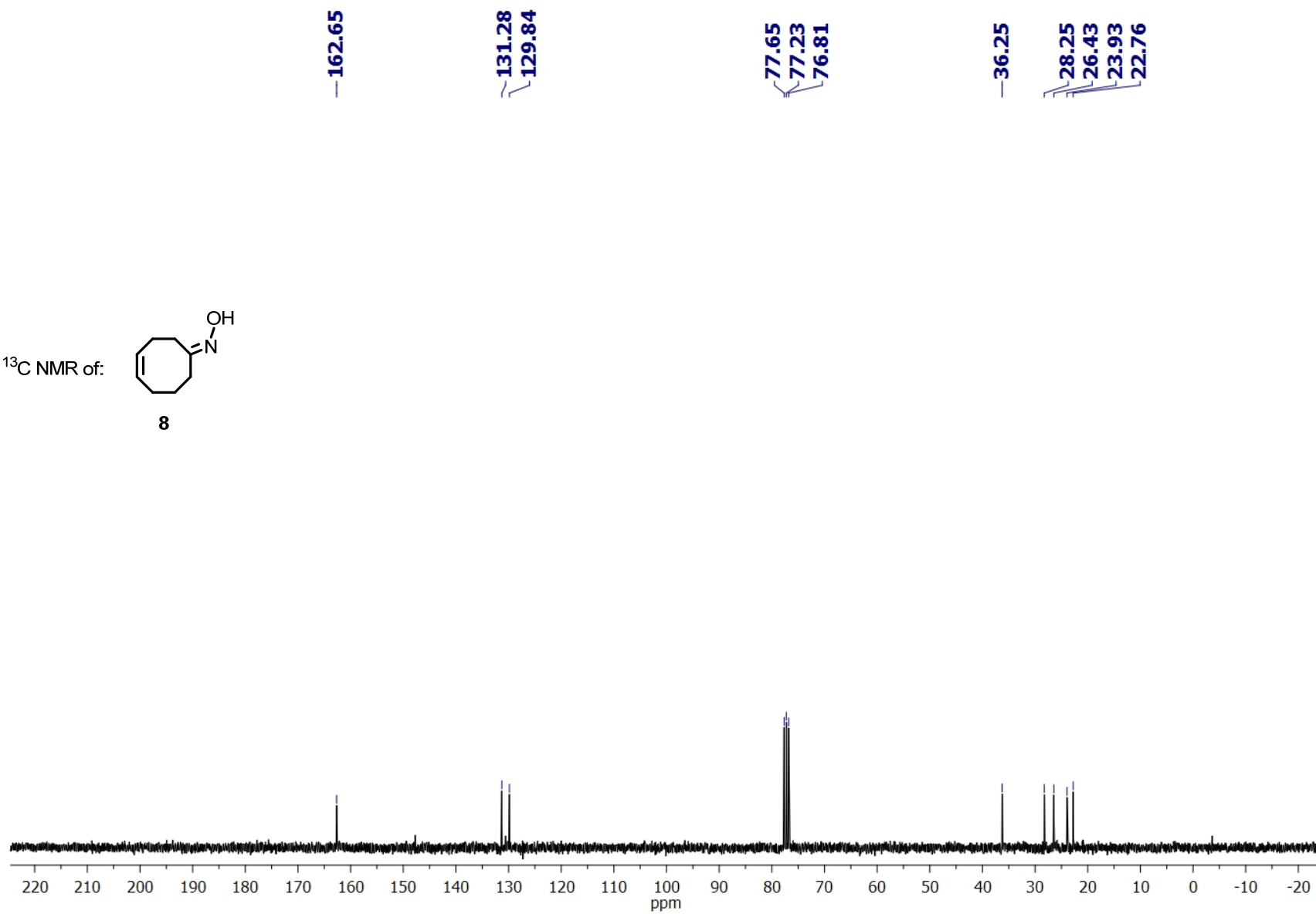
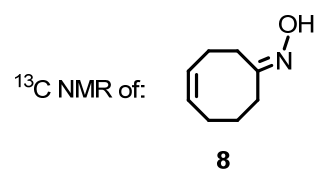


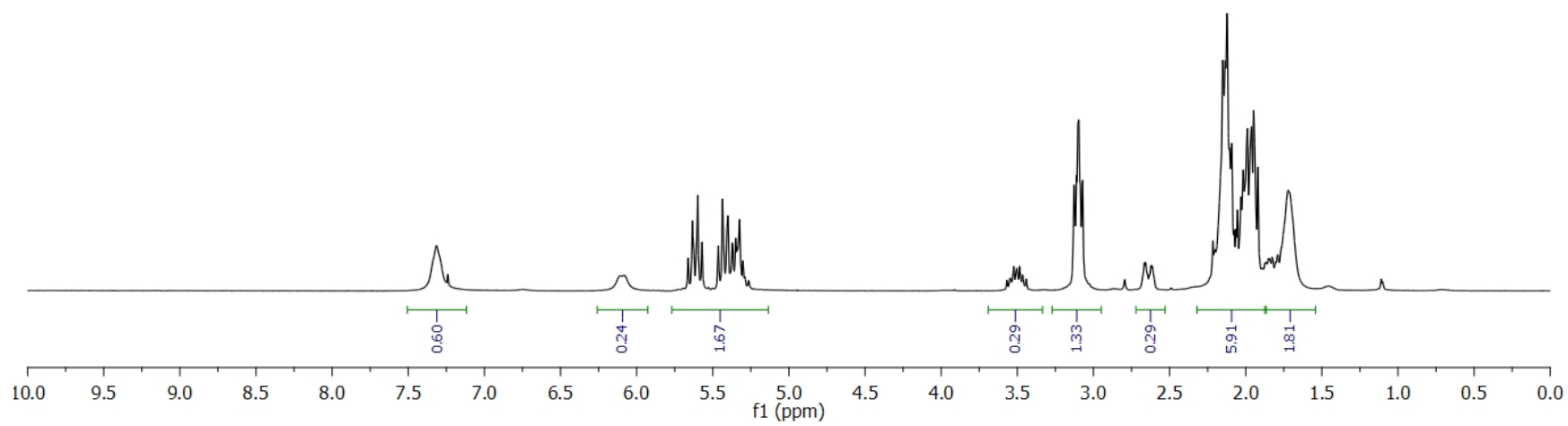
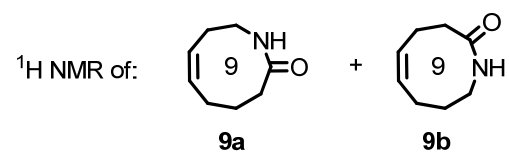


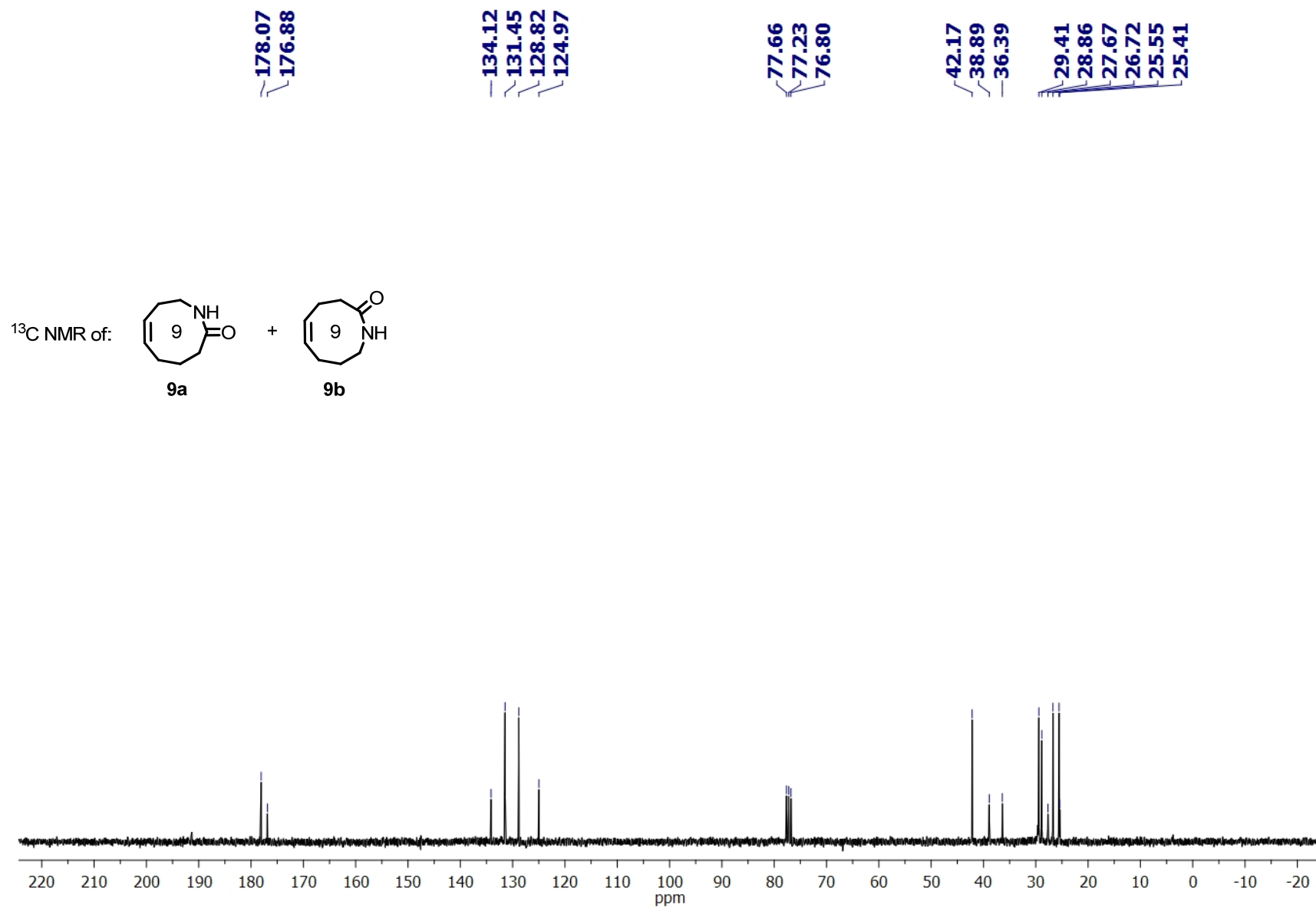




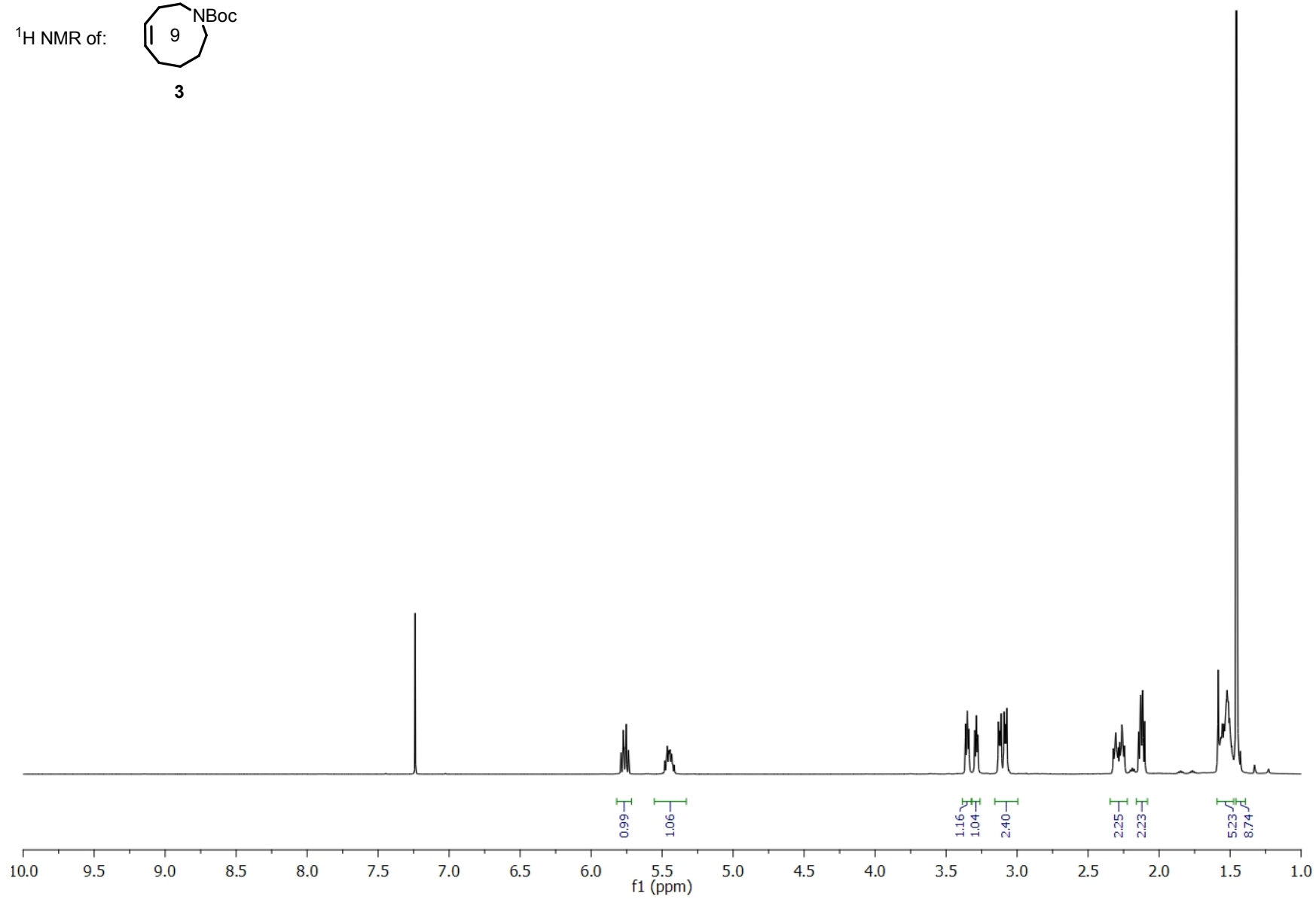
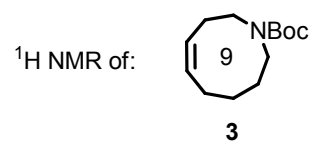










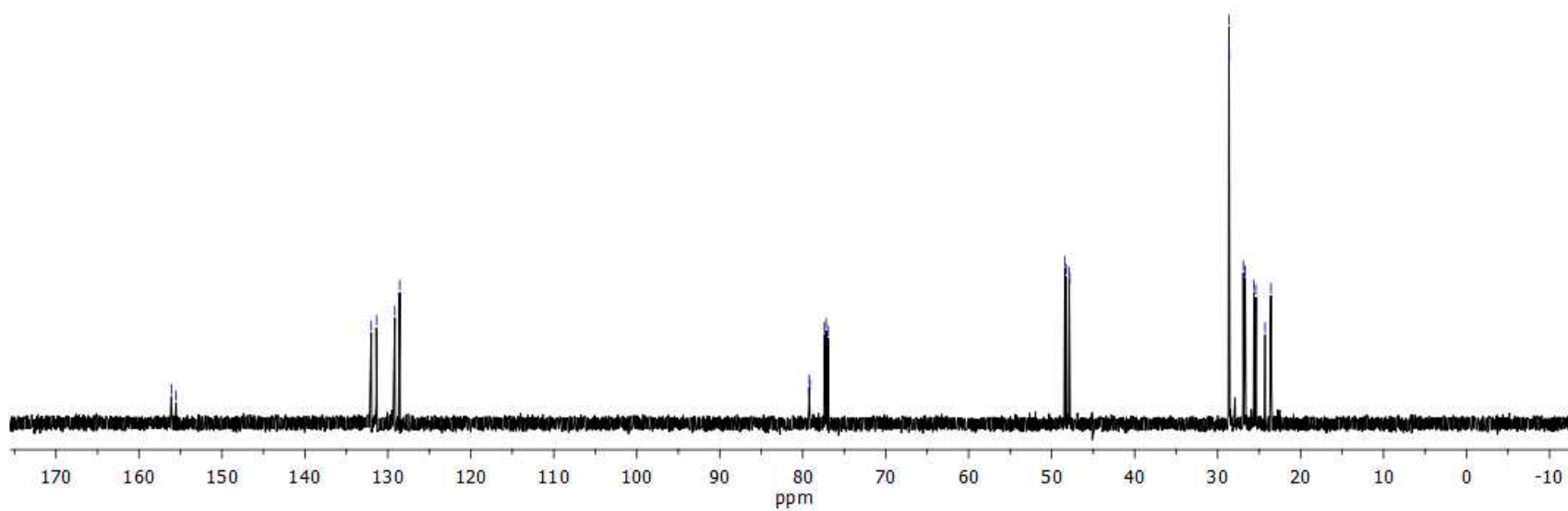
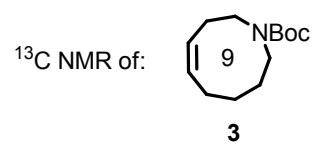


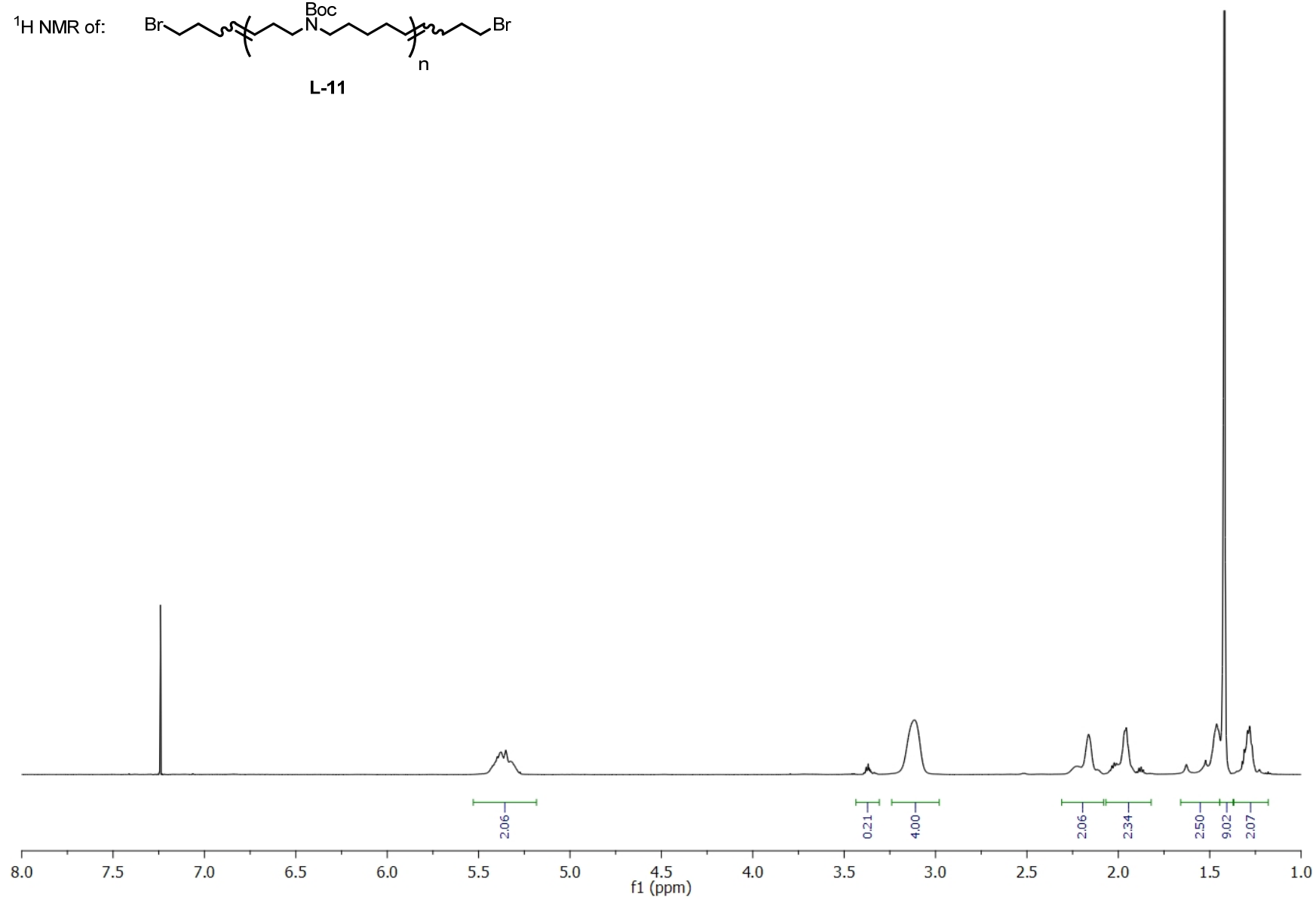
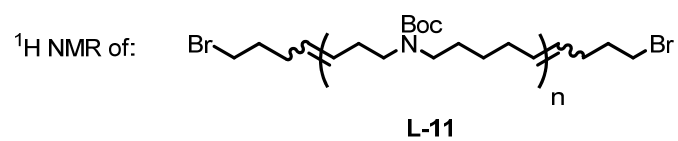
156.09  
155.51

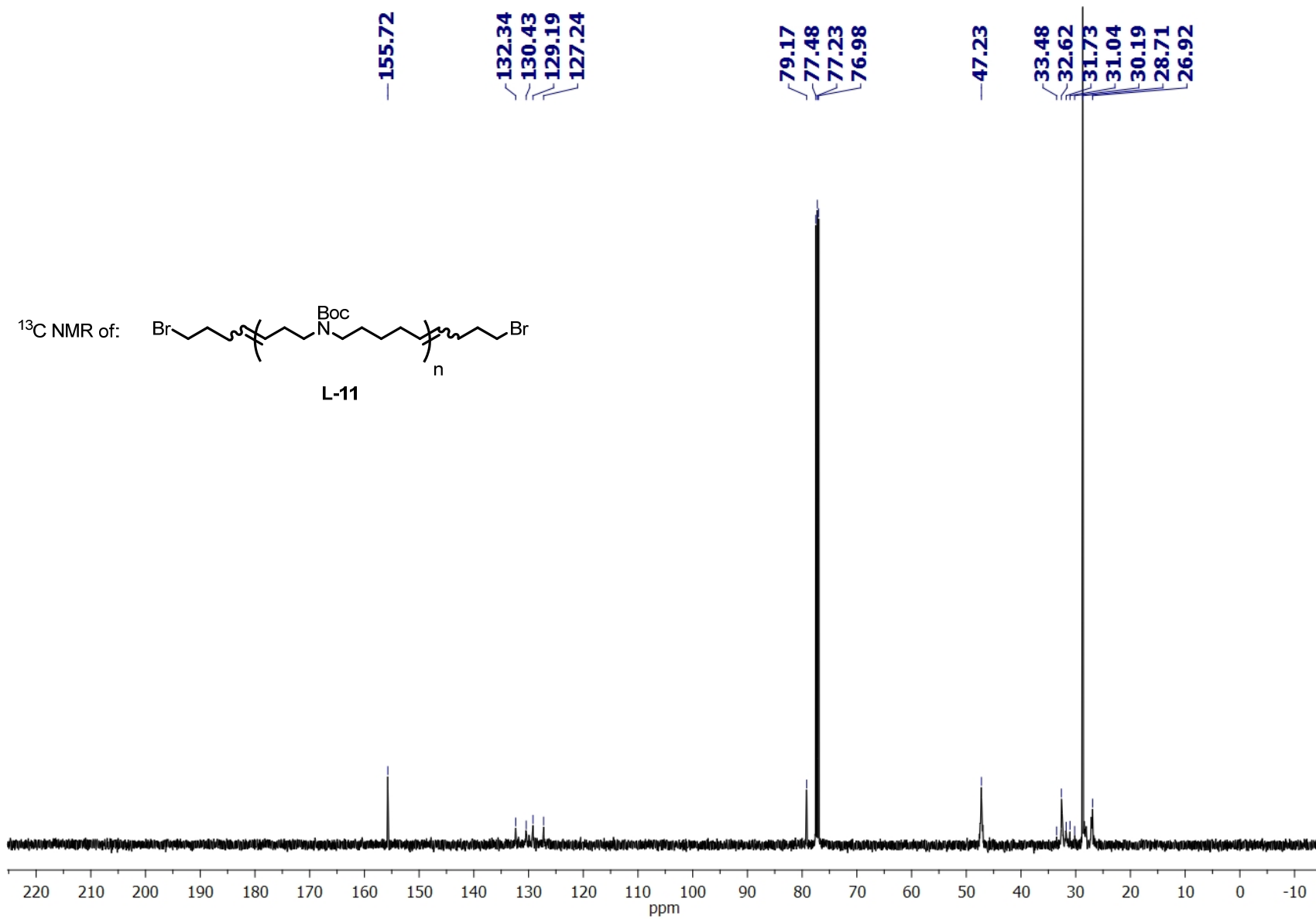
131.99  
131.37  
129.16  
128.58

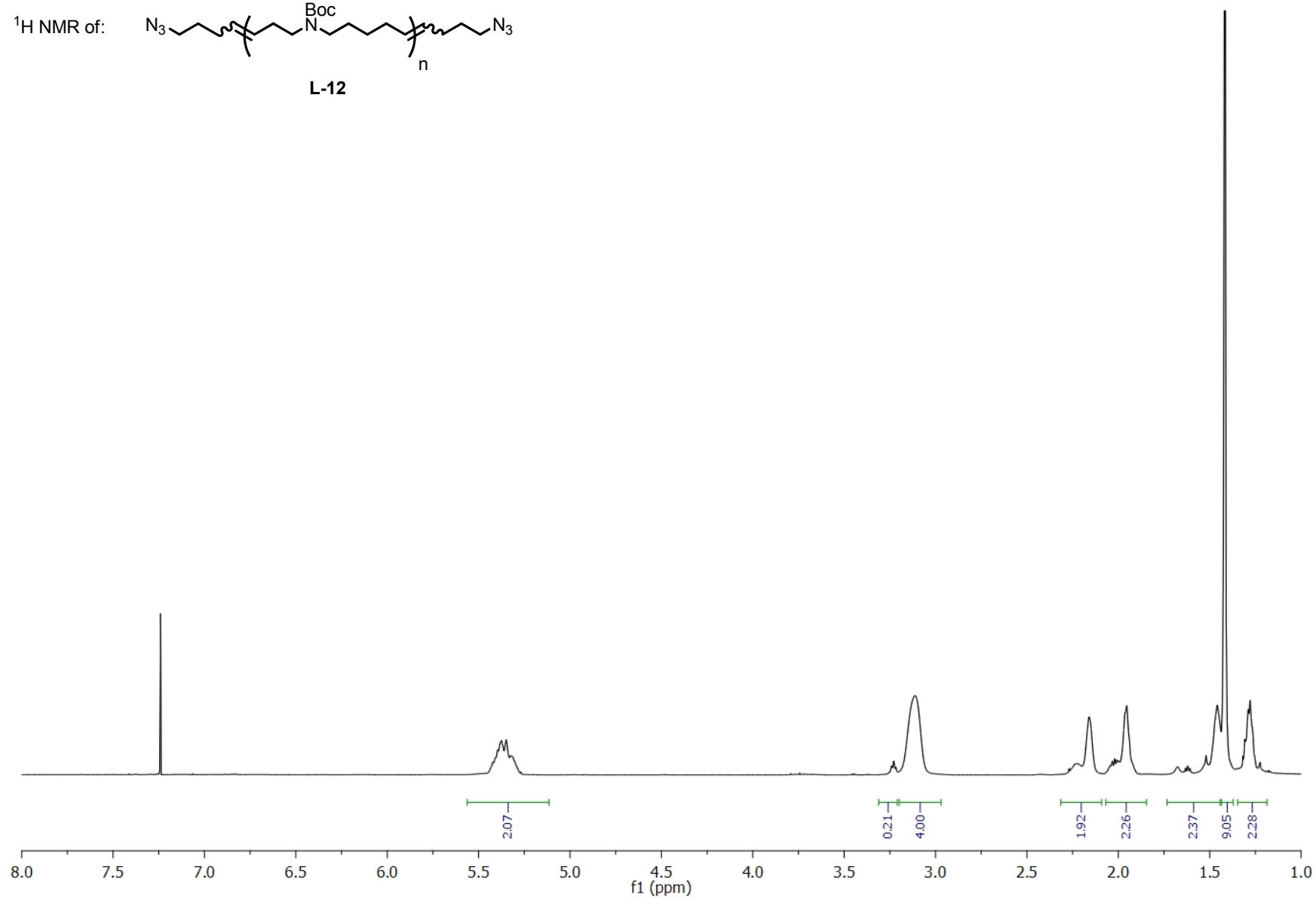
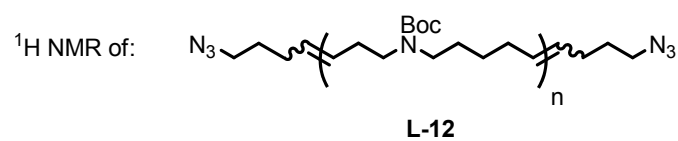
79.23  
79.12  
77.37  
77.16  
76.95

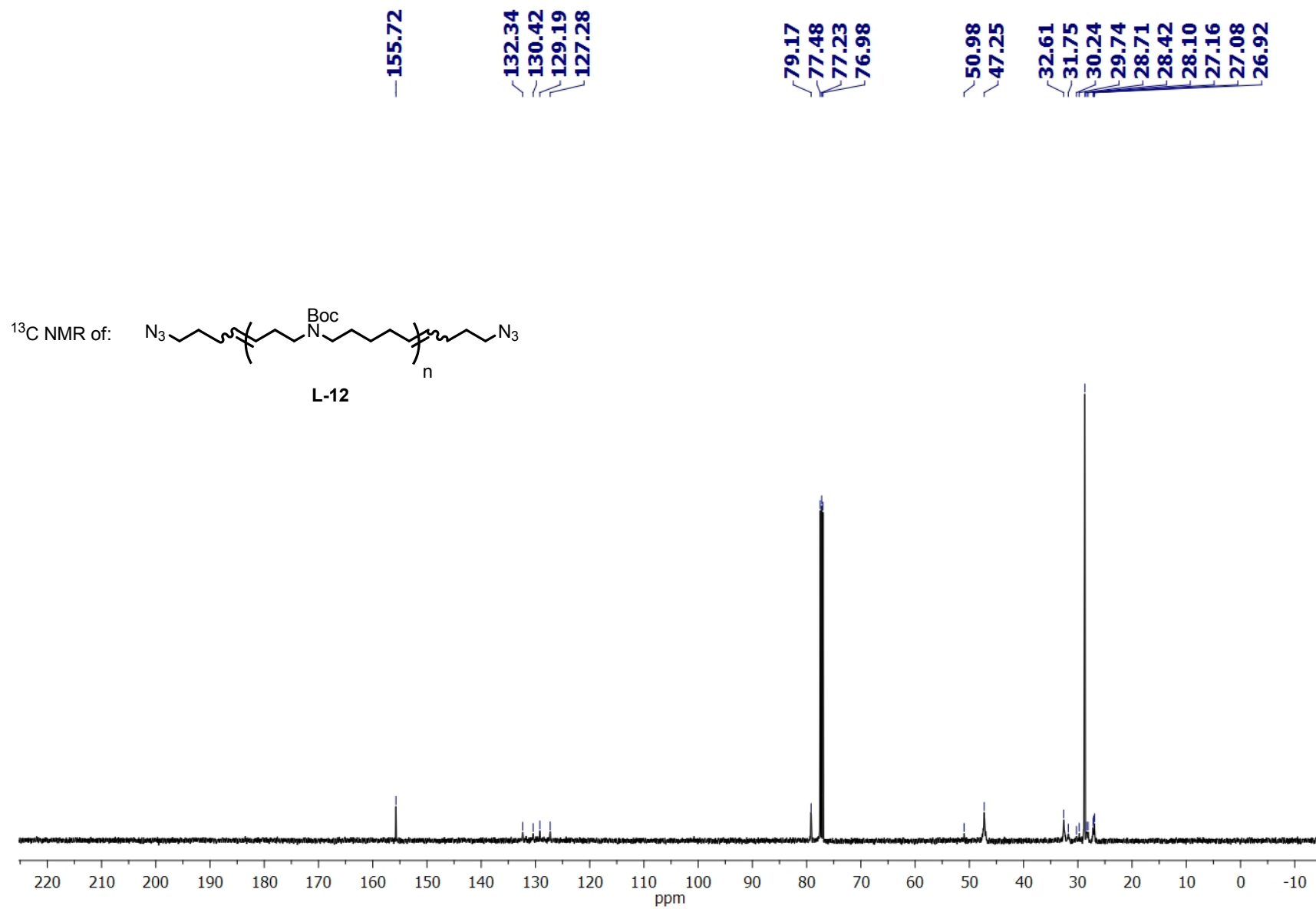
48.42  
48.26  
47.89  
47.82  
28.63  
28.58  
26.91  
26.77  
26.68  
25.63  
25.54  
25.38  
24.29  
23.58



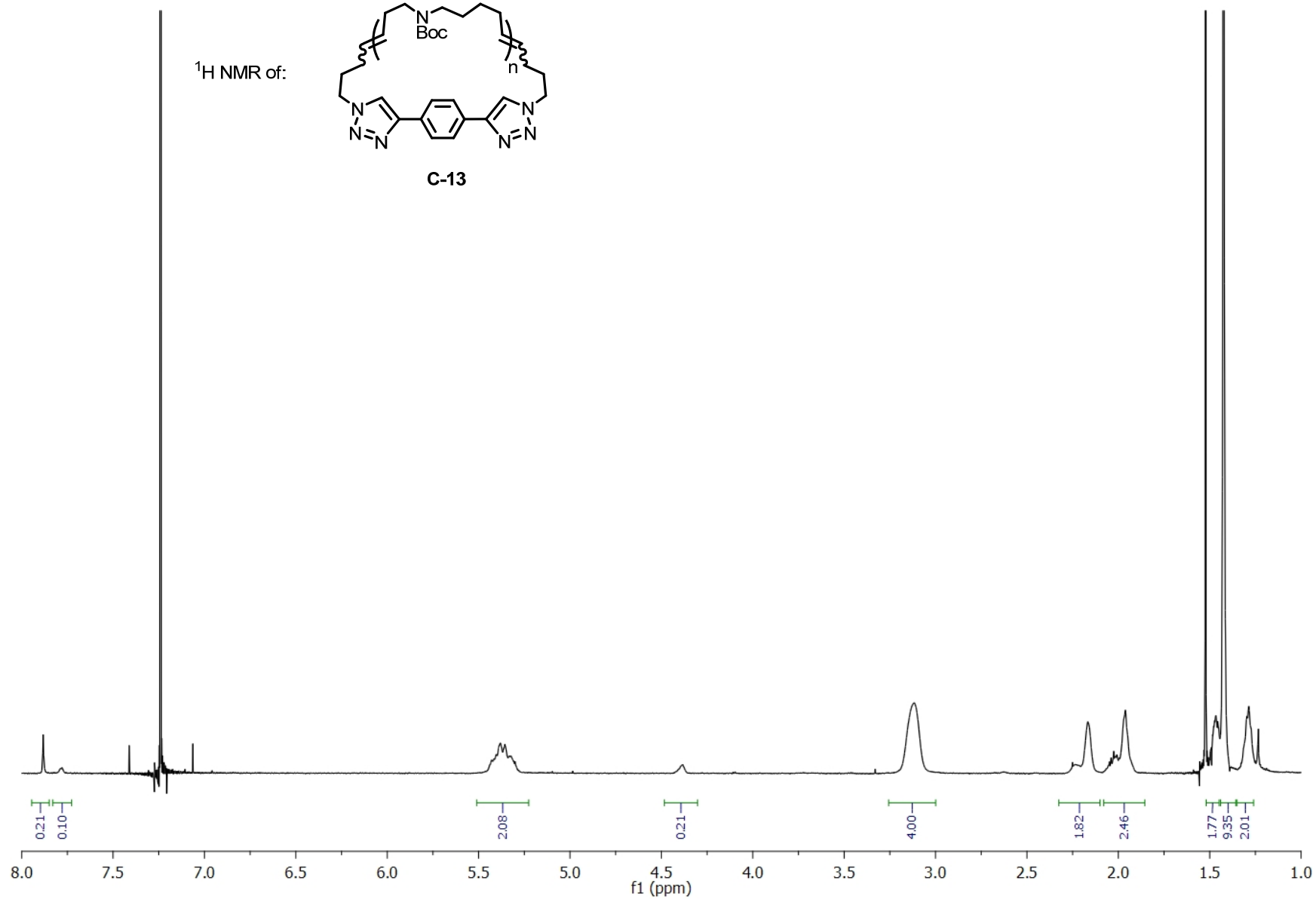
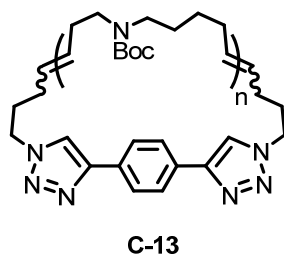






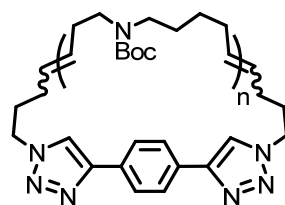


$^1\text{H}$  NMR of:

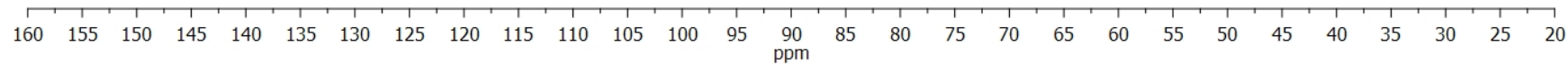


155.68  
155.66

147.49

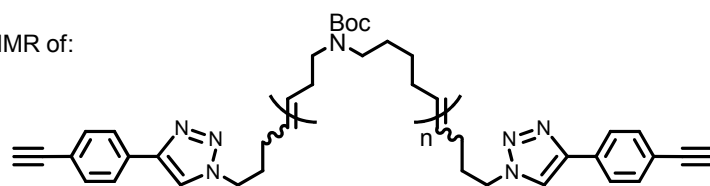
132.30  
131.72  
130.40  
129.87  
129.15  
128.26  
127.24  
126.56  
126.23  
119.80<sup>13</sup>C NMR of:

C-13

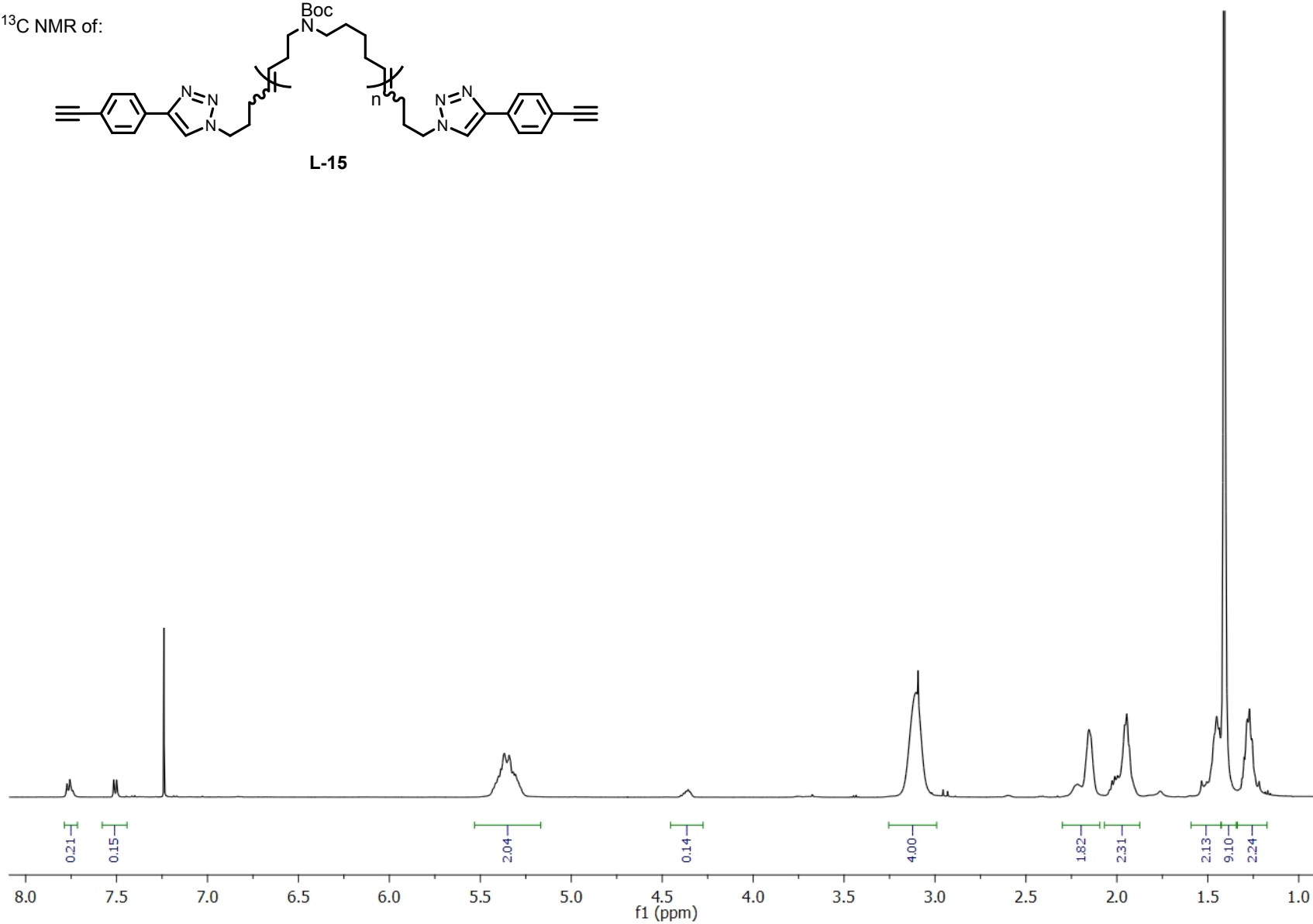
79.17  
79.13  
77.23  
76.9850.49  
49.87  
47.21  
46.9532.55  
30.49  
28.81  
28.66  
28.50  
28.96  
28.03  
27.17  
27.11  
27.00  
26.87

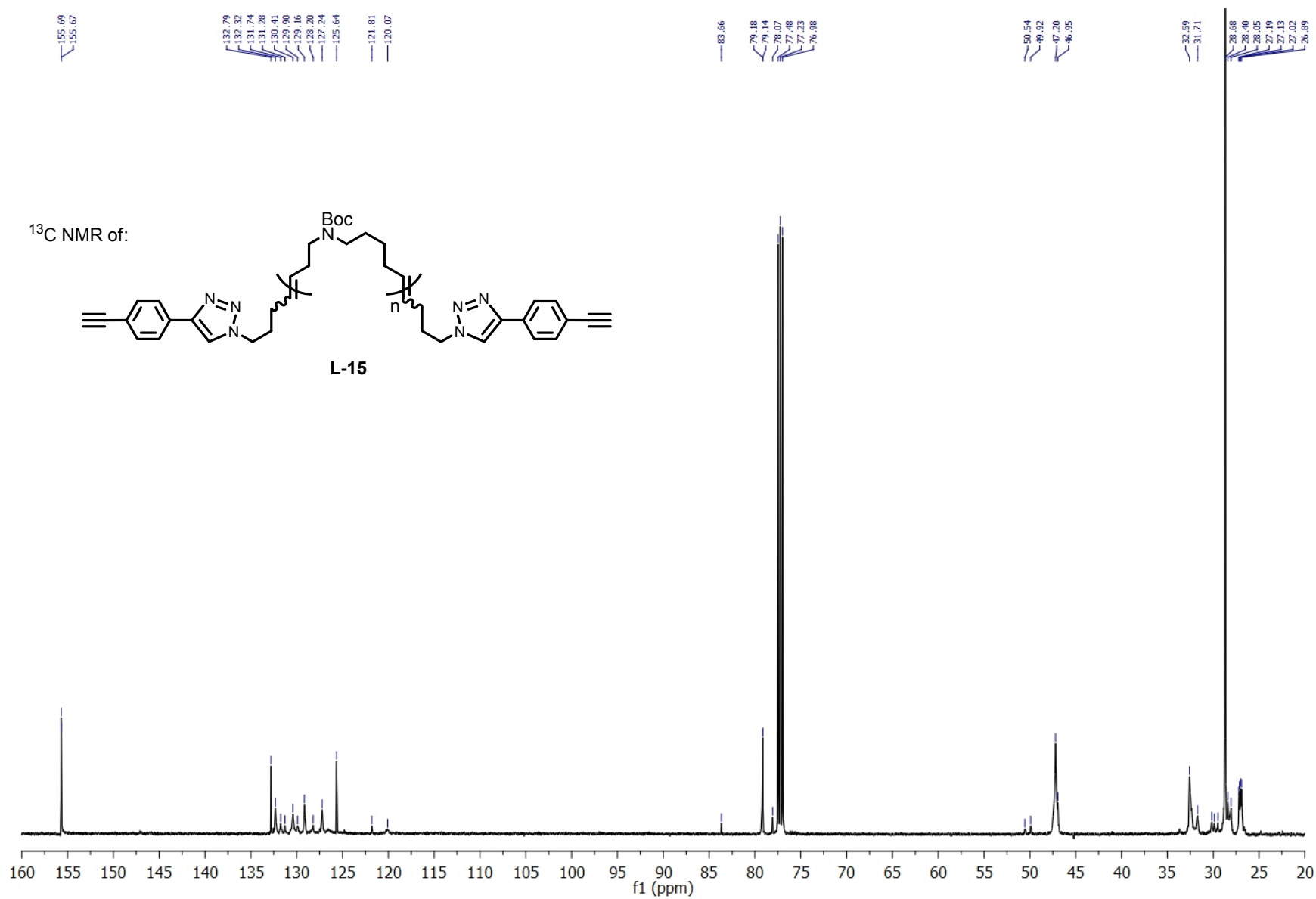


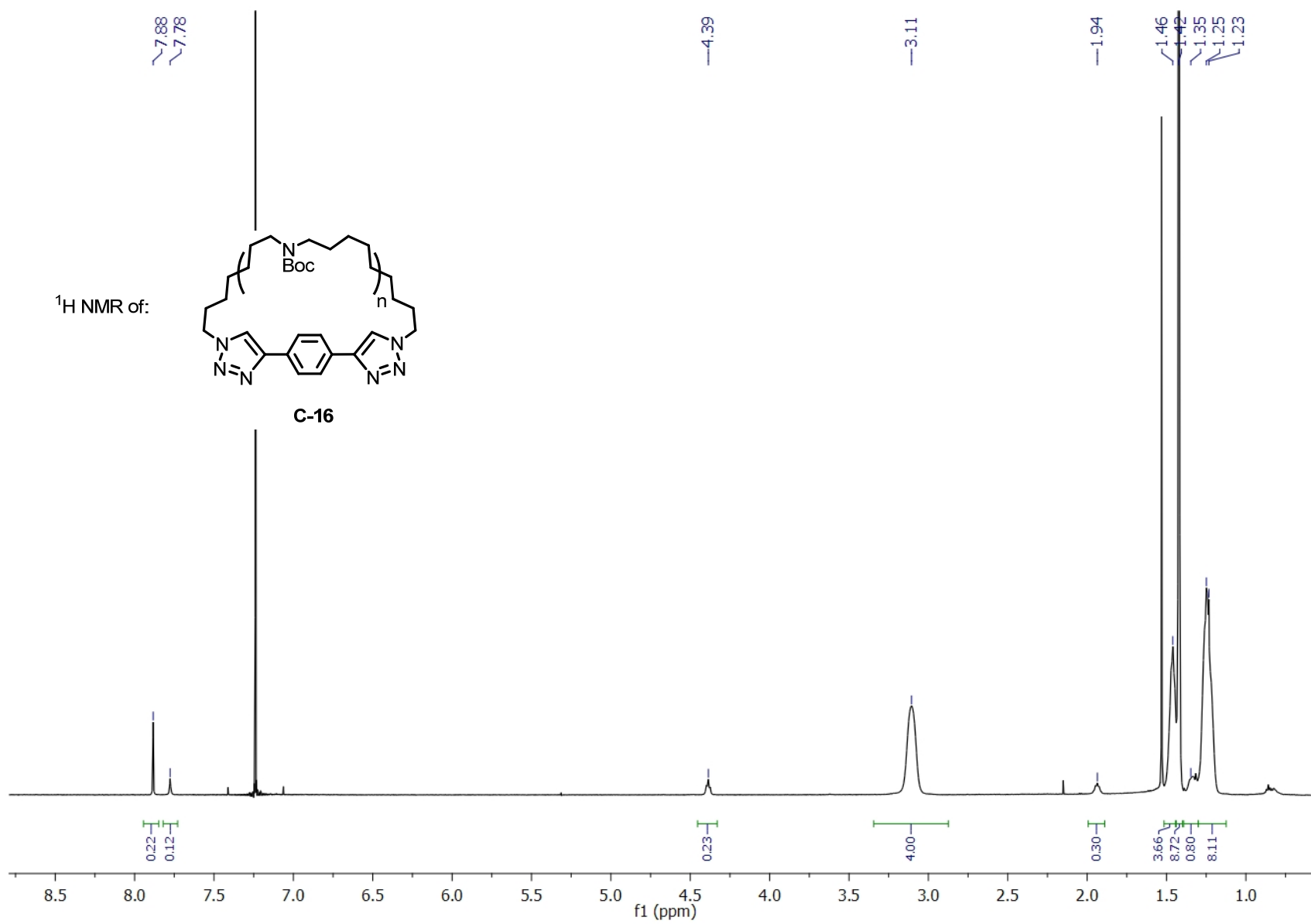
$^{13}\text{C}$  NMR of:

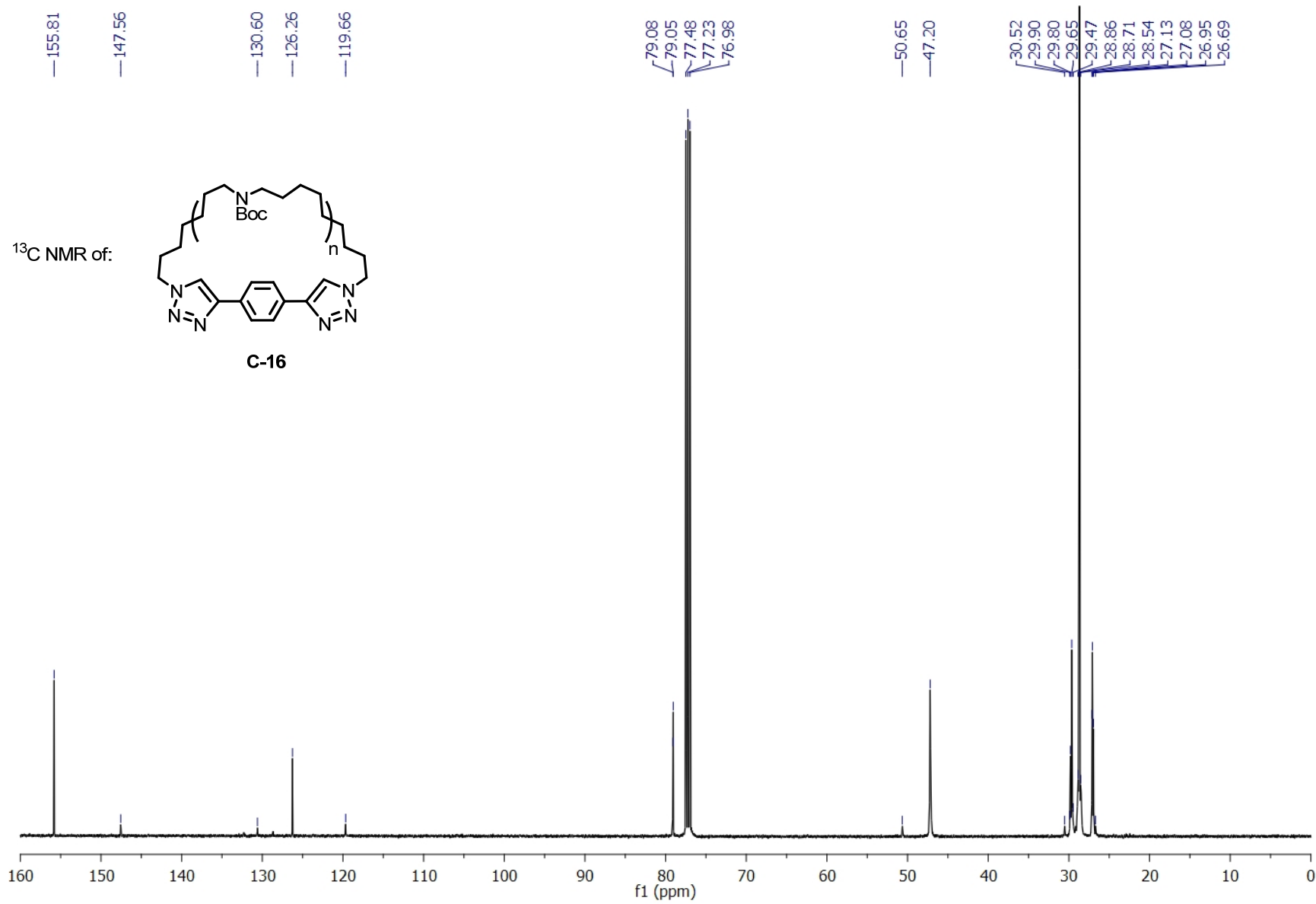


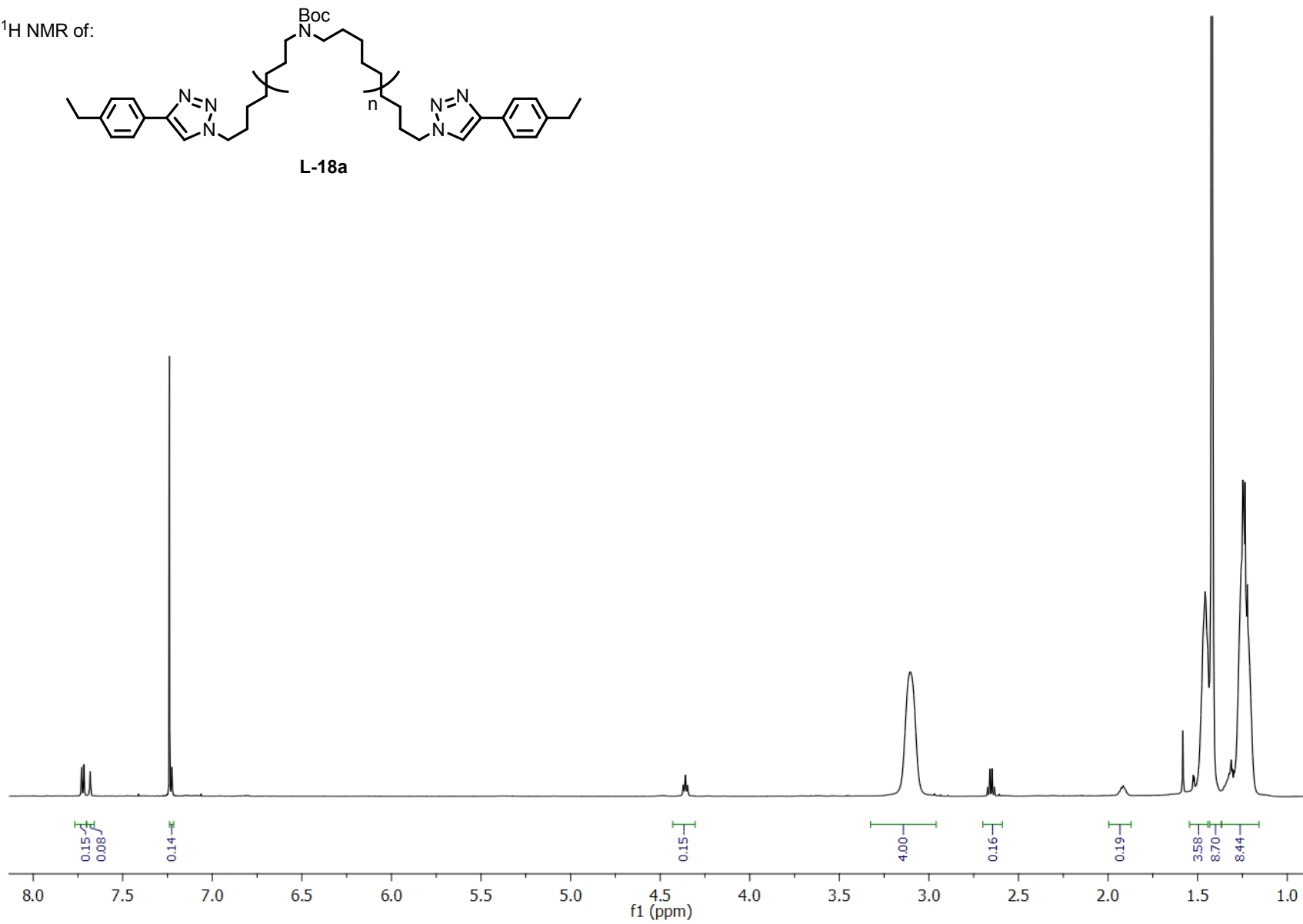
**L-15**



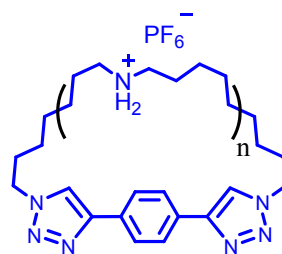




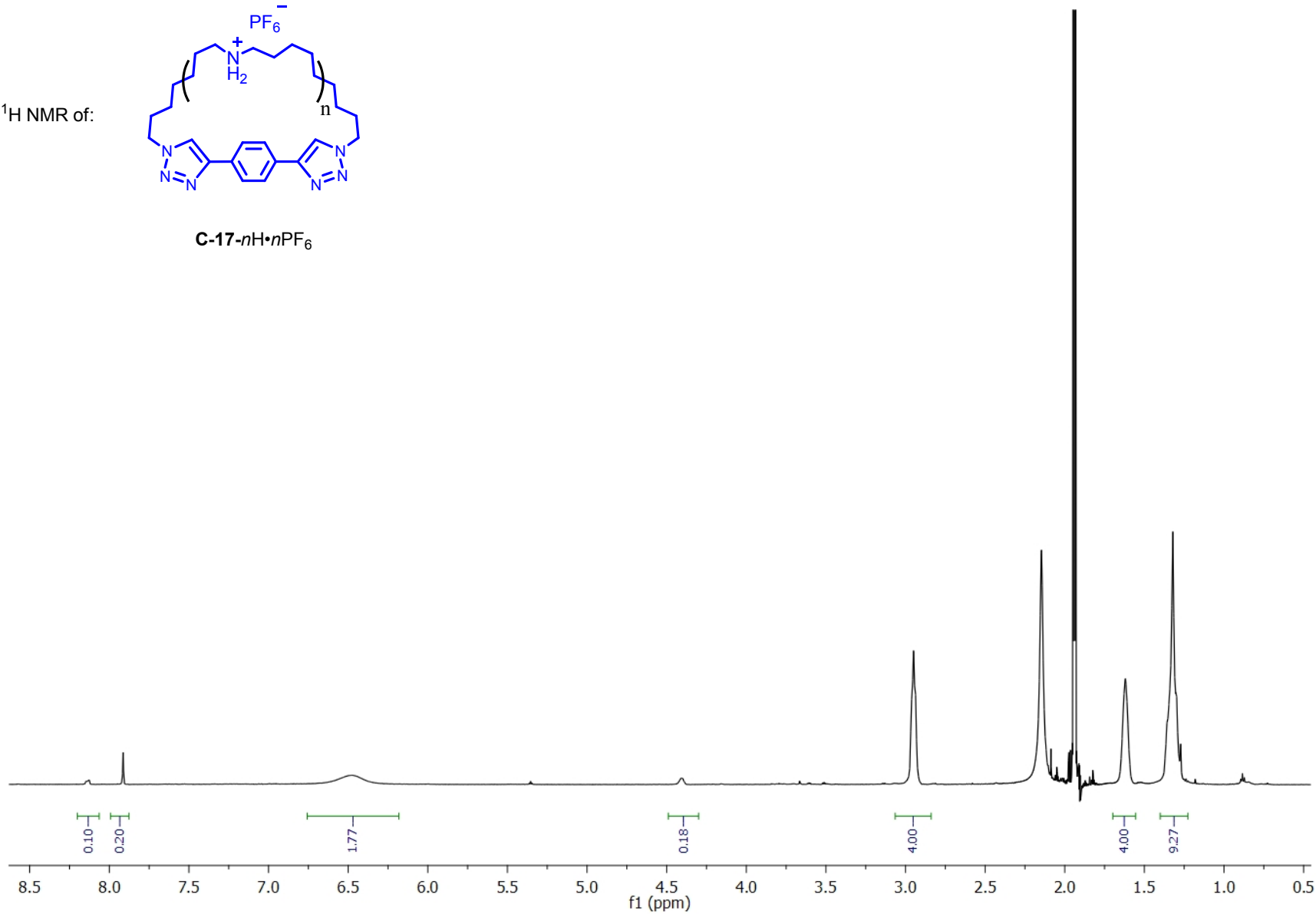


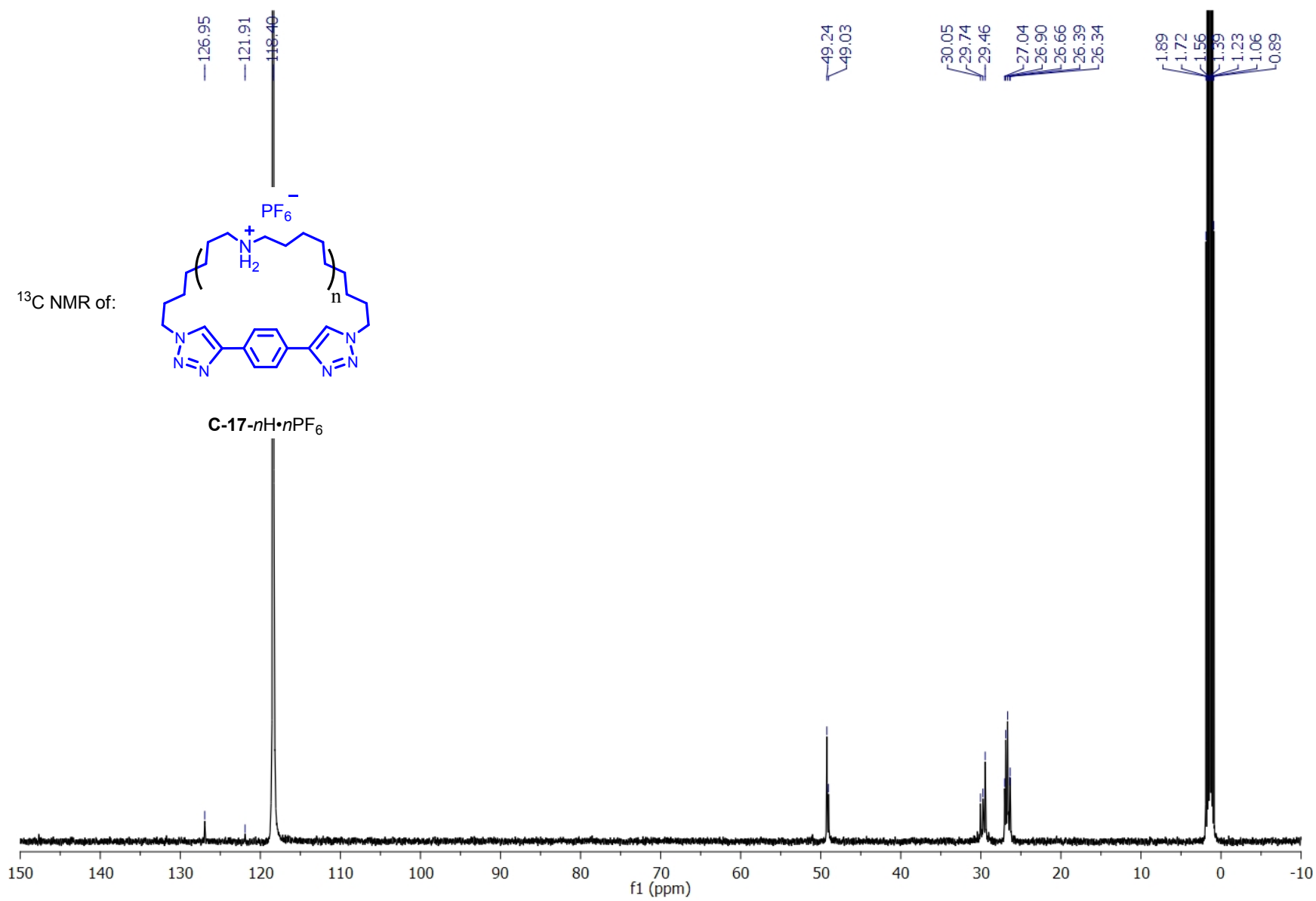


$^1\text{H}$  NMR of:

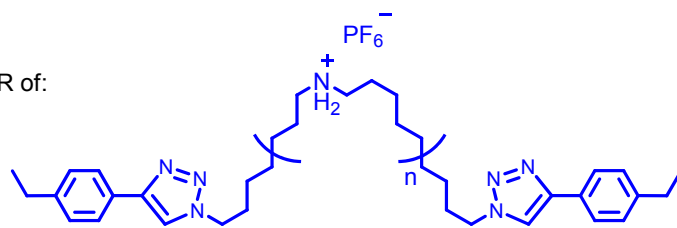


**C-17- $n\text{H}$ - $n\text{PF}_6$**

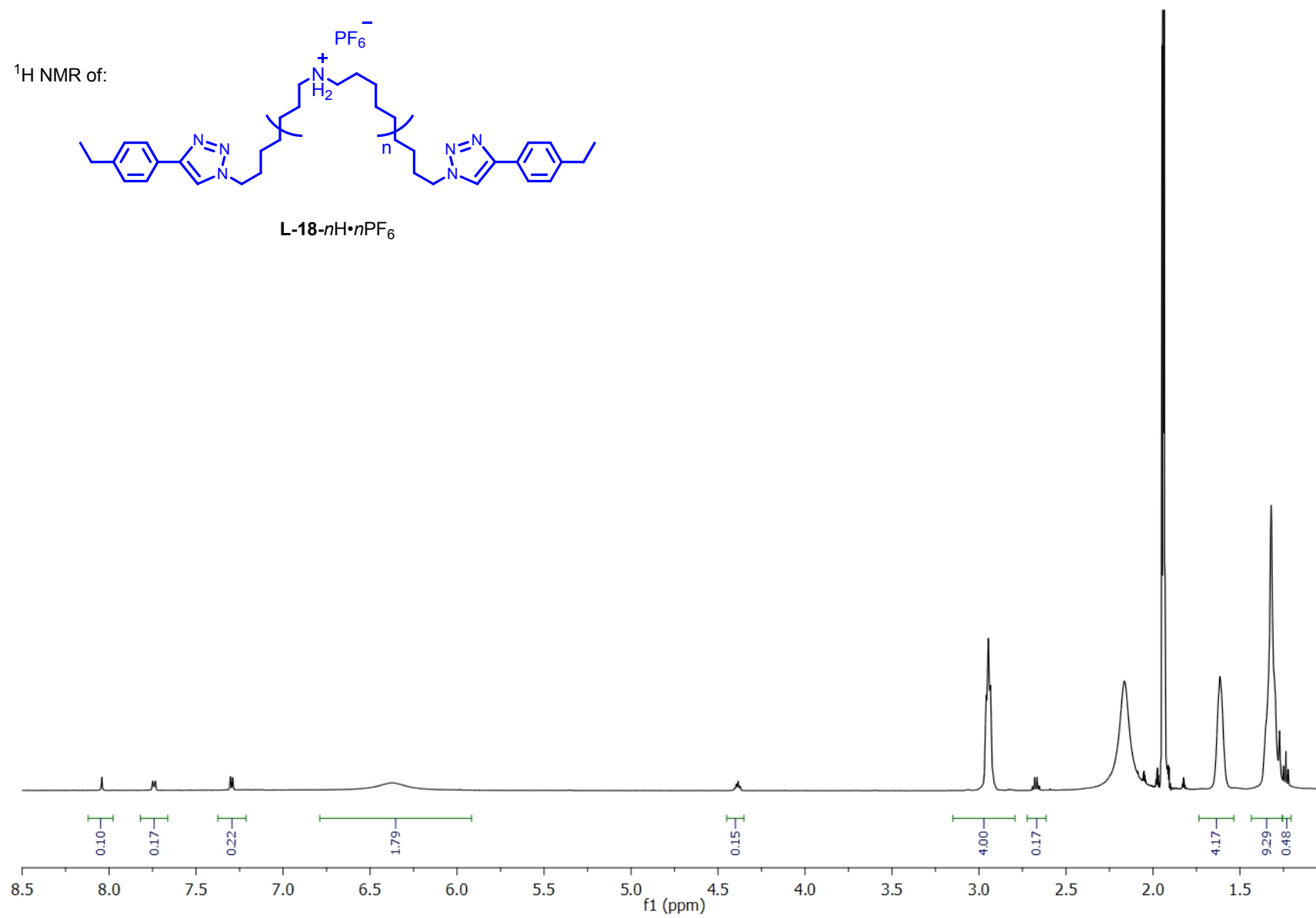




$^1\text{H}$  NMR of:

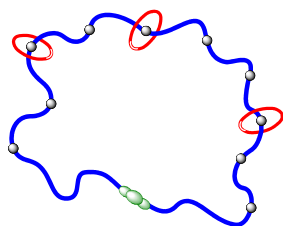


**L-18-*n*H•*n*PF<sub>6</sub>**



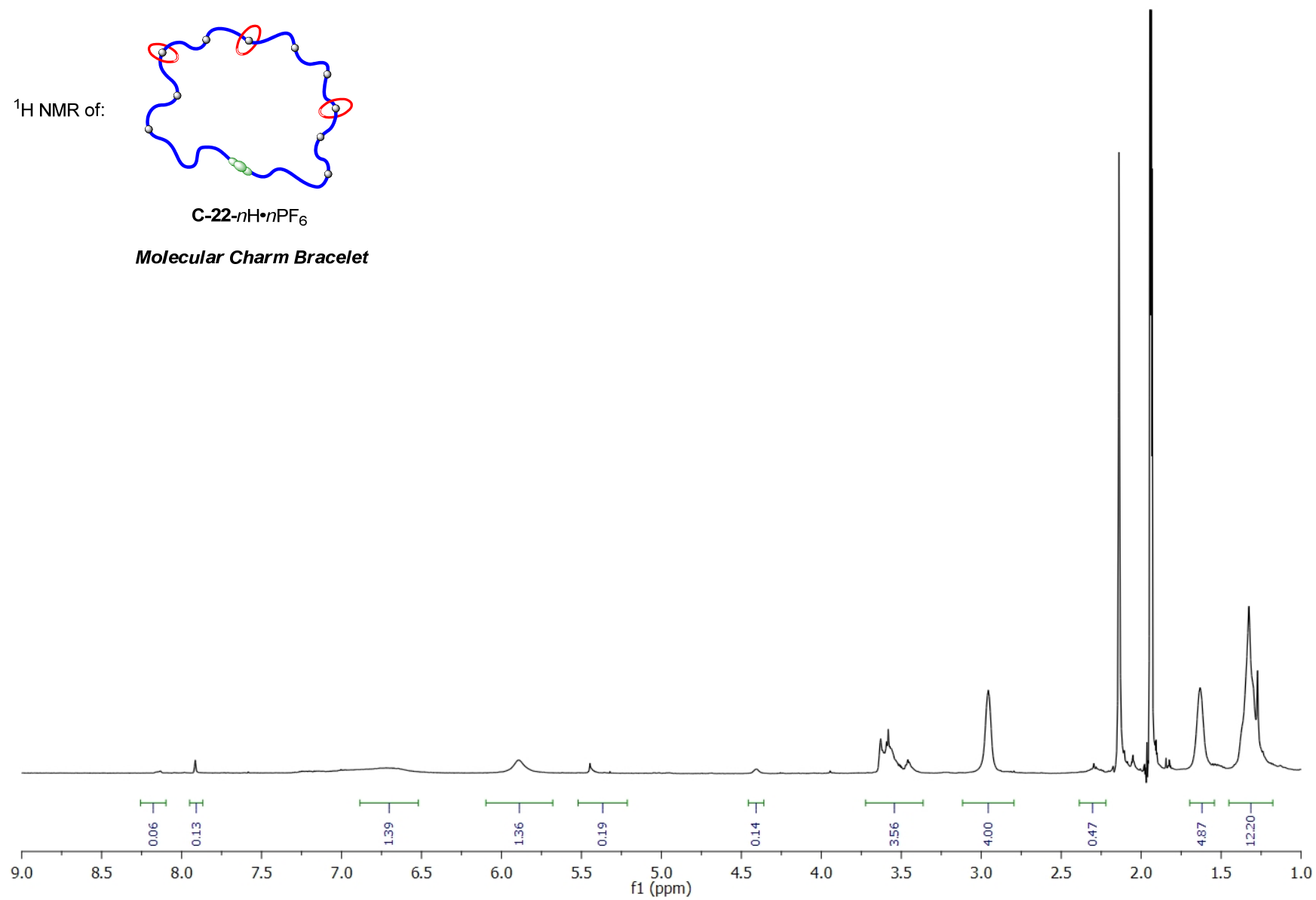


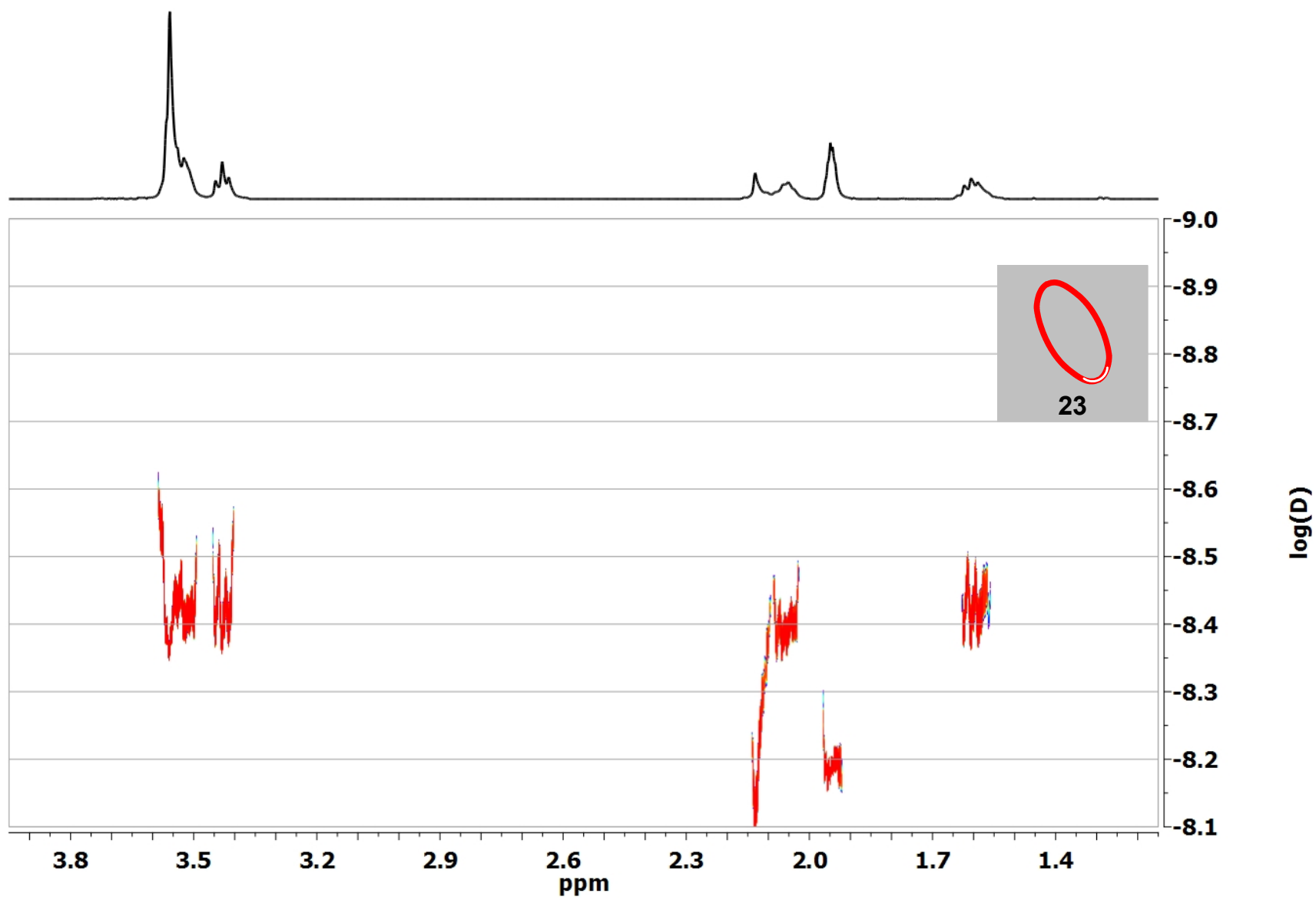
$^1\text{H}$  NMR of:

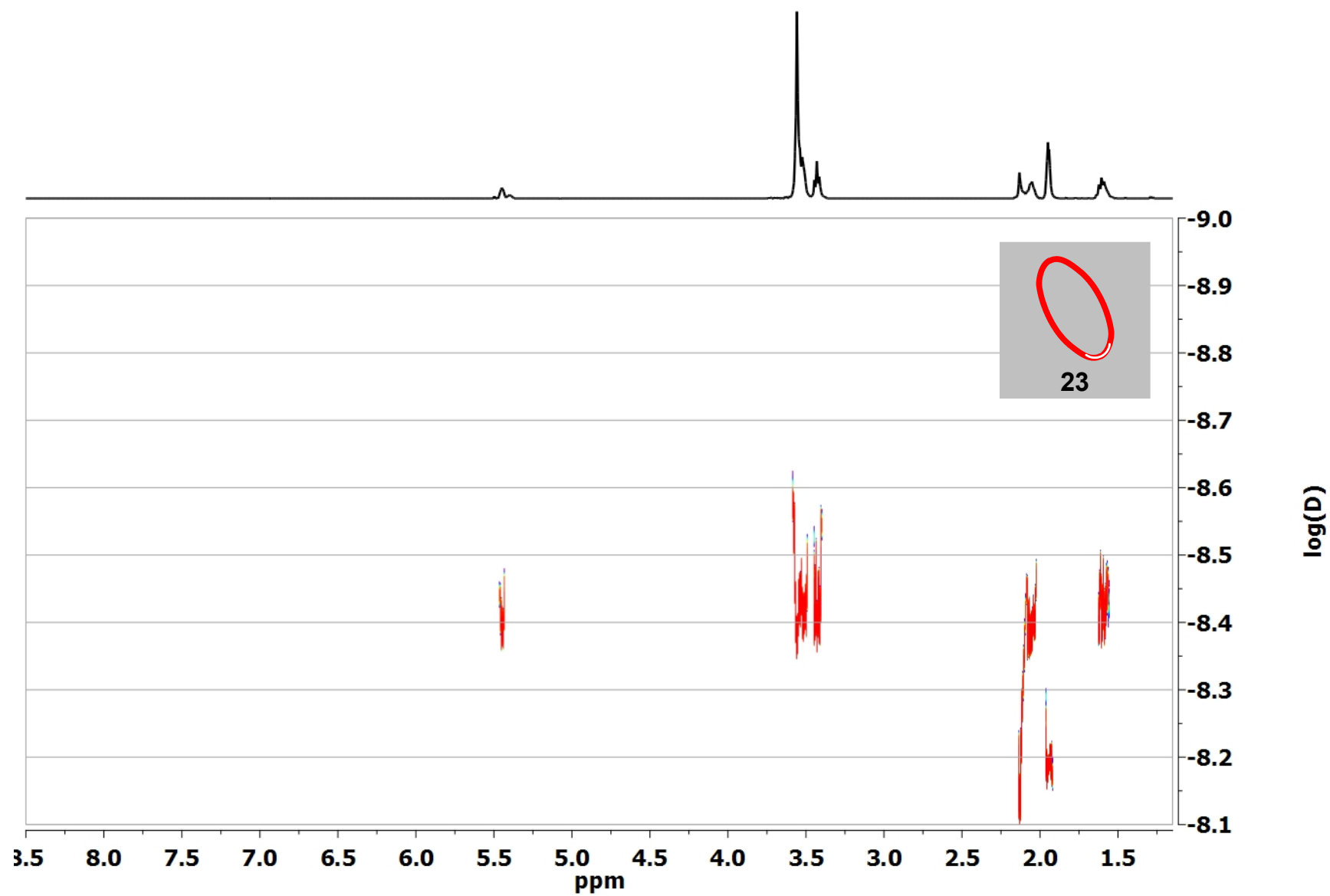


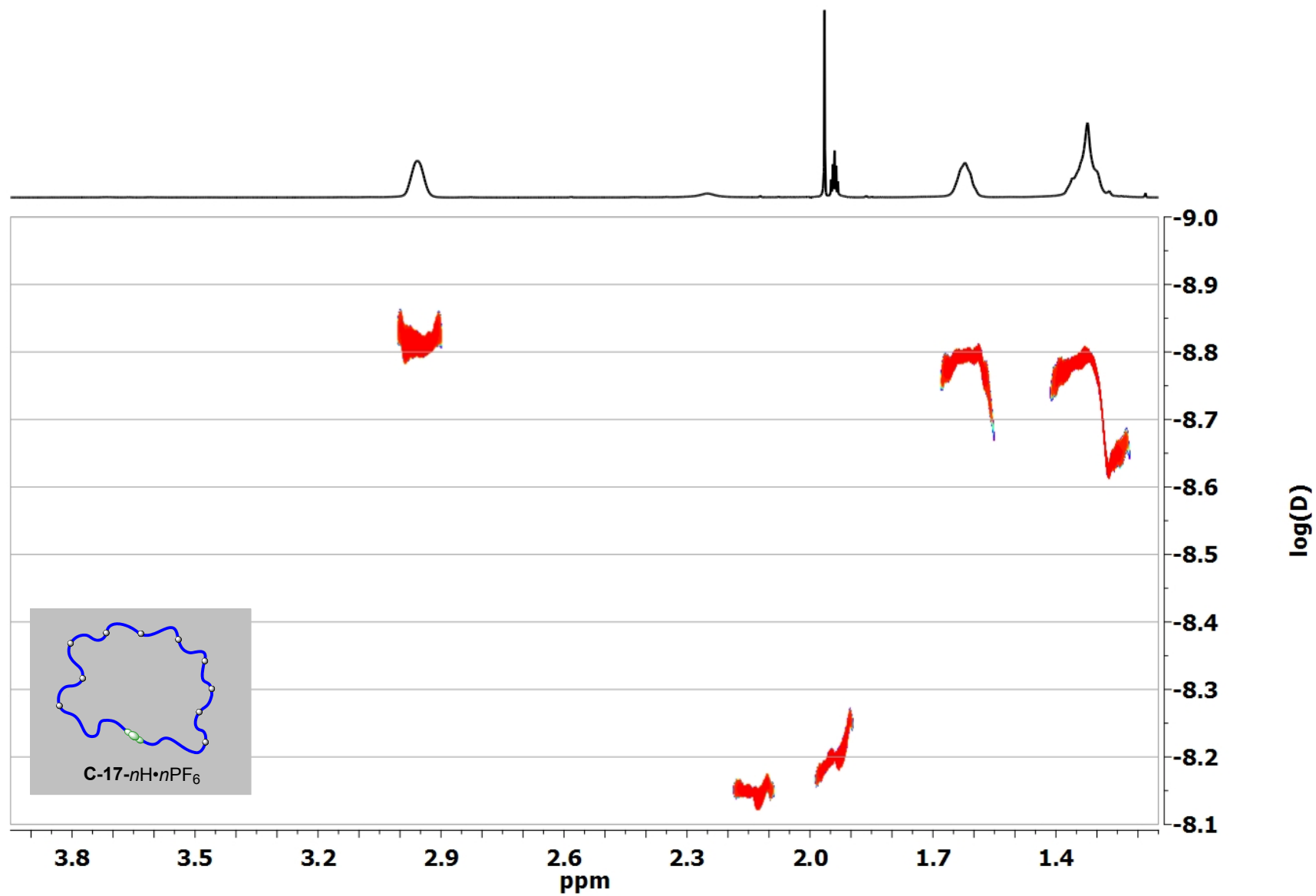
**C-22-nH-nPF<sub>6</sub>**

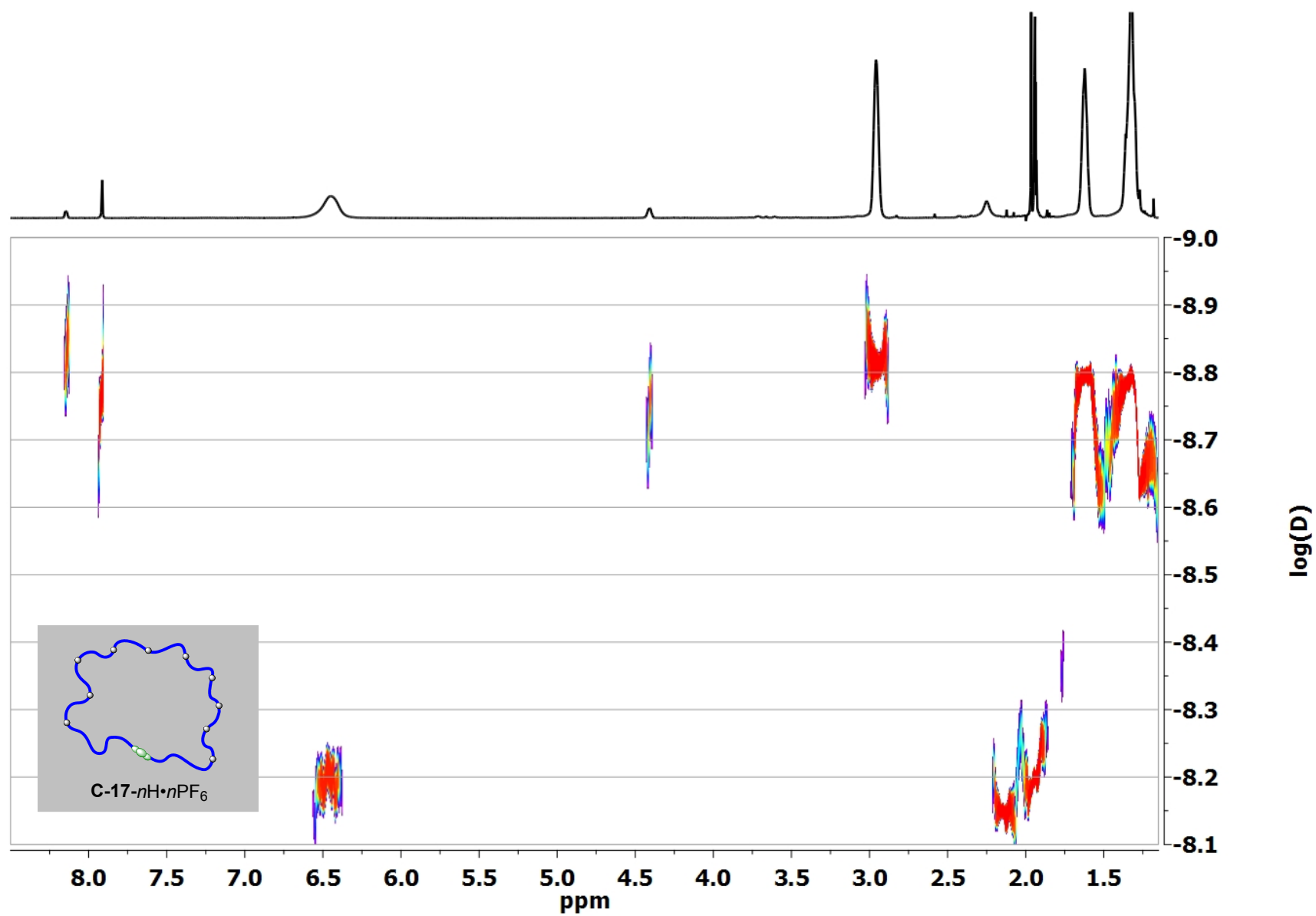
***Molecular Charm Bracelet***

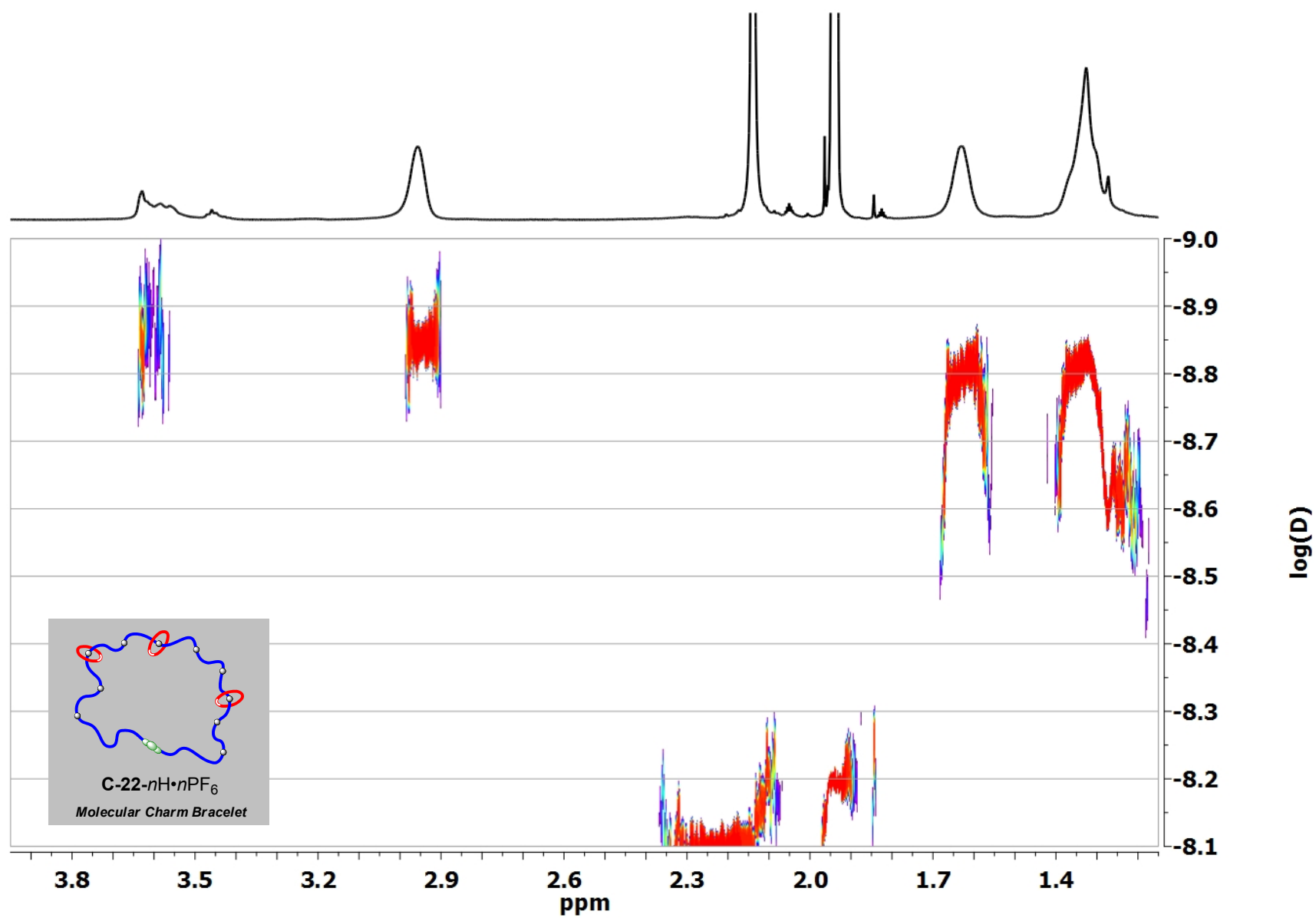


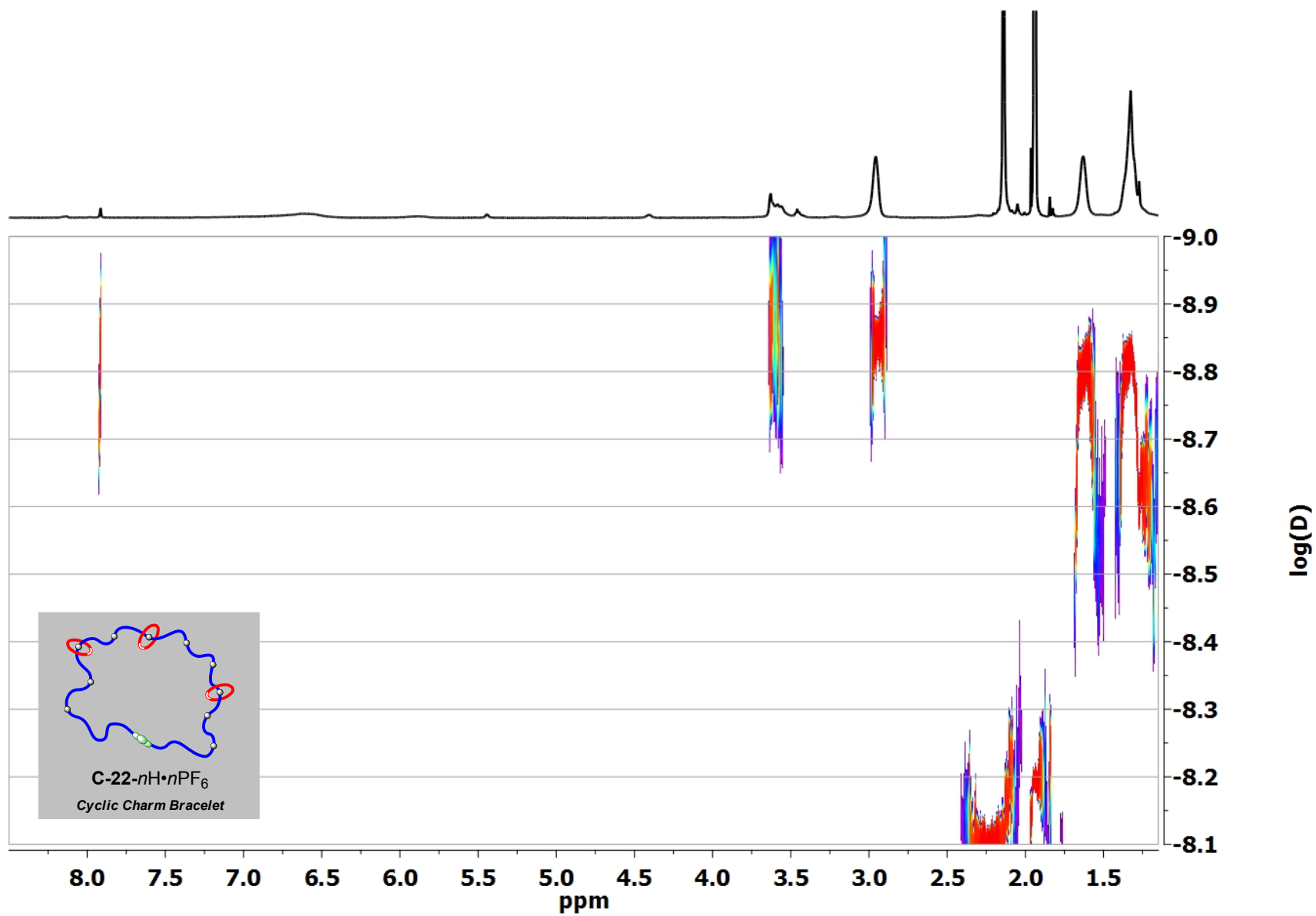


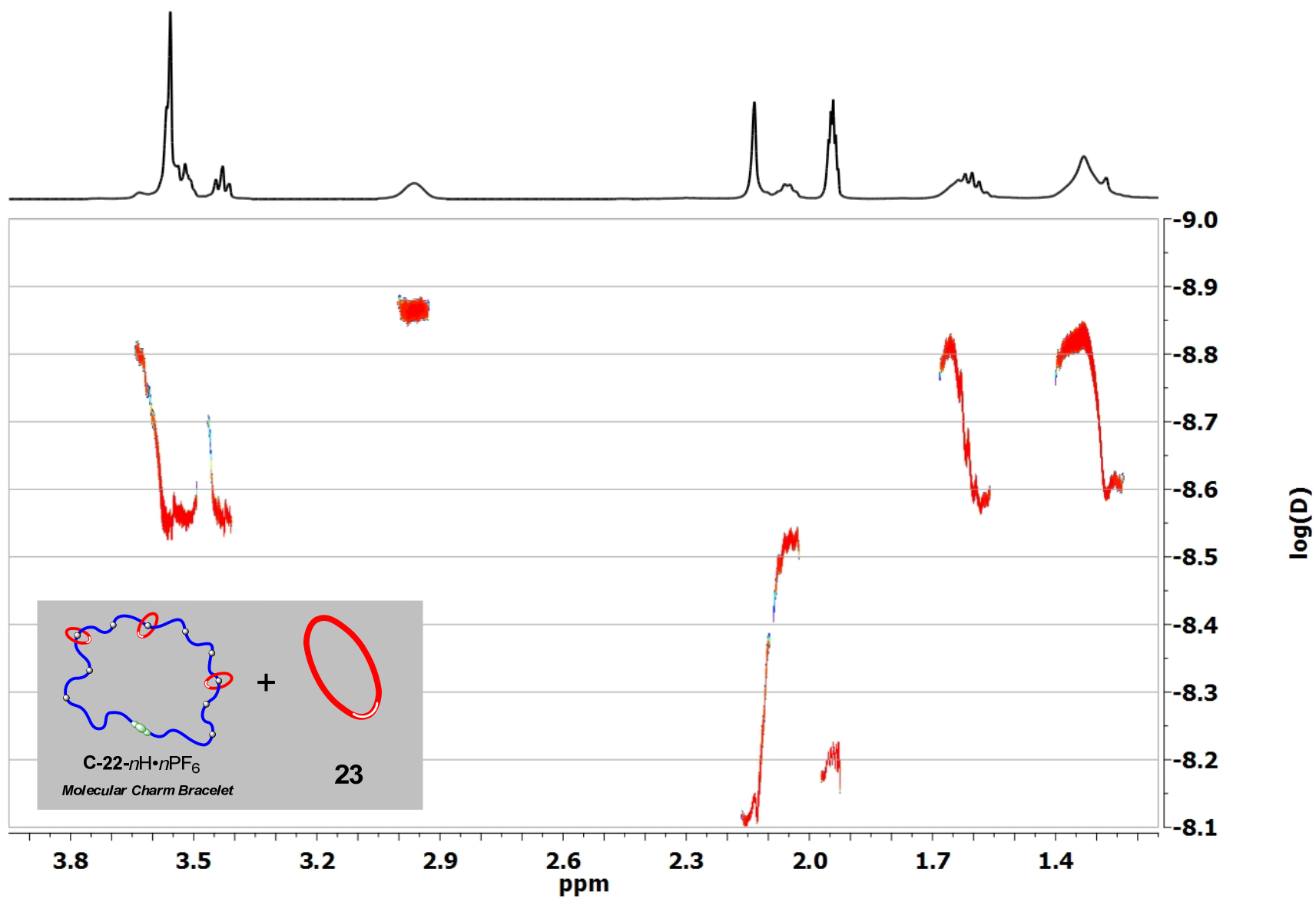




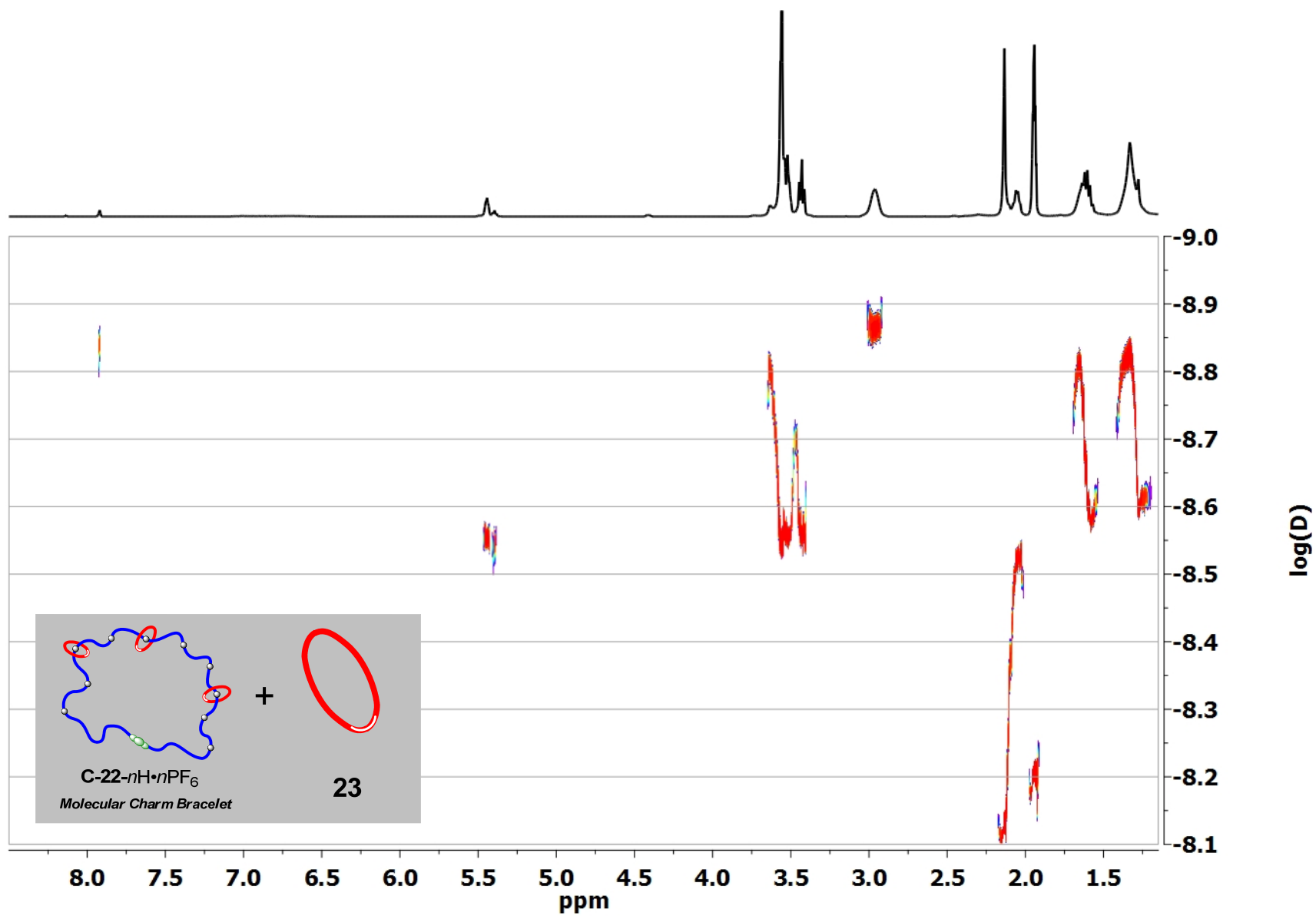




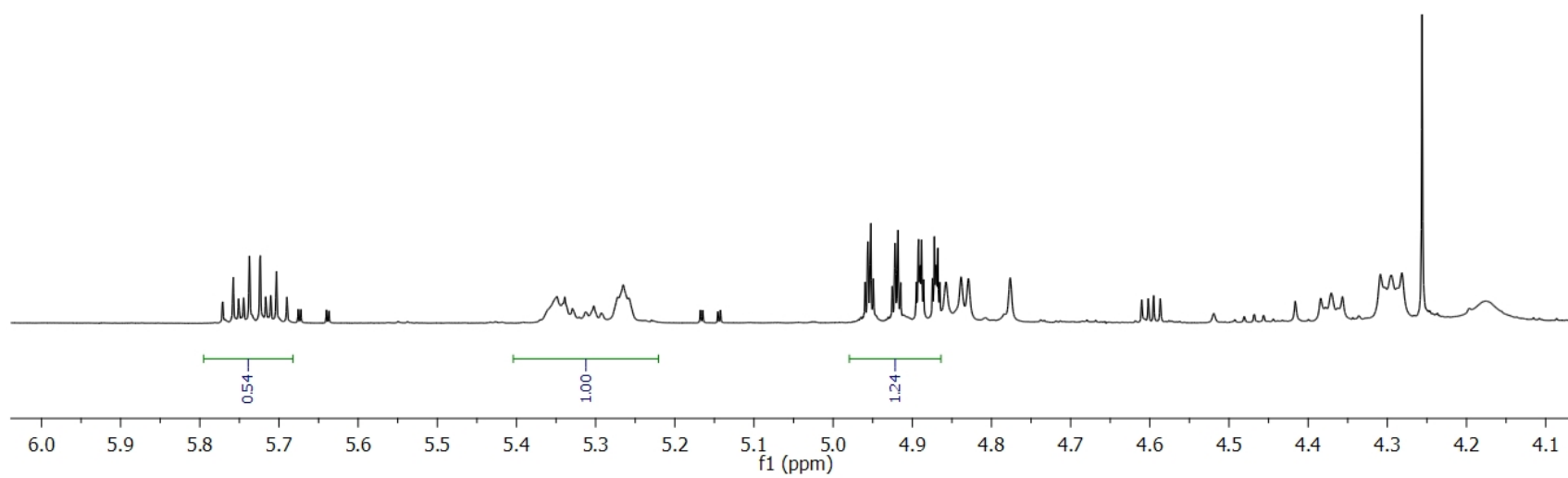
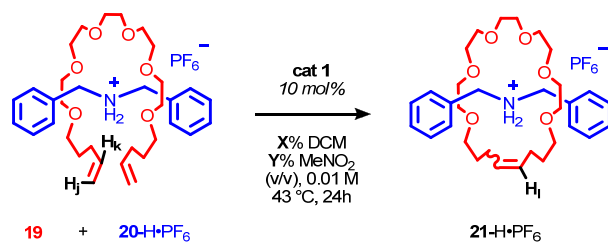




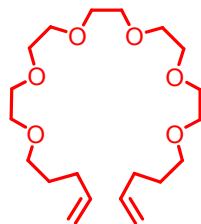




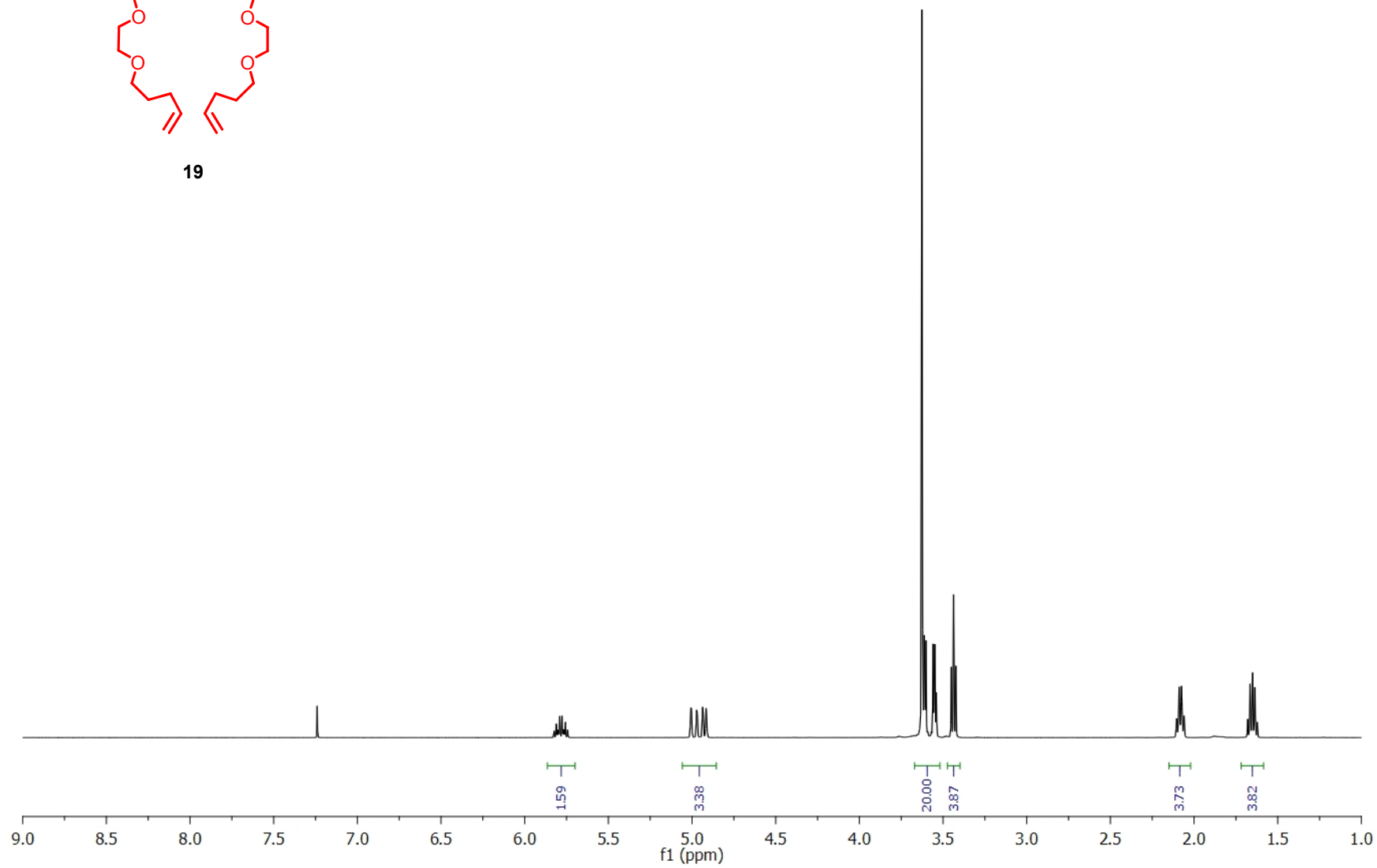
$^1\text{H}$  NMR of **ENTRY 5**:

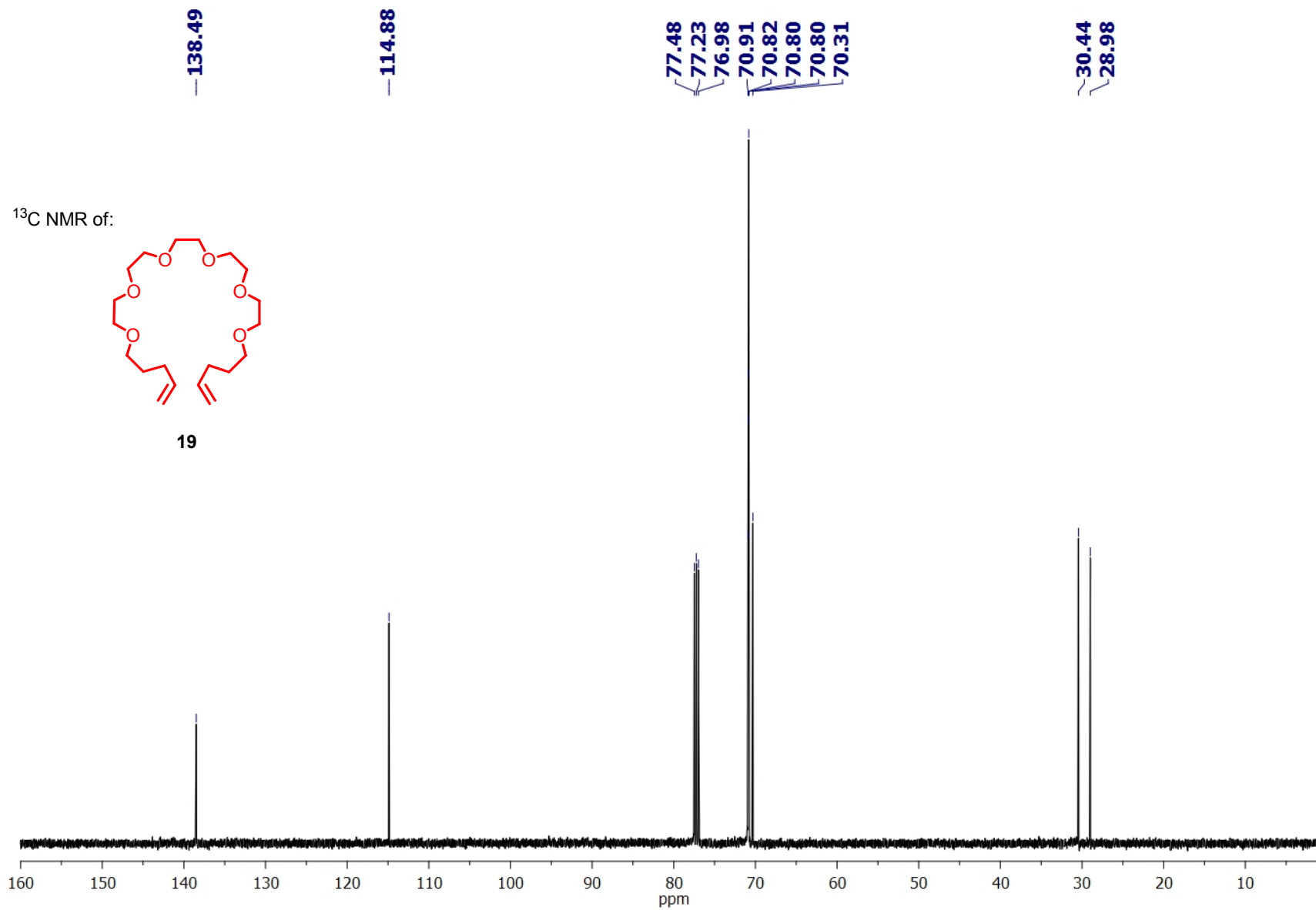


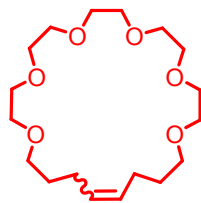
$^1\text{H}$  NMR of:



**19**

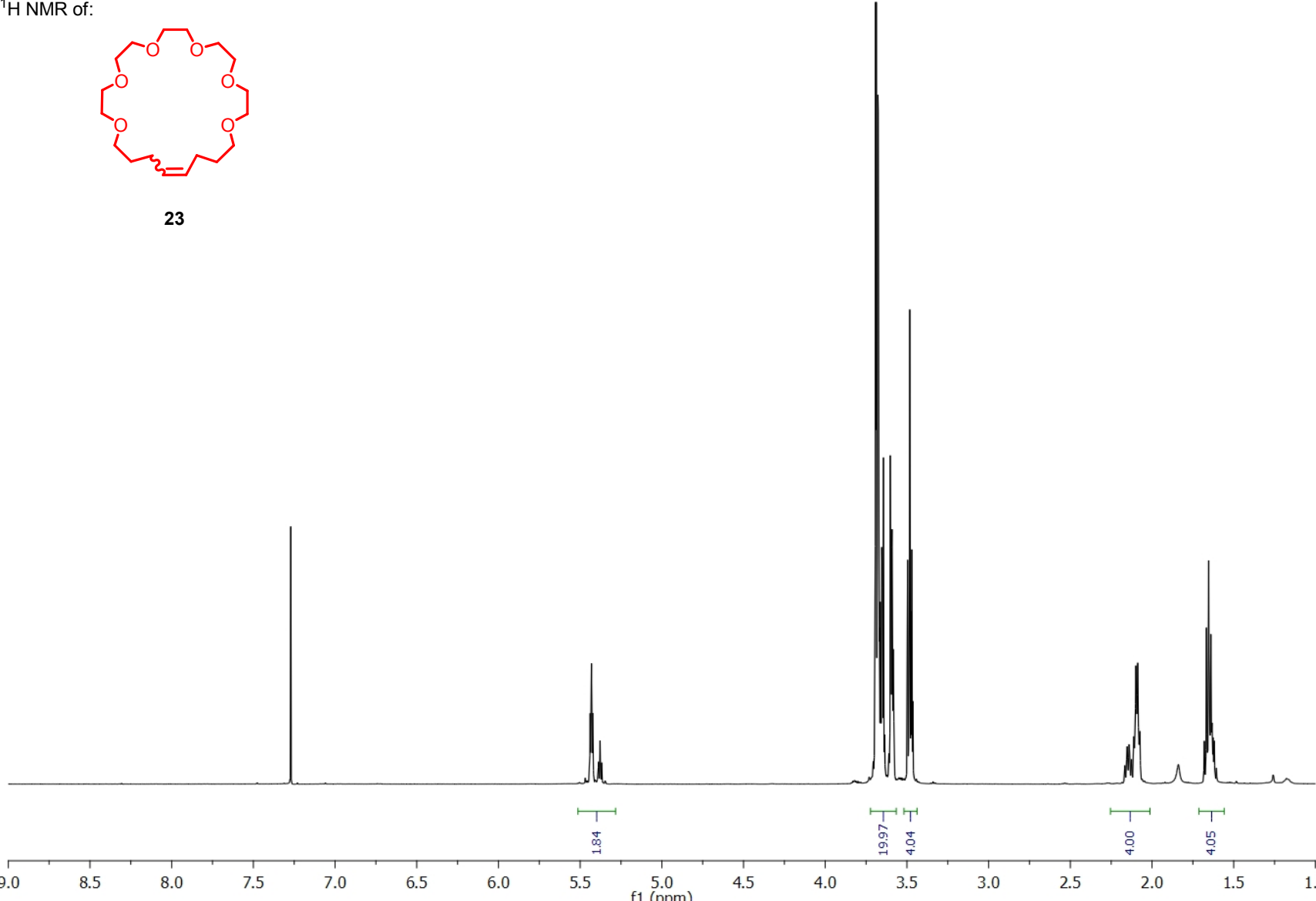




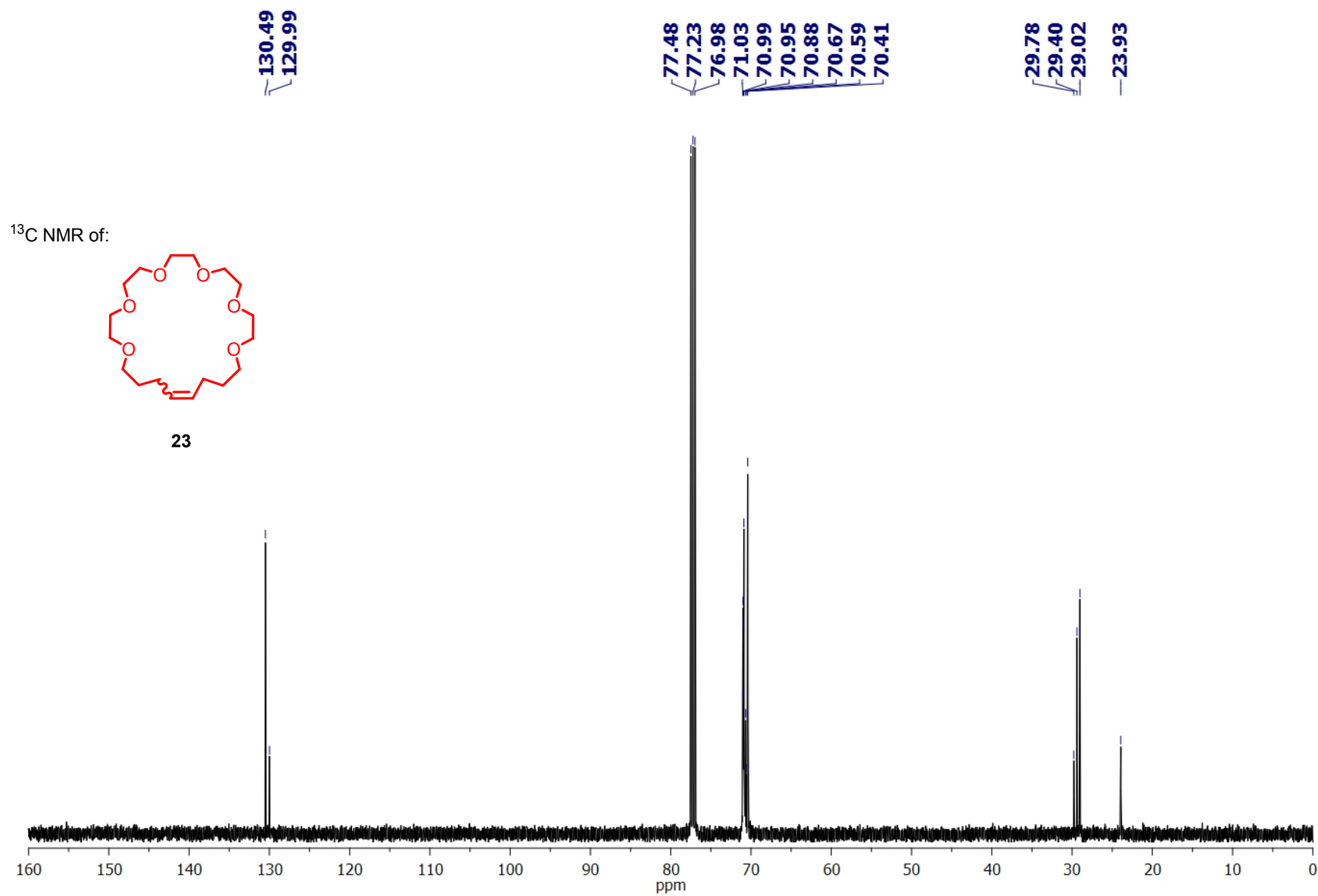


<sup>1</sup>H NMR of:

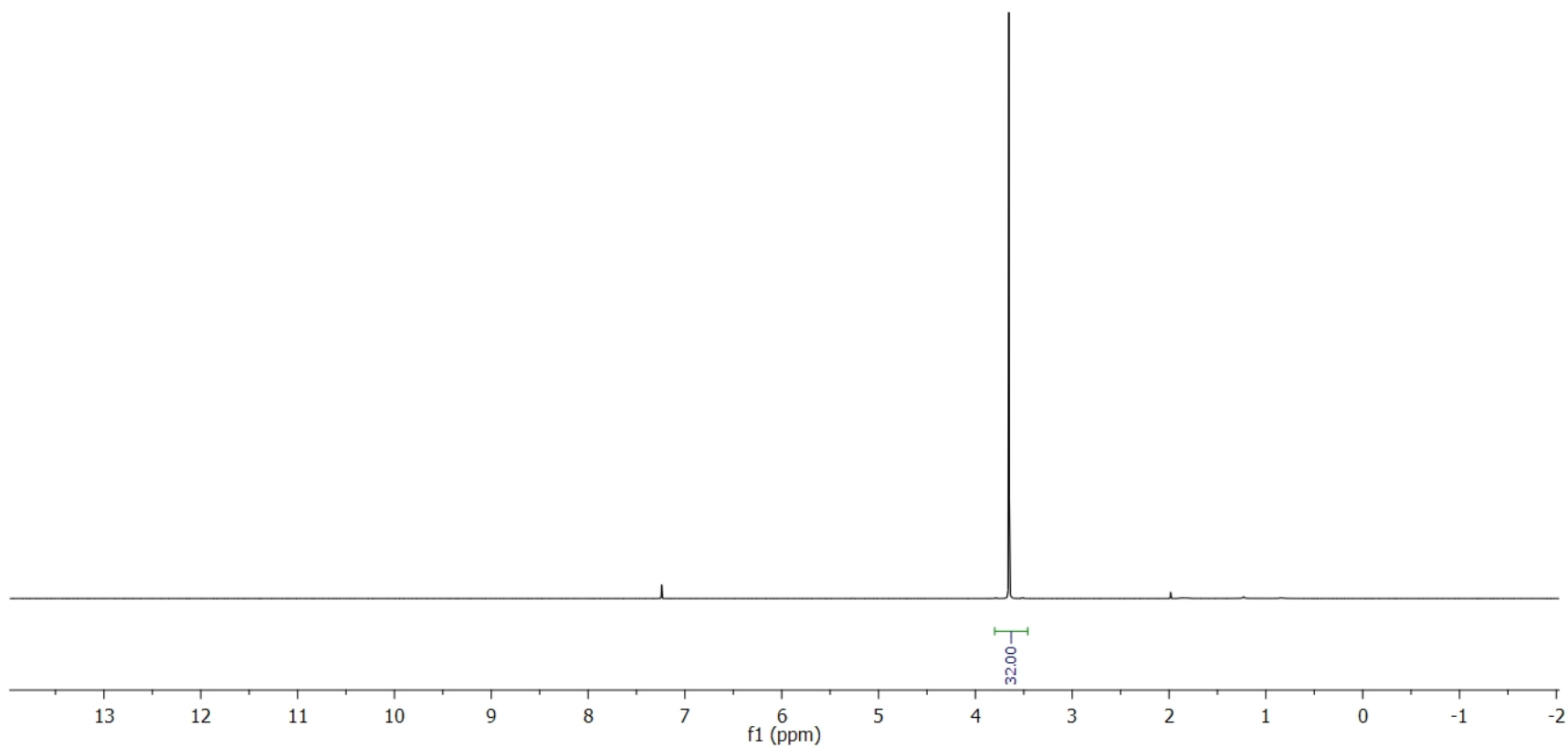
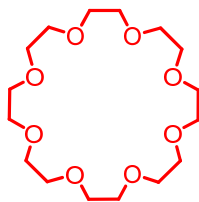
**23**



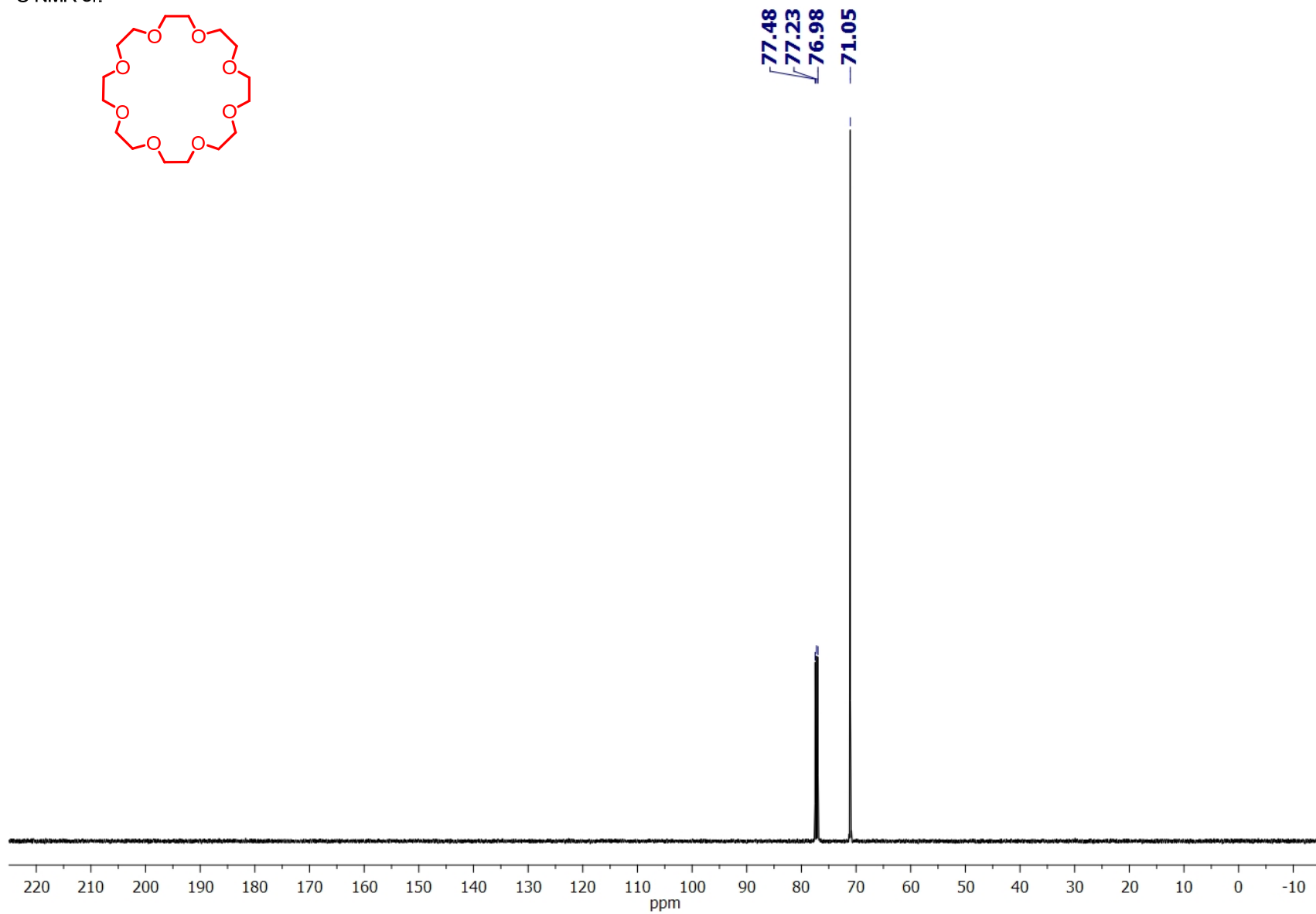
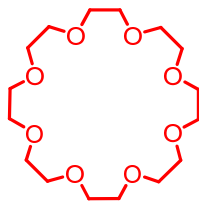
The <sup>1</sup>H NMR spectrum of compound 23 is displayed in the figure. The x-axis represents the chemical shift in ppm, ranging from 9.0 to 1.0. The spectrum shows several distinct signals: a sharp singlet at approximately 7.3 ppm, a multiplet between 5.4 and 5.6 ppm, a very large multiplet between 3.5 and 3.8 ppm, and two multiplets at approximately 2.1 ppm and 1.7 ppm. Integration values are provided for the signals between 1.5 and 5.5 ppm: 1.84 for the 5.4-5.6 ppm region, 19.97 for the 3.5-3.8 ppm region, 4.00 for the 2.1 ppm region, and 4.05 for the 1.7 ppm region.



$^1\text{H}$  NMR of:



$^{13}\text{C}$  NMR of:





## CHAPTER 4

### **Facile Synthesis of Polyrotaxanes via Acyclic Diene Metathesis Polymerization of Supramolecular Monomers**

This work was performed in collaboration with Nebojša Momčilović and Andrew J. Boydston. We are completing the necessary studies and will be submitting this for review by the end of July.

## Facile Synthesis of Polyrotaxanes via Acyclic Diene Metathesis

### Polymerization of Supramolecular Monomers

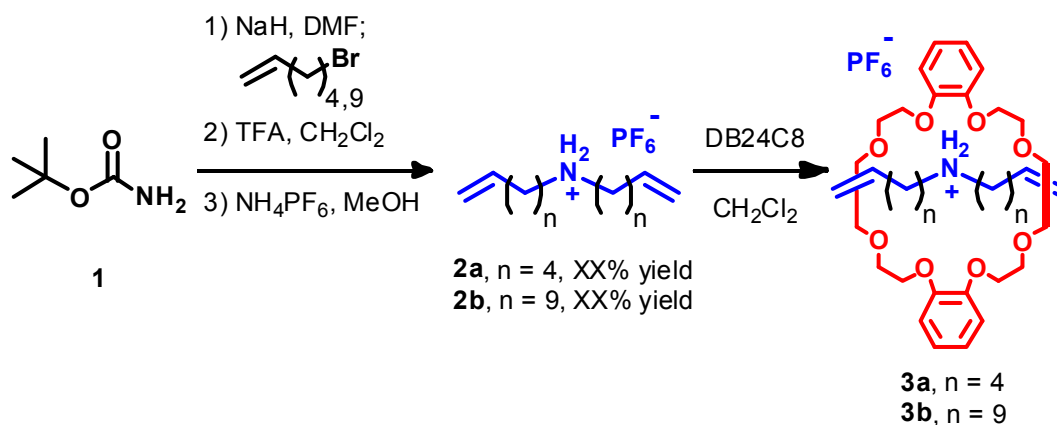
#### *Introduction/Motivation*

Advanced supramolecular and mechanically interlocked polymers such as polyrotaxanes, polycatenanes, and polypseudorotaxanes offer enticing synthetic targets and the promise of unique physical characteristics.<sup>1</sup> The ability to construct these complicated architectures in an efficient, scalable, and modular fashion is key to realizing their full potential. A particular challenge in the synthesis of polyrotaxanes, for example, is achieving a combination of both threading to form a polypseudorotaxane and end-capping to secure the interlocked nature of the ensemble – feats often executed in a step-wise fashion. Inspired by elegant examples that have successfully accomplished these objectives,<sup>2</sup> we sought a system of improved efficiency in which polyrotaxanes could be generated in one-pot from readily available, modular building blocks via a controlled polymerization. We envisioned that incorporating end-caps during polymerization, while also allowing threading to occur, would benefit from a dynamic, rapidly equilibrating polymerization strategy such as acyclic diene metathesis (ADMET) polymerization.<sup>3</sup> Herein we describe a method to accomplish a one-pot synthesis of polyrotaxanes via multi-component ADMET polymerization.

#### *Results and Discussion*

Starting from commercially available *tert*-butoxy carbamate **1**, acyclic dienyl ammonium salts **2a** and **2b** were prepared in three steps and good overall yields

**Scheme 4.1:** Synthesis of Dialkenyl Ammonium Salts **2a** and **2b** and Templatation with DB24C8 to Provide Supramolecular Monomers **3a** and **3b**



(Scheme 4.1). Specifically, alkylation of **1** using NaH and a bromoolefin in DMF furnished the corresponding dialkyl carbamate intermediates (not shown). Subsequent deprotection using TFA, followed by anion metathesis with NH<sub>4</sub>PF<sub>6</sub> provided the desired dialkenyl ammonium salts bearing 6- or 11-carbon chains (**2a** and **2b**, respectively).

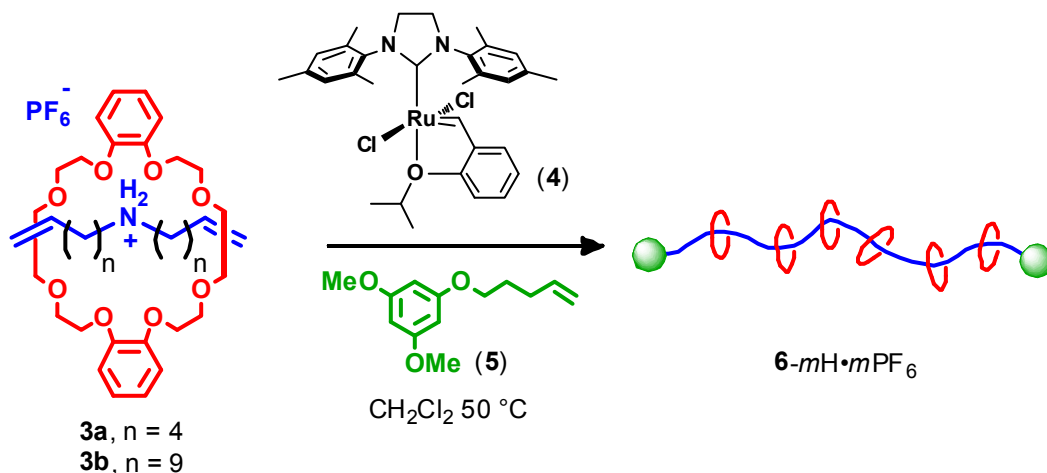
Efficient and quantitative threading of **2** using dibenzo-24-crown-8 ether (DB24C8) was confirmed via <sup>1</sup>H NMR spectroscopy of a 1:1 molar ratio of the two species in CD<sub>2</sub>Cl<sub>2</sub> (0.1 M in each).<sup>4</sup> Specifically, the CH<sub>2</sub> protons alpha to the ammonium moiety in **2** displayed resonances at δ = 3.0 ppm in the absence of DB24C8, and moved downfield to δ = 3.2 ppm in the presence of DB24C8. The resulting supramolecular complexes (**3a** and **3b**, Scheme 4.1) were concentrated under vacuum and subsequently used in ADMET polymerizations without any further purification.

To test the ability of the threaded supramolecular complexes to be polymerized via ADMET, we first subjected **3a** to polymerization conditions (Scheme 4.2) using Ru-alkylidene complex **4** as catalyst, and an end-capping chain transfer agent (CTA) (**5**) to ensure the structural fidelity of the interlocked macromolecules; key results are

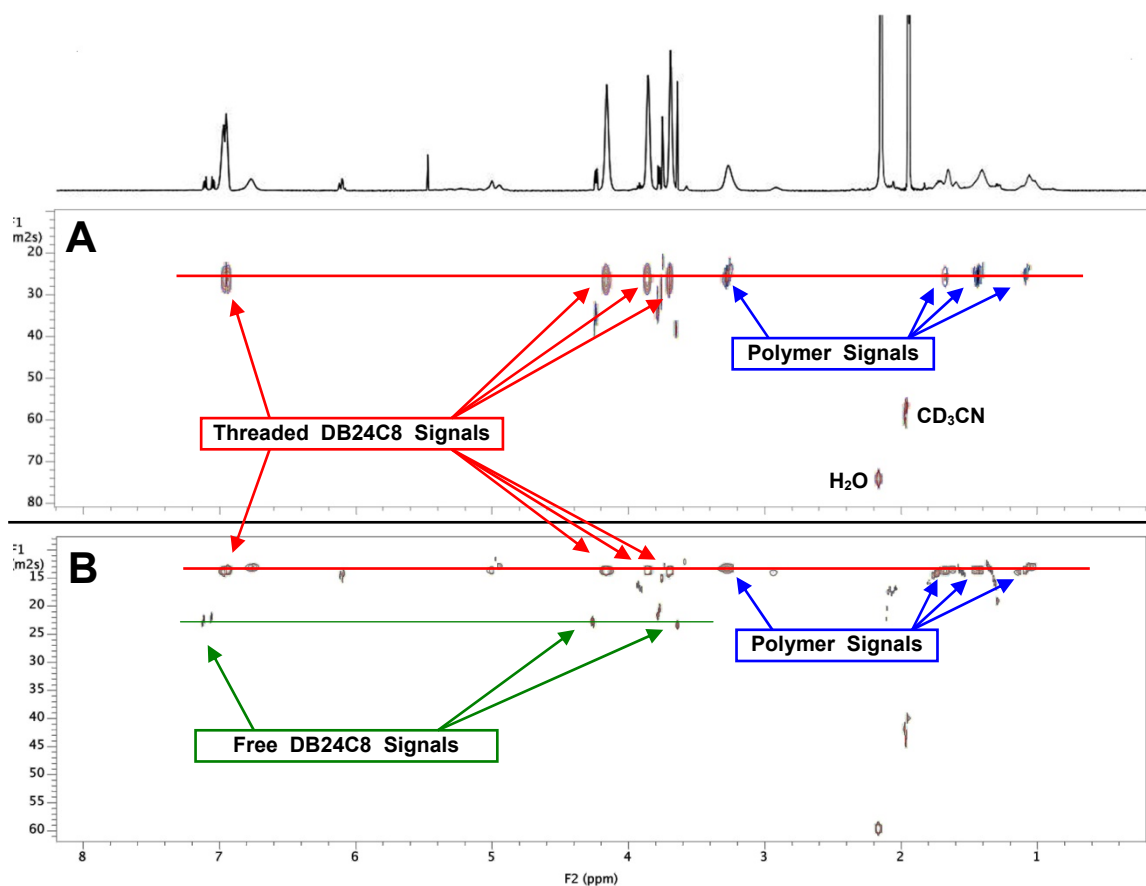
summarized in Table 1. Using  $[M/CTA]_0$  of 2.5:1, and  $[M/C]_0$  of 40:1 (entry 1), the reaction solution was prepared in dry  $CH_2Cl_2$  (3 mM in **3a**), sealed under Ar, and vigorously stirred in an oil bath at 50 °C for 2 h. The solution was then opened to vacuum to facilitate removal of ethylene, and then fresh  $CH_2Cl_2$  was added under Ar. The process of adding  $CH_2Cl_2$  and subsequently removing the solvent under vacuum was repeated after 6 h, and again after 9 h. After a total reaction time of ca 12 h, polyrotaxane **6-mH·mPF<sub>6</sub>** was concentrated under vacuum to give a thick tan foam. Analysis of the polyrotaxane via  $^1H$  NMR spectroscopy indicated ca 82% of the repeat units remained threaded, and GPC analysis revealed a  $M_w$  of 11.0 kDa (PDI = 1.42). The calculated  $M_n$  value of 7.8 kDa corresponds to a degree of polymerization (DP) of ca 10. The calculated DP was higher than the theoretical DP based on the  $[M/CTA]_0$ , implying full equilibration had not been reached.

To confirm the end-capped, mechanically locked nature of the polyrotaxanes we conducted DOSY experiments on both the protonated and deprotonated polymers (i.e.,

**Scheme 4.2:** ADMET Polymerization of Supramolecular Monomer **3a** to Form Polyrotaxane **6-mH·mPF<sub>6</sub>**



ammonium and amino backbones, respectively). As can be seen in Figure 4.1, the diffusion rates for both the polyammonium backbone of **6-*m*H·*m*PF<sub>6</sub>** and the DB24C8 moieties are consistent with one another. This supports the successful incorporation of the end-caps, but may also have been ascribed to strong ammonium-DB24C8 interactions. To investigate, **6-*m*H·*m*PF<sub>6</sub>** was treated with KOH (2 equiv relative to ammonium), producing the neutral amino repeat units. DOSY of this material also revealed consistent diffusion rates of the polymer backbone and the DB24C8 species, further indicating that end-caps were sufficiently incorporated and that dethreading was avoided.



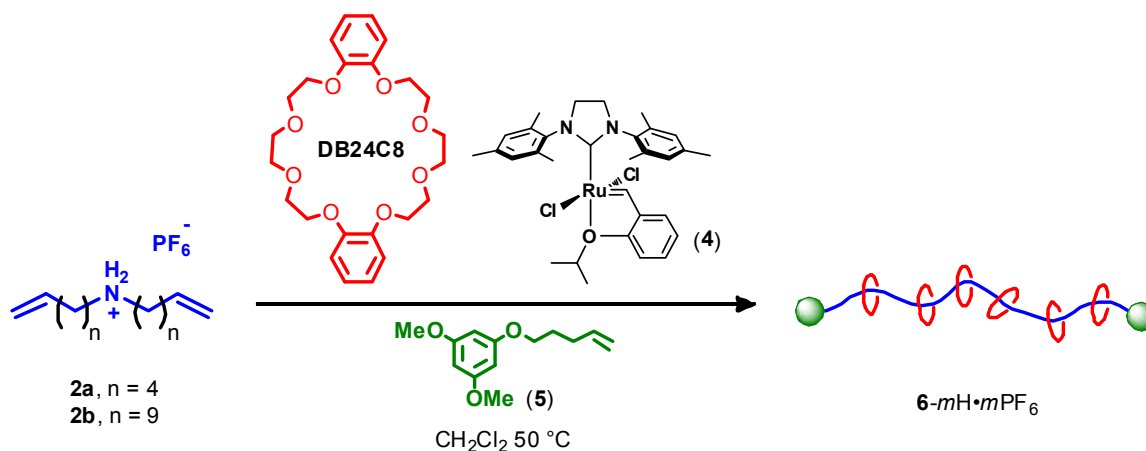
**Figure 4.1:** 2D-DOSY <sup>1</sup>H NMR spectrum in CD<sub>3</sub>CN at 600 MHz and 25 °C of polyrotaxane **6-*m*H·*m*PF<sub>6</sub>** (A) and polyrotaxane **6-*m*H·*m*PF<sub>6</sub>** with free DB24C8 (B).

Entry	Monomer	DB24C8 (eq)	Yield (%)	Threading (%)	Th. MW (kDa)	GPC $M_n$ (kDa)	GPC $M_w$ (kDa)	PDI
1	<b>3a</b>	1	94	82	4.6	7.8	11.0	1.42
2	<b>3b</b>	1	85	72	4.6	8.4	13.2	1.58
3	<b>2b</b>	1	80	82	4.6	16.4	19.3	1.18
4	<b>2b</b>	5	50	80	4.6	10.8	14.9	1.37

**Figure 4.2:** Data for ADMET polymerizations of various monomers to form polyrotaxane **6-mH**·*m*PF<sub>6</sub>.

To improve the efficiency of the ADMET polymerization, we next focused on monomer **3b** bearing longer undecenyl groups in comparison with **3a**. The reduced viscosity of the resulting reaction mixture appeared to indeed facilitate the polymerization, reaching full monomer conversion in ca 2 h (cf. 90% conversion at 6 h when **3a** was employed). After ca 12 h and three cycles of adding CH<sub>2</sub>Cl<sub>2</sub>/vacuum, the polyrotaxane was concentrated to yield a thick viscous oil (entry 2, Figure 4.2). Analysis as before revealed ca 72% threading, and  $M_w = 13.2$  kDa (PDI = 1.58). The DP (based on  $M_n$ ) was calculated to be ca 9. Notably, the amount of threading did not benefit from the addition of 5 equiv of DB24C8 relative to ammonium species (entry 4), suggesting that the maximum amount of threading for this particular system had been reached.

Encouraged by the ability to efficiently polymerization the congested supramolecular monomers via ADMET, and the rapid threading observed from ammonium salts **2** and DB24C8, we next attempted the polyrotaxane synthesis without pre-assembly of **3** (Scheme 4.3). Accordingly, **2b**, DB24C8, CTA **5**, and catalyst **4** were combined as a heterogenous mixture and degassed CH<sub>2</sub>Cl<sub>2</sub> was added. The

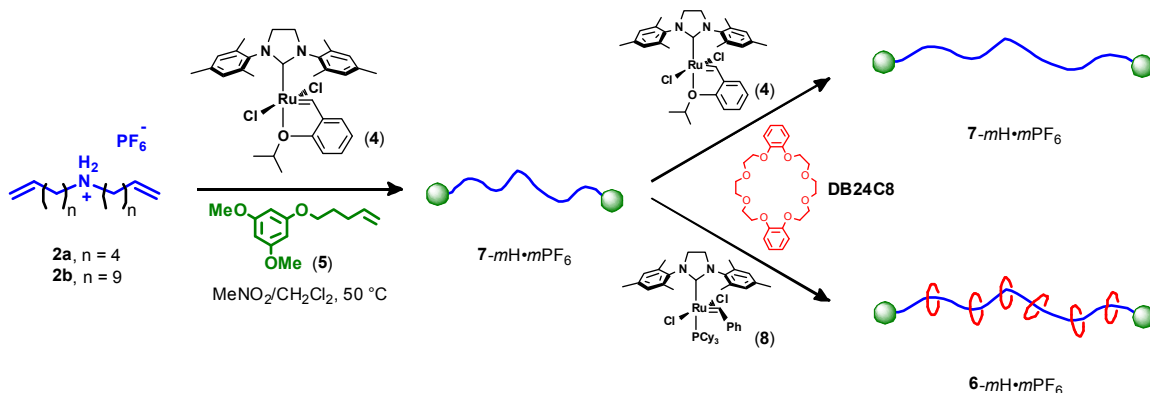
**Scheme 4.3:** One-Pot ADMET Polymerization to Form **6-*m*H·*m*PF<sub>6</sub>**

polymerization was conducted as described above. Analysis of the resulting polyrotaxane revealed similar threading and  $M_w$  values (75% threading,  $M_w = 13.2$  kDa, entry 3) as those obtained using the pre-assembled **3b** monomer (entry 3 and 4). In this way, polyrotaxanes could be obtained in a single operation from readily available building blocks.

### *Continuing Work*

The ability to thread, polymerize, and end-cap to form the polyrotaxanes may benefit from the rapid association between **2** and DB24C8, occurring prior to metathesis events. In addition, however, the ability to form a terminal olefin at the polymer chain end would also facilitate threading *during* polymerization. The olefin-terminated polymer can be generated, for example, via cross metathesis with a Ru-methylidene complex, or pseudo-degenerate metathesis between a Ru-terminated propagating polymer and monomer (i.e., chain transfer to monomer).<sup>5</sup> These events would allow the multi-

**Scheme 4.4:** Proposed Threading Equilibration Test of Capped Polyammonium Polymer  $7\text{-}m\text{H}\cdot m\text{PF}_6$  with Catalysts **4** and **8**



component polymerization to equilibrate toward formation of the polyrotaxane, imitating “magic-ring” rotaxation.

To investigate, we are preparing an end-capped polyammonium species  $7\text{-}m\text{H}\cdot m\text{PF}_6$  (Scheme 4.4) via ADMET of **2a** in the absence of DB24C8. Treatment of  $7\text{-}m\text{H}\cdot m\text{PF}_6$  with DB24C8 in  $\text{CD}_2\text{Cl}_2$  is not expected to result in threading, and will be determined by  $^1\text{H}$  NMR spectroscopy. This will confirm the end-capped nature of  $7\text{-}m\text{H}\cdot m\text{PF}_6$ . To facilitate chain transfer and polymer threading, the solution of  $7\text{-}m\text{H}\cdot m\text{PF}_6$  and DB24C8 (1:1 molar ratio) in  $\text{CD}_2\text{Cl}_2$  will be treated with second-generation metathesis catalyst **8** (ammonium/Ru = 40/1 molar ratio). After being allowed to react for several hours at room temperature, we would expect to observe nearly complete threading (80%), consistent with the amount of threading observed in the previous polymerizations (entries 1–4). We also plan to monitor the threading progress over time in an effort to obtain insight into the rate of chain transfer. For comparison, we will investigate catalyst **4** under similar conditions with  $7\text{-}m\text{H}\cdot m\text{PF}_6$ , but are not



anticipating any significant threading presumably due to the increased steric bulk of the benzylidene ether that can effectively serve as a polymer end-cap upon chain transfer.

### **Conclusions**

In conclusion, we have developed a simple strategy for a one-pot, multi-component synthesis of polyrotaxanes using acyclic diene metathesis polymerization. The efficiency and ease with which these mechanically interlocked macromolecules can be assembled should facilitate rapid modulation to achieve versatile polyrotaxane architectures.

### **References:**

- (1) (a) Huang, F.; Gibson, H. W. *Prog. Polym. Sci.* **2005**, *30*, 982. (b) Wenz, G.; Han, B.-H.; Müller, A. *Chem. Rev.* **2006**, *106*, 782. (c) Kang, S.; Berkshire, B. M.; Xue, Z.; Gupta, M.; Layode, C.; May, P. A.; Mayer, M. F. *J. Am. Chem. Soc.* **2008**, *130*, 15246. (d) Harada, A.; Hashidzume, A.; Yamaguchi, H.; Takashima, Y. *Chem. Rev.* **2009**, *109*, 5974. (e) Stoddart, J. F. *Chem. Soc. Rev.* **2009**, *38*, 1802.
- (2) (a) Yamabuki, K.; Isobe, Y.; Onimura, K.; Oishi, T. *Chem. Lett.* **2007**, *36*, 1196. (b) Wu, J.; He, H.; Gao, C. *Macromolecules* **2010**, *43*, 2252.
- (3) (a) Matloka, P. P.; Wagener, K. B. *J. Mol. Catal. A: Chem.* **2006**, *257*, 89. (b) Baughman, T. W.; Wagener, K. B. *Adv. Polym. Sci.* **2005**, *176*, 1.

- (c) Schwendeman, J. E.; Church, A. C.; Wagener, K. B. *Adv. Synth. Catal.* **2002**, *344*, 597.
- (4) Ashton, P. R.; Campbell, P. J.; Chrystal, E. J. T.; Glink, P. T.; Menzer, S.; Philp, D.; Spencer, N.; Stoddart, J. F.; Tasker, P. A.; Williams, D. J. *Angew. Chem. Int. Ed.* **1995**, *34*, 1865.
- (5) Stewart, I. C.; Keitz, B. K.; Kuhn, K. M.; Thomas, R. M.; Grubbs, R. H. *J. Am. Chem. Soc.* **2010**, in press (DOI: 10.1021/ja1029045)

## **APPENDIX 1**

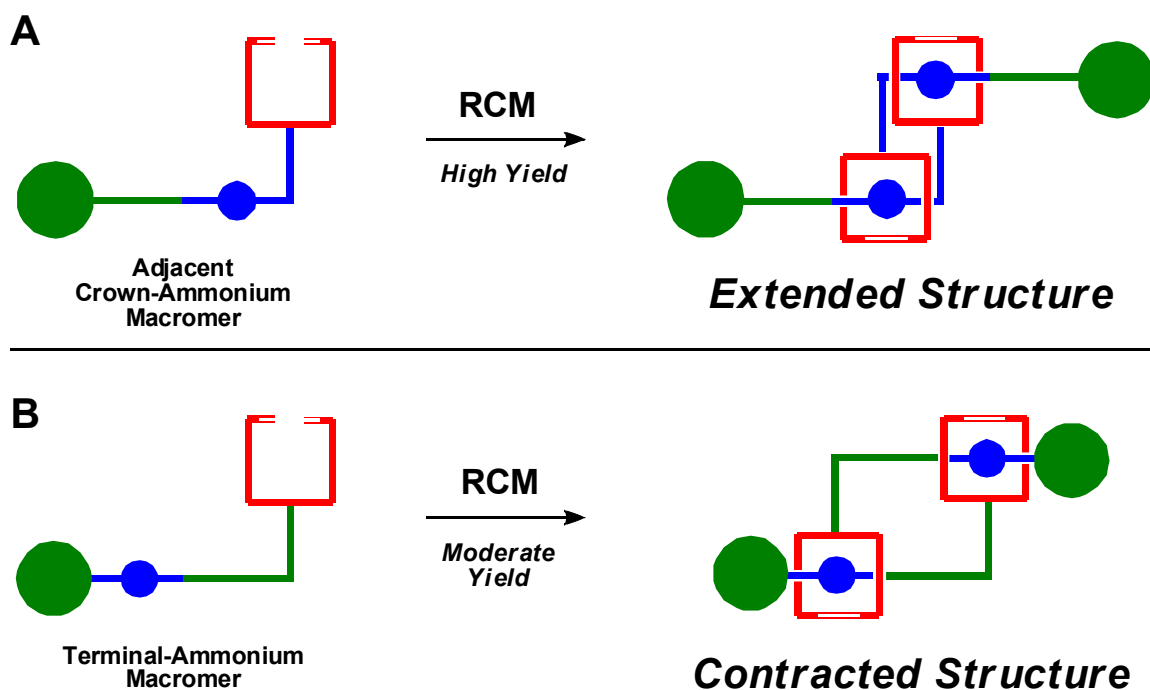
### **Flexible [c2]Daisy-Chain Dimers**

Parts of this work were performed in collaboration with Ryan Elmquist and Yuxioa Sun.

## Flexible [c2]Daisy-Chain Dimers

### Introduction/Motivation

In complement to the work presented in Chapter 2, we sought to explore flexible, switchable [c2]daisy-chain dimers (DCDs) where the macromer ammonium binding site was adjacent to the crown-type recognition structure and separated from the cap by an alkyl chain. A DCD of this topology would have an extended structure in the bound conformation (when the ammonium was coordinated to the crown). This DCD would not be a viable molecular muscle mimic, since coordination would induce *extension* of the structure rather than contraction (Figure A1.1). However, this structural motif was expected to more successfully generate DCD material in high yield via RCM because of the close proximity of the binding sites and recognition moieties. Because of the dilution



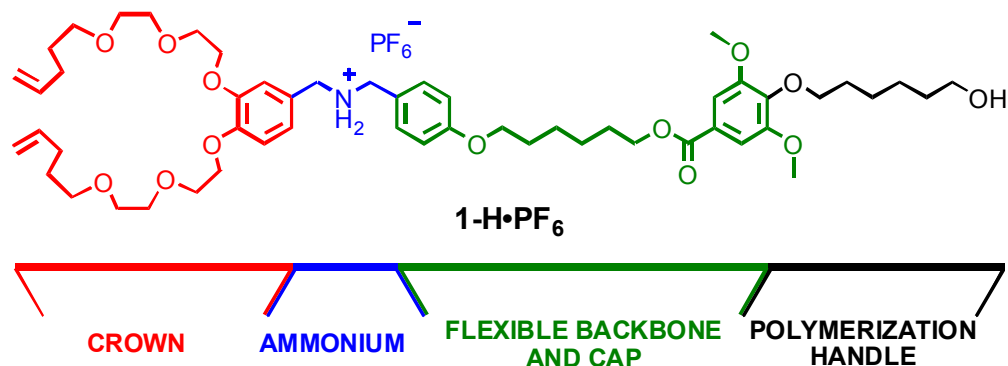
**Figure A1.1:** Graphical comparison of the [c2]daisy-chain dimers formed from a macromer structure containing adjacent recognition structure and binding site (**A**) or the terminal-ammonium macromer (**B**) presented in Chapter 2.

of the dimerization reaction (0.01 M), once one crown-type macrocycle encircled a partner macromer's ammonium residue, the probability of the second interlocking RCM reaction would be significantly greater than encountering a third macromer to form a trimeric structure. By contrast, the macromer structure introduced in Chapter 2 has a longer distance between the crown-type structure and the ammonium binding residue. This increased separation decreases the chance of engaging in the second interlocking reaction and decreases the yield of DCD relative to more traditional macromer architectures.<sup>1</sup>

Though DCDs formed from a macromer with an adjacent recognition moiety and binding site will not contract upon coordination, they still have the potential to undergo dimension changes upon switching. To enable comparison with DCD structures presented in Chapter 2, we designed several different macromers that were promising candidates to allow access to DCDs with flexible alkyl chains between the ammonium binding site and the cap.

### ***Synthesis of the First-Generation Flexible [c2]Daisy-chain Dimer***

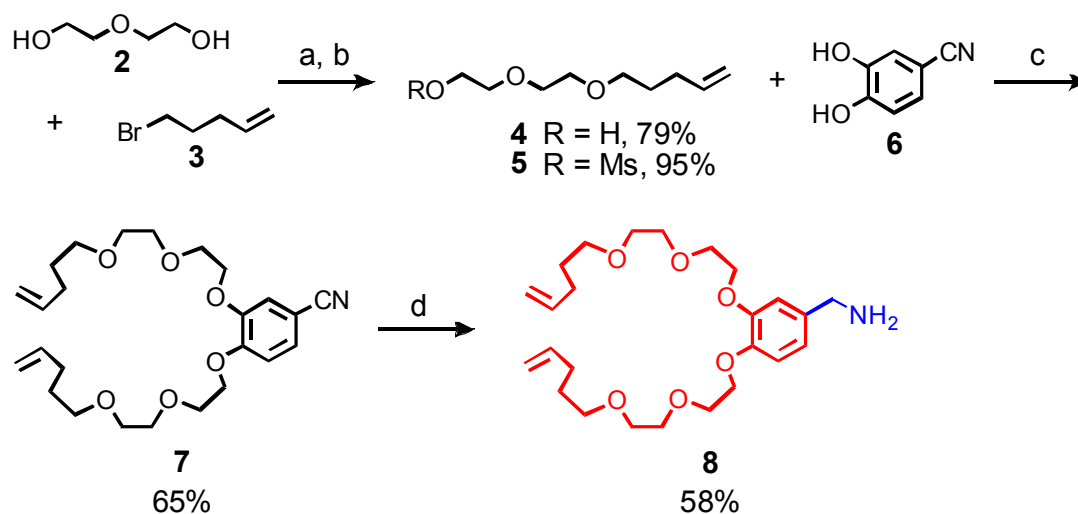
Previous dimer species synthesized by ring-closing metathesis had a very limited distance along the backbone from the coordination site to the cap, prohibiting any significant extension or contraction motion.<sup>1,2</sup> The target macromer structure **1**-H·PF<sub>6</sub> (Figure A1.2) was a promising precursor for the “first-generation” flexible DCD. Key to the assembly of the structure was an esterification to append the cap compound to the crown-ammonium section, with a linear alkyl chain linking the two fragments.



**Figure A1.2:** First generation [c2]daisy-chain dimer macromer **1-H·PF<sub>6</sub>** with a flexible alkyl linker between ammonium binding site and bulky cap.

Synthesis of the crown analogue **8** (Scheme A1.1) has been reported previously,<sup>1,3</sup> and can be accomplished in a straightforward manner. Diethylene glycol (**2**) was subjected to basic conditions in the presence of 5-bromopentene (**3**), giving the monoalkylated species **4**. Due to the conditions of this alkylation reaction, a statistical distribution of products was observed, contributing to a lower yield. It was found that

**Scheme A1.1:** Synthesis of Crown Fragment **8**

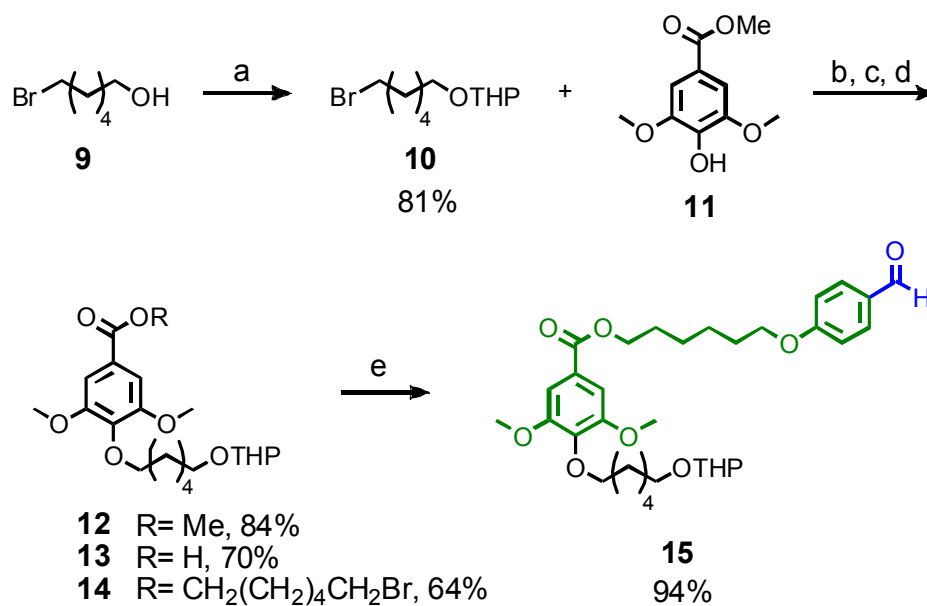


doubling the equivalents of **2** from the literature procedure significantly improved the ratio of monoalkylated to dialkylated **4**. Mesylation of **4** proceeded in excellent yield. Compound **5** was coupled to commercially available 3,4-dihydroxybenzonitrile (**6**) using potassium carbonate, giving the dialkylated benzonitrile crown analogue **7**. Reduction of nitrile **7** to amine **8** was achieved by treatment with lithium aluminum hydride (LAH) in refluxing THF. Having **8** in hand, attention was directed at the synthesis of the backbone and cap.

To obtain a more flexible DCD, the distance between crown and cap must be lengthened. This can be accomplished by incorporation of a flexible alkyl linker in the backbone. It has been shown that 3,5-dimethoxy substituted aromatic rings have sufficient bulk to prevent unthreading of [24]crown type macromers,<sup>1-5</sup> and several derivatives of such compounds are commercially available. Also, since the ultimate goal is formation of materials using the DCD, a synthetic handle must be present for future oligomerization or polymerization reactions. By functionalizing the cap, no interference with dimer sliding motion is expected. The envisioned backbone compound **15** (Scheme A1.2) meets all three of these requirements, possessing an alkyl unit for flexibility, dimethoxy substituents for capping purposes, and a terminal alcohol handle for future dimer polymerization. Synthesis of **15** began by mixing commercially available 6-bromo-1-hexanol (**9**) with dihydropyran and *p*-toluenesulfonic acid to give the tetrahydropyran (THP) protected alcohol **10**. Methyl 3,5-dimethoxy-4-hydroxybenzoate (**11**), also commercially available, was then subjected to alkylation conditions in the presence of **10** to afford methyl ester **12** in good yield. Lithium hydroxide saponification

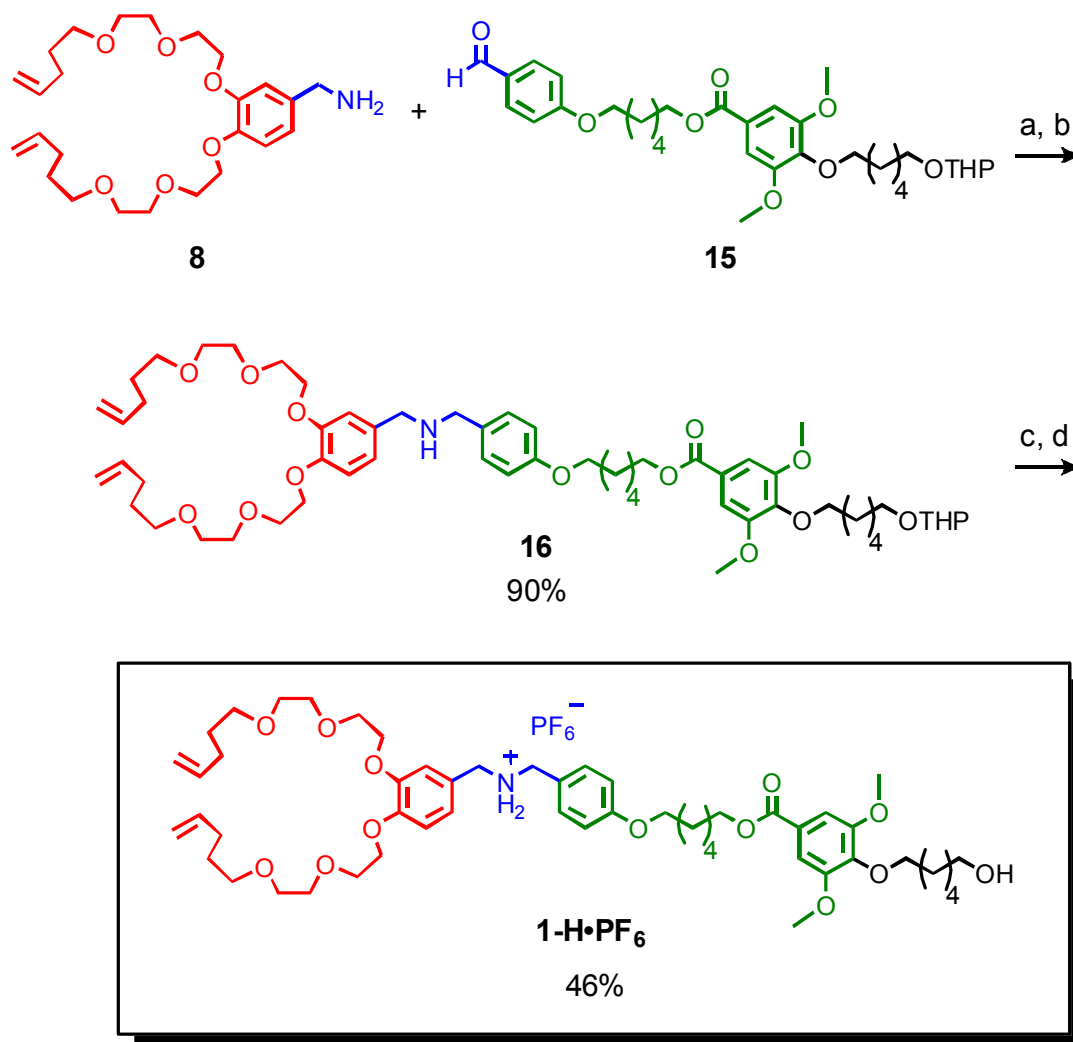
of the methyl ester produced the free acid **13**. A variety of standard ester coupling conditions, as well as several alcohol substrates, were used in an effort to obtain the ester linkage in **14**, but met with little success. After some further work, it was found that an alternate protocol using a mixture of DPTS, DMAP, **10**, **13**, and the well-known coupling agent EDC in DCM achieved formation of ester **14**, albeit in moderate yield. In the presence of potassium carbonate and commercially available 4-hydroxybenzaldehyde, **14** can be readily converted to the cap/backbone component **15** in excellent yield.

**Scheme A1.2:** Synthesis of Flexible Cap Fragment **15**



Reagents and conditions: a) DHP, *p*-TsOH, DCM, 0 °C to r.t., 16h; b) K<sub>2</sub>CO<sub>3</sub>, DMF, 80 °C, 2d; c) LiOH, 5:1 v/v THF:H<sub>2</sub>O, r.t., 3d; d) EDC, DPTS, DCM, r.t., 36h; e) 4-hydroxybenzaldehyde, K<sub>2</sub>CO<sub>3</sub>, DMF, 80 °C, 2d.



**Scheme A1.3:** Synthesis of Macromer **1-H**·PF<sub>6</sub>

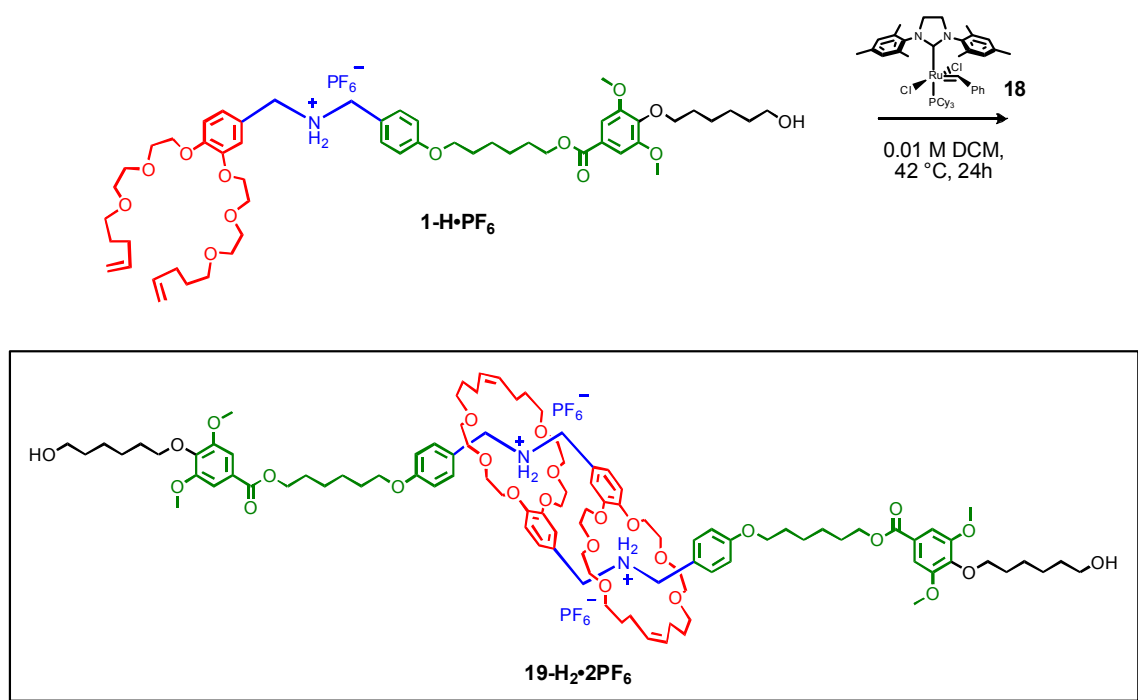
Reagents and conditions: a) D.S. Trap, C<sub>6</sub>H<sub>6</sub>, reflux, 3d; b) NaBH<sub>4</sub>, MeOH, r.t., 5h; c) 1.0M TFA, MeOH, THF, r.t., 1h; d) NH<sub>4</sub>PF<sub>6</sub>, MeOH, r.t., 4d.

With key fragments **8** and **15** in hand, attention was directed towards coupling and salt formation (Scheme A1.3). Since **8** is an unstable benzylic amine, prone to oxidation under atmospheric conditions, it was freshly prepared from nitrile **7** immediately before use. Amine **8** and aldehyde **15** were condensed under standard Dean-Stark conditions, followed by reduction with sodium borohydride to afford the coupled amine product **16**. Ideally, we wanted to affect both amine protonation and THP-deprotection of **16**

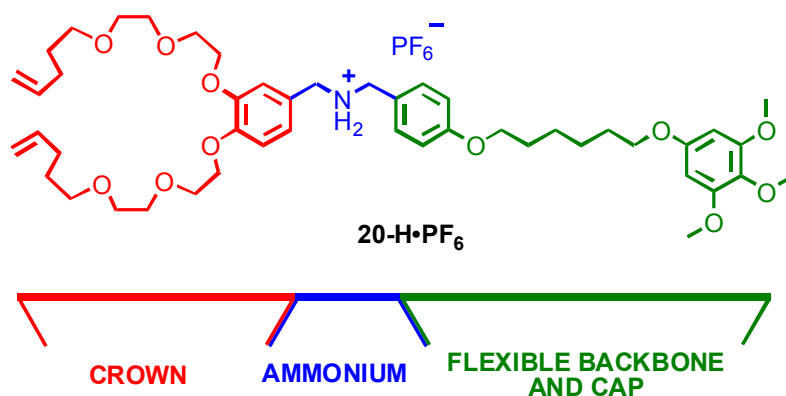
simultaneously. Because of the highly electron-rich nature of the cap, typical acidic conditions used to perform these transformations resulted in cleavage of the ester linkage attaching the cap to the flexible backbone. Consequently, we explored a number of amine protonation conditions and found that treatment of **16** with trifluoroacetic acid (TFA) successfully protonated the amine and revealed the primary alcohol. To enhance the organic solubility of the final macromer and increase the association constant ( $K_a$ ) of the ammonium moiety, the TFA adduct was mixed with ammonium hexafluorophosphate, completing the synthesis of **1-H·PF<sub>6</sub>**.<sup>6-9</sup>

Dimerization of **1-H·PF<sub>6</sub>** was achieved via addition of second-generation catalyst **18** (Scheme A1.4). To favor dimer formation instead of oligomerization, the RCM reaction was run at a dilute macromer concentration (0.01 M) to favor formation of ring-

**Scheme A1.4:** Dimerization of **1-H·PF<sub>6</sub>**



closed product instead of oligomeric species. Evidence of the success of the dimerization reaction was observed by NMR analysis. The  $^1\text{H}$  NMR spectrum, though very complicated due to the formation of two diastereomeric forms of the dimer, showed high conversion to the internal olefin product. There was also distinct broadening of the signals corresponding to the benzylic protons, as well as the signals corresponding to the aromatic protons (adjacent to the ammonium center). Proton resonances for the olefin region broadened as well, which can be attributed to the presence of both *cis* and *trans* isomers within the product mixture. Attempts to purify **19**-H<sub>2</sub>·2PF<sub>6</sub> via silica chromatography resulted in significant loss of material (presumably due to the acid sensitivity of the ester linkage), but some pure material was obtained and submitted for mass spectrum analysis. The species observed via MALDI-TOF MS had a measured mass one-half the calculated full mass of the dimer ( $[\text{M} - 2\text{PF}_6]^{+2} = 910.0195 \text{ m/z}$ ) with mass increments of 0.5 amu, indicative of a dicationic species of double the observed mass. Unfortunately, a yield was unable to be obtained, nor was any further work able to be done with **19**-H<sub>2</sub>·2PF<sub>6</sub> due to decomposition challenges. The ester linkage, which proved challenging to install, was unstable to further manipulations, and was expected to be intolerant of conditions necessary to induce switching of the dimer.

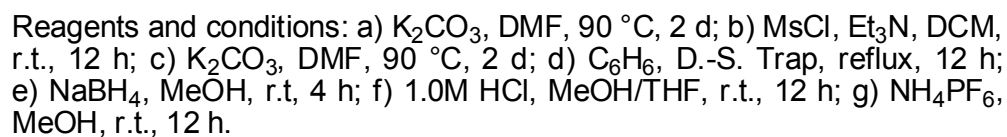


**Figure A1.3:** Second-generation macromer structure **20-H·PF<sub>6</sub>** containing an ether linkage between the cap and backbone.

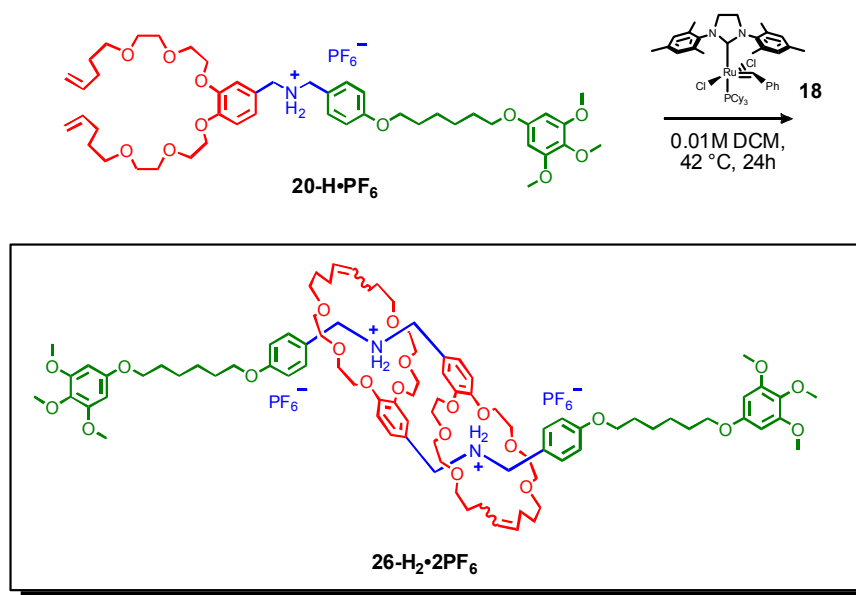
### Macromer Modifications

To increase the stability of the final dimer structure, the design of **1-H·PF<sub>6</sub>** was modified, installing an ether linkage in lieu of the ester linkage. Given the convergent synthesis of the macromer, achieving such a structural modification only requires alteration of the cap component. Because of the challenges encountered during formation of the ester linkage, we first wanted to observe whether the ether linkage would suitably inert. Consequently, we targeted “second-generation” macromer structure **20-H·PF<sub>6</sub>**. In this model system, we used commercially available 3,4,5-trimethoxyphenol (**24**) as our capping fragment. Though the DCD obtained upon dimerization of **20-H·PF<sub>6</sub>** would not contain a polymerization handle, it would allow us to explore the stability of the proposed ether linkage (and, concomitantly, the stability of the interlocked DCD structure).

To access the new macromer target, we revised the synthesis of the backbone-cap fragment (Scheme A1.5). Alkylation of *para*-hydroxybenzaldehyde (**21**) with **9** gave compound **22**, whose terminal alcohol was subsequently mesylated to yield derivative **23**. Displacement of the mesylate with model cap **24** produced the desired aldehyde **25**. Condensation of **25** with crown-type compound **8**, followed by reduction, salt formation,

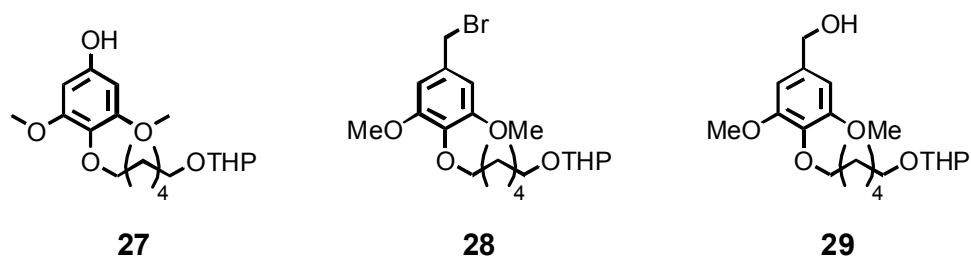


and anion metathesis completed the synthesis of macromer **20**-H·PF<sub>6</sub>. During salt formation, it was encouraging to observe that the phenolic cap linkage appeared to be highly stable to acidic conditions that were unsuitable for the ester bond in **1**-H·PF<sub>6</sub>.

**Scheme A1.6:** Dimerization of Second-Generation Macromer **20-H**·PF<sub>6</sub>

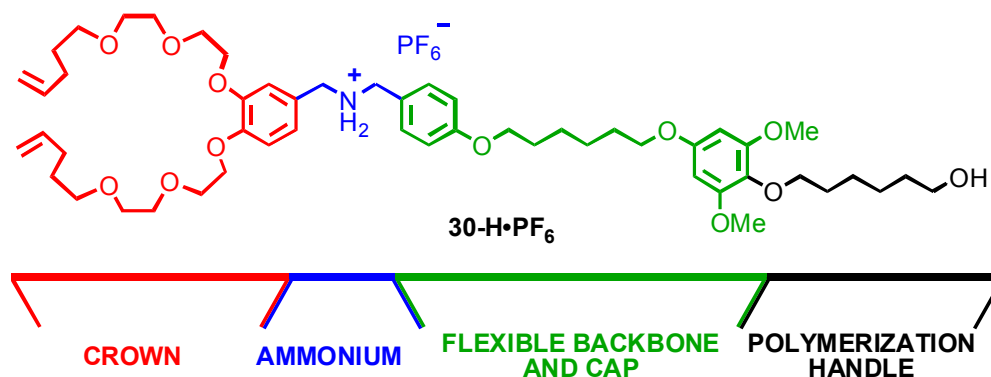
Treatment of second-generation macromer **20-H**·PF<sub>6</sub> with catalyst **18** readily produced DCD **26-H<sub>2</sub>·2PF<sub>6</sub>** (Scheme A1.6) and completed our efforts with the model system. Because of the lack of a handle with which to incorporate the dimeric structure covalently within a material, we did not pursue further work with **26-H<sub>2</sub>·2PF<sub>6</sub>**.

To obtain an analogue of **26-H<sub>2</sub>·2PF<sub>6</sub>** suitable for materials studies, we have pursued several cap compounds (Figure A1.4) that present a terminal functionality. Currently, phenol cap **27** has proven to be the most promising candidate. The high degree

**Figure A1.4:** Various cap structures suitable for producing a DCD that presents functional handles for incorporation in materials.

of oxygen substitution around the aromatic ring makes the benzylic derivatives highly reactive and unstable, and prevents purification and coupling of **28** or **29** with either alcohol **22** or mesylate **23**, respectively. In an effort to determine if coupling was feasible with these compounds, some crude material was reacted with an appropriate coupling partner. Though  $^1\text{H}$  NMR evidence indicated some coupling may be occurring (particularly for **29**), facile cleavage at the benzylic position appears to be occurring before the backbone-cap fragments can be isolated (no effort to fully characterize the decomposition materials was made). Because of the difficulties associated with **28** and **29** and because of the successful synthesis of DCD using 3,4,5-trimethoxyphenol **24** (a synthetic analogue of **27**), we believed a phenol linkage might prove more stable than a benzylic linkage and focused much of our attention on phenol **27**.

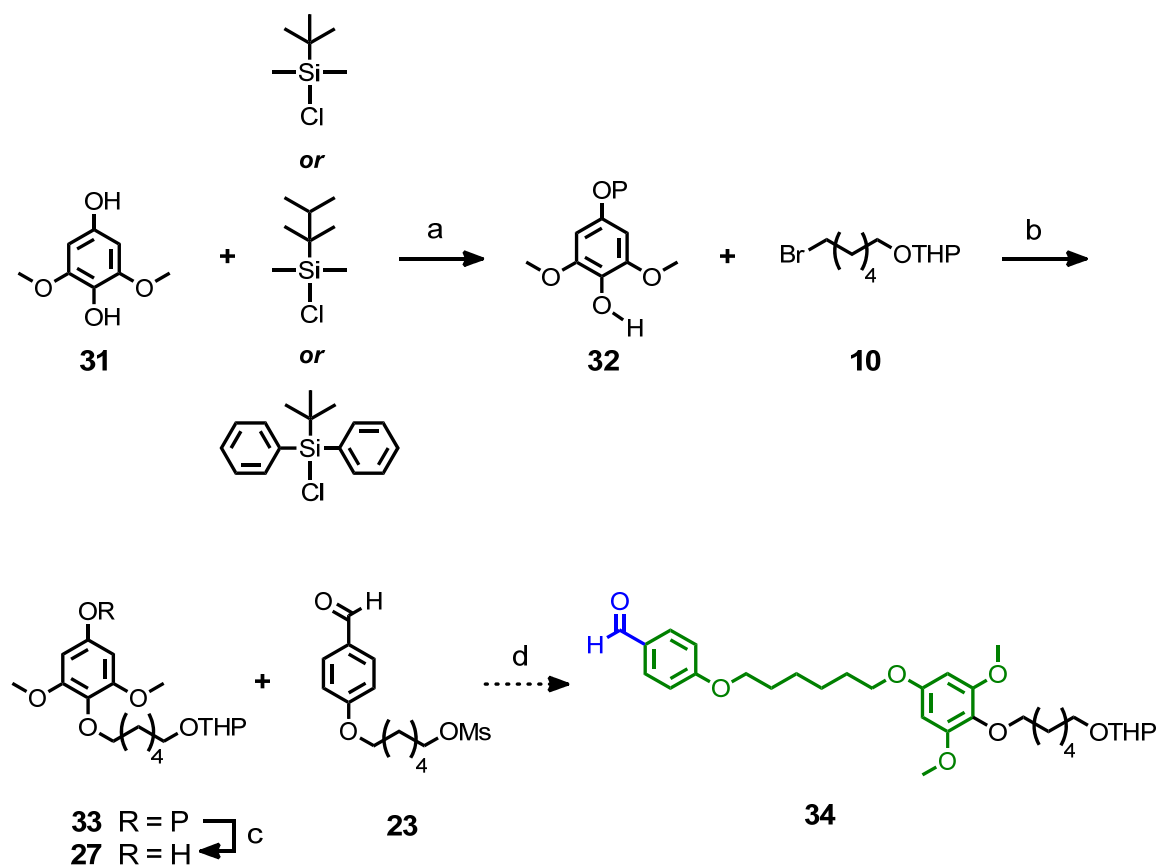
For this “third-generation” flexible DCD structure, we targeted macromer **30-H**· $\text{PF}_6$  (Figure A1.5). Cap compound **27** was accessed (Scheme A1.7) via selective protection of the less hindered phenol of 1,4-dihydroxy-2,6-dimethoxybenzene (**31**) using



**Figure A1.5:** Third-generation macromer **30-H**· $\text{PF}_6$

a bulky silyl protecting group. To perform the selective protection, we explored *tert*-butyldimethylsilyl (TBS), dimethylhexylsilyl (DMTS), and *tert*-butyldiphenylsilyl (TBDPS) groups, as the increased bulk of the latter two (especially TBDPS) was expected to limit reaction at the methoxy-shielded phenol. Interestingly, treatment of **31** with TBSCl afforded a mixture of regioisomeric products, but isolation proved challenging on larger (>0.1 g) scale. Work has continued with the other two protecting groups, but accessing reasonable yields of the desired product has proven elusive. One reason for the challenges we encountered was the ready oxidation of **31** to the

**Scheme A1.7:** Synthesis of Third Generation Flexible Backbone-Cap **34**



Reagents and conditions: a) Base ( $\text{Et}_3\text{N}$  or  $\text{K}_2\text{CO}_3$ ), DMAP, DCM, r.t., 24 h; b)  $\text{K}_2\text{CO}_3$ , DMF, 90 °C, 2 d; c) TBAF, THF, r.t.; d)  $\text{K}_2\text{CO}_3$ , DMF, 90 °C, 2 d;



benzoquinone derivative. Indeed, even the material obtained from a commercial vendor contained at least 30–40 percent of the unreactive benzoquinone contaminant. We did briefly pursue purification of the starting material, both via recrystallization and chromatographic methods, but met with little success. We also explored *in situ* reduction of the starting material to the desired diphenol, but the reductions did not proceed cleanly. Given the challenges encountered during isolation of **31**, we abandoned the reduction route. While a high-yielding selective protection was not able to be realized with TBS chloride or DMTS chloride, we could observe some monoprotected material by  $^1\text{H}$  NMR spectroscopy when using TBDPS as the protecting group. Believing that the desired derivative **33** would be more stable to isolation conditions than free phenol **32**, we subjected crude **32** to alkylation conditions in the presence of **10**. Unfortunately, we were unable to isolate any of protected, alkylated product **33**. The final steps to synthesize the backbone-cap fragment **34** would involve deprotection of the phenol of **33**, giving cap compound **27**, followed by alkylation with mesylate **23**. Subsequent coupling of **34** and **8** using standard conditions would produce the targeted macromer **30**-H·PF<sub>6</sub>. In future work, isolation of **32** prior to the alkylation reaction may successfully allow access to **33**, and, as a result, enable synthesis of **34**. Alternatively, other cap derivatives could be explored that do not possess such a highly electron-rich aromatic ring.

## Conclusions

Several different [c2]daisy-chain dimer syntheses via ring-closing metathesis were discussed, with particular focus on the incorporation of a flexible alkyl linkage

between the ammonium binding site and the bulky cap component. We varied the macromer structure in an effort to produce a stable bond between the cap and alkyl chain. In the first-generation, we installed an ester functionality. However, acidic conditions necessary during subsequent transformations of the macromer revealed that the ester would be unstable to dimer switching conditions. Consequently, we turned our attention to installing a phenolic ether linkage, which had proven highly stable in a model DCD system. Unfortunately, challenges were encountered during selective protection of the necessary starting material, and we are continuing our efforts to produce a suitably-functionalized cap.

### ***References***

- (1) Guidry, E. N.; Li, J.; Stoddart, J. F.; Grubbs, R. H. *J. Am. Chem. Soc.* **2007**, *129*, 8944-8945.
- (2) Cantrill, S. J.; Youn, G. J.; Stoddart, J. F. *J. Org. Chem.* **2001**, *66*, 6857-6872.
- (3) Badjić, J. D.; Cantrill, S. J.; Grubbs, R. H.; Guidry, E. N.; Orenes, R.; Stoddart, J. F. *Angew. Chem. Int. Ed.* **2004**, *43*, 3273-3278.
- (4) Schalley, C. A.; Weilandt, T.; Bruggemann, J.; Vogtle, F. *Top. Curr. Chem.* **2004**, *248*, 141-200.
- (5) Kilbinger, A. F. M.; Cantrill, S. J.; Waltman, A. W.; Day, M. W.; Grubbs, R. H. *Angew. Chem. Int. Ed.* **2003**, *42*, 3281-3285.
- (6) Ashton, P. R.; Cantrill, S. J.; Preece, J. A.; Stoddart, J. F.; Wang, Z.-H.; White, A. J. P.; Williams, D. J. *Org. Lett.* **1999**, *1*, 1917.

- (7) Montalti, M. *Chem. Commun.* **1998**, 1461.
- (8) Doxsee, K. M. *J. Org. Chem.* **1989**, 54, 4712.
- (9) Jones, J. W.; Gibson, H. W. *J. Am. Chem. Soc.* **2003**, 125, 7001.

## *Experimental Information*

### **Supporting Information**

Experimental procedures and characterization data ( $^1\text{H}$  and  $^{13}\text{C}$  and 2D NMR, IR, HRMS, GPC) for all compounds and their precursors.

**General Information.** Unless otherwise noted, all NMR spectra were obtained on Varian Mercury 300 MHz spectrometers using  $\text{CDCl}_3$  as solvent. Chemical shifts for both  $^1\text{H}$  and  $^{13}\text{C}$  spectra are reported in parts per million (ppm) relative to  $\text{Si}(\text{CH}_3)_4$  ( $\delta=0$ ) and referenced internally to the solvent resonance. Multiplicities are abbreviated as follows: singlet (s), doublet (d), triplet (t), quartet (q), quintet (qt), septuplet (sp), multiplet (m), and broad (br). Molecular mass calculations were performed with ChemDraw Ultra 10 (Cambridge Scientific). Mass spectrometry measurements (FAB, EI, and MALDI) were performed by the California Institute of Technology Mass Spectrometry Facility. Analytical thin-layer chromatography (TLC) was performed using silica gel 60 F254 precoated plates (0.25 mm thickness) with a fluorescent indicator. Visualization was performed using UV, CAM, and iodine stain. Flash column chromatography was performed using silica gel 60 (230-400 mesh) from EM Science. Grubbs second-generation catalyst  $(\text{H}_2\text{IMes})(\text{PCy}_3)(\text{Cl})_2\text{Ru}=\text{CHPh}$  (**1**) was obtained from Materia. X-ray crystal structure data was provided by the Caltech X-ray Crystallography Facility.

**Materials and Methods.** Anhydrous N,N-dimethylformamide (DMF) was obtained from Acros (99.8% pure, Acroseal), and dry acetonitrile was obtained from Aldrich (99.8%, anhydrous, sureseal). Dry tetrahydrofuran (THF), toluene, and dichloromethane (DCM) were purified by passage through solvent purification columns.<sup>1</sup> All water was deionized. 4-dimethylaminopyridinium *p*-toluenesulfonate (DPTS) was received as a gift from the Stoddart group. 1-ethyl-3-(3-dimethylaminopropyl)carbodiimide (EDC) was purchased from Aldrich and used as received. 4-dimethylaminopyridine (DMAP) was purchased from Aldrich (99%) and used as received. Methyl 3,5-dimethoxy-4-hydroxybenzoate (98%) was received from Acros and used as received. All other compounds were purchased from Aldrich, unless otherwise specified.

**General Freeze-Pump-Thaw Procedure.** A flask charged with reagents and solvent was frozen with liquid nitrogen. After the solution had frozen, the headspace of the flask was evacuated to low pressure. The flask was sealed and allowed to thaw to room temperature. The headspace of the flask was then backfilled with argon. The flask was sealed and the reaction mixture frozen again with liquid nitrogen. This process was repeated a total of four times to give a degassed reaction mixture.

---

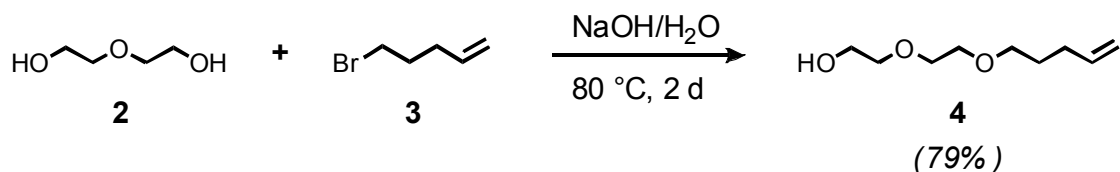
**References:**

- 1) Pangborn, A. B.; Giardello, M. A.; Grubbs, R. H.; Rosen, R. K.; Timmers, F. J. *Organometallics* **1996**, *15*, 1518-1520.

**General Phenol Alkylation Procedure.** To a cooled, flame-dried, two-neck round bottom flask, equipped with a stir bar and fitted with a septum, water condenser, and vacuum adapter was added, under argon, 3 equivalents (relative to each mole of phenol) of anhydrous potassium carbonate (J. T. Baker, 99.6%), anhydrous DMF (to make a ~0.1M solution), and 1 equivalent of phenol at room temperature. To this stirring mixture was added 1 equivalent of alkylating agent dissolved in a minimal amount of DMF. The reaction was heated to 80 °C in an oil bath for 3 to 4 days, and, upon completion, was quenched by cooling to room temperature. The reaction mixture was poured into a separatory funnel, and partitioned between water and ethyl acetate. The aqueous layer was extracted three times with fresh portions of ethyl acetate, and the combined organic layers were washed three times with fresh portions of water and brine. The washed organic layer was dried with anhydrous magnesium sulfate ( $\text{MgSO}_4$ ), filtered through filter paper, and evaporated to dryness under reduced pressure to give the alkylation product. Purification was achieved by flash chromatography on silica gel using various eluents.

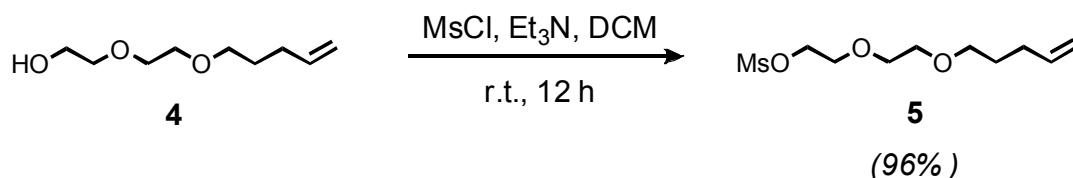
**General Lithium Aluminum Hydride Reduction Procedure.** To a cooled, flame-dried two-neck flask, equipped with a stir bar and fitted with a septum, water condenser, and vacuum adapter was added, under argon and at 0 °C, 3 equivalents of lithium aluminum hydride (LAH), dry THF, and, slowly, 1 equivalent of ester, acid, aldehyde, or nitrile dissolved in a minimal amount of dry THF. The septum was replaced with a glass stopper, and the reaction was heated to 87 °C overnight in an oil bath. To quench the

reaction mixture, the oil bath was removed and the reaction cooled to 0 °C. Water (1 ml per gram of LAH) was added very slowly to the stirring mixture, followed by very slow addition of a 10% sodium hydroxide solution (1 ml per gram of LAH). Water (3 ml for every gram of LAH) was added very rapidly, and the resulting slurry was allowed to stir for 4 hours at room temperature. After this time, a large excess of celite and anhydrous  $\text{MgSO}_4$  was added, and the mixture allowed to stir for an additional hour. The reaction was filtered into a separatory funnel and diluted with ethyl acetate, water, and brine. The water layer was extracted three times with fresh ethyl acetate, and the combined organic layer was washed with two fresh portions of water and brine, dried with anhydrous  $\text{MgSO}_4$ , filtered, and evaporated to dryness under reduced pressure to give the reduced product. Unless specified, the products were used with no further purification.



**Monoalkylated Diethylene Glycol (4).** A flask equipped with a stir bar was charged with diethylene glycol (**2**) (637 ml, 6.71 moles) and 5-bromo-1-pentene (**3**) (50 g, 0.3355 moles). A solution of sodium hydroxide and water (67.1 g NaOH, 1.6775 moles, and 67 ml of  $\text{H}_2\text{O}$ ) was added slowly over a period of 1 h via an addition funnel, resulting in turbidity of the reaction mixture. The reaction was heated to 80 °C for one day, and after cooling to room temperature, the mixture was poured into a separatory funnel, diluted with methylene chloride, water, and brine. The aqueous layer was extracted four times

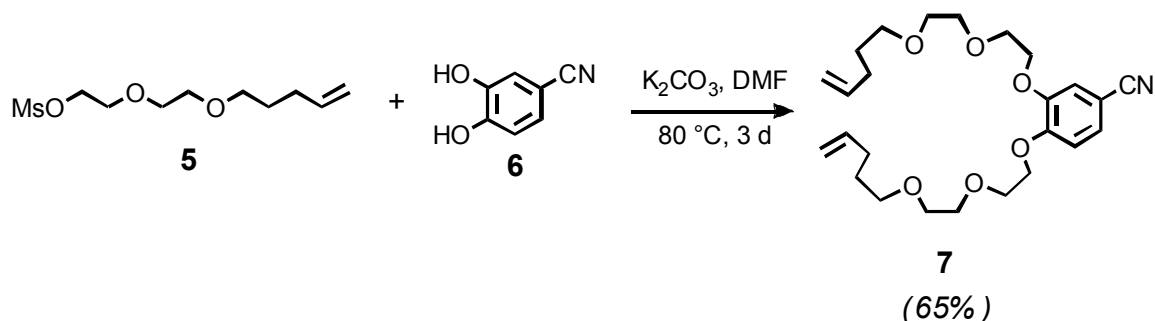
with fresh methylene chloride, and the combined organic layers were washed two times with fresh water and brine, dried with magnesium sulfate, filtered, and the solvent removed under reduced pressure. The resulting residue was purified by flash chromatography, eluting with a 3:1 to 1:1 hexanes to ethyl acetate gradient to give pure **4** (46.8 g, 79 % yield) as a brown oil.  $^1\text{H}$  NMR (300 MHz,  $\text{CDCl}_3$ ):  $\delta$  5.74 (m, 1H), 4.94 (m, 2H), 3.61 (m, 8H), 3.42 (m, 2H), 2.05 (m, 2H), 1.64 (m, 2H).  $^{13}\text{C}$  NMR (75 MHz,  $\text{CDCl}_3$ ):  $\delta$  138.0, 114.6, 72.4, 70.6, 70.2, 70.0, 61.5, 30.0, 28.5.



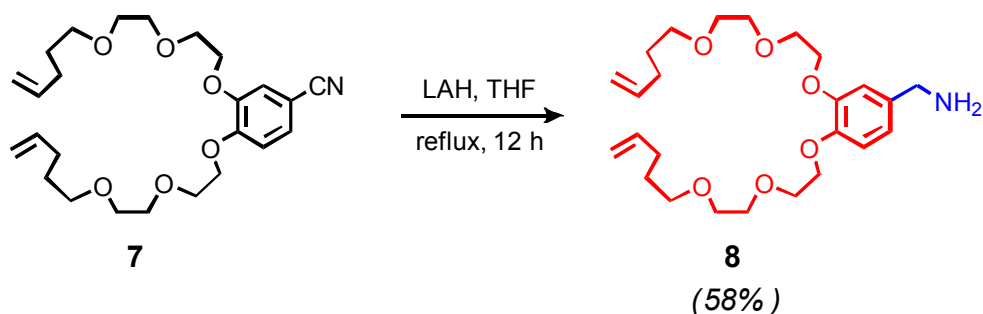
**Mesylated Arm Fragment (5).** A cooled, flame-dried flask equipped with a stir bar and septum was charged with **4** (46.3 g, 0.2657 moles) and dry DCM (~300 ml), then cooled to 0 °C. To the cooled reaction mixture was added mesyl chloride (31 ml, 0.3986 moles) and triethylamine (55.5 ml, 0.3986 moles) alternately in several batches. The reaction was warmed to room temperature and allowed to stir overnight. Stirring was stopped and the reaction mixture poured into a separatory funnel and partitioned with water and brine. The aqueous layer was extracted three times with fresh DCM, and the combined organic layers were washed three times with fresh water and brine, dried with magnesium sulfate, filtered, and the solvent removed under reduced pressure. The resulting crude oil was run through a plug of silica using 3:2 hexanes to ethyl acetate as eluent to afford **5** (64.2 g, 96 % yield) as a yellow oil.  $^1\text{H}$  NMR (300 MHz,  $\text{CDCl}_3$ ):  $\delta$  5.70 (m, center, 1H), 4.95-



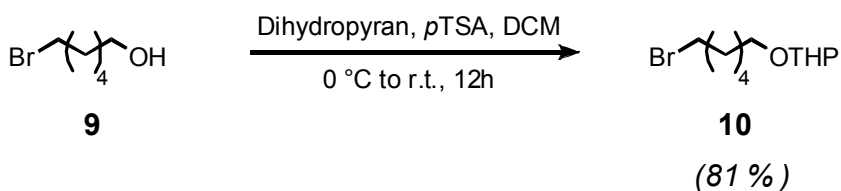
4.83 (br m, 2H), 4.29-4.26 (m, 2H), 3.68-3.65 (m, 2H), 3.65-3.61 (m, 2H), 3.57-3.53 (m, 2H), 3.49-3.45 (m, 2H), 3.37 (t,  $J = 10.2$  Hz, 2H), 2.99 (s, 3H), 2.04-1.96 (m, 2H), 1.56 (quint,  $J = 6.6$  Hz, 2H).  $^{13}\text{C}$  NMR (75 MHz,  $\text{CDCl}_3$ ):  $\delta$  138.10, 114.72, 70.55, 69.92, 69.45, 68.90, 52.57, 37.54, 30.11, 28.67. HRMS-FAB ( $m/z$ ):  $[\text{M} + \text{H}]$  calcd for  $\text{C}_{10}\text{H}_{21}\text{O}_5\text{S}$ , 253.1110; found, 253.1113.



**Nitrile Crown-Type Fragment (7).** Standard phenol alkylation conditions were used on a mixture of 3,4-dihydroxybenzonitrile (**6**) (7.0087 g, 0.05187 moles), **5** (26.1770 g, 0.1031 moles),  $\text{K}_2\text{CO}_3$  (21.5 g, 0.1031 moles), and dry DMF (1.0 L). Flash chromatography using 2:1 hexanes to ethyl acetate as eluent gave **7** (14.9910 g, 65 % yield) as a yellow oil.  $^1\text{H}$  NMR (300 MHz,  $\text{CDCl}_3$ ):  $\delta$  7.26-7.23 (m, 1H), 7.15-7.14 (m, 1H), 6.92 (d,  $J = 8.7$  Hz, 1H), 5.87-5.73 (m, 2H), 5.04-4.93 (m, 4H), 4.22-4.15 (m, 4H), 3.88 (qt,  $J = 5.1$  Hz, 4H), 3.71 (m, 4H), 3.59 (q,  $J = 3.3$  Hz, 4H), 3.49-3.44 (m, 4H), 2.10 (qt,  $J = 7.2$  Hz, 4H), 1.73-1.63 (m, 4H).  $^{13}\text{C}$  NMR (75 MHz,  $\text{CDCl}_3$ ):  $\delta$  152.89, 148.86, 138.24, 138.19, 126.77, 119.17, 117.08, 114.76, 114.73, 113.49, 104.10, 70.98, 70.96, 70.79, 70.77, 70.18, 70.16, 69.56, 69.42, 69.15, 68.69, 30.21, 28.74. HRMS-FAB ( $m/z$ ):  $[\text{M} + \text{H}]$  calcd for  $\text{C}_{26}\text{H}_{40}\text{NO}_6$ , 462.2856; found, 462.2857.

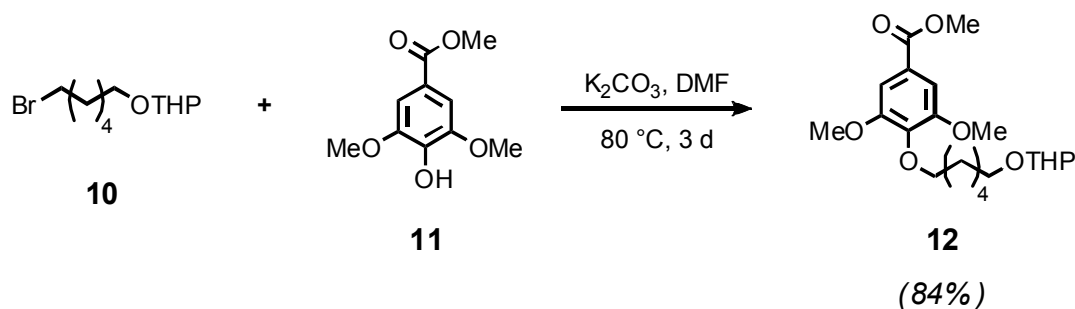


**Amine Crown-Type Fragment (7).** Standard LAH reduction conditions were used on **7** (0.6116 g, 1.367 mmol), LAH (0.1556 g, 4.101 mmol), and dry THF (20 ml). After workup, **8** (0.3578 g, 58 % yield) was obtained as a yellow oil.  $^1\text{H}$  NMR (300 MHz,  $\text{CDCl}_3$ ):  $\delta$  6.89-6.80 (m, 3H), 5.87-5.73 (m, 2H), 5.04-4.92 (m, 4H), 4.19-4.13 (m, 4H), 3.85 (q,  $J$  = 5.4 Hz, 4H), 3.77 (s, 2H), 3.73-3.70 (m, 4H), 3.60-3.57 (m, 4H), 3.46 (t, 6.9 Hz, 4H), 2.10 (q,  $J$  = 6.9 Hz, 4H), 1.67 (quint,  $J$  = 6.9 Hz, 4H).  $^{13}\text{C}$  NMR (75 MHz,  $\text{CDCl}_3$ ):  $\delta$  149.20, 147.91, 138.40, 120.02, 115.18, 114.85, 114.00, 70.97, 70.87, 70.32, 69.93, 69.24, 69.04, 46.27, 30.37, 28.90.

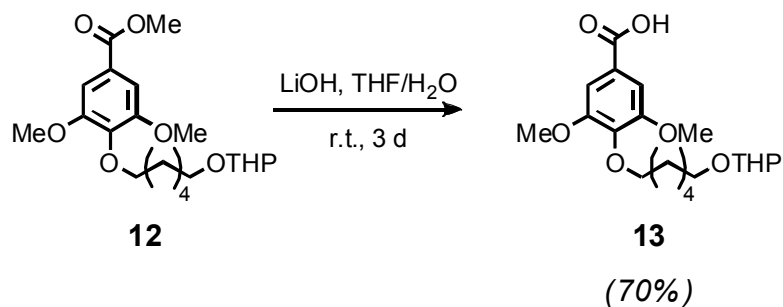


**2-(6-Bromohexyloxy)tetrahydro-2H-pyran (10).** A cooled, flame-dried round bottom flask equipped with a stir bar and septum was charged, under argon and at 0 °C, with **9** (7.6551 g, 42.28 mmol), dry DCM (10 ml), dihydropyran (4.25ml, 46.51 mmol), and *p*-toluenesulfonic acid (0.4030 g, 2.114 mmol). The reaction was allowed to stir at room

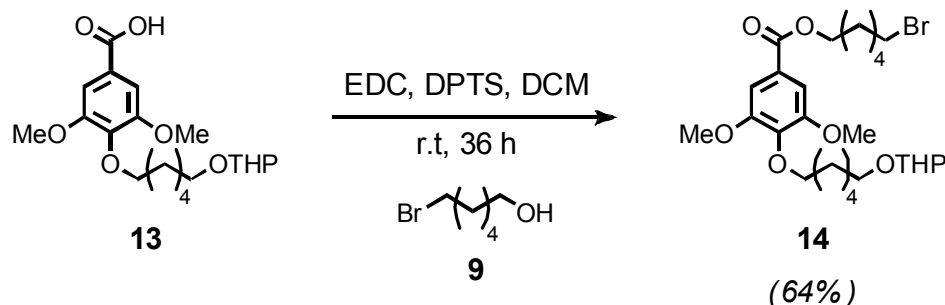
temperature overnight, and was quenched by diluting with water and DCM in a separatory funnel. The organic layer was washed three times with fresh water and brine, dried with magnesium sulfate, filtered, and the solvent removed under reduced pressure. Flash chromatography using 15:1 hexanes to ethyl acetate gave **10** (9.0902 g, 81 % yield) as a clear oil.  $^1\text{H}$  NMR (300 MHz,  $\text{CDCl}_3$ ):  $\delta$  4.56 (t,  $J = 2.75$  Hz, 1H), 3.85 (m, 1H), 3.72 (m, 1H), 3.51 (m, 1H), 3.40 (m, 3H), 1.95-1.36 (br m, 14H).  $^{13}\text{C}$  NMR (75 MHz,  $\text{CDCl}_3$ ):  $\delta$  99.09, 67.60, 62.58, 34.10, 32.95, 30.97, 29.76, 28.21, 25.69, 19.91.



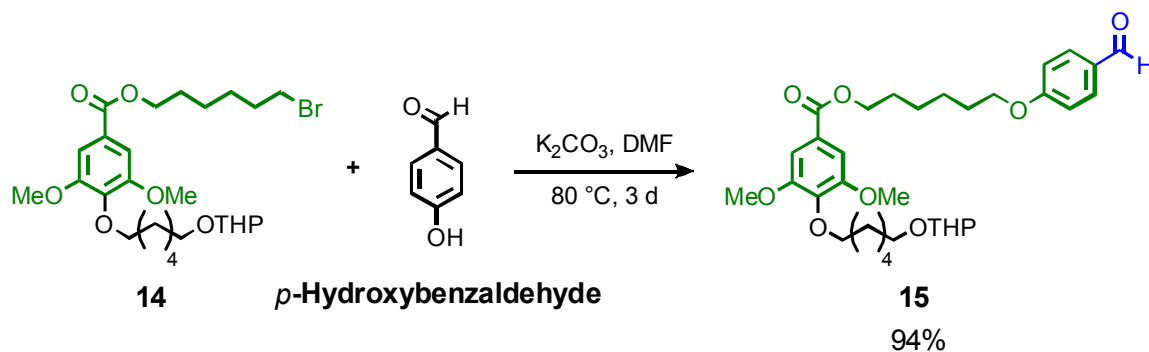
**Methyl Ester Cap (12).** Standard alkylation conditions were used with **10** (3.1637 g, 11.90 mmol), **11** (2.7847 g, 13.09 mmol),  $\text{K}_2\text{CO}_3$  (4.9465 g, 35.7 mmol), and dry DMF (~50 ml). After 3 days, the reaction was worked up. Flash chromatography using 4:1 hexanes to acetone as eluent gave **12** (3.8678 g, 84 % yield) as a viscous, colorless oil.  $^1\text{H}$  NMR (300 MHz,  $\text{CDCl}_3$ ):  $\delta$  7.27 (s, 2H), 4.56 (t,  $J = 2.75$  Hz, 1H), 4.01 (t,  $J = 6.88$  Hz, 2H), 3.88 (s, 3H), 3.87 (s, 6H), 3.83 (m, 1H), 3.72 (m, 1H), 3.47 (m, 1H), 3.37 (m, 1H), 1.89-1.34 (br m, 14H).  $^{13}\text{C}$  NMR (75 MHz,  $\text{CDCl}_3$ ):  $\delta$  166.88, 153.25, 141.55, 124.97, 106.85, 98.97, 73.53, 67.68, 62.48, 56.28, 52.28, 30.87, 30.12, 29.82, 26.12, 25.75, 25.57, 19.81.



**Benzoic Acid Cap (13).** A flask, equipped with a stir bar and septum, was charged with **12** (3.3962 g, 8.566 mmol), THF (47.6 ml), water (9.5 ml), and lithium hydroxide (1.0783 g, 25.698 mmol). The reaction was allowed to stir for 3 days at room temperature, after which the THF was removed under reduced pressure. The resulting mixture was dissolved in DCM, poured into a separatory funnel, and partitioned with water and brine. To this was added ~75ml of a 5 % citric acid solution in water. The aqueous layer was extracted three times with fresh DCM, and these organic layers were combined, dried with magnesium sulfate, filtered, and the solvent removed under reduced pressure. Flash chromatography using 2:1 hexanes to acetone as eluent gave **13** (2.0931 g, 63 % yield) as a colorless oil.  $^1\text{H}$  NMR (300 MHz,  $\text{CDCl}_3$ ):  $\delta$  10.60-9.75 (br s, 1H), 7.33 (s, 2H), 4.56 (t,  $J = 2.75$  Hz, 1H), 4.01 (t,  $J = 6.88$  Hz, 2H), 3.87 (s, 6H), 3.83 (m, 1H), 3.72 (m, 1H), 3.47 (m, 1H), 3.37 (m, 1H), 1.89-1.34 (br m, 14H).  $^{13}\text{C}$  NMR (75 MHz,  $\text{CDCl}_3$ ):  $\delta$  171.28, 153.22, 142.18, 124.27, 107.38, 98.88, 73.526, 67.66, 62.37, 56.23, 30.78, 30.09, 29.75, 26.07, 25.70, 25.51, 19.67.

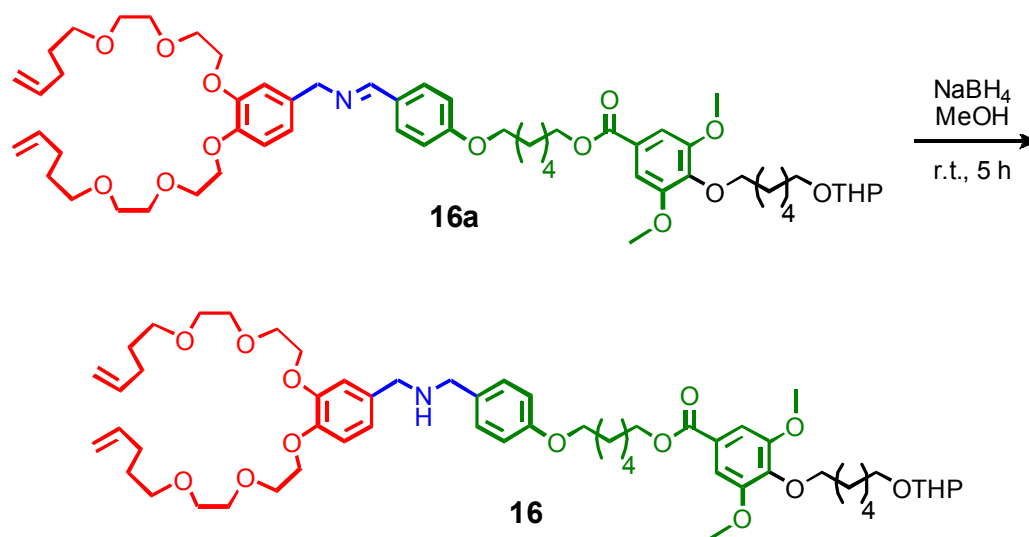


**Ester Backbone-Cap Fragment (14).** A cooled, flame-dried round bottom flask equipped with a stir bar and septum was charged, under argon, with 1-ethyl-3-(3-dimethylaminopropyl)carbodiimide (0.1504 g, 0.784 mmol), DPTS (75.0 mg, 0.255 mmol), DMAP (95.8 mg, 0.784 mmol), **9** (0.1420 g, 0.784 mmol), and **13** (0.3000 g, 0.784 mmol). This solid mixture was then solvated with dry DCM (7ml) and allowed to stir at room temperature for 1.5 days. The reaction mixture was stopped by dilution in a separatory funnel with water and brine. The first organic layer was collected, and the aqueous layer extracted two additional times with fresh EA. The combined ethyl acetate and DCM layers were dried with magnesium sulfate, filtered, and the solvent removed under reduced pressure. Flash chromatography using 4:1 hexanes to acetone as eluent and loading with benzene, gave **14** (0.2725 g, 64 % yield) as a pale-yellow oil.  $^1\text{H}$  NMR (300 MHz,  $\text{CDCl}_3$ ):  $\delta$  7.28 (s, 2H), 4.56 (t,  $J$  = 2.75 Hz, 1H), 4.31 (t,  $J$  = 6.88 Hz, 2H), 4.01 (t,  $J$  = 6.88 Hz, 2H), 3.89 (s, 6H), 3.83 (m, 1H), 3.74 (m, 1H), 3.56 (t,  $J$  = 6.60 Hz, 2H), 3.47 (m, 1H), 3.37 (m, 1H), 1.95-1.35 (br m, 22H).  $^{13}\text{C}$  NMR (75 MHz,  $\text{CDCl}_3$ ):  $\delta$  166.44, 153.27, 141.62, 125.27, 106.90, 98.98, 73.56, 67.70, 65.05, 62.49, 56.34, 33.80, 32.69, 30.89, 30.13, 29.84, 28.70, 27.89, 26.14, 25.77, 25.60, 25.33, 19.83. HRMS-FAB ( $m/z$ ):  $[\text{M} + \text{H}]$  calcd for  $\text{C}_{26}\text{H}_{41}\text{O}_7\text{Br}$ , 544.2036; found, 544.2034.



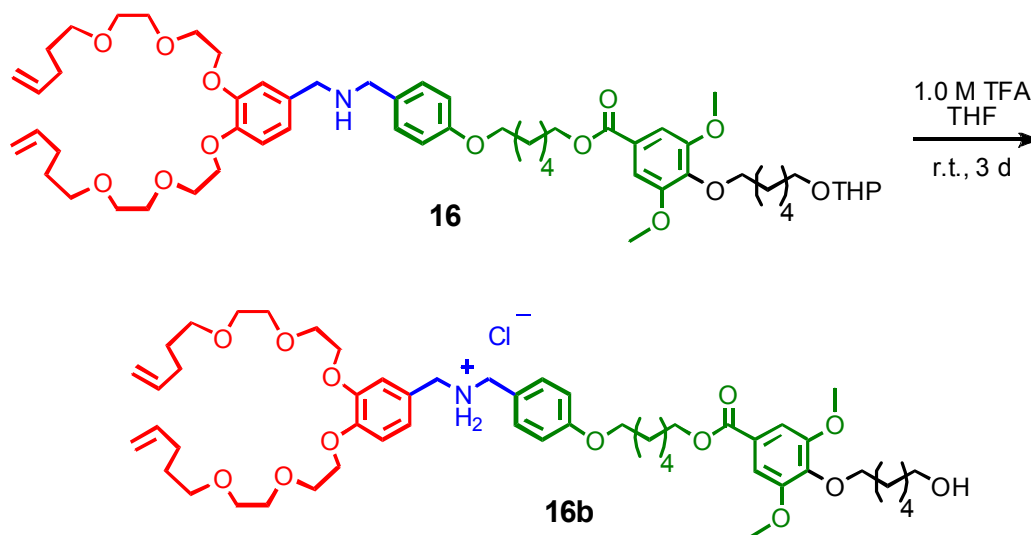
**Aldehyde Backbone-Cap Fragment (15).** Standard alkylation conditions were used with **14** (0.9508 g, 1.743 mmol), *p*-hydroxybenzaldehyde (0.2341 g, 1.917 mmol),  $K_2CO_3$  (0.2412 g, 5.229 mmol), and dry DMF (20 ml). Flash chromatography using 4:1 hexanes to acetone as eluent and benzene as the loading solvent gave **15** (0.9577 g, 94 % yield) as a colorless oil.  $^1H$  NMR (300 MHz,  $CDCl_3$ ):  $\delta$  9.78 (s, 1H), 7.72 (d,  $J$  = 8.79, 2H), 7.22 (s, 2H), 6.89 (d,  $J$  = 8.79, 2H), 4.49 (t,  $J$  = 2.75 Hz, 1H), 4.25 (t,  $J$  = 6.66 Hz, 2H), 3.96 (t,  $J$  = 6.52 Hz, 4H), 3.80 (s, 6H), 3.75 (m, 1H), 3.66, (m, 1H), 3.40 (m, 1H), 3.31 (m, 1H), 1.82-1.28 (br m, 22H).  $^{13}C$  NMR (75 MHz,  $CDCl_3$ ):  $\delta$  190.57, 166.14, 163.98, 153.03, 141.40, 131.83, 129.66, 125.05, 114.57, 106.67, 98.71, 68.02, 67.43, 64.84, 62.21, 56.06, 30.66, 29.92, 29.61, 28.83, 28.55, 25.91, 25.66, 25.57, 25.54, 25.38, 19.59.

**Ester Macromer (1-H·PF<sub>6</sub>).** A flask equipped with a stir bar, Dean-Stark trap, and water condenser was charged with **8** (0.5419 g, 1.200 mmol), **15** (0.6532 g, 1.117 mmol), and benzene (~50 ml). The reaction was heated to 100 °C for 4 days. The Dean-Stark trap was emptied several times, followed by addition of fresh benzene. The reaction was cooled and the benzene removed under reduced pressure to afford the imine condensation product **16a** (1.1397 g, quantitative yield) as a brown oil. The product was used without further purification. <sup>1</sup>H NMR (300 MHz, CDCl<sub>3</sub>): δ 8.35-8.19 (br s, 1H), 7.82 (d, J = 8.25 Hz, 2H), 7.28 (s, 2H), 6.98 (d, J = 8.8 Hz, 2H), 6.95-6.81 (br m, 3H), 5.79 (m, 2H), 5.08-4.88 (br m, 4H), 4.70 (s, 2H), 4.57 (t, J = 2.75 Hz, 1H), 4.32 (m, 2H), 4.16 (q, J = 4.67 Hz, 2H), 4.03 (qt, J = 6.81 Hz, 4H), 3.93-3.80 (br m, 11H), 3.78-3.66 (br m, 5H), 3.64-3.54 (br m, 5H), 3.52-3.34 (br m, 5H), 2.09 (qt, J = 6.88, 4 H), 1.92-1.34 (br m, 26H).

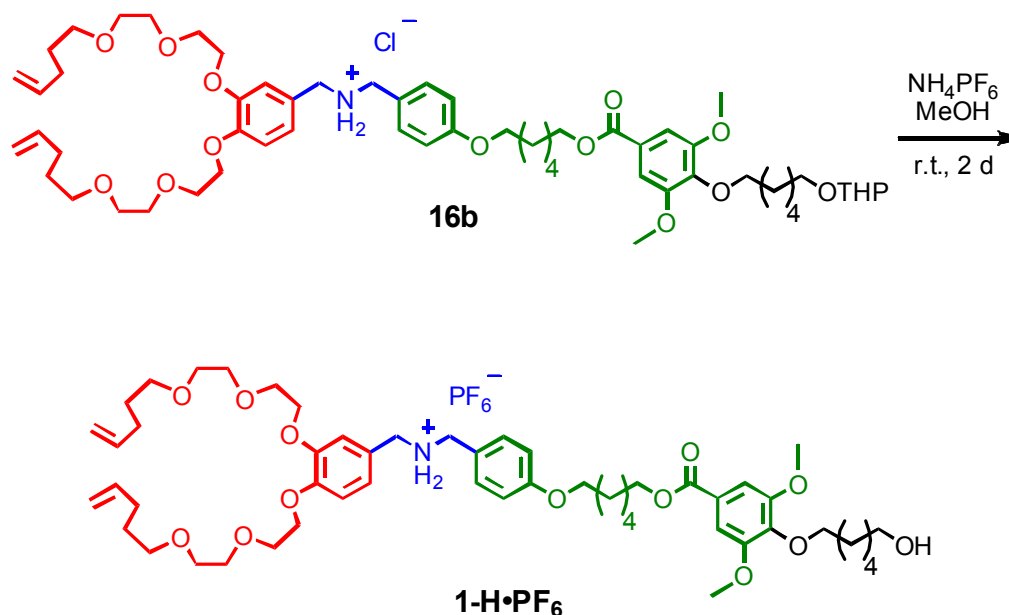


To a flask equipped with a stir bar was added crude imine **16a** (1.1397 g, 1.117 mmol) and methanol (13 ml). Sodium borohydride (0.1471 g, 3.891 mmol) was added in one portion to the stirring reaction mixture, resulting in much bubbling but no heat production. The reaction was stirred at room temperature for 5 hours, and was quenched by removal of methanol under reduced pressure. The product residue was dissolved in DCM, poured into a separatory funnel, and mixed with water and brine. The aqueous layer was extracted two times with fresh DCM, and the combined organic layers were dried with magnesium sulfate, filtered, and the solvent removed under reduced pressure to afford amine **16** (1.0373 g, 91 % yield) as a thick orange oil. The product was used without further purification. <sup>1</sup>H NMR (300 MHz, CDCl<sub>3</sub>):  $\delta$  7.25 (d, *J* = 6.60 Hz, 2H), 7.20 (d, *J* = 8.53 Hz, 2H), 6.89-6.72 (br m, 5H), 5.79 (m, 2H), 5.08-4.88 (br m, 4H), 4.55 (t, *J* = 2.75 Hz, 1H), 4.30 (t, *J* = 6.88 Hz, 2H), 4.14 (q, *J* = 4.83 Hz, 4H), 4.00 (t, *J* = 6.88 Hz, 2H), 3.93 (t, *J* = 6.47, 2H), 3.86 (s, 6H), 3.75-3.33 (br m, 24H), 2.09 (qt, *J* = 6.88, 4 H), 1.92-1.34 (br m, 26H).



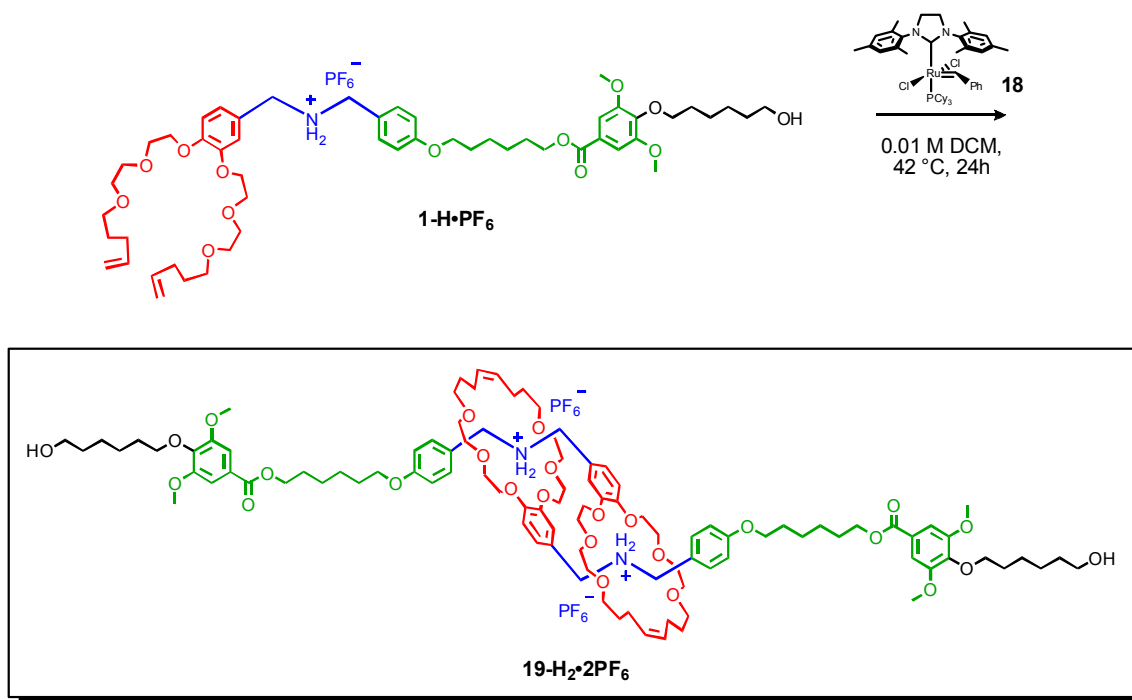


A flask equipped with a stir bar was charged with **16** (1.0373 g, 1.015 mmol), THF (17 ml), methanol (3.5 ml), and 1.0M TFA in water (10 ml, 10 mmol). The reaction mixture turned from pale yellow to bright orange over 3 days. The THF and methanol were removed under vacuum, and the residue was dissolved in DCM, poured into a separatory funnel, and mixed with water. The aqueous layer was extracted three times with fresh DCM, and the combined organic layers were dried with magnesium sulfate, filtered, and the solvent removed under reduced pressure to give deprotected, chloride salt macromer **16b** (0.7832 g, 68 % yield) as a bright orange oil. The product was used with no further purification.  $^1\text{H}$  NMR (300 MHz,  $\text{CDCl}_3$ ):  $\delta$  9.75-9.25 (br s, 2H), 7.37-7.18 (br m, 6H), 7.00 (s, 1H), 6.83 (m, 2H), 5.79 (m, 2H), 5.08-4.88 (br m, 4H), 4.32 (t,  $J = 6.88$  Hz, 2H), 4.11 (q,  $J = 4.83$  Hz, 4H), 4.07-3.42 (br m, 30H), 2.16-2.02 (br m, 4H), 1.88-1.32 (br m, 20H).



In a flask equipped with a stir bar, chloride salt **16b** (0.7832 g, 0.744 mmol) was dissolved in methanol (8 ml), and ammonium hexafluorophosphate (0.2427 g, 1.488 mmol) was added. The solution was stirred for several days, followed by removal of methanol under reduced pressure. The resulting residue was dissolved in DCM, and partitioned with water and brine. The organic layer was washed three times with fresh water and brine, dried with anhydrous magnesium sulfate, filtered, and the solvent removed under reduced pressure to give **1-H·PF<sub>6</sub>** (0.5459 g, 68% crude yield) as a brown viscous oil. The product was used without further purification. <sup>1</sup>H NMR (300 MHz, CDCl<sub>3</sub>): δ 8.47 (br s, 2 H), 7.42 (d, J = 8.25 Hz, 2H), 7.25 (s, 2H), 7.05-6.65 (m, 3H), 5.79 (m, 2H), 5.08-4.88 (br m, 4H), 4.29 (t, J = 6.6 Hz, 2H), 4.22-3.38 (br m, 34H), 2.05 (br m, 4H), 1.95-1.25 (br m, 20 H). <sup>13</sup>C NMR (75 MHz, CDCl<sub>3</sub>): δ 166.34, 159.91, 153.14, 148.09, 147.57, 141.45, 137.85, 137.57, 131.01, 125.23, 123.45, 123.17, 122.49, 115.25, 115.04, 114.90, 114.55, 113.47, 106.80, 73.38, 71.19, 70.99, 70.86, 70.80, 70.09,

70.00, 69.59, 69.51, 68.68, 68.21, 67.89, 65.84, 65.04, 62.75, 56.22, 50.77, 50.45, 32.68, 30.11, 30.02, 29.10, 28.66, 25.82, 25.75, 25.58, 25.48.



### Standard Binding Motif Ester [2]Rotaxane Dimer Molecular Muscle (**19-H<sub>2</sub>·2PF<sub>6</sub>**).

A cooled, flame-dried two-neck flask equipped with a stir bar, water condenser, gas port, and septum was charged, under argon, with **1-H·PF<sub>6</sub>** (0.5397 g, 0.498 mmol) and dry DCM (49.8 ml, 0.01M). This mixture was subjected to standard freeze-pump-thaw conditions, followed by catalyst **1** (21.1 mg, 0.0249 mmol) addition. The septum was replaced with a glass stopper, and the reaction heated to 42 °C overnight. The reaction was quenched by addition of ethyl vinyl ether (~2ml), and was allowed to stir at elevated temperature for 30 minutes. The solvent was removed under reduced pressure, yielding a brown foam. Flash chromatography using a 50:1 DCM to methanol to 20:1 DCM to

methanol gradient as eluent afforded some **20** mixed with impurities and decomposition products. No yield was obtained due to incomplete purification and decomposition.  $^1\text{H}$  NMR (300 MHz,  $\text{CDCl}_3$ ):  $\delta$  8.10-6.55 (br m, 11H), 5.415 (m, 2H), 4.82-3.36 (br m, 36H), 2.62-1.36 (br m, 24H).  $^{13}\text{C}$  NMR (75 MHz,  $\text{CDCl}_3$ ):  $\delta$  166.32, 159.77, 153.12, 146.55, 146.12, 141.45, 131.93, 130.35, 129.83, 125.88, 125.20, 123.49, 115.03, 114.78, 106.77, 99.53, 74.676, 73.41, 73.35, 70.71, 70.11, 69.65, 68.00, 65.23, 65.01, 62.73, 60.69, 56.20, 53.12, 52.07, 51.72, 32.66, 31.90, 30.00, 29.85, 29.65, 29.07, 28.91, 28.64, 26.75, 26.22, 26.01, 25.80, 25.73. ESI-TOF MS ( $m/z$ ):  $[\text{M} - 2\text{PF}_6]^{+2}$  calcd for  $\text{C}_{51}\text{H}_{76}\text{NO}_{13}$ , 910.5311; found, 910.5236.

## APPENDIX 2

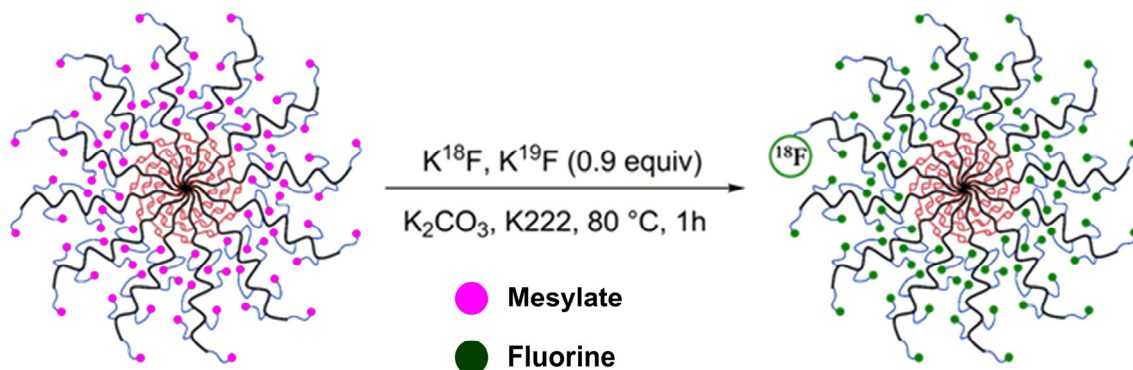
### Progress Toward $^{18}\text{F}$ Labeled Nanoparticles as *in vivo* Imaging Agents

For background and introduction to this appendix, see the thesis of Dr. John B. Matson, as well as the following published material: Matson, J. B.; Grubbs, R. H. *J. Am. Chem. Soc.* **2008**, *130*, 6731-6733.

### **Progress toward $^{18}\text{F}$ Labeled Nanoparticles as *in vivo* Imaging Agents**

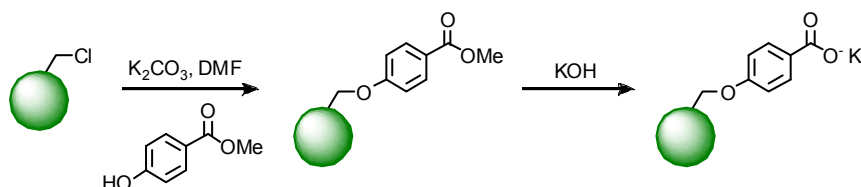
Recent Work: One of the efforts in our lab is directed at the synthesis of  $^{18}\text{F}$ -labeled nanoparticles to be used as tumor imaging agents for positron emission tomography. We have been encountering some challenges during radiofluorination of the mesylated nanoparticles (NPs, Scheme 1). One of these challenges involves the analysis of the crude reaction mixture after the one hour fluorination reaction via radio-thin layer chromatography (TLC) on silica, a technique identical to traditional TLC except that analysis of the developed TLC plate is performed by a radioactivity sensor. Because free  $^{18}\text{F}$  does not move off of the baseline, any radioactive spot higher up the plate indicates appending of a molecule of  $^{18}\text{F}$  to the species that is moving up the plate. Intriguingly, though we were seeing no radioactive spots higher up the TLC plate,  $^1\text{H}$  NMR analysis of our NPs after the  $^{18}\text{F}$  reaction indicated we were achieving  $\sim 12\%$  fluorine substitution of the mesylates. This led us to believe that radio-TLC of the NPs on silica gel may be an intractable analytical protocol, as reaction of a single mesylate on the surface of the NPs with the TLC silica surface could irreversibly bind the particles to the surface and prevent their movement off of the baseline. To test this theory, we analyzed a number of NP

**Scheme A2.1.** Fluorination of Mesylated Nanoparticles



samples, both before and after fluorination, via preparatory and two-dimensional TLC on silica. Though the preparatory TLC failed to yield conclusive evidence of particle decomposition or binding, the two-dimensional TLC showed very clear binding of mesylated NPs to the silica. Fluorine-labeled NPs appear to suffer from a similar fate, which is not surprising given the limited fluorination. It is likely that the surface of these fluorinated NPs contains functionality that can, similar to the mesylate, react with the silica and bind to the surface. Consequently, to solve this challenge and enable the direct analysis of the NP radiofluorination studies by TLC, we have explored other sorbents for NP TLC and are continuing our efforts to maximize fluorine coverage across the surface of the NPs. Initial work indicates that the NPs readily move up aluminum oxide TLC plates, and that the particles can be successfully recovered from the aluminum surface of the plate.

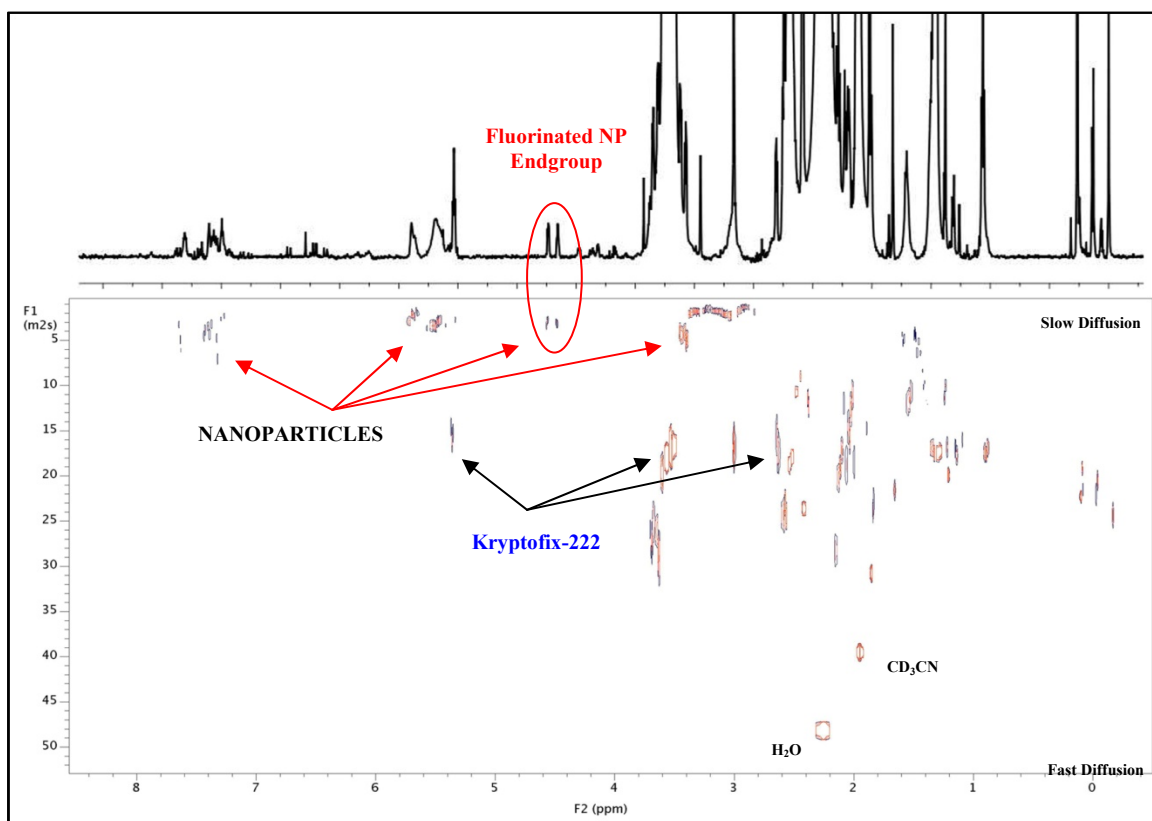
During the radiofluorination substitution of the NP mesylate groups, we had been employing potassium carbonate ( $K_2CO_3$ ) as both a base, to prevent loss of fluorine from the reaction as HF, and as a potassium ion donor to generate more potassium/kryptofix-222 (K222) phase transfer catalyst. Unfortunately, after NP fluorination in the presence of  $K_2CO_3$ ,  $^1H$  NMR analysis shows substitution of a portion of the mesylates with carbonate. The generation of a terminal carbonate can induce a number of side-reactions, including reaction with additional surface mesylates and concomitant decrease of available fluorination sites, or coupling between NPs, resulting in aggregation and decreasing the efficacy of the NPs as imaging agents. In an effort to eliminate the problematic  $K_2CO_3$  from the reaction, we have begun employing resin-bound potassium

**Scheme A2.2.** Synthesis of Resin-Bound Potassium Benzoate

benzoate (Scheme 2) as both a potassium ion source and proton sponge. Initial results indicate that we obtain similar amounts of NP fluorination when using the beads in lieu of  $K_2CO_3$ , but there appear to be far fewer side-reactions and degradation products. We are hoping that optimization of reaction conditions, including the quantity of resin, temperature, equivalents of other reagents, and possible solvent effects will increase the extent of fluorination while preventing NP degradation.

One of the major difficulties associated with NP functionalization is the analysis of the NPs after functionalization. Because TLC has not yet proven to be a viable technique, we have had to rely on NMR to ascertain the success of the fluorination. Unfortunately, the particle size results in significant line broadening in the one-dimensional  $^1H$  NMR spectrum and makes separation of product and reagent peaks exceptionally challenging. However, two-dimensional diffusion-ordered NMR spectroscopy (2D-DOSY) enables separation of proton signals based on the solution diffusion rate of the species generating those signals. In this way, signals corresponding to the protons on the rapidly diffusing small molecules (such as K222) are readily distinguished from the NP proton signals (Figure 1). Consequently, we will be using 2D-DOSY during optimization of the reaction conditions to help maximize fluorine incorporation in the NP shell. We are also beginning to explore the possibility of 2D-Fluorine-DOSY for NP study.

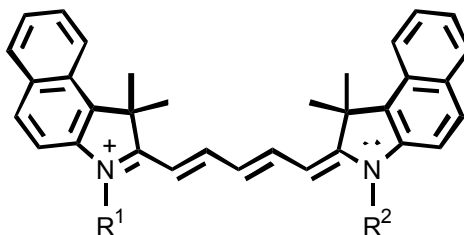




**Figure A2.1:** Two-dimensional diffusion-ordered  $^1\text{H}$  NMR spectrum of fluorinated nanoparticles.

### ***Future Work***

Currently, we are working to enhance the extent of fluorination through the inclusion of a small amount of water during the fluorination. While water can prove detrimental by reacting with surface mesylates and coupling two nanoparticles, we have observed that a small amount of water (contained as a component of the deuterated acetonitrile in which the NP fluorination reactions were performed) increased the quantity of NP surface fluorination. This phenomenon is still being explored, but it is likely that trace water helps solubilize the fluoride salts and bring them into the acetonitrile/NP solution, something that cannot be achieved if very dry acetonitrile is



**Figure A2.2:** General structure of Cy5.5 dye to be appended to the NPs.

used. We will be introducing controlled amounts of water into NP reaction solutions prepared in dry acetonitrile to determine the ideal quantity of water required to maximize fluorination and keep NP dimerization to a minimum.

In addition to the  $^{18}\text{F}$  labeling of the NPs, we also will be exploring the distribution of the NPs within the eye. These studies will be performed in collaboration with Prof. Raymond Iezzi and colleagues at the Mayo Clinic, and necessitates conjugation of a cyanine 5.5 dye (cy5.5, Figure A2.2) to the surface of the NP. We will be synthesizing three different sizes of the NPs for these studies.